VLÁKNA a TEXTIL

FIBRES AND TEXTILES

3

VÚTCH

CHEMITEX

Trenčianska univerzita
Fakulta priemyselných technológií v Púchove
Alexandra Dubčeka v Trenčíne

VÚCHV

Spoločnosť priemyselnej chémie
zSVTS

TECHNICAL UNIVERSITY OF LIBEREC
Faculty of Textile Engineering

STU
FCHPT

Fibres and Textiles (3) 2016
Vlákna a textil (3) 2016
September 2016

Special issue venue XXIV International Congress IFATCC

"TRADITION AND HIGH-TECH DEVELOPMENT KEYS TO THE TEXTILE MARKET"

held on June 13.- 16. 2016 in Pardubice, Czech Republic

CONTENT

DYEING OF POLYESTER FABRIC WITH BIO-BASED MADDER DYE AND ASSESSMENT OF ENVIRONMENTAL IMPACTS USING LCA TOOL

T. Agnhage[1,2,3,4], A. Perwuelz[1,2] and N. Behary[1,2]

[1]*ENSAIT, GEMTEX, F-59100 Roubaix, France*
[2]*Univ. Lille Nord de France, F-59000 Lille, France*
[3]*Univ of Borås, Swedish School of Textiles, S-501 90 Borås, Sweden*
[4]*Soochow Univ. College of Textile and Clothing Engineering, Suzhou, Jiangsu, China*
tove.agnhage@ensait.fr

Abstract: *In order to improve the environmental sustainability of textile dyeing processes, dyeing of polyester fabric with bio-based dye from the roots of madder plant (Rubia tinctorum L.) has been explored and the environmental impacts assessed.*

The influence of the main dyeing conditions (dyebath pH, time and temperature) on the dyeing performance was studied. The dyeing performance was evaluated with respect to color yield and fastness properties of the dyed samples. The potential environmental impacts were quantified using life cycle assessment (LCA) tool. Three impact categories were considered: Global warming potential (GWP), Water depletion (WD) and Water eutrophication (WE).

The optimum dyeing conditions were found to be pH of 5, dyeing temperature of 130°C and dyeing time of 45 min. LCA of a cradle-to-grave scenario (lifetime of a madder dyed polyester shirt) revealed that the dyeing process was the most important life cycle stage with respect to GWP whereas the use phase of the shirt was the most significant life cycle stage with respect to WD and WE. Gate-to-gate LCA of the dyeing process showed that the extraction of madder dyes indeed was a hotspot with respect to GWP.

Key Words: *natural dye, life cycle assessment, dye extraction, use phase*

1   INTRODUCTION

One of the oldest dye sources used throughout history is the tinctorial plant madder (*Rubia tinctorum L.*)*.* The plant was historically cultivated in Central and Western Europe and one of the most important dye plants in Europe at the end of the 19th century. At this time in history, mills in France (Provence - one of the main regions for production) produced as much as 33 million kilograms of powdered madder during 8 months of yearly production [1].   However, with the invention of synthetic dyes, in particular the preparation of alizarin by BASF as well as Perkin in 1869, madder almost completely disappeared from the world market [2].

Nevertheless, concerns over polluted textile wastewaters and limited supply of non-renewable fossil fuels have caused renaissance in research into the potential use of natural dyes, as alternatives to existing synthetic compounds. Drivas et al. (2011) used coloring species from madder as platform chemicals to synthesize sustainable alternatives to existing synthetic dyes for polyester. Indeed the madder roots contain anthraquinone derivatives (36 compounds have been identified so far), whereof the main dye is alizarin **(1)**. Other coloring species present are purpurin **(2)**, xantho-purpurin **(3)**, rubiadin **(4)**, pseudopurpurin **(5)**, munjistin **(6)** and lucidin **(7)** [3].

As natural dyes reach only low production volume and are restricted to small scale uses (such as handicraft), environmental impacts have been neglected. With an increased production and consumption it is essential that the environmental benefits exceed the present situation defined by synthetic dyes.
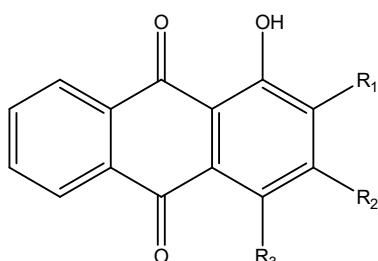
(1): R_1 = OH; $R_2 = R_3$ = H
(2): $R_1 = R_3$ = OH; R_2 = H
(3): $R_1 = R_3$ = H; R_2 = OH
(4): $R_1 = CH_3$; R_2 = OH; R_3 = H
(5): R_1 = COOH; $R_2 = R_3$ = OH
(6): R_1 = COOH; R_2 = OH; R_3 = H
(7): $R_1 = CH_2OH$; R_2 = OH; R_3 = H

To our knowledge, the environmental impacts related to the production and use of madder dye has not been quantified. Therefore, this study explores dyeing of polyester with madder dye and assesses the potential environmental impacts of the dyeing process. The work aims at identifying opportunities for environmental improvements in the dyeing process of polyester with madder dye, for the development of "green" bio-based textile dyeing.

2 MATERIALS AND METHODS

2.1 Materials

A polyester (polyethylene terephthalate – PET) plain woven fabric of the density 110 g/m^2, with 60 warp threads/cm and 34 weft threads/cm, was used. The fabric was dyed with G.O.T.S and REACH certified madder (*Rubia tinctorum L.*) dye (C03), used as received from Couleurs de plantes (France).

2.2 Experimental dyeing

The dye was prepared in 1, 3 and 5% owf. The influence of dyebath pH, temperature and time on the dyeing performance was studied while the liquor:fabric ratio (LR) of 15:1 was kept constant. pH was adjusted using aqueous formic acid, acetic acid or sodium hydroxide to obtain dyebath solutions of pH 3, 5, 7, 9 and 11.

Prior to dyeing, a light scouring (pre-wash) of the fabric was carried out using a conventional wash at 60°C. Samples (10 g) were dyed in 200 ml beakers in a laboratory-scale Labomat dyeing machine (Switzerland). Temperature / time profile is shown in Figure 1.

To remove surface sorbed dyes, a designed after-treatment was used, namely one wash according to ISO 105: C 10 (Labomat, Switzerland), which was the same as the one used for the standard wash fastness test.

Five consecutive standard washings (ISO 105:C 10) were carried out for wash fastness characterization. Rub fastness test was carried out according to ISO 105-X12.
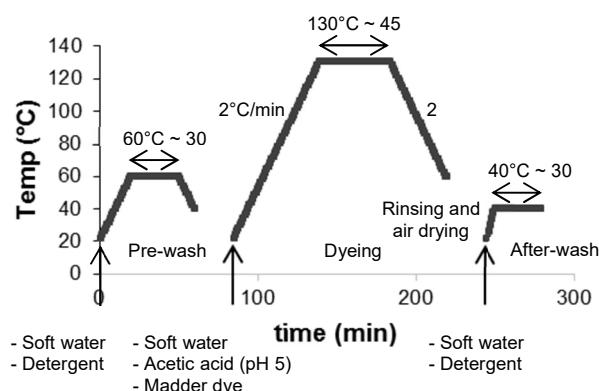
Figure 1 Temperature / time profile for the dyeing phase including the three textile wet-processes: pre-wash, dyeing and after-wash

Spectral reflectance factors of the dyed samples were measured using a Datacolor Spectraflash SF600 reflectance spectrophotometer (Datacolor International). The color yield (K/S value) was automatically calculated by the software using Kubelka-Munk equation [4]. CIELab values (*L**, *a**, *b**, *C** and *h**) were assessed under illuminant D65 using the 10° standard observer.

2.3 Life cycle assessment

The LCA was carried out using EIME software, Bureau Veritas CODDE (France). Two functional units (FU) were used: "Dyeing of 1 kg woven polyester fabric (110 g/m^2) with 3% owf madder dye" and "One madder dyed woven polyester shirt to be worn and cleaned, twice a month, for 2.5 years". Madder dye production included all the process steps shown in Figure 2. The system boundaries (Figures 3a, 3b) considered production and end of life treatment in Europe. It was hypothesized that the shirt was washed in France. Transportation, packaging and maintenance of machines were not considered.

The databases within the EIME software were the source of the secondary inventory data based upon which energy production, water softening treatment, raw and process materials, waste water treatment etc. were modeled.
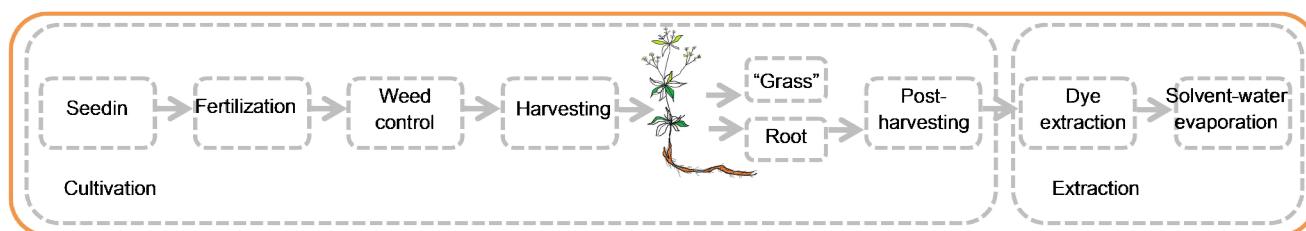
Figure 2 Flowchart of madder dye production
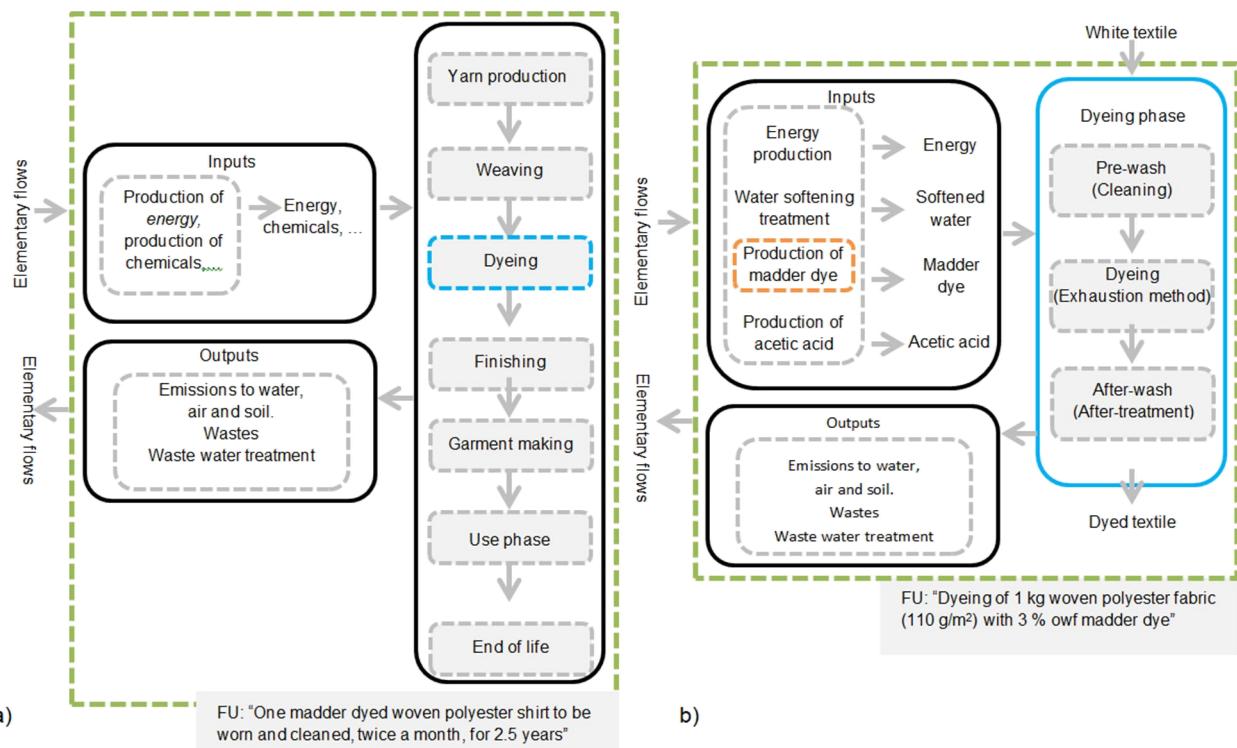
Figure 3 System boundaries for cradle-to-grave (a) and gate-to-gate (b) LCA

Table 1 Data sources for the inventory flows

Life cycle stage	Type of data	Source
Raw materials production (370 g)	Polyester yarn from secondary raw material	EIME-Tex database
Texturizing (185 g)	Energy consumption	[5]
Weaving (296 g)	Weaving with rapier loom, 110 g/m	EIME-Tex database
Dyeing (260 g)	Energy, water and material consumptions (including electricity mix and process steam, softened water, laundry detergent and acetic acid). Waste water treatment.	Experimental, [6]
Madder plant cultivation (0.031 m^2)	Resources used for seeding to post-harvest (drying)	EIME-Tex database, [2, 7, 8]
Madder dye production (8 g)	Energy, water and material consumptions for extraction and evaporation (including electricity mix, softened water and methanol)	Experimental, [9]
Finishing (255 g)	Antistatic finishing	EIME-Tex database
Sewing (250 g)	Energy consumption	[10]
Use phase (200 g) - Washing	Energy, water and detergent consumptions for 60 washings at 41°C, fully loaded machine.	[5, 6, 11]
End of Life (200 g)	ELCD – Waste incineration with energy recovery	EIME-Tex database
Textile waste (170 g)	ELCD – Waste incineration with energy recovery	[10]

Laboratory experiments were carried out to determine activity data related to the dyeing phase. Experimental data were then extrapolated to an industrial overflow machine using the EIMETex database. This was done since laboratory dyeing machines use electrical energy for heating water baths, whereas industrial machines require steam [5]. The pre-wash was modeled using a published source [6]. Input for the after-wash was based on experimental data (electricity consumption was measured with a power meter, Chauvin Arnoux C.A. 8332B).

Published sources were used for collecting activity data related to the other life cycle stages (yarn production, …, end of life), although the input for madder dye extraction had to be supplemented by experimental work in our research laboratory (energy consumption). The data sources for each stage are presented in Table 1. The use phase was modeled based on probable maintenance conditions (41°C wash, fully loaded machine, detergent, no drying or ironing) and the corresponding input of energy, water, and detergent. The impact categories considered and corresponding category indicators are listed in Table 2.

Table 2 Impact categories considered*

Abbreviation	Impact category	Category indicator
GWP	Global Warming Potential	kg CO_2 eq.
WD	Water Depletion	dm^3
WE	Water Eutrophication	kg PO_4^{3-} eq.

*Impact category: class representing environmental issues of concern to which the life cycle inventory analysis may be assigned (ISO 14040).

3   RESULTS AND DISCUSSION

3.1   Influence of dyebath pH

The dyed fabric showed a clearly visible color shift, with a change in pH of the dyebath, namely from yellow-orange (pH < 7) to red-purple (pH > 7). From Figure 4a, it is clear that the yellow value decreased with increasing pH (positive *b**: from 28 to 12), whereas the red value stayed almost the same (positive *a**: around 10.5). The color shift with a change in pH can be attributed to the halochromism of the coloring species in madder. In particular to the ability of alizarin to ionize in alkaline pH and the differences in the position of the absorption maxima of the neutral, anionic and di-anionic form which results in a red shift in the absorbance spectra with increased pH [12-13].

The color yield (K/S) decreased with increasing pH (Figure 4b). This can be explained by increased electrostatic repulsion between the anionic forms of alizarin and the fabric surface (which becomes more negatively charged in basic pH) [14].

Moreover, color fastness decreased with increasing pH, with gray scale ratings 4-5, 4-5, 4, 2 and 1-2 for pH values 3, 5, 7, 9 and 11, respectively.

To minimize inputs of dye and chemicals and reduce dye-release into the wastewater, pH 3 and 5 were studied in more detail whereof dyebaths of pH 5 are presented further in this paper.

3.2   Influence of dyebath temperature and time

The dyeing process was modified so that the dyeing temperature (90 or 130°C) was maintained during different durations (15, 30, 45, 90, 130 or 180 min). The color yield increased with temperature and time. At both temperatures, though, optimum dyeing was achieved after 45 min. Therefore, samples were dyed for 45 min and then subjected to color fastness tests.

3.3   Fastness properties

Color fastness to one wash was better for dyeing above boil than below, gray scale 4-5 for 130°C compared to 3-4 for 90°C (Figure 5). Nevertheless, after the first wash all samples showed very good wash fastness up to the 5 washing cycles studied. All samples exhibit good dry and wet rub fastness (4-5 to 5).
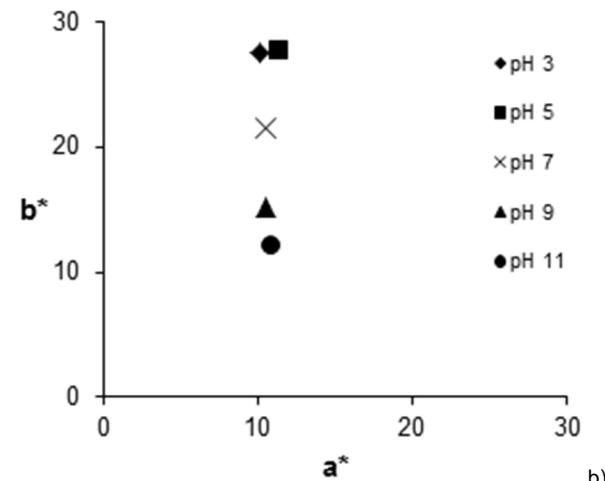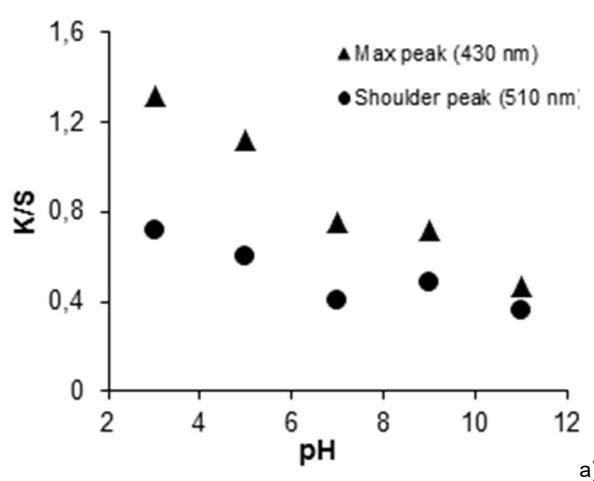
Figure 4 Effect of dyebath pH on *a** and *b** color coordinates (a) and on color yield K/S (b)
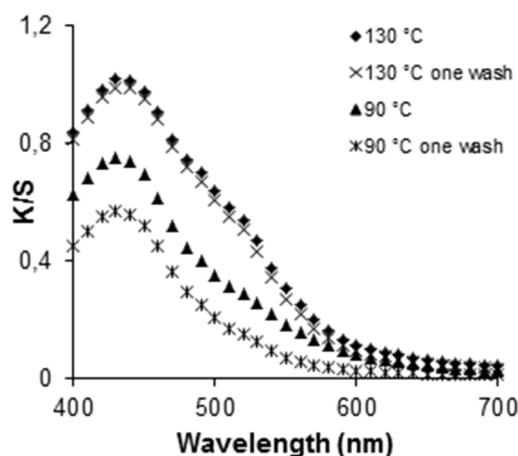
Figure 5 Effect of dyeing temperature on color yield (K/S), before and after wash (pH 5, 3% owf)

3.4 Scenario for environmental assessment

Dyebath of pH 5, with the dyeing temperature of 130°C for 45 min, was selected for LCA. Table 3 shows the colorimetric data for the dyed sample using these conditions and which corresponds to the FU: "Dyeing of 1 kg woven polyester fabric (110 g/m^2) with 3% owf madder dye".

Table 3 Colorimetric data for the FU: "Dyeing of 1 kg woven polyester fabric (110 g/m^2) with 3% owf madder dye".

L*	a*	b*	C*	h*	Dyed sample
74.9	11.3	27.6	29.9	67.7	

3.5 Impact assessment of the dyeing process

Three phases were considered in the dyeing process: (1) cultivation of madder plant (from seeding up to post-harvesting), (2) dye extraction (extraction and solvent evaporation) and (3) the dyeing phase (pre-wash, exhaustion dyeing and after-wash).

The relative contribution to each impact category (GWP, WD and WE) for the dyeing process is illustrated in Figure 6.
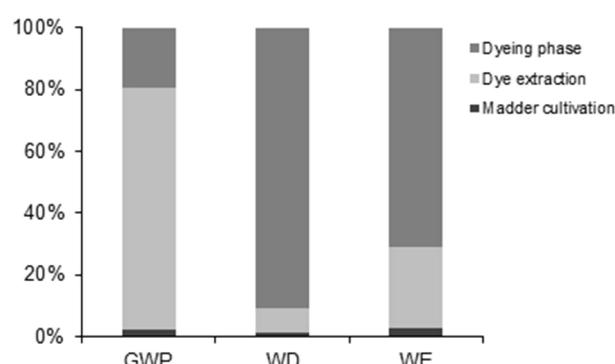
Figure 6 Relative contribution to impact categories for the dyeing process

Indeed the dye extraction was the most significant phase with respect to GWP, whereas the dyeing phase was the most important one for the water related impact categories (WD and WE). Sensitivity analysis on madder root yield, consumption of fertilizers, irrigation and extraction method indicated that environmental improvement, in particular, will be found with a more resource-efficient extraction method, with respect to energy and solvent use, without compromising on dye yield.

3.6 Impact assessment of a madder dyed polyester shirt – from yarn production to the end of life

The assessment was extended to include all the life cycle stages of a madder dyed polyester garment (Figure 7). The dyeing process was the major contributor to GWP, whereas the use phase of the shirt was the major contributor to WD and WE.
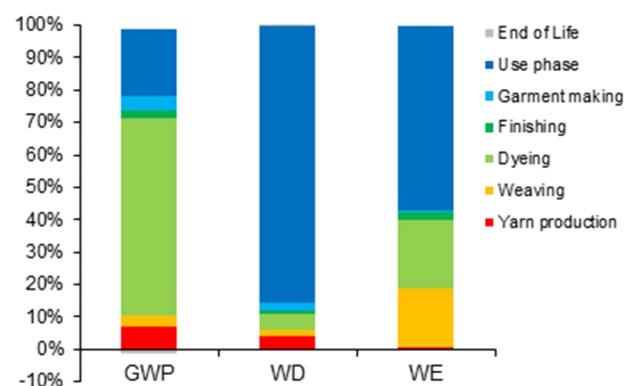
Figure 7 Relative contribution to impact categories for the scenario of a madder dyed polyester shirt

4 CONCLUSIONS

This study assesses the potential environmental impacts of dyeing of polyester with bio-based madder dye. Laboratory experiments were carried out to determine optimum dyeing conditions (pH 5, 130°C, 45 min) and corresponding input and output data flows. When the dyeing process was assessed using LCA tool, it became clear that environmental improvement will be found in any other dyeing process that replaces the conventional madder dye extraction with a more resource-efficient alternative, as well as reduces the water consumption in the dyeing phase.

When the life cycle of a madder dyed polyester end-product (shirt) was evaluated, the use phase together with the dyeing process were the major contributors to impact on the environment.

LCA is an interesting tool for the development towards sustainable bio-based textile dyeing. However, data concerning LCI (Life cycle inventory) of the production of natural dyes are not easily

available. Therefore, data collection for the design of such data base is encouraged.

5   REFERENCES

1. Cardon D.: *Natural Dyes Sources, Tradition,* Technology and Science, Archetype, London, 2007
2. Bechtold M., Mussak R.: Handbook of Natural Colorants, John Wiley& Sons, Ltd., 39-52, 2009
3. Drivas I., Blackburn R. S., Rayner C. M.: Natural anthraquinonoid colorants as platform chemicals in the synthesis of sustainable disperse dyes for polyesters. Dyes and Pigments 88, 7-17, 2011
4. Haddar W., Elksibi I., Meksi N., Mhenni F.M.: Valorization of the leaves of fennel (Foeniculum vulgare) as natural dyes fixed on modified cotton: A dyeing process optimization based on a response surface methodology. Industrial Crops and Products 52, 588-596, 2014
5. Van der Velden N. M., Patel, K. M., Vogtländer J. G.: LCA benchmarking study on textiles made of cotton, polyester, nylon, acryl, or elastane. The International Journal of Life Cycle Assessment 19, 331-356, 2014
6. Pesnel S.: Product Environmental Footprint (PEF) Category Rules (PEFCR) Pilot T-shirts 2014
7. Chenciner R.: Madder Red: A History of Luxury and Trade. Routledge, U.S.A., 2000
8. Hasler K., Bröring S., Omta S.W.F., Olfs H.-W.: Life cycle assessment (LCA) of different fertilizer product types. European Journal of Agronomy 69, 41-51, 2015
9. Cuoco G., Mathe C., Archier P., Chemat F., Vieillescazes C.: A multivariate study of the performance of an ultrasound-assisted madder dyes extraction and characterization by liquid chromatography-photodiode array detection. Ultrasonics Sonochemistry 16, 75-82, 2009
10. Cycleco Données semi-spécifiques proposées dans le cadre de l'élaboration des référentiels textiles v1.2, CYCLECO 2010
11. Kim J., Changsang Y., Park Y., Park C. H.: Post-consumer energy consumption of textile products during 'use' phase of the lifecycle. Fibers and Polymers 16(4), 926-933, 2015
12. Van der Schueren L., De Clerck K.: The use of pH-indicator dyes for pH-sensitive textile materials. Textile Research Journal 80(7), 590–603, 2010
13. Lofrumento C., Platania E., Ricci M., Mulana C., Becucci M., Castellucci E.M.: The SERS spectra of alizarin and its ionized species: The contribution of the molecular resonance to the spectral enhancement. Journal of Molecular Structure 1090, 98-106, 2015
14. Ran J., Bénistant G., Campagne C., Périchaud A., Chai F., Blanchemain N., Perwuelz A.: Characterization of Nonwoven Poly(ethylene terephtalate) Devices Functionalized with Cationic Polymer. Journal of Applied Polymer Science 124, 3583–3590, 2011

THE INTENSIFICATION OF THE PROCESSES OF PRINTING AND DYEING OF NATURAL PROTEIN FIBERS USING REDOX SYSTEMS

A. Aitova and A. Burinskaia

Department of Chemical Technology and Design of Textiles
St-Petersburg State University of Industrial Technologies and Design
Bolshaya Morskaya st. 18, 191186, St-Petersburg, Russia
alya190990@mail.ru

Abstract: *Woolen fabrics were printed with a paste containing a redox system (ammonium persulphate - glycerol) and amino acids (glutamic acid, arginine, lysine). The printed fabrics were evaluated in terms of their printability, color fastness and shrinkage properties as well as stiffness of the substrate. The surface morphology was characterized by comparative microscope images. Our results reveal that the combination of amino acids and redox system leads to an increased sorption and the formation of covalent bonds in addition to the usual ionic bonds between the dye and the wool fiber. The combination of amino acids and a redox system is found to be effective in enhancing the printability of wool fabrics with Acid Red dye. Furthermore, the process of low-temperature dyeing of wool was investigated. Proposed technology prevented the destruction of the material, contributing to an increase in strength and elasticity of the woolen substrate.*

Key Words: *Woolen fabric, redox system, amino acids, acid dye*

1   INTRODUCTION

Textile industry uses substantial quantities of wool fibers in terms of textile and technical products. Wool plays a significant role in the textile industry. It is the most useful fiber with outstanding properties. Its warmth, moisture absorbency, drapeability, resiliency, flame retardation allow us to consider wool as an ideal tool for numerous applications in apparel and interior. Wool can enhance other fibre properties when blended, extending its application into a new product. Moreover, it is "green" being a renewable resource and ecofriendly.

The conversion of fiber into fabric requires a technological intervention to obtain a variety of different kinds of products, while textile processing is used to enhance the value and functionality of the textile product. Textile processing other than dyeing and finishing, preparatory or pre-treatment process may be used in the textile processing conventionally or specifically, which depends on the end-uses of the products.

In the case of wool it has been observed that dyeing is the most commonly used technique to enhance aesthetic appeal. Printing is not commonly used either at small scale or large scale to produce beautiful attractive designs.

It has been reported that only 2% of total wool in the world is printed. The main reason of this is physical and morphological nature of wool. The hairy nature of woolen fabric operates against the production of fine, crisp designs which may be printed on smooth fabric. Wool does not absorb the print paste very well; this effect is connected with scales on its surface [1].

Chemical treatment brings about a change in the surface characteristics, in particular, in the scaly layer and in the chemical nature of wool fiber, which makes fibers more receptive to dyes, resulting in different color yield, fixation and color fastness properties. Treatment can be also introduced in textile processing, either to save energy or to reduce the amount of chemicals involved in the subsequent processing. A. Demir [2] has investigated how the surface characteristics of wool fabric depend on the various types of treatments, such as plasma, enzymatic and biopolymers treatments. All these processes induce high dyeing efficiency and shrink-resistance in wool fabric. The K/S values and fastness properties of the fabric are evaluated. For example, the plasma, enzyme and chitosan combination give the best K/S values compared to untreated dyed fabric. Since plasma pretreatment modifies the surface, enzymatic treatment can remove the hydrophobic layer of wool more efficiently, which makes dye migration higher after the application of chitosan.

Various chemicals and auxiliaries are used to produce modifications in physical structure or to help in swelling of fiber or dissolution of dyes.

Researchers Burkinshaw S.M. and Jiann Guand Lu investigated dyeing of various textiles - silk, polyester, nylon 6 and nylon 6.6 - in the presence of free radical initiators [6-8]. For example, dyeing of silk with acid and disperse dyes was carried out using ammonium persulfate, potassium periodate (KIO_4), hydrogen peroxide (H_2O_2) as oxidizing agents, and as a reducing agent, glucose, thiourea, thiourea dioxide and ferrous sulfate ($FeSO_4$). Buffer mixture was used in the dyeing. The redox system was added directly into the dyebath. Dyeing was carried out at a temperature of 40-70°C for 60 minutes. After dyeing, the fabrics were rinsed with cold water and soaped at 98°C for 5 minutes in a solution containing 2% surfactant Sandozin NIE, then the samples were rinsed and dried at room temperature. The enhanced wash fastness of each of the dyes on silk secured by the use of the radical initiators can be attributed to covalent attachment of the dye to the fiber.

It is conjectured that, in presence of the redox system, free radicals are formed in both the fiber and the dye and the interaction between these free radicals favors post fixation of dye on the fiber surface. It is possible that this could create a covalent fixation in addition to the usual ionic links, hydrogen bonds and van der Waals forces, J. Luo [9].

There also is evidence of influence of amino acids on the process of coloring textile materials, which improves quality of colors and their resistance to physical and chemical effects [10].

In this research work, woolen fabrics were printed with a paste containing a redox system (ammonium persulphate - glycerol) and different amino acids (glutamic acid, arginine, lysine).

The influence of the redox system and additions of various amino acids on the fastness properties of color, stiffness of substrate, shrinkage and printability of wool fabrics is investigated.

In the absence of the redox system, dyeing proceeds via electrostatic bonding between the dye anion and the protonated amino group, hydrogen bonding between the amido, hydroxy, amino groups in the protein fibers, and hydroxy and amino groups in the dye and/or van der Waals forces [11].

2   EXPERIMENTAL

Merino wool fabrics were used for the printing experiments. Prior to printing, the fabrics were scoured to remove any residual materials from previous processes using sodium carbonate and a non-ionic detergent. The fabrics were then rinsed several times with warm and cold water, squeezed and dried at room temperature.

Amino acids (glutamic acid, lysine and arginine), ammonium persulphate, glycerol, dimethyl-formamide (DMF) were laboratory-grade chemicals.

C.I. Acid Red 1 (milling type acid dye) was obtained from ColoRos. The dye was used without further purification.
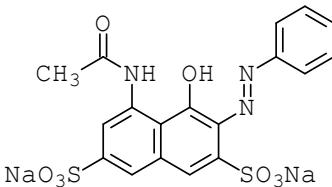
$C_{18}H_{15}N_3O_8S_2$. 2 Na

2,7-Naphthalenedisulfonic acid, 5-(acetylamino)-4-hydroxy-3-(2-phenyldiazenyl), sodium salt (1:2)

The redox system and the amino acids were added directly to the printing paste commonly used in printing of wool fabrics with an acid dye. The printing paste was applied to wool using the flat-screen printing technique.

The printed fabrics were dried at a temperature not exceeding 60°C, followed by steaming with saturated steam (102°C) for 30 - 40 min in a steam ager. The printed wool fabrics were finally washed thoroughly with warm and cold water to remove the thickener and any unfixed dye, and then dried.

Spectral reflectance measurements of the printed fabrics were carried out using a spectrophotometer Specol 11. The color intensity expressed as K/S values of the printed samples was determined by applying the Kubelka-Munk equation (1) [12]:

$$K/S = (1 - R)^2/2R \qquad (1)$$

where R is the decimal fraction of the reflectance of the dyed substrate, S is the scattering coefficient, K is the absorption coefficient.

The wool fabrics used in the presented study were printed with acid dye as follows: sample 1 – wool fabric was printed without intensifying additives (traditional technology); sample 2 – redox system additive; sample 3 – redox system + arginine; sample 4 – redox system + glutamic acid; sample 5 – redox system + lysine.

The color fastness to washing and to crocking was determined according to the ISO standard method 105-A01-99.

Printed samples were extracted with 50% dimethylformamide (DMF) at reflux temperature for detecting the presence of a covalent bond between the acid dye and wool fiber. The amount of dye bound to the fabric (expressed as percentage residual color strength) was calculated by equation (2):

$$C = K_1/K_0 \cdot 100\% \qquad (2)$$

where K_0 and K_1 are the color strength (expressed as K/S) before and after DMF extraction, respectively.

3   RESULTS

To observe the printing properties of fabrics, the Acid Red 1 dye was used. The *K/S* values and fastness properties of the color were evaluated.

The *K/S* values of printed fabrics are given in Figure 1. Analysis of the data shows that the intensity of the color printed fabric in the presence of a redox system and amino acids is higher than the sample printed without intensifiers, which indicates an increase of printability of the woolen fiber due to the formation of active sites and additional bonds.
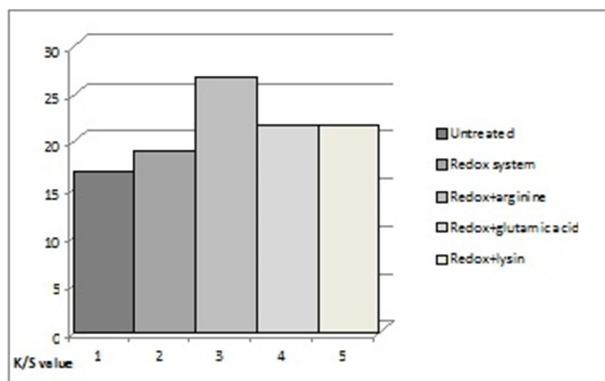
Figure 1 K/S Values of Acid Red 1 dyed fabrics

Table 1 shows the effect of treatment of these samples on their printability with Acid Red 1, as well as the fastness of the printed fabrics to washing and crocking and the dye fixation, expressed as percentage residual color strength after DMF extraction.

Table 1 Fastness properties for untreated and treated printed wool with Acid Red 1

Treatment	*K/S*	C [%]	Fastness to		
			Washing	Crocking	
				Dry	Wet
Sample 1	16.87	9.4	5/4/4	5	3
Sample 2	19.01	43.21	5/5/4	5	4
Sample 3	26.79	54.70	5/5/4	5	4
Sample 4	21.74	46.72	5/5/4	5	4
Sample 5	21.74	41.84	5/5/4	5	4

The residual color strength of samples printed using redox system and amino acids was 41.84 - 54.70% after DMF extraction, compared with 9.4% for sample without additives.

The superior fastness of the printed fabrics against washing and crocking and the higher fixation value obtained after DMF extraction show that combination of amino acids and redox systems lead to an increased sorption and the formation of covalent bonds in addition to the usual ionic bonds between the dye and the wool fiber.

The tentative mechanism for covalent bond formation between wool fiber and the acid dye is shown in Scheme 1, where W-NH$_2$, D-H, GL-OH represent wool, acid dye and glycerol.

$$S_2O_3^{2-} > 2\,SO_4^{-}\bullet$$
$$2\,SO_4^{-}\bullet + H_2O > H^{+} + SO_4^{2-} + HO\bullet$$
$$HO\bullet + GL\text{-}OH > H_2O + GL\text{-}O\bullet$$
$$W\text{-}NH_2 + HO\bullet\,(GL\text{-}O\bullet) > W\text{-}NH\bullet + H_2O\,(GL\text{-}OH)$$
$$D\text{—}H + HO\bullet\,(or\ GL\text{—}O\bullet) > D\bullet + H_2O\,(GL\text{—}OH)$$
$$D\bullet + Amino\text{-}NH > D\text{-}Amino\text{-}NH\bullet$$
$$W\text{-}NH\bullet + D\text{-}Amino\text{-}NH\bullet > W\text{-}NH\text{-}Amino\text{-}NH\text{-}D$$
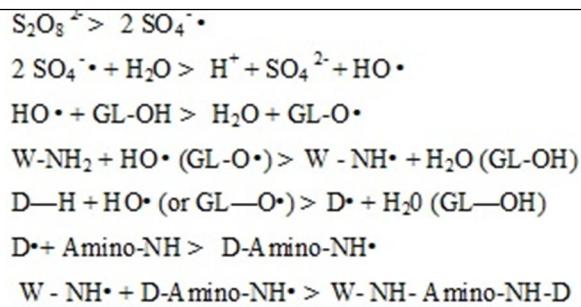
Scheme 1 The tentative mechanism for bond formation between wool fiber and acid dye

Table 2 shows the color specifications and color coordinates of printed wool fabrics in the CIE LAB, under the light source A – approximating incandescent light with a color temperature 2854 K, and a source D 65 – scattered sunlight including ultraviolet component, having a color temperature of 6500°C.

Table 2 Color specifications and color coordinates of wool fabric printed with the Acid Red 1

Sample	Color specifications in the CIELAB									
	Standard light source D65					Standard light source A				
	*L**	*C**	*h**	*a**	*b**	*L**	*C**	*h**	*a**	*b**
1	7.7	0.5	6.3	3.6	0.4	4.1	9.2	3.1	1.3	7.7
2	5.9	1.5	6.5	9.4	9.6	2.8	0.9	3.2	6.5	2.3
3	6.1	9.3	5.7	9.0	7.2	3.0	8.6	5.6	6.2	9.8
4	7.6	6.3	6.4	2.2	3.5	5.3	6.1	3.1	8.9	6.8
5	6.1	4.0	6.9	0.4	2.1	3.2	3.6	3.5	7.3	4.8

The analysis of the data given in Table 2 shows that the lightness (*L**) of samples of woolen fabrics printed in the presence of a redox system and amino acids is lower than the substrate printed without additives, which indicates higher intensity prints.

Color saturation (*C**) and hue (*h**) of samples of wool fabric, printed in the presence of redox systems and by the traditional technology, practically coincide. This fact indicates that the presence of redox systems in the printing paste does not change the color hue of obtained samples, which is important in the case of wool material printing into a predetermined tone of coloration.

Textile printing process involves the pattern formation on the material surface, which sometimes leads to an increase in its stiffness. Comfort of finished products is ensured by the use of special textile auxiliaries – softeners.

In this paper, a comparative evaluation of the stiffness of the samples of wool fabric printed in the presence of intensifiers was carried out.
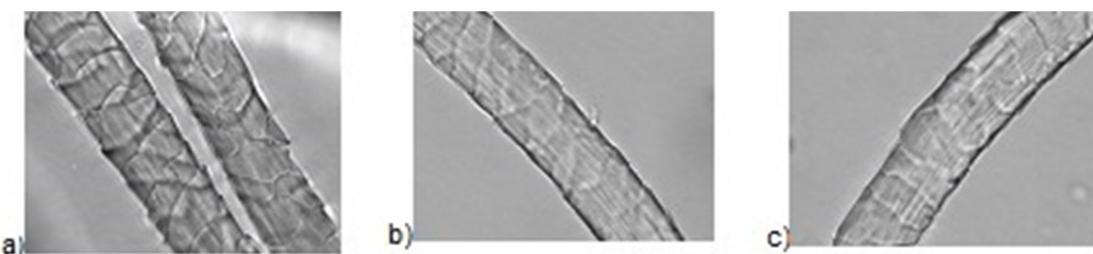
Figure 2 Images of untreated (a) and treated: redox system (b), redox system+arginine (c) wool samples (zoom in 500x)

Stiffness of samples printed with the addition of a redox system and amino acids reduced the average by 3 times (390 mN.cm^2) compared to the control sample (stiffness - 1250 mN.cm^2). It avoids the subsequent processing operation by special textile auxiliaries.

Moreover, felting properties of printed wool samples were investigated by the standard method which characterizes the change in the area of the sample after the milling process. Shrinkage of the sample printed without additives is 52%, and that of the samples printed in the presence of the studied additives, 15 - 20%. This fact is connected with the impact of the additives on the scaly layer of wool fiber.

The surface appearance of untreated and treated wool fibers is presented on the photograph (Figure 2). It can be observed that the untreated fiber has more signified scales with well-defined scale edges, which is typical for wool.

As seen from the images, redox system and combination of redox system and amino acid lead to degradation of the scales on the surface of the fiberA reduction of shrinkage of wool fabric indicates a decrease of felting as well as an improvement of dimensional stability of the product, which, in turn, increases the overall level of their consumer qualities.

Consequently, the application of printing paste with the addition of a redox system (ammonium persulfate – glycerol) and amino acids essentially improves the wool quality, which was measured by a number of indices. The spectral characteristics of color of the printed samples, reduction of the stiffness of the substrate, increase in the strength of color characteristics, and reduction of shrinkage of fabric show the effectiveness of the developed technology discussed in this paper.

Furthermore, the process of low-temperature dyeing of wool was investigated for the purposes of better study of the effects of the redox system and of the amino acids on the properties of wool fibers.

The weighed wool yarn samples were introduced into a dyebath containing the requisite amount of dye, buffer, glutamic acid and the redox system (ammonium persulfate – thiourea) at the liquor ratio

of 50:1. Dyeing was performed at the temperature of 80°C for 60 min with continuous stirring. At the end of the dyeing, the dyed samples were rinsed and dried at ambient conditions.

Dyed samples were extracted with 50% dimethylformamide (DMF) at reflux temperature for detecting the presence of a covalent bond between the dye and the wool fiber (Figure 3).
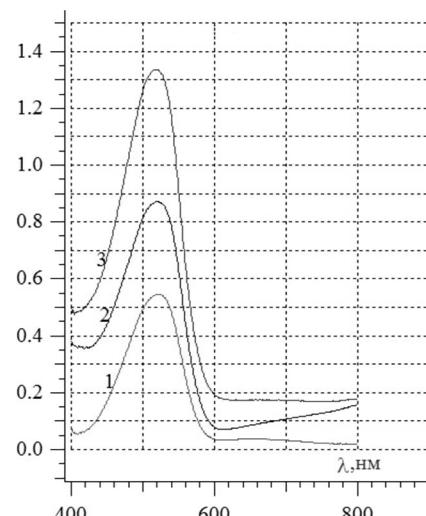
Figure 3 The adsorption spectra of dyed wool single fibers after extraction with DMF: 1 – sample dyed according to the conventional recipe: 2 – dyed in the presence of glutamic acid; 3 – dyed in the presence of redox system and glutamic acid

The data shows that in the processes of dyeing, best result of dye fixation was obtained in the case of dyeing the substrate in presence of redox system and glutamic acid.

Submitted results can indicate the presence of a covalent bond between the fiber and the dye and/or dye polymerization.

Tensile tests were made using the Instron 1122 instrument. All the tests were performed with the strain rate of 100 mm/min under standard conditions at 25°C and 65 percent relative humidity.

Tensile strength (σ, cN/tex), strain at failure (ε, %) and initial modulus of rigidity (cN/tex) were determined on the basis of the tensile diagram and presented in Table 3.

Table 3 Mechanical properties of wool yarns

Sample	Tensile strength [cN/tex]	Modulus of rigidity [cN/tex]	Strain at failure [%]
Untreated	7.0	36.9	27.3
Treated with glutamic acid	7.5	37.6	28.7
Treated with redox + glutamic acid	7.6	38.4	30.7
Untreated Dyed at 100°C	6.8	41.5	27.3
Dyed in presence of glutamic acid	9.0	36.9	31.2
Dyed in presence of redox + glutamic acid	7.8	39.2	27.6

Higher tensile strength is observed for the sample dyed in the presence of glutamic acid and redox system + amino acid. This can be explained by a decrease of thermal destruction of filaments in the case of dyeing wool at lower temperatures and/or increase of amounts of cross-linking in the presence of amino acids.

Yarn dyed by traditional technology at 100°C showed the maximum stiffness, which increased by 12% compared with the original sample. That can be associated with damage of the α-structure of wool fiber in the process of dyeing at the boiling temperature.

Proposed technology of low-temperature dyeing in the presence of investigated enhancers provides lower hardness and higher elasticity of yarn.

4   CONCLUSION

Selected acid dye exhibits enhanced fixation on woolen materials when printing and dyeing is carried out in the presence of redox-systems and amino acids. This effect may be due to either the formation of dye polymers or dye-fiber covalent bonding. Proposed initiator increases the sorption of dye to the substrate.

Low-temperature dyeing of wool yarn with the acid dye in the presence of glutamic acid and redox system (APS-thiourea) provides a deeper and stronger color of woolen material.

Proposed technology prevented the destruction of the material, contributing to an increase in strength and elasticity of the woolen substrate.

5   REFERENCES

1. Allam O.G.: Improving functional characteristics of wool and some synthetic fibres, Open journal of organic polymer materials, pp. 8-19, 2011

2. Demir A., Karahan H. A., Özdoğan E., Oktem T., Seventekin N.: The Synergetic Effects of Alternative Methods in Wool Finishing, FIBRES & TEXTILES in Eastern Europe J 2, 86-94, 2008

3. Burinskaia A., Petrova O., Mogilnaia L., Gusakov A.: A method of dyeing of textile materials, Patent 2211265, RF, 2003

4. Petrova O., Grebennikov S., Burinskaia A.: Changes in the structure of the wool fiber due to dyeing in redox conditions, The Journal of Applied Chemistry 78(4), 616-617, 2005

5. Haggag K. Kantouch F., Allam O. G., El-Sayed H.: Improving Printability of Wool Fabrics Using Sericin, Textile Research Division, National Research Centre, Dokki, Cairo, Egypt. 270-275, 2009

6. Burkinshaw S.M., Jiann Guand Lu: Dyeing in the Presence of Free Radical Initiators. Part 7: The Dyeing of Silk Fibres // Department of Colour Chemistry and Dyeing, The University of Leeds, Leeds LS2 9JT, UK &Department of Textile Engineering, Van Nung Institute of Technology, Chung-Li (320), Taiwan, 1994

7. Burkinshaw S.M., Jiann Guand Lu: Dyeing in the Presence of Free Radical Initiators. Part 1: The Dyeing of Polyester Fabric with CI Disperse Yellow 54 4 Department of Colour Chemistry and Dyeing, The University of Leeds, Leeds LS2 9JT. UK & Department of Textile Engineering, Van Nung Institute of Technology, Chung-Li (320), Taiwan, 1993

8. Burkinshaw S.M., Jiann Guand Lu: Dyeing in the Presence of Free Radical Initiators. Part 2: The Dyeing of Nylon 6 with Disperse Dyes // Department of Colour Chemistry and Dyeing, The University of Leeds, Leeds LS2 9JT, UK N Department of Textile Engineering, Van Nung Institute of Technology, Chung-Li (320). Taiwan, 1993

9. Luo J.: Low Temperature dyeing of real silk fabrics using a redox system, Zhejiang Textile School, Ningbo, China, 117-119, 1991

10. Burinskaia A.A. Okulovskaia N.V., Baruzdina L.V., Gromov F. Stotskii A.A. Gurtovenko S.I.: A method of dyeing textile material made of wool or a mixture of polyamide fiber, Patent 4909293/05, RF, 1993

11. D M Lewis: Rev. Prog. Coloration, 8-10, 1977

12. Abidi N. and Hequet E.:J.Appl.Polym.Sci., 145, 2004

TOWARDS A CIRCULAR ECONOMY IN TEXTILES: RESYNTEX AND THE EUROPEAN UNION

A. Aneja[1], R.Pal[2], K. Kupka[3] and J. Militky[4]

[1]*Department of Engineering, East Carolina University, Greenville, NC 27858, USA*
[2]*Department of Business Administration and Textile Management, Swedish School of Textiles, University of Borås, Borås 50190, Sweden*
[3]*TriloByte Statistical Software, Ltd., St. Hradiste 300, CZ 53352 Pardubice, Czech Rep*
[4]*The Technical University of Liberec, Department of Materials, Liberec, Czech Republic*
anejaap@gmail.com

Abstract: *Europe is at crossroads in terms of growth and living standards. The nexus between circular economy, RESYNTEX and textile provides direction and opportunity for seamless prosperity. The current strategy consisting of a linear economy for resource utilization, a surprisingly wasteful model of value creation, is leading to decline in prosperity and concomitant global influence. It must develop a more resource savvy circular economy, with the biological and mineral nutrients of modern society continuously circulating. Rather than face a bleak and uncertain future dependent on resources from overseas, Europe needs to develop technologies towards self-sufficiency in energy and water and keep materials required for consumption flowing [1]. This will insure reduction in virgin resources and treat waste as a valuable input rather than a burden for welfare of society and the environment.*

RESYNTEX, the European Union's Horizon 2020 research and innovation funded program, will produce secondary raw materials from blends and pure components of unwearable textile waste and is expected to have a strong circular economy focus. The project will develop and demonstrate a strategic design for closed loop textile recycling throughout the value chain.

Key Words: *textiles, circular economy, key drivers, circular thermodynamics, recycling.*

1 INTRODUCTION

The party is over – finito! The current Linear Economy Model, with its roots in the Industrial Revolution and focus on productivity and efficiency, has been exceptionally successful, with global GDP growing twenty-fold between 1900 and 2000 in the process providing affordable products to consumers and material prosperity to billions. However now, under the same system, each year, humanity uses resources and ecosystem services that would require 1.5 Planets Earth to be able to keep up with our societies and to support them. Since industrialization, human activities have destabilized the Earth's systems and natural cycles and forced the environment into a state out of balance. The earlier environmental changes were moving slower and mostly occurring locally whereas current changes are dramatic in geological speed and are of a global nature. The result could be irreversible when reaching a tipping point with abrupt environmental changes and with catastrophic consequences for human development. These consequences can be summed up in terms of the following challenges: climate crises, financial crises, global poverty, ozone depletion, extinction of species, pandemics, deforestation, armed conflicts, fresh water shortage, social anxiety, natural disasters and the list goes on. Daily we are faced with alarming reports about the state of nature and humanity. The different aspects are often treated separately but are all interlinked and have to be dealt with simultaneously in order to create a sustainable future. What is the remedy for this chaotic state of affairs?

2 WHAT GOT US HERE - THE LINEAR SYSTEM

A major cause of the continued deterioration of the global environment is the current pattern of production and consumption – often referred to as the Linear Economy. This is a system with a tendency to accumulate waste and of wasting natural resources built upon the assumption that they are in abundance forever. We need to consider three different kinds of capital; natural, real and human capital which underlie our way of living and which are at risk. Natural capital being all natural resources and ecosystem services. Real capital meaning man-made capital such as money, buildings, cars etc. Human capital being human resources available for economic activity, thus skills, technology and knowledge about how to use natural and real capital and also institutions to rationally manage production. Within the current economic model, these types of capital are seen as interchangeable. In today's economy, natural resources are mined, turned into products and finally discarded. While the recycling of waste and strategies of efficient extraction of raw materials reduce consumption, this remains fundamentally an open, linear system which places unsustainable demands on the environment as a waste reservoir.
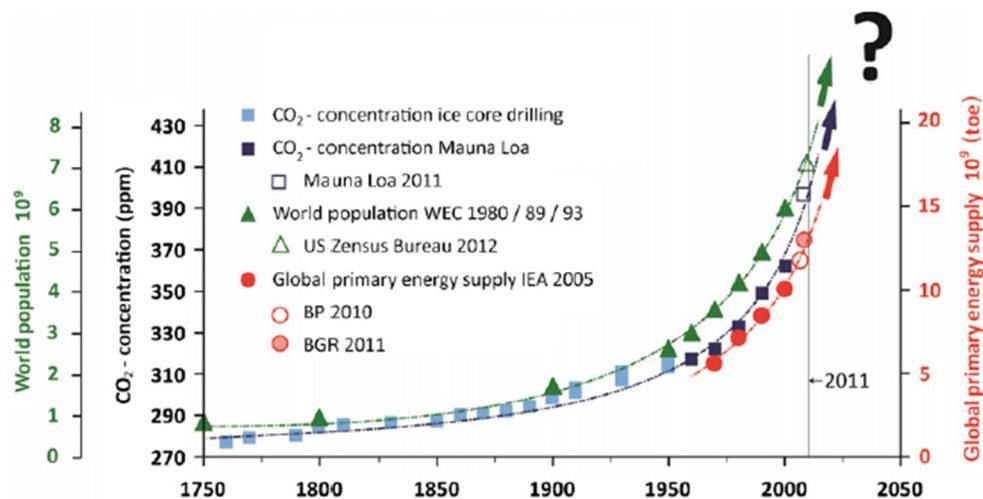
Figure 1 Global Developments

Furthermore, major challenges to society through Linear Economy are imposed by the following constraints on global development: population growth, carbon footprint, energy consumption, resource (mineral & natural) utilization, skyrocketing commodity and energy costs, new and better technology availability, water shortage, and urbanization [2] (Figure 1). All of these trends are rapidly advancing the "judgment day" of mankind perhaps finally reaching the limits of this "run-away" economic system.

A crucial element in the current economic system is the high use of fossil fuel. It is a relatively easy access to cheap energy which, to a large extent, has fueled the accelerating economic growth since industrialization. According to IPCC, however, three fourths of the remaining fossil resources need to stay in the ground if we should have a reasonable chance to restrict the global temperature rise to two degrees. Climate researchers' message is crystal clear, the transition of the world's fossil-dependent energy system has to start now. However, economic growth is related to resource consumption with resultant increase of carbon footprint (CO_2 intensity) causing the unfolding mayhem in global climate we potentially face. The solution is to break this correlation and become prosperous and carbon free by creating Kuznets curve of de-carbonization for global safety and national security. This is possible by the use of alternate sources of energy. The concept was successfully demonstrated in the creation of environmental Kuznets curve (Figure 2) relationship between environmental quality and economic development) during the 70's and 80's.

Today's linear "take, make, waste" economic model which relies on large quantities of cheap, easily accessible materials and energy, has been at the heart of industrial development and has generated an unprecedented level of growth.

Yet recent sharp price rises, increased volatility and growing pressure on resources have alerted business leaders and policy makers about the necessity of rethinking materials and energy use – the time is right, many argue, to develop something new. Increasingly, however, the linear approach to industrialization has come under strain.
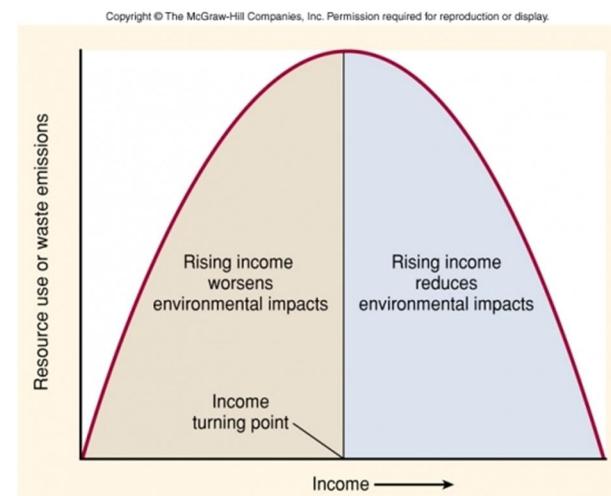
Figure 2 Environmental Kuznets Curve

Some three billion consumers from the developing world will enter the middle class by 2030. The unprecedented size and impact of this shift is squeezing companies between rising and less predictable commodity prices on the one hand, and blistering competition and unpredictable demand on the other. The turn of the millennium marked the point where a rise in the real prices of natural resources began erasing a century's worth of real-price declines. The biggest economic downturn since the Great Depression briefly dampened demand, but since 2009, resource prices have rebounded faster than global economic output (Figure 3). Clearly, the era of largely ignoring resource costs is over.

Indexes: Q1 2007 = 100 (nominal data)

Source: Food and Agriculture Organization of the United Nations (FAO); International Monetary Fund (IMF); Organisation for Economic Co-operation and Development (OECD); Oxford Economics; World Bank; UN Comtrade database; McKinsey Global Institute (MGI) analysis
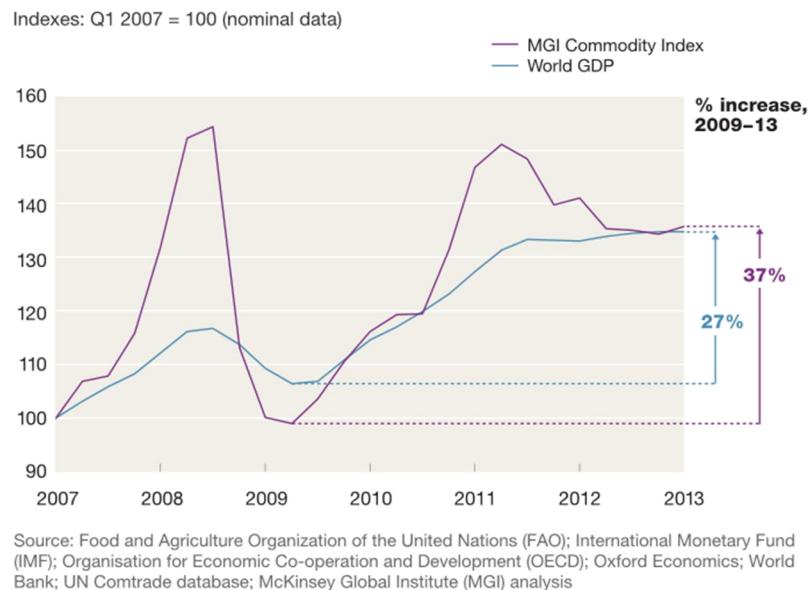
Figure 3 Global GDP versus Commodity Price Rise

In the light of volatile markets for resources, and even worries about their depletion, the call for a new economic model is getting louder. In response, we are questioning the assumptions which underpin how products are made and sold. In an effort to keep control over valuable natural resources, companies are finding novel ways to reuse products and components. Their success provokes bolder questions – could economic growth be decoupled from resource constraints? Could we develop an industrial system that is regenerative by design?

3   THE IDEA OF CIRCULAR ECONOMY

Circular economy [3] has the aim to regenerate capital, no matter if it is financial, manmade, human, social or physical, and have production and transport systems that run on renewable energy. The starting point for the ideas on CE (circular economy) has been to change the linear economic system of "take-make-dispose" so as to lower resource use and waste of natural capital. It builds on the notion of cycles in nature fueled by alternate sources of energy, where nothing is wasted but just goes around in loops. Hence, it is restorative and regenerative by design, and aims to keep products, components and materials at their highest utility and value at all times, distinguishing between technical (non-biodegradable nutrients, e.g. metals, plastics etc.) and biological (biodegradable nutrients, e.g. cotton) cycles. Each product produced in a circular economy is designed so that the biological and technical components could be easily separated and re-circulated in the system and the focus is on effectiveness rather than efficiency. As Figure 4 illustrates, the difference between a linear and circular economy is that CE replaces one assumption – disposability – with

another – restoration. At the core, it aims to move away from incessant waste creation by designing and optimizing products for multiple cycles of disassembly and reuse. Indeed, tight component and product cycles of use and reuse aided by product design create positive cost arbitrage opportunities. This distinguishes it from linear economy which loses large amounts of embedded materials, energy and labor. It also builds on ideas of performance economy with new business models that focuses on selling services instead of products to lower the resource use [4]. While the linear growth model is based on exploitation of resources and labor efficiency gains, the growth in the circular economy is based on increased quality of products and services.

CE proponents claim it to be a new paradigm for industry since it aims at generating ecological, social and economic value resulting in effectiveness, improving the state of the environment and even going beyond sustainability. A global systems level change it involves so much opportunity, and it is the aim … to help further develop understanding and engagement in its realization.

This definition implies that the concept of CE should be considered an economic concept, with 'closed material loops' as an important prerequisite. 'Closed material loop' implies that material is reused again, either as bulk material, as products, or as components. Specific processes (or economic activities) are needed to facilitate this, such as refurbishment or recycling. How closed loops influence the essence of an economy, the production, distribution and consumption of goods and services has been suggested by Ellen MacArthur Foundation [5]. One of the most important implications of closing material loops is

the potential minimization of extraction of material from nature and the emission of waste to nature. Problems with extraction, such as resource scarcity, and with emissions, such as environmental impact, can potentially be solved.

Figure 5, referred to as the 'butterfly diagram', visualizes a CE. Several archetypes of closed material loops are visible, such as reuse, recycling and soil restoration (fertilizing soil with organic waste). Important to note is that Figure 5 gives the impression that material loops should be closed literally, in the sense that materials or components must go back to the original parts or product manufacturer. However, material can be used by another manufacturer, as long as the materials can flow back in the *original* material pool. In that case the original manufacturer can use the material again and *down-cycling* is prevented. This is called open loop recycling.

The same should be noted about product life extension (PLE) or strategies for increased durability of products, enabling a longer use of products. These strategies are often related to CE and indeed support a CE when, for example, a product is made more durable to enable reuse (and thus closes a loop). However, making a product durable to bring it to the dump a few years later does not support a CE.
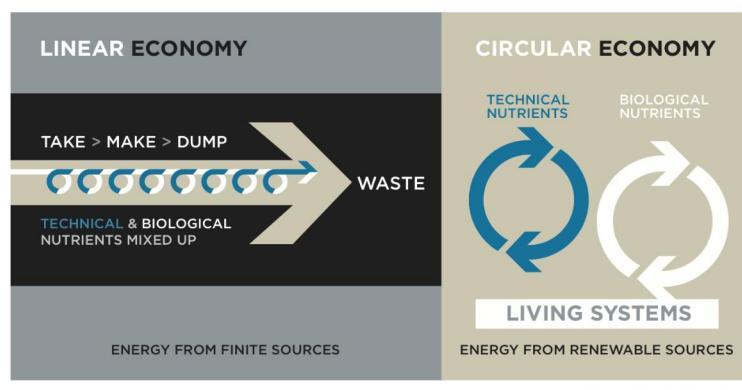
Figure 4 Linear versus Circular Economy
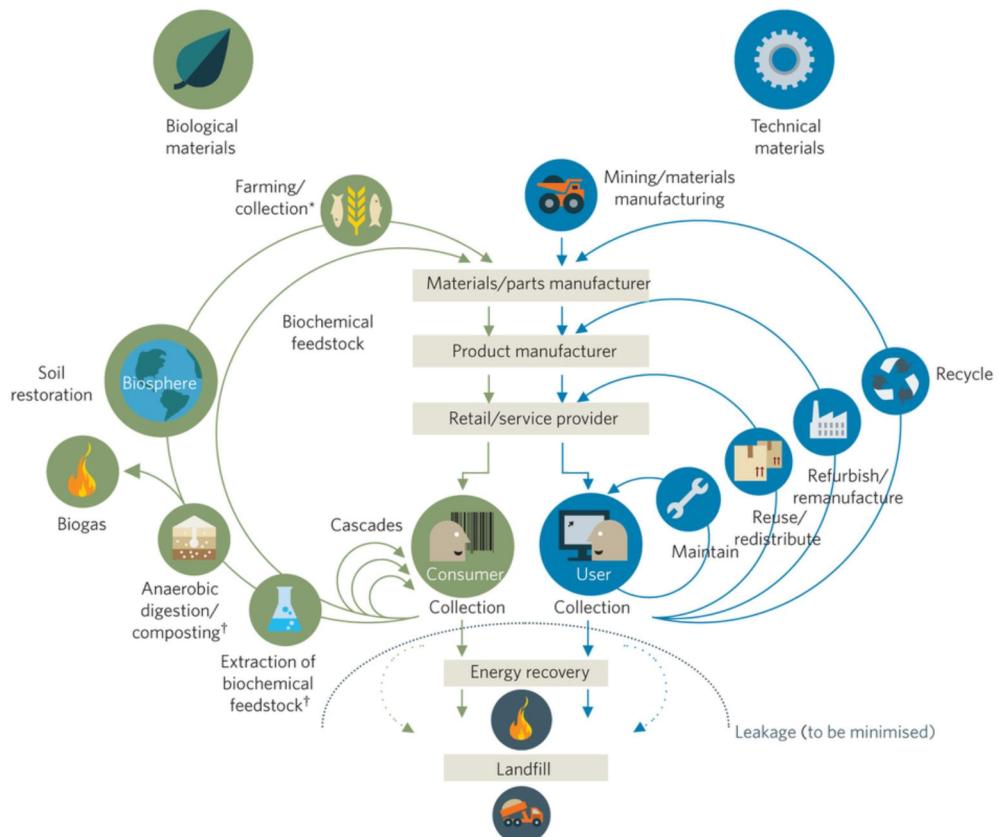
Figure 5 Circular Economy Concept

4 HOW MONEY IS MADE – THE CIRCULAR BUSINESS MODEL

A circular business model is the rationale of how an organization creates, delivers and captures value with and within closed material loops. It consists of the following components:

- Value proposition: **what** value does a company create with its product/service?
- Infrastructure management or Supply chain: **how** is the value proposition created, i.e. the **process?**
- Customer interface: **who** are the customers?
- Financial model: costs and benefits – **why** is the value proposition created, or how is value captured?

In CE, the Business Models are decoupling growth from scarce resources and, thus, gaining a competitive edge – circular advantage. Humanity is rapidly approaching a point where the linear growth model is no longer viable for companies. This is due to the rising global affluence, the inability of many non-renewable resources to keep up with demand, the strained regenerative capacity of renewable resources, threatened planetary boundaries, and exposure of a company of tangible and intangible value to serious risks. This leads to an inescapable situation: continued dependence on scarce natural resources for growth not acceptable to risk averse profit oriented entities. For businesses and firms, the answer lies in circular economy – where growth is decoupled from the use of scarce resources through disruptive technology and business models based on longevity, renewability, reuse, repair, upgrade, refurbishment, capacity sharing and dematerialization. This will lead to companies gaining a circular advantage – driving both resource efficiency and customer value, and delivering at the heart of a company's strategy, technology and operations. Possible new business models are:

1. Circular supplies: Provides fully renewable, recyclable or biodegradable resource inputs that underpin circular production and consumption systems.
2. Resources recovery: Enables a company to eliminate material leakage and maximize the economic value of product return flows.
3. Product life extension: Allows companies to extend the lifecycle of products and assets. Value that would otherwise be lost through wasted materials is instead maintained or even improved by repairing, upgrading, remanufacturing or remarketing products.
4. Sharing platforms: Promotes a platform for collaboration among product users, either individuals or organizations.
5. Product as a service: Provides an alternative to the traditional model of "buy and own." Products are used by one or many customers through a lease or pay-for-use arrangement.

These business models turn incentives for product durability and upgradability upside down, shifting them from volume to performance.

5 QUANTITATIVE JUSTIFICATION – CIRCULAR THERMODYNAMICS

Thermodynamics is the science of material and energy transformation, the circular thermodynamics of organisms is therefore none other than living economy: the transformation of energy and materials that enable organisms including human beings to survive and thrive. For isothermal processes, the change in Gibbs free energy ΔG (thermodynamic potential at constant temperature and pressure) is $\Delta G = \Delta H - T\Delta S$

where ΔH is the change in enthalpy (heat content), T is the temperature in Kelvins, and ΔS the change in entropy. Thermodynamic efficiency requires that ΔS approaches 0 (least dissipation) as reflected by the Carnot Cycle, and $\Delta H = 0$; or ΔG approaches 0 via entropy-enthalpy compensation, i.e. entropy and enthalpy changes cancelling each other out [6].

The zero-entropy circular economy is patterned after and integrated with the circular economy of nature versus the dominant economic model (Linear) of infinite unsustainable competitive growth that utilizes Earth's resources and exports massive amounts of wastes and entropy with maximum dissipation (entropy generation). The two are contrasted in Figure 6. The dominant linear input-output system grows relentlessly, swallowing up the earth's resources, laying waste to everything in its path. There is no closed cycle to hold resources within, to build up stable organized social or ecological structures. That is the essence of our "boom and bust" suicidal economy.
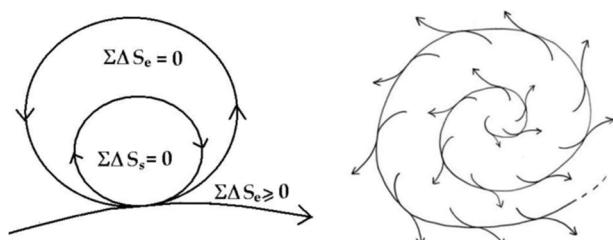
Figure 6 Entropy Change- Circular versus Linear Economy

The zero entropy circular economy, on the other hand, is embedded within and integrated with the circular economy of the natural ecosystem. It builds up space-time structures within to store and mobilize renewable energy and materials through values added in various ways to the primary productivity from sunlight and photosynthesis.

The components of the circular economy ensure that all space-times are bridged, and are optimized for capturing, storing, and mobilizing resources

efficiently and rapidly while conferring local autonomy on all scales. It also maximizes diversity: numerous small entities scaling up to very few large ones. Another key feature is that activities requiring energy or material are coupled to those that generate them; and the giving and taking can be reversed as the need arises. In other words, the system maximizes symbiosis, reciprocity and cooperation. It is a fair and just reciprocal exchange of materials and energy that maintains and ensures the survival of the whole. This is indeed the biggest lesson for the commercial sector that has hitherto operated on exploitation and competition.

6   HOW TO OPERATIONALIZE CIRCULAR ECONOMY

The required innovations in transitioning to a circular economy go beyond new and more efficient technologies; practices need to radically change as well. Examples of new practices include extending the producer responsibility to the entire life-cycle of a product, including its recycling. If properly set up, this so called 'Extended Producer Responsibility' creates strong incentives for more eco-responsible design; Selling services rather than products, thereby creating incentives for long-lasting products and refurbishing and develop the sharing economy in order to get more service from fewer products.

There are five generic principles based upon several 'schools of thought' [7] in which the description of CE is rooted. They are:

- Design out waste

Delivering benefits in new ways by shifting to service. Thus world's largest taxi company (Uber) owns no taxis, while the largest software vendors (Apple & Google) do not write apps. In addition it would require new design of products and processes such as modular products, purer material flows, and easier disassembly. In addition, an emphasis placed on rethinking, redesigning of benefits by integrating environmental concerns in product design and business strategy development.

- Build resilience through diversity (balance efficiency with adaptability)

Modularity, versatility, and adaptivity are the prized features that need to be promoted in an uncertain and fast-evolving world. Production systems should be flexible to use many different inputs.

- Shift to renewable energy sources

Systems should ultimately run on renewable energy, enabled by reduced threshold energy levels required by restorative circular economy. In addition to use of alternate sources of energy, the products must avoid use of heavy metals and reduce weight for dematerialization.

- Think in systems

The ability to understand how parts influence one another within a whole, and the relationship of the whole to parts is critical. The elements of the system are considered in relation to these environmental and social contracts. We must create strong supply chain collaboration (new value networks) and aligned business models to have a strong revenue model. This involves redesign of value chains both up-stream and down-stream.

- Think in cascades

Development of core competences and technologies along reverse cycles as cascades.
The value creation lies in the opportunity to extract additional value from products and materials by cascading them through other applications. Thus, in case of textiles, clothes entering the second hand market and cascading down to fibers for use in furniture followed by conversion to insulation material. They are finally returned to basic feedstock in the technical cycle and to biosphere during natural material biodegradability.

7   RESYNTEX

The underpinnings of RESYNTEX project which aims at designing, developing and demonstrating industrial symbiosis between textile waste and the chemical industry is rooted in CE. This is based on the chemical/enzymatic transformation of textile waste into a form that facilitates easy acceptance as feedstock by the chemical industry in order to produce high value added products at competitive prices. The project will consider and demonstrate the viability of complete value chain beginning with the citizen behaviour change and the textile collection of unwearable textiles demonstrating the production of the transformed textile into chemical feedstock. Interdisciplinary information exchange between various industrial and societal sectors (symbiosis) involved is vital for successful project performance.

8   CONCLUSION

Moving toward a circular economy can be daunting. Yet, by adopting circular economy principles, more and more companies are gaining real competitive advantage. They are getting ahead of rivals by innovating for both resource efficiency and customer value, and creating change at the intersection of a company's strategy, technology and operations.

In the face of runaway resource scarcity and rising customer and policy expectations for better, more sustainable products, there has never been a better time to start. By developing a proactive strategy – built on a clear understanding of the motivation to leave behind the linear model and underpinned by innovative business models, technologies and

capabilities critical to success – companies can create superior value and capture the circular advantage.

For this to be true, circular transition needs to be more than a catchy slogan; it needs to go beyond mere process efficiency improvements. Real breakthroughs are required – not just in the way corporates do business but also in the way consumers consume. We all play a part; our attitude towards consumption also needs to go circular. RESYNTEX is a strong start to achieve this lofty goal for the textile sector.

9   REFERENCES

1. Clark J.: A greener and circular economy, Chemistry & Industry, December 2012

2. Reh L.: Process engineering in circular economy, Particuology 11, 119-133, 2013

3. Pearce D, Turner RK.: Economics of natural resources and the environment, Harvester Wheatsheaf, London, 1990

4. Wijkman Anders & Rockström Johan: Bankrupting Nature - Denying our planetary boundaries, Routledge, Oxon, 2012

5. Webster K.: The Circular Economy – A Wealth of Flows, Ellen MacArthur Foundation Publ., UK, 2015

6. Shaely B.: Towards a Better Understanding of the Full Life-Coherence Principle, 2016

    http://bsahely.com/2016/02/10/towards-a-better-understanding-of-the-full-life-coherence-priciple/

7. Aneja A. & Pal R.: Textile Sustainability: Major Frameworks & Strategic Solutions, Handbook of Sustainable Apparel Production, CRC Press, 2014

EFFECT OF 3-DIMENSIONAL KNITTED SPACER FABRIC CHARACTERISTICS ON ITS THERMAL AND COMPRESSION PROPERTIES

V. Arumugam, R. Mishra, J. Militky, D. Kremenakova, J. Salacova, M. Venkatraman and V. B. Ramanisanthi Subramanian

Department of Materials Engineering, Faculty of Textile Technology, Technical University of Liberec
Studentská 2, 461 17 Liberec, Czech Republic
veerakumar27@gmail.com, arumugam_veerakumar@tul.cz

Abstract: *Spacer fabrics consist of three layers of fabrics which have ability to complement and maximize the essential thermal clothing comfort for various applications. Clothing comfort is also defined by the tactile sensations felt by a subject through the mechanical interactions between the body and the garment. In this research work, the thermal and compression properties of polyester/polypropylene and polyester/polypropylene/Lycra blended knitted spacer fabrics have been studied in relation to density, thickness, stitch density and type of spacer yarns (monofilament or multifilament).The objective of this study was to determine the influence of spacer fabric factors such as the constituent fibres, density, thickness, stitch density, type of spacer yarns and knit characteristics on the fabrics properties such as air permeability, relative water vapour permeability, thermal conductivity and work of compression. The experiment results show that the thermal conductivity and effusivity are closely related to the fabric characteristics such as the raw materials, type of spacer yarn, density, thickness and tightness of surface layer. Also, this study established that the compression resilience of the fabric made up of monofilament spacer yarn was better than that of the multifilament spacer yarn in spacer knitted fabrics.*

Key Words: *knitted spacer fabrics, air permeability, thermal conductivity, compression resilience*

1   INTRODUCTION

The main factors which affect human beings during the selection of clothing or functional materials are aesthetic, appearance and fashion. Apart from these factors, comfort properties of functional clothing during usage are important. Nowadays, people have become much more demanding when it comes to the properties of clothing, particularly those of leisure and sportswear. One of the textile properties that have steadily gained importance among is breathability, because this property seems to be directly linked to comfort ability of functional fabric materials. To be comfortable and to maintain the state of comfort, clothing must be designed to allow the body's heat balance to be maintained under a wide range of environmental conditions and activities of body. Comfort is considered as a fundamental property when a clothing product is evaluated. There are three parameters mainly influencing clothing comfort such as thermo-physiological, sensorial and psychological comfort [1, 2]. Clothing comfort is an extremely complex phenomenon and has drawn the attention of many textile research workers. The thermal comfort is the factor governed by the movement of heat, moisture, and air through the fabric. Maintaining a balance is probably the most important attribute of clothing and has drawn the attention of many textile research workers. The main problem associated with thermal comfort is the incompatibility between the requirement of heat conservation during low metabolic activity and heat dissipation at high energy level. Air permeability is a biophysical feature of textiles which determines the ability of the air to flow through the fabric. Airflow through textiles is mainly affected by the pore characteristics of fabrics. The pore characteristics of the fabric are mainly determined by their structure and density. Water vapour permeability determines breathability of the clothing material. It has the ability to transmit vapour from the body to the environment. The mechanism involved in water vapour transmission through fabric from the skin to the outer surface is diffusion and absorption-desorption method. The ability of clothing to transport water vapour is an important determinant of physiological comfort. Spacer fabrics is a three dimensional fabrics which has two outer surfaces connected to each other with spacer yarns. Since the middle layer comprises monofilaments, the fabrics possess special characteristics [3]. Components in spacer fabrics differ depending on the yarn type and production method [4]. There are two types of spacer fabrics: warp-knitted spacer fabric and weft-knitted spacer fabric. The first type can be produced by using a rib raschel machine which has two needle bars [5] while the second can be knitted with double jersey circular machine which has a rotatable needle cylinder and a needle dial [6].

The properties of spacer fabrics such as 3D fibre location, possibility to use different materials and production in one step allow for the use of spacer fabrics in different application areas, with the major application areas such as automotive textiles, medical textiles, geotextiles, protective textiles, sportswear and composites [7, 8].

Due to spacer yarn between the surface layers, spacer fabrics have the ability to trap and hold air and insulate. This, along with the ability to wick away moisture, maintains the body's microclimate, and thus keeps the person dry and comfortable. There are many outdoor/active apparel manufacturers who still employ the layering concept in order to achieve all the desirable properties in active apparel. According to previous researches, the outermost layer should protect the wearer from environmental elements such as wind, rain, or snow, the middle layer should provide the wearer with warmth, and the innermost layer should have an insulating factor and have the capabilities to wick moisture away from the skin; it is also noted that all layers should be breathable and should have wicking capabilities in order to provide the greatest comfort to the wearer. Three layers of outerwear could create a bulk and be a good outfit. Spacer fabrics can accomplish all of these desirable characteristics. The thermal insulation properties of both warp and weft knit spacer fabrics are excellent when being considered for active wear. A lower density in the pile yarns of the spacer fabrics will yield a higher thermal resistance which is ideal for active wear fabrics as it will keep the wearer warm [9].

Weft knitted spacer fabrics have significantly better air permeability than the warp knitted fabric [9]. However, it should be noted that the density of the fabric, regardless of whether it is a warp knit or a weft knit, will have a substantial impact on the air permeability and thermal regulation properties. The denser spacer fabric will have a higher thermal conductivity value, but a low air permeability value; therefore end use must be taken into consideration to find an optimum density for the fabric.

The compression properties including compression resilience are very many attributes of spacer fabrics which are related to sensation of comfort. Many outdoor activities of athletes are seasonal (i.e. skiing), therefore during the off-season it is likely that the garments are stored away in containers, or other means, where they are under a heavy load. During the season, these garments are packed in suitcases for traveling. The athlete or outdoor enthusiast expects the garments to not be distorted in any way when they are removed from storage, as they should be ready to be utilized for the new season. Spacer fabrics are very resilient and will resist and recover from pressure that may be applied on them, thus deformation is not a problem in apparel made using spacer fabrics, and this may prolong the life of the garment. The lack of comprehensive studies on thermal and compression characteristics of knitted spacer fabrics are a sound basis for this research. Hence, it is necessary to understand the influence of characteristics of spacer fabric on thermal and compression properties. So, this study presents the effect of thickness, density, stitch density, composition and types of spacer yarn on thermal and compressional behaviour.

2   EXPERIMENTAL

Six different spacer fabrics were knitted using Mayer & Cie, OVJA 1.6 E 3 WT circular knitting machine with 5 feeders, 14 gauge and 80 cm diameter. In the present study, different types of yarns were used to produce spacer fabric samples. Among six different types of samples, the first three were produced using Polyester/Polypropylene blend with three different proportions and the other three (KSF4 – KSF6) with Polyester/Polypropylene/Lycra blend having another 3 different compositions. Furthermore, for spacer (middle layer), samples KSF1 AND KSF4 were knitted with Polyester monofilament yarn and the remaining samples are knitted with polyester multifilament. These sample classifications are clearly shown in Table 1.

Table 1 Weft knitted spacer fabrics particulars

Fabric Samples	KSF1	KSF2	KSF3	KSF4	KSF5	KSF6
Face Layer	POP - 14.5 tex	POP - 14.5 tex	POP - 14.5 tex	POP - 14.5 tex Lycra - 44dtex	POP - 14.5 tex Lycra - 44dtex	POP - 14.5 tex Lycra - 44dtex
Middle Layer (Spacer)	PES Monofil - 88 dtex	PES - 14.5 tex	PES - 167 dtex	PES Monofil - 88 dtex	PES - 14.5 tex	PES - 167 dtex
Back Layer	POP - 14.5 tex	POP - 14.5 tex	POP - 14.5 tex	POP - 14.5 tex	POP - 14.5 tex	POP - 14.5 tex
Fibre Composition [%]	58% POP 42% PES Monofil	45% POP 55% PES	41%POP 59% PES	55%POP 39%PES Monofil 6%Lycra	42% POP 52% PES 6% Lycra	39% POP 55% PES 6% Lycra

*KSF – Knitted Spacer Fabrics, POP - Polypropylene, PES Monofil - Polyester Monofilament, PES - Polyester Multifilament

Table 2 Characteristics of knitted spacer fabrics

Fabric samples	KSF1	KSF2	KSF3	KSF4	KSF5	KSF6
Areal density [g/m^2]	493	443	477	632	657	695
Thickness [mm]	4.4	2.62	2.74	4.4	3.5	3.4
Density [kg/m^3]	112	169.1	174.1	144.8	187.7	205.4
Wale/cm	10	10	10	14	14	14
Course/cm	20	15	15	25	20	20
Stitch Density [stitches/cm^2]	200	150	150	350	280	280

The fabric characteristics of interest including yarn linear density and fabric weight per unit area were determined according to ASTM D1059 standard using electronic weighing scales. The density (D) of the fabric was calculated using the relationship

$$D = \frac{W}{t} \quad [\text{kg/m}^3] \qquad (1)$$

where W is areal density (weight per unit area), which was determined following the standard method ASTM D 3776. Thickness t was determined using SDL thickness gauge as per ASTM D 5736 standard. The fabric characteristics such as areal density, stitch density, structure, thickness, are presented in Table 2. All the experiments were carried out under standard ambient conditions.

2.1 Air permeability

The spacer fabric samples were conditioned for 48 hours in atmospheric conditions of 20±2°C temperature and 65±2% relative humidity before the tests were performed. The air permeability of the samples in L/m^2/s was measured according to the method specified by Standard ISO 9237 using a Textest FX3300 air permeability tester. The measurements were performed at a constant pressure drop of 100 Pa. For each of the 6 spacer samples, we repeated this measurement for 10 times and average values are reported.

2.2 Water vapour permeability

The water vapour permeability was measured on the Permetest by following the standard ISO 11092. Slightly curved porous surface of the instrument is moistened (either continuously or on demand) and exposed in a wind channel to parallel air flow of adjustable velocity. A sample is located in a small distance from the wetted area of the diameter of about 80 mm. The amount of evaporation heat of liquid water taken away from the active porous surface is measured by a special integrated system. Thus, very low time constant of the whole system is achieved, resulting in short measurement time. The relative water vapour permeability ($RWVP$) of the fabric sample is calculated as the ratio of heat loss from the measuring head with fabric (q_s) and without fabric (q_0) as given in Eq. (2) [10]:

$$RWVP = \frac{q_s}{q_0} \times 100\% \qquad (2)$$

where q_s - loss with the fabric on the measuring head, q_0 - heat loss from the bare measuring head.

2.3 Thermal properties

Thermal conductivity measurements were performed using C-Therm Thermal Conductivity Analyzer Tci (Figure 1).

Figure 1 Thermal conductivity (Tci) analyzer (C-Therm)

The TCi is based on the modified transient plane source technique. This system consists of an external sensor, software for computer and control electronics. The guard ring which is spiral in shape surrounds the heating element or sensor. It generates heat in addition to the spiral heater wire, approximating a one-dimensional heat flow from the sensor into the material under test in contact with the sensor. The voltage drop on the spiral heater is measured before and during the transition. The voltage data is then translated into the effusivity and conductivity value of the tested material [11]. The system automatically compensates for variations in sensor temperature, thus enabling reliable measurements at a wide range of temperatures from -50 to +200°C so that it can test solids, liquids, foams, powders and pastes. The testing of the materials can be performed by placing the sample on the heating element (sensor) for about 0.8 seconds. A known current is passed through the sensors heating element which results in a raise in temperature at the interface between the material and the samples. This temperature rise at the interface induces a change in the voltage drop of the sensor's spiral heating element [12]. The standard test method EN 61326-2-4:2006 was used for this testing using TCi [9]. This test was performed at room temperature. The results are reported in Table 3.

2.4 Compression test

The KES-FB3-A compression tester was used for testing the compression properties of the spacer fabrics. The testing method was carried out according to the instruction manual from Kato Tech Co., Ltd. (Kawabata & Niwa, 1996). The parameters obtained from the compression hysteresis curves are defined in Table 3. The sample size used in the compression test was 20 × 20 cm and the maximum pressure used was

50 gf/cm^2. In each case, 10 specimens were tested and the average values were reported.

3 RESULTS AND DISCUSSION

3.1 Relation between fibre composition and density on water vapour permeability

The water vapour permeability of fabric depends upon a number of factors including thickness and density of fabrics, wetting and wicking behaviour of yarns, and the relative humidity and temperature of the atmosphere. The relative vapour permeability is greatly reduced by the presence of 6% of lycra in spacer samples. This is due to normally elastomeric fibres which have moisture regain percentage of about 0.6-0.8, so they have a tendency to hold water vapour to restrict permeability in fabrics. Moreover, decrease in the fibre composition ratio between polypropylene and polyester shows a significant effect in both water vapour permeability and evaporative resistance. It is also observed that with the increase in density of samples in dry state, the relative water vapour permeability increases in all samples, as plotted in Figure 2. The research also showed that the ability to transmit water vapour decreases with the reduction in the percentage of polyester fibre content. But the trend is reversed in the case of evaporative resistance. So, the results demonstrate the apparent influence of fibre composition and density on the water vapour permeability of weft knitted fabrics. Figure 3 also shows that there is no dependent correlation between water vapour permeability and air permeability. Therefore, the designing of clothing for active leisure with only air permeability or water vapour permeability in mind is not right, because water vapour permeability depends on the structure of fabrics not in the same order as air permeability.
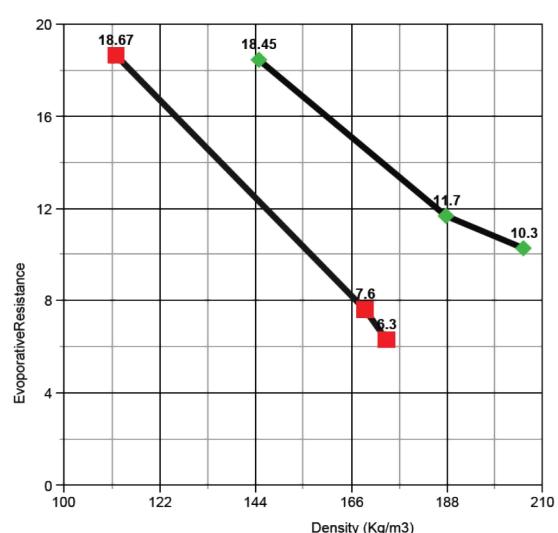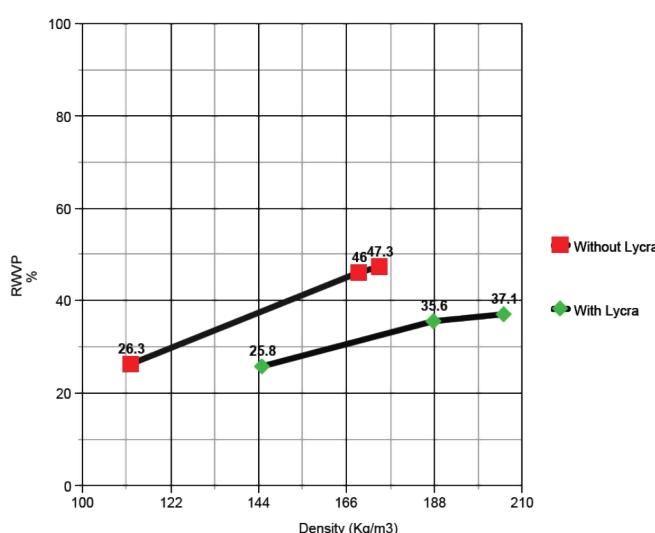
Figure 2 Effect of density and fibre content on RWVP and R$_{et}$
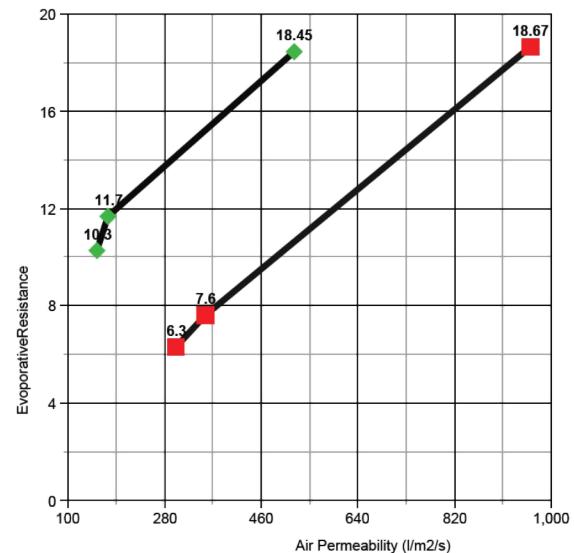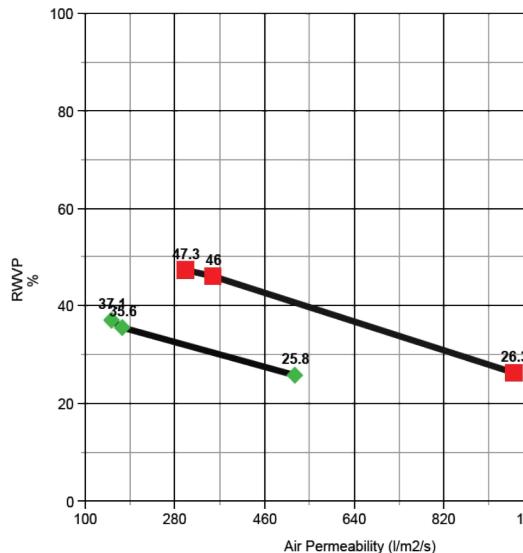
Figure 3 Influence of air permeability on RWVP and R_{et}

3.2 Influence of spacer fabric properties on thermal behaviour

The properties mentioned above are considered as the most important for thermal comfort in extreme environmental conditions. It was also possible to apply other thermal properties of fabrics, for instance their density, air permeability mass per square meter or thickness. All properties are important from the point of view of thermal comfort. Higher mass and thickness give better thermal insulation of the fabrics. Nevertheless, bigger mass and thickness can lead to a worsening of utility comfort, especially the freedom of movement.

The three dimensional nature of spacer fabric has a higher thickness and lower mass which leads to lots of air being trapped in the fabric structure. If the fabric is in contact with air from one side, the trapped air will circulate between the outer surface layers because of the higher air permeability in these fabrics. This feature causes the transfer of moisture and heat from skin surface via the circulating air. So, 3D spacer structure will be greatly thermally isolated. The thermal conductivity and effusivity of different spacer fabrics was presented here. Since a lower value of thermal conductivity indicates a lower heat transfer from the skin to the fabric surface, this is usually associated with a warm feeling. This study found that lower fabric density will have a lower thermal conductivity (shown in Figures 4 and 5), as there will be more space to trap air inside. Also, denser fabric has better thermal ventilation.
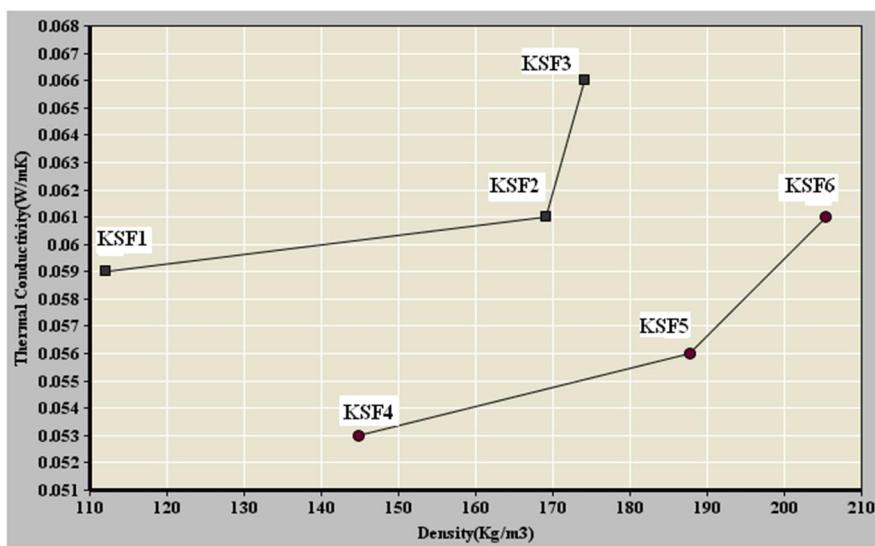
Figure 4 Effect of density on thermal conductivity
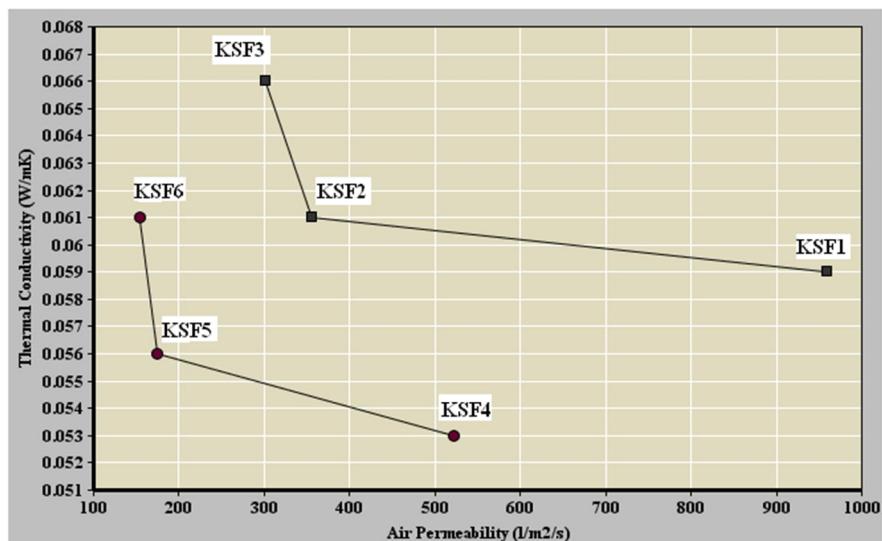
Figure 5 Influence of air permeability on thermal conductivity
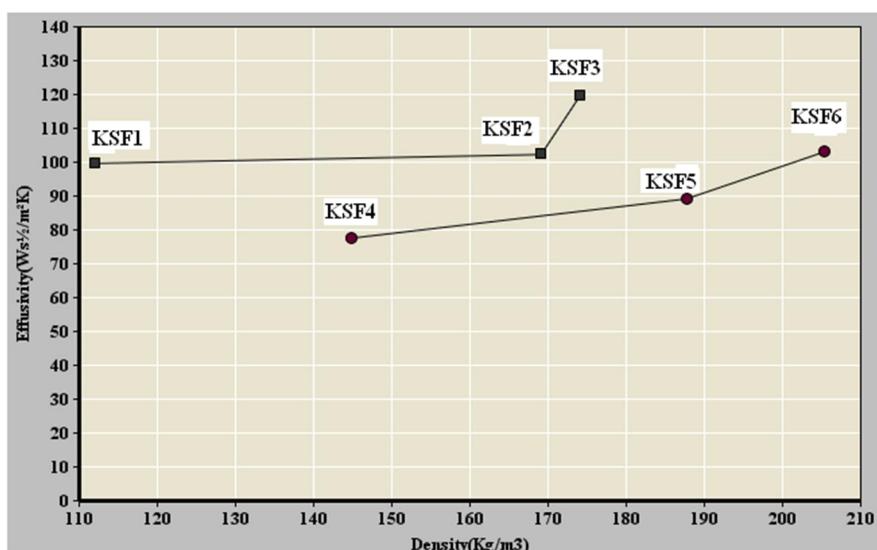
Figure 6 Effect of density on effusivity
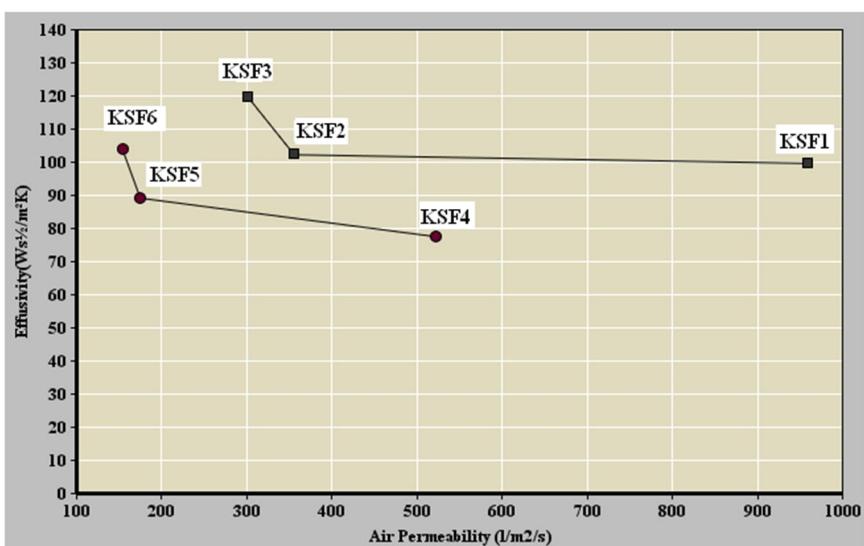
Figure 7 Influence of air permeability on effusivity

Remarkable differences between the heat transfer rates of all six spacer fabrics are also justified here. Fabrics with a low value of thermal effusivity give us a ''warm'' feeling, as shown in Figure 6. 3D Spacer fabrics have a much lower value of thermal absorption then, so they give us warmer feelings than other commercial 2D fabrics, which is not ideal for summer clothes. Thermal effusivity is a very important parameter from the point of view of thermal insulation, and is proportional to the fabric structure. Due to increase in density between the samples KSF1 to KSF3 and KSF4 to KSF6, we can observe the increase of thermal effusivity (Figure 6), and, in contrast, effusivity decreases as air permeability increases (shown in Figure 7). So spacer fabric with low thermal conductivity and effusivity is a perfect option for winter wear.

3.3 Compressional behaviour of knitted spacer fabrics

It is observed from the Table 2 that there is a decreasing trend in wales/cm and course/cm in both groups due to monofilaments used as spacer yarn. It can also be found that the thickness of the spacer fabrics made of monofilaments as spacer yarns is higher than that of fabric with multifilaments as spacer yarn. The areal density is higher for group 2 samples, which is due to elastic yarn (polypropylene/lycra) causing the surface loops/courses to come closer after the fabric is removed from the knitting machine, which leads to an increase in areal density and course/cm. The number of wales per centimetre (WPC) and courses per centimetre (CPC) can be influenced by the type of yarns (monofilament or multifilaments).

Table 3 Compression properties

Samples	LC	WC	RC
KSF1	0.462	0.649	62.51
KSF2	0.635	1.24	44.36
KSF3	0.5922	0.979	48.72
KSF4	0.384	0.715	61.14
KSF5	0.6746	1.737	49.24
KSF6	0.6464	1.44	52.15

WC - Work of compression (gf.cm.cm^{-2}), RC-Resilience (recoverability) of compression (%), LC-Linearity of compression

The compression properties of all the spacer fabrics are listed in Table 3. A series of two-way ANOVA tests was performed for each dependent variable to determine whether there were any significant differences due to different spacer yarns. It clearly shows that none of the six samples including samples made up of multifilaments and monofilaments have any significant difference in the compression resilience (RC). So, spacer fabrics have good compression resilience properties compared to any other form of fabrics. Obviously, the compression resilience increases in the samples (KSF1 and KSF4) which have monofilament as spacer yarn. It is also observed

that linearity of compression (LC) between the samples decreases with the increase in the distance between the two layers. Among the two groups, the samples containing lycra (KSF4-KSF6) have relatively lower compressibility than samples (KSF1 – KSF3). Also, the sample which has monofilament as spacer yarn has a significantly lower linearity of compression than fabrics containing multifilament as spacer yarn. Moreover, the compression energy (WC) has the same trend as the LC, and the effects of the spacer yarn, thickness and stitch density and their interaction were all highly significant. A higher WC value corresponds to a higher compressibility of the fabric.

4   CONCLUSIONS

The knitted spacer fabric offers lower thermal conductivity than the normal form of fabrics. It is due to the characteristics of spacer fabrics such as bulkiness, lower density and air layer in the middle part. Therefore, spacer fabric might be the proper choice for winter clothing thanks to its suitability.

It is also observed that the spacer fabrics with lycra content has higher compression than the fabric without lycra. Also, the spacer fabrics made up of monofilament as spacer yarn have more compression resilience irrespective of the surface layer. The effect of distance between two layers and the stitch density also have a significant effect on compression behaviour of spacer fabrics. The surface layer with higher course/cm leads to lower work of compression but fabric with monofilament spacer has higher compression recovery. These results have proved the importance of behaviour of spacer fabrics during compression, they further require more studies on compression properties of spacer fabrics.

5   REFERENCES

1. Skenderi Z., Cubric I.S., Srdjak M.: Water Vapour Resistance of Knitted Fabrics under Environmental Conditions, Fibres & Textiles in Eastern Europe 73(2), 72-75, 2009
2. Wang F., Zhou X., Wang, S.: Development processes and property measurement of moisture absorption and quick dry fabrics, Fibres & Textiles in Eastern Europe 73(2), 46-49, 2009
3. Bruer S.H., Powel N., Smith G.: Three dimensionally knit spacer fabrics: A review of production techniques and applications, Journal of Textile and Apparel Technology Management 4, 1-31, 2005
4. Mecit D., Marmarali A.: Application of spacer fabrics in composite production, Usak University Journal of Material Sciences 1, 71-78, 2012
5. McCartney P.D., Allen H.E., Donaghy J.G.: Underwire brassiere, warpknitted textile fabric for use in fabricating same, and method of warp knitting such fabric, USPTO Patent Full Text and Image Database, U S Patent No. 5669247, 1999

6. Shepherd A.M.: Weft-knitted spacer fabrics, USPTO Patent Full Text and Image Database, U S Patent No. 6779369 B2, 2004

7. Xiaohua Y.E., Hong H., Feng X.: Development of the warp knitted spacer fabrics for cushion applications, Journal of Industrial Textiles 37(3), 213, 2008

8. Gross D.: 3D spacer knit fabrics for medical applications, Journal of Textile and Apparel Management 4, 26-28, 2003

9. Pause B.: Studies of the thermo-physiological comfort provided by knitted spacer fabrics, Melliand International 8(1), 57-58, 2002

10. Hes L., Dolezal I.: A new portable computer-controlled skin model for fast determination of water vapour and thermal resistance of fabrics, Asian Textile Conference, New Delhi, 2003

11. Kuvandykova D.: A new transient method to measure thermal conductivity of asphalt, C-Therm Technologies 7, 1-10, 2010

12. Cha J., Seo J., Kim, S.: Building materials thermal conductivity measurement and correlation with heat flow meter, laser flash analysis and TCi, Journal of Thermal Analysis and Calorimetric 109, 295-300, 2012

THE EFFECT OF PREPARED SAMPLES OF SEQUESTERING AGENTS AND CHELATING SURFACTANTS ON MODEL WASHING

P. Bayerová, L. Burgert, M. Černý, R. Hrdina and A. Vojtovič

Faculty of Chemical Technology, University of Pardubice,
Department of Synthetic Polymers, Fibers and Textile Chemistry, Czech Republic
petra.bayerova@upce.cz

Abstract: This work presents the results of model washing with addition of prepared samples of sequestering agents and chelating surfactants. After 20× repeated washing in hard water of 22°dH (given in German degrees of hardness) the content of ash and Ca^{2+} ions were determined. The image of fabric after the model washing was evaluated by means of images from a scanning electron microscope.

Key words: sequestering agents, chelating surfactants, washing of textile materials

1   INTRODUCTION

It is well known that water has an irreplaceable role in textile industry. Any textile production is dependent on water and sufficiency of water of good quality and it is a basic precondition for textile plants. Water is almost the only solvent which is used in textile industry for washing and dissolution of finishing agents, dyes and sizes and it is also used for steam production.

Washing is one of the most important activities in the treatment and maintenance of textiles. A detergent is a complex mixture containing various systems – surfactants, builders and auxiliary agents.

The adverse effect of alkaline earth metal ions (Ca^{2+}, Mg^{2+}) which cause water hardness and also the effect of heavy metal ions (Fe^{3+}, Cu^{2+}, Mn^{2+}) on fundamental processes of textile industry have been generally well known. An important property of sequestrants is the disabling of $CaCO_3$ precipitation. This slightly soluble compound precipitates at high temperature as limescale on equipment and may affect its functioning, temperature regime etc. Besides of this, $CaCO_3$ can deposit on treated textile causing a rough handle. It also affects the efficiency of textile auxiliary agents and the run of other textile finishing processes. Besides $CaCO_3$, calcium silicate can also have a negative effect which is created if waterglass is present.

Therefore the usage of sequestering agents is recommended even in pre-treatment. Sequestrants are the most frequent agents used as components of detergents, not only in the area of textile finishing (mainly in pre-treatment) but also in other areas, e.g. dyeing cellulose materials and water softening. Sequestering agents are generally compounds creating chelates, i.e. specific kinds of complex compounds surrounding the cation.

Chelating surfactants should combine the properties of surfactants and sequestering agents. Then the sequestering substance reduces the hardness of water and improves the washing effect of surfactants. [1-3]

New types of sequestering agents and chelating surfactants (derivatives of aspartic acid) were synthetized at the Institute of Chemistry and Technology of Macromolecular Materials of University of Pardubice. Prepared samples are biodegradable. [4] These substances were tested in repeated model washing in hard water.

2   EXPERIMENTAL

2.1   Samples of sequestering agents and chelating surfactants

Two types of sequestering agents (Table 1) and three types of chelating surfactants (Table 2) were tested in this study.

Table 1 Structures of sequestering agents

Sample	Chemical structure
No. 1	H₂C—COONa HC—NH—CH—CH₂—COONa COONa COONa *N*-(1,2-dicarboxyethyl)aspartic acid tetrasodium salt
No. 2	H₂C—COONa HC—NH——CH₂—COONa COONa *N*-carboxymethyl aspartic acid trisodium salt
Trilon M	CH₂—COONa NaOOC——CH—N H₃C CH₂—COONa methylglycindiacetic acid trisodium salt

Table 2 Structures of chelating surfactants

Sample	Chemical structure
No. 3	H_2C——COOK HC—NH—$(CH_2)_{15}$—CH_3 COOK *N*-hexadecyl aspartic acid dipotassium salt
No. 4	H_2C——COOK HC—NH—$(CH_2)_n$—CH_3 COOK n = 10-18 *N*-cocoyl aspartic acid dipotassium salt
No. 5	H_2C——COONa HC—NH—$(CH_2)_{11}$—CH_3 COONa *N*-dodecyl aspartic acid disodium salt

The commercial sequestering agent Trilon M (Table 1) was used for the comparison of their efficiency.

2.2 Model washing process

The prepared agents were analyzed under conditions for model washing. The chosen model detergent consisted of waterglass (soln. of sodium metasilicate), carboxy-methylcellulose, sodium carbonate, and sodium sulfate [5]. The analyzed sequestrants were added to this basic mixture when the washing filling had contained 7 g/l of model washing agent. The washed material was a batch of 20 grams of cotton textile, at a bath ratio of 1:20.

The washing was repeated 20x in hard water 22 °dH (given in German degrees of hardness) for 30 min at 90°C (Figure 1). The hard water was prepared by dissolving $CaCl_2.6 H_2O$ in distilled water (1°dH = 39.06 mg $CaCl_2.6 H_2O$).
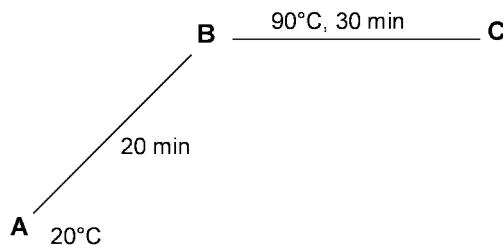
Figure 1 Process of model washing

2.3 The evaluation of content of ash and Ca^{2+} ions

After 20× repeated washing in hard water of 22°dH for 30 min at 90°C, the content of ash and Ca^{2+} ions were determined. After 20× repeated washing, the

textile was incinerated in a platinum crucible and the amount of calcium was evaluated in ash. The titration was carried out with Chelaton III (13.270 g/l) according to the recommended procedure [6]. Finally, the image of fabric after the model washing was evaluated by means of images from a scanning electron microscope (JEOL JSM – 5500LV).

3   RESULTS AND DISCUSSION

Due to the fact that a significant part of the world production of the sequestering agents is used for manufacturing of detergents and cleaning agents, the prepared samples were tested under model washing conditions. The washing with model detergent without sequestering ingredients increased the content of inorganic deposits in cotton textile. The content of ash and calcium in textile is relatively high: 3.18% ash and 15.20 g/kg Ca^{2+}. The addition of prepared samples with sequestering effect improved the result as documented by the data in Table 3.

Table 3 Content of ash and calcium ion in the cotton textile after twenty times repeated washing in hard water 22°dH

Sample	Ash content (mass %)	Content of Ca^{2+} (g/1kg)
no. 1 + model detergent	0.08	0.08
no. 2 + model detergent	0.50	1.76
no. 3 + model detergent	0.50	1.87
no. 4 + model detergent	1.08	4.22
no. 5 + model detergent	1.14	4.81
Trilon M + model detergent	0.06	0.43
no. 5 + no. 1 (2:1) + model detergent	1.80	7.83
no. 5 + no. 2 (2:1) + model detergent	1.91	7.97
no. 5 + Trilon M (2:1) + model detergent	1.30	5.11
no. 4 + no. 1 (2:1) + model detergent	0.66	2.67
no. 4 + no. 2 (2:1) + model detergent	0.96	3.90
no. 4 + Trilon M (2:1) + model detergent	0.02	0.11
Washing without sequestering agents	3.18	15.20
Commercial washing agent Bonux	5.30	16.70
Commercial washing agent Colon	4.55	18.50

Reduction of the content of ash and calcium was observed mainly in typical sequestering agents (Trilon M, sample no. 1, sample no. 2). The lowest content of Ca^{2+} was shown by sample no. 1: N-(1,2-dicarboxyethyl)aspartic acid tetrasodium salt - see Figure 4.

With the addition of chelating surfactants, the content of ash and calcium is lower than without prepared samples, too. Measured values are higher than for sequestering agents.

As chelating surfactants have lower value of sequestering capacity, their combination with sequestering agents was performed. These combinations achieved best results with surfactants prepared from cocoylamin (sample no. 4). The combinations with sample no. 5 did not lead to better results. Synergic effect did not occur. The reason may be the influence of dispersion and solubilization. The combination of sample no. 4 with Trilon M has the best effect in the bath: 0.02 % ash and 0.11 g/kg Ca^{2+}.

The image of fabric after the model washing was evaluated by means of images from a scanning electron microscope (Figures 2 – 10). With the addition of agent with sequestrant, the resulting effect was improved, which was the case of commercial washing agents, too.
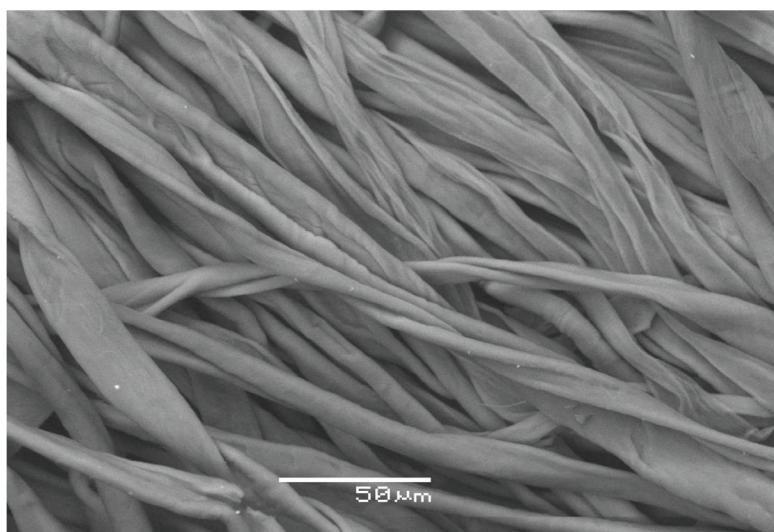
Figure 2 EMS of fiber surface of cotton textile (magnification 500x)
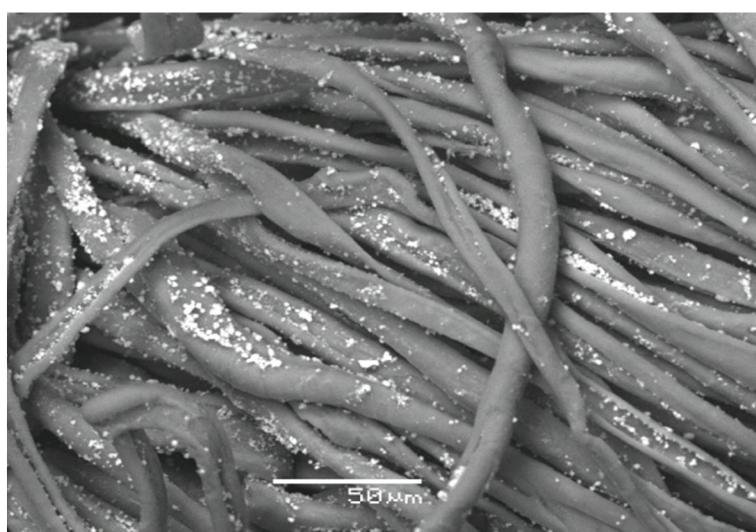
Figure 3 EMS of fiber surface of cotton textile washed without sequestering agent with model detergent (magnification 500x)
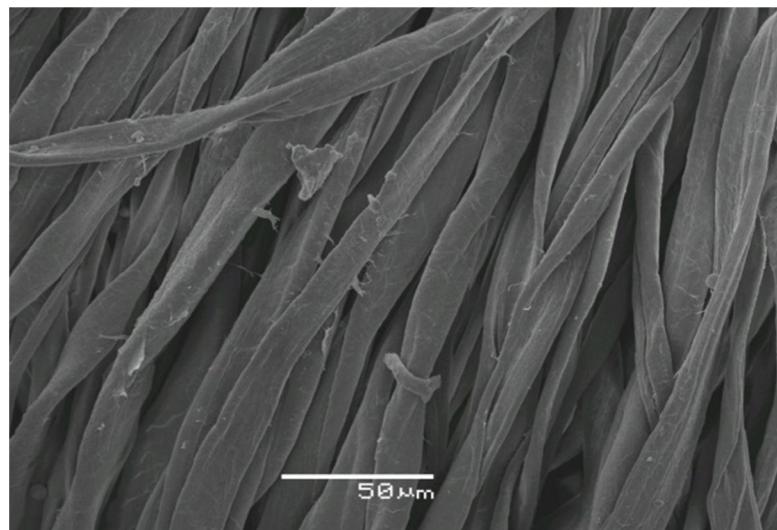
Figure 4 EMS of fiber surface of cotton textile washed with sequestering agent no. 1 (magnification 500x)
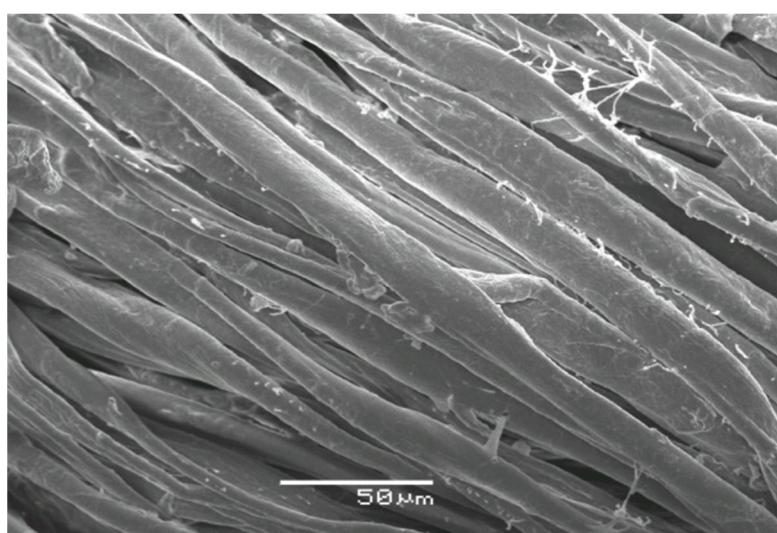
Figure 5 EMS of fiber surface of cotton textile washed with chelating surfactant no. 3 (magnification 500x)
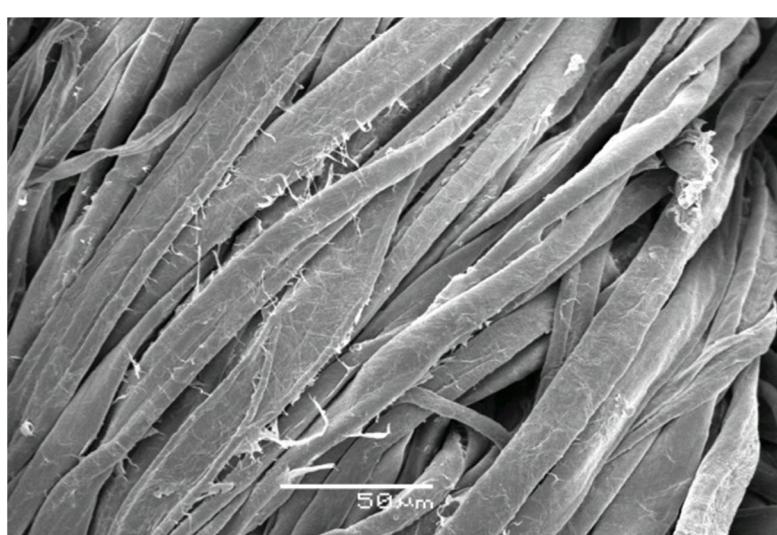
Figure 6 EMS of fiber surface of cotton textile washed with chelating surfactant no. 4 (magnification 500x)
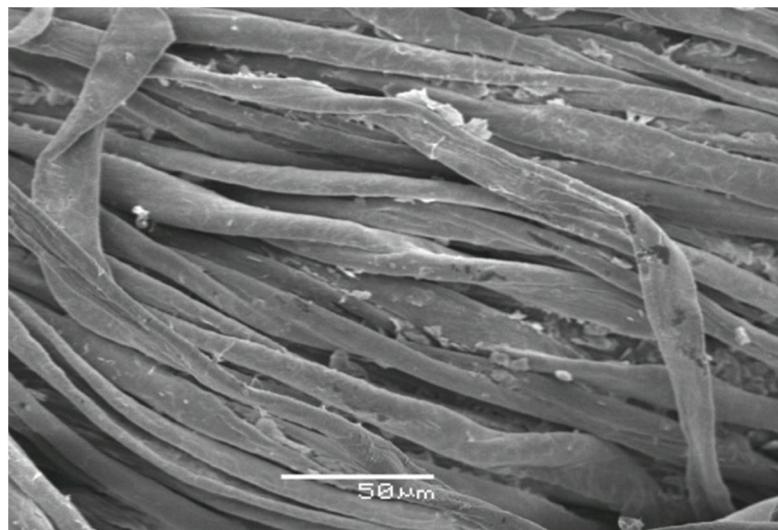
Figure 7 EMS of fiber surface of cotton textile washed with combination no. 4 + no. 1 (magnification 500x)
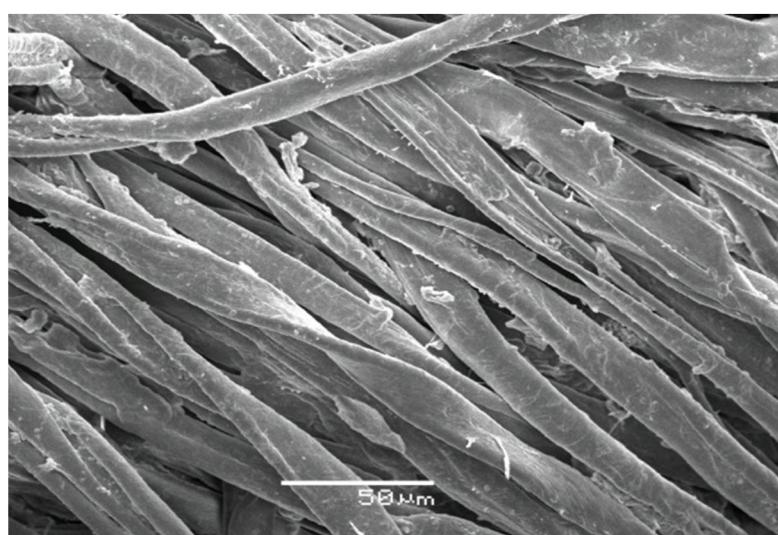
Figure 8 EMS of fiber surface of cotton textile washed with combination no. 4 + no. 2 (magnification 500x)
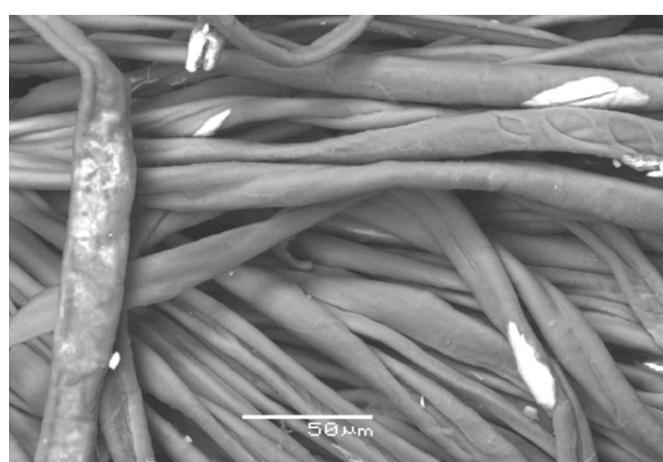
Figure 9 EMS of fiber surface of cotton textile washed with commercial agent I (magnification 500x)
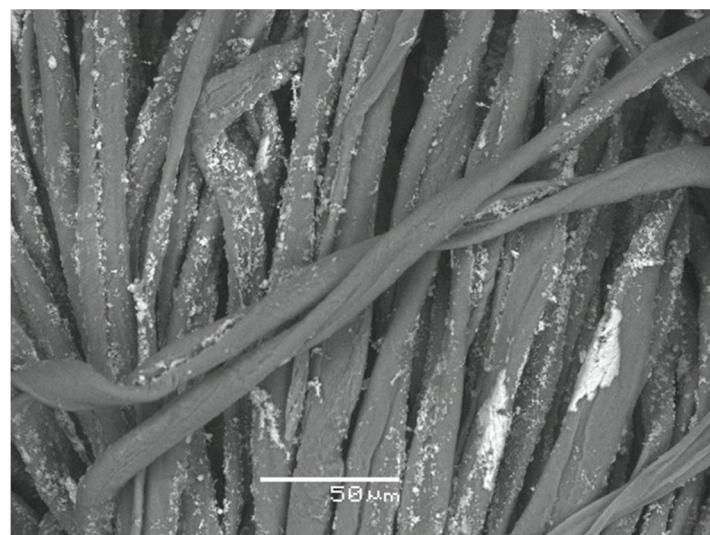
Figure 10 EMS of fiber surface of cotton textile washed with commercial agent II (magnification 500x)

4   CONCLUSIONS

The results of repeated model washing with the addition of prepared samples of sequestering agents and chelating surfactants were evaluated in this work. These additions of such prepared samples have a positive effect in the bath. The content of calcium ion is reduced, limiting its negative effect.

Washing effect of the prepared samples is comparable with commercial detergents, and the results of the determination of values ash and calcium ion are more favourable for prepared sequestering substances. Pictures of fiber surface of cotton textile from a scanning electron microscope confirm the idea of lower content of sediment in washed material.

It can be concluded that the prepared sequestering agents are applicable in many detergent formulas and as textile auxiliary agents for some finishing operations. Sample no.1 could be recommended as a replacement for existing sequestering agents. Sample no.3 would be suitable as a chelating surfactant.

5   REFERENCES

1. Choudhury A.K .Roy: Textile Preparation and Dyein, Enfield NH, USA: Science Publichers, 40-60, 2006, ISBN 1-57808-402-4

2. Dembický J., Kryštůfek J., Machaňová, D., Odvárka J., Prášil M., Wiener J.: Zušlechťování textilií. Liberec: Technická univerzita v Liberci, 13-19, 2008, ISBN 978-80-7372-321-7

3. Macháňová D., Prášil M.: Ekologické aspekty textilních procesů, Liberec: Technická univerzita v Liberci, 79-85, 2005, ISBN 80-7083-940-6

4. Popovová E.: The Evaluation of Development Types of Sequestering Agents and Chelating Surfactants, Pardubice, 2014, Diploma thesis, University of Pardubice

5. Hüls Chemische Werke A.-G. Waschmittelformulierungen mit biologisch abbaubaren Polymeren. Inventors: Beck R., Krause F., Schönkäs U. Int. Cl.: C 11 D 3/37. Ger. Offen. DE 43 19 807, 1994 -11 - 17

6. Voříšek J., Tulach J., Čermák F., Tóth J.: Analytical Chemistry (in Czech), Prague: SZN, 268, 1965

NEW TYPES OF SEQUESTERING AGENTS AND CHELATING SURFACTANTS

P. Bayerová, L. Burgert, M. Černý, R. Hrdina and A. Vojtovič

Department of Synthetic Polymers, Fibers and Textile Chemistry
Faculty of Chemical Technology, University of Pardubice, Czech Republic
petra.bayerova@upce.cz

Abstract: This work evaluates the development of sequestering agents and chelating surfactants. These agents are the substances capable of removing a metal ion from a solution system via formation of a complex ion that does not possess the reaction activity of the removed ion. These agents are used to eliminate water hardness and some metals, such as iron; both having found a wide applicability in the textile industry. Surface activity of chelating surfactants was measured by stalagmometric method. The sequestering capacity was measured at 20°C and 90°C using media with different pH and in combination with precipitating opacity titration - the so-called Hampshire test.

Key words: sequestering agents, chelating surfactants, surface activity, sequestering capacity

1   INTRODUCTION

Sequestering agents and surfactants are textile auxiliary agents. Textile auxiliary agents can be defined as compounds produced by chemical way and their mixtures. These mixtures make technological treatment easier, speed it up, improve it or enable it at all and are used in production and textile finishing. They are most frequently used as a component of detergents, in the areas of textile finishing (mainly in pre-treatment) but also in other areas, e.g. dyeing cellulose materials or softening of water.

Sequestering agents are generally compounds creating chelates, which are specific kinds of complex compounds surrounding the cation (such as Ca^{2+}, Mg^{2+}, Fe^{3+}, Cu^{2+}, Mn^{2+}). The polyvalent cation is the central atom and it is strongly locked by other negatively charged ions or by a neutral molecule. Nowadays, several types of sequestering agents are in use, namely: polyphosphates, aminopolycarboxylates, hydroxycarboxylates, polyaminophosphonate and polyhydroxyphosphonate or polymeric carboxylic acids [1].

Most traditional chelating agents do not break down readily in the environment. An increasing pressure on cleanness of wastewater and on the use of biodegradable washing components and finishing baths in textile production leads to new opinions on recently used sequestrants. These new types of sequestering agents are for example: polycarboxylic compounds containing nitrogen (nitrolotriacetic acid [2], glutamic acid [3], aspartic acid and its derivatives [4-6], agents based on imidodisuccinic acid, polyaspartic acid, hydroxyethylimidoacetic acid [7, 8]); copolymers of acrylic acid with monosaccharides or oligosaccharides [9]; copolymers of acrylic acid with vinyl acetate [10]; grafted polysaccharides [11].

Surfactants are surface-active substances. Surfactants have a bipolar chemical structure – each contains one hydrophilic and one hydrophobic part. Surfactants accelerate technological processes, reduce friction, stabilize disperse systems and affect physico-mechanical properties. Since surfactants reduce the surface tension of solvents, they facilitate the dissolution and removal of impurities [12]. The oldest and most widely used surface active agent is soap. Its disadvantage is poor stability in hard water, which limits its utilization.

Then the chelating surfactants should combine the properties of surfactants and sequestering agents. There are various ways of preparation of chelating surfactants, where the starting materials are phthalic anhydride, citric acid and polyethylene glycol [13], or the synthesis of itaconic acid, phthalic anhydride, citric acid and oxypropylated diols [14] or fumaric acid with polyoxyethylated stearyl ether [15]. Another option is to prepare a mixture of amides of polyaminopolycarboxylic acids and their salts, alternatively mixtures of detergents containing self-sequestering molecules of surfactants [16].

New types of biodegradable sequestering agents and chelating surfactants (derivatives of aspartic acid) were synthetized at the Institute of Chemistry and Technology of Macromolecular Materials of University of Pardubice. Basic properties (sequestering capacity and surface activity) were tested in this work.

2 EXPERIMENTAL

2.1 Samples of sequestering agents and chelating surfactants

Four types of chelating surfactants (Table 1) and three types of sequestering agents (Table 2) were tested in this study. Commercial product (sodium dodecylsulphate – Table 1) was used for the comparison of surface activity. Commercial sequestering agent Trilon M (Table 2) was used for the comparison of sequestering capacity.

2.2 Evaluation of sequestering capacity

The sequestering capacity was evaluated with model agents and compared to that of the commercially marketed sequestering agent. Evaluation of the sequestering capacity was carried out for the Ca^{2+} ions using precipitating opacity titration — the so-called Hampshire test [17], at two different temperatures of 20°C and 90°C. For the latter, a solution of sequestering agent was tempered at 90°C and then titrated when a solution of $CaCl_2.6H_2O$ had been selected as volumetric solution. The equivalence point was determined via the respective absorbance of the opacity formed during the reaction that was measured at the wavelength of 650 nm in a glass cell (thickness: 1 cm). For this purpose, a spectrophotometer (model Spekol 11; Carl Zeiss Jena, Germany) was used and the data obtained were consequently evaluated with the aid of a standard method of quantitative analysis.

Table 1 Structures of chelating surfactants

Sample	Chemical structure
No. 1	H$_2$C——COONa HC—NH—(CH$_2$)$_{11}$—CH$_3$ COONa *N*-dodecyl aspartic acid disodium salt
No. 2	H$_2$C——COOK HC—NH—(CH$_2$)$_n$—CH$_3$ COOK n = 10-18 *N*-cocoyl aspartic acid dipotassium salt
No. 3	H$_2$C—COONa HC—NH—(CH$_2$)$_8$—CH=CH—CH$_2$—CH$_3$ COONa *N*-oleyl aspartic acid disodium salt
No. 4	H$_2$C——COOK HC—NH—(CH$_2$)$_{15}$—CH$_3$ COOK *N*-hexadecyl aspartic acid dipotassium salt
	H$_3$C—(CH$_2$)$_{10}$—CH$_2$—O——SO$_3$H Sodium dodecylsulphate

Table 2 Structures of sequestering agents

Sample	Chemical structure
No. 5	H$_2$C—COONa HC—NH——CH$_2$—COONa COONa *N*-carboxymethyl aspartic acid trisodium salt
No. 6	H$_2$C—COONa HC—NH—CH—CH$_2$—COONa COONa COONa *N*-(1,2-dicarboxyethyl)aspartic acid tetrasodium salt
No. 7	H$_2$C—COOK CH$_2$—COOK HC—NH——CH$_2$—CH$_2$—NH—HC COOK COOK *N,N'*-ethylenediamine diaspartic acid tetrapotassium salt
Trilon M	NaOOC—CH—N(CH$_2$—COONa)(CH$_2$—COONa) H$_3$C methylglycindiacetic acid trisodium salt

2.3 The evaluation of surface tension

For the measurement a stalagmometric method was used. It is a relative method in which the numbers of drops of a known liquid n_1 of known surface tension y_1 are compared with the number of drops of the measured liquid n_x, in which we find the surface tension. Between the measured and reference liquid (in this case distilled water) the following relation holds:

$$n_x \cdot y_x = n_1 \cdot y_1 \rightarrow y_x = n_1 \cdot y_1 / n_x \qquad (1)$$

$$y_1 = 72.75.10^{-3} \text{ N.m}^{-1} \text{ (at 20°C)}$$

3 RESULTS AND DISCUSSION

Tables 3 – 6 state values of the sequestering capacity of chelating surfactants for pH 9-12. The measured values are relatively low. This was to be expected due to the number of carboxyl groups contained in the molecule.

Values of the sequestering capacity were expected based on the chemical structure of the samples. Content of functional groups necessary for the sequestration is important. The best results were achieved by sample no. 1 (N-dodecyl aspartic acid disodium salt) at 20°C and by sample no. 4 (*N*-hexadecyl aspartic acid dipotassium salt) at 90°C.

Tables 7 - 9 state values of the sequestering capacity of prepared samples of sequestering agents for pH 10-13. Table 10 states values of the sequestering capacity of commercial agent Trilon M. The sequestration efficiency depended on the increasing temperature and pH value. It is possible to say that the sequestration efficiency decreases with increasing temperature. Measured

values of prepared samples no. 5, 6, 7 at 20°C are comparable with the commercial sequestering agent Trilon M. The sequestering ability at 90°C of these samples is lower. The best results were achieved by sample no. 6 [N-(1,2-dicarboxyethyl)-aspartic acid tetrasodium salt]. Sequestering ability is a question of dissociative equilibria of complexes forming with Ca^{2+} ion and the sequestering agent.

Table 3 Values of sequestering capacity [mg Ca^{2+}/g] at 20°C and 90°C for sample no. 1 (N-dodecyl aspartic acid disodium salt)

	pH	S [mg Ca^{2+}/1g]		pH	S [mg Ca^{2+}/1g]
20°C	9	9.3	**90°C**	9	0.3
	10	18.7		10	5.8
	11	32.7		11	3.5
	12	35.0		12	6.9

Table 4 Values of sequestering capacity [mg Ca^{2+}/g] at 20°C and 90°C for sample no. 2 (N-cocoyl aspartic acid dipotassium salt)

	pH	S [mg Ca^{2+}/1g]		pH	S [mg Ca^{2+}/1g]
20°C	10	14.8	**90°C**	10	6.6
	11	3.3		11	6.6
	12	6.6		12	1.6

Table 5 Values of sequestering capacity [mg Ca^{2+}/g] at 20°C and 90°C for sample no. 3 (N-oleyl aspartic acid disodium salt)

	pH	S [mg Ca^{2+}/1g]		pH	S [mg Ca^{2+}/1g]
20°C	9	7.7	**90°C**	9	-
	10	21.3		10	21.4
	11	22.2		11	7.0
	12	29.9		12	22.5

Table 6 Values of sequestering capacity [mg Ca^{2+}/g] at 20°C and 90°C for sample no. 4 (N-hexadecyl aspartic acid dipotassium salt)

	pH	S [mg Ca^{2+}/1g]		pH	S [mg Ca^{2+}/1g]
20°C	9	9.7	**90°C**	9	48.4
	10	29.1		10	58.1
	11	19.4		11	77.5
	12	24.2		12	67.9

Table 7 Values of sequestering capacity [mg Ca^{2+}/g] at 20°C and 90°C for sample no. 5 (N-carboxymethyl aspartic acid trisodium salt)

	pH	S [mg Ca^{2+}/1g]		pH	S [mg Ca^{2+}/1g]
20°C	10	173.2	**90°C**	10	92.8
	11	165.4		11	68.5
	12	173.1		12	52.5

Table 8 Values of sequestering capacity [mg Ca^{2+} g] at 20°C and 90°C for sample no. 6 (N-(1,2-dicarboxyethyl)-aspartic acid tetrasodium salt)

	pH	S [mg Ca^{2+}/1g]		pH	S [mg Ca^{2+}/1g]
20°C	11	194.4	**90°C**	11	169.3
	12	142.1		12	113.4
	13	209.8		13	101.3

Table 9 Values of sequestering capacity [mg Ca^{2+}/g] at 20°C and 90°C for sample no. 7 (N,N'-ethylenediamin diaspartic acid tetrapotassium salt)

	pH	S [mg Ca^{2+}/1g]		pH	S [mg Ca^{2+}/1g]
20°C	10	110.1	**90°C**	10	47.2
	11	104.9		11	47.1
	12	99.8		12	41.9

Table 10 Values of sequestering capacity [mg Ca^{2+}/g] at 20°C and 90°C for Trilon M

	pH	S [mg Ca^{2+}/1g]		pH	S [mg Ca^{2+}/1g]
20°C	11	203.7	**90°C**	11	166.6
	12	197.5		12	154.3
	13	222.3		13	154.2

Surface activity of prepared chelating surfactants was measured by stalagmometric method. The presence of sufficiently high alkyl is a precondition for the ability of the product to behave as a surface-active substance. Measured surface tension is comparable with the commercial product sodium dodecylsulphate – Table11; Figure 1. Sodium dodecylsulphate is a commonly used anion-active surfactant. The surface activity of samples no. 2 and no. 3 is significant. It is reflected already at a low concentration 0.1 g/l. Samples no. 1 and no. 4 show lower solubility at room temperature, which may affect the measured value of the surface tension.

Table 11 Values of surface tension [mN/m] measured by stalagmometric method

c [g/l]	SDS	γ [mN/m]			
		no. 1	*no. 2*	*no. 3*	*no. 4*
0.1	71.12	63.26	46.56	60.94	71.56
0.25	62.69	60.63	43.33	49.32	68.47
0.5	53.31	58.39	42.90	46.68	65.39
0.75	48.91	57.25	42.59	44.77	62.36
1	45.00	56.14	42.28	44.10	60.63
1.5	38.46	54.56	41.67	41.87	57.25
2	35.42	52.75	41.08	41.57	56.14

SDS sodium dodecylsulphate
Sample no. 1 (N-dodecyl aspartic acid disodium salt)
Sample no. 2 (N-cocoyl aspartic acid dipotassium salt)
Sample no. 3 (N-oleyl aspartic acid disodium salt)
Sample no. 4 (N-hexadecyl aspartic acid dipotassium salt)
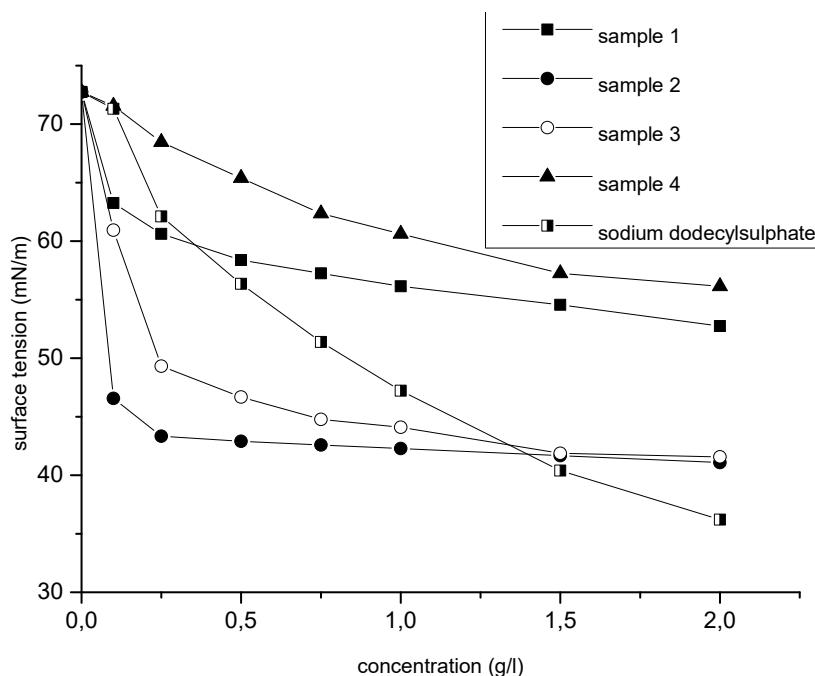
Figure 1 Dependence of surface tension on concentration of prepared samples and of commercial surfactant

4   CONCLUSIONS

Basic properties of four prepared samples of chelating surfactants and of three samples of sequestering agents were evaluated in this work. These developed samples were prepared by reaction of the appropriate amino compound with maleic anhydride. The prepared samples of chelating agents have a good surface activity. Measured surface tension is comparable with commercial product sodium dodecylsulphate. The sequestering ability of chelating surfactants is relatively low. There is always a necessary compromise between efficiency and possible biodegradability. Obtained results are materials for next research. Sequestering capacity of prepared sequestering agents is good, comparable with the commercial agent. The three tested samples could be used in various operations in the processing of textile materials (e.g. for water softening).

5   REFERENCES

1. Choudhury A.K. Roy: Textile Preparation and Dyeing, Enfield NH, USA: Science Publichers, 49-53, 2006, 88-130. ISBN 1-57808-402-4

2. Brouwer V.M., Terpstra P.M.J.: Tenside Surfactants Detergents 32, 225, 1995

3. Montedipe: Polyaminoacids as builders for detergent formulations, Inventors: du Vosel A., Francalanci F., Maggiorotti P., Int. Cl.: C 11 D 3/37. Eur. Pat. Appl. EP 454 126 A1, 1991-04-25

4. Matsumura S., Takahashi J.: Macromol. Chem., Rapid. Com. 9, 1, 1988

5. Sutuki T., Ichihara Y.: Agr. Biol. Chem. 37, 747, 1973

6. Matsumura S. et al.: JAOCS 70, 659, 1993

7. Lanxess [online], Baypure, 23-30, October 2005 [cit. 2014-8-29], www.aniq.org.mx/pqta/pdf/baypure%20DS%201004 0%20(HT).pdf

8. Roweton S., Huang S.J., Swift G.: Journal of environmental polymer degradation 5(3), 175, 1997

9. Basf aktiengesellschaft.: Pfropfcopolymerisate von monosacchariden, oligosacchariden, polysacchariden und modifizierten polysacchariden, verfahren zu ihrer herstellung und ihre verwendung, Inventors: Dezinger W., Hartmann H., Kud A., Baur R., Feldmann J., Raubenheimer H.J., Int. Cl.: C 08 F 251/00, Ger. Offen. DE 4 003 172 A1. 1991-08-08

10. Matsumura S. et al.: J Am Oil Chem Soc. 70, 659, 1993

11. Rhone-Poulenc Chemie SA, Grafted polysacharides, process for their preparation and their application as sequestering agents, Inventors: Vidil Ch., Vaslin S., Int. Cl.: C 08 F 251/00, Eur. Pat. Appl. EP 04 65 286, 1992-01-08

12. Machaňová D.: Pretreatmet of Textiles I. (in Czech: Předúprava textilií I.) Liberec: Technická univerzita v Liberci, 21-22, 35-63, 2005, ISBN 80-7083-971-6

13. Chen K.M., Wang H.R.: Synthesis and surface activity of self-sequestering surfactants, JAOCS 69(1), 60-63, 1992

14. Chiu-Chun Lai, Keng-Ming Chen: Preparation and properties of novel water-soluble surfactants, Journal of Applied Polymer Science 102, 3559-3564, 2006

15. Azab M.M., Bader S.K., Shaaban A.F.: Synthesis and surface activity of self-sequestering surfactants, Pigment and Resin Technology 31(3), 138-147, 2002

16. Montedison S.p.A., Italy: Detergent compositions containing self-sequestering surfactants, Inventors: Gafa Salvatore; Burzio Fulvio, Int. Cl. C 11D1/04. US 4 174 306, 1979-11-13

17. Degussa: Polyoxycarbonsäuren, Inventors: Haschke H., Bäder E., Int. Cl.: C 08 f 3/00. Ger. offen. DE 1904941(A1), 1970-08-0

INFLUENCE OF CURING TEMPERATURE OF CHITOSAN TREATED COTTON ON WHITENESS INDEX

E. Bou-Belda, M. Bonet-Aracil, P. Díaz-García and I. Montava

Textile and Paper Department, Universitat Politècnica de València
Plaza Ferrándiz y Carbonell s/n, Alcoy, Spain
maboar@txp.upv.es

Abstract: *Cotton treated with chitosan has many positive functionalities such as antimicrobial effect. Some authors have demonstrated that functional groups of chitosan can react with functional groups of cellulose. However, it is necessary to apply high temperatures to carry this reaction out. Cellulose is degraded by heat and the degradation involves oxidation and chain scission. Presence of aldehyde groups in oxidized cellulose makes it unstable and causes yellowing. The aim of this work is to study the colour change and the loss of tensile strength of treated cotton fabrics using different chitosan concentrations and temperatures in the curing process.*

Key Words: *chitosan, cotton, cellulose, yellowness, tensile strength.*

1 INTRODUCTION

Chitosan is an N-deacetylated biopolymer derivative of chitin (2-acetamido-2-deoxy-β-D-glucose through a β (1-4) linkage). The deacetylation is never complete. There is no specified nomenclature that describes the degree of deacetylation [1]. Chitin can easily be acquired from crab or shrimp shells. Its N-deacetylation is performed under alkali environment. The chitin that has been formed from the shells is deacetylated in 40% sodium hydroxide at 120°C for 1-3 h. This produces 70% deacetylated chitosan. Most natural polysaccharides are neutral or acidic, but chitin and chitosan are highly basic polysaccharides [2]. The bond between chitosan and cotton is a difficult one because of the likeness of the two polymers. To improve the bond, chitosan is dissolved in an acid. After that, chitosan is able to react with oxidised cotton fabric, for this reason it has a wide range of applications, for example it is most known for its use in wound dressing [3-5]. However, it can be used in a lot of other ways, such as cosmetics, as artificial skin, as contact lenses, for heavy metal capturing in polluted water, colour removal in textile mills, paper finishing, as a drug delivery system, etc. But its most important feature might be the fact that it is an antibacterial agent [2, 6-7]. This property is very attractive for many fields, such as textile industry. There are many studies which study the application of chitosan in fabrics of different compositions, cotton fabric being one of the most used.

It should be pointed out that to carry out the covalent bond formation between the -OH groups of cellulose and the -NH_2 groups of chitosan, it is necessary to apply high temperature of curing after the treatment, giving better fixation in this case [8].
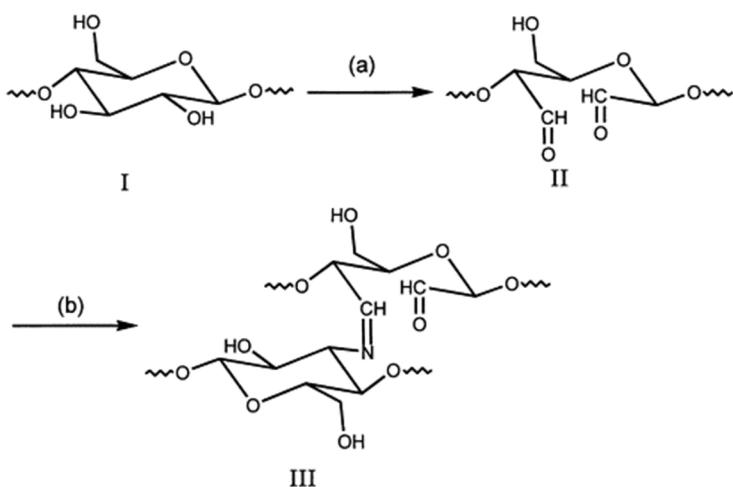
Figure 1 Oxidation of cotton (a) and reaction with chitosan (b) described by Liu et al. [8]

In order to study the influence of the concentration of chitosan used to treat the cotton fabric and the optimum temperature in the curing process, whiteness test was performed to see the change of colour in the cotton. Cellulose is degraded by heat and the degradation involves oxidation and chain scission. The presence of aldehyde groups in oxidized cellulose makes it unstable and causes yellowing.

There are many applications of textiles such as in civil engineering, in which colour differences are not considerably important, however, when textiles are used for garments, colour can be really important. Clothes cannot present differences between their different parts except for design issues. Yellowness is not only important for white clothes but for dyed ones as well. It can modify the final colour of the dyed fabric causing undesired side effects.

The Comision Internationale de l'Eclairage (CIE) defined CIELAB colour space parameters as the measurement of colour measurement for surface. It is based on colour appearance and offers an objective measure of the visual perception of colours. This is based on three tristimulus values, and mathematical expressions allow to convert them into an approximately uniform three dimensional space in which each colour has specific coordinates based on three axes *L**; *a**; and *b**. *L** shifts from Black (*L*=0) to white (*L**=100). As for *a**, it varies from red (*a**>0) to green (*a**<0), and *b** from yellow (*b**> 0) to blue (*b**<0). According to these parameters some White index or yellowing effects can be studied.

In this paper we study the effect of concentration of the chitosan and curing temperature used on the loss of fabric's mechanical strength, which can be attributed to two main factors, depolymerisation or the cellulose degradation and crosslinking of cellulose molecules due to fabrics being exposed to high temperatures in the curing process [9].

2   EXPERIMENTAL

2.1   Material

Medium molecular weight chitosan (from Sigma-Aldrich) was dissolved in acetic acid solution (mass concentration of 1%). Bleached cotton fabric with 210 g/m^2 was padded with chitosan solutions of various concentrations getting a wet pick-up of around 85%. The padded fabrics were then dried at 80°C for 5 minutes and cured using different temperatures (Table 1) for 3 minutes.

2.2   Treatment of the cotton fabric

Many parameters have been modified to treat the cotton fabric. In order to summarise them, Table 1 shows the samples treated using different chitosan concentrations and different temperatures in the curing process.

Table 1 Different cure temperatures of the chitosan for different concentrations of chitosan

Chitosan concentration [g/L]	Curing temperature [°C]						
3	80	100	120	140	160	180	200
5							
10							
15							

2.3   Whiteness test

Treated samples were prepared for colour measurement, which was carried out by following a standard procedure. Colour values were evaluated in terms of CIELAB values (*L*, a*, b*, c*, h*) using illuminant D65/10° observer on a Minolta CM-3600d UV-visible spectrophotometer using white ceramic and black hole as calibration standards.

On the basis of the results from the spectrophotometer for each cotton sample, additional colour parameters were calculated: the Whiteness Index, which was calculated according to CIE formulas as follows:

$$W_{CIE} = Y + 800 (x_O - x) + 1700 (y_O - y) \qquad (1)$$

2.4   Testing the traction resistance

Tensile strength of cotton fabrics was measured according to UNE EN ISO 13934-1 procedure, using dynamometer Zwick/Roell Z005. Samples were cut into strips which allowed 200 mm length and 50 mm width. Five samples were tested for each specimen.

2.5   FTIR spectroscopy of finished cotton fabric

A BRUKER IFS 66/S FTIR spectrometer was used to analyze the chemical structure, untreated sample and chitosan used with resolution of 4 cm^{-1} and 40 scans for each spectrum.

3   RESULTS AND DISCUSSION

The main influence to study is the thermal effect on cotton yellowing. In the first stage, we investigated the effects of drying process at 80°C on the yellowness of the cotton fabric. To study the behaviour the treated fabric with chitosan shows at different concentrations, we compared the treated fabrics with untreated fabric results.
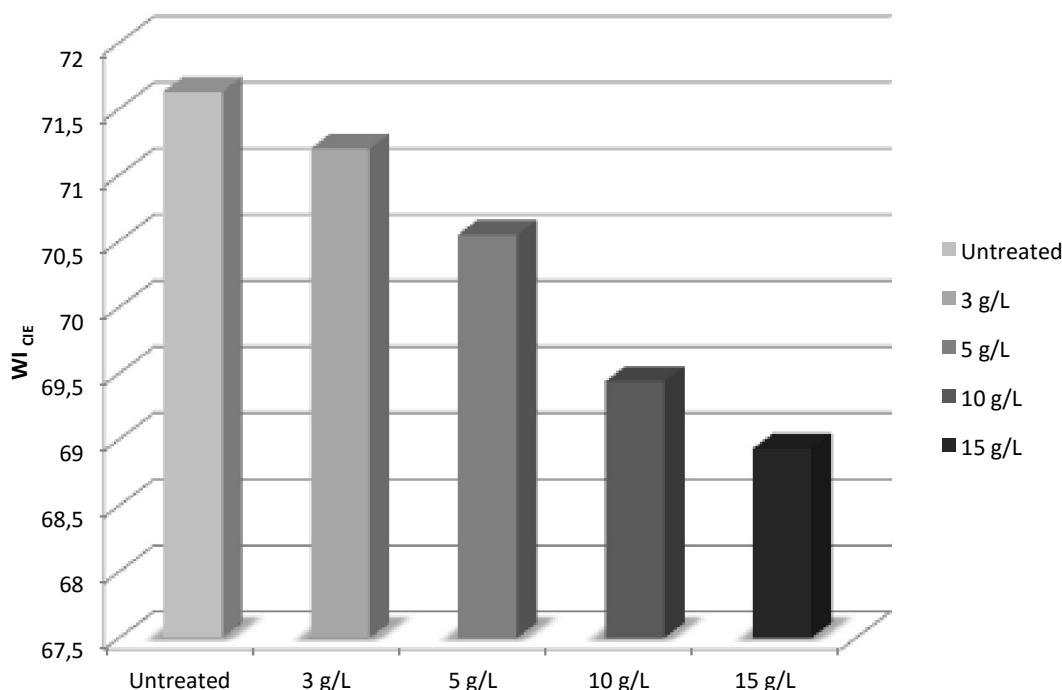
Figure 1 The whiteness results of untreated and treated fabrics exposed to 80°C

The results in Figure 1 show the effect of drying temperature on the cotton fibres. A decreasing tendency of the White Index (WI) is clearly seen, which consequently implies increase in the yellowness. It seems that when the fabric is treated with chitosan, the whiteness is lower. Furthermore, we can see that there is a relationship between the concentration of chitosan used in the treatment and the loss of whiteness index. The higher the concentration of chitosan applied onto cotton fibres, the lower WI is observed.

With the intention of comparing the behaviour of the treated fabric with chitosan cured at different temperatures, untreated fabric was exposed to the same range of temperatures from 80 to 200°C for 3 minutes. The results in Figure 2 show that the whiteness of the fabric decreases faster after reaching a curing temperature of 160°C. This can be explained by the decomposition of cotton at high temperatures. As a reference, an untreated sample was cured at the same temperatures. The decrease in whiteness for the untreated sample starts at 180°C, but if the cotton fabric is treated with chitosan, this shows yellowness after subjecting the treated cotton fabric to curing process at temperatures higher than 150°C. The results for temperatures below 160°C are similar for both treated and untreated fabric.

Cellulose degradation implies a reduction in mechanical properties; in order to check if the conducted treatment has had any influence, tensile strength was tested. Tensile strength is plotted against temperature in Figure 3. We can observe that there is not a significant difference between the concentrations of chitosan used in the treatment and the tensile strength of the treated fabrics. However, there is an important influence of the temperature used in the curing process to carry out the reaction between chitosan and cellulose. Similarly to what has been explained previously about Whiteness index (WI), it is for temperatures higher than 150°C that a significant loss of tensile strength is observed.

Treated fabrics show a gradual decrease of tensile strength, whereas these results decrease exponentially for the untreated fabric when it reaches more than 180°C. The untreated cotton fabric shows the worst result at 200°C. Apparently, cotton treated with chitosan does not show such an important decrease in traction resistance as untreated cotton. The maximum traction resistance loss is about 10% when the fabric is treated at high temperatures, whereas at 200°C it is around 40%.
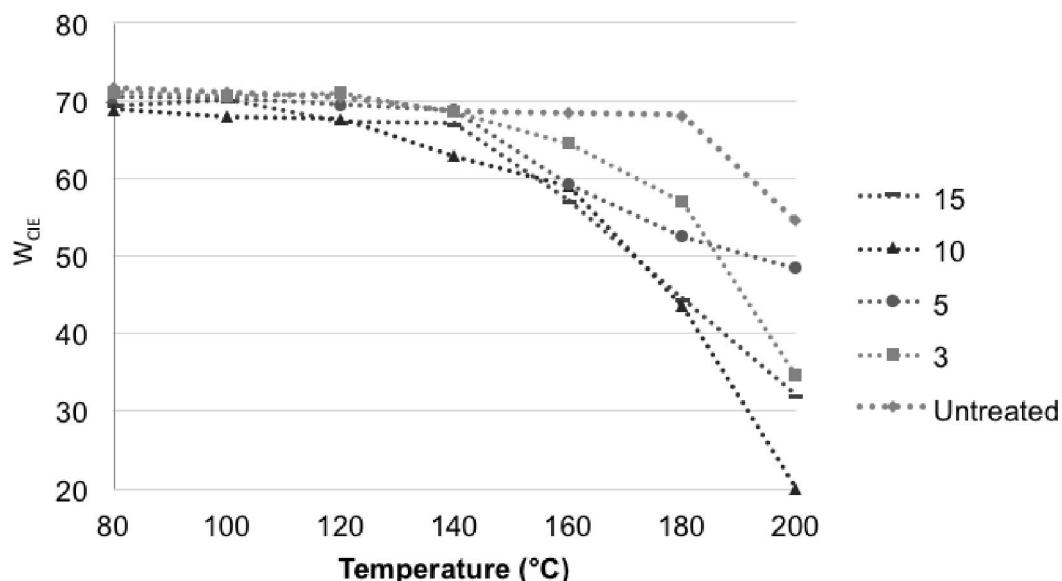
Figure 2 Whiteness after treatment with chitosan curing at different temperatures
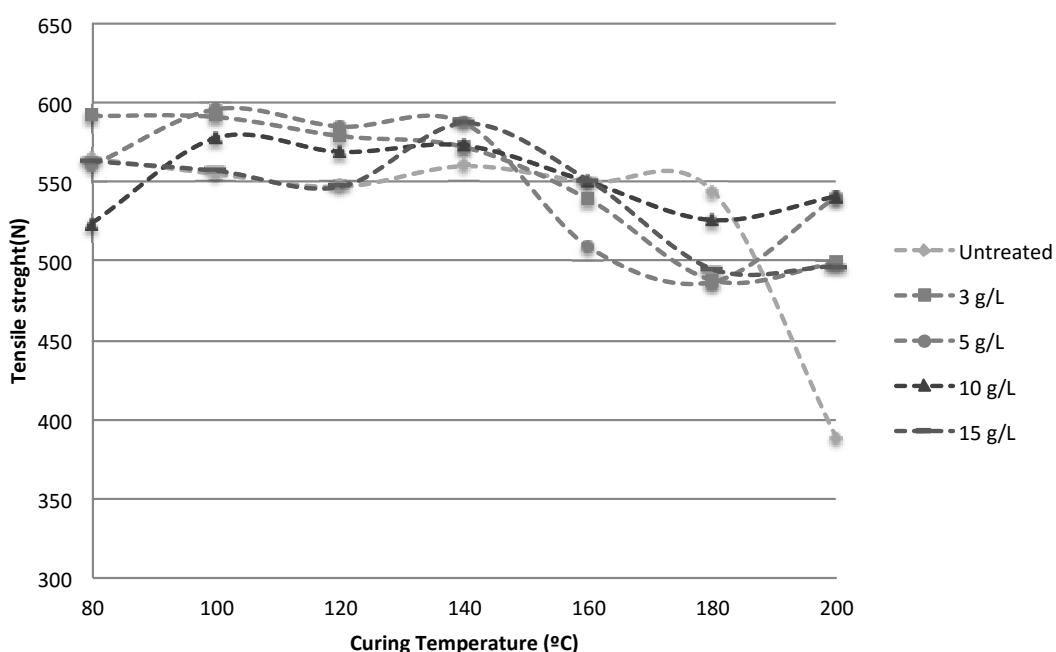
Figure 3 Tensile strength after treatment with chitosan curing at different temperatures

Infrared spectroscopy (FTIR) was as well used to obtain chemical information about treated fabrics with chitosan cured at different temperatures. We analyzed the fabric treated with the maximum concentration of chitosan, 15 g/L, in order to see the differences between using different curing temperatures. Figure 4 shows the FTIR spectra of treated and cured samples, untreated fabric and spectra of chitosan used to treat the cotton fabric. The chitosan and cellulose structure are very similar, for this reason the FTIR spectra present hardly any differences.

The spectrum of chitosan shows C=O and N-H bands at 1650 and 1550-1560 cm^{-1}, respectively, because of acetamide groups. The acetamide groups in chitin are changed into amide groups in chitosan by deacetylation, for this reason the chitosan spectrum shows a peak at 1590 cm^{-1} due to the NH_2 formation [10].
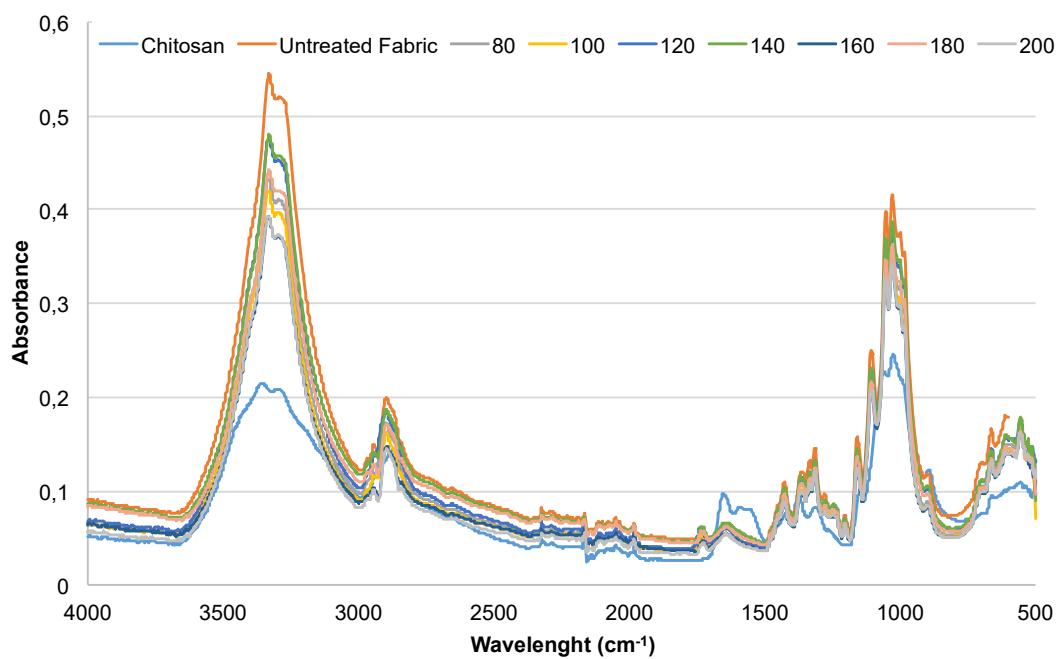
Figure 4 FTIR spectrum of untreated, treated and cured fabrics at different temperatures and chitosan
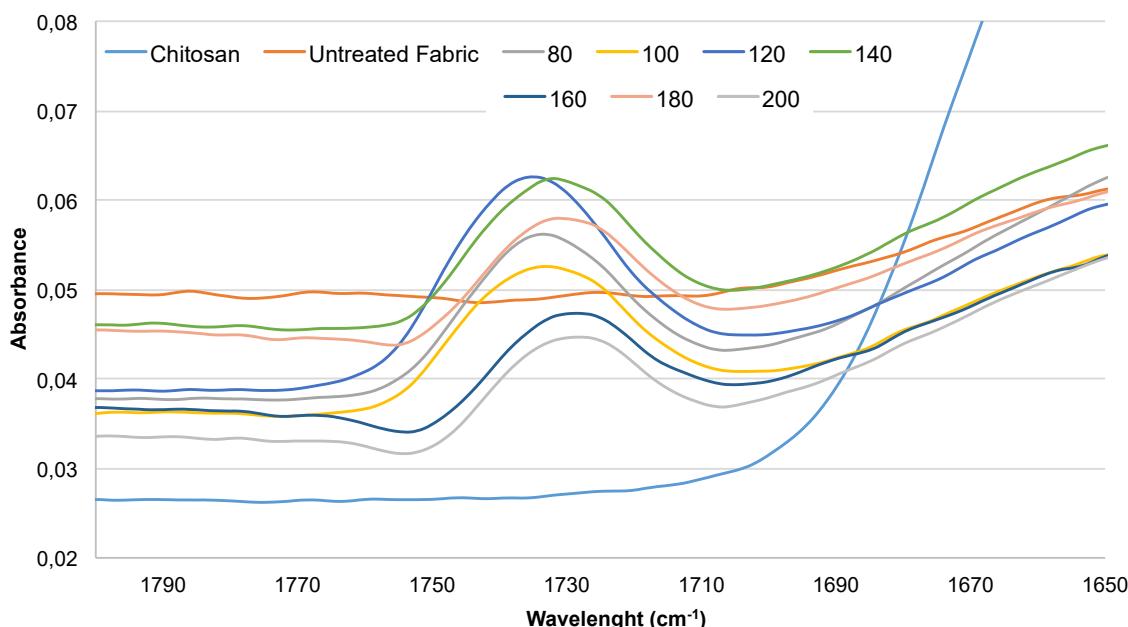
Figure 5 Enlargement from FTIR spectrum of untreated, treated and cured fabrics at different temperatures and chitosan (1800-1650 cm^{-1})

As can be seen from the spectrum of the treated and cured fabrics, a new peak was seen between 1700-1600 cm^{-1}. In Figure 5 the spectrum in this wavelength range has been enlarged and this figure is shown in order to analyze this peak.

The peak at 1735 cm^{-1} appears after the thermal treatment, belonging to the carboxyl group [11]. This peak is shown neither in the chitosan nor in untreated fabric spectra. Therefore we can confirm that the appearance of this signal confirmed the ester bond as being responsible for the formation of aldehyde groups and demonstrating that oxycellulose has been formed. Thus, the first stage of the reaction cotton-chitosan described by Liu et al and showed in Figure 1 has been demonstrated.

4 CONCLUSIONS

In this work we have impregnated cotton fabrics with different concentrations of chitosan, and we dried the samples at 80°C and cured them at different temperatures, ranging from 140 to 200°C. We could observe whiteness index and tensile strength differences, which were compared with the untreated cotton fabric.

The whiteness test shows a decrease in whiteness after reaching temperatures higher than 160°C. This can be explained by cellulose degradation. Although the loss of whiteness is not influenced by the concentration of chitosan used in the treatment, as there is no relationship between the chitosan concentration used in the treatment and the loss of whiteness caused by the curing process.

Concerning the loss of tensile strength, the results show that the tensile strength of the fabrics decreases with the increase of curing temperature, but samples treated with chitosan presented a more gradual decrease than untreated samples, which show the worst result at 200°C.

5 REFERENCES

1. Muzzarelli R.A.: Natural chelating polymers; alginic acid, chitin and chitosan, In Natural chelating polymers; alginic acid, chitin and chitosan, Pergamon Press, 1973

2. Kumar M.N.R.: A review of chitin and chitosan applications, Reactive and functional polymers 46(1), 1-27, 2000

3. Gupta D. & Haile A.: Multifunctional properties of cotton fabric treated with chitosan and carboxymethyl chitosan, Carbohydrate Polymers 69(1), 164-171, 2007

4. Fei Liu X., Lin Guan Y., Zhi Yang D., Li Z. & De Yao K.: Antibacterial action of chitosan and carboxymethylated chitosan, Journal of Applied Polymer Science 79(7), 1324-1335, 2001

5. Shirvan A.R., Nejad N.H. & Bashari A.: Antibacterial finishing of cotton fabric via the chitosan/TPP self-assembled nano layers, Fibers and Polymers 15(9), 1908-1914, 2014

6. Vartiainen J., Rättö M., Tapper U., Paulussen S. & Hurme E.: Surface modification of atmospheric plasma activated BOPP by immobilizing chitosan, Polymer Bulletin 54(4-5), 343-352, 2005

7. Wen Y., Yao F., Sun F., Tan Z., Tian L., Xie L. & Song Q.: Antibacterial action mode of quaternized carboxymethyl chitosan/poly (amidoamine) dendrimer core–shell nanoparticles against Escherichia coli correlated with molecular chain conformation, Materials Science and Engineering: C, 48, 220-227, 2015

8. Liu X.D., Nishi N., Tokura S. & Sakairi N.: Chitosan coated cotton fiber: preparation and physical properties, Carbohydrate Polymers 44(3), 233-238, 2001

9. Kang I.S., Yang C.Q., Wei W. & Lickfield G.C.: Mechanical strength of durable press finished cotton fabrics part I: effects of acid degradation and crosslinking of cellulose by polycarboxylic acids, Textile Research Journal 68(11), 865-870, 1998

10. Shin Y., Yoo D.I. & Jang J.: Molecular weight effect on antimicrobial activity of chitosan treated cotton fabrics, Journal of Applied Polymer Science 80(13), 2495-2501, 2001

11. Dehabadi V.A., Buschmann H. J. & Gutmann J.S.: Durable press finishing of cotton fabrics with polyamino carboxylic acids, Carbohydrate polymers 89(2), 558-563, 2012

THE IMPORTANCE OF OIL CONTENT TO OBTAIN MICROCAPSULES

E. Bou-Belda, M. Bonet-Aracil, P. Monllor and J. Gisbert

Textile and Paper Department, Universitat Politècnica de València, Plaza Ferrándiz y Carbonell s/n, Alcoy, Spain
maboar@txp.upv.es

Abstract: Microencapsulation is a process in which tiny drops of an active material (core substance) are surrounded by a shell to give small capsules. There are many systems to achieve active material dispersion, which is the first step in obtaining microcapsules. However, emulsion is the most used in different applications. In this work the effect of the amount of the active material added in the emulsion is studied.

Key Words: microcapsules, emulsion, active material, microencapsulation.

1 INTRODUCTION

Nowadays nanotechnology is becoming more and more interesting in different fields, including the textile one [1, 2]. Microencapsulation is the process which allows to obtain microcapsules of micrometric sizes but the shell thickness is about nanometres and can be considered as nanotechnology. Microcapsules (MICs) sometimes are considered as microspheres (MISs) and the main difference among them is focused on the basis of their definition. Microspheres are different spherical particles with a diameter between 1-1.000 μm.

Microcapsule properties can be characterised by:

a) Their properties are due to the material composition and chemical structure.

b) They are not damaged by use.

c) They can be reused.

On the other hand, microcapsules are based on two or more active ingredients and are characterised by:

a) Properties are due to the active ingredients and can be more than one.

b) They usually are damaged by use.

c) They cannot be reused.

Microcapsules for textile usage can be made of a polymeric shell and oil acting as active ingredient. There can be a wide variety of microcapsules active products [2-8]. The production of those microcapsules concerns the control of different parameters. The one presented in this work is the oil concentration added in the emulsion, that is, the first step to produce microcapsules in a chemical method.

Chemical microencapsulation methods are based on polymerisation or polycondensation mechanisms that may be implemented in a variety of different ways. Among them, interfacial and in situ polymerisation processes gained most scientific and industrial attention, and became an important alternative to coacervation microencapsulation processes. In situ polymerisation is one of the chemical microencapsulation processes taking place in oil-in-water emulsions. The procedure followed to obtain the microcapsules is very important. The microcapsules characteristics, such as size, shape and shell thickness, depend on the parameters and conditions used during emulsification process.

In this paper we discuss the importance of the oil content when preparing the emulsion and how it would influence the final result of the polymerization, obtaining the shell and consequently the microcapsules.

2 EXPERIMENTAL

Fragrance oil (was supplied by Disaromas, SA, Colombia), was used as the core material. 2,4-toluene diisocyanate (TDI, was supplied by Alfa Aesar) and 1,6-hexamethylenediamine (HDMI, was supplied by Panreac) were used as monomers for polyurea wall-forming materials. Tween 80 (was supplied by Panreac) was used as the stabilizing agent.

The procedure used to develop the microcapsules is interfacial polymerization. The first step in this process is to produce a stable emulsion. Emulsions are based on a mixture of oil in water (O/W) if oil is dispersed in water or water in oil (W/O) if water is dispersed in oil. Usually an emulsifier is used to stabilise the system.

The ratio oil/water is really important for both W/O and O/W. In this paper we show different ratios and study their influence.

The emulsification was carried out at 5000 rpm for 5 min with homogenizer (Benchtop, Pro Scientific Inc., Oxford). The size and shape of drops obtained

by different procedures were observed using optical microscope.

Table 1 Parameters to control during the emulsification procedure

REF	oil [g]	water [g]	surfactant [g]
1	20		0
2	50		0
3	100	100	0
4	20		1
5	50		1
6	100		1

We completed the microencapsulation process carrying out the shell stabilization using interfacial polymerization.

To obtain the microcapsules, 2,4-toluene diisocyanate (TDI, supplied by Alfa Aesar) and 1,6-hexamethylenediamine (HDMI, suministrated by Panreac) were used as monomers for polyurea wall-forming materials. Tween 80 (supplied by Panreac) and polyvinyl alcohol (PVA, Mw, 1500) (supplied by Sigma Aldrich) were used as the stabilizing agent.

After the W/O emulsification using different formulations which are shown in Table 1, the process that we followed to finish the microencapsulation of the fragrance oil is showed in Figure 1.
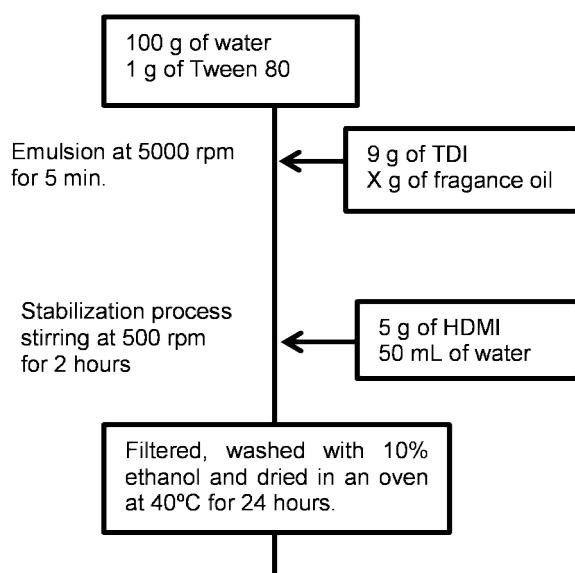
Figure 1 Microencapsulation of fragance oil by interfacial polymerization using polyurea as wall material

Emulsions were observed in an optical microscope. The procedure was carried out as follows: A drop of the emulsion was placed on the glass and immediately covered with a protective plastic. Once the sample was ready, an appropriate magnification was used to observe the samples.

For surface observation of the microcapsules, a PHENON scanning electron microscope (FEI company, United States) was used. Each sample was fixed on a standard sample holder and sputter coated with gold. Samples were then examined with suitable acceleration voltage and magnification.

3   RESULTS AND DISCUSSION

As we defined previously, the aim of this paper is to define the influence of oil content on the microcapsule formation in order to obtain a product capable of being applied onto fibres' surface. Thus, we prepared three emulsions with different oil concentrations. Figure 2 shows images from the three different emulsions obtained with different oil ratios. It is directly related with references 4, 5, and 6 shown in Table 1. Figure 2a shows the lowest concentration (20 g of oil) whereas Figure 2c was obtained from the emulsion with a higher concentration of oil (100 g/l); consequently, Figure 2b shows the medium concentration (50 g/L). References 1, 2 and 3 could not be observed as they were not offering a consistent emulsion and after a few minutes of having been prepared, water and oil were clearly separated into two different phases. Due to their fast separation and considerable instability we could not even prepare the sample to be observed through microscope and this is the reason why we cannot offer any image for references 1 to 3.

It can be clearly seen that different drops appear in each image obtained from the emulsion. The results show that the higher the concentration of oil, the more drops the emulsion shows, and consequently the number of microcapsules obtained when the polymerization occurs is considerably higher. We complete the microencapsulation process using these emulsions.

The morphology of the microcapsules was studied by scanning electron microscopy (SEM). Figure 2 shows the micrographs of fragrance microcapsules using 20, 50 and 100 g of fragrance oil when preparing the emulsion.

Observing the SEM images (Figure 3), it is easy to conclude that microencapsulation process using emulsion 5 (Figure 3b) yielded the best result, where most of the microcapsules have spherical shapes into which there is fragrance oil. However, if emulsion 4 (20 g/L of oil) is used to obtain microcapsules, we can see in Figure 3a that there is too much presence of polymer. On the other hand, if the oil concentration used in the emulsion is higher than 50 g/L, like emulsion 6 (100 g/L of oil), then it seems that there is not a sufficient amount of polymer to complete the polymerization around the drops of oil in the interface between water and oil solutions. For this reason, we don't get the stabilization of the microcapsules obtained in the emulsification process.
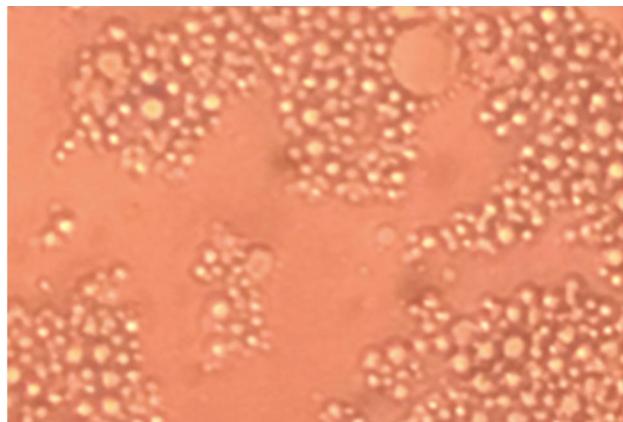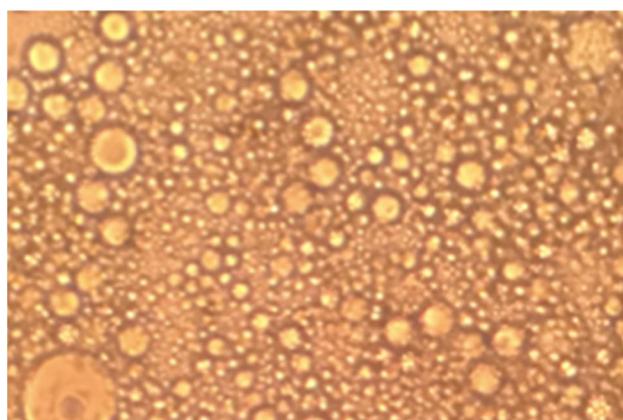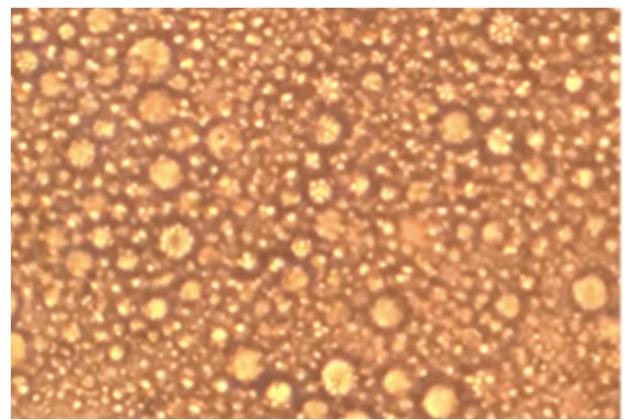
Figure 2 Drops of emulsion obtained by different formulation a) emulsion 4, b) emulsion 5, c) emulsion 6

Figure 3 SEM images of microcapsules obtained from a) emulsion 4 (Figure 2a); b) emulsion 5 (Figure 2b); c) emulsion 6 (Figure 2c)

4   CONCLUSIONS

During preparation we could observe high levels of instability in the emulsions prepared without surfactant, and they could not be evaluated with independence on the oil content. Considering samples that showed some stability to be studied, at first sight, it could be easy to conclude that the concentration of oil in the formulation has influence on the quality of the microcapsules obtained. It seems that if we use high concentration of oil in the microencapsulation process, we obtain high level of productivity of MICs. However, there can be a problem with the emulsion stability as drops can collapse because of the instability of emulsion when time passes by. On the other hand, if the amount of oil is lower, we get excess polymer. In this study, we conclude that using this type of oil and microencapsulation process, the optimum ratio of oil/water is 1/2.

5   REFERENCES

1. Sawhney A.P.S., Condon B., Singh K.V., Pang S.S., Li G., Hui D.: Modern applications of nanotechnology in textiles, Textile Research Journal 78(8), 731-739, 2008

2. Patra J.K.   &   Gouda S.:   Application of nanotechnology   in   textile   engineering: An overview, Journal of Engineering and Technology Research 5(5), 104-111, 2013

3. Nelson G.: Microencapsulates in textile coloration and finishing, Review of Progress in Coloration and Related Topics 21, 72-85, 1991

4. Nelson G.: Microencapsulation in textile finishing, Review of Progress in Coloration and Related Topics 321, 57-64, 2001

5. Miró Specos M., Escobar G., Marino P., Puggia C., Defain Tesoriero M.V., Hermida L.: Aroma finishing of cotton fabrics by means of microencapsulation techniques, Journal of Industrial Textiles 40(1), 13-32, 2010

6. Gisbert G., Ibañez F., Bonet M., Monllor P., Díaz P. and Montava I.: Increasing hydration of the epidermis by microcapsules in sterilized products, Journal of Applied Polymer Science 113(4), 2282-2286, 2009

7. Hong K., Park S.: Melamine resin microcapsules containing fragant oil: synthesis and characterization, Materials Chemistry and Physics 58, 128-131, 1999

8. Bonet M., Monllor P., Capablanca L., Gisbert J., Díaz P., Montava, I.: A comparison between padding and bath exhaustion to apply microcapsules onto cotton, Cellulose 22(3), 2117-2127, 2015

DECOLOURIZATION OF WASTEWATER FROM THE PRODUCTION AND APPLICATION OF ACID BLUE 62

L. Dušek and V. Kočanová

Faculty of Chemical Technology, University of Pardubice, Studentská 95, 532 10 Pardubice, Czech Republic
libor.dusek@upce.cz

Abstract: *The aim of this work was to evaluate the possibility of bleaching effluents containing aminoanthraquinone dyes Acid Blue 62 selected by indirect electrochemical oxidation of single-chamber laboratory electrolysers. To evaluate the effectiveness of model solution decolorized wastewater containing Acid Blue 62, UV-VIS spectroscopy was chosen as a suitable method. During electrochemical oxidation velocity changes were measured in model bleach solutions depending on the amount of supporting electrolyte, which was sodium chloride. Furthermore, decolourization rate was observed depending on the voltage of electrodes, which remained constant during the measurement. The samples were taken at various time intervals corresponding to chromaticity change of the electrolyzed solution. For the analysis of samples, (TOC, COD_{Cr}, AOX) and GC-MS (gas chromatography with mass spectrometer assigned) and liquid chromatography were used as auxiliary methods. The results of GC-MS established reaction mechanism of Acid Blue 62.*

Key Words: *Acid Blue 62, decolourization of wastewater, indirect oxidation*

1   INTRODUCTION

Anthraquinone dyes constitute the second largest class of reactive dyes after azo dyes and have been extensively used in the textile industry not only to colour cotton, but also wool and polyamine fibres due to their wide variety of colour shades and ease of application [1]. In previous publications [2], we have described oxidizing agents on chlorine base for wastewater treatment by the method of indirect electrochemical oxidation. In this study, we report on the indirect oxidation of the anthraquinonic dye Acid Blue 62, (sodium 1-amino-4-(cyclohexylamino)-9,10-dihydro-9,10-ioxoanthracene-2-sulfonate), in model wastewaters in presence of sodium chloride.

C.I.62045

Acid Blue 62
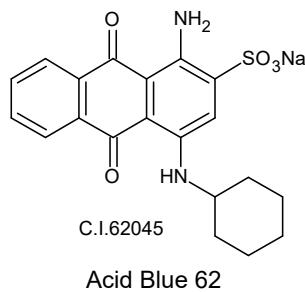
During electrochemical oxidation, the inorganic or organic pollutant is not oxidized directly on the surface of the anode, but via an oxidant which is continuously generated by the anode. Consequently, the oxidizing agent is generated in-situ. The most commonly used oxidizing agent is chlorine, but it depends on pH medium, that organic pollutant is attacked by chlorine, respectively hypochlorous acid or perchlorate, Figure 1 [3-6].

1.1 *Forms* of active chlorine

- generation of chlorine on the anode

$$2Cl^- \rightarrow Cl_{2(g)} + 2e^- \tag{1}$$

- dissolution of chlorine in water

$$Cl_{2(g)} \rightarrow Cl_{2(l)} \tag{2}$$

- formation of trichloride

$$Cl_2 + Cl^- \leftrightarrow Cl_3^- \tag{3}$$

- hydrolysis of chlorine

$$Cl_{2(l)} + H_2O \leftrightarrow HClO + H^+ + Cl^- \tag{4}$$

- dissociation of hypochlorous acid

$$HClO \leftrightarrow ClO^- + H^+ \tag{5}$$
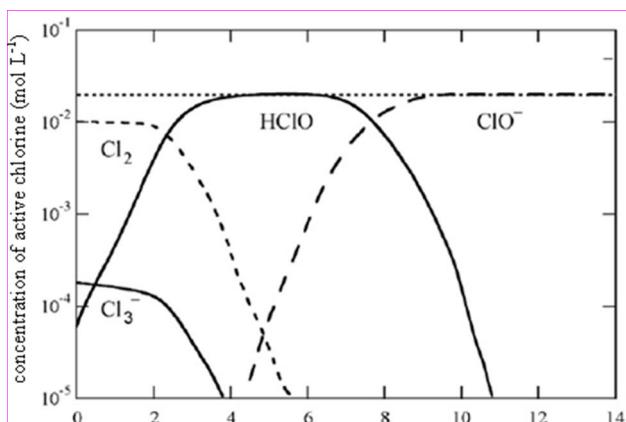
Figure 1 Diagram describing concentration dependence of chlorine-based active agents depending on pH during electrooxidation at concentration of 1.10^{-4} mol.L^{-1}. Active agents were generated in-situ via electrolysis of 0.1 mol.L^{-1} solution of NaCl in a non-divided single-chamber electrolytic cell at the temperature 25°C [7]

2   EXPERIMENTAL

2.1 Materials

The athraquinone dye AB 62 (the commercial name is Midlon Blue 2R) was supplied by Synthesia a.s. andit was used without further treatment. Sodium hydroxide and 0.1 M hydrochloric acid were of the highest purity available.

2.2 Electrochemical decolourization

The electrochemical oxidation was carried out in the single-chamber laboratory electrolytic cell with the volume of 400 mL. The electrolytic cell had a double-case. For measurements the dye solution was tempered to 20°C by thermostat Julabo ED 5. The model wastewater was prepared by mixing distilled water, NaCl and AB62. The initial concentration of electrolyzed solutions was $1-1.5.10^{-4}$ for kinetic measurements and 688 mg.L^{-1} ($1.628.10^{-3}$ mol.L^{-1}) for the analysis TOC, COD and AOX. The anode of the electrolytic cell (dimensions: 25x100x0.4 mm) was made of polished platinum, the cathode was made of austenitic stainless steel AISI – 316 (CSS 17.346, dimensions: 25 x 100 x 0.4 mm, composition: C 0.08%, Cr 16-18%, Ni 10-14%, Mn 2%, Mo 2-3%, P 0.045%, S 0.03% and Si 1%) with a declared corrosion resistance in sea water. The active area of electrodes was 13.5 cm^2 at specified conditions. Stabilized DC Power Supply Matrix MPS-3005 L-3 was used for the electrolysis of the solution. The laboratory DC Power Supply provides voltage from 0 to 30 V and current from 0 to 5 A. For kinetic measurements the electrolytic cell was equipped with a closed circulation circuit composed of peristaltic pump PP1B-05, connecting tubes and 1 cm quartz flow cell which was located in the temperate block of UV-VIS spectrophotometer Libra S22. The electrolyzed solutions were stirred by magnetic stirrer Heidolph MR Hei-Tec (300 rpm). During the electrooxidation the actual concentration of dyes was determined using UV-Vis spectrometer Libra S 22 according to Lambert-Beer law at the dye's maximum wavelength (λ_{max}= 662 nm). The determination of TOC, COD and AOX was carried out by standard analytical methods [8-11].

2.3 TOC analysis

The total organic carbon was measured by Protoc® 300 analyzer. The samples were taken at time intervals 1-48 hours for the analysis.

2.4 Determination of COD

The cuvette tests for determination of chemical oxygen demand (LCK 514, HACH LANGE), thermostat LT 200 (HACH LANGE) and spectrophotometer DR 2800 (HACH LANGE) were used for the determination of COD. The samples were taken at time intervals 1-48 hours for the analysis. The COD value of solution dyes was

established through electrolysis before and after the electrooxidation by the standard method determining the chemical oxygen consumption by potassium dichromate based on oxidation of organic substances by potassium dichromate in strongly acidic conditions of sulfuric acid in 2 hours-boiling at the temperature 148°C ± 3°C.

2.5 AOX analysis

Adsorbable organohalogenic compounds were determined by AOX/TOX multi X® 2500 analyzer. The samples were taken at time intervals 1-48 hours for the analysis. The sample was acidified with HNO$_3$. The adsorption of organic compounds was carried out by batch system on activated carbon (Analytik Jena, particle size 30-63 µm). The inorganic chlorides were removed by NaNO$_3$ washing. Then the activated carbon was burned in oxygen atmosphere at the temperature of 950°C. Incurred halohydrogens were determined by argentometry.

2.6 GC/MS analysis

The degradation products were identified using gas chromatography coupled with a mass spectrometry (GC/MS) system. The operating condition of GC/MS is: Instrument GC 2010 (Shimadzu, Japan), injection mode – splitless, carrier gas Helium (99.9999%), injector temperature 250°C, sample volume 1 µl, column HP-5MS, 30 m (length) x 0.25 mm (I.D.) with 0.25 m film thickness, temperature program 40°C (5 min), 300°C (20°C/min), 300°C for 7 min holding. Instrument MS QP 2010plus (Shimadzu, Japan), mode SCAN, m/z 10-900. The intermediate compounds formed were identified by comparison with the standard mass spectrum of NIST 147 and NIST 27 and WILEY 229 library.

3   RESULTS AND DISCUSSION

Before measurement of kinetic dependencies, UV-VIS spectra of aqueous solution AB62 and wavelengths of absorption maxima were determined. For monitoring kinetic dependence of decolourization of model wastewater, the band with the highest wavelength and calibration dependence of absorbance on concentration of pure dye was chosen, see Figure 2.

UV/VIS spectroscopy was used for monitoring kinetics of indirect electrochemical oxidation. Relatively cheap sodium chloride was chosen as a supporting electrolyte for increasing the conductivity of model wastewater. Sodium chloride is added to the bath during dyeing process for higher use of dye. Amount of sodium chloride was in the range of mass concentration 2.5-10.0 g.L^{-1}.

During electrochemical oxidation amino-anthraquinone dyes were measured for changes

of velocity of colourization of model solutions at a concentration cca 1-1.5.10^{-4} mol.L^{-1} with dependence on the amount of sodium chloride as a supporting electrolyte at concentrations 2.5; 5; 7.5 and 10 g.L^{-1}.

And then velocity with dependence on voltage of electrodes was monitored. Voltage was constant at values 3; 5; 7.5; 10; 12.5 and 15 V (in some cases where the conditions allowed, voltage was increased up to 22.5 V). Results of kinetic measurements are clearly summarized in Table 1. Generally, the oxidation rate decreased with the decrease of voltage and conductivity of the electrolyte, which depends on the amount of sodium chloride in the wastewater.

In the next step, decolourization of model waters which contained dye AB 62 was tested for dependence on pH from 3 to 11, especially for values 3; 5; 7; 9 and 11, because in context of different pH we can expect different decomposition products of oxidation. Applied voltage was held constant during measurement at the value 5 V, current density was 0.16 A/cm^2. Duration of electrooxidation was 24 h. After that, samples were collected from the discoloured model water and parameters AOX, COD$_{Cr}$, TOC and TN were measured. Obtained values of measurements are summarized in Table 2.
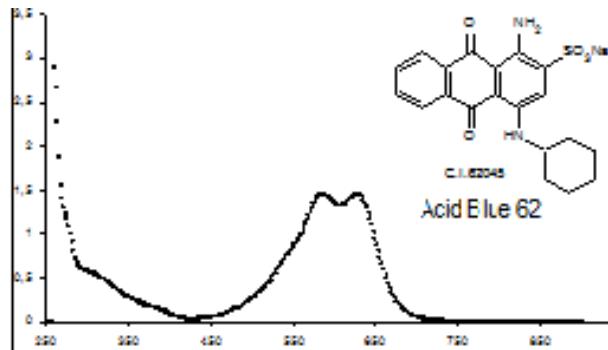
Acid Blue 62 before electrochemical oxidation
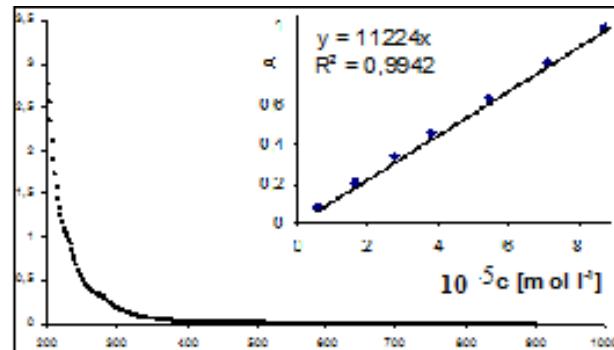
Acid Blue 62 after electrochemical oxidation

Figure 2 Absorption spectra dependence of absorbance on the wavelength of amino-anthraquinone dyes before and after electrochemical oxidation, measured in distilled water, t=25°C, λ=190-900 nm

Table 1 Kinetic measurement of electrochemical oxidation of Acid Blue 62 in distilled water, observed rate constant, half of reaction and its standard deviation with dependence on concentration of salt NaCl 2.5; 5; 7.5 and 10 g.L^{-1}, V=0.4 l, t=25°C, λ=626 nm, pH=7

Acid Blue 62											
	2.5 g NaCl.L^{-1}			5 g NaCl.L^{-1}			7.5 g NaCl.L^{-1}			10 g NaCl.L^{-1}		
U [V]	k [s^{-1}]	t ½ [s]	s	k [s^{-1}]	t ½ [s]	s	k [s^{-1}]	t ½ [s]	s	k [s^{-1}]	t ½ [s]	s
3	1.64E-04	4214.80	76.60	1.04E-04	6655	107.3	2.76E-04	2508.6	51.58	7.64E-04	906.78	3.27
5	5.71E-04	1218.36	68.75	6.01E-03	115.33	3.65	1.27E-02	54.44	0.37	7.12E-03	97.37	0.22
7.5	2.17E-03	320.13	8.41	1.14E-02	60.65	1.22	2.15E-02	32.23	0.41	3.93E-02	17.65	0.39
10	5.37E-03	129.24	3.71	1.35E-02	51.34	0.98	2.95E-02	23.44	0.23	5.55E-02	12.48	0.23
12.5	8.13E-03	85.27	1.38	1,55E-02	44.69	0.61	3.54E-02	19.60	0.23	7.75E-02	8.95	0.03
15	9.56E-03	72.47	0.31	1.67E-02	41.41	0.24	3.97E-02	17.47	0.21	8.20E-02	8.45	0.03
17.5	1.08E-02	64.06	0.10	2.33E-02	29.77	0.66	5.17E-02	13.41	0.27			
20	1.16E-02	59.58	0.31	2.93E-02	23.65	0.53	8.29E-02	8.37	0.14			
22.5	1.55E-02	44.62	0.26									

Table 2 Results of analysis COD, TOC, TN and AOX before and after indirect electrochemical oxidation of AB 62 for the pH range 3-11, t=25°C and concentration of NaCl 5 g.L^{-1}, U=5 V, i=0.16 A.cm^{-2}

	Before oxidation	After oxidation at pH				
		3	5	7	9	11
COD [mg.L^{-1}]	841	62	118	116	141	161
TOC [mg.L^{-1}]	33.33	20.53	25.27	26.30	27.15	29.11
TN [mg.L^{-1}]	3.35	1.43	1.73	2.07	2.42	2.72
AOX [mg.L^{-1}]	-	6.44	10.40	8.68	5.57	5.35
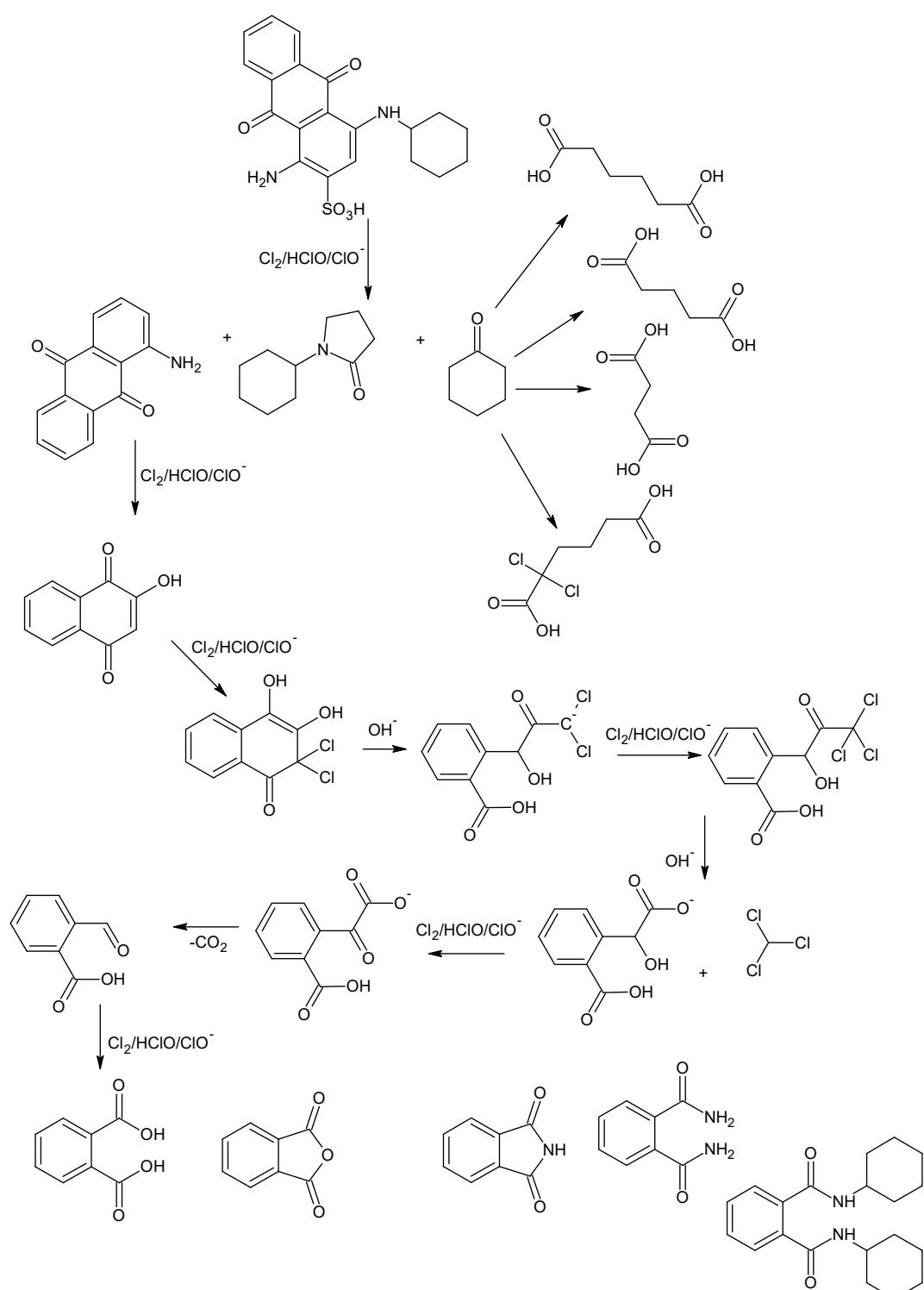
Scheme 1 Expected mechanism of decomposition of dye Acid Blue 62

In analogy with literature, decomposition of this amino-anthraquinone dye was expected. After decomposition of chromophore, it leads to discoloration of the solution and cyclohexane and cyclohexanol occurred among intermediates. Based on the results of the analyses GC-MS and AOX, expected mechanism of decomposition of dye Acid Blue 62 was proposed, see Scheme 1.

4   CONCLUSIONS

During decolourization respective decomposition of amino-anthraquinone dye Acid Blue 62 via indirect electrochemical oxidation in an aqueous solution of sodium chloride was detected by GC-MS analysis which was performed in the reaction mixture after total decolourization of the solution

of AB 62, the presence of some of the expected decomposition products, e.g. cyclohexanone. Together with that, GC-MS clearly showed the presence of chloroform, followed by dichloro carboxylic acid and chloro carboxylic acid which are generated by chlorination of cyclohexanol.

The presence of chlorinated hydrocarbons was also confirmed by an independent analysis, where a positive determination of AOX in the same reaction mixture was carried out.

From the obtained results we can already deduce some partial conclusions. Primarily, and that is unchallengeable, it is necessary to correct the classical conception of the reaction mechanism. Final products of the chloration are chloroform and mono- and dicarboxylic acids. These compounds are generated in all of studied pH range 3-11 and they are influenced by their ratio and total amount, based on the GC-MS analysis and determination of the parameter AOX.

Maximal concentration of AOX is ca 5 to 11 $mg.L^{-1}$ and this value is achieved within ca 24 h of electrooxidation. Consequently, the volume of AOX decreases, probably due to volatilization of POX compounds (purgeable organic halogens, which can be released from water at 60°C). A representative of POX is chloroform which was detected in the reaction mixture. Maximal amount of AOX, more than 11 $mg.L^{-1}$, is generated at pH 5, which corresponds to oxidation and chloration of electrochemically generated acid HClO (pKa = 7.5). Acid HClO is practically unique, but simultaneously also the most powerful oxidizing and chlorinating agent, at this pH value.

In the context of determined values of AOX, it is necessary to note the Government Order of the Czech Republic No. 82 from March 22nd, 1999, where the threshold limit of AOX is 0.025 $mg.L^{-1}$ for watercourses, and for other surface waters, 0.05 $mg.L^{-1}$. The comparison of these limits and experimentally determined values of AOX, which are 100-200 times higher in optimal pH range, indicates a detriment of indirect electrochemical oxidation in the sodium chloride medium.

During decolourisation of highly saline process waters and wastewater from paper mills, textile mills, dye houses and in other industrial branches using AB 62 and other amino-anthraquinone dyes with analogous structure, it is necessary to not operate this very effective treating and decolourizing process as the final technological stage. It may be better to use indirect electrochemical oxidation only for pretreatment of wastewater or complete it with a suitable final process, e. g. adsorption on activated carbon.

5   REFERENCES

1. Alkan M., CelikCapa S., Demirbas Ö., Dogan M.: Dyes and Pigments 65(2), 251-259, 2005
2. Dušek L., Horňáková B., Novotný L.: Chemické listy 106(11), 1054-1060, 2012
3. Carlos A., Martínez H., Brillas E.: Applied Catalysis B Environmental 87, 105-145, 2009
4. Perkowski J., Kos L., Ledakowicz S., Zylla R.: Fibres & Textiles in Eastern Europe 11(2), 88-94, 2003
5. Morsi M.S., Al-Sarawy A.A., El-Dein W.A.: Desalination and Water Treatment 26(1-3), 301-308, 2011
6. Maljaei A., Arami M., Mahmoodi N.M.: Desalination 249(3), 1074-1078, 2009
7. Boxall C.; Kelsall G.H.: Inst. Chem. Eng. Symp. Ser. *127*, 59, 1992
8. Horáková M. et al.: Analztics of water }in Czech:*Analytika vody), 2nd Ed.*, VŠCHT, Praha 2007
9. ČSN EN ISO 9562 (75 7531) Jakost vod – Stanovení adsorbovatelných organicky vázaných halogenu. ČNI Praha 1995
10. Standard Methods for the Examination of Water and Wastewater, 21st Ed., APHA, AWWA and WEF, Washington 2005
11. U.S. EPA 1650 Adsorbable Organic Halides by Adsorption and Coulometric Titration

PHYCOBILIPROTEINS – NEW NATURAL DYES FROM ALGAE AS A SUSTAINABLE METHOD

M. Ferrándiz[1], S. Moldovan[1], E. Mira[1], J. L. G. Pinchetti[2], T. Rodriguez[2], H. Abreu[3], A. M. Rego[3], B. Palomo[4], P. Caro[4]

[1]*Biotechnology Department, Textile Technological Institute, Spain, Plaza Emilio Sala, 1, Alcoy (Alicante)*
[2]*University of Las Palmas de Gran Canaria; Banco español de Algas, Spain*
[3]*Algaplus, production and commercialization of algae, Portugal*
[4]*Asebio, Spanish Bioindustry Association*
MFerrándiz@aitex.es

Abstract: *The aim of this work was to study the application of natural pigments extracted from algae, one of the majoritarian organisms in the aquatic environments, in the dyeing process. In this study two different pigments were employed, a blue one, phycocyanin, extracted from the cyanobacterium Arthrospira platensis, and a red one, phycoerythrin, extracted from the red macroalgae Gracilaria vermiculophylla. The extracted pigments were applied to cotton and wool fabrics by means of exhaustion dyeing process. The results were quantified by measuring the chromatic coordinates, colour strength and laundering and rubbing fastness. These results showed that the extracted phycobiliproteins presented a difference in colour if they had been treated with ammonium sulphate, as a stabilizer and presented higher colour strength when applied to cotton than to wool. The laundering and rubbing fastness showed good to excellent results.*

Key Words: *Arthrospira platensis, Gracilaria vermiculophylla, algal pigment, cotton fabric, wool fabric, chromatic coordinates, K/S value, wash and rubbing fastness*

1   INTRODUCTION

One of today's major challenges is represented by the increasing poverty of the natural resources. This natural reserve decrease of oil, water and land needs to satisfy an increasing demand. The principles of the basic economical law affirm that increasing demand by declining supply heads to higher prices, forcing the industries to find new ways to manage these challenges. Also the textile industry is subjected to this type of development, which already faces price volatilities in raw material procurement.

Taking into consideration ecological claims, Corporate Social Responsibility, led by the stakeholders of the companies, represents another extrinsic factor which is forcing the increase in the efficiency of resource allocation [1].

Various technical improvements need to be implemented, such as the usage of natural, renewable sources for obtaining pigments, as a sustainable industrial method.

Natural organic pigments were a significant part of historical pigments before modern era, particularly for bodily ornamentation, cosmetics and textile dyeing. Natural organic pigments are generally extracted from fruits, vegetables, seeds, roots, microorganisms and algae (micro and macro algae). [2]

Focusing on one of the resources populating the main resources of the earth, the aquatic systems, the algae, which are photosynthetic organisms, represent the primary producers containing organic pigments for harvesting light energy. There are three major classes of algal pigments: chlorophylls, carotenoids and phycobilins. Chlorophylls are green, carotenoids are yellow or orange pigments and phycobilins are hydrophilic and can be divided to phycoerythrin-red pigment and phycocyanin-blue pigment [3].

Many scientific sources note the diversity of pigments that exist within the specific algal divisions. It needs to be taken into consideration that pigment composition is not entirely uniform even within groups [4].

Gracilaria vermiculophylla [5] is a red macroalga that is cartilaginous, cylindrical and up to 50 cm long. It is native and widespread throughout the Northwest Pacific Ocean. It is used primarily as a precursor for agar, which is widely used in the pharmaceutical and food industries [6].

Arthrospira platensis [5] is a blue-green cyanobacterium, photolithoautotroph, meaning it derives its energy from sunlight and uses carbon dioxide as its carbon source. It has been harvested for food, starting since ancient times. Nowadays its usage presents ecological and commercial benefits like: it is superior to all plants as source of protein, it has minimal growth requirements and due to its high content in vitamins and proteins it represents a subject of interest in scientific research [7].

Probably the most commercially valuable groups of pigments are carotenoids and phycobilins [8, 9]. Phycobiliproteins (phycoerythrin, different phycocyanins and allophycocyanins) from red algae and Cyanobacteria have a long tradition of use as dyes in food, cosmetics and fluorescent markers in biomedical research. Numerous more recently discovered bioactivities of different phycobiliproteins include several antioxidant and radical scavenging activities, anti-inflamatory and anti-cancer properties [10]. The specificity of certain phycobiliproteins from particular species should be noted.

Much research has focused on optimising the extraction of specfic algal compounds or systematically screening selected algae for the occurrence of bioactive compounds [11]. Current search strategies for algal bioactive discovery include screening of known compounds for bioactive potential [12, 13].

Research regarding the extraction and purification of phycobiliproteins has been intensively realized, fact proven by the multitude of existing patents in this domain [14].

The aim of the present study was to study these pigments in textile industry. For that, the first task was the study of the extraction of phycobiliproteins (phycoerythrin and phycocyanin, blue and respectively red pigments) with provenience form the macro and micro algae.

The second task was the study of the dyeing process focused on natural materials, cotton and wool with these pigments.

The third task was the evaluation of the finished fabric to determine the colour strength and wash/rub fastness.

As expected results, the following can be mentioned: the substitution in the use of synthetic chemicals by a natural and renewable source that will turn dyeing into a more eco-friendly and economic procedure.

2   EXPERIMENTAL

2.1   Pigment preparation

2.1.1 Organisms and culture conditions

Gracilaria vermiculophylla was obtained from AlgaPlus, producer of algae and their derivatives from Portugal; the strain was cultured in a large scale culture in an open-system.

Arthrospira platensis was obtained from BEA (Banco Español de Algas), University of Las Palmas, Gran Canarias, Spain; the strain was cultured at laboratory scale, in 5 L flasks, and the biomass was produced with enriched medium.

2.1.2 Preparation of extracts from micro and macro algae

Concentrated (by filtration or centrifugation methods) fresh algal material was used to start extraction procedures. Pigments were extracted after biomass was broken by freeze (-20°C) and defreeze (4°C), and/or sonication, depending on the morphological characteristics of strains assayed (unicellular or filament forming; no cell wall vs. strong cell wall). Extracts were obtained in distilled water.

2.1.3 Quantitative analysis of phycobiliproteins

For the quantitative analysis of phycobiliproteins, spectrophotometric (UV spectrophotometer, Thermoscientific Evolution 60S) measurements were realized for the extracted biomass. Phycoerythrin (PE) was measured at 562 nm, phycocyanin (PC) at 615 nm and allophycocyanin (APC) at 652 nm.

The phycobilins containing solutions were used in order to calculate the concentration of PE, PC, APC quantities from the measurement of absorbance at 562, 615 and 652 nm using the equation established by Bennett and Bogorad (1973) [15] with the extinction coefficients from Bryant et al. (1979) [16].

$$APC = \frac{A_{562} - 0.208(A_{615})}{5.09} \quad [\text{mg.mL}^{-1}] \quad (1)$$

$$PC = \frac{A_{615} - 0.474(A_{652})}{5.34} \quad [\text{mg.mL}^{-1}] \quad (2)$$

$$PE = \frac{A_{562} - 2.41PC - 0.849APC}{9.62} \quad [\text{mg.mL}^{-1}] \quad (3)$$

2.2   Textile finishing process

2.2.1 Cotton and wool pre-treatment

In order to increase the fabrics' acceptability for dyes, the fabrics were subjected to a pre-treatment process of being immersed in 6% cream of tartar solution (supplied by Sigma Aldrich) for 45 minutes at 85°C.

2.2.2 Dyeing process

The solutions for dyeing process were prepared with the 1% of each pigments extract (red pigment extract from Gracilaria vermiculophylla and the blue pigment extract from Arthrospira platensis) and 6% of cream of tartar and 20% of ammonium sulphate (supplied by Sigma Aldrich).

The sample fabrics, cotton (supplied by INTEXTER UPC, Spain) and wool (supplied by James Heal, England) were immersed in the solution and subjected to the exhaustion dyeing process (apparatus supplied from Ugolini Redkrome, Italy) with the following characteristics: time=90 minutes,

temperature=50°C, bath relation=1/40. After the dyeing process, the samples were dried at ambient temperature.

2.3 Evaluation of finished fabric

2.3.1 Chromatic coordinates

Determination of CIELAB coordinates (UNE-EN ISO 105-J01:2000)

The chromatic coordinates of cotton and wool fabrics were determined with the DATACOLOR DC 650 (supplied by DATACOLOR, Spain) apparatus with an illuminant D_{65} and an observant at an angle of 10° and a diffuse measuring geometry.

2.3.2 Determination of colour strength

The colour strength of cotton and wool fabrics can be determined by calculating the *K/S* value of the dyed material. This value is directly proportional to the amount of dye present in the material. The finished cotton and wool fabrics were evaluated for the dye uptake, *K/S* value, using UV-Vis spectrophotometer (Spectrophotometer Lambda 950, from Perkin Elmer, Spain) by applying the formula developed by Kubelka and Munk [17]:

$$K/S = \frac{(1-R)^2}{2R} \qquad (4)$$

where - *K* is the coefficient of adsorption, *S* is the coefficient of scattering, *R* is the reflectance value of the fabric at λ_{max}

2.3.3 Wash fastness and rub fastness

Colour fastness to domestic and commercial laundering (Standard UNE-EN ISO 105-C06:2010)

Samples of about 10x4 cm were taken from both types of fabrics, wool and cotton. The samples were tested with the Gyrowash apparatus (supplied by James Heal, United Kingdom), at a temperature of 25°C, for 45 minutes, into the canister were added 10 steel balls and detergent. In each

canister 150 mL of water were added and 0.6 g of detergent. At the end of the test, the samples were dried in forced-air circulation dryer.

Colour fastness to rubbing (Standard UNE-EN ISO 105-X12:2003)

Samples of about 14x5 cm were taken from both types of fabrics, wool and cotton. The samples were tested with the Crockmeter apparatus (supplied by Atlas, Spain) at the temperature of 20°C, with an applied force of 9 N.

Two types of colour fastness to rubbing are tested: in dry conditions, where the rubbing was made at 1 cycle per second, exercising the rubbing on the fabric and at the same time applying the mentioned force. The wet rubbing was realized in the same manner as the dry method, but the difference was represented by the conditioning of the fabric in distilled water until it reached an impregnation between 95% and 100%.

3   RESULTS AND DISCUSSION

3.1.1 Chromatic coordinates

The chromatic characteristics of the tested fabrics were represented through the CIELab coordinates, and are presented in the following table. Starting from this information, it was possible to identify if there exists a difference between the untreated fabrics (without stabilizer) and the treated ones (with stabilizer), in means of colour intensity.

The value of ΔE^* confirms that a specific difference of colour exists between the treated and untreated samples, in the cases of cotton and wool. The value of ΔL^* in the case of the blue pigment extracted from *Arthrospira platensis* shows a slightly lighter result on cotton fabric and much lighter on wool fabric. The red pigment extracted from *Gracilaria vermiculophylla* presents a little darker treated sample of cotton fabric, and, in contrary, a much lighter color on the wool fabric.

Table 1 CIELab coordinates of the cotton and wool fabrics dyed with extracts from *Arthrospira sp*. and *Gracilaria sp*.

Cotton	L	a	b	C	H	X	Y	Z	x	y
Arthrospira sp. -no stab	88.47	-1.00	3.58	3.71	105.66	68.80	73.05	73.81	0.3190	0.3387
Arthrospira sp. -stab	88.88	-1.14	3.36	3.55	108.78	69.55	79.91	74.97	0.3184	0.3384
Gracilaria sp.-no stab	93.25	0.85	3.85	3.94	77.49	79.64	83.54	84.26	0.3218	0.3376
Gracilaria sp.-stab	93.15	0.85	3.41	3.52	76.04	79.41	83.30	84.61	0.3211	0.3368
Wool										
Arthrospira sp. -no stab	81.09	-2.47	12.37	12.61	101.32	54.61	58.63	49.98	0.3346	0.3592
Arthrospira sp. - stab	87.56	0.11	11.30	11.30	89.45	67.50	71.15	62.74	0.3352	0.3533
Gracilaria sp.-no stab	79.70	-4.57	9.49	10.53	115.73	51.49	56.16	50.45	0.3257	0.3552
Gracilaria sp.-stab	87.53	-1.15	16.24	16.28	94.06	66.88	71.09	57.30	0.3425	0.3641

Table 2 Differences in colour and intensity between the treated (with stabilizer) and untreated fabrics (reference) of cotton and wool treated with *Arthrospira sp*., and *Gracilaria sp*.

	Cotton *Arthrospira sp.*	Wool *Arthrospira sp.*	Cotton *Gracilaria sp.*	Wool *Gracilaria sp.*
ΔL^*	0.41	6.47	-0.1	7.83
ΔE^*	0.49	7.05	0.45	10.89

3.1.2 Colour strength

In the following table are presented the obtained values referring the colour strength of the employed pigments on wool and cotton.

Table 3 Colour strength for the treated samples of wool and cotton with the algal pigments of *Arthrospira sp.* and *Gracilaria sp.*

	K/S-*Arthrospira sp.*	K/S- *Gracilaria sp.*
wool	21.63	24.37
cotton	29.69	36.79

The red and blue colour from the pigment extracts were used in this study. Together with the cream of tartar, they were coated on cotton and wool fabrics. It was observed that the treated fabrics generated the following values for the K/S value,

29.6 for cotton for the blue *Arthrospira sp.* extraction and 21.6 for wool and 36.7 for cotton for the red *Gracilaria sp.* and 24.3 for wool.

3.1.3 Wash fastness and rub fastness

The results obtained after the test of the colour fastness properties of the treated fabrics to washing and rubbing according to ISO standard methods are shown in the following tables. According to the standard grey scale for colour change, the results were good.

From the results obtained in the above tables, it can be observed that the tested fabrics present good to excellent level of laundering fastness. Similar results were obtained in dyeing with pink pigment obtained from natural sources, and applied to cotton [18], and when brown dye extracted from natural sources was used for dyeing wool [19].

Table 4 Colour fastness to laundering of *Arthrospira sp.* and *Gracilaria sp.* applied on cotton

		Cotton 25ºC			
		Arthrospira sp. - no stab	*Arthrospira sp.* - stab	*Gracilaria sp.* -no stab	*Gracilaria sp.* -stab
Change in colour		1	3	2	4-5
Staining	Wool	5	5	5	5
	Acrylic	5	5	5	5
	Polyester	5	5	5	5
	Polyamide	5	4-5	4-5	5
	Cotton	5	4-5	4-5	5
	Acetate	5	4-5	4-5	5

1-Very poor 2-Poor·3-Moderate 4- Good 5- Excellent

Table 5 Colour fastness to laundering of *Arthrospira sp.* and *Gracilaria sp.* applied on wool

		Wool 25ºC			
		Arthrospira sp. - no stab	*Arthrospira sp.* -stab	*Gracilaria sp.* -no stab	*Gracilaria sp.* -stab
Change in colour		3	3	4-5	5
Staining	Wool	4-5	4-5	4-5	4-5
	Acrylic	4-5	4-5	4-5	4-5
	Polyester	4-5	4-5	4-5	4-5
	Polyamide	4-5	4-5	4-5	4-5
	Cotton	4-5	4-5	4-5	4-5
	Acetate	4-5	4-5	4-5	4-5

1-Very poor 2-Poor·3-Moderate 4- Good 5- Excellent

Table 6 Colour fastness to rubbing of *Arthrospira sp.* and *Gracilaria sp.* applied on cotton

	Cotton			
	Arthrospira sp. - no stab	*Gracilaria sp.* -no stab	*Arthrospira sp* -stab	*Gracilaria sp.* -stab
Dry staining	4-5	5	5	5
Wet staining	4-5	5	5	5

1-Very poor 2-Poor·3-Moderate 4- Good 5- Excellent

Table 7 Colour fastness to rubbing of *Arthrospira sp.* and *Gracilaria sp.* applied on wool

	Wool			
	Arthrospira sp. - no stab	*Gracilaria sp.* -no stab	*Arthrospira sp* -stab	*Gracilaria sp.* -stab
Dry staining	5	5	5	5
Wet staining	5	5	5	5

1-Very poor 2-Poor·3-Moderate 4- Good 5- Excellent

Regarding the colour fastness to rubbing, all of the samples showed good to excellent results, taking into consideration the two types of tests applied. No stains were obtained when performing the tests in wet and dry conditions.

4   CONCLUSIONS

The extracts of red pigment from the macroalgae *Gracilaria vermiculophylla* and the blue pigment from the cyanobacteria *Arthrospira platensis* showed even distribution on the cotton and wool fabrics, moreover giving them a pleasant appearance.

As the pigments employed in this study are represented by proteins, phycobiliproteins, which denature with temperature, the stabilizer used in the experiments, ammonium sulphate, showed improved results in terms of colour strength and fastness when compared to untreated samples. The stabilizer allows a temperature of 50°C for the dyeing process, giving the expected colour on the fabrics.

By means of colour difference it was observed that in both cases, a dissimilarity existed between the treated (with stabilizer) and untreated samples. When considering brightness comparison, in the case of the blue pigment, treated fabrics of wool and cotton were found lighter. On the other hand, in the case of red pigment, it appeared darker on treated cotton fabric and in the case of wool, a lighter treated fabric emerged.

If we compare the values obtained from the calculation of the color strength by using the reflectance values of the fabrics, it can be observed that the more powerful colors are achieved on the wool fabric, in both cases, with the blue and the red pigments.

Good to excellent results were obtained in the staining tests realized for the extracted pigments, through the fastness to laundering and to rubbing tests. These results represent a proof of the viability and the quality of the naturally dyed textiles.

The usage of natural pigments and natural fibers represents an ecofriendly approach in the textile industry. As the Corporate Social Responsibility promotes the usage of sustainable sources for the raw materials employed in the industry, adopting these concepts in the company will definitely establish a base for this more and more popular volunteer policy.

By employing natural sources, the sustainability concept, encompassed in the environmental policies, is used, giving to the final product, the textile, a higher value when taking into consideration the negative effects produced by the utilization of synthetic dyes.

5   REFERENCES

1. Mundinger A.K.: Resource scarcity and textile production, Overview Report. Düsseldorf: ZTC Working Paper, No7/2009

2. Green C.L.: A review of production, markets and development potential, Natural colourants and dyestuffs, Rome, 1995

3. Edward C.K., Loveson.: Role of Microalgae Pigments in Aquaculture. Aqua international., 34-37, August 2005

4. Prasanna R.A., Sood A., Jaiswal S., Nayak S., Gupta V., Chaudhary V., et al.: Rediscovering Cyanobacteria as valuable sources of bioactive compounds (review), Applied Biochemistry Microbiology No.(46), 119-34, 2010

5. Guiry M.D.: AlgaeBase, World-wide electronic publication, National University of Ireland, Galway, Available at: http://www.algaebase.org, Accesed: 2016-05-10

6. Thomsen M.S.: Gracilaria vermiculophylla (aquatic plant), Available from: http://issg.org/database/species/ecology.asp?si=1698&fr=1&sts=&lang=EN , Accesed: 2016-05-10

7. Barnett M.: Arthrospira Platensis: Brief History and Description, Biology, No.(221), University of Missouri-Rolla, 2007

8. Chaneva G., Urnadzhieva S., Minkova K., Lukavsky J.: Effect of light and temperature on the cyanobacteryum Arthronema africanum-a prospective phycobiliprotein-producing strain, Journal of Applied Phycology No.(19), 537-44, 2007

9. Prasanna R.A., Sood A., Suresh S., Nayak S., Kaushik B.D.: Potentials and applications of algal pigments in biology and industry, Acta Biologica Hungarica No.(49), 131-56, 2007

10. Eriksen N.: Production of phycocyanin-a pigment with applications in biology, biotechnology, foods and medicine, Applied Biochemistry Microbiology No.(80), 1-4, 2008

11. Dagmar B.S., Solene C., Popper Z.A.: Algal chemodiversity and bioactivity: Sources of natural variability and implications for commercial application, Biotechnology Advances No.(29), 483-501, June 2011

12. Li B., Lu F., Wei X., Zhao R.: Fucoidan: structure and bioactivity, Molecules No.(13), 1671-1695, 2008

13. Onofrejova L., Vasickova J., Klejdus B., Stratil P., Misurcova L., Kracmar S. et al.: Bioactive phenolics in algae: the application of pressurized-liquid and solid-phase extraction techniques, Journal of Pharmaceutical and Biomedical Analysis No.(51), 464-470, 2010

14. Soundaeapandian S., Muruganandham C.: Phycobiliproteins as a commodity: trends in applied research, patents and commercialization, Journal

of Applied Phycology No.(20), 113-136, August 2008

15. Bennett A. and Bogorad.: Complementary chromatic adaptation in a filamentous blue-green alga, The Journal of Cell Biology No.(58), 419-35, 1973

16. Bryant D.A., Guglielmi G., de Matsac N.T., Castets A. and Cohen-Bazire G.: The structure of cyanobacterial phycobilisomes: a model, Archives of Microbiology No.(123), 113-127, 1979

17. Munk, Kubelka.: The Kubelka-Munk Theory of Reflectance, Zeit. Fur Tekn. Physik No.(12), 593, 1931

18. Selvi, Rajendran R., Thamarai B.: Natural dyeing of cotton fabrics with pigment extracted from Roseomonas Fauriae. Universal Journal of Environmental Research and Technology 4(1), 54-59, 2014

19. Mabrouk A.M., El-khrisy E.A.M., Youssef Y.A., Asem A.M.: Production of textile reddish brown dyes by fungi, Malaysian Journal of Microbiology No.(1), 33-40, 2011

REUSE OF RECOVERED DYES IN CYCLODEXTRINS IN DYEING PROCESS

E. Franco[1], M. Ferrandiz[1], S. Moldovan[1], P. Fini[2], Paola Semeraro[3], P. Cosma[3], E. Núñez[4], J. A. Gabaldón[4], I. Fortea[4], E. Pérez[5] and M. Ferrándiz[5]

[1]Biotechnology Departm., Textile Industry Research Association (AITEX), Alcoy, Spain, Plaza Emilio Sala 1, (Alicante), E-03801
[2]Consiglio Nazionale delle Ricerche CNR-IPCF, UOS Bari, Bari, Italy
[3]Università degli Studi "Aldo Moro" di Bari, Dip. Chimica, Bari, Italy
[4]Departamento Ciencia y Tecnología de Alimentos, Universidad Católica San Antonio de Murcia, Guadalupe, Murcia, Spain
[5]Colourprint Fashion, SL, Avda. Fco. Vitoria Laporta, Muro de Alcoy (Alicante), Spain
EFranco@aitex.es

Abstract: *The purpose of the paper is to describe the possibility of reuse of encapsulated textile dyes into the structural cavity of CDs for a new dyeing process. The dyes to be reused represent the unfixed dyes that remain in the textile waste water after the dyeing process. Three types of cyclodextrins were tested individually with each dye and the best results were tested in a tricomy using the CDs with a larger cavity, the γ CDs. The complexes formed between the dyes and CDs were proved by FTIR analysis, and the fabrics were characterized by spectrophotometric and by CIELab coordinates in order to determine their differences. It has been demonstrated that direct dyes form inclusion complexes with the CDs. It can be affirmed that the cyclodextrins are capable of encapsulating a tricomy mix wastewater successfully. Regarding the dyeing process, it was observed that the colour of the dyed fabrics presents just a minor difference compared with the original dye without the involvement of the cyclodextrins technique, making it viable.*

Key Words: *cyclodextrins, encapsulation, recovered dye, dyeing process, reuse*

1   INTRODUCTION

The textile industry is energy, water, and chemical-intensive: from 15 to 19% of the total costs in the wet textile processes are energy costs [1]. In 2009, 954 million kg of textile were produced in Europe, requiring between 40 and 386 liters of high quality water to produce 1 kilogram of textile [2]. This water is polluted with a huge variety of chemicals, specifically synthetic dyes.

Synthetic dyes are common water pollutants, the dyestuffs are partially lost during the dyeing process and released with the effluent, which are more difficult to degrade [3]. Depending on the type of dye this quantity can range between 5% and 50%. The release of those colored wastewaters in the environment is a considerable source of non-aesthetic pollution since the presence of even small amounts of dyes (below 1 ppm) is clearly visible. Dye wastes can also generate eutrophication and dangerous by-products through oxidation, hydrolysis or other chemical reactions taking place in the wastewater-phase. Many of these dyes are also toxic and even carcinogenic and these pose a serious hazard to aquatic living organisms [4-6].

Due to the large degree of aromatics present in dye molecules and the stability of modern dyes, biological treatment is ineffective for their degradation. Various chemical and physical processes are currently in use for the removal of dyes by conventional treatment technologies including biological and chemical oxidation, chemical coagulation, foam flotation, electrolysis, biodegradation, advanced oxidation, photocatalysis, membrane filtration and adsorption processes.

However, among all the techniques, solid-phase extraction (SPE) using sorbents is one of the most efficient and popular methods for the removal of organic compounds from wastewater. The sorbents may be of mineral or organic origin; silica beads, activated carbon, zeolites, polyamine beads, polyurethanes resins, gels, calixarenes [7]. Much attention has recently been focused on biopolymers and natural molecules such as starch [8], chitosan [9-11], or cyclodextrins (CDs) [12-16].

Cyclodextrins (CDs) are cyclic oligosaccharides that consist of (α-1,4)-linked α-D-glucopyranose units. CDs are shaped like a truncated cone rather than perfect cylinders. The hydroxyl functions are oriented to the cone exterior, with the primary hydroxyl groups of the sugar residues at the narrow edge of the cone and the secondary hydroxyl groups at the wider edge. The central cavity gives a lipophilic character, and the external surface is hydrophilic, so they are soluble molecules [17].

The most common types are: α-cyclodextrin, β-cyclodextrin and γ-cyclodextrin which are composed of six, seven and eight α-(1,4)-linked

glycosyl units, respectively [18] and the size of CDs depends on the number of the glycosyl units. The CDs can be modified to design their qualities which increase the number of available applications on the selection and allow for optimization of the results of the complexation system [19].

An alternative approach to CD modification is the use of CD polymers, which can offer the advantages of the amorphous state and CD-type complexation without toxic effects, and better handling. Polycondensation of CDs or CD derivatives with epichlorohydrin or other epoxy compounds such as ethylene glycol bis (epoxypropyl) ether or butylenes glycol bis (epoxypropylether) in aqueous solution offers the formation of α,β,γ-CDs Epi [20].

The most notable feature of cyclodextrins is their ability to form solid inclusion complexes (host–guest complexes) with a very wide range of solid, liquid and gaseous compounds by a molecular complexation, especially aromatics, through host–guest interactions [21].

In these complexes, a guest molecule is held within the cavity of the cyclodextrin host molecule. Complex formation is a dimensional fit between host cavity and guest molecule [22]. The lipophilic cavity of cyclodextrin molecules provides a microenvironment into which appropriately sized non-polar moieties can enter to form inclusion complexes [23]. No covalent bonds are broken or formed during formation of the inclusion complex [24].

The textile industry always works with a three-color system (mixture of three dyes): yellow, red, and blue that are mixed in different amounts in order to obtain the final colour for fabrics. Exceptionally, black is the only one that employs special dyes because, if done with the three-color system method, the consumption of dyes would be very high and the results would have low quality. Other colours are used for special nuances.

The aim of the present study was to study the reuse of the encapsulated dyes in different CDs and to check if the encapsulation realized with a wastewater mix was obtained in the same proportion as the original, in order to reuse the recovered dye to obtain the same colour on the fabrics as the original ones.

2   EXPERIMENTAL

2.1 Materials

Epichlorohydrin-cyclodextrin polymers were synthetized in the lab. Materials purchased for the realization of the experiments were epichlorohydrin, β-CDs, HP-βCD, γ-CD, and sodium hydroxide from Sigma-Aldrich (Spain). Sodium borohydride was provided by Panreac (Barcelona, Spain).

Supplies necessary for the dyeing experiments: Cotton fabric EMMPA 222 supplied by Intexter (Spain) and dyestuff: Direct Yellow 106 (Comercial Química Massó, Spain), Direct Red 83:1 (Comercial Química Massó, Spain) and Direct Black 112 (Auxicolour, Spain). Sodium sulphate anhydrous from Sigma-Aldrich (Spain).

2.2 Methods

2.2.1 Polymer synthesis

EPI-CDs is a polymer system where the epichlorohydrin is the crosslinker and the different CDs are the monomers. This system facilitates an easy recovery of CDs after the dye encapsulation. EPI-βCDs, EPI-HP-βCDs and EPI-γCDs polymer was obtained with the procedure described by Solms and Egli (1965) [25] and extended by Kominaya et al (1985) [26].

Briefly, the amount of cross-linking agent was increased to obtain mechanically stable polymers containing the same amounts of γ-CD.

A typical polymerization reaction was carried out as follows. Firstly, a solution of NaOH (13 mL, 40% w/w) containing $NaBH_4$ (30 mg) was introduced in a thermostatic reactor (at 50°C), gradually adding 12 g of CD until complete dissolution. After that, 132 g of EPI was added drop-wise and the mixture was vigorously stirred at a constant speed with a paddle stirrer. After two hours of continuous stirring, the viscosity of the solution started to increase and a solid precipitate could be observed. At this time, acetone (supplied by Scharlab, Spain) (80 mL) was added to the reaction mixture, leaving under stirring at constant temperature (50°C) for 10 min.

After cooling, the insoluble polymer was poured into a large beaker of water, filtered and the solid was purified by several Soxhlet extractions with acetone and water for 2 h. Finally, the polymer was filtered and dried at 60°C for 5 h.

2.2.2 Preparations of standard solutions

To check the formation of the inclusion complex between dyes and EPI-CDs polymers, solutions of Direct Yellow 106, Direct Red 83:1 and Direct Black 112 were prepared individually at the concentration of 0.2 g/L. Direct dyes were dissolved directly in distilled water and used as received without further purification.

2.2.3 Complexation process

The complexation process was done introducing the EPI-βCDs, EPI-HP-βCDs and EPI-γCDs with a proportion of 50/1 (v/w) in the standards solution bath maintained in agitation (Heating Magnetic Stirrer FB 15001 from Fisher Scientific) for 30 minutes at 25°C. After that the formed complex was recovered by filtration (Whatman[TM] GE Healthcare Life Sciences n. 5) and dried in an oven

at 100°C for 2 hours (Memmert oven, Model 100-800, Germany).

2.2.4 Complex characterization

Fourier transform infrared spectroscopy (FTIR) was used to confirm the formation of the inclusion complex between β-CDs, HP-βCDs γ CDs and the direct dyestuff analyzed (FTIR Spectrum BX from Perkin Elmer).

2.2.5 Dyeing process

Once obtained, the complex was used as raw material in a new dyeing process replacing the dyes concentration with 6% w.p.f of the complex dyes/ EPI-βCDs, EPI-HP-βCDs and EPI-γCDs.

The dyeing conditions for all the dyeing processes were: temperature = 95°C, time = 60 minutes, liquor rate = 1/15. To these were added auxiliaries like: sodium sulphate 15 g/L (apparatus supplied by Ugolini Redkrome, Italy).

The following textile concepts were taken into account:

- Liquor ratio: is the relation between weight of fabrics and amount of water employed.
- % weight per fiber (w.p.f.): is the amount of dye employed to dye 100 g of fiber.

To obtain the wastewater with the unfixed dye molecules, a dyeing bath with 0.440% w.p.f. Direct Yellow 106, 0.920% w.p.f. Direct Red 83:1, and 0.014% w.p.f. Direct Black 112 was prepared. The dyed fabrics obtained served as reference in the analysis.

The complexation process was done introducing the EPI-γCDs in the previously obtained wastewater by maintaining it in agitation (Heating Magnetic Stirrer FB 15001 from Fisher Scientific) for 30 minutes at 25°C in relation 50/1 (v/w). After that the formed complex was recovered by filtration (Whatman™ GE Healthcare Life Sciences nº 5) and dried in an oven at 100°C for 2 hours (Memmert oven, Model 100-800, Germany).

The complex was used as raw material in a new dyeing process replacing the dyes concentration with 25% w.p.f, 50% w.p.f and 100% w.p.f of the complex dyes/ EPI-γCDs.

2.2.6 Textile characterization

The techniques employed to characterize the textiles were:

- Spectrophotometry of the textile was measured in order to prove the reproducibility of the original colour in the textile after the reuse of the encapsulated dye from the waste water in a new dyeing process. (Spectrophotometer Lambda-950 from Perkin Elmer).

- CIELab coordinates represent a method for measuring and ordering an object's colour. The CIELab colour space can be visualized as a three-dimensional space where every colour can be uniquely located. The location of any colour in the space is determined by its colour coordinates; L^*, a^*, and b^* (Datacolor DC 650, from Datacolor).

3   RESULTS AND DISCUSSION

First are shown the results of the capacity of cyclodextrin to form inclusion complexes with direct dyes.

3.1 FTIR

In order to evaluate the encapsulation application process, FTIR analyses were realized, validating the encapsulation process and comparing the encapsulation in the EPI-βCDs, EPI-HP-βCDs and EPI-γ-CDs.

From all the diagrams presented below it can be observed that approximately at the peak value of 1000 cm^{-1}, the line corresponding to the complex formation presents a band resulting as the sum of corresponding bands of the dye and the cyclodextrin.
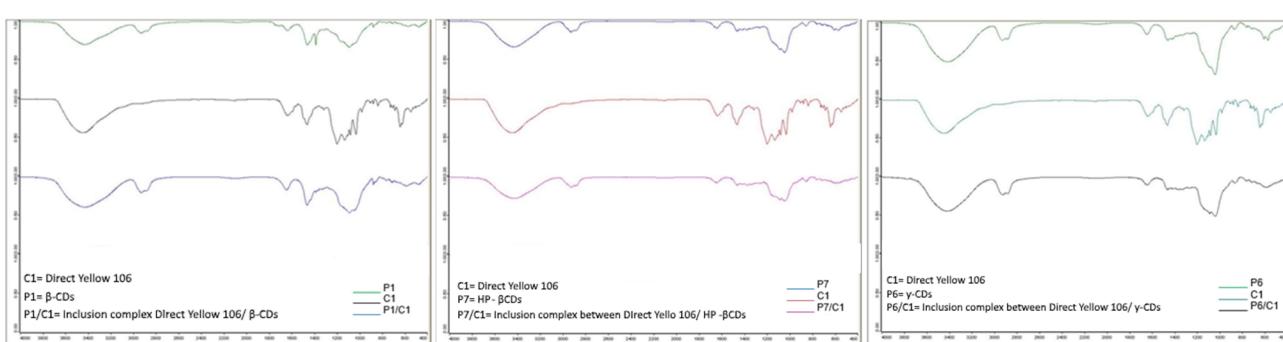
Figure 1 FTIR spectra comparing Direct Yellow 106 with β-CDs (left), HP-βCDs (center) and γCDs (right)
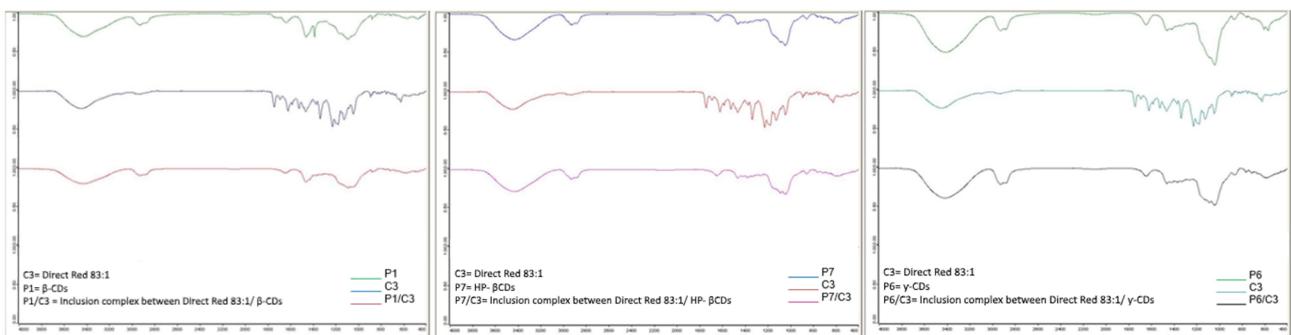
Figure 2 FTIR spectra comparing Direct Red 83:1 with β-CDs (left), HP-βCDs (center) and γCDs (right)
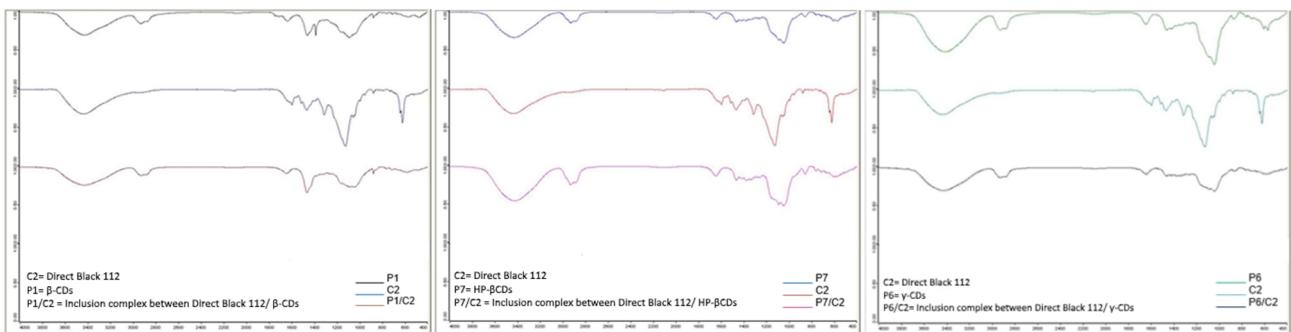
Figure 3 FTIR spectra comparing Direct Black 112 with β-CDs (left), HP-βCDs (center) and γCDs (right)

Below are presented the results of the characterization of obtained textiles using the conventional dyeing process and the ones in which the cyclodextrin technique was employed.

3.2 Textile spectrum

The textile spectra of different dyed fabrics show that the release of the dye from different cyclodextrins varies depending on the obtained dye in different intensities on the fabric.

EPI-βCDs achieved the lightest fabrics with Direct Yellow 106 and Direct Black 112 and the darkest with Direct Red 83:1.

EPI-HP-βCDs achieved medium intensity fabrics with Direct Yellow 106 and Direct Black 112 and the lightest with Direct Red 83:1

EPI- γCDs achieved the darkest fabrics with Direct Yellow 106 and Direct Black 112 and medium intensity with Direct Red 83:1, so it was selected to be the best in two of the dyes and second-to-best in the remaining one.

In Figure 7 the spectrum of the fabrics obtained with the original dye and with the complex, obtained after the treatment of the wastewater with the EPI-γCDs and by modifying their concentration with 25% w.p.f, 50% w.p.f and 100% w.p.f., can be observed.
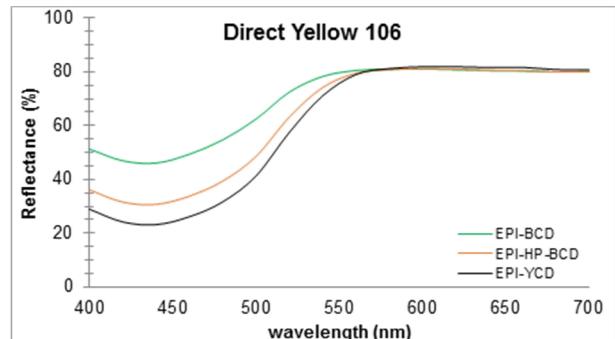
Figure 4 Spectrum of fabrics dyed with the complex formed by Direct Yellow 106 and EPI-βCDs, EPI-HP-βCDs and EPI- γCDs, respectively
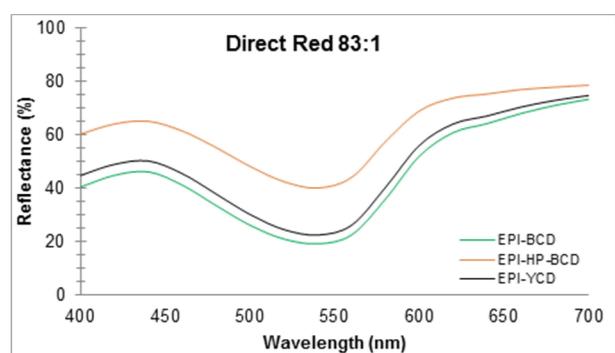
Figure 5 Spectrum of fabrics dyed with the complex formed by Direct Red 83:1 and EPI-βCDs, EPI-HP-βCDs and EPI-γCDs, respectively
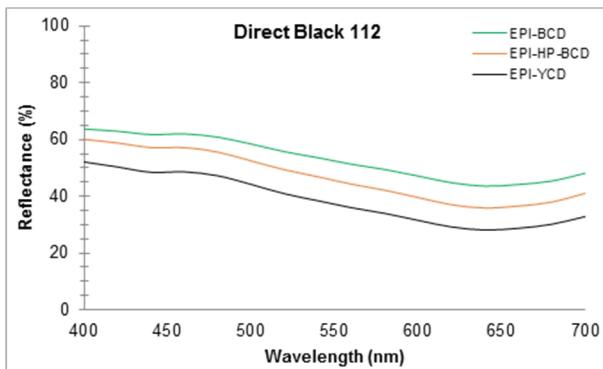
Figure 6 Spectrum of fabrics dyed with the complex formed by Direct Black 112 and EPI-βCDs, EPI-HP-βCDs and EPI-γCDs, respectively.

Figure 7 Spectrum of the fabrics dyed with the original dye and the complex formed in different concentrations

From the comparison spectrum of the original dye without the use of cyclodextrins and different percentages of complexed cyclodextrins/dye, it can be observed that there is a small difference in reflectance only in the range of 400-500 wavelength, in the other ranges the difference is relative to the intensity.

3.3 CIELab coordinates

In the following table are presented the results obtained regarding the CIELab coordinates.

CIELab system organizes colours so that numeric differences between colours agree consistently with visual perceptions.

Table 1 CIELab measurement of Direct Yellow 106 with different CDs

Sample	L	a	b	C	H	X	Y	Z	x1	y1
DY106/EPI-βCD	89.38	-1.50	23.45	23.49	93.66	70.37	74.97	53.15	0.3545	0.3777
DY106/EPI-HP-βCD	87.08	0.99	37.82	37.84	88.50	66.98	70.17	36.74	0.3852	0.4036
DY106/EPI-γCD	85.85	3.32	46.80	46.92	85.95	65.65	67.70	28.67	0.4052	0.4178

Table 2 CIELab measurement of Direct Red 83:1 with different CDs

Sample	L	a	b	C	H	X	Y	Z	x1	y1
DR83:1/EPI-βCD	63.49	35.02	-11.92	37.01	341.22	40.86	32.18	44.35	0.3481	0.2740
DR83:1/EPI-HP-βCD	77.37	21.89	-8.88	23.62	337.92	57.95	52.15	66.75	0.3296	0.2966
DR83:1/EPI-γCD	66.45	32.96	-11.65	34.95	340.53	44.53	35.91	48.82	0.3440	0.2781

Table 3 CIELab measurement of Direct Black 112 with different CDs

Sample	L	a	b	C	H	X	Y	Z	x1	y1
DB112/EPI-βCD	77.57	-4.04	-8.92	9.49	245.62	48.28	52.48	66.19	0.2892	0.3144
DB112/EPI-HP-βCD	73.36	-4.64	-11.68	12.57	248.31	41.80	45.72	61.09	0.2813	0.3077
DB112/EPI-γCD	67.61	-5.04	-12.84	13.79	248.58	34.04	37.45	51.92	0.2758	0.3035

Table 4 CIELab measurement of the wastewater mix with EPI-γ CD

Sample	L	a	b	C	H	X	Y	Z	x1	y1
Original	39.17	33.65	6.35	34.25	10.68	15.17	10.76	9.38	0.4296	0.3046
25% CDs+dye	47.04	33.56	9.46	34.87	15.72	21.58	16.05	13.11	0.4254	0.3163
50% CDs+dye	40.93	35.45	2.99	35.57	4.83	16.80	11.82	11.56	0.4181	0.2942
100% CDs+dye	35.79	35.01	0.22	35.01	0.36	13.06	8.90	9.48	0.4155	0.2830

Table 5 CIELab differences between the original and the samples dyed with the complex Dye+CDs

Sample	ΔE	ΔL
25% CDs+dye	8.46	7.87
50% CDs+dye	4.20	1.76
100% CDs+dye	7.13	-3.38

The value of *ΔE* shows a difference of tone between the original and the samples obtained with the complex, the most similar being the one obtained using 50% w.p.f. On the other hand, *ΔL* confirms that only the sample with 100% w.p.f is darker than the original.

4   CONCLUSIONS

It is possible to efficiently encapsulate dyes into EPI-CDs polymers and to recover the unfixed dyes from the wastewater and reuse them in a new dyeing process.

FTIR tests confirm the formation of the complex between the dye and the EPI-CDs polymers. They also show that the dye does not suffer any transformation during the encapsulation process.

It is easy to substitute the dyes with the complex formed by CDs/dye in the dyeing process, taking into account that the weight of the complex has to be higher than the dye alone, due to the fact that in this case the weight is composed of the cyclodextrin and the dye contributions.

The release of the dye depends on the dye and the CDs employed. So it can be concluded that a single CDs capable of the encapsulation of all the existent dyes with the best efficacy does not exist.

Different fabrics were obtained successfully with the recovered dyes, using the cyclodextrin technique reducing the environmental impact of dyeing process. This allows for a reduction in polluted wastewater, in the production of synthetic dyes and in the chemicals used to treat the wastewater.

Is difficult to reproduce the same colour because the dyeing is based on a tricomy and not all the dyes are encapsulated and released in the same way from the cyclodextrins. In this case, as the colour was formed by Direct Yellow 106, Direct Red 83:1 and Direct Black 112, the principal difference in the textile spectrum was generated by the change in the reflectance peak of the yellow.

Adopting the cyclodextrin technique can represent a difference in the Social Corporate Responsibility in the companies and open a new window for the development of new sustainable methods of dyeing by applying the three R principles of the environmental concepts: Reduce, Recycle and Reuse.

5   REFERENCES

1. Evolutia: Textile Sectorial Study, 2010
2. Shaikh A.M.: Water conservation in Textile Industry, Physical Therapy Journal, 2009
3. Shahabuddin M., Mustafa Y., Yilmaz E.: Removal of direct azo dyes and aromatic amines from aqueous solutions using two B-CD based polymers, Journal of hazardous materials 174(1-3), 592-597, 2010
4. Baban A.,Yedilir A., Clilz N.K.: Integrated water management and CP implementation for wool and textile blend processes, Clean 38(1), 84-90, 2010
5. Suteu D., Zaharia C., Malutan T.: Removal of orante 16 reactive dye from aquous solution by wasted sunflower seed shells, Journal of the Servian Chemical Society.1783, 9007-9024, v
6. Zaharia C., Suteu D., Muresan A., Muresan, R., Popescu A.: Textile wastewater treatment by homogenous oxidation with hydrogen peroxide, Environmental Engineering and management journal 8(6), 1359-1369, 2009
7. Crini. G.: Non-Conventional low-cost adsorbents for dye removal: a review, Bioresource Technology, 1061-1081, 2006
8. Renault F., Morini-Crini N., Gimbert F., Badot P.M., Crini G.: Cationized Starch-based material as a new ion-exchanger adsorben for the romoval of C.I. Acid Blue 25 from aqueous solutions, Biosurce Technology 99(16), 7573-7586, 2008
9. Crini G., Gimbert F., Capucine R., Martel B., Adam O., Morini-Crini N., De Giorgi F., Badot P.M.: The removal of Basic Blue 3 from aquous solutions by chitosan-based adsorbent: Batch studies, Journal of Hazardous Material 153(1-2), 96-106, 2008
10. Crini G., Martel B., Torri G.: Adsorption of C.I. Basic Blue 9 on Chitosan-based Materials, International Journal of Environment and Pollution 34(1-4), 451-465, 2008
11. Rizzi V.: Applicative Study (Part I): The Excellent Conditions to Remove in Batch Direct Textile Dyes (Direct Red, Direct Blue and Direct Yellow) from Aqueous Solutions by Adsorption Processes on Low-Cost Chitosan Films under Different Conditions, Advances in Chemical Engineering and Science 4, 454-469, 2014
12. Crini G., Peindy H.N., Gimbert F., Bapucini R.: Removal of C.I. Basic Green 4 (malachite Green) from aqueous solution by adsorption using cyclodextrin-based adsorbent: Kinetic and equilibrium studies, Separation and Purification Technology 53(1), 97-110, 2007
13. Crini G.: Studies on adsorptioni of dyes on beta-cyclodextrin polymer, Biosurce technology 90(2), 193-198, 2003
14. Crini G.: Kinetic and equilibrium studies on the removal of cationic dyes from aqueous solution by adsorption onto a cyclodextrin polymer, Dyes and Pigments 77(2), 415-426, 2008
15. Semeraro P., Rizzi V., Finni P., Matera S., Cosma P., Franco E., Garcia R., Ferrandiz M., Nunez E., Gabaldon J.A., Fortea I., Perez E., Ferrandiz M.: Interaction between industrial textile

dyes and cyclodextrins, Dyes and Pigments, 84-94, 2015

16. DYES4EVER, Available on:
    http://www.dyes4ever.eu/

17. Marques H., Cabral M.: A review on cyclodextrin encapsulation of essential oils and volatiles, Flavour and fraagance journal 25(5), 313-326, 2010

18. Tao B.Y., Eastburn S.D.: Application of modified cyclodextrins, Biotechnology Adv 12, 235-329, 1994

19. Sanjoy K.D., Rajan R., Shba D., Gani N., Khanam J., Arunabha N.: Cyclodextrins-The molecular container, Research journal of pharmaceutical, biological and chemical sciences 4(2), 1694, 2013

20. Renard E., Deratani A., Volet E., Sebille G.: Preparation and characterization of water soluble high molecular weight B-cyclodextrin-eplichlorohydrin polymers, European polymer journal 33(1), 49-57, 1997

21. Szetjli. J.: Introduction and general overview of cylodextrin chemistry, Chemical Reviews (98, 1998, pp. 1743-1753

22. Muñoz-Boteela S., Del Castillo B., Martyn M.A.: Cyclodextrin properties and applications of inclusion complex formation, Ars Pharmaceutica 37, 187-198, 1995

23. Loftsson T., Brewster M.E.: Pharmaceutical applications of cyclodextrins: drug solubilisation and stabilization, Journal of Pharmaceutical Science 85, 1017-1025, 1996

24. Schneiderman E., Stalcup A.M.: Cyclodextrins: a versatil tool in separation science., Journal of Chromatography B. 745, 83-102, 2000

25. Solms J., Egli R.: Harze mit Einschlusshohlräumen von Cyclodextrin struktur, Helvetica Chimica acta 48(6), 1225-1228, 1965

26. Komiyama S.: Inmobilized B-cyclodextrin catalyst for selective synthesis of 4-hydroxybenzoic acid Polym. 17, 1225-1227, 1985

ANTIMICROBIAL ACTIVITY OF SOME NOVEL 2-AMINO-5-ARYLTHIAZOLE DISPERSE DYES AND THEIR APPLICATIONS FOR DYEING OF POLYESTER FABRICS

H. E. Gaffer[1], M. M. G. Fouda[1] and M. Khalifa[2]

[1]*Textile Research Division, National Research Center, Dokki, Giza, P.O. 12622, Giza, Egypt*
[2]*Department of Chemical Engineering, Higher Institute for Engineering and Technology, New Damietta, Egypt*
hatem197@yahoo.com

Abstract: *The present work describes the synthesis of a series of four novel biologically active 2-amino-5-arylazothiazole disperse dyes containing sulfa drugs' nucleus. The structures of the synthesized thiazole derivatives are confirmed using UV-Spectrophotometer, Infra-Red, Nuclear Magnetic Resonance techniques and elemental analysis as well. The synthesized dyes are applied to polyester fabrics as disperse dyes and their fastness properties to washing, perspiration, rubbing, sublimation, and light are evaluated. The synthesized compounds exhibit promising biological efficiency against selected Gram-positive and Gram-negative pathogenic bacteria as well as fungi.*

Key Words: *Azo dyes; 2-aminothiazole; sulfaguanidine; polyester; dyeing; antimicrobial activity*

1   INTRODUCTION

Azo dyes, containing at least one N=N structure in molecule, are the most important group of disperse dyes [1, 2] and globally comprise over 50% of disperse dyes because of their strong tinctorial strength compared to anthraquinone dyes, ease to make, and a low cost of manufacture. Azo dyes have a vivid color in the yellow to blue-green region by varying between azo components with electron withdrawing groups and coupling components with electron donating groups such as aminobenzene. 2-Aminothiazoles are mainly known as biologically active compounds with a broad range of activities and as intermediates in the synthesis of antibiotics such as the well-known sulfa drugs [3]. Several papers have been published on the use of these compounds as antimicrobial [4], antifungal [5], anti-inflammatory [6], anesthetic [7], anti-hypertensive [8] and antiviral drugs [9]. 2-Aminothiazoles and their derivatives are also used in the syntheses of various types of dyes [10-13]. In continuation of our interest in the synthesis of arylazo-thiazole derivatives [14-16], this paper reports the synthesis of some 2-amino-5-arylazo-thiazoles and their application as disperse dyes on polyester fabrics.

In addition, the antibacterial activities of the synthesized dyes against various pathogenic bacteria and fungi were also investigated.

2   RESULTS AND DISCUSSION

2.1 Synthesis

Treatment of 2-aminothiazole derivatives **1** with the diazonium chloride derived from sulfaguanidine **2** afforded the corresponding 2-amino-5-arylazothiazole derivatives **4** and **5**. The structures of **4** and **5** were established on the basis of their elemental analyses and spectral data. For example, the IR spectrum of **4** revealed absorption bands at 3346, 3232, 3173 cm^{-1} due to NH_2 and NH functions, while the absorption band at 1610 cm^{-1} was attributed to (C=N) function. The ^{1}H NMR spectrum displayed a triplet signal at δ 7.05 ppm due to NH proton, two doublet signals at δ 7.74 and 8.04 ppm corresponding to the aromatic protons, a singlet signal at δ 8.16 ppm characteristic for the C-4 thiazole-H, two signals at δ 8.51 and 8.67 due to two NH_2 groups and a singlet signal at δ 11.88 ppm due to NH proton.

Moreover, coupling of 2-aminothiazole derivatives **1** with the diazoium chloride derived from sulfapyrimidine **3** yielded the corresponding 2-amino-5-arylazothiazole derivatives **6** and **7**. The structures of these substituted thiazole dyes **6** and **7** were elucidated based on their elemental analyses and spectral data. The IR of the dye **6** showed absorption peaks at 3364, 3286, 3142 cm^{-1} due to the presence of NH_2 and NH functions, in addition to the characteristic absorption peak of C=N group at 1612 cm^{-1}. The ^{1}H NMR spectrum of dye **6** showed a triplet signal at 6.88 ppm due to C-5 pyrimidine proton, a singlet signal at 7.13 ppm for NH group, two doublet signals at 7.66 ppm and 8.04 ppm for four aromatic protons and a singlet signal at 8.22 ppm for the C-4 thiazole proton. The presence of a doublet signal at 8.40 was attributed to the C-4 and C-6 pyrimidine-H protons, while the NH_2 group is downfield shifted to 8.70 ppm.

2.2 Dyeing and fastness properties

The functionalized 4-arylazo-3-methyl-2-substituted-thiophene disperse dyes **4-7** were applied to polyester fabrics (o.w.f. 2%) using high-temperature pressure technique (130°C), and the visual color shades varied from red to reddish violet. Dyeing of polyester fabrics was assessed in terms of their fastness properties (e.g. fastness to washing, perspiration, rubbing, sublimation, and light) *via* a standard method [17]. All results are provided in Table 1, which disclose that these dyes have good fastness properties to washing, perspiration, rubbing and sublimation.

The light fastness of the synthesized dyes on polyester shows fading of these dyes, where it is significantly affected by the presence of azo group due to its decomposition by oxidation, reduction and/or photolysis [18]. The rate of this process depends on the chemical structure, treatment conditions, as well as the nature of substrate. The use of polyester fabric (*i.e.*, non-proteinic fabric type), explains that the fading process likely occurs by oxidation [19]. The ease of oxidation of azo linkages should be a function of electron density. Therefore, electron-donating substituent on this moiety should increase the fading rate. This proposal is in agreement with the observed results (Table 1) which demonstrate that the presence of a phenyl group attached to the synthesized dyes causes a decrease of light fastness to 4-5.

2.3 Color assessment

Dyeing colors of polyester fabrics are expressed in terms of CIELAB values (Table 2) and the following CIELAB coordinates are defined by lightness (L^*), chroma (C^*), hue angle from 0° to 360° (H), (a^*) value exemplifies the degree of redness (positive) and greenness (negative) and (b^*) signifies the degree of yellowness (positive) and blueness (negative). A reflectance spectrophotometer (Gretag Macbeth CE 7000a) was utilized for the colorimetric assessments of the dyed samples. K/S values provided by the reflectance spectrometer are calculated at λ_{max} and are directly associated with the dye concentration on the dye substrate.
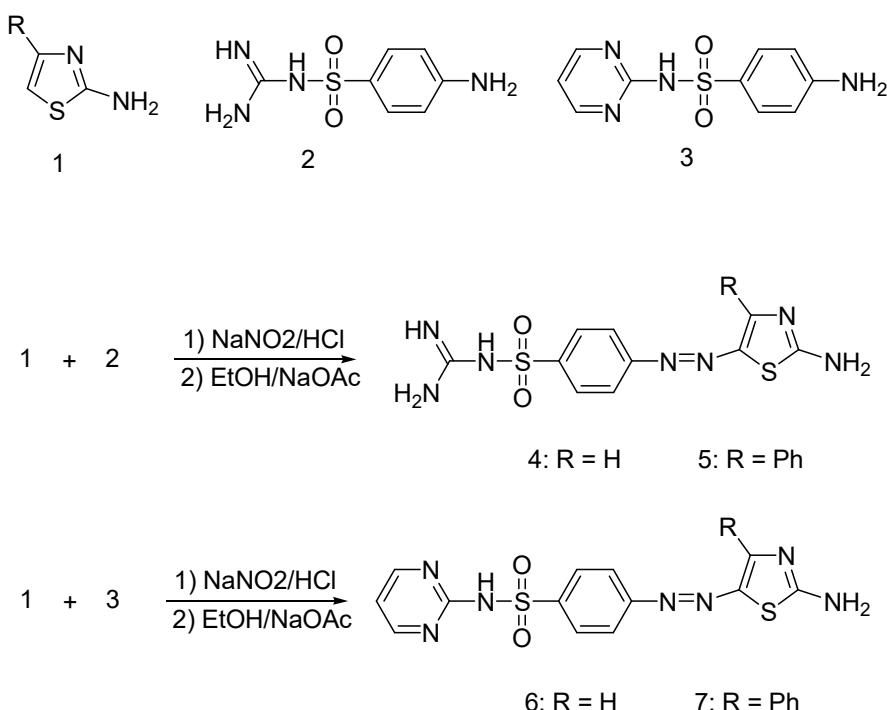
Scheme 1 Synthesis of 2-amino-4-arylazo-thiazole disperse dyes **4-7**

Table 1 Fastness properties of the synthetic dyes on polyester fabrics

Dye	Washing	Perspiration		Rubbing		Sublimation		Light [60 h]
		Acid	*Alkali*	*Dry*	*Wet*	*Staining at 180℃*	*Staining at 210℃*	
4	4-5	4-5	4-5	3-4	4-5	4	3	5
5	4-5	3-4	4-5	3	3	5	4	4-5
6	4-5	4-5	4-5	3-4	4-5	5	4	5
7	4-5	4	4	4	4	3	3	4-5

Table 2 Optical measurements of the synthetic dyes on polyester fabrics

Dye	% Exhaustion	Absorption λ_{max}/nm	K/S	L*	a*	b*	C*	H
4	65	446	9.26	81.09	3.35	20.42	40.58	80.71
5	71	444	12.67	73.23	-1.48	23.13	43.88	76.75
6	69	463	11.33	74.22	8.17	37.20	48.71	76.21
7	66	458	9.37	89.35	-1.78	3.14	43.51	85.84
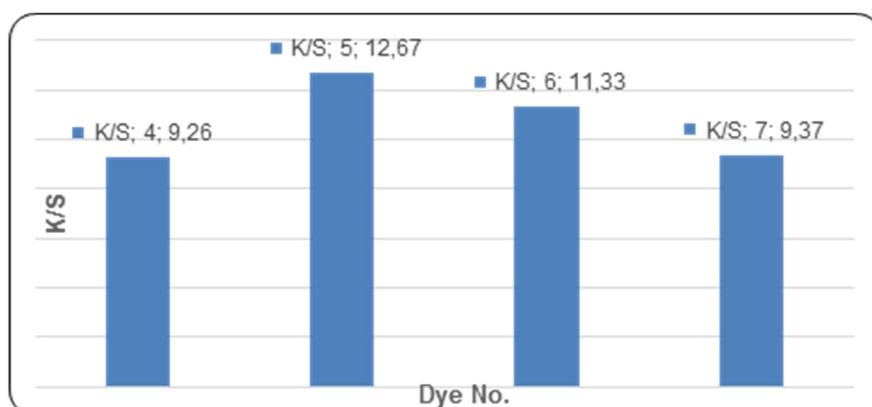
Figure 1 Comparison of K/S values for the synthesized disperse dyes **4**–**7** series

Generally, the color hues of the thiazole dyes **5** and **7** on polyester fabric are shifted to the greenish directions, this is showed by the negative values of *a** (red-green axis). The positive values of *b** (yellow-blue axis) designate that the color hues of the thiazole dyes **6** and **8** on polyester fabric are shifted to the yellowish directions.

Application of the synthesized compounds **4-7** as disperse dyes showed a good affinity of such dyes to polyester fabrics, as indicated by the satisfactory color yields and the acceptable *K/S* values. Figure 1 illustrates the relationship between the dyeing bath concentrations and the strengths of the synthesized **4-7** disperse dyes (*K/S*), under high temperature (HT) dyeing conditions where no direct correlation between the relative molecular mass of these dyes to the build-up was apparent. This probably reflects the importance of other parameters such as dye solubility, which in turn is dictated by the type of structural features within the dye. These results are in line with the ones previously reported by Müller [20] on the relation between substituents and dye structure.

2.4 Antimicrobial activity

Table 3 showed that all samples exhibited an acceptable antimicrobial activity against tested bacteria at different concentrations 0.01, 0.5, 1 mg. At high concentrations, regarding *C. albicans*; however, the extract exhibited an acceptable antifungal activity. The inhibition zone of all synthetic products was at range 0.6 to 1.7 mm.

2.5 Scanning electron microscope

Scanning electron microscope was used to observe the morphological alteration of the cells after treatment with the synthesized compounds (e.g. the higher active compound **7**). As shown in Figures 2 and 3, the bacterial cells (*S. aureus*) and fungal cells (*Candida albican*) treated with the synthesized compound, compared to untreated cells exploring that the treated cells appeared to be shrunk and there was a degradation of the cell walls.

Table 3 Antibacterial and antifungal activities of the synthesized compounds **4-7** with different concentrations [mg]

Compd.#	Gram +ve bacteria									Gram –ve bacteria						Fungi	
	S. aureus			S. pyogenes			S. typhi			P. aeruginosa			K. pneumoniae			C. albicans	
	0.01	0.5	1.0	0.01	0.5	1	0.01	0.5	1	0.01	0.5	1	0.01	0.5	1.0	0.005	0.05
4	0.6	0.7	1	0.4	0.6	0.65	0.6	0.9	1.2	0.3	0.6	0.8	0.2	0.6	0.7	0.7	1.1
5	0.6	0.8	1.2	0.1	0.2	0.6	0.6	0.8	1	0.2	0.4	0.6	0.2	0.6	0.7	0.9	1.3
6	0.6	1	1.7	0.3	0.6	1.6	0.6	1	1.2	0.7	1	1.4	0.3	0.5	1.2	0.7	1.4
7	0.6	1.2	1.3	0.6	1.1	1.9	0.7	1.2	2	0.1	0.3	0.7	0.4	1	2	0.8	1.3
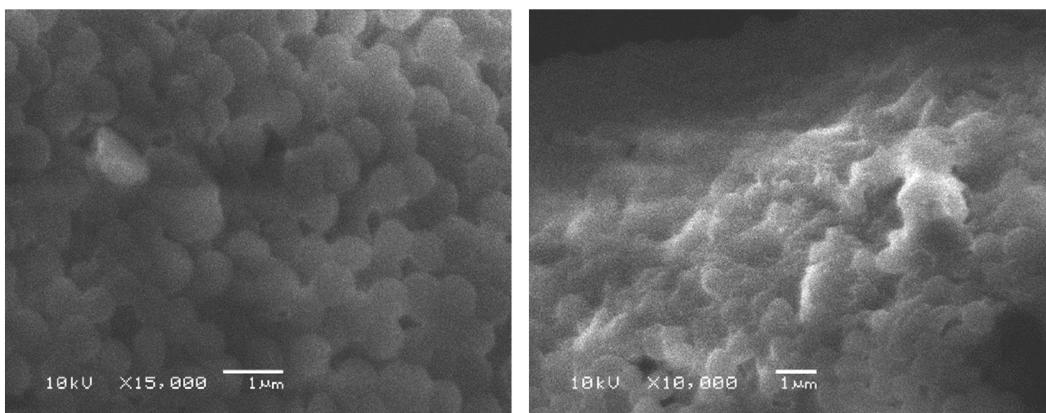
Figure 2 *S. aureus* in ethanol as control (left); treated *S. aureus* with synthesized compound **7** (right)
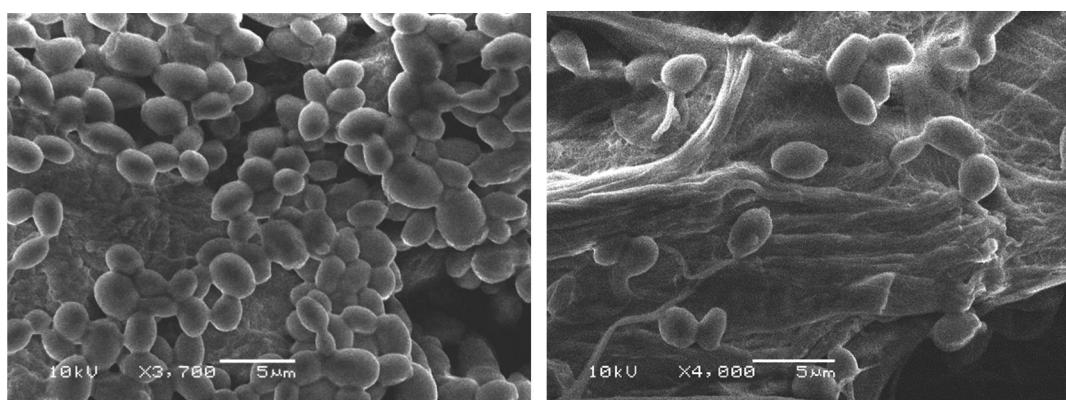
Figure 3 *Candida albicans* in ethanol as control (left); treated *Candida albicans* with synthesized compound **7** (right)

Table 4 Minimum Inhibitory Concentration (μg/mL) of the synthesized compounds **4-7** against Gram positive (e.g. *S. aureus* and Gram negative (e.g. *S. typhi*) bacteria at different concentrations [μg.mL^{-1}]

Compd.	Control conc. [%]	S. aureus				Control conc. [%]	S. typhi			
		5	*10*	*60*	*150*		*5*	*10*	*60*	*150*
4	$49.32×10^3$ (0%)	$37.65×10^3$ (23.7%)	$31.44×10^3$ (36.3%)	$24.80×10^3$ (49.7%)	$19.39×10^3$ (60.7 %)	$36.09×10^3$ (0%)	$34.22×10^3$ (5.2%)	$25.36×10^3$ (29.7%)	$22.71×10^3$ (37.1%)	$16.64×10^3$ (53.9%)
6	$49.32×10^3$ (0%)	$48.94×10^3$ (0.8%)	$48.19×10^3$ (1%)	$46.31×10^3$ (6.1%)	$28.24×10^3$ (42.7 %)	$36.09×10^3$ (0%)	$32.67×10^3$ (9.5%)	$20.22×10^3$ (44%)	$19.44 10^3$ (46.1%)	$16.18×10^3$ (55.2%)
5	$49.32×10^3$ (0%)	$43.47×10^3$ (11.9%)	$26.16×10^3$ (47%)	$25.22×10^3$ (48.9%)	$17.32×10^3$ (64.9 %)	$36.09×10^3$ (0%)	$36.56×10^3$ (1.3%)	$31.89×10^3$ (11.6%)	$22.24 10^3$ (38.4%)	$15.56×10^3$ (56.9%)
7	$49.32×10^3$ (0%)	$48.21×10^3$ (21.2%)	$37.65×10^3$ (23.7%)	$20.52×10^3$ (58.4%)	$19.20×10^3$ (61.1 %)	$36.09×10^3$ (0%)	$31.89×10^3$ (11.6%)	$24.00×10^3$ (33.5%)	$21.78 10^3$ (39.7%)	$16.33×10^3$ (54.8%)

2.6 Minimum inhibitory concentration (MIC)

A strong inhibition of the synthesized compounds **4-7** against the tested pathogenic bacteria was noticed (5 to 150 μg.mL^{-1}) as described in Table 4 to be vulnerable to all of them and their minimum inhibition concentration (MIC) values ranged from 5-10 μg.mL^{-1}, with noticeable inhibitory action. In this study, synthesized compounds **4** and **7** showed the highest antibacterial activity against the tested bacteria with the lowest MIC value of 5 μg.mL^{-1}. According to the obtained results, it is obviously clear that, all synthesized compounds **4-7** had higher activities against Gram positive bacteria than Gram negative bacteria.

3 EXPERIMENTAL SECTION

3.1 Materials and Methods

3.1.1 Materials, Chemicals and reagents

All the chemicals and solvents used in this study were obtained from Acros Chemicals Company (New Jersey, USA), and of pure grades. Polyester fabrics were kindly supplied by Misr for Spinning and Weaving Company (Mahalla El-Kobra, Egypt).

The dispersing agent Setamol WS was supplied by BASF Company (Germany). Source of bacteria strains: ATCC, American Type Culture Collection, were purchased from MicroBioLogics Inc., (St Cloud, MN, USA). The tested microorganism strains in ethanol were used as controls for biological experiments.

3.1.2 Instrumentation

All melting points were measured by an electrothermal Gallenkamp melting point apparatus (capillary method, Gallenkamp Co., London, UK) and are uncorrected. Elemental analyses were carried out at the Microanalytical Unit, National Research Centre, Giza, Egypt; the results were in satisfactory agreement with the calculated values. The IR spectra (KBr) were recorded in KBr disks by a Mattson 5000 FTIR spectrometer (Shimadzu Co., Kyoto, Japan, not all frequencies are reported). The NMR spectra (^{1}H and ^{13}C) were acquired using a WP 300 spectrometer (Bruker Co., Billerica, MA, USA) at 300 MHz using *TMS* as an internal standard and DMSO-d_6 as solvent. The colorimetric measurements for the dyed polyester fabrics were carried out using a reflectance spectrophotometer (GretagMacbeth CE 7000a, GretagMacbeth Co., Windsor, UK). Fastness to washing was carried out using the automatic Rotadyer launder (sponsored by the British Standard Institute—Society of Dyers and Colourists), fastness to perspiration was assessed according to the test sponsored by the (BSS), fastness to rubbing was carried out according to the standard method of testing (BSS) using a Crockmeter FD-17 apparatus (Electric Hungarian Co., Budapest, Hungary), fastness to sublimation was carried out using scorch tester M247 A (Atlas Electric Devices Co., Chicago, IL, USA) and fastness to light was carried out using the "Weather-o-meter" (Atlas Electric Devices Co., Chicago, IL, USA) according to the AATCC standard test method.

3.2 Synthesis

3.2.1 General procedure for the synthesis of 2-amino-4-arylazo-thiazole disperse dyes (4-7)

A solution of aryl diazonium chloride was prepared by adding cold sodium nitrite solution (0.7 g in 10 mL H_2O) to a cold suspension of aryl amine **2** and/or **3** (0.01 mol) in 3 mL concentrated HCl with stirring. The freshly prepared solution was added with continuous stirring to a cold solution (0-5 C) of 2-aminothiazole **1** (1 g; 0.01 mol) in 30 mL ethanol and 4.0 g sodium acetate. The reaction mixture was stirred at 0-5°C for 2 hours, diluted with water, and then filtered. The obtained 2-amino-5-arylazothiazole **4-7**, were dried and recrystallized from ethanol.

2-Amino-5-{[4-(carbamimidoyl-sulfamoyl)-phenyl]azo}-thiazole (4)

Red solid, yield 74%, m.p. 220-221°C. IR (KBr, cm^{-1}): 3346, 3232, 3173 (NH$_2$ and NH), 1610 (C=N). s^{1}H NMR (DMSO-d_6, δ ppm): 7.05 (t, 1H, NH), 7.74 (d, 2H, Ar-H), 8.04 (d, 2H, Ar-H), 8.16 (s, 1H, C-4 thiazole-H), 8.51 (d, 2H, NH$_2$), 8.67 (s, 2H, NH$_2$), 11.88 (s, 1H, NH). ^{13}C NMR (DMSO-d_6, δ ppm): 121.99 (2C), 129.51 (2C), 139.79, 144.88, 152.80, 155.20, 158.91, 173.40. Anal. calcd. for C$_{10}$H$_{11}$N$_7$O$_2$S$_2$ (325.37): C, 36.91; H, 3.41; N, 30.13, found: C, 36.83; H, 3.45; N, 30.20.

2-Amino-5-{[4-(carbamimidoyl-sulfamoyl)-phenyl]azo}-4-phenylthiazole (5)

Red solid, yield 77%, m.p. 241-241°C. IR (KBr, cm^{-1}): 3388, 3256, 3206 (NH$_2$ and NH), 1611 (C=N).^{1}H NMR (DMSO-d_6, δ ppm): 7.10 (t, 1H, NH), 7.27-7.50 (m, 7H, Ar-H), 8.00 (d, 2H, Ar-H), 8.55 (d, 2H, NH$_2$), 8.87 (s, 2H, NH$_2$), 11.62 (s, 1H, NH). ^{13}C NMR (DMSO-d_6, δ ppm): 121.46 (2C), 126.55 (2C), 128.21, 129.38 (2C), 130.86 (2C), 137.32, 140.64, 144.32, 151.08, 154.56, 160.27, 174.38. Anal. calcd. for C$_{16}$H$_{15}$N$_7$O$_2$S$_2$ (401.47): C, 47.87; H, 3.77; N, 24.42, found: C, 47.73; H, 3.84; N, 24.50.

2-Amino-5-{[4-(pyrimidin-2-yl-sulfamoyl)-phenyl]azo}-thiazole (6)

Red solid, yield 80%, m.p. 234-235°C. IR (KBr, cm^{-1}): 3364, 3286, 3142 (NH$_2$ and NH), 1612 (C=N). ^{1}H NMR (DMSO-d_6, δ ppm): 6.88 (t, 1H, C-5 pyridine-H), 7.13 (t, 1H, NH), 7.66 (d, 2H, Ar-H), 8.04 (d, 2H, Ar-H), 8.22 (m, 1H, C-4 thiazole-H), 8.40 (d, 2H, C-4 and C-6 pyridine-H), 8.70 (d, 2H, NH$_2$). ^{13}C NMR (DMSO-d_6, δ ppm): 112.82, 122.48 (2C), 127.75 (2C), 131.84, 138.79, 140.11, 142.68, 156.21 (2C), 167.86, 173.36. Anal. calcd. for C$_{13}$H$_{11}$N$_7$O$_2$S$_2$ (361.40): C, 43.20; H, 3.07; N, 27.13, found: C, 43.38; H, 3.15; N, 27.24.

2-Amino-4-phenyl-5-{[4-(pyrimidin-2-yl-sulfamoyl)-phenyl]azo}-thiazole (7)

Red solid, yield 72%, m.p. 181-182°C. IR (KBr, cm^{-1}): 3374, 3292, 3196 (NH$_2$ and NH), 1611 (C=N). ^{1}H NMR (DMSO-d_6, δ ppm): 6.90 (t, 1H, C-5 pyridine-H), 7.11 (t, 1H, NH), 7.32-7.60 (m, 7H, Ar-H), 8.00 (d, 2H, Ar-H), 8.33 (d, 2H, C-4 and C-6 pyridine-H), 8.62 (d, 2H, NH$_2$). ^{13}C NMR (DMSO-d_6, δ ppm): 113.64, 123.71 (2C), 127.06 (2C), 128.46, 129.18 (2C), 130.69 (2C), 135.74, 136.62 138.08, 141.26, 144.59, 157.27 (2C), 167.38, 172.91. Anal. calcd. for C$_{19}$H$_{15}$N$_7$O$_2$S$_2$ (437.50): C, 52.16; H, 3.46; N, 22.41, found: C, 52.02; H, 3.57; N, 22.57.

3.3 Disperse dyeing application

3.3.1 Dyebath Preparation, Dyeing procedure

The synthesized disperse dyes under investigated **4–7** series were applied to polyester fabrics (0.04 g dye/2 g fabric; 2% shade) by a convenient method for dyeing polyester fabrics in the laboratory at 130°C and high-pressure (24-30 psi). A laboratory model glycerin-bath of high-temperature beaker-dyeing apparatus was utilized. A dispersion of dye was formed by dissolving a proper quantity of dye (o.w.f. 2%) in 1 mL of acetone as solvent. 1% Setamol WS as anionic dispersing agent obtained from BASF was added drop-wise under stirring to the dye bath. The liquor ratio was 20:1, and the pH was adjusted to 5.5 using aqueous acetic acid.

Then, the wetted-out polyester fabrics were added. The dyeing process was accomplished by raising the dyebath temperature to 130°C, at the interval of 3°C/min, the reaction was left for 60 min under pressure. After cooling to 50°C, the dyed fabrics were rinsed with cold water, and then reduction cleared using a mixture of 1 g/l sodium hydroxide, 1 g/l sodium hydrosulfite for 10 min. at 80°C. The dyed fabrics were rinsed again with hot water followed by cold water and finally left for air drying.

3.3.2 Dyeing Characteristics on Polyester Fabrics

Color Fastness Tests

The color fastness properties of the dyed fibres to washing, perspiration, rubbing, sublimation and light were evaluated using standard methods [17]. The staining of adjacent cotton and nylon fabrics was assessed using the grey scale: 1-poor, 2-fair, 3-moderate, 4-good and 5-excellent, other than light fastness which scaled from 1–8 on the grey scale.

Color Properties of the Dyes on Polyester

A reflectance spectrophotometer (GretagMacbeth CE 7000a; D65 illumination, 10° observer) was used for the colorimetric measurements of the dyed samples. K/S values given by the reflectance spectrometer are calculated at λ_{max} and are directly correlated with the dye concentration on the dye substrate according to the Kubelka–Munk equation:

$$K/S = \frac{(1-R)^2}{2R} \qquad (1)$$

where K = absorbance coefficient, S = scattering coefficient, R = reflectance ratio.

3.4 Biological assessment

3.4.1 Test-pathogens

The antibacterial activity was performed against five bacteria strains: Gram positive (*Staphylococcus aureus* ATCC 25923 and *Streptococcus pyogenes* ATCC 19615) and Gram negative (*Salmonella typhi* ATCC 6539, *Pseudomonas aeruginosa* ATCC 27853 and *Klebsiella pneumoniae* ATCC 700603), and *Candida albicans* strain ATCC 90028 for antifungal activity, which were grown on sabouraud agar. The microbial strains were conserved in Brain Heart Infusion medium (BHI) at –20°C. 300 µL of each stock-culture were added to 3 mL of BHI broth. Cultures were kept for 24 h at 37°C ± 1°C and the purity of cultures was checked after 8 h of incubation. After 24 h of incubation, bacterial suspension was diluted with sterile sodium chloride solution, and bacterial suspension was diluted with BHI broth to a density of approximately 10^9 CFU/mL (McFarland standard 3).

3.4.2 Antimicrobial and antifungal activity

The antimicrobial activities of the dyes **4-7** were assessed *in vitro* using the agar diffusion method [21]. In this method, the medium was incubated with freshly prepared cells for each tested bacteria or fungi. After solidification of the agar, a number of clean disks were immersed into the solvents (negative controls) or extract solutions and located on the plates. After incubation at 37°C for 24 h, the antimicrobial activity was assessed in terms of diameter of the inhibition zone. Each test was repeated three times and the average results (mm of zone of inhibition) are tabulated.

3.4.3 Minimum inhibitory concentration (MIC)

The selected bacteria for MIC were *Staphylococcus aureus* ATCC 25923 and *Salmonella typhi* ATCC 6539. MIC of four different samples was calculated by the two-fold serial dilution method [21, 22]. The levels dose of 5, 10, 60, 150 µl/mL were utilized for MIC evaluation. 5 µl of standardized suspension of tested bacteria (10^8 CFU mL^{-1}) well was used for 1 mL of the broth. The test tubes were incubated at 37°C for 24 h. The growth was calculated by spectrophotometer at 600 nm. MIC for bacteria was determined as the lowest concentration of the compound inhibiting the visual growth of the test cultures on the agar plate. Each test in this experiment was repeated three times and the average results in term of (mm of zone of inhibition) were tabulated.

3.4.4 Scanning electron microscopy

Scanning Electron Microscope (SEM) was used to evaluate the susceptible bacteria that were subjected to the synthetic products. A small piece of agar was cut from the inhibition zone and fixed in glutaraldehyde solution 3% (v/v) buffered with 0.1 M sodium phosphate (pH 7.2) for 1 hr at 25°C. Subsequently, the samples were washed with sodium phosphate buffer. All pieces were then post-fixed in 1% (w/v) osmium tetroxide (OsO$_4$) for 1 hr and then washed again in buffer. Dehydration steps were performed using propylene oxide (CH$_3$CH.CH$_2$.O). The specimens were left to dry and were mounted onto stubs using double-sided carbon tape, and then were coated with a thin layer of gold by a Polaron SC 502 sputter coater. All of them were observed in a Jeol JSM 6060 LV Scanning Electron Microscope [23].

4 CONCLUSIONS

A series of novel 2-amino-5-arylazothiazole disperse dyes was synthesized. The newly synthesized dyes were applied as disperse dyes for dyeing polyester fabric, where they exhibited very good dyeability and fastness properties. The novel compounds displayed antibacterial efficiency upon screening against selected Gram positive and Gram-negative bacteria, as well as fungi.

It will be possible to discover new synthetic drugs serving as chemotherapeutic agents for treatment of nosocomial pathogens and they could control antibiotic-resistant bacteria.

5   REFERENCES

1. Dawson J.F.: Developments in disperse dyes, Color. Technol. 9, 25-35, v

2. Malik G.M., Zadafiya S.K.: Thaizole based disperse dyes and their dyeing application on polyester fiber and their antimicrobial activity, Chem. Sin. 1, 15-21, 2010

3. Ibatullin U.G., Petrushina T.F., Leitis L.Y. Minibaev I.Z., Logvin B.O.: Synthesis and transformations of 4-substituted 2-aminothiazoles, Chem. Heterocycl. Comp. 29, 612-615, 1993

4. Gaffer H.E, Abdel-Latif E.: Antimicrobial Activity of Some New 4-Arylazo-3-methylthiophene Disperse Dyes on Polyester Fabrics, J. Appl. Polym. 122, 83-89, 2011

5. Beuchet P., Varache-Lembège M., Neveu A., Léger J.-M., Vercauteren J., Larrouture S., Deffieux G., Nuhrich A.: New 2-sulfonamidothiazoles substituted at C-4, synthesis of polyoxygenated aryl derivatives and in vitro evaluation of antifungal activity, Eur. J. Med. Chem. 34, 773-779, 1999

6. Geronikaki A., Vicini P., Dabarakis N., Lagunin A., Poroikov V., Dearden J., Modarresi H., Hewitt M., Theophilidis G.: Evaluation of the local anaesthetic activity of 3-aminobenzo[d]isothiazole derivatives using the rat sciatic nerve model, Eur. J. Med. Chem. 44, 473-481, 2009

7. Papadopoulou C., Geronikaki A., Hadjipavlou-Litina D.: Synthesis and biological evaluation of new thiazolyl/benzothiazolyl-amides derivatives of 4-phenyl-piperazine, Il Farmaco 60, 969-973, 2005

8. Gouda M., Gaffer H. E., Gouda M.A.: Synthesis and anti-hypertensive activity of novel sulphadimidine derivatives, J. Med. Chem. Res. 21, 3902-3906, 2012

9. Kreutzberger A., Schimmelpfennig H.: Antivirale Wirkstoffe 18. Mitt. 2-Aminothiazole durch Spaltung der S-S-Bindung des Disulfidodicarbamidins, Arch. Pharm. 314, 385-391, 1981

10. Keil D., Flaig R., Schroeder A., Hartmann H.: Synthesis and characterization of methine dyes derived from N,N-disubstituted-2-aminoselenazoles and some of their heterocyclic sulfur analogues, Dyes Pigments 50, 67-76, 2001

11. Metwally M.A., Abdel-latif E., Khalil A.M., Amer F.A., Kaupp G.: New azodisperse dyes with thiazole ring for dyeing polyester fabrics, Dyes Pigments 62, 181-195, 2004

12. Singh K., Singh S., Taylor J. A.: Monoazo disperse dyes-part 1, synthesis, spectroscopic studies and technical evaluation of monoazo disperse dyes derived from 2-aminothiazoles, Dyes Pigments 54, 189-200, 2002

13. Yen M.S., Wang I.J.: Synthesis and solvent characteristics of bishetaryl monoazo dyes derived from polysubstituted-2-aminothiophene derivatives, Dyes Pigments 67, 183, 2005

14. Khalifa M.E., Abdel-Latif E., Gobouri A.A.: Disperse Dyes Based on 5-Arylazothiazol-2-ylcarbamoyl-thiophenes, Synthesis, Antimicrobial Activity and Their Application on Polyester, J. Heterocycl. Chem. 52, 674-680, 2015

15. Abdel-Wahab B.F., Gaffer H.E., Fahmy H.M., Fouda M.E.: Synthesis of some new 2-[(2,3-dihydroinden-1-ylidene) hydrazinyl]-4-methylthiazole derivatives for simultaneous dyeing and finishing for UV protective cotton fabrics, J. Appl. Polym. Sci. 112, 2221-2228, 2009

16. Abdel-Latif E., Amer F.A., Metwally M.A., Khalifa M.E.: Syntheses of some 5-arylazo-2-(arylidenehydrazino)-thiazole disperse dyes for dyeing polyester fibers, Pigm. Resin. Technol. 38, 105-110, 2009

17. Anonymous, Standard Methods for the Determination of the Color Fastness of Textiles and Leather, 5th Ed., Society of Dyes and Colorists Publication, Bradford, England, 1990

18. Al-Etaibi A.M., El-Apasery M.A., Ibrahim M.R., Al-Awadi N.A.: A facile synthesis of new monoazo disperse dyes derived from 4-hydroxyphenylazopyrazole-5-amines, evaluation of microwave assisted dyeing behavior, Molecules 17, 13891-13909, 2012

19. Chipalkatti H.R., Desai N.F., Giles C.H., Macaulay N.: The influence of the substrate upon the light fading of azo dyes, J. Soc. Dyers Color. 70, 487-501, 1954

20. Müller C.: Recent developments in the chemistry of disperse dyes and their intermediate, Amer. Dyestuff Rep. 59, 37-44, 1970

21. Chandrasekaran M., Venkatesalu V.: Antibacterial and antifungal activity of Syzygium jambolanum seeds, J. Ethnopharmacol. 91, 105-108, 2004

22. Adesokan A., Akanji M.A. and Yakubu M.T.: Antibacterial potentials of aqueous extract of Enantia chlorantha stem bark, A. J. Biotechnol. 6, 2502-2505, 2007

23. Hayat M.A.: Principles and techniques of electron microscopy, Vol. 1. London, Edward Arlond Lt., 522, 1981

MASS CUSTOMIZED TECHNICAL TEXTILES - CHALLENGES TO THE TEXTILE INDUSTRY FOR TOMORROW

R. Gebhardt[1], L. Grafmüller[2], M. Barteld[1] and T. Mosig[2]

[1] STFI - Saxon Textile Research Institute, Annaberger Str. 240, 09125 Chemnitz, Germany
[2] HHL Leipzig Graduate School of Management, Jahnallee 59, 04109 Leipzig, Germany
rainer.gebhardt@stfi.de

Abstract: The last years have shown an increasingly greater shift of classical manufacturing of textile products in large quantities to countries and regions with low salaries. The European textile and clothing industry has experienced a reduction in employment, which has stabilized at a low level. One reason for the stabilization can be seen in the increased focusing of companies on technical textiles, a field with high growth rate in general. Usually, this field is addressed with individualized products in small quantities but with a high degree of innovation due to consistent use of cutting-edge technologies, which is a great opportunity for the European textile industry. Mainly business customers from different industries demand these complex products. This context is typically referred to as engineer-to-order or solution business in the literature. Prerequisite for the actions in this field is the continuous penetration of the production chain, an intense interaction with the customer and its IT system linkage. In addition to that, the individual processes need to be further analyzed to effectively produce small quantities, down to the batch size of one, under industrial conditions with regard to the mass customization (MC) principles.

In this paper, we take stock of the current challenges for specialized textile companies to implement MC. Data collected in 80 companies show a stocktaking of the current positioning, technical possibilities as well as typical customer-manufacturer interactions. The data contains 39 surveys and 38 interviews conducted with CEOs, sales personnel and heads of development. Basic results of studies on the individualization of textile processes and possible diversification potential for new applications will be presented.

Key Words: mass customization, supply chain, B2B, B2C, individualization

1 INTRODUCTION

The last years have shown an increasingly greater shift of classical manufacturing of textile products in large quantities to countries and regions with low salaries.

The European textile and clothing industry has experienced a reduction in employment, which has stabilized at a low level.

One reason for the stabilization can be seen in the increased focusing of companies on technical textiles. Thus in Germany, about 50% of companies work in this field with diverse application areas. Nevertheless the relationship of clothing, home textiles and technical textile in European regions is different.

Usually, it is about special products with small quantities but with a high degree of innovation, which is a great opportunity for the European textile industry.

Prerequisite for the actions in this field is the continuous penetration of the production chain and its IT system linkage.

In addition to that, the individual processes need to be further customized to effectively produce small quantities, down to the batch size of one, under industrial conditions.

The finishing has a special role since the crucial features and functionality for special applications are generated there. At the same time, distribution channels will change through customizing and new marketing strategies will come along.

Particular attention will be paid to the closer integration of the customer in the development and manufacturing processes. This will also lead to a possible change in the business models.

First examples of individualization have been reached in knitting and embroidery production, as well as the use of digital printing for different applications.

However, not every technology has sufficient individualization potential.
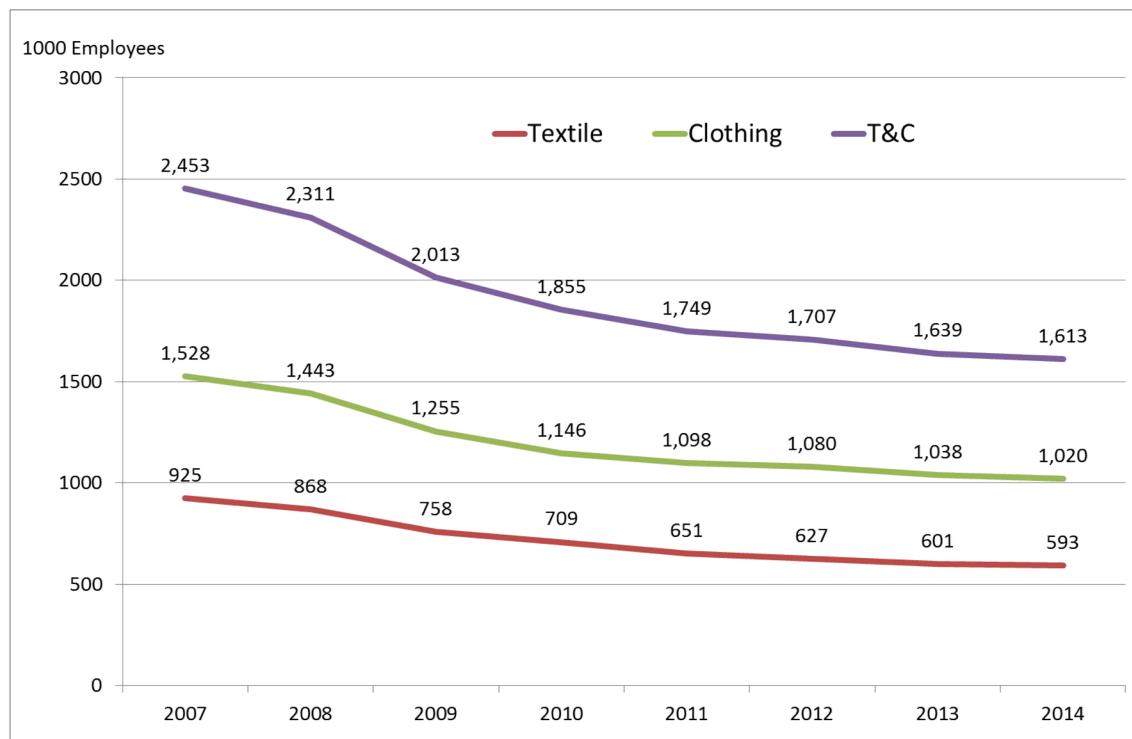
Figure 1 Numbers of employees in textile and clothing industry of Europe (Source: Euratex). In Germany the situation is more stabilized

Figure 2 Numbers of employees in textile and clothing industry of Germany (Companies with more than 20/50 employees). Source: textile+mode and vti
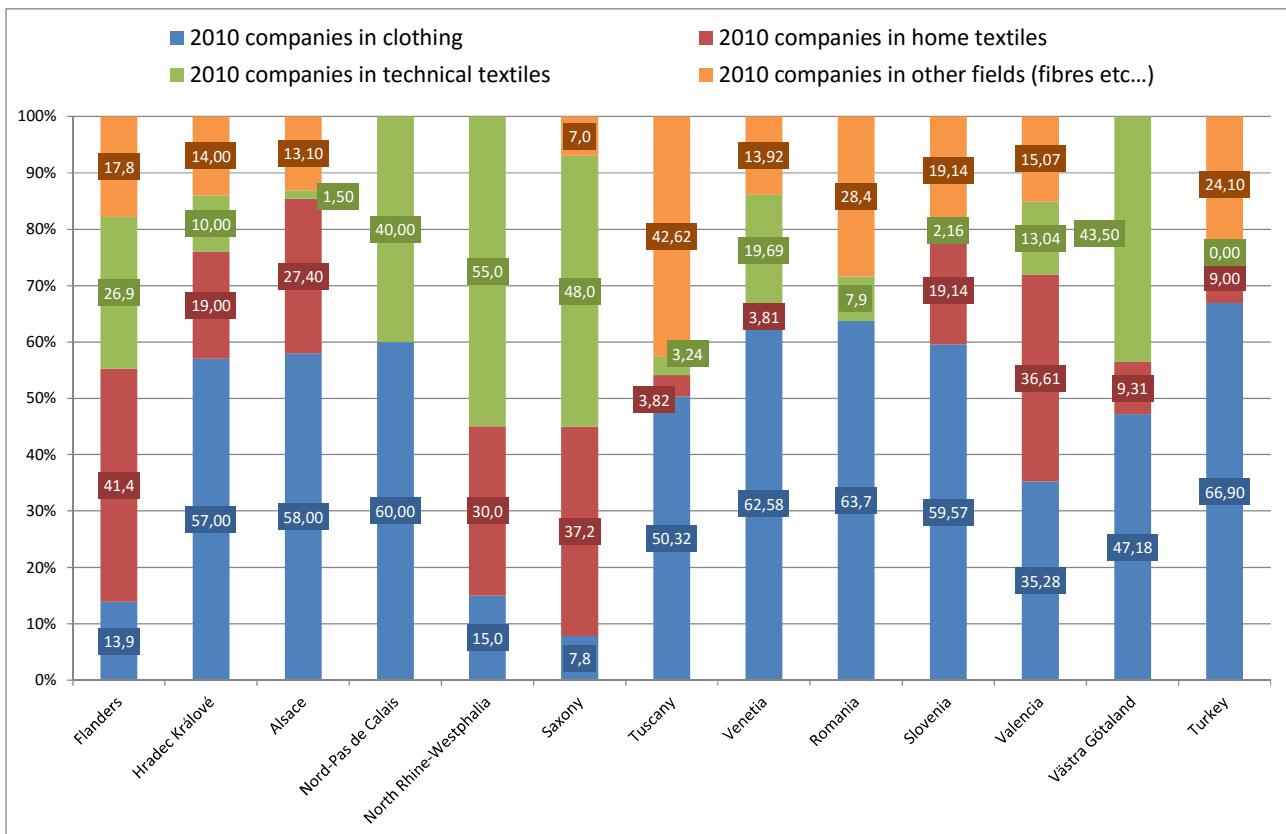
Figure 3 Relationship of companies in clothing, home textiles, technical textiles and others in European textile regions (Source: Crosstexnet)

2   MASS CUSTOMIZATION & THE INDUSTRIAL CONTEXT: A BUSINESS PERSPECTIVE

More and more customers are demanding individualized products and therefore challenge the traditional mass production. MC offers a solution in order to provide products which are both inexpensive and individualized (Pine 1992). The increase of output diversity without losing cost advantages of mass production was considered to be the main challenge of MC. MC relies on a number of principles for its realization. Among the frequently stressed principles are the modularization of production, often combined with technologies which enable a direct conversion between digital and real world (e.g., 3D scanning, 3D printing), and high customer integration, in particular in the process of outcome design which is usually supported by toolkits (Da Silveira, Borenstein, & Fogliatto, 2001; da Silveira, Giovani J.C., 2011).

Since Pine's seminal work (1992), much has been written about MC drivers, success factors, enablers, the customer-manufacturer interaction or the solution space of individualization on B2C markets (Da Silveira et al., 2001; Fogliatto, da Silveira, Giovani J.C., & Borenstein, 2012). However, less attention has been paid to

the industrial context, and thus B2B markets. The case of business customers differs fundamentally from the situation of end consumers. For instance, a single business customer is usually much more important than a single consumer. As a consequence, business customers have always been attended to with individualized offers. They exhibit different characteristics and goals that impose other requirements on the design of the customer interaction process. For instance, they buy rather for economic than for emotional reasons (Eggert & Ulaga, 2002) and are capable of handling much more complex configuration tasks (Tuli, Kohli, & Bharadwaj, 2007; Ulaga & Loveland, 2014). Furthermore, whereas toolkits for end consumers are designed for non-experts, i.e., they represent relatively small solution spaces, business customers are typically seen as experts, which is especially relevant with regard to the co-design process. In the literature, individualized B2B offers are typically discussed under engineer-to-order (ETO), solution selling and solution business (Keränen & Jalkala, 2013). In these markets, the solution is created within an individual and personal customer-manufacturer interaction, a time-consuming process with a high degree of product customization and hence complexity (Davies, Brady, & Hobday, 2006; Tuli et al., 2007; Ulaga & Loveland, 2014). The offer does not only

encompass products and services, but it fulfills specific functions for the customer through assistance in internal processes and provision of certain resources (Grönroos, 2011; Ulaga & Reinartz, 2011). Hence, the promise of MC with respect to business customers is rather the opposite. It revolves around questions such as: How can the established degree of individualization be managed while moving from ETO production or solution-oriented approaches to a more standardized MC offer? What are the central customer value components of MC for business customers? How can these value components be addressed? In order to answer and solve these questions and to respond properly to the values customers are demanding, the business models of the companies need to be adjusted accordingly (Pine 1992). Core of such a MC business model is the customer-manufacturer relationship and the value provided to customers. Therefore, companies need to be aware of their value propositions which are the activities of a corporation it is providing value to the customer with (Osterwalder, 2014). These value-providing activities are in this case represented by consulting and prototyping services. These services are essential for the individualization and finally the fit of the product regarding the customer's needs.

3   MASS CUSTOMIZATION IN TEXTILES

Since 1999 in textile and clothing the number of publications in mass customization has been increasing. But in the same time only 6 mass customization publications in relation to technical textiles were published.

4   EXAMINATIONS AND RESULTS

In the official statistic 2015 – companies with more than 50 employees – of the new eastern states of Germany are 86 companies listed with 9.577 employees. The statistic of companies with more than 20 employees shows 192 companies with 13.063 employees [vti-statistics]. Based on internal statistics by STFI about smaller companies, we have a company structure listed in Table 1.

The percentage of Technical Textiles in the new German countries is more than 50%. Especially in Saxony it is higher. The distribution of the interviewed companies is shown in Figure 5.

Table 1 Structure of textile and clothing industry in East Germany

Employees / Company	Number	Percentage
<10	160	30.2%
10-19	171	32.3%
21-50	104	19.6%
51-100	48	9.1%
101-250	34	6.4%
>250	13	2.4%

Table 2 Numbers and percentage of textile and clothing companies in East Germany

	New Countries		Saxony		Thuringia	
TC-Companies	530		333		89	
Technical Textiles	269	50.8%	186	55.9%	40	44.9%
Home Textiles	176	33.2%	125	37.5%	22	24.7%
Clothing	184	34.7%	106	31.8%	35	39.3%
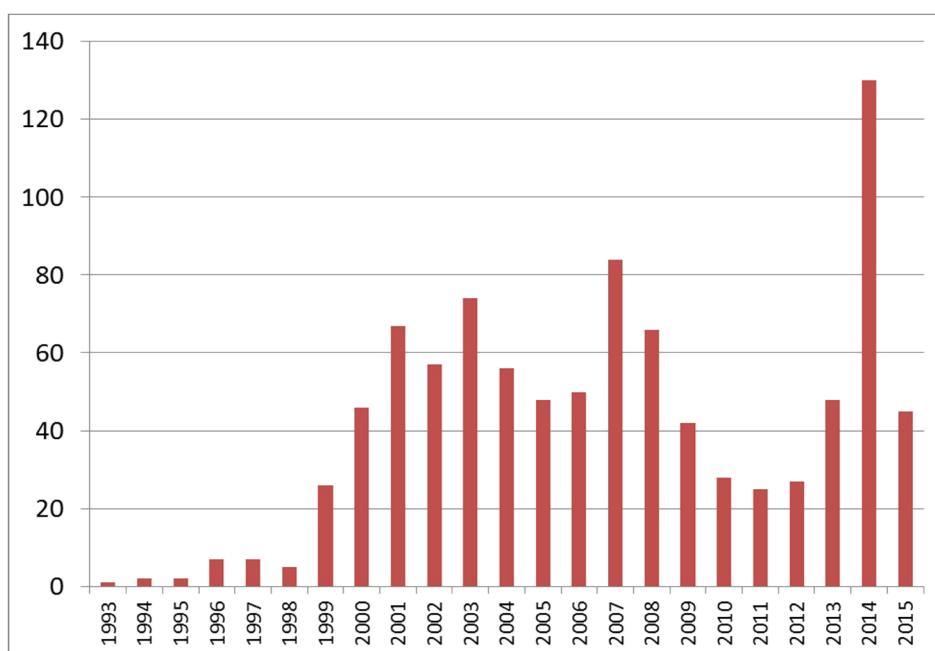
Figure 4 Numbers of mass customization publications (Source: WTI)
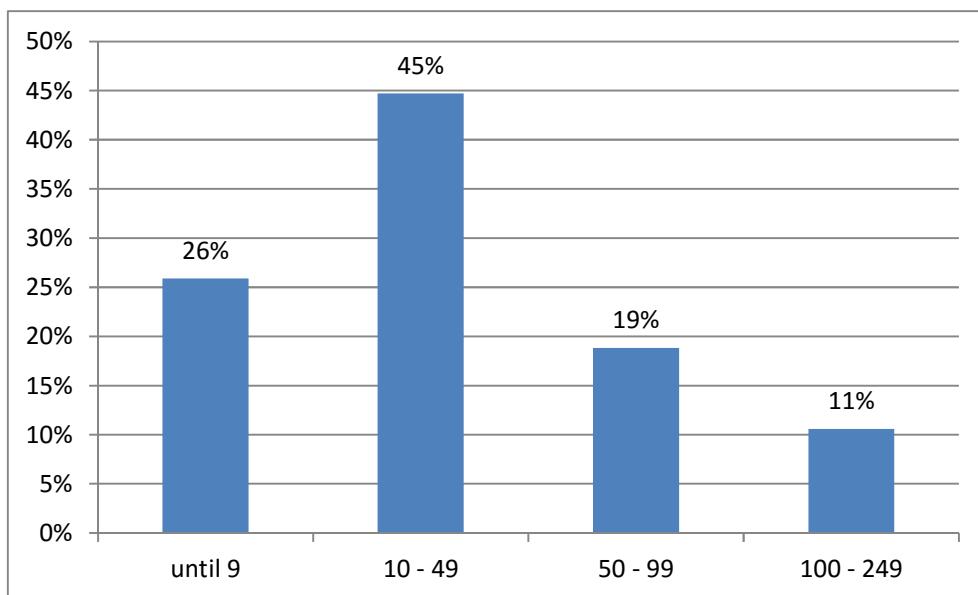
Figure 5 Numbers of employees in companies

4.1 Results of the quantitative analysis

In the first study, 60 companies were selected [Varga et al.]. Over 50% are interested in individualization and mass customization.

The basic project "Key technologies and core competencies to transform traditional textile value chains in sustainable customer oriented value networks based on mass customization strategies" is a part of the futureTEX project. The production of customized and cost-effective products is not new. However, since the research focus until now is strongly oriented to the retail markets and to the end-user (B2C). The project tries to close the backlog and the research gap in the B2B and to technical textiles. In the project the feedback of statistical data from 80 companies will be analyzed. 40 companies will be interviewed.

These are the first results of the quantitative analysis:

Action towards individualization: 39% of the companies urgent, 39% in 1-2 years and 22% later.

In 86 % of the companies the consumers are integrated in the production or distribution process.

67 % of the companies manufacture a single, individual product, but 33% with too high cost.
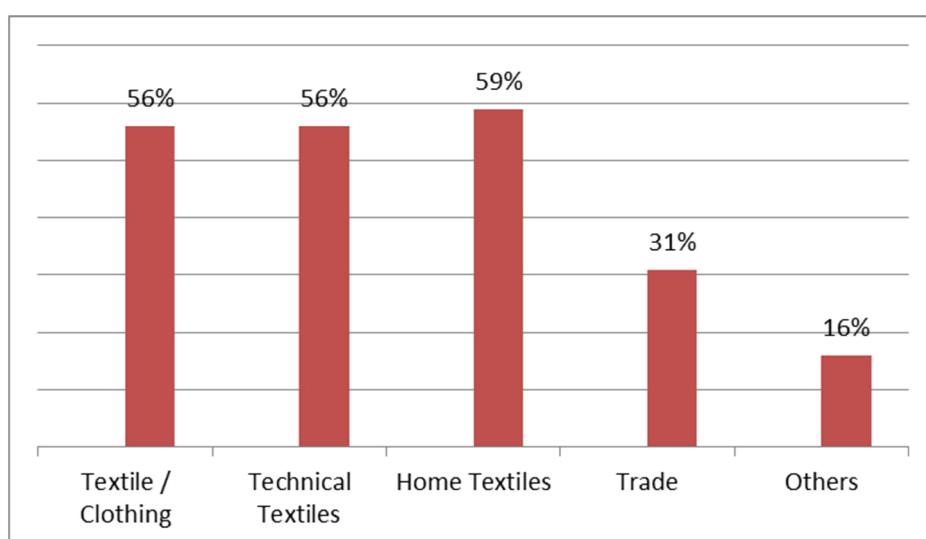
Figure 6 Percentage in the branch segment (multiple selection)
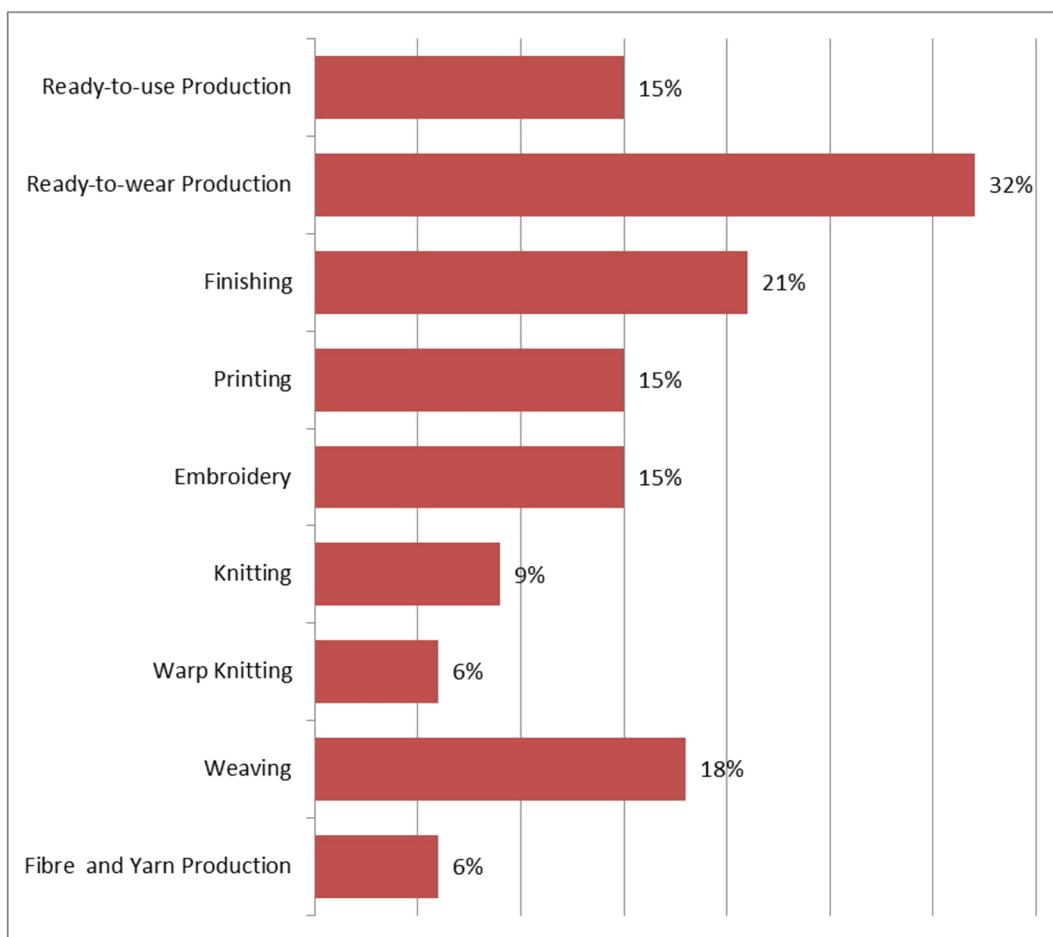
Figure 7 Fields of textile technology (multiple selection)
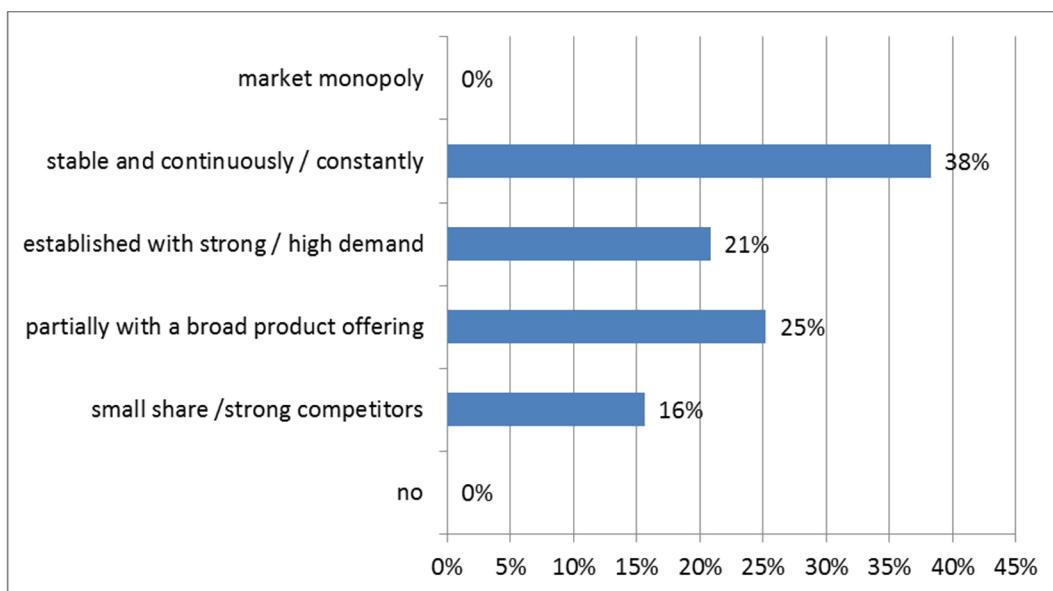
Figure 8 Position of the companies in the market
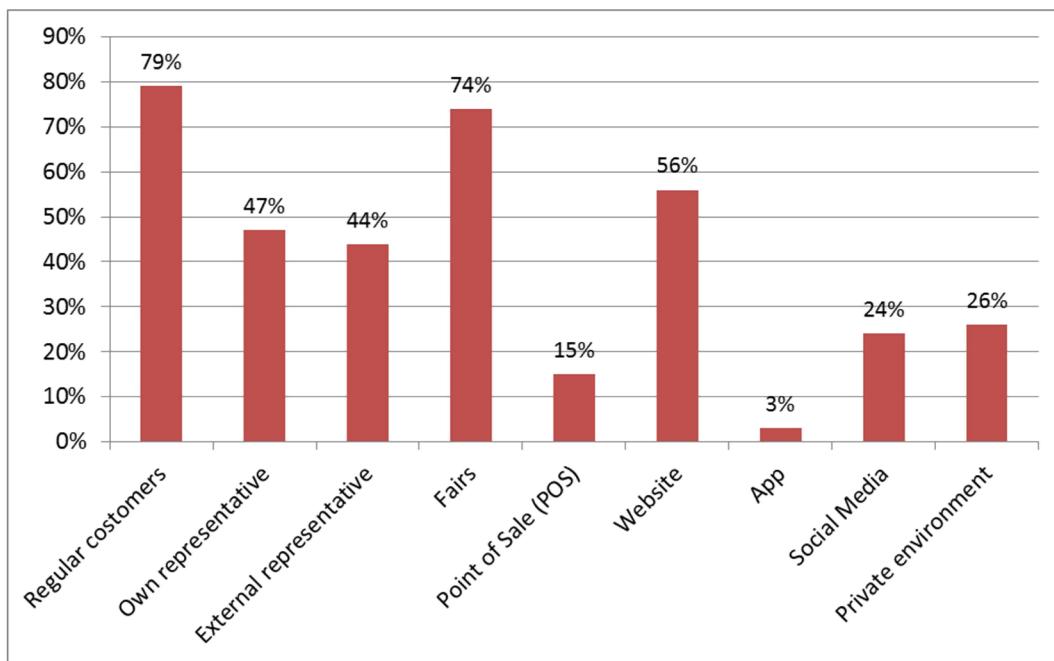
Figure 9 Kind of orders
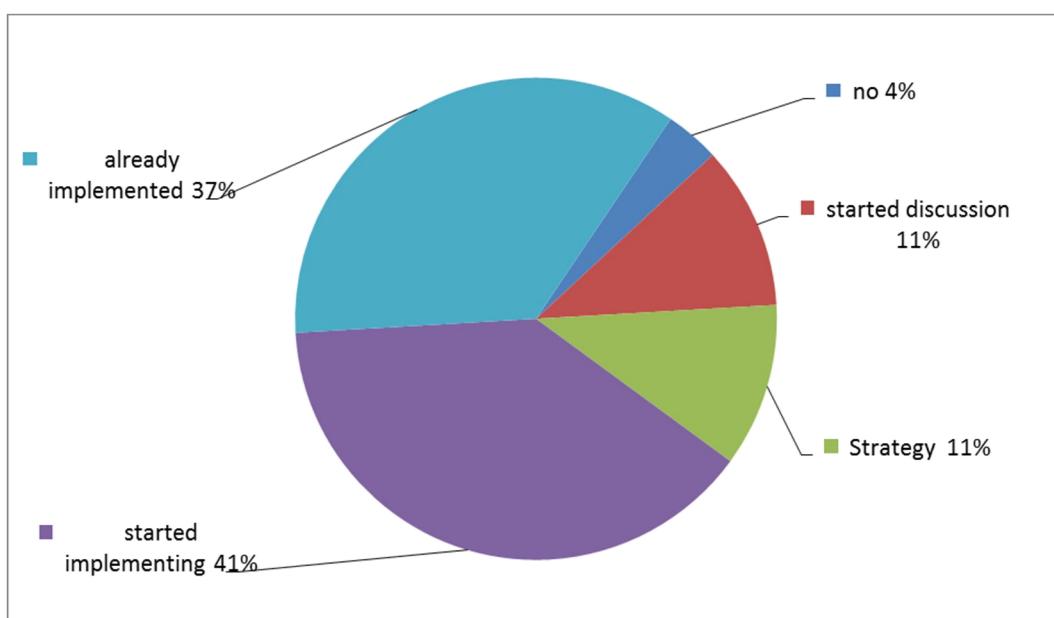
Figure 10 Approaches / Considerations for Individualization
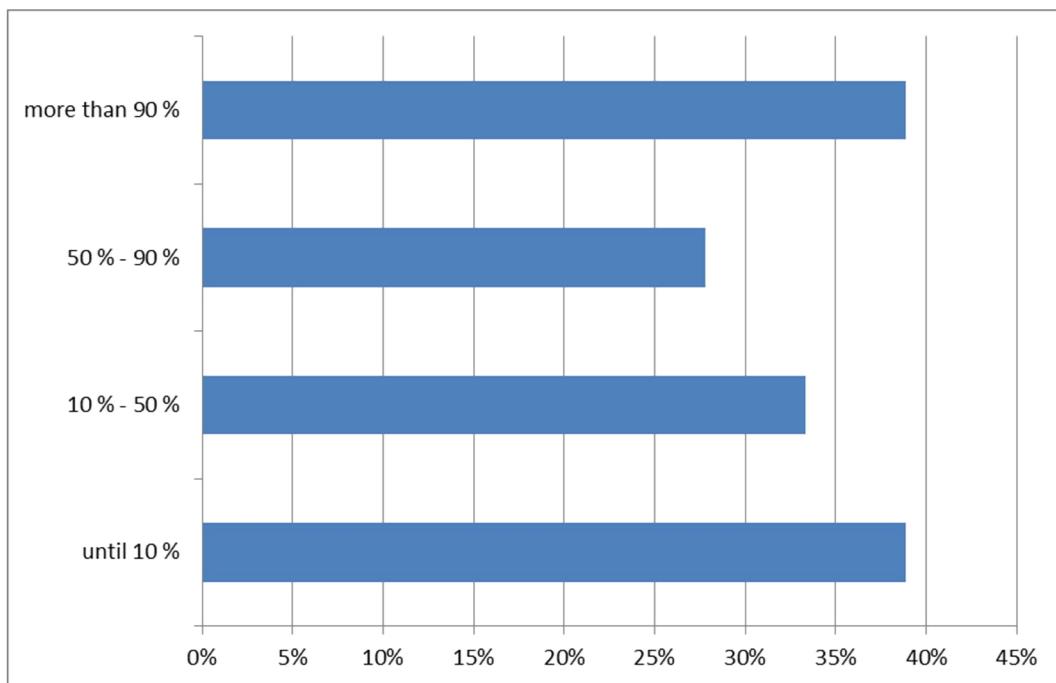
Figure 11 Proportion of special or custom-made total sales
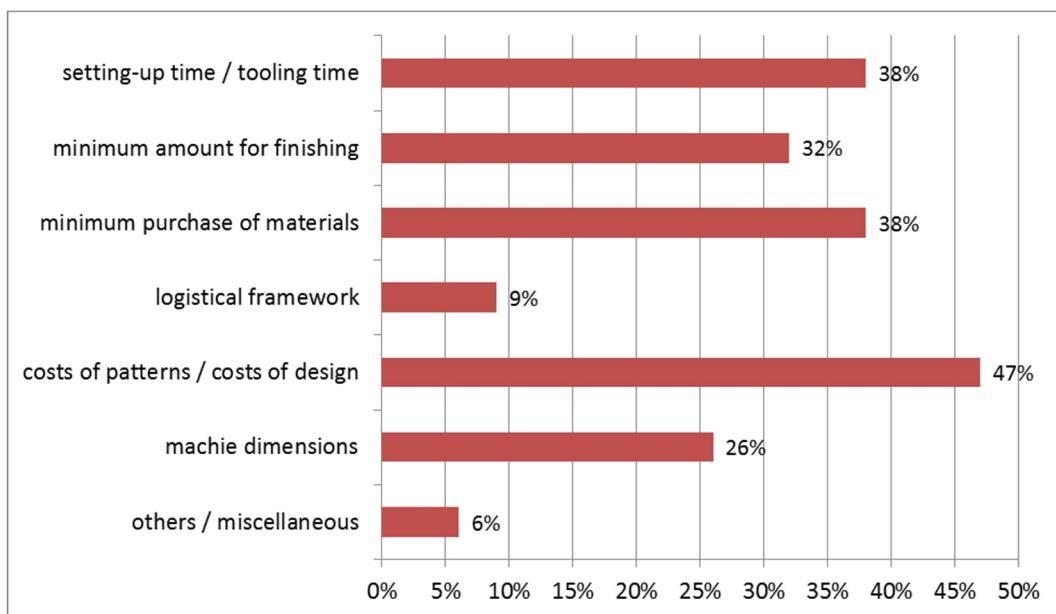
Figure 12 Problems and impediments of mass customization in companies

Figure 13 Online shop participation

4.2 Results of the qualitative data analysis

In total, 38 interviews were conducted with CEOs, sales personnel and heads of development and analyzed following the grounded theory approach by (Glaser & Strauss, 1967). This approach seems appropriate since it allows identifying new concepts and exploring new phenomena, which is particularly necessary due to the low number of studies in the addressed field. We identified two areas which constitute a hotspot for future research, namely the business models and the co-creation or rather the co-design process.

The interviews revealed that companies often underestimate the impact of the services included in their business model and the importance of them for their customers. For them, still their products are the main value drivers. On the one hand, this is correct in respect to the utility of the products. On the other hand, it is incorrect because the interviews have shown that also business customers often have to rely on the expertise of the mass customizer.

This also shows that business customers cannot always be perceived as experts, as mentioned earlier. About the complexity of the products in the B2B context also numerous business clients are not aware of or cannot handle it properly. Characteristics for technical textiles in particular need to fit together and not override each other in order to achieve the desired utility. Furthermore, the fact that textile manufacturers mainly deal with designers who are changing regularly often impedes the set-up of expert knowledge on the business customer's side. Therefore, the need for consulting services appears even more important. Furthermore, all the consulting effort is highly time intense for the corporation. Therefore, it would be necessary to standardize at least parts of this consulting process. The interviews have shown that sales people often follow a standardized procedure during the consulting phase with the customer which could be a starting point for an automation of the process. In contrast, companies stated the personal contact between the business customer and them during the consulting process to be another important value proposition. This neglects the approach to automate the entire consulting process by introducing a toolkit like a configurator for example which often is used in the B2C context (Fogliatto et al., 2012). Nevertheless, also business customers could be approached by a web-based tool asking for the purpose of the product and leading them afterwards to the relevant product characteristics. This tool would narrow down the perceived complexity for the customer. In the end, the information will be sent to the sales people, on which basis they can consult the customer more target-oriented. Thereby, the time a sales person has to invest decreases without losing the personal contact with them.

Regarding the business model, the interviews have shown so far that the companies' value propositions need to be redefined and especially the customer-supporting services have to be promoted proactively to them. Furthermore, sales personnel need to be supported in their work as well as customers in their choice by automating parts of the consulting process. The potential for improvements as well as the effectiveness of the proposed adjustments need to be investigated further and are part of future research.

With regard to the co-design process, we argue that it needs to be redesigned. We see three reasons as follows. First, in line with the latter executions, business customers are typically experts themselves and possess a relatively high degree of knowledge (Franke & Piller, 2004). Consequently, the identification of the customers'

requirements can draw on a more elaborate picture of actual customer needs. This is in line with Franke and Piller (2004) who state that toolkits (as means of eliciting needs) for B2B markets are expert toolkits that allow real innovation. From a broader perspective, the higher level of expertise of business customers calls for conceptualizing the co-design process as interaction among experts. Furthermore, the emphasis on strong technical knowledge on the provider side indicates that real expertise is needed, and systematically stressed, within the co-design process. Secondly, end customers clearly value hedonic and creative elements within the configuration process. This is in line with the outcome-related value of uniqueness or self-expression, which we propose to consider 'fun' components, since customers make use of MC voluntarily in their free time. In B2B contexts, it is typically the task of procurement personnel to source inputs professionally, which represents a different context for decision making, hence, a different design of the co-creation process seems necessary, i.e., with customer efficiency as its main goal. Thirdly, in many B2B markets personal salesforces are used to perform one-to-one marketing and personalization. Hence, the co-design process is highly dependent on the personal interaction between sales personnel of the provider organization and procurement personnel of the customer organization, which is underpinned by the commitment of learning and collaborating drawn from the literature review.

5 CONCLUSIONS

Individualization and mass customization are a big chance for the textile industry in Europe. 37% of the interviewed companies situated in the eastern part of Germany have already finalized and 41% have started with the implementation of mass customization. The most important potential was recognized in the field of Technical Textiles.

6 REFERENCES

1. Da Silveira G., Borenstein D., Fogliatto F.S.: Mass customization: Literature review and research directions, Int. J. of Production Economics 72(1), 1-13, 2001

2. da Silveira Giovani J.C.: Our own translation box: Exploring proximity antecedents and performance implications of customer co-design in manufacturing, Int. J. of Production Research 49(13), 3833-3854, 2011

3. Davies A., Brady T., Hobday M.: Charting a Path Toward Integrated Solutions, MIT Sloan Management Review 47(3), 39-48, 2006

4. Eggert A. & Ulaga W.: Customer perceived value: A substitute for satisfaction in business markets? Journal of Business & Industrial Marketing 17(2/3), 107-118, 2002

5. Fogliatto F.S., da Silveira Giovani J.C., Borenstein D.: The mass customization decade: An updated review of the literature, Int. Journal of Production Economics 138(1), 14-25, 2012

6. Franke N., Piller F.: Value Creation by Toolkits for User Innovation and Design: The Case of the Watch Market, Journal of Product Innovation Management 21(6), 401-415, 2004

7. Gebhardt Rainer: CROSSTEXNET- Textiles at the Cross Roads of New Applications, Deliverables 2.1 & 2.2, Revised version, March 2013

8. Glaser B.G., Strauss A.L.: The discovery of grounded theory: Strategies for qualitative research, New York NY u.a.: Aldine de Gruyter, 1967

9. Grönroos C.: A service perspective on business relationships: The value creation, interaction and marketing interface, Industrial Marketing Management 40(2), 240-247, 2011

10. Keränen J., Jalkala A.: Towards a framework of customer value assessment in B2B markets: An exploratory study, Industrial Marketing Management 42(8), 1307-1317, 2013

11. Osterwalder A.: Value proposition design: How to create products and services customers want, get started with, Strategyzer series, Hoboken NJ u.a.: Wiley, 2014

12. Pine II J.: Mass Customization: The New Frontier in Business Competition. Boston, Mass.: Harvard Business School. Tuli K.R., Kohli A.K. & Bharadwaj S.G. Rethinking Customer Solutions: From Product Bundles to Relational Processes, Journal of Marketing 71(3), 1-17, 2007

13. Ulaga W., Loveland J.M.: Transitioning from product to service-led growth in manufacturing firms: Emergent challenges in selecting and managing the industrial sales force, Industrial Marketing Management,43(1), 113-125, 2014

14. Ulaga W., Reinartz W.J.: Hybrid Offerings: How Manufacturing Firms Combine Goods and Services Successfully, Journal of Marketing 75(6), 5-23, 2011

15. Varga J., Scholta C., Munzert P.: Studie strategische Ausrichtung textiler sächsischer Mittelstand 2020, Chemnitz 2015

16. Vti Statistik – Verband der Nord-Ostdeutschen Textil- und Bekleidungsindustrie e.V., 2015

PLASMA AND CHITOSAN TREATMENTS FOR IMPROVEMENT OF NATURAL DYEING AND ANTIBACTERIAL PROPERTIES OF COTTON AND WOOL

A. Haji[1], M. K. Mehrizi[2] and S. Hashemizad[3]

[1]*Textile Engineering Department, Birjand Branch, Islamic Azad University, Birjand, Iran*
[2]*Textile Engineering Department, Yazd University, Yazd, Iran*
[3]*Textile Engineering Department, Yadegar-e Imam Khomeini (RAH) Branch, Islamic Azad University, Tehran, Iran*
Ahaji@iaubir.ac.ir

Abstract: *In this study, the effect of low pressure oxygen plasma treatment and subsequent chitosan treatment on the dyeability of cotton and wool fabrics is investigated. Raw, plasma treated and chitosan coated wool and cotton samples were dyed with natural dye extracted from dried cotton pods. The effect of each modification on the color strength of the dyed samples was examined and the order of the K/S for both fibers was as follows: chitosan treated > plasma treated > raw. The samples were also tested for antibacterial properties before dyeing. The samples coated with chitosan after plasma treatment showed excellent antibacterial activity.*

Key Words: *Cotton, Wool, Plasma, Chitosan, Dyeing*

1   INTRODUCTION

Recently there has been a great tendency to revive the tradition of using safe, biodegradable, and eco-friendly natural dyes [1-2]. The majority of natural colorants need metal mordants to dye wool fiber satisfactorily [3]. The metal mordants mainly are considered as toxic and researchers are exploring environmentally friendly alternatives to reduce or eliminate the use of metal mordants in natural dyeing recipes. Low temperature plasma treatment, a water-free and clean process, provides a new alternative for surface modification of textile fibers. Oxygen plasma treatment has a great influence on wettability of natural fibers and the plasma treated sample absorbs water very quickly and the water wicking and dyeability are remarkably improved after plasma treatment [1, 4, 5]. Chitosan as a natural biopolymer can be applied on cotton and wool fibers by different techniques and enhance their dyeability with anionic dyes [6]. Coating of fibers with chitosan can introduce amine groups to the fiber, leading to the improved affinity towards natural dyes.

In a paper recently published by Haji et al, cotton fabric was successfully coated with chitosan using oxygen plasma as a pretreatment. The chitosan treated samples showed better dyeability beside good build up with direct and acid dyes used in this study. The application of chitosan on cotton fabric reduced the need for electrolyte in the dyebath markedly. The optimum dyeing time for the direct and acid dye was 90 and 30 min, respectively. The wash fastness of both dyes was significantly higher in the case of chitosan treated samples [7].

Plasma treatment can impart functional properties to textiles when applied in conjunction with chitosan. In this study, the effect of low pressure oxygen plasma treatment and subsequent chitosan treatment on the dyeability and antibacterial properties of cotton and wool fabrics with natural dye extracted from the valves of capsules of cotton plant is investigated.

2   EXPERIMENTAL

Plasma treatment: Plain woven pure cotton and wool fabrics were cut in size 10x15 cm^2. Samples were pretreated using radio frequency low pressure plasma equipment (Junior plasma, Europlasma, Belgium) with oxygen gas (chamber pressure: 100 mTorr; Oxygen flow rate: 100 sccm; Plasma power: 150 W; Time: five minutes).

Chitosan treatment: Plasma treated samples were immediately impregnated in 0.5% w/v solution of chitosan containing 1% v/v acetic acid for 30 min. Padding with 100% wet pick up, drying at 80°C for 30 min and washing (1% w/v Triton X-100 in distilled water, at 50°C for 15 min) were the next steps of the coating process.

Dyeing: Dyeing of the samples was performed using 20% owf of the natural dye (L:G= 40:1, pH=5 for wool and pH=7 for cotton samples). The dyeing was started at 40°C and the temperature was raised to boil at the rate of 2°C per minute. Then the samples remained in that condition for 1 hour, and then were rinsed and air dried.

Color strength measurements: The reflectance of dyed samples was measured on a Color-eye 7000A spectrophotometer using illuminant D65 and 10° standard observer. Color strength (*K/S*) of each dyed sample was calculated using Kubelka-Munk equation:

$$K/S = \frac{(1-R)^2}{2R} \qquad (1)$$

where *R* is the observed reflectance at wavelength of maximum absorbance, *K* is the absorption coefficient and *S* is the light scattering coefficient.

Color fastness test: Color fastness to washing and to light was measured according to ISO 105-C01: 1989(E), and ISO 105-B02: 1994(E), respectively.

Scanning electron microscopy (SEM): Scanning electron micrographs were taken on an AIS2100 scanning electron microscope (Seron Technology, South Korea) to study the effect of plasma and chitosan treatments on the surface morphology of cotton and wool fibers [5, 7].

3   RESULTS AND DISCUSSION

Raw, plasma treated and chitosan coated wool and cotton samples were dyed with the same concentration of natural dye extracted from dried cotton pods. The effect of each modification on the color strength of the dyed samples was examined and the order of the *K/S* for both fibers was as follows: chitosan treated > plasma treated > raw. Figure 1 shows that the natural dye is exhausted on wool better that cotton fibers in raw, plasma treated and chitosan coated states. It can be seen that the highest color strength was obtained when the sample was pretreated with oxygen plasma, then coated with chitosan. Plasma treatment has etched the surface layer of fibers and enhanced the wettability of the samples and improved the attachment of chitosan to the surface of fibers. The attachment of chitosan introduced amino groups to the surface of cotton fibers and increased the amino groups onto wool fabric and enhanced their anionic dye uptake to a great extent [8]. The most abundant flavonoids present in the valves of capsules of cotton are glycosides of kaempferol and quercetin [9]. Figure 2 shows the chemical structures of chitosan, kaempferol and quercetin.

Figure 3 shows the effect of plasma treatment and chitosan coating on surface morphology of cotton and wool fibers.
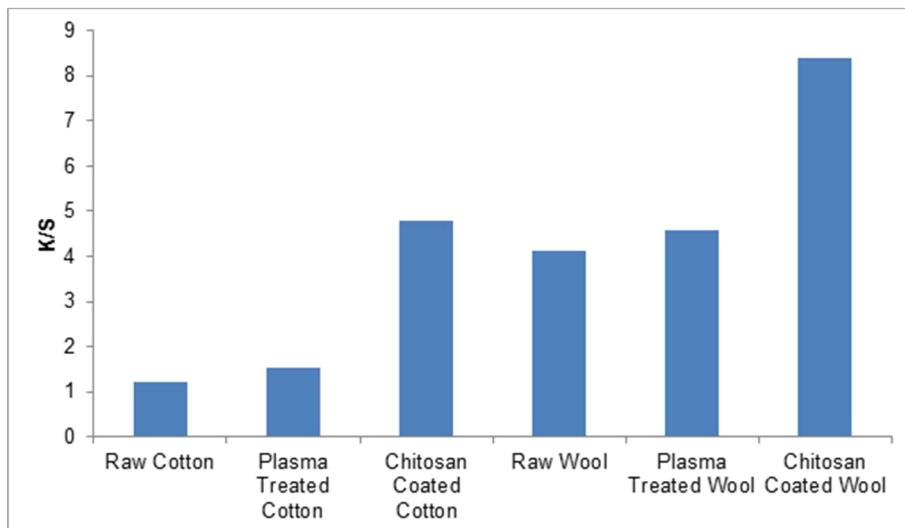
Figure 1 Colour strength of raw, plasma treated and chitosan coated cotton and wool samples
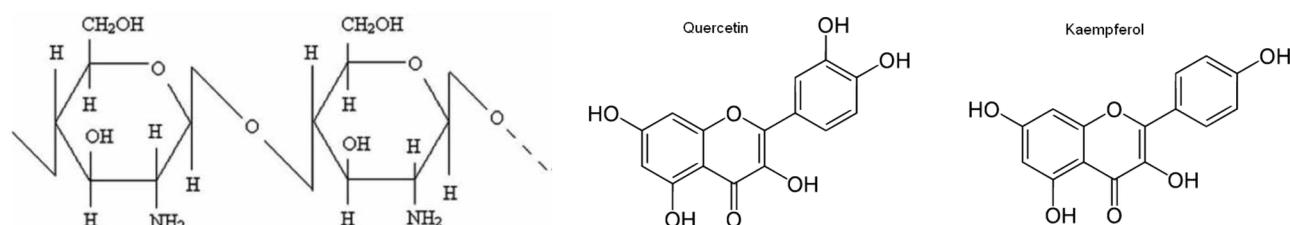
Figure 2 Structures of chitosan (left), quercetin (middle) and kaempferol (right) [10]
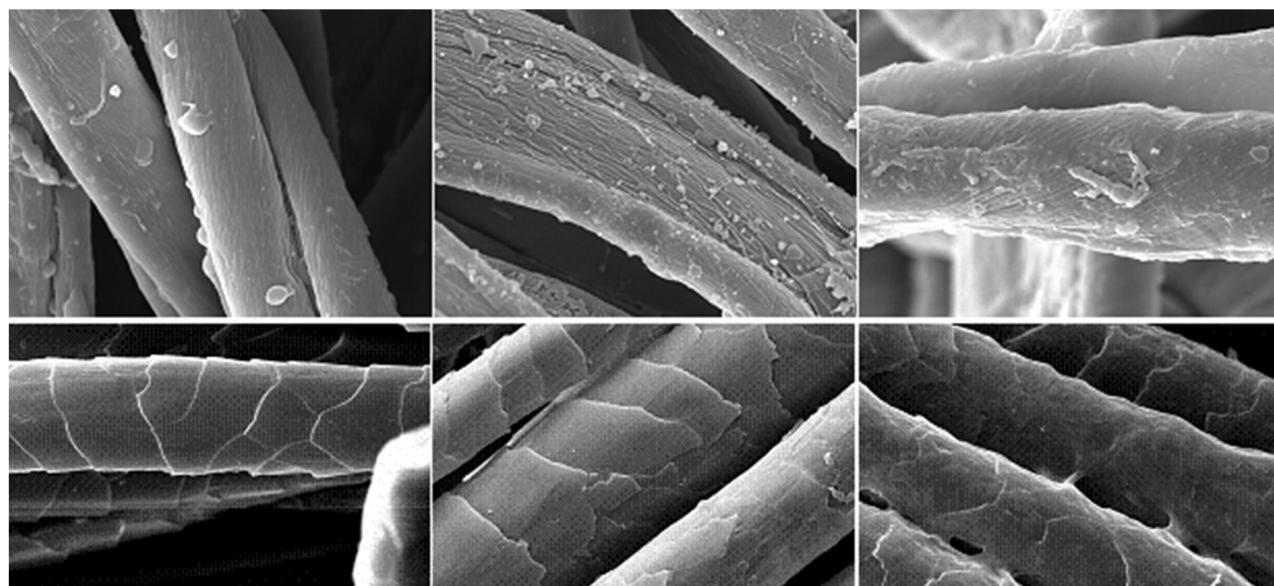
Figure 3 SEM images of (left to right) raw, plasma treated and chitosan coated cotton (top) and wool (bottom) samples

Table 1 Percent reduction in number of two bacteria on the surface of different samples

Bacteria	Raw wool	Plasma treated wool	Chitosan coated wool	Raw cotton	Plasma treated cotton	Chitosan coated cotton
S. aureus	0	0	99.9	0	0	99.9
E. coli	0	0	99.9	0	0	99.9

Table 2 The color fastness properties of samples prepared at different conditions

	Raw wool	Plasma treated wool	Chitosan coated wool	Raw cotton	Plasma treated cotton	Chitosan coated cotton
Wash fastness	4-5	4-5	5	4	4	4-5
Light fastness	7-8	7-8	7-8	7	7	7-8

Etching of wool scales and cotton surface layer after 5 min plasma treatment which can accelerate the diffusion of dye molecules into the fibers is evident. The images in the right side of Figure 2 show the surface morphology of the chitosan coated cotton and wool samples where the deposition of chitosan is visible on the surface of both fibers.

Due to antibacterial properties expected from chitosan, the plasma treated and chitosan coated samples were tested for antibacterial property and compared with the untreated sample. Both cotton and wool samples showed high antibacterial activity against both Gram negative and Gram positive bacteria after coating with chitosan. Table 1 shows the results of antibacterial test confirming the high antibacterial activity of the finished samples.

Table 2 shows the fastness properties of different samples after dyeing with the same recipe. Although the fastness properties of untreated sample were acceptable, plasma and chitosan treatments improved it. The highest wash and light fastness were obtained when the wool and cotton fabric samples were treated with oxygen plasma and coated with chitosan.

4   CONCLUSIONS

Cotton and wool fabrics were successfully coated with chitosan using oxygen plasma as a pretreatment. The chitosan treated samples showed high antibacterial activity and better dyeability with the used natural dye compared with raw and plasma treated samples. The wash fastness properties were better in the case of chitosan treated samples. The method used in this study can increase the dye uptake and wash fastness of natural dyes on cotton and wool fibers.

5   REFERENCES

1. Haji A., Qavamnia S.S.: Fibers and Polymers 16(1), 46-53, 2015

2. Haddar W., et al.: Journal of Cleaner Production 66(1), 546-554, 2014

3. Prabhu K.H., Teli M.D., Waghmare N.: Fibers and Polymers 12(6), 753-759, 2011

4. Haji A., Khajeh Mehrizi M., Akbarpour R.: Journal of Inclusion Phenomena and Macrocyclic Chemistry 81(1-2), 121-133, 2015

5. Haji A., Shoushtari A.M.: Industria Textila 62(5), 244-247, 2011

6. Jabli M., et al.: Journal of Engineered Fibers and Fabrics 6(3), 1-12, 2011

7. Haji A. Qavamnia S.S., Bizhaem F.K.: Industria Textila 67(2), 109-113, 2016

8. Gawish S.M., et al.: Journal of the Textile Institute 102(2), 180 - 188, 2011

9. Ismailov A.I., et al.: Chemistry of Natural Compounds 30(1), 1994, pp. 1-14

10. Haddar W., et al.: Industrial Crops and Products 52(0), 588-596, 2014

DEVELOPMENT OF TICK PROTECTIVE TEXTILE MATERIALS

M. Janickova[1], J. Marek[1], F. Rettich[2] and T. Bubova[2]

[1]INOTEX Ltd, Stefanikova 1208, 544 01 Dvur Kralove, Czech Republic
[2]NIPH Prague, Srobarova 48, 100 42 Prague, Czech Republic
janickova@inotex.cz

Abstract: People try to protect themselves against the annoying insects from time out of mind. Ticks are a group of parasites attacking humans and transmitting many diseases, especially Lyme borreliosis, and tick-borne encephalitis. Over the past 30 years, the occurrence of ticks and of tick-borne diseases has increased significantly. The species Ixodes ricinus is present across the whole Europe [1].

For the protection against the tick attack, people most often use chemical substances like DEET, permethrin or IR 3535-ethyl butylacetylaminopropionate. These agents are usually used in spray form and can be applied on the skin or on the clothing directly before the „possible" tick attack; the effectiveness is a few hours. Many natural substances derived from plants contain substances which can repel ticks [2-4]. The work was focused on exploration of two essential oils (eucalyptus and lavender) as the active substances for functional treatment of textiles with tick repellency. Used essential oils were obtained by steam distillation of plant materials. The efficiency of the tick repellency was tested at NIPH Prague using conventional assessment methods (Carroll test, Circular test, Fall off method). Microencapsulation technique was used for the protection and slow release of the essential oils. The possibility of using cyclodextrins as alternative carriers of repellent functional components (essential oils) on the fabric was verified.

Key Words: tick Ixodes ricinus, essential oil, repellency

1   INTRODUCTION

Vectors are small organisms that can carry pathogens between living entities and from place to place. Tick *Ixodes ricinus* covers a wide geographic area including: Scandinavia, British Isles, Central and Eastern Europe, France, Spain, Italy, the Balkans and North Africa. Occurrence of ticks has had an upward trend in recent years. *Ixodes ricinus* has also been found at higher altitude in Bosnia & Herzegovina and Czech Republic. These changes have been attributed to a combination of factors including climate change [1]. At present, Lyme borreliosis is the most commonly reported vector-born disease in these areas. Second significant human dangerous disease transmitted by ticks is encephalitis.

People have been trying for a long time to protect themselves against annoying insects. The most commonly used protection against insect bites at this moment is based on the direct spray of synthetic repellent agents (Picaridin, IR 3535, DEET, Permethrin, Fipronil).

Also some of the natural substances derived from plants (such as essential oils) show repellent activity [2-4].

Since the Middle Ages, essential oils have been widely used for bactericidal, fungicidal, medicinal and cosmetic applications. Essential oils (EOs) are easily produced by steam distillation of plant material and contain many volatile compounds, low-molecular-weight terpenes and phenolics. Some essential oils have repellent insecticidal effects on a wide variety of insects. Chemical finishing is crucial for giving textiles new functionalities and making them appropriate for special applications.

Research was focused on the application of essential oils on the textile substrate in the final finishing phase and on the selection of test method for the determination of repellent effectiveness of the treated textile substrate against ticks. Due to the fact that the volatility of EOs significantly reduces their activity during and after application, encapsulated form of essential oil was verified. Microencapsulation of a core-functional substance in a melamine wall is one of existing micropackaging techniques that enables reduction of volatility by slow release of encapsulated active substance through the thin polymeric shell [5, 6]. Active substances are encapsulated in the form of small particles of solids or droplets of liquids. Apart from the capsule wall permeability the encapsulated compound release can be determined by external conditions. In case of volatile content (like the EOs) its leakage increases with the vapour tension. This can be actuated by external effects like surface friction of the textile fabric carrier by functionalized garment wear. Beside functionality of the encapsulated core substance and the slow release sufficiency, the effective life of the protective effect significantly

depends on the durability of the capsule – textile substrate interaction.

Cyclodextrins are cyclic oligosaccharides consisting of 6, 7, or 8 (respectively) glucopyranose units. The solubility of natural cyclodextrins is very poor. However, chemical substitutions at the 2-, 3-, and 6-hydroxyl sites would greatly increase solubility. A frequently used approach is to use cyclodextrin as a "carrier" molecule to facilitate the dissolution of compounds. Cavity size is the major determinant as to which cyclodextrin is used in complexation. The cavity diameter of β-cyclodextrins has been found to be the most appropriate size; for this reason, β-cyclodextrin is most commonly used as a complexing agent. Cyclodextrins cyclic oligosaccharide structures contain a lipophilic central cavity and a hydrophilic outer surface. Hydrophobic molecules are incorporated into the cavity of cyclodextrins by displacing water. This effectively encapsulates the molecule of interest within the cyclodextrin [7]. In the textile field, CDs may find many applications such as: they can absorb unpleasant odours, they can complex and release fragrances [8]. The property of cyclodextrins to act as hosts and to form inclusion compounds with essential oils was investigated.

Determınation of tick repellency comprises an inseparable part of the study. In collaboration with the NIPH – National Reference Laboratory for Vector Control (NIPH-NRLVC) Prague, alternative tick repellency methods were investigated to specify the functional protection effectiveness of treated textiles. The true picture of protective fabric repellency was carried out by the use of Circular test [9] and Fall off method, which uses the negative geotropism of the tick crawling up on vertically hung textile swatch [10].

2   EXPERIMENTAL

2.1   Materials

The essential oils of Eucalyptus and Lavender were obtained from the E! TickoTEX project industrial partner Hofigal, Romania. DEET and 2-hydroxypropyl-ß-cyclodextrin (HP BCD) were obtained from Porta, Prague, sodium hypophosphite-SHPI (Penta).

The 100% cotton twill (bleached) fabric 175 g/m^2 was obtained from CNM Textile Ltd, Oskava (CZ), blend of 63% cotton/ 31% polyester/ 6% elastan satin (bleached) 200 g/m² from Kivanc (TR – industrial project partner). The other used agents (TexaromaCap S Eucalyptus – melamine capsules with eucalyptus oil) Texafix HY, Texafix SW,

Texawet RN) are part of Inotex textile speciality chemicals (TAA) portfolio.

Padd application of active components – W.Mathis lab. foulard. Drying/couring – lab. W.Mathis LTE hot air device.

2.2 Essential oils effectiveness

In this study two essential oils (lavender, eucalyptus) selected with respect to the recent EC biocide regulation were used [11]. As the first step, the anti-tick effectiveness of these potential natural agents was determined. Repellent effectiveness against *Ixodes ricinus* of diluted (1:9) essential oils in ethyl alcohol was evaluated by Circular test, in comparison with commonly used synthetic DEET (Figure 1).
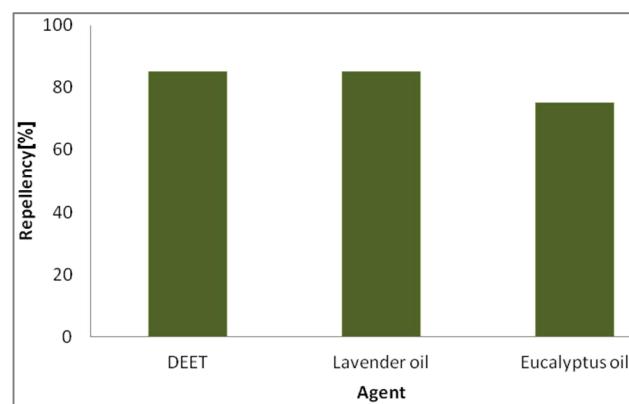
Figure 1 Comparison of tick repellency (essential oils, DEET) - Circular test on the carton

2.3 *Alternative application of essential oils on cyclodextrin pre-activated textile substrate*

To identify the efficiency of direct application of eucalyptus oil on the textile substrate and possible prolongation of repellent effect by the means of alternative embedding of EOs into β-cyclodextrin cavities, the 100% cotton fabric was treated alternatively by using the two step padding procedure under the conditions mentioned in Table 1. Each sample was wrapped separately in a polyethylene bag after the 2nd step drying and sent to NIPH testing.

2.4 Application of the encapsulated essential oil

Fabric (Co/PES/elastane blend) was treated by using the padding procedure under the conditions defined in Table 2.

Table 1 Composition of the bath and condition of application on 100% cotton – influence of B-CD pre-modification followed by 2nd step EO impregnation on the repellency of Eucalyptus/Lavender essential oil

1st step	Sample 1	Sample 2	Sample 3	Sample 4
		57 g/L citric acid 21 g/L SHPI 30 g/L HP ß CD		57 g/L citric acid 21 g/L SHPI 30 g/L HP ß CD
Wet pick up		75%		76%
Drying		10 min. 60°C		10 min. 60°C
Curing		10 min. 160°C		10 min. 160°C
2nd step				
	10% Eucalyptus oil 10% ethanol 80% distilled water	10% Eucalyptus oil 10% ethanol 80% distilled water	10% Lavender oil 10% ethanol 80% distilled water	10% Lavender oil 10% ethanol 80% distilled water
Wet pick up	78%	78%	78%	77%
Drying	35°C	35°C	35°C	35°C

Table 2 Composition of the bath and conditions of TEXAROMA CAP application on blended fabric

	Sample 5
	100 g/L TEXAROMA CAP S Eucalyptus 20 g/L TEXAFIX (acrylic co-polymer, soft) 20 g/L TEXAFIX SW (aliphatic PU dispersion) 0.5 g/L TEXAPAL RN (nonionic wetting agent)
Wet pick up	80%
Drying and curing	120°C

Presence of capsules and their homogeneous surface distribution was detected by SEM (at TU Liberec).
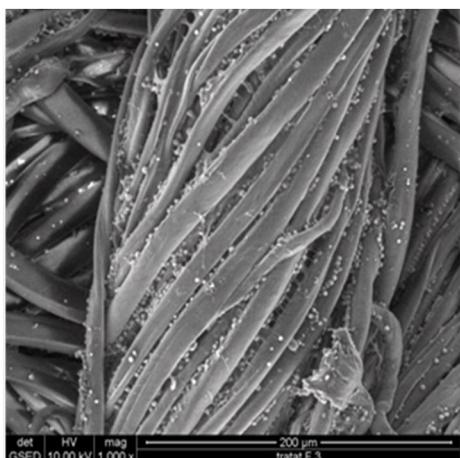
Figure 2 SEM – Sample 5 – Treated substrate (Co/PES/elastane blend) even distribution of capsules with Eucalyptus oil confirmed

3   RESULTS AND DISCUSSION

In the first stage the tick-repellency effect of the selected essential oils was confirmed. Repellency was tested after dilution, on the carton by use of simple Circular test. Obtained results confirmed (Figure 1) that both essential oils have repellency against tick greater than 70%.

The following experiments were focused on the application of the essential oils on textile substrates. The essential oils were dispersed in a mixture of ethyl alcohol and distilled water and applied on cotton substrate and on cotton substrate that was pre-modified by cyclodextrin. The testing of the effectiveness was carried out by Fall-off test. Results presented in the Figure 3 show that cotton pre-modified by cyclodextrin and post-impregnated with eucalyptus oil has the best repellency.
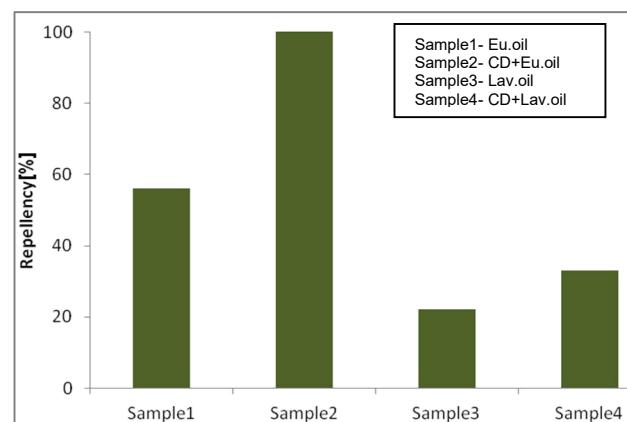
Figure 3 Fall off test – repellency of treated fabric

The critical point of this application is the efficiency decreasing with time. This is a logical consequence of the EO's volatility. Just this seems to be one of the logical attributes of their repellent effect. Figure 4 shows that the embedding treatments lost the repellent effect in three weeks. Eucalyptus oil was applied on the blended fabric construction (Co/PES/elastane) in encapsulated form.
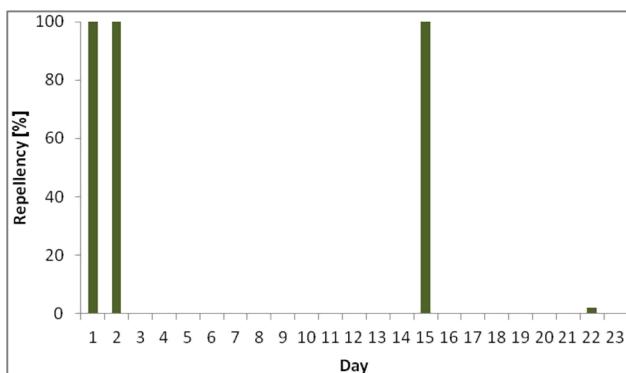
Figure 4 Fall off test – repellency of treated fabric versus time after application – Sample 2 CD + Eu.oil

In the case of encapsulated volatile EO, the positive effect of mechanical surface friction (simulated by brushing) on the repellency enhancement was confirmed.
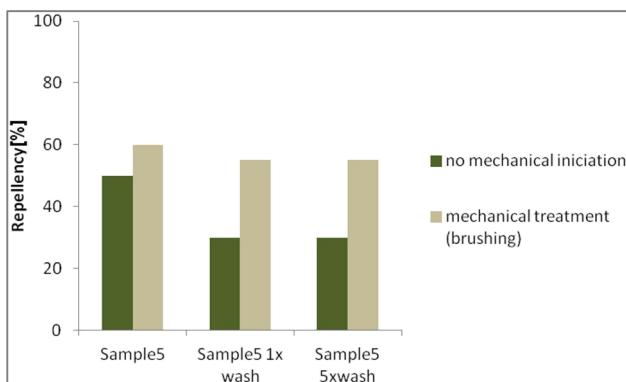
Figure 5 Fall off test - repellency of treated fabric- influence of mechanical exposure (surface friction) on the encapsulated repellent efficiency (eucalyptus oil)

4   CONCLUSIONS

This work describes the application of essential oils as the natural tick repellent substances on textile substrate as the final finishing.

Effectiveness of tested essential oils (lavender and eucalyptus – plant extracts).

The effectiveness by testing with species *Ixodes ricinus* was confirmed. The main problem is their high volatility and thus related certain technological limitation of application as a final treatment of the textile substrate. The limiting factor connected with high volatility of the essential oils as such is the loss of effect in a short time after application. Therefore the key task of this study focused on the prolongation of selected EOs effect by the means of embedding in alternative carrier structures with subsequent slow release of these repellent substances. Both studied systems – encapsulation (melamine-formaldehyde resin shell) and β-cyclodextrin pre-activation of textile substrate followed by embedding of EOs proved their

efficiency as the functionalization tools by prolongation of tick repellency. Better results were achieved by the use of cyclodextrin pre-modified substrate. Fabric treated with encapsulated eucalyptus oil shows a repellency of fifty per cent. However, this activity increases by mechanical fabric surface exposure (simulated by brushing). Gained results confirm that the risk of *Ixodes ricinus* tick attack can be reduced by functional textiles treated with natural plant-based repellent essential eucalyptus oil protecting in the moderated mode.

5   REFERENCES

1. ECDC   website,   Available   from http://ecdc.europa.eu/en/healthtopics/vectors/ticks/Pages/ixodes ricinus.aspx, Accessed 2015-10-25

2. Specos M.M., García J.J., Tornesello J., Marino P., Vecchia M.D., Tesoriero M.V., Hermida L.G.: Microencapsulated citronella oil for mosquito repellent finishing of cotton textiles, Transactions of the Royal Society of Tropical Medicine and Hygiene 104(10), 653-658, 2010

3. Sumei Fitz Gerald, Available from http://www.ehow.com/list 6550945 essential-oils-kill-ticks.html

4. Pesticides and You, A Beyond Pesticides Factsheet, Accessed: 2015-05-19, Available from http://www.beyondpesticides.org/assets/media/documents/pesticides/factsheets/oillemoneucalyptus.pdf

5. Hong K., Park S.: Melamine resin microcapsules containing fragrant oil: synthesis and characterization, Materials Chemistry and Physics 68(2), 128-131, 1999

6. Hwang J-S., Kim J-N., Wee Y-J., Yun J-S., Kim S-H., Ryu H-W.: Preparation and Characterisation of Melamine - Formaldehyde Resin Microcapsules Containing Fragrant Oil, Biotechnol. and Bioprocess Engineering 11, 332-336, 2005

7. Caligur V., BioFiles 3.3, 2008, p. 32

8. Vojcina B., Vivod V.: Chapter 3, Cyclodextrins in Textile Finishing, In Eco -Friendly Textile Dyeing and Finishing, In Tech 2013, Available from http://www.intechopen.com/books, Accessed 2015-03-15

9. Dautel H.: Test systems for tick repellents, International Journal of Medical Microbiology 293, Suppl. 37, 182-188, 2004

10. Sonenshine D.E.: Biology of Ticks, Oxford University Press, Vol. 2, 1993

11. The Biocidal Product Regulation, Available from http://echa.europa.eu/regulations/biocidal-products-regulation

COMPARISON OF THREE DIFFERENT METHODS FOR IMMOBILIZING REDOX ENZYMES ON A MULTI-FILAMENT CONDUCTIVE CARBON YARN

M. Kahoush[1, 2], N. Behary [1, 2] and A. Cayla[1, 2]

[1]*Ecole Nationale Supérieure des Arts et Industries Textiles (ENSAIT),*
[2]*allée Louise et Victor Champier BP 30329, 59056 Roubaix CEDEX 1, France*
[2]*Université Nord de France*
may.kahoush@ensait.fr

Abstract: This study focuses on the comparison of three different methods of immobilizing redox enzymes on electrically conductive carbon multifilament yarn to be used as electrodes for different applications. Glucose oxidase and Laccase enzymes were immobilized separately on conductive carbon multifilament yarns to produce anode and cathode electrodes, respectively. Three different enzyme immobilization methods were used: (M1) Adsorption on clean carbon yarns, (M2) Adsorption on carbon yarns coated with a conductive PEDOT PSS (Poly (3, 4-ethylenedioxythiophene) polystyrene sulfonate) polymer as a mediator, and (M3) Entrapment in PEDOT PSS coating on carbon yarns. The electrodes obtained by these methods were tested later in biofuel electrical cell fuelled by D-Glucose (10%) and powered by electrical voltage of 1.5 V. The maximum current value (20.5 µA) was achieved by using enzyme adsorption on carbon coated with PEDOT PSS (M2). PEDOT PSS coating brought enhanced electrical conductivity to carbon yarns in aqueous solutions and had good affinity with the immobilized enzymes. Results showed that except for the entrapment method, the current value generated is proportional to the quantity of enzyme immobilized on both electrodes in the case of enzyme adsorption methods. Finally, the current values showed to depend also on the glucose concentration and the total surface area of electrode exposed to the fuel in all cases.

Key Words: Redox enzymes, immobilization, carbon multifilament, electrodes

1   INTRODUCTION

Immobilization of redox enzymes on conductive fibres and textiles is a method that can be used to produce small size flexible equipment for use as biosensors or biofuel cells for promising applications in the fields of medicine, environment, energy production, pollution control, and in food industry. In the medical field, applications as biosensors allow monitoring of changes in physiological substances such as glucose sensing for diabetic patients. Implantable medical devices have increased the demand for the biofuel cells. In the food industry, many biosensors are used for pathogen detection. In pollution detection, biosensors are used to detect soil or air pollutants (toxic polycylic aromatic hydrocarbons (PAHs), mercury).

Electrodes of the biosensors or biofuel cells are fabricated by immobilizing Oxidoreductases or Redox enzymes (EC1) enzymes on electrically conductive supports [1]. In a biofuel cell, oxidase and reductase enzymes are immobilized on the anode and cathode, respectively. This allows the catalysis of electron transfer from one molecule (the oxidant) to another molecule (the reductant), creating an electron flow though the electrically conductive supports to produce a pulse of electricity in biofuel cells or electrical signal in biosensors. However, like all enzymes, they are affected by changes in pH and temperature which can lead to enzyme denaturation, making them lose their efficiency.

Many supporting conductive materials have been used in fabrication of electrodes (anode or cathode). Noble metals and conductive polymers charged with nanotubes have been used because they are resistant to corrosion when placed in an aqueous medium. Some conductive materials used are MWCNT/PEDOT combination, platinum black, gold coated porous silicon with nanotubes, carbon fibres, graphite and gold [2-7].

Enzyme immobilization on supporting conductive materials has been achieved using many immobilization methods like, covalent bonding, cross linking, adsorption, and mechanical confinement into the support by compression [6-9].

In some cases, a mediator is used to facilitate the electron transfer from the enzyme to the conductive support of the electrode, and hence, increase the speed of reaction. Many metal based products have been used as mediator, for example, osmium based mediators, carboxy ferrocene and vitamin K3 [2, 10, 7]. In other cases,

direct electron transfer can be achieved and no mediator is used [4, 6].

This study focuses on the comparison of three different methods of immobilizing redox enzymes on electrically conductive carbon multi-filament yarn to be used as anode or cathode electrodes for different applications such as biofuel cells and biosensors.

2   EXPERIMENTAL

2.1   Materials

The Carbon multi-filament yarn chosen in our study is HTA40 extracted from a woven Tenax®-J/E HTA40 E13. PEDOT PSS (Poly (3, 4-ethylenedioxythiophene) polystyrene sulfonate) was provided by HERAEUS - Clevios CPP 105D [11, 12]. Both Glucose Oxidase from *Aspergillus niger* - G 7141 EC (1.1.3.4) and Laccase from *Trametes versicolor* - 38429 EC (1.10.3.2) [13, 14] were purchased from Sigma-Aldrich along with D-Glucose.

2.2   Methods

2.2.1 Carbon yarns coating with PEDOT PSS

As the provided carbon multifilament yarns bear an epoxy coating in (1.3% w/w), heat treatment at 300°C for 3 hours followed by treatment with acetone using ultrasound was applied to desize the resin and clean the yarns in order to get a good electrical conductivity.

The process used to coat the carbon multifilament yarn with PEDOT PSS is the "Dip coating" process, which produces uniform and controlled thickness of film coating as a function of speed of yarn withdrawal. The 10 cm long carbon yarn was completely dipped in the conductive polymer, and then withdrawn at constant speed. As the withdrawal speed increases, so does the mass drain in the same time interval. Equation 1 relates the PEDOT PSS coating thickness to other parameters [15]:

$$h = C \sqrt{\frac{\mu U}{g\rho}} \qquad (1)$$

where h is the thickness (µm), U is the withdrawal speed (mm.min^{-1}), C is a function of the capillary number, ρg is the weight per unit volume and μ is the coefficient of viscosity.

Hence, to obtain a thin coating, the withdrawal speed used was fixed to 35 mm.min^{-1}.

2.2.2 Enzyme immobilization

Three different immobilization methods were used to fix both enzymes (Glucose Oxidase and Laccase) on desized carbon yarn (Figure 1):

1. Adsorption on clean carbon yarn (M1).

2. Adsorption of enzyme on PEDOT: PSS coated carbon yarn (M2).

3. Coating with enzyme entrapped in conductive mediator PEDOT: PSS (M3).
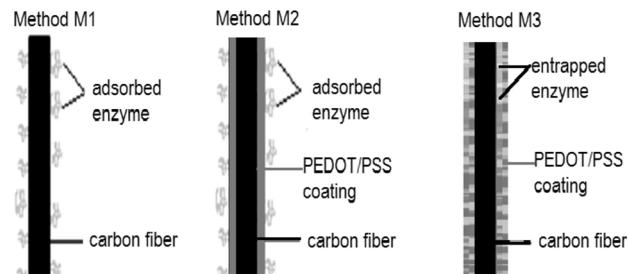
Figure 1 The three types of enzyme immobilization methods used on conductive carbon yarns

By adsorption

A 10 cm long carbon multifilament yarn was placed in 5 mL of enzyme solution of a 1 mg.mL^{-1} concentration (138.4 U.mL^{-1} for Glucose Oxidase and for Laccase, 0.62 U.mL^{-1}) at pH=5.5 for Glucose Oxidase and pH=4.5 for Laccase and 4°C for 24 hours. The yarn with adsorbed enzymes was then rinsed in successive water baths, each containing 12 mL of distilled water for 10 minutes, to remove all releasable non fixed enzymes. The carbon yarn was then hanged and dried at 4°C for 3 hours. All carbon yarns with immobilized enzymes (electrodes) were kept at 4°C until use. The amounts of enzymes in the residual solutions after adsorption, as well as in the rinsing baths, were quantified. The same enzyme adsorption procedure was used for the dried PEDOT PSS coated carbon yarn (see section 1).

By entrapment

0.125 g of each enzyme (17.3*10^3 U of Glucose Oxidase and 77.5 U of Laccase) was dissolved in 2.5 mL of distilled water (pH=5.5 for Glucose Oxidase, pH=4.5 for Laccase). This 2.5 mL of enzyme solution (5% enzyme) was mixed with 2.5 mL of pure PEDOT PSS. Each carbon yarn was placed in the resulting solution for 5 minutes, shaken to remove excess enzyme solution, and then hanged to dry at 4°C.

Electrode weight was recorded in each step in order to determine the amount of enzyme fixed.

2.2.3 Electrical set-up

Electrodes with immobilized Glucose Oxidase were used as anodes because of the enzyme's ability of catalysing oxidation reaction of D-Glucose, with release of electrons as shown in equation 2.

Electrodes with immobilized Laccase were used as cathodes because of the Laccase's ability of catalysing reduction reaction of oxygen which

captures electrons to form water as shown in equation 3.

$$D\text{-Glucose} \rightarrow \text{Gluconic acid} + 2e^- + 2 H^+ + O_2 \quad (2)$$

$$\tfrac{1}{2} O_2 + 2e^- + 2 H^+ \rightarrow H_2O \quad (3)$$
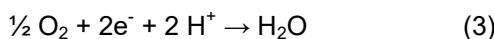
2.2.4 Quantifying enzymes immobilized

To quantify the enzyme amount immobilized on each carbon yarn, the following formula (4) was used:

$$Q_I = Q_M - Q_W \quad (4)$$

Q_I - theoretical quantity of enzyme immobilized and fixed on carbon yarn (mg)

Q_M - Total Quantity of enzyme in the initial enzyme solution (before sorption) (mg)

Q_W - Quantity of enzyme eliminated during rinsing from the carbon yarn (mg)

Calibration curves were used to quantify the activity of different concentrations of enzymes in presence of a determined amount of substrate after a determined time interval. These curves allowed quantifying free enzyme in aqueous solutions.

Quantifying the amount of free Glucose Oxidase

The Glucose oxidase used in the experiments has a maximal UV absorption at wave length of $\lambda=280$ nm. A UV spectrophotometer scanner was used (UV-Vis Scanning UV-3100PC Spectrophotometers) to determine the UV absorption of different concentrations of aqueous enzyme solution at pH 5.5, and from these values, a calibration curve was plotted.

Quantifying the amount of free Laccase

To quantify the Laccase quantity in a solution, Malachite Green dye was selected as a substrate because it is decolorized by Laccase enzyme. Indeed, this enzyme can cause decolorization of the dye by up to 96% [16, 17]. 0.018 g/L of Malachite Green has an absorption ≈ 1, at a maximum absorption wave length $\lambda=616$ nm. A calibration curve was plotted by measuring the absorbance of the dye solution after degradation of 1 mL of 0.018 g/L of Malachite Green with 1 mL of varying concentrations of Laccase enzyme, at 40°C for 1 hour. A UV-Vis Scanning UV-3100PC Spectrophotometer was used to measure the absorption at $\lambda=616$ nm.

2.2.5 Electrical characterization

An electrical energy source KEITHLY: 617 Programmable Electrometer and the complementary software was used. Tweezers were attached on one end to the electrical supply and the other end was fixed to each electrode. A 6 cm length of each of these electrodes was immersed in 15 mL of fuel solution in a glass U-tube as shown in Figure 2.
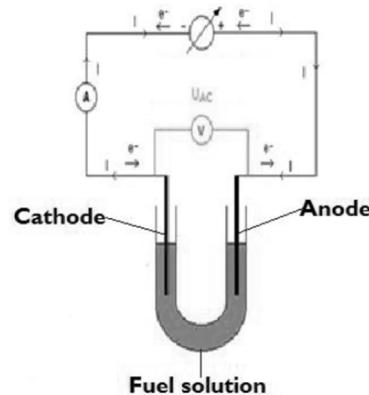
Figure 2 Electrical circuit used fueled by D-Glucose (10%) and powered by electrical voltage of 1.5 V

3   RESULTS AND DISCUSSION

3.1 Effect of electrode length

To choose the working length of the electrodes, several lengths were tested for both clean carbon yarns and yarns coated with PEDOT PSS without immobilized enzymes (6000 monofilaments per multifilament yarn with a monofilament diameter 7 μm), and using an electrolyte solution (aqueous NaCl 0.1 M). For electrodes with a working length of 4 cm and 6 cm, the calculated surface area was 0.005 m^2, and 0.008 m^2 respectively. The 6 cm electrodes gave better current values: 0.148 mA and 0.531 mA for the clean and coated electrodes respectively, compared to 0.132 mA and 0.490 mA for the shorter 4 cm electrodes. The results obtained show clearly that the longer is the electrode used, the lower is the cell resistance, and the higher the electrical current generated.

The electrode length of 6 cm was selected for all the experiments for the three methods of immobilization.

3.2 Effect of Glucose concentrations on the Electrical current generated

The impact of Glucose concentration on the cell performance and the currents generated for the three immobilization methods was studied for three different concentrations of aqueous glucose solutions (2.5%, 5% and 10%). From the results shown in Figure 3, it can be observed that the higher the glucose concentration, the higher the electrical current for the three different methods of enzyme immobilization. Above 10% glucose, no further increase in electrical current is detected. Moreover, for the entrapment method, maximum current is obtained using 5% Glucose solution. Very small increase occurs with 10% Glucose.
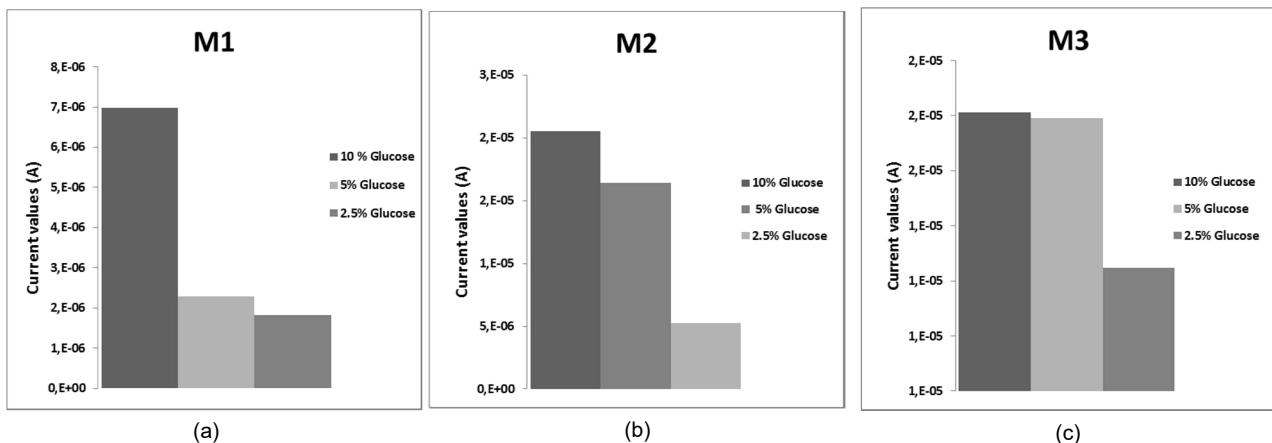
Figure 3 Effect of Glucose concentration on the current, for the different methods of enzyme immobilization (a) adsorbed on carbon (M1), (b) adsorbed on coated carbon with PEDOT (M2) and (c) entrapped in PEDOT (M3)
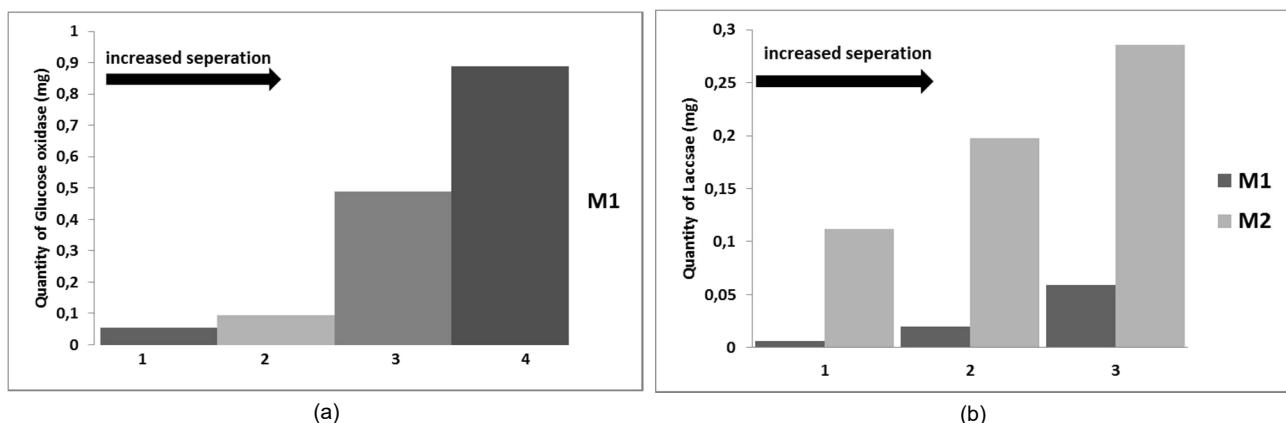
Figure 4 Quantities of immobilized enzymes on different batches of electrodes (a) Glucose Oxidase by method M1, (b) Laccase by methods M1 and M2

3.3 The quantities of the enzymes immobilized on carbon yarn electrodes

3.3.1 Using adsorption method

The results shown in Figure 4 present the quantity of Glucose oxidase and Laccase enzymes immobilized by (M1) and (M2) methods. Varying amounts of enzymes could be adsorbed on clean carbon yarns according to the different separation levels between the filaments; this is shown in the results by means of a high dispersion around the mean value. The amounts of enzymes adsorbed by (M2) method tend to be higher than the amount adsorbed by (M1) method.

3.3.2 Using entrapment method

The quantity of enzymes immobilized by the method of entrapment in PEDOT PSS coating was calculated by measuring the weights of the fibres before and after coating in the wet state. Hence, the amount of the enzyme entrapped within the polymer is proportional to its percentage in the original coating mixture; which is 2.5% of enzyme. Results show that the amounts obtained

from both enzymes used are close. This indicates that the amount of enzyme immobilized by this method is better controlled than the adsorption method.

3.4 The electrical data analysis of the electrodes obtained by the three methods of enzyme immobilization in 10% Glucose solution

From the results shown in Figure 5, electrodes obtained by the adsorption of enzyme on PEDOT PSS coated carbon yarn (M2), yield the highest electrical current (20.5 µA) in comparison with enzyme entrapment method (M3) (15 µA) and the enzyme adsorption on clean carbon yarns (M1) (7 µA).

Figure 6 shows the electrical current as a function of increasing voltage for the three immobilization methods. The cell resistance can be calculated from these plots using Ohm's Law in the linear curve case; hence, the gradient of the linear line indicates the inverse of the cell resistance. The calculated resistance values are shown

in Figure 7. It can be shown clearly that the resistance of the cell obtained by the (M1) method is the highest, whereas the lowest resistance is obtained by the (M2) method.
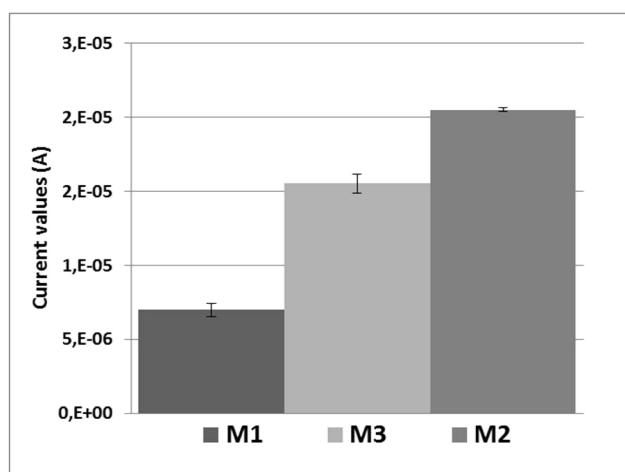
Figure 5 Electrical current recorded for the three immobilization methods for electrical voltage of 1.5 V and 10% D-Glucose
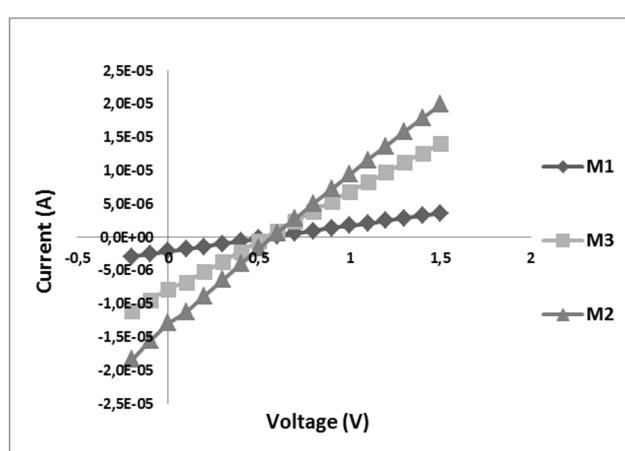
Figure 6 Current evaluation with the voltage
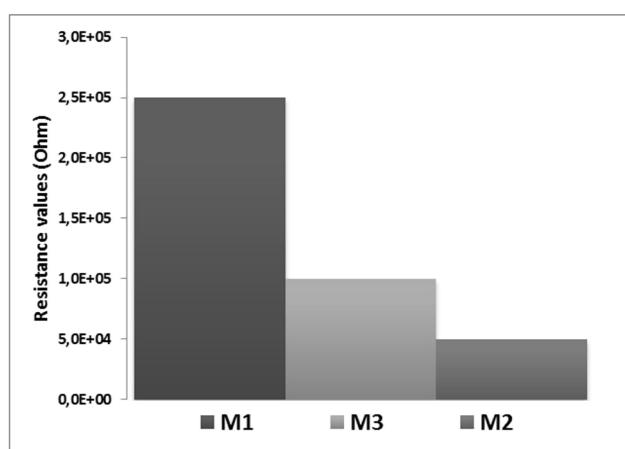
Figure 7 Cell resistance

3.5 Influence of electrolyte (NaCl 0.1M) on the electrical behaviour of electrodes with immobilized enzymes

A study was carried out to understand the influence of 0.1 M electrolyte (NaCl) on the electrical current measured using electrodes with immobilized enzymes. The three methods of enzyme immobilization were compared. In the cell used, the results shown in Figure 8a indicate clearly that the use of NaCl electrolyte in a weak concentration (0.1 M) enhances the electrical current of the biofuel cell for the three enzyme immobilization methods used.

When the electrical currents (generated at 1.5 V) are compared for electrodes with or without immobilized enzyme (Figure 8b), it is clear that activity of immobilized enzymes enhances electrical conductivity of electrodes in the presence of NaCl electrolyte.

3.6 Discussion

Our study shows that biocatalytic active electrodes can be obtained from the three immobilization methods used (M1, M2 and M3). The success of this process showed to be dependent on many factors like the specific surface area, the substrate concentration and the quantities of the immobilized enzymes.

Indeed, increased surface area for which a long electrode with sufficiently separated filaments is used allows more interfacial areal contact between the carbon yarns and the enzyme solution, hence higher quantities of enzymes are immobilized. Furthermore, when these electrodes are exposed to the substrate solution, higher rates of electron exchange occur especially for adsorption methods, where there is a direct contact between the immobilized enzymes and the substrate solution.

It is clear from our results that coating with the conductive polymer PEDOT PSS increases the electrodes' conductivity in the aqueous solutions by accelerating electron transfer process (resistance value: 1250 Ω and 10000 Ω in NaCl solution and in air respectively). Furthermore, swelling of the PEDOT PSS film coating, caused by hydrophilic PSS surrounding the hydrophobic PEDOT, may allow this higher adsorption or diffusion of enzyme at the outer surface of the coating.

Concerning the substrate concentration in the methods M1 and M2, when the Glucose concentration increases, more substrate can directly access the active sites of the immobilized enzymes, which results in higher electrical currents obtained. However, when all the enzymes' active sites are occupied for a certain moment, the increased Glucose concentration does not give any augmentation of the electrical current.
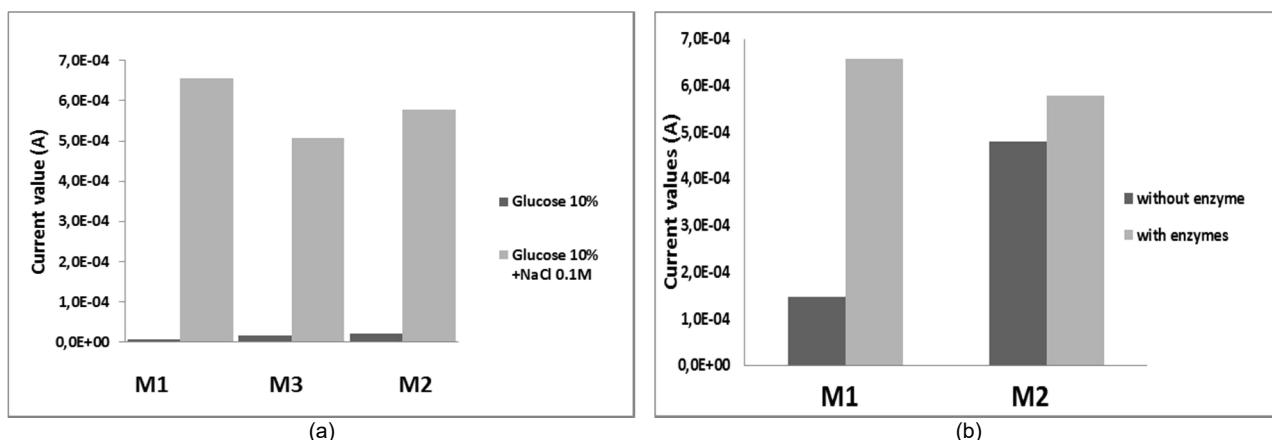
Figure 8 Effect of added NaCl 0.1 M to the fuel on the current obtained (a) comparison between the presence and absence of NaCl, (b) the combined effect of enzymes and electrolyte

For the entrapment method M3, time is needed for the Glucose to diffuse through the conductive polymer to reach the enzyme, and that limits the amount of enzymes available and consequently limits the amount of electrons generated over specific time intervals. Hence, increasing concentration of the Glucose solution does not increase the current value accordingly, which is considered as a limitation for this method.

The obtained results show that the quantities of the enzymes immobilized by the method M2 are greater than in method M1, which refers to the good affinity of PEDOT/PSS with the enzymes due to its composition of a mixture of cation/anion without blocking the active sites.

The method M3 enabled to fix higher amounts of enzymes on the yarns than the other methods, but the electrical current measured at 1.5 V was not the highest. Indeed, enzymes entrapped in the polymer matrix need the polymer to be swollen so that there can be an easy access of the Glucose to the active sites of entrapped enzymes. In this case, the diffusion time factor can play an important role in determination of the current evaluation.

The use of NaCl electrolyte was studied because it is interesting in the biofuel cells and sensors that may be oriented toward health issues, due to its natural presence in the body and blood.

As can be seen from the results, the presence of electrolyte reduces the resistance of the Glucose solution and enhances the ability of the fuel solution to allow the current to pass. Furthermore, the oxidation/reduction reactions that happen at the electrodes enhance the effect of the oxidation and reduction obtained by the immobilized enzymes, which increase the potential difference between the cathode and anode above a certain threshold to generate electrical current that can be measured. The electrolyte is a substance that can be ionized when it is put in a proper solvent,

and this gives the electrolyte solution the property of electrical conductivity.

4 CONCLUSIONS

Three different enzyme immobilization methods were successfully achieved. Immobilization by adsorption on the carbon coated with PEDOT/PSS yielded the highest electrical current. Electrical current values depend on the quantities of immobilized enzymes, also on the glucose concentration and the total surface area of electrode exposed to the fuel. The electrodes obtained by these methods aim to be used later in biofuel cells and for biosensing applications which are interesting and promising areas of research oriented towards better health and environment in the future.

5 REFERENCES

1. A Medical Terminology Dictionary Published at the Dept. of Medical Oncology, University of Newcastle upon Tyne © Copyright 1997-2005

2. Kwon C.H., Lee S.-H., Choi Y.-B., Lee J.A., Kim S.H., Kim H.-H., Kim S.J.: High-power biofuel cell textiles from woven biscrolled carbon nanotube yarns, Nature Communications 5, 3928, 2014, doi:10.1038/ncomms4928

3. Jia W., Wang X., Imani S., Bandodkar A.J., Ramirez J., Mercier P.P., Wang J.: Wearable textile biofuel cells for powering electronics, Eneregy & Environmental Science, doi:10.1039/c4ta04796f, 2012

4. Wang S.C., Yang F., Silva M., Zarow A., Wang Y., Iqbal Z.: Membrane-less and mediator-free enzymatic biofuel cell using carbon nanotube/porous silicon electrodes, Electrochemistry Communications 11(1), 34-37, 2009, doi:10.1016/j.elecom.2008.10.019

5. Mano N., Mao F., Heller A.: A miniature membrane-less biofuel cell operating at +0.60 V under physiological conditions, ChemBioChem 5, 1703-1705, 2004, doi:10.1002/cbic.200400275

6. Ramanavicius A., Kausaite A., Ramanaviciene A.: Enzymatic biofuel cell based on anode and cathode powered by ethanol, Biosensors and Bioelectronics 24, 761-766, 2008, doi:10.1016/j.bios.2008.06.048

7. Togo M., Takamura A., Asai T., Kaji H., Nishizawa M.: An enzyme-based microfluidic biofuel cell using vitamin K3-mediated Glucose oxidation, Electrochimica Acta 52, 4669-4674, 2007, doi:10.1016/j.electacta.2007.01.067

8. Willner I., Arad G., Katz E.: A biofuel cell based on pyrroloquinoline quinone and microperoxidase-11 monolayer-functionalized electrodes, Bioelectro-chemistry and Bioenergetics 44, 209-214, 1998, doi:10.1016/S0302-4598(97)00091-3

9. Zebda A., Cosnier S., Alcaraz J.P., Holzinger M., Le Goff A, Gondran C., Cinquin P.: Single Glucose biofuel cells implanted in rats power electronic devices, Scientific Reports 3, 1516, 2013, doi:10.1038/srep01516

10. Liu Y., Dong S.: A biofuel cell harvesting energy from Glucose-air and fruit juice-air, Biosensors and Bioelectronics 23, 593-597, 2007, doi:10.1016/j.bios.2007.06.002

11. "Toho Tenax Europe GmbH, Tenax®-J/E HTA40 E13," 2011

12. C. P. Division, "Clevios^{TM} p form. cpp105d," no. 81076866, 1-3, 2011

13. "Glucose Oxidase from Aspergillus Niger -G 7141, Sigma-Aldrich," vol. 3802, 6-7, 1990

14. "Laccase from Trametes versicolor TruPAGE TM Pre cast Documentation", 6-8, 2015

15. Horowitz and Michels: Optical monitoring 47(13), 1790-1794, 2005

16. Balan K., Sathishkumar P., Palvannan T.: Decolorization of malachite green by laccase: Optimization by response surface methodology, J. Taiwan Inst. Chem. Eng. 43(5), 776-782, 2012

17. Maalej-Kammoun M., Zouari-Mechichi H., Belbahri L., Woodward S., Mechichi T.: Malachite green decolourization and detoxification by the laccase from a newly isolated strain of Trametes sp., Int. Biodeterior. Biodegrad. 63(5), 600-606, 2009

COMPARISON OF DIFFERENT METHODS USED FOR COLOR MEASUREMENT OF COTTON

N. Khan, M. Vik and M. Vikova

Department of Material Engineering, Faculty of Textile Engineering, Technical University of Liberec
Studentska 2, Liberec 46117, Czech Republic
nayab.khan@tul.cz

Abstract: Economic value of cotton fiber is by far superior to that of any other natural fiber. And when it comes to trade, cotton fiber and its value added products, the grading of cotton fiber is of high importance which depends upon different properties. Color is one of those important properties which play a vital role in the cotton selection. Currently used system for the color classification in the cotton world is not that much reliable when keeping in view the importance of fiber. Mostly before the purchase of cotton fiber, a professionally trained visual cotton inspector gives grade to the cotton which is later on confirmed in the mills by HVI which measures Rd and +b values in order to grade the cotton fiber. The grade given by visual inspection not only varies from the HVI grading but, also has contradiction among the cotton classers who are professionally trained. In this study we will try to find out the relationship between the visual classification and the instrumental classification of cotton fiber by keeping in view the universal standards for cotton grading. So, different instrumental methods for color measurements will be used and their relationships will be the main objective of the study.

Key Words: cotton, Rd, +b, HVI, Non-contact method

1   INTRODUCTION

Globally the classification of cotton is done by the AMS of the United States department of Agriculture (USDA) by using the HVI. Although there are different parameters measured by HVI unit like fiber length, length uniformity, micronaire, trash content and color. The properties of color which are measured by the HVI are *Rd* and *+b*. For the color analysis of cotton fiber, the HVI unit uses a camera based system with two broad band filters (two wavelengths) to determine *Rd* and *+b*. The AMS supplies two sets of cotton standards for the HVI color measurement – a set of five ceramic tiles and a set of 12 uniform cotton batts. There is no doubt that HVI does a very good job but it is also true that the parameters of cotton measured by the HVI are specific to cotton only. And the origin of these values dates back to the 1930s.

Parameters of cotton do not relate to the other well-known and globally recognized color systems like CIELAB, where *L** is the lightness, *a** is the redness/greenness and *b** is the blueness/yellowness of the sample. As a two wavelength based system, the HVI does not include information about other regions of the color space which might play a vital role in the cotton color measurement. The values of the specific wavelengths used are proprietary to Uster and it was not possible for the others to have access to these values. If these improvements can be added into the HVI, then this system will be a much improved color analysis system for the color evaluation of cotton fiber [1]. Modern spectrophotometers and colorimeters include diffuse reflectance measurements of the sample over full visible spectral region of the electromagnetic spectrum (at minimum, 400-700 nm), they use globally recognized color systems and units, and an NIST traceable white standard.

The Nickerson equations for *Rd* and *+b* are:

$$Rd = 100Y \qquad (1)$$

$$+b = 70fy(Y - 0.847Z) \qquad (2)$$

$$Fy = 0.51[(21 + 20Y)/(1 + 20Y)] \qquad (3)$$

where *Y* and *Z* are the tristimulus color parameters *Y* and *Z* (Illuminant C, 2° Observer).

So, the direct use of color spectrophotometer for the cotton color measurement of parameters *Rd* and *+b* is not that simple because the advanced spectrophotometer is capable of examining the entire visible region (400-700 nm) while on the other hand the HVI is only a two filters colorimeter, as we mentioned earlier. Thus, direct measurement of *Rd* and *+b* is not possible, so the internationally recognized three dimensional color space system has been used. Primarily the color system based on tristimulus color (*XYZ*) [2].

There are some problems connected with color measurement using the HVI, which uses a two-dimensional system: the (*Rd*) and (*+b*) to assess the color of a sample and the color grade. However, the HVI approach is insufficient in comparison with visual human perception. HVI color results are correlated with the visual grading, but the agreement between the HVI and the classer grading is not satisfactory. Although the HVI is used all over the world for the grading of cotton, be it the color property or other properties of the cotton fibers, but as far as the color property is considered, the final grading of cotton was performed by the grader till the end of 2000. Using standard tiles and cotton batts provided by the Agricultural Marketing Service (AMS) of the USDA, color results of a series of color spectrophotometers have established good correlations between standard CIE color parameters and HVI colorimeter color parameters ($L^* \leftrightarrow Rd, b^* \leftrightarrow +b$) [3]. L^* is normally higher than *Rd*, whereas a very good agreement is observed between b^* and *+b*. Good to excellent agreement was observed between bench and portable color units but the color agreement was decreased when glass was used. The use of non-contact method for the color measurement of cotton fiber is still not in use in the cotton industry. In the previous study, a comparative evaluation was performed to establish a relationship between the HVI Rd and *+b* and portable spectrophotometer *L*a*b** and *XYZ* color parameters with Illuminant D65 and C and at the degree of observer of 10° and 2° [4]. And it was found that there was an excellent linear relationship between the given parameters [5].

2   EXPERIMENTAL

In this experiment, 5 ceramic tiles and 12 cotton sample (standards) were used. These standards were provided by the AMS USDA. These ceramic tile standards were well prepared and possessed a smooth surface for the evaluation. White, Brown, Yellow, Grey and Central, these five colors for set of box were provided with the standards readings. Figure 1 shows the standards and samples used for the measurement.

The ceramic tiles were measured with the HunterLab MiniScan portable color spectrophotometer. As discussed earlier, AMS provided the HVI *Rd* and *+b* values as reference values, then the data obtained from the HunterLab MiniScan were compared with the provided data. For all the measurements, five replications were made and average per sample was taken; then average HunterLab values were compared with the HVI values. All the measurements were performed at the laboratory conditions (70±2°F and 65±2% RH).
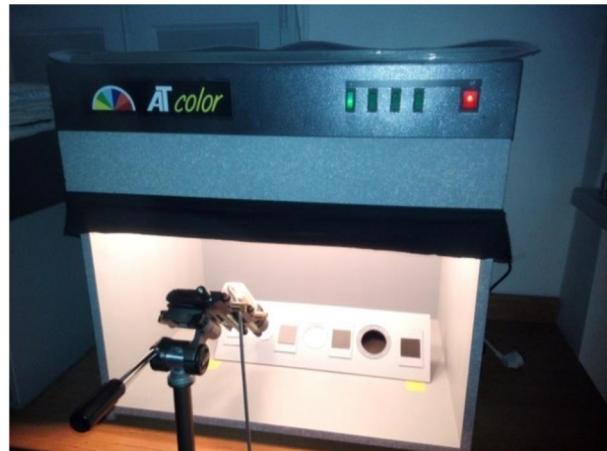
Figure 1 Non-contact method used for testing

Figure 2 AMS standards Ceramic tiles which are used for the HVI calibration (Left to right: White, Brown, Yellow, Grey, Central)

For the visual grading of cotton, samples in a light cabinet AT color were used and common observers were invited for the color measurement of cotton samples instead of professionally trained cotton classer. These observers were asked to grade the cotton samples by taking the ceramic tiles as reference measurement. Five replications again were taken from each observer on five different days. Each observer was fully aware of the international cotton grading system but they never performed cotton grading so they were just common people. This phenomenon was performed for a set of standards (xenon, incandescent) to measure the non-contact method color measurement. Konica Minolta CA-210 was used for telescope measurement in the Laboratory of Color and Appearance Measurement, Technical University of Liberec. An illuminant D65 was used at the 2° observer. As this is a non-contact method, the distance from the probe of the telescope and the sample was 7 cm. A light cabinet as mentioned

earlier was again used to illuminate the sample and the readings of *x, y* and *Lv* were taken. We used some color space conversion calculations to convert these readings into the *Rd* and *+b* values and then the relationship between the visual grading and non-contact method was studied. So, two relationships are studied here: in the first relationship it was studied whether the HVI standard provided by the AMS, Memphis TN has a relationship with the non-contact measurement method, and then the visual inspection was compared with the instrumental color measurement taken in the laboratory by taking the AMS standards as reference standards. The spectral values of the cotton samples were taken from HunterLab and were used for the conversion of *Rd* values in the color space conversion formulas. The new telescopic method is never used in the cotton color measurement which can be called the Non-contact method.

3   RESULTS AND DISCUSSION

For the AMS standard ceramic tiles, the reference *Rd* values were obtained from the master HVI-1000 colorimeter in Memphis, TN. The HVI colorimeter uses two filters to measure the samples diffuse reflectance at two visible spectrum regions and the value of *Rd* and *+b* obtained from Uster algorithms. In the Laboratory of Color and Appearance Measurement at the Technical University of Liberec, two sets of tiles were measured again with the non-contact method. One set with incandescent and the second with xenon light source. Then the values of *Rd* and *+b* were compared with the HVI-1000 and with the non-contact method.
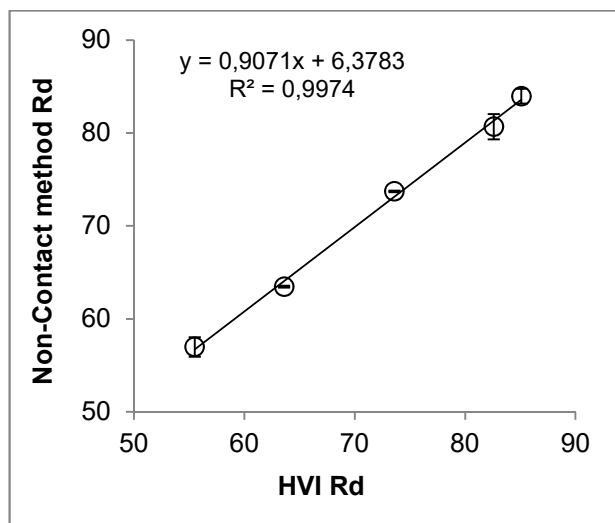
Figure 3 AMS standard ceramic tiles (xenon). HVI *Rd* vs non-contact method *Rd*

In the table it is clearly visible that there is a strong relationship between the HVI measurement and

with the non-contact method measurements. In both the parameters (*Rd, +b*), the values are very close to each other with R^2 values of 0.99 and 0.98, respectively.
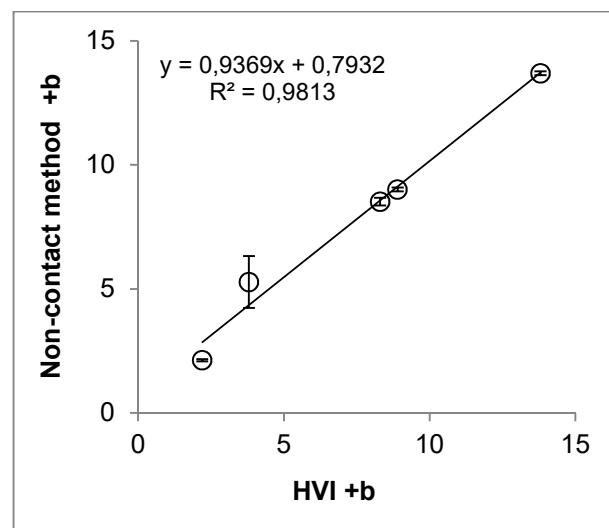
Figure 4 AMS standard ceramic tiles (xenon). HVI *+b* vs non-contact method *+b*

Table 1 Comparison of a classer with the non-contact method as well as with the contact method

No.	Classer Grade	Non-Contact method *Rd*	Contact method *Rd*
1	Y	69.94	69.38
2	Y	64.63	64.07
3	B	67.49	66.83
4	C	56.96	56.48
5	C	56.87	56.36
6	C	65.86	65.23
7	C	56.54	56.05
8	C	63.58	63.08
9	C	56.75	56.24
10	C	55.14	54.65
11	W	60.78	60.32
12	C	58.24	57.79

Table 2 Comparison of *Rd* values

Sample No.	HVI	Non-contact method	Image analysis (mean of *L* value)
1	78.5	77.38	81.24
2	68.9	68.34	78.07
3	59.3	58.91	62.74

The cotton samples which were examined by three methods: visual inspection, contact method and non-contact method. Figure 5 shows that the comparison between the contact method and the non-contact method is a great result and indicates that the relationship between these two methods is very strong under the same illuminant D65 [6, 7]. *Rd* values measured by the contact method were slightly lower compared to those obtained by the non-contact method. It shows us that this method is usable for the measurement of color property of cotton fiber.
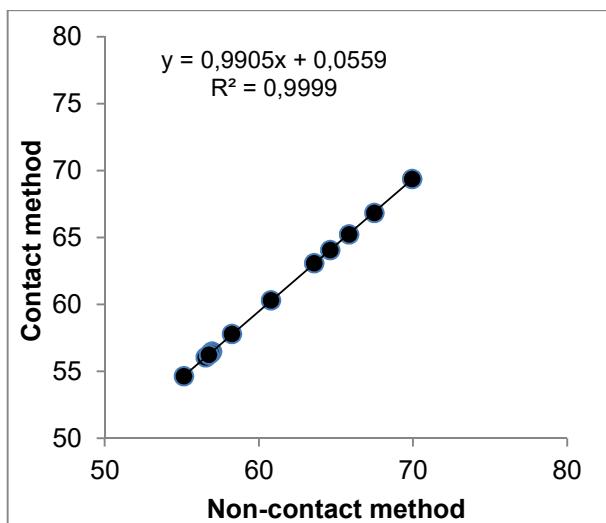
Figure 5 Relationship between contact and non-contact methods in *Rd* values of cotton samples
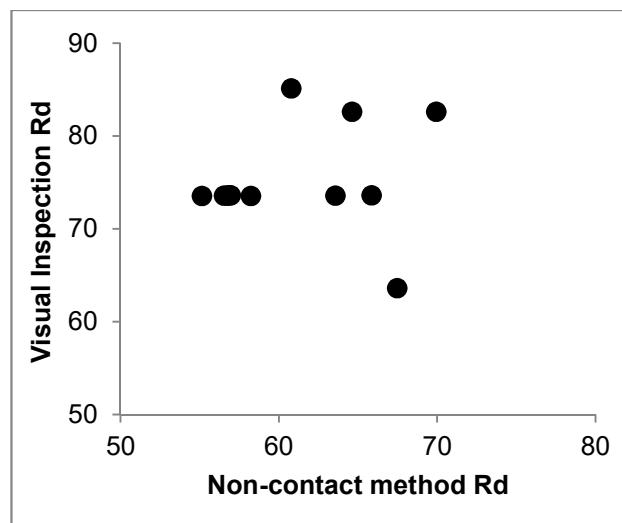
Figure 6 Spearman's rank correlation coefficient. Non-contact method *Rd* and visual Inspection *Rd*. *Rs*=0.26
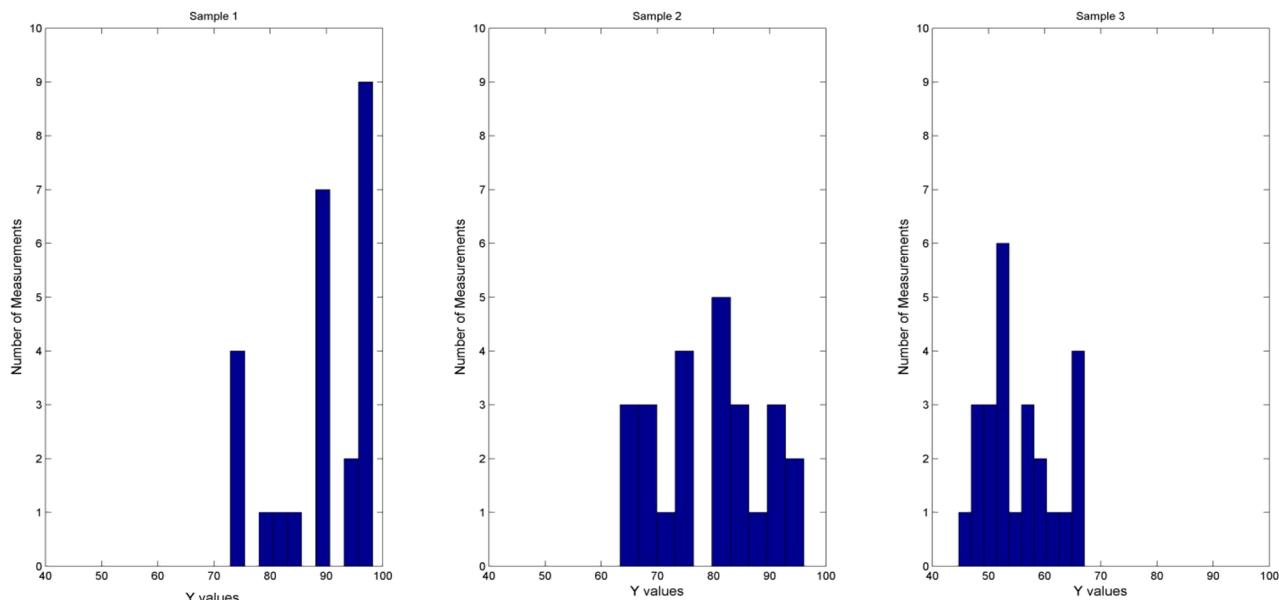
Figure 7 Histograms of Y values obtained from non-contact method

The values obtained through visual inspection data, though, cannot be very well trusted and we cannot say anything authentic about these values because these values are taken by common inspectors and the classers are not professionally trained for cotton color grading. But still, the contradiction between the visual inspection data and the other instrumental methods is present in the cotton grading during our research work.

In this comparison, the image analysis method is also used to analyze the two different methods. In the image analysis method, the RGB values are converted to the *L*a*b** values and used to compare these values with the HVI values used globally for the color measurement of cotton, and also with the new non-contact method used for the color measurement as well by using luminance values. This comparison also confirms the strong relationship between the non-contact method and the image analysis method.

4   CONCLUSIONS

The color standards provided by the AMS for the cotton color measurement were confirmed through non-contact method and it was confirmed that the results show a strong relationship between the two methods.

The measurement of *Rd* values of cotton samples with the two methods mentioned above also shows

a strong relationship between the two methods but a contradiction with visual inspection.

Disagreement between visual inspection and instrumental grading continues as presented in previous research.

The new method (non-contact) can be implemented for the cotton color measurement with some more focus in this method.

5   REFERENCES

1. Nickerson D.: New automatic cotton colorimeter for use in cotton quality specification, Textile Research Journal 21, 33-38, 1951

2. Cheng L., Hossein G., Kermit D., Terezie Z., Michae W.: Color Grading of Cotton Part II: Color Grading with an Expert System and Neural Networks, Textile Research Journal 69(12), 893-903, 1999

3. Matusiak M .: Digieye application in cotton color measurement, Autex Research Journal 15(2), 77-86, 2015

4. Matusiak M., Anetta W.: Important aspects of cotton colour measurement. Fibres & Textiles in Eastern Europe 18(3), 17-23, 2010

5. Guild J.: The colorimetric properties of the spectrum, Philosophical Transactions of the Royal Society of London, Series A, Containing Papers of a Mathematical or Physical Character 230, 149-187, 1931

6. Rodgers J., Jacqueline C., Xiaoliang C., Devron T.: Feasibility of traceable color standards for cotton color, AATCC Review, 42-47, 2009

7. Nickerson D., Richard H., Marshall P.: New automatic colorimeter for cotton, Journal of the Optical Society of America 40(7), 446-449, 1950

FUNCTIONALIZATION OF TEXTILES USING 3D PRINTING – ADD-ON TECHNOLOGY FOR TEXTILE APPLICATIONS TESTING NEW MATERIAL COMBINATIONS

M. Korger, J. Bergschneider, J. Neuss, M. Lutz, B. Mahltig and M. Rabe

Hochschule Niederrhein – University of Applied Sciences, Research Institute for Textile and Clothing (FTB)
Richard-Wagner-Str. 97, 41065 Mönchengladbach, Germany
michael.korger@hs-niederrhein.de

Abstract: *3D printing, also known as additive manufacturing (AM), offers new ways of textile surface modification or functionalization using fused deposition modelling technology (FDM). In addition to textile applications like buttons, accessories or 3D structured elements for home textiles (roller blinds, curtains) the possibilities of integrating a local reinforcement and protection function for sportswear as well as protective clothes can be considered as application fields. For this, a good adhesion and stability of the 3D printed structures on textiles are essential.*

In this paper, the adhesion strengths of the thermoplastic Soft PLA printed on different textile surfaces were tested, which included the adaptation of an existing testing method with respect to separation force measurements. In this context, in addition to 3D printer settings and different combinations of Soft PLA and textile materials, the influences of textile physical and chemical surface properties such as weaves, surface roughness and after plasma treatment or washing were investigated.

The experimental results demonstrated that the adhesion strength is mostly influenced by both the form-locking connections of the thermoplastic and the textile material (above and inside the textile) and the textile surface energy (i.e. the wetting behaviour of the molten polymer on the textile surface).

These results can serve as a valuable basis for the application of 3D elements on textiles with improved and added functionalities like antistatic or conductive paths or plugs using adequate printing materials to be developed in the future.

Key Words: *3D printing, textile surface, fused deposition modelling, adhesion, Soft PLA*

1   INTRODUCTION

3D printing counts as a flexible and quick prototyping and manufacturing process which has a great potential to become more and more important in addition to well-established technologies and production processes in the coming years. Combining 3D printing with textiles, new possibilities of individual product and process design present themselves in textile and clothing industry. 3D printing offers new ways of textile surface functionalization using thermoplastic materials from hard (such as acrylonitrile butadiene styrene ABS, polylactide PLA, polyamide PA) to flexible (such as Soft PLA, thermoplastic elastomers TPE) [1-4]. Furthermore, when different thermoplastic and textile materials are combined, multicomponent textiles can be produced which show new property profiles [4-7]. In one study the dieless forming of carbon fiber reinforced plastic parts was examined performing static and fatigue tests with tensile specimens manufactured by 3D printing [8].

3D printing investigations on textiles are generally carried out using the low-cost fused deposition modelling technique (FDM), which was developed by Stratasys Inc. (Minnesota) [9] and is easy to handle. In FDM a wire-shaped thermoplastic filament is molten in an extruder nozzle and deposited in layers on a heatable printing bed, which is lowered according to the selected layer thickness each time one layer had been printed. In this way the 3D element according to a previously designed CAD model is built up step by step.

When application fields like printing decorative or functional features onto textiles are taken into account, a sufficient adhesion of the printed polymers on the textile material is necessary even under stress conditions. Recently a quite extensive study has been published, where the adhesion characteristics of printed ABS, PLA and PA on different types of fabric were investigated. This was done by visual and tactile inspection of printed 3D forms using a scale rating (1-10) concerning warping, bonding, quality and flexural strength of the prints [10]. But in order to get comparable results for adhesion evaluation, a quantitative analysis of the adhesion strength according to a standardized testing procedure is reasonable.

Now this article concentrates on the influence of different chemical and physical surface properties of the textiles on the adhesion of the prints. Textile surface treatments like roughening, washing and plasma treatment were performed before the printing. The adhesion strengths of Soft PLA prints on the differently treated textiles were systematically measured following a textile testing standard. So this study provides a deeper insight into the bonding mechanisms which are most responsible for a good adhesion between the printed polymer and the textile substrate.

2   EXPERIMENTAL

3D printing experiments were performed using the FDM printers X400 manufactured by German RepRap GmbH and Prodim XXL^{PRO} manufactured by Prodim International BV (The Netherlands). The latter was used for printing samples after textile roughening with the use of a Martindale device and sandpaper (BOSCH C355 P600). The selected nozzle diameters were 0.5 mm and 0.4 mm, respectively.

When testing the adhesion strength, rectangles were created as CAD models, exported as stl files and imported in the Repetier-Host software for slicing. Rectangle dimensions for the prints were 150 mm x 50 mm; the layer thickness was set to 0.3 mm. Two layers were printed, selecting a rectilinear infill pattern and a fill angle of 45°. In variation from this, using ProdimXXL^{PRO}, the rectangle dimensions were 90 mm x 30 mm, layer thickness 0.2 mm and 3 layers were printed.

Soft PLA (shore hardness 42-44 D) was used as printing filament (with 3 mm diameter for use with X400 and 1.75 mm diameter for use with ProdimXXL^{PRO} purchased by German RepRap and Orbi-Tech, respectively). The temperatures of the nozzle / printing bed were set to 210°C / 70°C (X400) and 240°C / 60°C (ProdimXXL^{PRO}). Textile cotton (CO) and polyester (PES) materials under investigation are depicted in Table 1. When printing the first layer, it was ensured that the nozzle moves in close contact to the textile surface.

Adhesion tests were performed according to DIN 53530 (test for separating layers of laminated woven fabrics) using a Zwick Roell testing device. For evaluation, the average peak values of the tensile forces in the recorded stress-strain-diagrams were given following the standard specifications.

Washing and desizing of textile samples were performed for 45 min at 60°C, adding the enzyme amylase and the washing agent Kieralon CD (BASF).

Low pressure plasma treatments (50 Pa, 2.45 GHz microwave discharge) of textile samples were performed under carbon dioxide and argon pressure using parameter settings as follows: 600 W (power), 250 sccm (gas flow), 30 s (duration of treatment).

3   RESULTS AND DISCUSSION

According to results of a former study, where the hairiness of a wool surface in comparison to smoother textile surfaces was made responsible for a comparatively good connection to FDM printed Soft PLA [1], the importance of mechanical interlocking caused by textile roughening for obtaining high adhesion strengths was investigated. Figure 1 (left) shows the adhesion strengths for Soft PLA printed on woven PES fabric dependent on the degree of textile roughening before the print. After 200 Martindale cycles using sandpaper, the hairiness of the PES surface is enhanced (see Figure 1 right) without further destruction of the textile, which results in a nearly three times as big adhesion strength. This can be attributed to added form-locking connections of the printed polymer to the increased fiber loops and ends on the textile surface. Applying higher numbers of Martindale cycles did not result in better adhesion properties. Even after 1000 Martindale cycles, when at least two yarns are broken, no significant improvement of the adhesion can be obtained; rather, a bigger deviation of the measured adhesion strength values becomes obvious. In this case a more destructed textile surface contains more loose fibers which do not have any longer a strong connection to the textile bulk material and can be pulled out easily during the adhesion strength tests.

In order to examine physical and chemical bonding mechanisms dependent on the textile substrate surface in a larger scale, different CO and PES woven fabrics mainly used for technical applications were selected of a similar fabric thickness between 0.21 mm and 0.33 mm (Table 1). The CO textile substrates are made out of natural staple fiber yarns and have different weaves, whereas the PES fabrics with plain weaves contain synthetic yarns made out of filaments (smooth or texturized). The respective textile surface structures are shown in Figure 2.
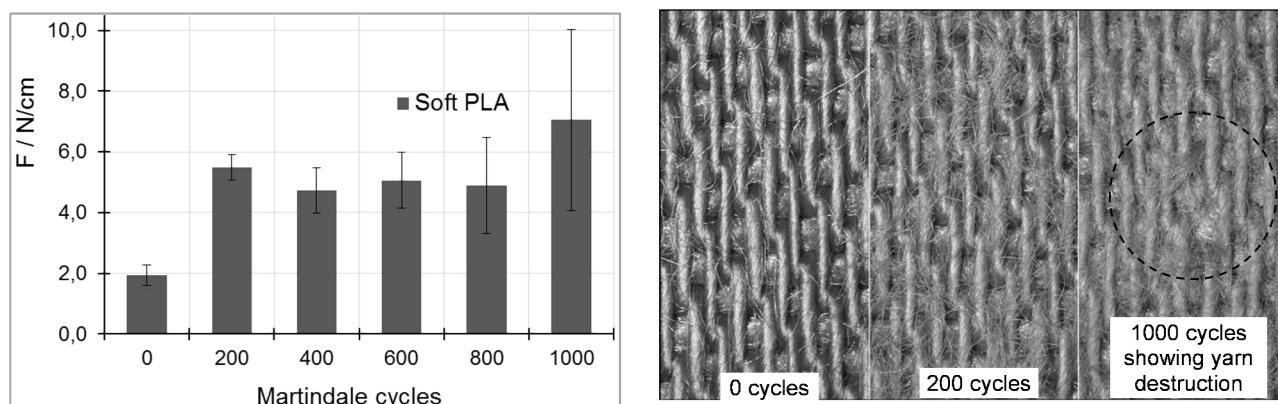
Figure 1 Adhesion strengths of Soft PLA prints on rough PES fabric (satin weave, thickness 0.5 mm) dependent on Martindale cycles (load of 9 kPa using sandpaper) (left); light microscope images of PES samples (magnification 50x) after roughening (0, 200 and 1000 Martindale cycles from left to right) (right)

Table 1 Textile material specifications (cotton CO and polyester PES) under investigation

fabric samples	weave	yarn count (warp/weft) [Nm]	weight per unit area [g/m^2]	thickness [mm]
CO gross plain	plain	50/50	128	0.22±0.1
CO fine plain	plain	68/68	126	0.24±0.1
CO twill	twill	34/50	177	0.30±0.1
CO satin	satin	100/100	116	0.21±0.1
PES hop	hopsack	6.0/6.0	621	0.33±0.1
PES 1 plain	plain	9.1/9.1	343	0.24±0.1
PES 2 plain	plain	9.1/9.1	333	0.21±0.1
PES tex	plain (texturized)	60/50	255	0.27±0.1
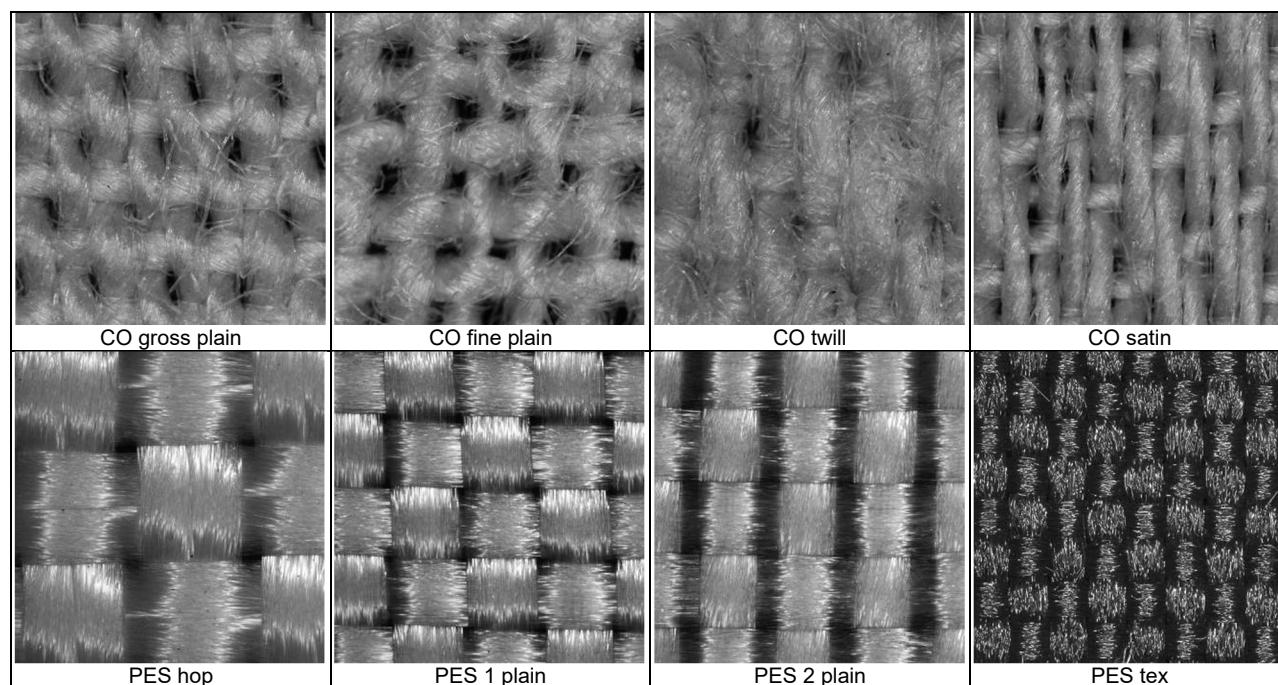
Figure 2 Light microscope images of textile materials (CO: magnification 150x; PES: magnification 50x)
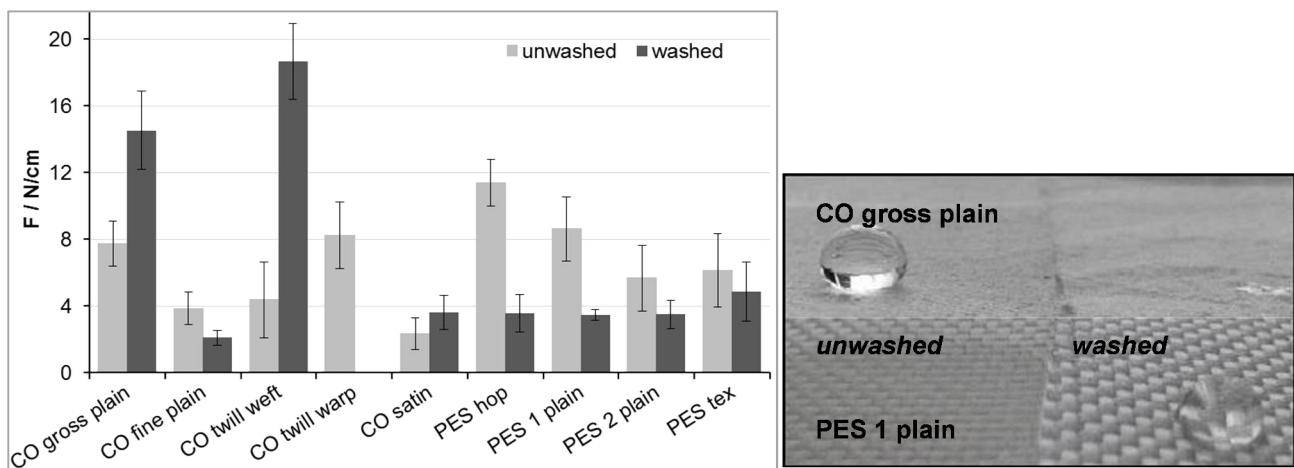
Figure 3 Adhesion strengths of Soft PLA prints on different unwashed and washed fabrics (left); wetting test (water droplet on textile CO and PES surfaces) before and after washing procedure (right)

Figure 3 depicts the influence of washing of the woven fabrics before the print on the adhesion strength of printed Soft PLA. During these washing cycles, sizes and chemicals used for textile finishing should be removed.

Looking at the CO samples first, the determined values for the adhesion strength vary widely. *CO gross plain* and *CO twill* show the best adhesion, especially the latter providing a very nappy textile surface. Also a difference in adhesion strength occurs if the textile is oriented either in warp or weft direction on the printing bed. When oriented in warp direction, the rectilinear infill of the print fits exactly into the rib structure of the textile resulting in a better adhesion strength.

Compared to *CO twill*, the *CO satin* textile surface is quite smooth, leading to worse adhesion properties. The likewise low adhesion strength of *CO fine plain* demonstrates that a more open textile structure as can be seen in Figure 2 does not support a good connection between the polymer and the textile due to decreasing form-locking connections of the printed polymer to the fibers.

Except for *CO fine plain*, after washing and desizing the adhesion strength increases. For *CO twill* the adhesion strength even gets four times as high as without washing, resulting in 18.7 N/cm, so that it becomes impossible to remove the print by hand. The water droplet test (Figure 3, right) demonstrates that after washing, the CO surface becomes hydrophilic owing to removal of waxes or lubricants. So the wettability of the textile surface and therewith the textile surface energy is enhanced. Additionally, the mechanical strain during washing treatment roughens the textile surface. This way bigger a surface area is provided, offering more connection points for the molten polymer.

The adhesion strengths of Soft PLA prints on the selected PES fabrics are not so different from each other. Especially after washing, almost the same reduced adhesion strength (of about only 4 N/cm) was measured. In contrast to the CO fabrics, washing treatment of the PES fabrics led to hydrophobization of the PES surface, so that surface energy and wettability were reduced. This resulted in worse adhesion characteristics of the printed Soft PLA on the PES surface. Here the formerly applied hydrophilic finish functions as a penetration and adhesion promoter.

Since hydrophilicity and good wettability of the textile surface seem to improve the adhesion strength of the printed Soft PLA, the PES textiles were treated with low pressure carbon dioxide (CO_2) and argon (Ar) plasma to create polar groups on the textile surface before the print. Figure 4 shows the resulting adhesion strengths which were obtained.

Both CO_2 and Ar plasma treatment of unwashed PES samples resulted in much lower adhesion strengths for printed Soft PLA. Apparently, this kind of treatment only had a cleaning effect on the textile surface, removing the hydrophilic finish. Plasma treatments of washed samples were conducted with *PES hop* and *PES tex*, whereat CO_2 plasma treatment of the latter resulted in a nearly twice as high adhesion strength as without plasma treatment. This was the only plasma treatment which definitely caused the creation of polar groups on the textile surface, which was proven by the water droplet test (immediate wetting of the textile surface with no water drop formation). With regard to the other plasma treatments, no better wetting of the textile surface could be achieved and, on the contrary, a nearly repulsive behavior between the textile and the printed polymer was observed leading to only very low adhesion forces.
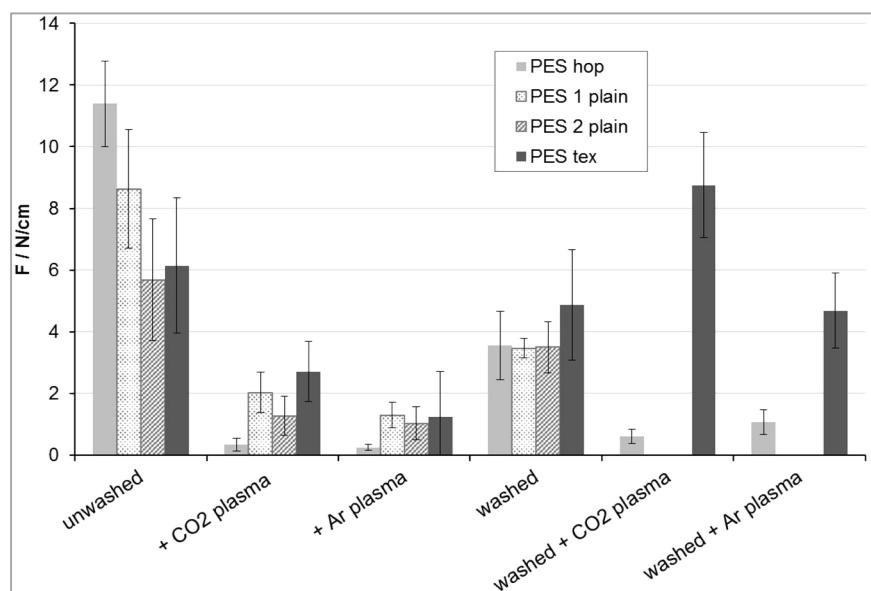
Figure 4 Adhesion strengths of Soft PLA prints on different unwashed and washed PES fabric samples before and after low pressure CO_2 and Ar plasma treatment

Figure 5 shows cross section images of printed CO and PES samples, where the upper panels visualize good adhesion strengths. The textile surface is sufficiently wetted by the polymer.

Looking at the *CO twill* image (upper left), the polymer penetrates deep into the textile, building up strong form-locking connections.

CO twill washed [18.7 N/cm]

PES tex washed + CO_2 plasma [8.8 N/cm]

CO satin unwashed [2.3 N/cm]

PES tex unwashed + Ar plasma [1.3 N/cm]
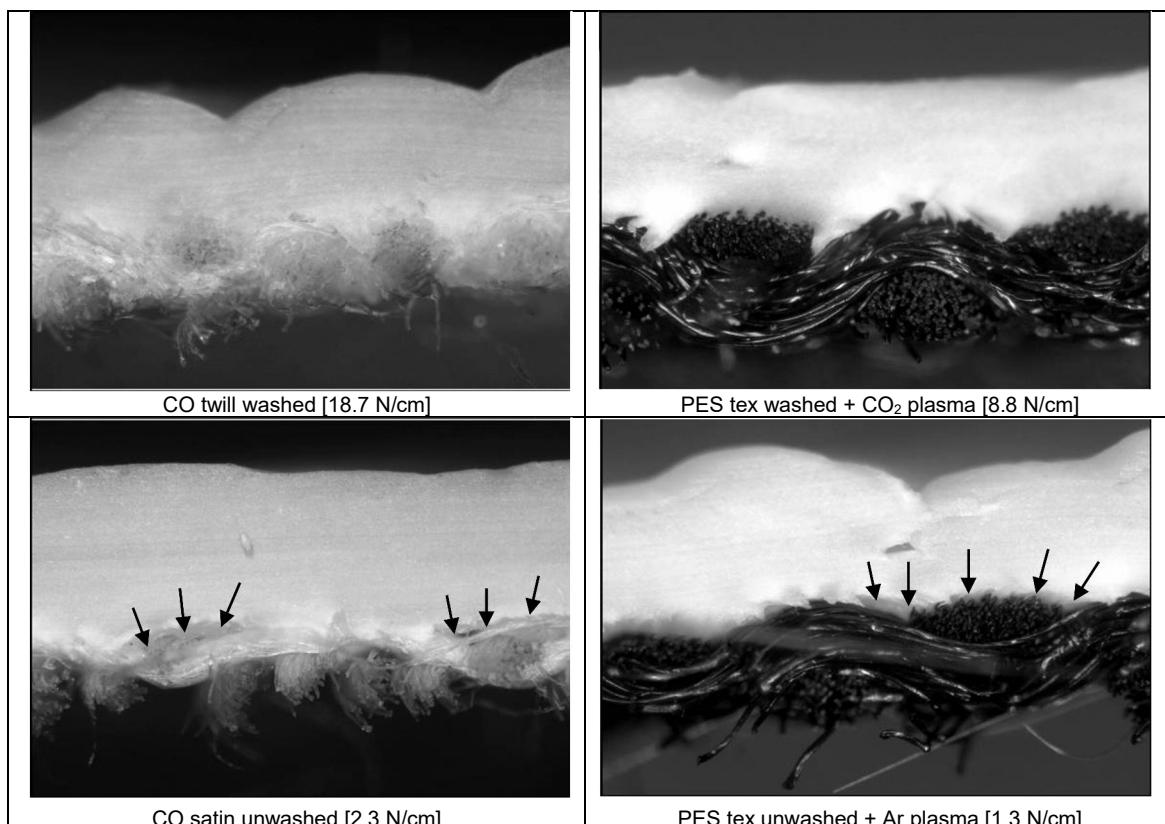
Figure 5 Cross section analysis of CO (left panels) and PES (right panels) samples printed with Soft PLA using light microscope (magnification 150x); arrows indicate air space between the textile and Soft PLA on the top leading to low adhesion (adhesion forces are given in square brackets)

The lower panels visualize bad adhesion results. Low adhesion forces can be attributed to bad wetting and bad connections of the polymer to the textile. When looking at the interface between polymer and textile, air spaces are visible, creating a kind of "air layer" between the two materials. These air layers were observed to a great extent in the case of printed PES samples which had been plasma treated and showed very low adhesion strengths. In this case, only small intermolecular attractions exist between the molecules of the polymer and the textile.

4   CONCLUSIONS

Deposition of polymers onto textiles using FDM printing technology can contribute to new textile applications and individual manufacturing of functional products. In this study, the influence of textile surface properties on the adhesion strength of a printed flexible polymer (Soft PLA) was examined considering mechanical / physical and chemical adhesion mechanisms. Basically, FDM prints on cotton and polyester textiles can result in great adhesion properties. The obtained adhesion strength is decisively influenced by the form-locking connections of the molten polymer with the textile substrate. These connections can occur on the textile surface (if roughened and hairy) and in the textile structure itself corresponding to the type of yarns and weave. Another important factor which affects the adhesion strength is the wettability of the textile surface and so the textile surface energy. In this regard, intermolecular interactions like hydrogen bonding or dipole-dipole interaction between the molecules of the polymer and the textile surface become important to obtain good adhesion properties. This is or can be specifically controlled by washing (desizing), finishing or plasma treatment of the textile before the print.

Further investigations will concentrate on other printing materials and on the influence of their polymer characteristics like melt strength or viscosity on the adhesion strength. Additional textile surface energy measurements can be a useful step to identify suitable polymer-textile combinations to reach the desired adhesion strength.

5   REFERENCES

1. Korger M., Lutz M., Rabe M.: 3D-Druck kombiniert mit Textil – Eine Hybrid-Technologie zur individuellen Erzeugung von Multikomponenten-Textilien, TextilPlus 11/12(3), 25-28, 2015
2. Deleersnyder K.: 3D-Druck auf Textilien, TextilPlus 07/08(3), 23-25, 2015
3. Rabe M., Korger M.: 3D Printing on Textiles – New Ways to Textile Surface Modification, Man-made Fibers Congress, 16.09.2015, Dornbirn, Austria
4. Richter C., Schmülling S., Ehrmann A., Finsterbusch K.: FDM printing of 3D forms with embedded fibrous materials, Design, Manufacturing and Mechatronics, 961-969, 2015
5. Sabantina L., Kinzel F., Ehrmann A., Finsterbusch K.: Combining 3D printed forms with textile structures – mechanical and geometrical properties of multi-material systems, IOP Conf. Ser.: Mater. Sci. Eng. 87, 012005, 2015
6. Julius A., Lutz M., Finsterbusch K., Ehrmann A.: Integration of woven fabrics in 3D printed elements to enhance the mechanical properties, Technical Textiles, accepted
7. Melnikova R., Ehrmann A., Finsterbusch K.: 3D printing of textile-based structures by Fused Deposition Modelling (FDM) with different polymer materials, IOP Conf. Ser.: Mater. Sci. Eng. 62, 012018, 2014
8. Mori K.-i., Maeno T., Nakagawa Y.: Dieless forming of carbon fibre reinforced plastic parts using 3D printer, Procedia Engineering 81, 1595-1600, 2014
9. Chua C.K., Leong K.F., Lim C.S.: Rapid Prototyping: Principles and Applications, 2nd Edition, World Scientific Publishing Co. Pte. Ltd., Singapore, 2003
10. Pei E., Shen J., Watling J.: Direct 3D printing of polymers onto textiles: experimental studies and applications, Rapid Prototyping Journal 21/5, 556-571, 2015

ENZYMATIC ENHANCED ADHESION OF CELLULOSIC WOVEN FABRICS COMPOSITES

T. Linhares, A. Zille and G. Soares

2C2T –Center for Textile Science and Technology, Textile Engineering Department, University of Minho, Campus de Azurém, 4800-058 Guimarães, Portugal
gmbs@det.uminho.pt

Abstract: *The purpose of this work was to produce and characterize enzymatically treated fabric composites using different mixtures of two commercial cellulase enzyme solutions in dosages of 0.1% and 0.5% in order to improve the fabric's adhesion. Three cellulosic taffeta plain weave fabrics of 100% flax, cotton and bamboo viscose were used in different combinations. The properties of the woven fabrics and produced composites were characterized using several mechanical tests. The cotton & viscose composite appears to be the best materials combination, exhibiting improved breaking force (0.5% of Xylanase PLUS^{TM}) and percentage of elongation at maximum force (0.1% of Xylanase PLUS^{TM}), as well as better results on the peel adhesion test (0.5% of AlternaFuel® MAX^{TM}). The flax & cotton combination did not show any improvement for all the tested properties. Flax & viscose combination, despite not having shown peel strength improvement, exhibits remarkable elongation and breaking force (0.5% of Xylanase PLUS^{TM}). Since there is no posterior emission of volatile products, one can expect a great public acceptance. However, higher enzymatic concentrations should be studied to clarify the contribution of this parameter to the surface modification and adhesion promotion.*

Key Words: *biotechnology, enzymes, surface modification, pressure adherence, woven cellulosic composites*

1   INTRODUCTION

Biotechnology applied to the textile processes has been an increasing tendency during the last years. Textile composites produced via enzymatic modification of the material's surface is a recent and increasing investigation field and might be the complement or the alternative to the conventional process by applying polymeric matrices. However, there are few studies about composite fabrics produced with reinforced structures from natural fibres and biodegradable matrices using enzymes [1]. Composites can be defined as multiphase materials with enhanced characteristics due to the geometric conception to maximize inherent properties of the individual components [2]. Polymer composites can be produced from a polymer matrix, by thermoset or thermoplastic or by the use of different types of binding, adjoined to the matrix in the form of fibres, yarn, mats, fabrics, foams, honeycombs, etc. [3]. The binding of the composites on synthetic materials can be done by joining polymer layers followed by consolidation of their interfaces due to pressure and heat fusion [4]. The most recurrent and increasingly important composites for structural applications consist of a polymer matrix reinforced with fibres, where a combination of high strength, relatively low weight and durability are required [5]. The consumption of composites with natural-based matrices is a small fraction of the total composites

market [3]. However, there is an increasing interest in research and development of cellulosic materials combined with man-made fibres, in which adherence is made by crosslinking polymers or selective melting of fibres and where the interaction for adherence is enhanced by the irregularity of natural fibres [6]. Cellulose is the main organic compound in the biosphere and constitutes the basic material of all plant fibres [7, 8]. The macromolecule structure is formed by linear condensation of D-anhydroglucopyranose units linked by β1,4-glycosidic bonds [9]. The absence of side branches increases its crystallinity and leads to efficient intermolecular and intra-chain hydrogen bonding due to the hydroxyl groups, which results in dimensionally stable fibres [10]. The chemical composition on natural vegetable fibres depends on the plant's origin. Generally, plant composition can be divided in major components, such as cellulose, hemicellulose and lignin, and minor components, like protein and mineral substances, fatty and resinous acids, phenols, etc. [11, 12]. In the case of cellulosic materials, the matrix phase has to be prepared by modification of the surface, also using biotechnology approaches, unlike the thermoplastic polymers [6, 13]. The main advantage of biotechnology, compared with conventional technologies, consists in their specificity for a particular reaction over a specific substrate. Enzyme technology has the unique potential for the modification of surface of textile

and synthetic materials thanks to the high specificity of enzymes which allows diversified advanced functionalities [14]. Since the late 80's those enzymatic processes which are relevant for the textile industry have been intensively studied, with obvious results on the use of enzymes in the replacement of conventional chemical treatments [14, 15]. Enzymatic surface modification of textile materials comprises processing of fibres or biopolymers in order to change their physical and chemical surface properties, or the introduction of functional groups on the surface [14]. Cellulases are enzymes which are capable to cleave the glycosidic linkages in oligosaccharides and polysaccharides, including cellulose and hemicelluloses [16]. In order to optimize the enzymatic treatments of surface modification, enzyme mixtures were successfully conceived according to the desired effect on the fibres' or material's surface [17]. Cellulases are widely used for textile finishing of cellulosic materials as well as for development of new products [18]. There are several benefits in using cellulases or enzymes in general: its implementation is easy and the processes might be adjusted to the available equipment at different stages of the wet process; the application conditions are moderate in terms of pH and temperature; enzymes are organic compounds, so totally biodegradable, not contributing to environmental wastes; treatment with enzymes has economical advantages due to the lowest temperatures and reduction of the processing time [18]. Cellulosic materials are hydrolysed by the synergistic action of three general types of cellulases: Endoglucanases, which hydrolyse amorphous cellulose randomly into smaller polymers, thus creating new ends; Exoglucanases, which attack the extremities of the cellulose polymer, thereby producing cellobiose. Cellobiose is hydrolysed by β-glucosidase, yielding glucose [14]. There are also other species of cellulases with some importance: hemicellulases, which modify the structure of xylan and glucomannan in pulp fibres to improve chemical delignification, and endoarabinases, which hydrolyze the α-1,5-linkages of arabinan polysaccharides that are present as side chains of pectin [19].

This work is intended to study the production of composite using enzymatically modified woven cellulosic fabrics made up from fibres of cotton, linen and bamboo viscose. The adhesion of the fabric will be promoted using different mixtures of cellulase enzymes. The properties of the woven fabrics and produced composites were characterized using several standard mechanical tests.

2   EXPERIMENTAL

Materials

The composites were conceived by combining three taffeta weaved woven fabrics: 100% linen, 177 g/m^2; 100% cotton, 156 g/m^2; 100% bamboo viscose, 133 g/m^2. Two commercial enzymatic formulations were used. AlternaFuel® MAX[TM] (Dyadic International, USA) a liquid cellulase preparation produced from *Myceliophthora thermophila*, which converts lignocellulosic substrates into glucose. Dyadic Xylanase PLUS (Dyadic International, USA) a concentrated liquid acid-neutral endo-1,4-β-D-xylanase produced by *Trichoderma longibrachiatum*. All other reagents were of analytical grade purchased from Sigma-Aldrich and used without further purification.

Enzymatic treatment process

Cleavage of the glycoside bonds of the polymers' surfaces were achieved by hydrolysis with the two commercial cellulase preparations opportunely diluted in 0.1 M phosphate buffer. Fabrics of flax, cotton and viscose (3.16 g, 2.89 g, 2.41 g, respectively) with the dimensions of 30 x 6 cm were incubated in a liquor rate of 1/20 and with two cellulase enzymatic dilutions of 0.1 and 0.5%. The solutions with the immerged fabrics were processed under continuous agitation at the temperature of 50ºC for 30 minutes. After the treatment, each sample was rinsed with 250 mL of distilled water, at room temperature, with slight agitation, for 10 seconds. Excess water was removed by compression of the sample wrapped on a tweezers, against beaker walls. The control test has also been made by immersion of the three samples in the buffer solution, using the same treatment conditions but without enzyme formulation. Parameters of enzyme dosage preparations are outlined in Table 1.

Table 1 Enzyme dosage [mg], sample mass [g] and volume of solution [mL] in a liquor rate of 1:20 for sample dimension of 30 x 6 cm

Materials	Solution [mL]	Sample mass [g]	Enzyme formulation			
			AlternaFuel® MAX™		Dyadic® Xylanase PLUS	
			0.10%	0.50%	0.10%	0.50%
			Enzyme dosage [mg]			
Flax	127	3.16	10.1	49.9	10.2	49.6
Cotton	116	2.89	11.7	50.0	10.4	49.1
Viscose	96	2.41	10.4	10.7	51.2	51.6

Adhesion of composites

The combinations of fabrics that were made for the development of textile composites can be seen in Table 2. All sample-composites were pressed for 10 minutes after the enzyme treatment. Then, the adhesion was promoted by compression in a uniaxial hydraulic press under the load of 10 tonnes at 200ºC for 60 seconds.

Table 2 Enzyme and fabrics combinations for composite production and respective codex

| Composites | Enzyme formulation | | | |
| | AlternaFuel® MAX™ | | Dyadic® Xylanase PLUS | |
	0.10%	0.50%	0.10%	0.50%
Flax&Cotton	B	D	A	C
Flax&Viscose	F	H	E	G
Cotton&Viscose	J	L	I	K

Fabric characterization

The three woven fabrics were characterized by physical tests as per following standards: Determination of mass per unit area using small samples (NP EN 12127:1999); Determination of number of threads per unit length (ISO 7211-2: 1984 modified; NP EN 1049-2: 1995); Determination of crimp of yarns in fabrics (NP 4115: 1991); Determination of linear density of yarn removed from fabric (NP 4105: 1990); Determination of thickness of textiles and textiles products (NP EN ISO 5084: 1999); Standard Test Method for Breaking Force and Elongation of Textile Fabrics (Strip Method, ASTM D5035: 93); Standard Test Method for Pilling Resistance and other Related Surface Changes of Textile Fabrics (Martindale Pressure Tester Method, ASTM D 4970–89).

Composite characterization

The composites were characterized by physical tests as per following standards: Determination of thickness of textiles and textiles products (NP EN ISO 5084: 1999); Standard Test Method for

Breaking Force and Elongation of Textile Fabrics (Strip Method, ASTM D5035: 93); Standard Test Method for Peel or Stripping Strength of Adhesive Bonds (ASTM D903: 93); Standard Test Method for Pilling Resistance and other Related Surface Changes of Textile Fabrics (Martindale Pressure Tester Method, ASTM D 4970–89).

3   RESULTS AND DISCUSSION

The physical properties of a textile product are vital to its performance, determining its suitability for the intended application [20, 21]. On the original materials as well as on the final composite products, basic characterization physical tests and mechanical strength tests were made, as stated in the following tables.

Yarn characterization demonstrates that there tends to be a major dispersion of results in linen yarns when compared with viscose (Table 3). This can be understood due the fibres' different origins - due to the manufacturing process of viscose, these fibres present a greater uniformity, hence the lower value of the coefficient of variation on the ring spun yarns.

The results of the test of Determination of Peel or Stripping Strength of Adhesive Bonds in the flax & cotton composite show lower values than in the control, which can indicate that treatment conditions are not favourable for this combination (Table 4). The results of the testing of Breaking Force and Elongation of Textile Fabrics were also worse than for the control composite. Mass per unit surface was not determined due to the contamination of the composite samples by a large amount of solid particles during the pressing process. The results of the test of Determination of Peel or Stripping Strength of Adhesive Bonds on the flax & cotton composite show lower values than in the control, which can indicate that treatment conditions are not favourable for this combination. The results of the testing of Breaking Force and Elongation of Textile Fabrics were also worse than for the control composite.

Table 3 Characterization of woven fabrics

	Flax	Cotton	Viscose
Mass per unit area [g/m^2]	177.01±0.28	155.76±4.75	132.91±0.35
Number of threads (warp) [Nº/cm]	19.6±0.6	17.8±0.5	48.7±2.5
Number of threads (weft) [Nº/cm]	19.4±0.9	15.6±0.5	33.7±0.6
Crimp (warp) [%]	5.7±0.9	9.6±0.4	11.18±0.45
Crimp (weft) [%]	4.1±0.4	4.2±0.2	6.5±0.5
Linear density (warp) [tex]	45.1±4.6	30.9±2.2	14.6±1.2
Linear density (weft) [tex]	41.3±5.0	60.8±1.5	14.8±0.8
Thickness [mm]	0.37±0.02	0.47±0.01	0.27±0.01
Breaking Force (warp) [N]	390.6	164.1	233.3
Elongation (warp) [%]	24.05	11.17	24.05
Pilling resistance	5	4-5	4-5

Table 4 Characterization of woven composite of flax & cotton

	Control	A	B	C	D
Thickness [mm]	0.46±0.02	0.55±0.03	0.52±0.02	0.53±0.04	0.50±0.03
Breaking Force (warp) [N]	371.6	295.2	339.6	348.4	352.4
Elongation (warp) [%]	9.33	8.13	8.93	9.55	8.60
Peel Strength [N]	0.18	0.18	0.18	0.08	0.08
Pilling resistance	4	5	4	4	5

Table 5 Characterization of woven composite of flax & viscose

	Control	E	F	G	H
Thickness [mm]	0.40±0.02	0.45±0.02	0.44±0.02	0.44±0.03	0.42±0.04
Breaking Force (warp) [N]	372.8	395.6	424.0	474.0	372.4
Elongation (warp) [%]	8.48	10.27	9.60	10.33	9.20
Peel Strength [N]	1.325	0.825	1.175	0.925	1.075
Pilling resistance	4-5	5	5	5	5

Table 6 Characterization of woven composite of cotton & viscose

	Control	I	J	K	L
Thickness [mm]	0.35±0.04	0.45±0.02	0.43±0.02	0.46±0.03	0.40±0.02
Breaking Force (warp) [N]	248.0	281.6	275.6	287.2	274.4
Elongation (warp) [%]	19.93	22.65	22.35	23.25	22.33
Peel Strength [N]	0.675	1.000	1.075	1.000	1.25
Pilling resistance	5	5	5	5	5

On the flax & viscose composite it can be seen that, based on the result of Breaking Force and Elongation of Textile Fabrics (Strip Method) test, there is some improvement in the end product, where the breaking force increased up to the maximum of ≈12% (Table 5). However, on the essay of the Determination of Peel or Stripping Strength of Adhesive Bonds, the outcomes are worse than in the control composite, which can perhaps be explained by induced adherence due to the enzymes which restricts the elongation of composite material.

The cotton & viscose composite presented the best behaviour of all combinations - the Breaking Force increased by 11 to 15%, depending on base materials, and the peel adhesion was also slightly higher than composite control (Table 6). It can also be noted that the abrasion resistance was slightly improved, based on the results of the Evaluation of Pilling Resistance; nevertheless, the results in this essay were already good in the composite control. Another aspect that can be very interesting is the fact that the thickness of all composites was significantly smaller than the sum of the two individual materials, which can perhaps be explained by the absence of the usual polymeric matrix which can eventually reduce the entanglement of the fibres resulting in a thicker end product.

4   CONCLUSIONS

The purpose of this work was to study the possibility of making composites from cellulosic textile materials by enzymatic surface modification of materials as an alternative to conventional polymeric matrices. The combination cotton & flax did not work probably due to the relatively greater linear density of the yarns that may restrict the entanglement of the fibres and minimize the adhesion between components. The flax & viscose combination did not show peel strength improvement, however for Dyadic® Xylanase PLUS it exhibited a remarkable effect on elongation and breaking force at the 0.5% dosage. The cotton & viscose composite appears to be the best combination, exhibiting improved breaking force (0.5% of Xylanase PLUS[TM]) and percentage of elongation at maximum force (0.1% of Xylanase PLUS[TM]), as well as better results in the peel adhesion test (0.5% of AlternaFuel® MAX[TM]). The abrasion resistance has also been slightly improved, based on the results of the evaluation of pilling resistance, despite of the good results on the control composites. Due to the small dosages that had been used, it is very difficult to assess the influence of the enzyme concentration on the obtained results, however higher enzymatic concentrations should be studied to clarify the contribution of this parameter on the surface modification and adhesion promotion.

5   REFERENCES

1. Porras A., Maranon A., Quijano A.: Development and Characterization of a Laminated Composite Material from Polylactic Acid (PLA) and Woven Bamboo Fabric. In: Binetruy C, Boussu B, editors. Advances in Textile Composites, Lancaster: DEStech Publications, Inc, 546-554, 2010

2. Mobasher B.: Mechanics of fiber and textile reinforced cement composites. Boca Raton: Taylor & Francis Group, LLC; 2012

3. Biron M.: Thermosets and Composites-Material Selection, Applications, Manufacturing and Cost Analysis, 2nd ed. Oxford: Elsevier Ltd, 2014

4. Ageorges C., Ye L.: Fusion Bonding of Polymer Composites, London: Springer-Verlag, 2002

5. Plackett D.: Biodegradable polymer composites from natural fibres, In: Smith R, editor. Biodegradable polymers for industrial applications, Boca Raton: CRC Press LLC, 189-218, 2005

6. Soykeabkaew N., Sian C., Gea S., Nishino T., Peijs T.: Cellulose 16, 2009, pp. 435-444

7. Huber T., Mussig J., Curnow O., Pang S., Bickerton S., Staiger M.P.: J Mater Sci 47, 1171-1186, 2012

8. Fedorak P.M.: Microbial processes in the degradation of fibers, In: Blackburn RS, editor, Biodegradable and sustainable fibres, Cambridge: Woodhead Publishing Limited, 1-35, 2005

9. Thomas S., Paul S.A., Pothan L.A., Deepa B.: Natural Fibres: Structure, Properties and Applications, In: Cellulose Fibers: Bio- and Nano-Polymer Composites – Green Chemistry and Technology, Kalia S, Kaith BS, Kaur I, editors, Berlin: Springer-Verlag, 3-42, 2011

10. Keenan T.M., Tanenbaum S.W., Nakas J.P.: Biodegradable polymers from renewable forest resources, In: Smith R, editor, Biodegradable polymers for industrial applications, Boca Raton: CRC Press LLC, 219-250, 2005

11. Asunción J.: The Complete Book of Papermaking. New York: Lark Books; 2003

12. Strezov V., Evans T.J., Nelson P.F.: Carbonization of Biomass Fuels, In Michael D. Brenes, editor, Biomass and Bioenergy: New Research, New York: Nova Science Publishers, Inc., 91-123, 2006

13. Murphy J.F.: Safety Considerations in the Chemical Process Industries, In: Kent J.A., editor, Handbook of Industrial Chemistry and Biotechnology Vol. 1, 2, 12th ed. New York: Springer Science + Business Media, 46-105, 2012

14. Nierstrasz V.A.: Enzyme surface modification of textiles, In: Wei Q, editor, Surface Modification of Textiles, Cambridge: Woodhead Publishing in Textiles: Number 97, 2009

15. Nierstrasz V., Cavaco-Paulo A.: Preface. In: Nierstrasz V., Cavaco-Paulo A., editors, Advances in Textile Biotechnology, Cambridge: Woodhead Publishing Series in Textiles: Number 107, 139-163, 2010

16. Kubicek C.P.: Fungi and Lignocellulosic Biomass, Ames: John Wiley & Sons, Inc, 2013

17. McKelvey S.M., Murphy R.: Biotechnological Use of Fungal Enzymes, In: Kavanagh K., editor, Fungi Biology and Applications, 2nd ed. Oxford: John Wiley & Sons, Ltd., 2011

18. Miettinen-Oinonen A.: Cellulases in the Textile Industry, In: Polaina J., MacCabe .AP., editors, Industrial Enzymes Structure, Function and Applications, Dordrecht: Springer, 51-63, 2007

19. Bajpai P.: Environmentally Benign Approaches for Pulp Bleaching, 2nd ed, Oxford: Elsevier, 2012

20. Pickering K.L., Aruan Efendy M.G., Le T.M: Composites: Part A 83, 98-112, 2016

21. Hu J.: Introduction to fabric testing, In: Hu J., editor, Fabric Testing, Cambridge: Woodhead Publishing Limitedp., 1-27, 2008

EFFECT OF FATLIQUORING AND FINISHING
ON MOISTURE ABSORPTION-DESORPTION OF LEATHER

A. M. Manich[1], J. Barenys[2], L. Martínez[2], M. Martí[1], J. Carilla[1] and A. Marsal[1]

[1]*IQAC-CSIC, Jordi Girona 18-26, 08034 Barcelona, Spain*
[2]*TRUMPLER Española S. A., carrer Llobateres 15, Barberà del Vallès, Spain*
albert.manich@iqac.csic.es

Abstract: *The purpose of the paper is to investigate the moisture absorption-desorption kinetics of leather, a natural collagen fibrous structure, by the application of Vickerstaff's method that enables to determine the diffusion coefficient of dyes in fibres, to the diffusion coefficient of moisture in leather. Leather has been fatliquored and finished in order to evaluate the effect of these treatments on moisture diffusion. Samples were subjected to ascending and descending steps of relative humidity, to cause absorption/desorption of moisture in leather. The amount of moisture absorbed/desorbed is measured as regain (% odw). At each step, the final regain (at equilibrium) X, the half absorption/desorption time $t_{1/2}$, the ratio $X_{1/2}/t_{1/2}$ being $X_{1/2}=X/2$ that corresponds to the diffusion rate were calculated. Following Vickerstaff's method, the maximum slope of the normalized absorption plot X(t)/X vs. $\sqrt{t}$ enabled us to derive the square root of the apparent coefficient of diffusion D_A which is based on the % of moisture absorbed/desorbed by a unit of sample mass per unit of time.*

Hysteresis depends on the water activity (RH%/100) of the environment and points out the energy at which the moisture absorbed at this humidity level is linked to the substrate. The higher the relative humidity, the lower the bonding energy of moisture. At lower water activities, the absorbed moisture is linked to collagen as primary water. The comparison of the regain in desorption Xd vs. regain in sorption Xa at different humidity levels yields the hysteresis at each humidity level: Hyst (%) = 100 * (Xd-Xa)/Xa.

Fatliquors mainly affect the maximum sorption capacity of leather, decrease the size of the monolayer although they make the bonding energy ascend. Significant differences in the apparent diffusion coefficients between fatliquors have been observed. The highest coefficients were those of sulphited triglycerides of colza oil and sulphited fish oil, while the lowest were those given by the non fatliquored leather and that fatliquored by the combination of sulphited triglycerides of colza oil and fatty polymer.

As regards the effect of finishing according to the relative humidity, finishing enhances the diffusion coefficient in the intermediate range of humidities between 30 and 65% while differences decrease at the extreme values.

Key Words: *leather, collagen, fatliquoring, finishing, moisture, absorption, desorption, diffusion coefficient, hysteresis, sulphited triglycerides of colza oil, sulphited fish oil, fatty polymer.*

1   INTRODUCTION

When collagen is placed in a given atmosphere, it acts as a moisture buffering body that gradually takes up or loses water until reaching equilibrium. This is a dynamic equilibrium which occurs when the number of water molecules evaporating from the specimen in a given time equals the number of water molecules absorbed. The moisture content of collagen/leather influences its properties [1-3], can develop driving forces causing spatial displacement of the substrate [4] and, by over drying, leather properties are modified in an irreversible way [5, 6]. The property of absorbing moisture is a valuable characteristic of articles in contact with the human body. This avoids problems caused by accumulation of sweat on the skin and in shoes [7]. The sorption of water causes the leather to act as a heat reservoir, protecting the body from sudden changes in external conditions. The moisture buffering ability of leather is determinant in comfort feeling and, when used in upholstery, enhances the indoor air quality of a room [8]. Moisture content affects its microbial resistance, aspect and durability [9].

The fibrous structure and the large concentrations of hydrophilic groups of collagen account for its high water sorption capacity. In a study on water-collagen interactions using rat-tail tendons, Pineri et al. [10] described different mechanisms of water fixation. Grigera et al. [11] reported two types of water. One type of water is hydrogen-bonded to the macromolecular backbone at well-defined positions and the other type interacts weakly with a number of different sites, forming a multilayer with more liquid-like properties. This is consistent with the view of Caurie [12], who described three types of water: a) water adsorbed onto the most energetic sites known as strongly bonded primary sites, b) water consisting of weakly bonded secondary molecules, and c) unbounded free liquid water that condenses at saturation pressure.

1.1 Sorption isotherms

It is common knowledge that there is a good correlation between the number of water molecules in a monolayer and the number of polar side chains using the classic Brunauer, Emmett and Teller (BET) multilayer sorption equation. This suggests that each polar group initially sorbs one molecule of water followed by multimolecular sorption at a higher humidity. Despite its limitations, BET equation is still used to calculate monolayer values in very different physicochemical fields, yielding data sorption specific area values. The BET equation is used because of its simplicity and because it has been approved by the International Union of Pure and Applied Chemistry (IUPAC). In 1985, the Commission on Colloid and Surface Chemistry recommended the so-called BET plot for a standard evaluation of monolayer values in the relative vapour pressure (water activity) interval between 0.05 and 0.30.

The Guggenheim, Andersen and de Boer (GAB) sorption equation also provides monolayer sorption values. It has become more popular because the range of the relative vapour pressure interval is much wider than that of the BET equation (from 0.05 to 0.8-0.9) [13]. The BET and the GAB isotherms are closely related since they are based on the same statistical model. The GAB, which is an improvement on the BET model, shares with it the two original BET constants: a) the monolayer capacity Xm, and b) the energy constant C. The GAB model owes its greater versatility to the introduction of a third constant K.

The energy constants determine the sigmoid shape of the isotherms. Constant C determines the shape of the "knee" at the lower activity range and is proportional to the ratio between the attachment rate constant and the escape rate constant per unit pressure for the primary sites [13]. Constant K determines the profile at the higher water activity range, regulating the upswing after the plateau following the "knee" at medium water activity range, and is related to the attachment rate constant and the escape rate for all higher layers in the system [14]. The lower the value of K, the less structured the state of the sorbate in the multilayers above the monolayer, which is less structured than in the pure liquid state. K increases with stronger interactions between sorbate and sorbent [13].

Hysteresis gives rise to two different paths between sorption and desorption. The extent of it is related to the nature and state of the components of the sample, reflecting their potential for structural and conformational rearrangements, which alter the accessibility of the water to the energetically favourable polar sites [15]. The general shape of the equilibrium water sorption isotherm for collagen can be described by a Type II or Type III

isotherm with a small amount of water that persists at very low relative humidity and a large amount of water at high relative humidity [16]. Table 1 shows the sorption isotherms and the parameters used to fit the experimental sorption/desorption data.

The basic mechanism of equilibrium depends on the balance between the rate of attachment and detachment of water molecules in the sorbed material. The monolayer moisture content calculated from the equilibrium sorption isotherms is essential for the physical and chemical stability of dehydrated materials. At lower water activities, water is held by strong hydrophilic sites. When sorbed, water molecules can become attached to additional water molecules which are transformed into less firm sorption sites. When the water activity is increased, sorption enters a second region, where sorbed water is more loosely held by hydrogen bonds. This "multilayer region" can be considered a transition phase between the initial and final regions of the isotherm. The least firmly bonded water is produced when the water activity attains the highest levels. In this region, "condensed water" is mechanically entrapped within the voids of the fibre, and has many of the characteristics of liquid water. According to Dent [14] it is possible to calculate the fractions of the total sorption as a function of water activity a_w: variation of empty sites, monolayer moisture content, "primary" and "secondary" water bonded molecules, and the ratio between them.

Table 1 BET and GAB models. Parameters used to fit the experimental sorption data

Model	Mathematical equation
BET [21]	$X = X_m C a_w / [(1-a_w)(1-a_w+C a_w)]$
GAB [22]	$X = X_m C K a_w / [(1- K a_w)(1- K a_w+C K a_w)]$
Parameter	**Definition**
a_w	Water activity expressed as vapour relative pressure p/p_0, where p_0 is the saturated vapour pressure
X	Equilibrium moisture content at a_w in g sorbed/100 g of sorbent on dry basis
X_m	Monolayer moisture content in g sorbed/100 g of sorbent on dry basis d.b
C	Energy constant related to the difference between the free enthalpy of the water molecules in the pure liquid state and in the monolayer. This is proportional to the rate between both the attachment and the escape rate constants for the primary sites
K	Ratio between the standard vapour pressure of the liquid and the vapour pressure of the sorbate in the secondary (upper) layers. Proportional to the rate between the attachment rate constant and the escape rate for all higher layers.

Among the post-tannig operations, fatliquoring, together with retanning, is one of the most influencing treatments on leather characteristics, in particular those related to handle and comfort [17, 18]. Fatliquors are added to leather for similar reasons as plasticizers to polymers (the improvement of their flow properties) [19], they enhance fiber mobility due to the reduction of the friction between microfibrils [20] and prevent fiber adhesion by filling the spaces between the network structure, resulting in a greater fiber mobility [20]. Fatliquors are placed between collagen fibrils and act as lubricant, improving handle and making easy the relative displacement of microfibrils when are subjected to mechanical stresses. Fatliquors modify the size of the leather internal sorbing surface of moisture, affecting their comfort feeling.

1.2 Objective

The main aim of this study is to evaluate the absorption/desorption behaviour of leather explained by the half adsorption/desorption rate, the apparent coefficient of diffusion and their relationships according to fatliquoring, finishing, test mode (adsorption/desorption) and relative humidity.

2   EXPERIMENTAL

2.1 Materials

The experimental work was carried out at the pilot plant of Trumpler Española SA. Wet-blue sides from Ireland, shaved to a thickness of 1.2-1.4 mm, were used. After washing, rechroming and neutralization, leathers were retanned and dyed following a conventional process and, then, they were fatliquored with five fatliquoring agents of different chemical composition in order to compare their effect on moisture absorption/desorption. Fatliquoring was carried out by applying a 7% of active matter on shaved weight. After final washing and drying, moisture absorption/desorption tests were carried out. To evaluate the effect of finishing, a light standard finishing was applied to each of the samples. Results before and after finishing were compared with those of the non fatliquored sample before and after finishing.

Fatliquors were identified by their main characteristic component:

- Sulphited triglycerides of rapeseed oil TCSi
- Fatty Polymers (non water repellent) PGR
- Phosphoric Ester ESF
- Sulphited fish oil PSi
- The standard fatliquoring agent used as reference is the combination (TCSi/PGR).

2.2 Methods

Sorption and desorption plots of samples around 12 mg in mass were measured for moisture absorption/desorption by the Q5000SA Dynamic Vapour Sorption DVS Analyzer (TA Instruments), according to the following procedure:

1) Initial Drying: temperature 60°C, relative humidity 0%, time 1 h.

2) Pre-stabilization: temperature 25°C, relative humidity RH 0% and then, initial adsorption at RH 5%.

3) Sorption steps: the sample previously stabilized at 5% RH is subjected to absorption tests that progressively increase from 15% to 25%, 35%, 55%, 75% and 95% of RH.

4) Desorption steps: the sample stabilized at 95% RH after the sorption kinetics is subjected to desorption tests that progressively decrease from 75% to 55%, 35%, 25%, 15% and 5%.

5) Final step conditions: each step lasts a maximum time of 500 min. If variation in weight is lower than 0.02% for 10 min, the step is considered to have reached a quasi-equilibrium condition.

Based on the moisture content at the end of each step, the software provided by TA Instruments fits the BET and GAB models to the experimental data. Figure 1 shows the results of the absorption/desorption test and the isothermal plot using final regains at each step.

The exhaustive description of the absorption phenomena under particular conditions of temperature and relative humidity under which the sample is placed, is completely given by the sorption isotherm vs. time plot. It normally shows an initially rapid absorption/desorption which tends asymptotically towards the equilibrium. The main feature of the plot describes the gain or loss of regain at quasi-equilibrium X and the rate at which this is achieved. The absorption/desorption rate can be numerically characterized by the time of half-sorption $t_{1/2}$ which is the time required for the substrate to absorb/desorb half as much regain $X_{1/2}$ as is interchanged with the environment when the quasi-equilibrium conditions are reached. The rate of half sorption $v_{1/2}$ is given by $X_{1/2}/t_{1/2}$. As explained, the increasing/decreasing intervals of relative humidities between 5% and 35% are of 10%, while those from 35% to 95% are of 20% of relative humidity. Then, rates of half absorption in the range 35-95% are twice as high as those in the range 5-35%. For comparative purposes, the rates of the upper humidity range will be reduced by half, yielding the corrected half sorption rate $v^*_{1/2}$.

a)

b)
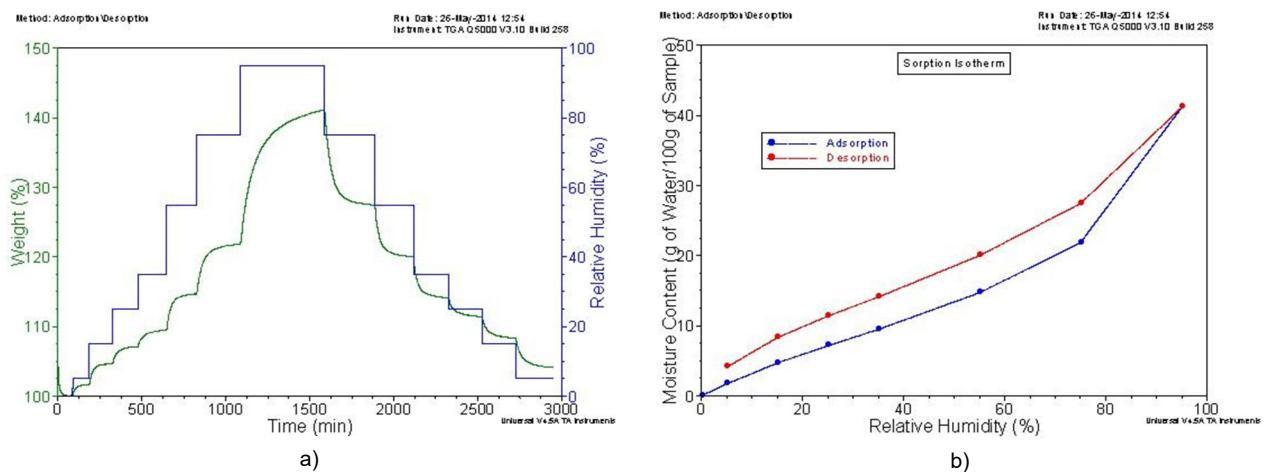
Figure 1 a) Sample mass variation in (% odw) at different relative humidity levels of absorption/desorption according to measuring procedure; b) Absorption/desorption isotherm using the final regain of each step

The existence of a water content gradient between the external surface and inside the specimen causes moisture to diffuse toward the centre of the specimen at a rate proportional to the gradient. If water content gradient is expressed in terms of weight of moisture per unit volume of substrate, the diffusion coefficient D will be the amount of moisture diffusing in unit time across a unit area of the specimen under a unit gradient of adsorbable water. Thus, D will be a measure of both the diffusing properties of moisture and the permeability of the specimen. It is not easy to evaluate the volume and the external surface of a leather specimen. If we replace the volume by the mass of the specimen, the gradient of moisture concentration gradient is expressed in grams of absorbable moisture per 100 g of dry specimen, resulting in an "apparent diffusion coefficient" D_A, which will be equal

to the grams of moisture adsorbed in unit time by 100 g of dry specimen under a unit concentration gradient of absorbable moisture, measured in min^{-1}, which is obtained using the Vickerstaff's method [21] used to study the diffusion of dyes in fibres. Diffusion is well fitted by an expression derived from Fick's equation that we apply in diffusion of moisture. This expression gives surprisingly satisfactory results in the early stages of moisture adsorption as in dye diffusion. If the fractional absorbed/desorbed moisture is plotted against the square root of the absorption/desorption time, the points lie on a straight line:

$$X(t)/X = \sqrt{D_A}\,\sqrt{t} \qquad\qquad (1)$$

being the maximum slope of the square root of the apparent diffusion coefficient D_A.

a) Regain $X(t)$ in % odw

b) Fractional regain
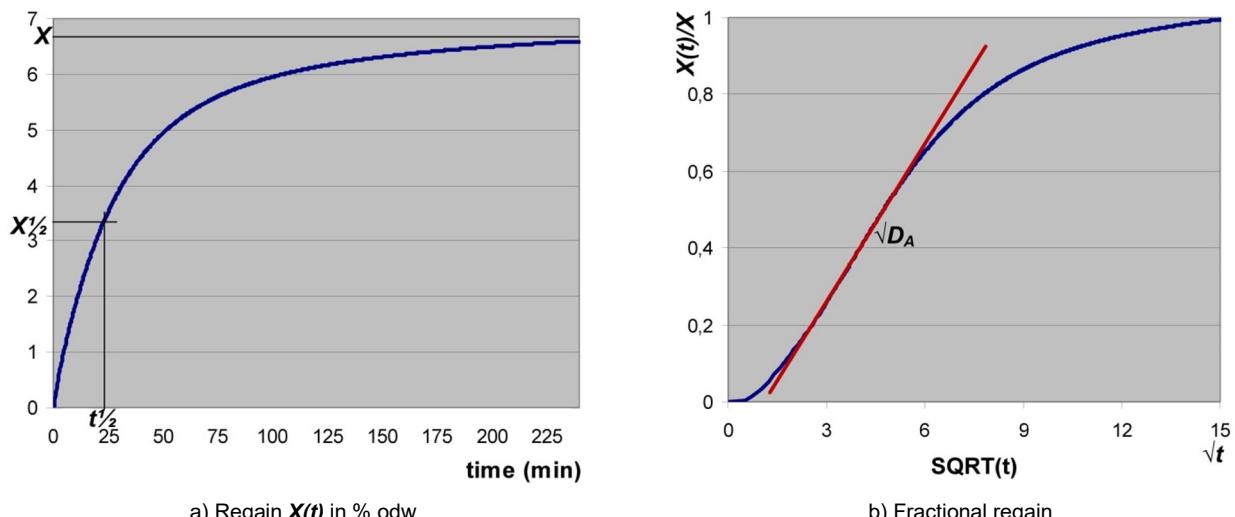
Figure 2 a) Mass increase in % odw caused by moisture absorption at one step along time, up to the equilibrium X. including values of half regain $X_{1/2}$ and half absorption time $t_{1/2}$; b) Fractional absorption $X(t)/X$ vs. square root of time. The maximum slope reflects the square root of the apparent diffusion coefficient D_A

3   RESULTS AND DISCUSSION

Table 2 summarizes the results of the parameters of fitted GAB model in absorption, the specific surface of absorption, mean values of hysteresis between 5 and 75% of relative humidity, the apparent density and tearing energy of non fatliquored and fatliquored samples at the two steps (before finishing, i.e. in crust C, and after finishing F), according to the different fatliquors applied. Methods are explained elsewhere [22, 23].

In order to analyze moisture absorption/desorption kinetics, the corrected rates of half absorption/desorption $v^*_{1/2}$, the time elapsed to attain the maximum diffusion t_{max} yielded by the plot of the fractional absorption/desorption vs. the square root of time and the apparent diffusion coefficient given by the square of the slope D_A at t_{max} are considered. The results for non

fatliquored leather and that fatliquored by the standard fatliquoring agent used as reference (TCSi/PGR) are shown in Table 3, those of their components TCSi and PGR, in Table 4, and the results corresponding to ESF and PSi, in Table 5.

The application of the ANOVA to the experimental results enabled us to estimate the effect of fatliquoring agent, step (crust, finished), mode (absorption, desorption) and relative humidity on the diffusion parameters (rate of half absorption corrected to a gradient of 10% RH $v^*_{1/2}$, time for maximum diffusion t_{max} and apparent coefficient of diffusion D_A), which explain the easiness of moisture interchange between leather and its environment. Table 6 summarizes the signification of the effects and interactions.

Table 2 GAB model parameters in absorption (X_m, C, K), estimated maximum absorption capacity X_1 at RH 100%, specific surface of absorption S, mean value of hysteresis between 5 and 75% of relative humidity H, apparent density D and tearing energy TE of the samples according to the fatliquor and step (C in crust and F finished) applied

Fatliquor	No		TCSi/PGR		TCSi		PGR		ESF		PSi	
Step	C	F	C	F	C	F	C	F	C	F	C	F
X_m [%]	10.55	9.46	11.32	9.00	9.87	8.23	10.59	7.95	10.45	8.79	9.98	8.85
C	5.01	5.81	4.92	5.83	4.78	5.91	4.59	6.37	4.50	5.35	5.09	5.51
K	0.81	0.82	0.80	0.82	0.79	0.82	0.79	0.84	0.79	0.81	0.80	0.81
X_1 [%]	52.59	51.10	49.18	47.46	43.62	43.33	47.73	47.88	46.9	44.35	46.86	45.84
S [m²/g]	374.2	335.5	401.5	319.2	350.1	291.9	375.6	282.0	370.6	311.8	354.0	313.9
H [%]	69.0	64.7	65.3	61.8	62.1	62.2	62.2	67.7	60.2	60.7	59.3	61.5
D [g/cm³]	0.621	0.650	0.588	0.649	0.640	0.689	0.637	0.678	0.632	0.653	0.656	0.699
TE [N/mm]	25.30	39.77	39.74	57.26	49.60	89.34	73.53	74.21	68.22	103.0	57.89	87.43

Table 3 Results of corrected rates of half absorption/desorption $v^*_{1/2}$, times for maximum diffusion t_{max} and apparent diffusion coefficients D_A, of non fatliquored leather **No** and that fatliquored by the **TCSi/PGR** combination in crust C and after finishing F. Absorbed and desorbed regains according to step are included

Fatliquor	No						TCSi/PGR					
Parameter	$v^*_{1/2}×10^2$ [%/min]		t_{max} [min]		$D_A×10^2$ [min⁻¹]		$v^*_{1/2}×10^2$ [%/min]		t_{max} [min]		$D_A×10^2$ [min⁻¹]	
Step	C	F	C	F	C	F	C	F	C	F	C	F
Absorption												
5→15%	11.25	11.32	7.58	7.75	3.18	3.36	13.56	9.02	6.25	9.00	4.10	2.89
15→25%	7.35	7.58	3.79	4.50	2.25	2.39	8.67	6.46	3.00	5.75	2.73	2.11
25→35%	5.68	5.88	3.16	2.50	1.74	1.94	6.53	5.24	1.75	4.75	2.20	1.72
35→55%	4.83	7.44	2.97	13.75	1.24	2.65	5.58	6.23	1.88	14.25	1.58	2.38
55→75%	5.33	7.22	34.04	16.25	1.06	1.90	6.26	5.87	25.38	20.00	1.24	1.57
75→95%	7.33	7.78	46.57	28.75	0.77	0.76	7.99	6.47	37.87	35.25	0.86	0.68
Desorption												
95→75%	10.30	12.03	19.37	20.00	1.43	1.86	11.36	9.76	15.87	25.25	1.67	1.60
75→55%	8.27	9.91	8.38	11.00	1.77	2.39	9.47	8.11	7.25	12.50	2.19	2.08
55→35%	7.32	9.06	5.37	8,50	1.88	2.56	8.50	7.42	4.12	10.25	2.45	2.28
35→25%	7.43	7.34	4.50	4,50	2.02	2.24	8.72	6.33	3.50	5.25	2.53	2.04
25→15%	8.36	7.91	5.25	5,00	2.15	2.02	9.23	6.76	4.50	6.50	2.45	1.84
15→5%	9.39	8.73	14.49	13.25	1.72	1.67	9.91	7.40	8.25	17.25	1.92	1.56
In crust: Regain absorbed (5 - 95%): 41.17% *Regain desorbed (95 - 5%): 38.55%* *Finished: Regain absorbed (5 - 95%): 39.44%* *Regain desorbed (95 - 5%): 37.03%*							*In crust: Regain absorbed (5 - 95%):38.85%* *Regain desorbed (95 - 5%): 36.33%* *Finished: Regain absorbed (5 - 95%): 36.81%* *Regain desorbed (95 – 5%):34.61%*					

Table 4 Results of corrected rates of half absorption/desorption $v^*_{1/2}$, times for maximum diffusion t_{max} and apparent diffusion coefficients D_A, of leathers fatliquored with **TCSi** and **PGR** in crust C and after finishing F. Absorbed and desorbed regains according to step are included

Fatliquor Parameter Step	TCSi						PGR					
	$v^*_{1/2}\times10^2$ [%/min]		t_{max} [min]		$D_A\times10^2$ [min⁻¹]		$v^*_{1/2}\times10^2$ [%/min]		t_{max} [min]		$D_A\times10^2$ [min⁻¹]	
	C	F	C	F	C	F	C	F	C	F	C	F
Absorption												
5→15%	11.19	12.45	7.50	5.75	3.61	4.32	11.08	9.95	8.08	8.33	3.40	3.23
15→25%	7.79	8.58	4.00	2.50	2.72	3.36	7.79	7.30	5.00	4.58	2.58	2.87
25→35%	6.03	6.48	2.67	2.08	2.21	2.80	5.93	5.86	3.00	3.50	2.16	2.65
35→55%	7.47	8.17	13.08	10.13	2.55	3.09	7.14	6.26	12.63	12.58	2.22	2.26
55→75%	7.81	8.19	14.78	12.17	2.34	2.63	7.56	6.17	16.67	15.92	1.99	1.79
75→95%	7.34	8.17	25.17	22.79	0.82	0.91	7.31	6.51	27.42	34.67	0.76	0.65
Desorption												
95→75%	11.58	13.37	20.00	16.25	2.09	2.35	11.34	10.33	20.83	23.17	1.83	1.72
75→55%	9.74	10.70	9.58	8.50	2.73	3.05	9.63	8.53	11.67	12.13	2.46	2.30
55→35%	8.90	9.65	6.92	7.13	2.91	3.38	8.77	7.76	9.08	9.42	2.65	2.49
35→25%	7.36	8.18	4.17	3.83	2.52	3.20	7.36	6.71	4.67	4.08	2.29	2.28
25→15%	7.72	8.61	5.00	4.38	2.18	2.62	7.81	7.08	6.42	7.92	2.01	1.93
15→5%	8.33	9.55	14.58	9.58	1.72	2.04	8.68	7.75	14.00	16.33	1.65	1.57
In crust: Regain absorbed (5 - 95%): 34.99% *Regain desorbed (95 - 5%): 32.91%* *Finished: Regain absorbed (5 - 95%): 33.78%* *Regain desorbed (95 - 5%): 31.85%*							*In crust: Regain absorbed (5 - 95%):38.13%* *Regain desorbed (95 - 5%): 35.98%* *Finished: Regain absorbed (5 - 95%): 36.21%* *Regain desorbed (95 – 5%):34.15%*					

Table 5 Results of corrected rates of half absorption/desorption $v^*_{1/2}$, times for maximum diffusion t_{max} and apparent diffusion coefficients D_A, of leathers fatliquored with **ESF** and **PSi** in crust C and after finishing F. Absorbed and desorbed regains according to step are included

Fatliquor Parameter Step	ESF						PSi					
	$v^*_{1/2}\times10^2$ [%/min]		t_{max} [min]		$D_A\times10^2$ [min⁻¹]		$v^*_{1/2}\times10^2$ [%/min]		t_{max} [min]		$D_A\times10^2$ [min⁻¹]	
	C	F	C	F	C	F	C	F	C	F	C	F
Absorption												
5→15%	12.19	10.64	6.75	7.75	3.81	3.62	12.04	12.05	6.00	6.00	3.43	4.08
15→25%	7.99	7.51	2.75	4.25	2.67	2.71	5.35	8.14	2.00	2.75	2.56	2.95
25→35%	6.25	6.07	2.50	3.50	2.07	2.29	3.56	6.34	1.50	2.25	1.99	2.27
35→55%	7.98	7.11	13.00	10.50	2.68	2.63	6.70	7.89	15.50	11.50	2.29	3.00
55→75%	8.02	7.09	16.00	16.00	2.10	1.99	8.20	7.41	16.50	14.75	2.18	2.04
75→95%	7.78	7.42	25.75	26.50	0.83	0.83	7.88	7.69	26.25	28.50	0.84	0.83
Desorption												
95→75%	11.83	11.53	20.50	19.75	1.91	1.96	12.22	11.72	18.25	20.75	1.95	1.98
75→55%	10.14	9.59	11.25	10.00	2.63	2.62	10.49	9.97	10.25	11.00	2.74	2.70
55→35%	9.64	8.87	8.50	8.00	2.92	2.93	9.74	9.34	7.25	8.00	3.00	3.00
35→25%	8.04	7.46	4.25	4.50	2.59	2.59	8.22	7.88	3.75	4.00	2.74	2.74
25→15%	8.68	7.81	5.25	5.25	2.33	2.30	8.95	9.14	5.00	4.75	2.43	2.45
15→5%	9.78	8.59	10.00	10.00	1.99	1.90	10.06	9.73	9.50	10.75	2.07	2.09
In crust: Regain absorbed (5 - 95%): 37.38% *Regain desorbed (95 - 5%): 35.16%* *Finished: Regain absorbed (5 - 95%): 34.67%* *Regain desorbed (95 - 5%): 32.62%*							*In crust: Regain absorbed (5 - 95%): 37.11%* *Regain desorbed (95 - 5%): 34.81%* *Finished: Regain absorbed (5 - 95%): 35.66%* *Regain desorbed (95 – 5%): 33.32%*					

Table 6: Summary of the signification of **F**atliquor, **S**tep (crust, finishing), **M**ode (absorption, desorption), **R**elative **H**umidity and their interactions (**FxS**, **FxM**, **FxRH**, **SxM**, **SxRH**, **MxRH**) on diffusion parameters: rate of half absorption $v^*_{1/2}$, time for maximum diffusion t_{max} and apparent diffusion coefficient D_A

Diffusion parameters	Main effects				Interactions					
	Fatliquor	Step	Mode	RH	FxS	FxM	FxRH	SxM	SxRH	MxRH
$v^*_{1/2}$	0.0%	2.5%	0.0%	0.0%	0.0%	n.s.	n.s.	n.s.	5.0%	0.0%
t_{max}	1.0%	n.s.	0.0%	0.0%	5.0%	n.s.	n.s.	n.s.	n.s.	0.0%
D_A	0.0%	0.1%	n.s.	0.0%	0.0%	n.s.	n.s.	n.s.	5.0%	0.0%

Note: n.s. – non-significant effect.

As shown in Table 6, diffusion parameters are significantly influenced by fatliquor, step (crust, finished), mode (absorption, desorption) and relative humidity and the interactions between fatliquor and step, and between relative humidity and both step and mode. Consequently, discussion will be based on interaction plots in which the effect of all factors can be assessed. Figure 3 shows the effect of relative humidity and step in diffusion parameters. Regardless of fatliquoring, it can be observed that the initial half sorption rate decreases up to 30% RH but when exceeded, turns to ascend. At 10% RH, initial sorption rate is higher in crust than in finished samples, which can be related with their higher size of the monolayer. Moisture initially absorbed by leather hinders the entrance of subsequent moisture, decreasing the initial rate up to 30% RH but the increase in partial pressure of moisture by the increase in relative humidity balances the hindering and makes the initial rate increase with partial pressure or relative humidity. From 20% of RH, no significant differences in the initial diffusion rate between crust and finished are observed. No differences between crust and finished samples are observed as regards the time to attain the steady diffusion regime that decreases up to 30% RH and then turns to ascend, probably due to the fact that moisture is located in the inner parts of the sample. As regards the apparent coefficient of diffusion, finishing favours diffusion especially for relative humidities around 45%. At higher RH, secondary water is located in multilayers: this explains the decrease of the coefficients and the growth in time for maximum diffusion.

Figure 4 shows the effect of relative humidity and mode in diffusion parameters. It appears that the initial rate of sorption is higher in desorption than in absorption except when primary water strongly linked to leather at lower RH is involved [24]. As regards the time for maximum diffusion (to reach the steady state) variation in desorption is more balanced than that in absorption, being longer at lower RH and shorter in higher RH. Similar evolution is observed in relation with the diffusion coefficient. Variation in desorption is more balanced than that in absorption. The diffusion of primary strongly linked water can be observed at lower RH, that of the secondary weakly linked one, at medium values of RH, and the diffusion of free water, at the higher RH levels. Figure 5 shows that the effect of finishing on diffusion parameters depends on the fatliquor used. Finishing in non fatliquored leather makes the initial diffusion rate ascend, reaching faster the steady (lower t_{max}) and increasing the diffusion coefficient.
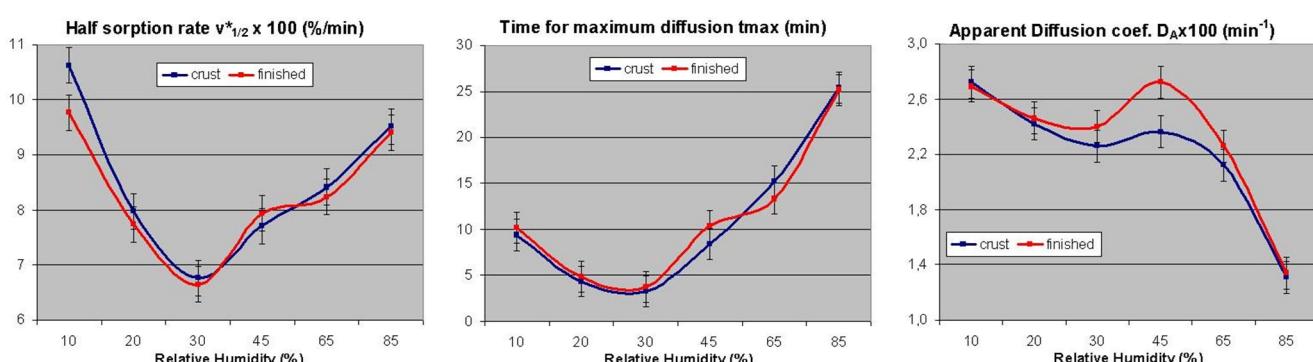

Figure 3 Effect of the relative humidity and step (crust, finishing) on diffusion parameters (corrected half sorption rate, time for maximum diffusion and apparent diffusion coefficient)
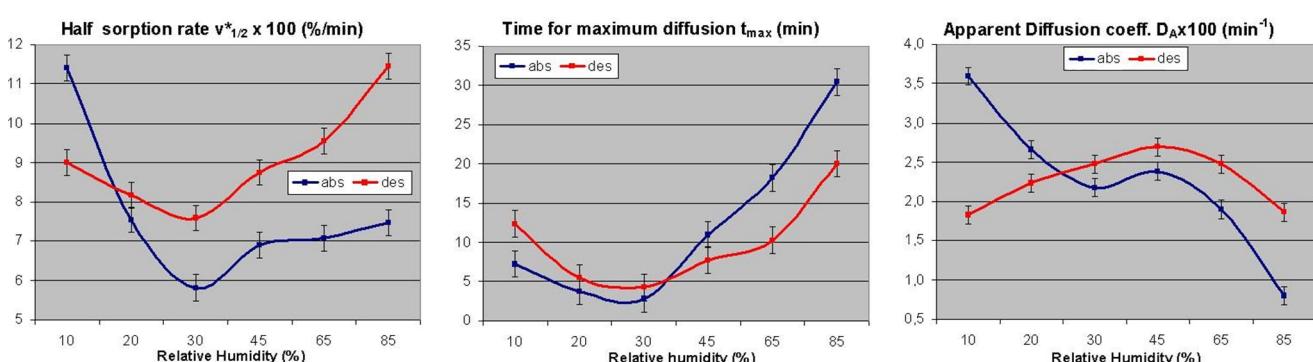

Figure 4 Effect of the relative humidity and mode (absorption, desorption) on diffusion parameters (half sorption rate, time for maximum diffusion and apparent diffusion coefficient
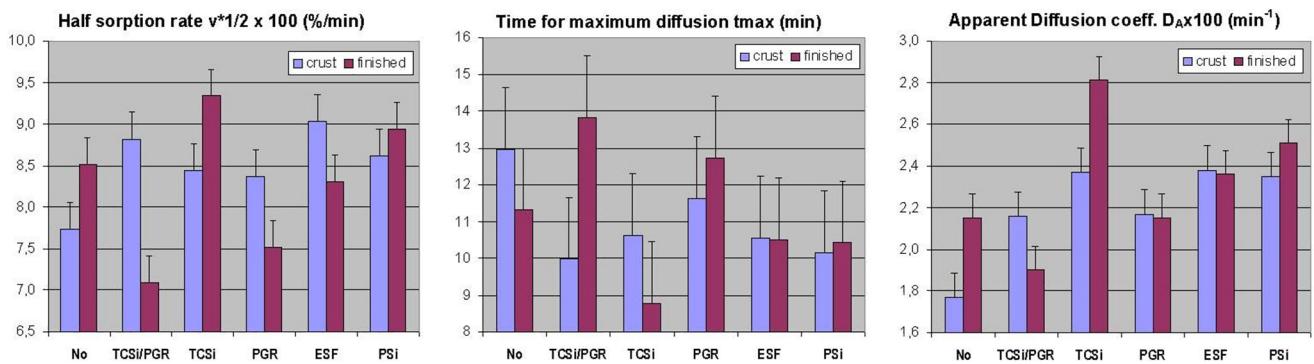
Figure 5 Effect of fatliquor and step (crust, finishing) on diffusion parameters (half sorption rate, time for maximum diffusion and apparent diffusion coefficient
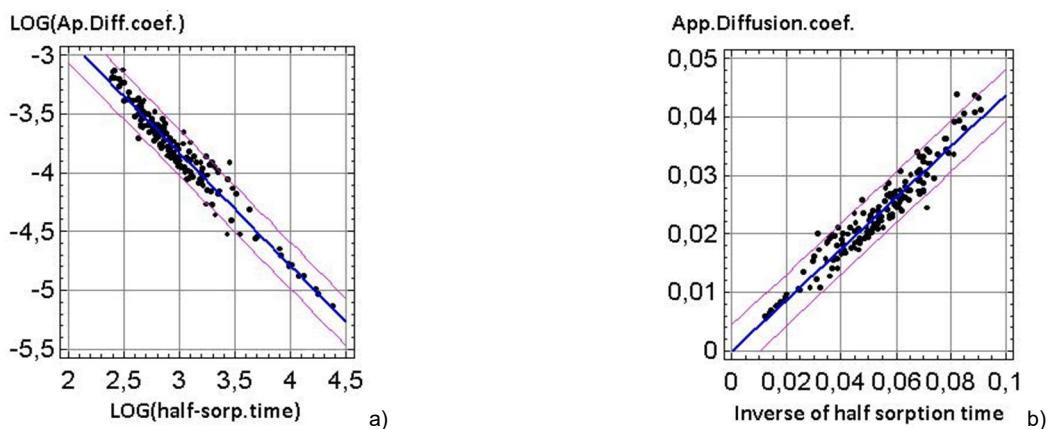

Figure 6 Linear relationships between a) the logarithms of the apparent diffusion coefficient and the half of sorption time, and b) that of the apparent diffusion coefficient and the inverse of half-sorption time

Similar effects of finishing can be are observed when leather is fatliquored with TCSi although it shows the highest initial rates, the lowest times for steady diffusion and the greatest diffusion coefficients. As regards leather finished with standard mixture (TCSi/PGR), finishing causes the opposite effects: a strong decrease in the initial rate, a significant ascent in time for maximum diffusion and a decrease in the diffusion coefficient. These seem to be the expected effects of finishing, taking into account that this operation causes an increase in the apparent density of leather. When leather is fatliquored with the other component of the mixture, PGR, the effects, although shorter, show the same tendencies for the initial rate and the time for maximum diffusion. The diffusion coefficient after finishing remains the same. When we consider leathers fatliquored with ESF and PSi, no significant effects of finishing are observed in the time for maximum diffusion and the diffusion coefficient, although the initial diffusion rate of ESF significantly decreases while the initial rate for PSi is non significantly modified.

As regards the diffusion parameters, no differences between crust and finished steps are observed

in non fatliquored leather at low relative humidities up to 30%. Focusing on the apparent coefficient of diffusion, a continuous decrease with relative humidity can be observed in non fatliquored sample and that fatliquored with standard fatliquoring in crust state. But, after finishing and with the other fatliquors regardless of the step, the evolution of the diffusion coefficient with the relative humidity is similar to that shown in Figure 4.

Boulton, Reading and Neale studied the relationship between the rate of dyeing and diffusion inside the fibre and the results are explained by Vickerstaff [21]. As regards the diffusion of direct dyes on viscose rayon, these authors plotted the apparent diffusion coefficients against the half-times of dyeing in logarithmic basis. According to them, all points lie close to a straight line whenever the rate of dyeing is determined by the rate of diffusion inside the fibre. We applied the same criteria to evaluate the rate of moisture absorption/desorption and the diffusion inside all treated leather samples. Figure 6a) confirms the linear relationship between the logarithms of the apparent diffusion coefficient and the time of half sorption.

A deeper examination of the relationship between half adsorption time and the apparent diffusion coefficient suggests another linear relationship that is closer and more simple, [25] i. e. the regression between the inverse of the half time of sorption and the apparent diffusion coefficient, yielding the equation shown in Figure 6b), $D_A = 0,437/t_{\frac{1}{2}}$ with a correlation coefficient of 0.996. Prediction intervals at 95% are included.

4   CONCLUSIONS

In the light of our findings, the following conclusions may be drawn:

– Diffusion parameters explain the kinetics of sorption that is independent of sorption results reached at the equilibrium.

– Diffusion parameters are significantly influenced by fatliquor, step (crust, finished), mode (absorption/desorption) and relative humidity.

– The initial half-sorption rate tends decreases up to 30% RH and then tends to ascend. At lower relative humidities, crust samples show higher initial rates than finished ones, and the diffusion coefficient of finished samples is higher than that of crust ones when RH is around 45%.

– As regards the time for maximum diffusion that shows a minimum at 30% RH, no differences are observed between crust and finished samples.

– When mode of sorption is considered, higher half-sorption rates and diffusion coefficients are observed at lower relative humidities, while the contrary occurs at higher relative humidities.

– The evolution of the apparent diffusion coefficient of all crust and finished samples follows the plot shown in Figure 4, except for crust samples non fatliquored and fatliquored with TCSi/PGR which progressively decrease as relative humidity increases.

– The linear relationship between the logarithmic form of the time of half adsorption and the apparent diffusion coefficient suggests that the rate of adsorption is governed by the diffusion of moisture inside the sample.

5   REFERENCES

1. Bajza Z., Vrcek I.V.: J Mater Sci 36, 5265-5270, 2001

2. Mitton R.G.: J Soc Leath Tech Ch 54, 248-266, 1970

3. Komanowsky M.: J Am Leather Chem As 86, 269-280, 1989

4. Tuckerman M., Mertig M., Pompe W., Reich G.: J Mater Sci 36, 1789-1799, 2001

5. Bienkiewicz K.: "Physical Chemistry of Leather Making", RE Kriger Publishing Company, Malabar, Florida, 110, 1983

6. Bosch T, Manich A.M., Carilla J., Cot J., Marsal A., Kellert H.J., Germann H.P.: J Am Leather Chem As 97, 441-450, 2000

7. Hole L.G.: J Soc Cosmet Chem 24, 43-63, 1973

8. Svennberg K., Lengsfeld K., Hardekup L.E., Holm A.: J Build Phys 30(3), 261-274, 2007

9. Dernovšková J., Jirasová H., Zelinger J.: Restaurator 16, 31-44, 1995

10. Pineri M.H., Escoubes, M., Roche, G.: Biopolymers 17, 2799-2815, 1978

11. Grigera J.R., Berendsen H.J.C.: Biopolymers 18, 47-57, 1979

12. Caurie M.: Int J Food Sci Tech 40, 283-293, 2005

13. Timmermann, E.O.: Colloid Surface A 220, 235-260, 2003

14. Dent R.W.: Text Res J 47, 145-152, 1977

15. Al-Muhtaseb A.H., McMinn W.A.M., Magee T.R.A.: J Food Eng 61, 297-307, 2004

16. Kneule F.: "Enciclopedia de la Tecnología Química. Tomo I: El Secado", Ed. Urmo, S. A., Bilbao (Spain), 32-33, 1976

17. Palop R., Manich A.M., Marsal A.: J Am Leather Chem As 102(5), 145-153, 2007

18. Palop R., Manich A.M., Marsal A.: J Am Leather Chem As 101(11), 399-407, 2006

19. Higgins R A: "Properties of engineering materials", Edward Arnold, London, 1991

20. Otunga M.G.: "Effect of drying under strain on the mechanical properties of leather", PhD Thesis, University of Leicester, UK, 2002

21. Vickerstaff T.: "The Physical Chemistry of Dyeing", Oliver and Boid, London, 1954

22. Manich A.M., Barenys J., Martínez L., Lloria J., Carilla J., Marsal, A.: "Efecto del engrase en las características de confort de la piel. Parte III: Absorción y desorción de humedad", Proceedings 64 AQEIC Congress, Barcelona, 2016 (in Spanish)

23. Manich A.M., Barenys J., Martínez L., Lloria J., Marsal A.: J Am Leather Chem As, (in press) April 2016

24. Ussman M., López-Santana D., Carilla J., Manich A.M.: "Cellulosic Fibres and Water Sorption Isotherms", 10th Mediterranean Conference on Calorimetry and Thermal Analysis MEDICTA 2011, Proceedings, Porto, 2011

25. Manich A.M., Maldonado F., Carilla J., Catalina M., Marsal A.: J Soc Leath Tech Chem. 94(1), 15-20, 2010

MITIGATION OF ENVIRONMENTAL IMPACT CAUSED BY DWOR TEXTILE FINISHING CHEMICALS STUDYING THEIR NONTOXIC ALTERNATIVES

M. Martí and A. M. Manich

IQAC-CSIC, Jordi Girona 18-26, 08034 Barcelona, Spain
meritxell.marti@iqac.csic.es

Abstract: *DWOR (Durable Water and Oil Repellents) are textile finishing products made of long chain fluorocarbon polymers to give repellency to water, oil and dirt to fabrics. These chemicals are persistent and bioaccumulative. Many perfluorochemicals have already been listed in different European regulations to put emphasis on their risk for humans and the environment.*

These products have been used in the textile industry since many years ago and tentative to replace them has been done since 2000. Alternative products are currently being proposed by different chemical companies for textile applications, however, the toxicity and environmental impact of these new alternatives is still unknown. The substitution of toxic and persistent perfluorochemicals is of high importance as they occupy a high place in the market and almost all alternatives are perfluorocarbons based products (fluorocarbons polymers with shorter chain length).

The main objective of the project is to mitigate the environmental, health and safety impacts of current and future Durable Water and Oil Repellents (DWOR) alternatives by analyzing their environmental impact and technical performances, in order to assess manufacturers on the best available technologies for repellent finishing. Moreover, the risks of the DWOR alternatives will be evaluated for human and environmental health in the textile finishing industry. In this perspective, policy recommendations will be set in order to promote the widespread implementation of the less toxic and most effective DWOR alternatives to fulfill REACH Regulation.

Key Words: *Durable Water and Oil Repellents*

1   INTRODUCTION

Durable water and oil repellents (DWORs) are finishing treatments normally applied to fabrics to provide protection against water, oil and dirt. DWOR finishes add value to textile products. In addition to providing protection against water, oil and soil, these finishes also extend the life of products and keep them looking newer longer. DWOR technology has historically been achieved with textile finishes that contain a polymer to which long-chain perfluoroalkyl groups have been attached. These long-chain fluorinated polymers often contain residual raw materials and trace levels of long-chain perfluoroalkyl acids (PFAAs) as impurities. The residual raw materials and the product themselves may degrade in the environment to form long-chain PFAAs.

Since the 1950's, long-chain PFAAs as well as polymers and surfactants containing long-chain perfluoroalkyl functionality which may degrade to form long-chain PFAAs have been widely used in numerous industries and commercial applications. As a result of the widespread uses, long-chain PFAAs including PFOA and PFOS have been detected globally in the environment, wildlife and humans. PFOA and PFOS, the most widely known and studied long-chain PFAAs [1, 2], have been shown to be persistent in the environment, have long elimination half-life in wildlife and humans, and have toxicological properties of concern. Due to these properties, regulatory actions have been put in place or are being considered in several countries to manage these substances. There is also a shift within industries towards DWOR chemistries containing shorter perfluoroalkyl chains as well as non-fluorinated chemistries.

1.1 Alternative techniques to DWOR:

Templating, lithography, imprinting

These structure modification techniques aim at mimicking the nature, reproducing the nanometric surface structure of plants (lotus leaves or rice leaves) or animals (butterfly wings).

Plasma

Plasma is a gas partially ionized composed of electrons, ions, photons, atoms and gas molecules in any state of excitation. Plasma treatments are used to provide hydrophobic properties to textile substrates, and depend on the pressure (low pressure plasma, atmospheric plasma). Surface polymerization, grafting and

surface activation can be achieved by using this method [3].

Electrospinning

Electrospinning is a new technique to spin nanometric sized fibers obtained from a polymeric fluid pulverized on a collecting surface. The coaxial electrospinning method has been used to produce nanofibers with a nanometric roughness on its surface responsible for imparting hydrophobic properties to the substrate.

1.2 Alternative finishings to DWOR

Conventional paraffin-based repellents:

Paraffin repellent finishing was one of the first repellent finishings used before fluorinated polymers. Paraffin finishings are usually composed of a paraffin wax emulsified in water with stearic acid, triethanolamine and a salt acting as a deactivating agent of the hydrophilicity of the emulsifying agent (aluminum chloride, aluminum sulfate, zinc sulfate, barium chloride, etc.). Once the emulsion is obtained; it can be applied on the fabric by padding or exhaustion. The final structure obtained on the fabric is a comb-like structure with hydrophobic long chain of paraffin wax. The main inconvenience of this type of repellent is that they do not have oil repellency properties and they have low domestic washing fastness [4].

Conventional stearic acid melamine based repellents:

Stearic acid melamine repellents are another type of conventional finishing applied on textile for water repellency. This product is made of stearic acid and formaldehyde mixed with melamine, resulting in a complex molecule imparting hydrophobic properties to textiles. The solution is applied by impregnation techniques such as exhaustion and padding. Stearic acid melamine repellents' advantage is that they have good washing fastness due to the covalent links they can produce with the fabric [4].

Silicone based repellents:

Silicone repellents are also commonly used in the textile industry to give water repellency to fabrics. These finishings are generally made of elastomeric polydimethylsiloxanes which can coat the fabric surface after curing. The structure obtained after finishing by padding of the fabric surface is a three-dimensional, flexible and hydrophobic layer bonded to the fabric's fibers. Silicone repellents finishings have moderate washing fastness due to the hydrolysis of the siloxane during laundry.

Sol gel

The sol gel process is one of the new processes of the inorganic chemistry which doesn't require reactions at very high temperatures (>700°C)

to develop new mineral structures [5]. It consists in developing three-dimensional inorganic or organometallic matrix from liquids monomers at low temperature and normal pressure. This process is employed to obtain hydrophobic coating on textiles by means of conventional textile application techniques (padding and exhaustion). The precursors are usually organosilicates (for example, Tetraethyl orthosilicate, TEOS). The sol gel coating obtained once applied on textile is transparent, has good light and heat fastness and doesn't affect the hand of the fabric due to its nanometric structure [6, 7].

Perfluorosilicones (PFSi)

Perfluorosilicones are alternative products to perfluoroacrylates materials and are linear polydimethylsiloxane (Si–O–Si) chains composed of short fluorinated side chains [4]. This material is widely used in the textile sector to provide hydrophobic and oleophobic properties. They have been extensively studied due to the problematic related to long chain fluorocarbon based finishing and due to their possibility of providing good technical performance and lower environmental impact.

Perfluoropolyethers (PFPE)

Like perfluorosilicones, perfluoropolyethers represent an alternative to perfluoroacrylates as they don't present long fluorocarbon side chains but are made of fluorine atoms responsible for giving high hydrophobicity. PFPE finishings are well-known to provide hydrophobic and oleophobic properties to textiles.

Dendrimers and hyperbranched polymers

The hyperbranched polymers group includes dendrimers, dendrons, dendrigraft polymers and branched polymers. They are all cascade polymers of different sizes or branch extensions. Dendrimers are considered the fourth macromolecular generation (Figure 1) and are used to obtain hydrophobic and oleophobic textiles [8].


Dendrímero   **Polímero hiperramificado**
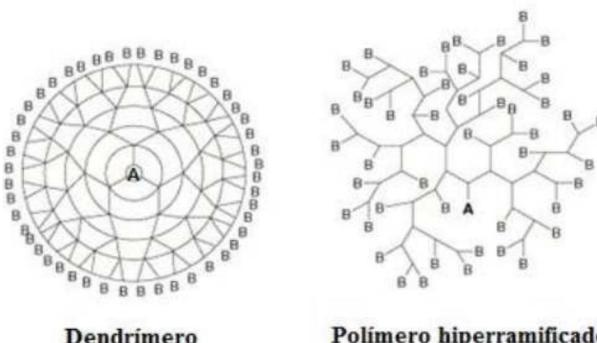
Figure 1 Dendrimer's and hyperbranched polymer's architecture

2 PROJECT OBJECTIVES AND PARTICIPANTS

This LIFE+Environmental Policy and Governance project groups three textile clusters from Spain, Italy and Czech Republic (AEI Textil, CLUTEX and CS-POINTEX) which group the industrial textile sector of their countries and also, joins two technological Spanish centres (LEITAT and CETIM) and a Spanish research centre (IQAC) that belongs to the Spanish Research Council (CSIC) for the next three years. The technological cluster "AEI Textil" is the Leader of the Project.

The main objective of this project is to mitigate the environmental, health and safety impacts of current and future DWOR alternatives, by analyzing their environmental impact and their technical performances, in order to help manufacturers to move on to the best available technologies for water, oil and dirt repellent finishing. This main objective will be reached as a consequence of the completion of more specific objectives that are listed below, in order to mitigate the use of PFOA and PFOS toxic compounds in the industry:

- Evaluation of the environmental impact of DWOR and their available alternatives

- Evaluation of the risks posed by DWOR and their alternatives for human and environmental health

- Elaboration of a complete report for the European textile and other related industries that use DWOR on accepted repellent finishing technologies by 2018, including the following topics:
  - Good practices guidelines on DWOR selection, use and disposal
  - Innovative tools enabling the industries to identify and compare the environmental impact, risk assessment and technical performance of diverse repellent finishing.

The preliminary work of the MIDWOR project has been focused on the selection of the most representative textile materials and finishing technologies normally used in the textile sector. This is the base over which the project will be developed. A complete exploratory study of the market has been performed in order to determine the most common chemical products used to give water, oil and dirt repellence of fabrics, and also the type of textiles on which this finishing is applied as regards their main characteristics (areal density, fabric structure, weave, composition and application).

3 EXPERIMENTAL

The identification of the Durable Water and Oil Repellent (DWOR) products normally used by the textile industry has been based on a screening design completed by the partners and directed to the industries, in order to get this information.

The three cluster associations included as partners in the project reached out to their local industry (Spain, Italy and Czech Republic) to collect the replies. Two target groups where defined for this survey:

1. Finishers for third-parties or manufactures of finished fabric, and
2. Producers or formulators of finishing products for the textile industry.

After processing the information obtained from surveys and the technical information available about water and oil repellent finishes that are normally used in the market, the survey leads to the selection of seven alternative DWOR products, two conventional long chain fluorocarbon based DWOR for comparative purposes, and the application of all these products on five different representative fabrics that differ between each other in areal density (weight), composition and structure.

4 RESULTS AND DISCUSSION

The project team collects technical and scientific data about DWOR conventional treatments, alternatives and innovations, and during for a 4-month period, the cluster managers look for the answers of their contacts to write a survey report that enables them to know the current DWOR industrial state.

80% of the questionnaires were answered by finishers for third-parties or manufacturers of finished fabric and the remaining 20% by producers or formulators of finishing products for the textile industries from Italy, Czech Republic and Spain.

Figure 2 summarizes the ratio of the collected answers for the first group in a circular sector plot.

It has to be noted that the two following questions were only answered by companies which had replied "Yes, but with some drawbacks" to the question "Does the market accept them?":

- What are the main issues that your company faces while using finishing products containing fluorocarbons?
  - Environmental restrictions/Conflict with EU regulations (50%)
  - Demand for alternative products
  - Regulations about treatment of emissions to the atmosphere
  - Performance drawbacks (allowed percentages/feel of fabric (fashion sector))

- What solutions or alternatives to fluorocarbons does your company offer?
  - Fluorine-free products
  - HF ecological adaptation
  - Silicones
  - Microencapsulate waxes
  - None (30%)

Does your company produce finished fabrics with durable water and oil repellents (DWOR)?

- Yes
- No

25%

75%

FOR WHICH SECTOR?

- FASHION
- HOME
- SPORT
- PPE
- OTHER

21,6%

32,4%

21,6%

18,9%
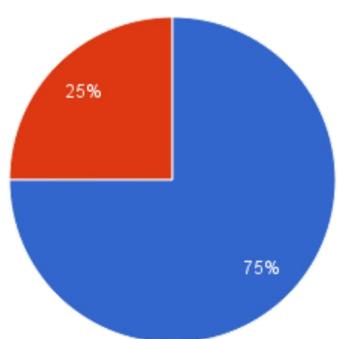
Does your company use products containing fluorocarbons to provide water and oil repellency properties?

- No
- Yes

16,7%

83,3%

Does the market accept them?

- Yes, but with some drawbacks
- Yes, no questions asked

40%

60%
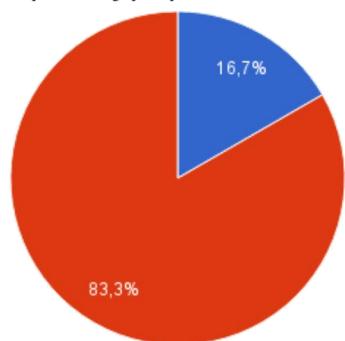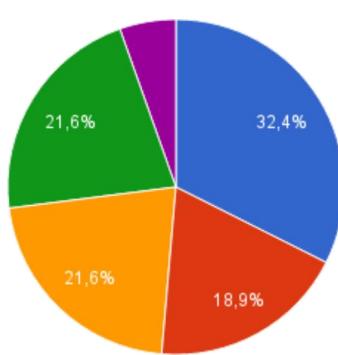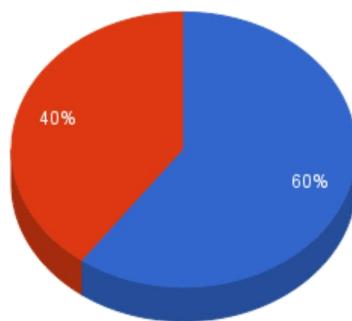
Figure 2 Different questions and answers obtained from finishers for third parties or manufacturer.

For which fiber compositions?

- Wool
- Polyester
- Cellulose
- Cotton
- Mixed

21,4%

28,6%

14,3%

14,3%

21,4%
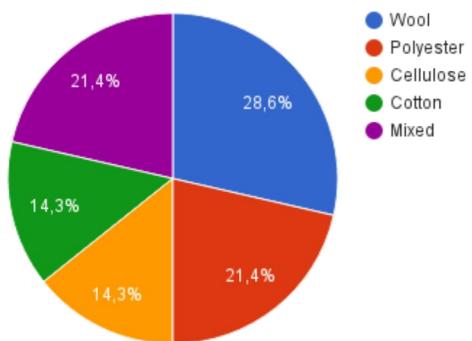
Which application method is recommended?

- Impregnation
- Exhaustion
- Coating

18,2%

54,5%

27,3%
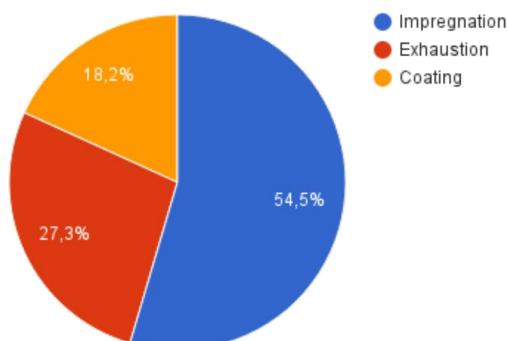
What PFOA / PFOS -free alternatives do you believe will take over in the future of the textile industry?
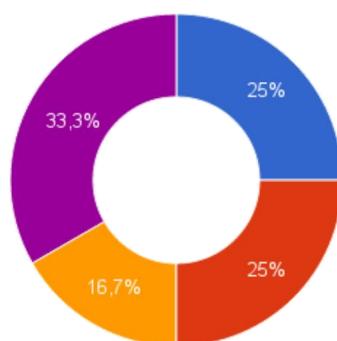
- i. Fluorocarbons with very short chains
- ii. Branched / structured polymers
- iii. PUR
- v. Modified silicones

25%

33,3%

25%

16,7%

Figure 3 Questions and answers from the producers / formulators of finishing products for the textile industry

Table 1 Final selection of different DWORs

| Number	Technology	Characteristic component	Comments
1	CONVENTIONAL	Long Chain Fluorocarbon (c8)	-
2	CONVENTIONAL	Long Chain Fluorocarbon (c8)	-
3	ALTERNATIVE	Short Chain Fluorocarbon (c6)	PFOA-free
4	ALTERNATIVE	Short Chain Fluorocarbon (c6)	PFOA-free,Nano-dispersion of fluoropolymer
5	ALTERNATIVE	Short Chain Fluorocarbon (c6)	PFOA-free dendrimer and 3D hyperbranched polymer
6	ALTERNATIVE	Short Chain Fluorocarbon (c6)	PFOA-free
7	ALTERNATIVE	SOL-GEL	SOL GEL without fluorine, PFOA-Free
8	ALTERNATIVE	Perfluorosilicones	Structured coating: C6 + silicone
9	ALTERNATIVE	Silicones	Completely Fluorine-free

Table 2 Five selected representative fabrics

Number	Weight [g/m^2]	Composition	Sector
1	230	100% PES	Automotive
2	195	100% PES	Sport (mountain)
3	180	100% WO	Fashion (suit)
4	250	49%PP / 47%PES / 4%CO	Home (sofa)
5	175	100% PES	Workwear (polo)

As regards the second group "Producer / Formulator of finishing products for the textile industry", it has to be noted that the answer to the question "Does your company offer products with durable water and oil repellent (DWOR) finishes for the textile industry?" was "Yes" for all the companies.

Figure 3 summarizes in a circular sector plot the ratio of the collected answers for other questions made to this group.

The majority of respondents are finishers (80%) and 75% of them use DWOR products. The sectors which they work for are fashion, sport, personal protective equipment and home textiles. Most of the companies work only for one, two or maximum three sectors, for one sector being the most representatives of the respondents. It is observed that most companies solve the problems related with water and oil repellency by using fluorocarbon-based finishing, but most of them inform us that the market begins to ask about environmental issues.

With the information obtained from the survey, conventional DWORs were looked for to choose two of them as the most used representatives. Five different commercial producers were assessed, and two commercial long chain fluorocarbons (C8) were selected.

Regarding DWOR alternative products, the tendency is to replace the C8 fluorocarbon chemistry by C6 or C4 fluorocarbon products or even fluorine-free water repellents. In fact, currently, new commercial DWOR finishes are coming onto the market which are based on short chain fluorocarbons, hybrid systems or they are fluorine free.

The selection of the other alternatives has been done according to the reported interest of the companies about them, based on the state

of the art that has been done. Three commercial products were selected, one per each alternative that seems to be an alternative for the future: SOL-GEL technology, perfluorosilicones and modified silicones. Additional four C6 fluorocarbon products were also included in the studied possible alternatives (Table 1).

Another selection was that of the fabrics where DWOR products would be studied. An initial list of 93 different fabrics were examined in order to select the most representative ones according to the different sectors that are interested in water and oil repellence, such as automotive, sport, fashion, work wear and home textiles. After grouping them for composition and application, five different fabrics were selected as representative compositions (Table 2).

5   NEXT STEPS

Based on alternative products and representative selected fabrics, the project is now engaged in the preindustrial demonstration of DWOR and alternative material processing that will be followed by the industrial demonstration of the new feasibilities to confer water, oil and dirt repellence to the fabrics using safer products, to conclude by the validation of the alternatives on site showing the risk assessment of the new finishing process.

5.1 Pre industrial demonstration of DWOR and alternative material processing

This task will be done by first applying the finishing solution on the fabrics and then will be followed by the characterization of them. The application will be done with a pre-industrial padding machine (ROACHES padding machine) working in the same conditions as industrial padding machines. The repellent finishing will be introduced inside the padding machine and the fabric will be

squeezed between the machine rolls after having been impregnated with the solution. Different processing conditions will be considered. Then the textiles will be dried and cured in a preindustrial stenter (MATHIS stenter machine) in the same conditions as at industrial scale. The characterization of the treated fabrics will be done following different standardized essays using the AATCC methods, ISO standards and ASTM standards to evaluate the performance of the finished fabrics.

5.2 Industrial demonstration of DWOR and alternatives material processing

The results obtained from the previous characterizations will be tested at industrial level in a scaling-up attempt to reproduce the optimal treatment conditions. The application process of the repellent products will be performed at industrial level in 6 different textile manufacturing companies, members of the three clusters. Industrial padding machines will be employed to reproduce the processes performed at laboratory scale, looking for the best conditions in scaling-up. In these finishing companies, at least 50 meters of fabric will be impregnated and then squeezed between the rolls of the industrial padding machine. The fabric will then be inserted into an industrial stenter whose temperature ranges from 100 to 180°C maximum. Then the treated fabric will be collected on a roll. The textiles treated at industrial scale will be characterized using the same European standards and essays as previously done on fabrics obtained at lab. If needed, AATCC methods and ASTM standards will be applied to evaluate the performance of the finished fabrics.

The demonstration scenario has 2 dimensions: on one hand, to determine the technical performance of DWOR and to quantify environmental and health impacts of their application; on the other hand, to demonstrate with 6 pilot industries that the textile sector can lower its environmental and health impact.

It is expected that the main value resulting from the pilot experiences and industrial demonstrations will be rigorous technical evidences on the desirability of replacing toxic DWOR repellents by sustainable alternatives.

5.3 Validation on site, at industrial scale, of the risk assessment of the project finishing applications

The risks of the water, oil and dirt repellent finishing application will be evaluated for human and environmental health during their laboratory and industrial application. These studies on risk will be carried out in relevant exposure scenarios, that is to say in the industrial textile companies, by analyzing each step of the industrial process.

The performance of the pilot industries will be monitored with the aim of identifying all possible risks.

The participation of the three clusters on the project also assures the demonstration character of the project, especially at industrial scale. The three clusters have different kinds of members which may be involved, in different ways, on the project: textile manufacturers (including yarn spinners, fabric weavers and dyers and finishers), garment makers, textile trade associations, research institutes or technological centers.

Each cluster will select two finishing companies that will be considered the most representative among its members, in order to develop demonstration activities at industrial scale that can easily be implemented to the other members of the cluster and also to all the industries.

6   CONCLUSIONS

Based on the main objective of the project to look for a mitigation of the environmental, health and safety impacts of current DWOR products actually applied on finishing, the first step of the project has been based on the selection of the finishing additives and of textile materials.

The repellent finishing available on the market has been studied mainly by collecting information from the Association's members, the textile and chemical companies and other European Associations supporting the project.

The direct contact with the industry has provided accurate information about the repellent products available and their available alternatives, of which it has been the basis to select two conventional DWOR products of C8 and seven safer alternatives to be applied on five different representative fabrics to be studied in the next steps of the project.

The project is now engaged in the preindustrial demonstration of DWOR and alternative material processing that will be followed by the industrial demonstration of the new feasibilities to confer water, oil and dirt repellence to the fabrics using safer products.

It is expected that the project will conclude with the validation on site of the alternatives showing the risk assessment of the new finishing process to help the industry to adopt them as a technologically feasible and safer alternatives.

7   REFERENCES

1. Heckster F.M., Laane RWPM, Voogt P.: Perfluoroalkylated Substances: Aquatic Environmental Assessment, July 2002, Retrieved July 2012 from http://edepot.wur.nl/174379
2. Danish Environmental Protection Agency, More Environmentally friendly Alternatives to PFOSCompounds and PFOA, March 2005. Retrieved July 2012 from http://www2.mst.dk/udgiv/publications/2005/87-7614-668-5/pdf/87-7614-669-3.pdf
3. Genzer J., Efimenko K.: Science 290, 2130-2133, 2000
4. Schlinder W.D., Hauser PJ.: Chemical Finishing of Textiles, Woodhead Publishing Ltd., Cambridge, England, 2004
5. Brinker C.J. et al.: The Physics and Chemistry of Sol Gel Processing, Academic Press of Altanta, 1989
6. Grundwurmer M.: Wear 263, 318-329, 2007
7. Wang Z.: Rare Metal Materials and Engineering 36, 629-631, 2007
8. Namligoz E.S., Bahtiyari M.I., Hosaf E., Coban S.: Fibres and Textiles in Eastern Europe 17(5), 76-81, 2009

ATERBIO – ENVIRONMENT FRIENDLY FUNCTIONAL BARRIER TEXTILES BASED ON PHOTOACTIVE PHTHALOCYANINE DYEINGS

L. Martinková[1], R. Kořínková[2], M. Karásková[2], M. Vrtalová[3] and V. Špelina[3]

[1]*INOTEX, spol. s r.o., Štefánikova 1208, 544 01 Dvůr Králové n. L., Czech Republic*
[2]*Centre for Organic Chemistry, Ltd, Pardubice, Czech Republic*
[3]*National Institute of Public Health, Prague, Czech Republic*
martinkova@inotex.cz

Abstract: An innovative photoactive phthalocyanine based antimicrobial system used for textile barrier finishing was studied and optimized as a new tool for photo-initiated antimicrobial functionality of textiles. A range of photoactive phthalocyanines containing Zn or Al and reactive groups capable to create a covalent bond with cellulosic fibres was synthesized and applied on the cotton fabric by the reactive dyeing process. The antimicrobial efficiency of the finished fabrics was determined according to a modified standard relevant for health-care textiles evaluation during repeated washing and chemo-thermo-disinfection maintenance cycles. The unique properties of textiles dyed with photoactive phthalocyanine derivatives were confirmed. This type of textile finishing can be used for simultaneous dyeing and preparation of antimicrobial/self-cleaning textile materials with a long-lasting wash-permanent barrier effect as an effective, safe and less environmentally risky alternative of conventional antimicrobial systems.

Key Words: textile finishing, photocatalysis, phthalocyanines, reactive dyeing, antimicrobial activity

1   INTRODUCTION

Photoactivity of phthalocyanine compounds (PTCs, Figure 1) containing certain metals as a central atom is based on production of singlet oxygen $^1O_2$ when exposed to light.
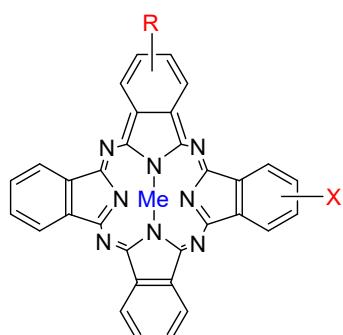

Figure 1 General structure of synthesized phthalocyanines (Me=metal, R=reactive group/s, X=solubilizing group/s)

There are two singlet states of oxygen, denoted as $^1\Sigma_g$ and $^1\Delta_g$. The singlet states of oxygen are 158 and 95 kilojoules per mole higher in energy than the triplet ground state of oxygen. Under most common laboratory conditions, the higher energy $^1\Sigma_g$ singlet state rapidly converts to the more stable, lower energy $^1\Delta_g$ singlet state usually abbreviated $^1O_2$, to distinguish it from the triplet ground state molecule, $^3O_2$. Singlet oxygen in the gas phase is an extremely long-lived (72 minutes) species, although the interaction with solvents reduces its lifetime to microseconds or even nanoseconds [1].

This highly reactive form of oxygen is able to kill the majority of microorganisms and to destroy some pollutants. The lifetime of singlet oxygen is only several microseconds and therefore the field of its effect is up to 20 nm distance from a surface modified by these PTC derivatives.

These unique properties of photoactive PTCs were used for the preparation of antimicrobial/self-cleaning textile materials with long-lasting wash-permanent barrier effect as an effective and safe alternative of conventional antimicrobial systems because firmly fixed on textile fibre [1, 2].

A range of PTCs containing Zn or Al in their structure and reactive groups capable to create a covalent bond with the cellulosic fibre was synthesized at the Centre for Organic Chemistry, Pardubice. These derivatives were applied on cotton fabric in INOTEX, Dvůr Králové n. L. as reactive dyestuffs under optimized conditions. Resulting colour-fastnesses were evaluated according to relevant standards. Testing of photoactivity of the finished textiles was conducted at the Centre for Organic Chemistry by the means of iodide method. Antimicrobial activity of the finished textiles was evaluated in the National Institute of Public Health, Prague according to the modified standard EN ISO 20743 after dyeing and repeated maintenance cycles: washing at 60°C (EN ISO 6330, Wascator, 6N, EEC - standard phosphate-free detergent, conducted at INOTEX) and chemo-thermo-disinfection prescribed for health care sector

(washing 60-65°C followed by rinsing with solution of Persteril - peracetic acid 36%, conc. 0.2 mL/L conducted at the Commercial Laundry & Dry Cleaning Company, Náchod, Czech Republic).

2 EXPERIMENTAL

2.1 Photoactive PTCs

Several greenish-blue derivatives of photoactive PTCs containing Zn or Al as a central metal atom and reactive vinylsulfone (VS) or monochlorotriazine (MCT*) groups typical for reactive dyestuffs were synthesized and prepared in a purified powder form ready for dyeing process. The prepared compounds are listed in Table 1.

2.2 Reactive dyeing – antimicrobial finishing

The reactive PTC derivatives were applied on a cotton fabric (100% cotton CARLTON - Mileta a.s. CZ, plain weave, square weight 120 g/m^2, pre-treated and pre-bleached for dyeing, without optical brighteners), as reactive dyes using a conventional exhaustion process on Labomat dyeing lab device at a liquor ratio 1:10 (Figure 2).

2.3 Evaluation of photoactivity of PTC dyed fabrics

Testing of photoactivity of the finished textiles is based on evaluation of their capability to produce singlet oxygen. These tests were performed using an iodide method determining a rate of triiodide production at the presence of the singlet oxygen (Eq.1). Triiodide forming at singlet oxygen presence:

$$^1O_2 + 2I^- \xrightarrow{H^+} I_2 \qquad (1)$$

$$I_2 + I^- \rightarrow I_3^-$$

The triiodide content growth was observed spectrophotometrically (absorption at λ = 351 nm). The photocatalytic effect of the fabrics had to be initiated: a LED light source emitting a red radiation suitable for PTCs excitation under defined conditions was used (Figure 3).

Only the $^1\Sigma_g$ form of singlet oxygen participates in the iodide formation.
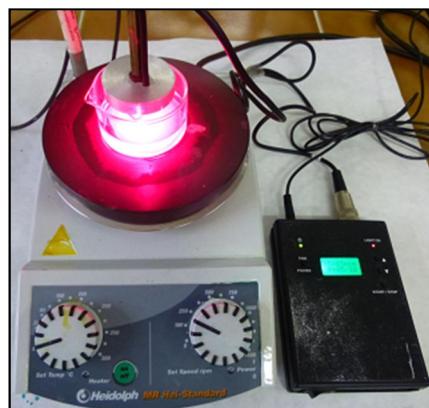
Figure 3 Testing of photocatalytic activity of fabrics

Table 1 Synthesized reactive phthalocyanine derivatives

Dye	Me	R	X
PTC 1164/75-Zn/VS	Zn	-SO$_2$-NH-C$_6$H$_4$-SO$_2$-CH$_2$-CH$_2$-OSO$_3$H	(-SO$_3$H)$_{2.1}$
PTC 1146/139	Zn	(-SO$_2$-NH-CH$_2$-CH$_2$-NH-CH$_2$-CH$_2$-OSO$_3$H)$_{1.8}$	(-SO$_3$H)$_{0.4}$
PTC 1146/37	Zn	(-SO$_2$NHCH$_2$CH$_2$Cl)$_{1.8}$	(-SO$_3$H)$_{1.1}$
PTC 1151/208	Zn	(-SO$_2$NHCH$_2$CH$_2$NHCH$_2$CH$_2$OSO$_3$H)$_{2.2}$	(-SO$_3$H)$_{0.1}$
PTC 1134/298	Zn	[-NH(CH$_2$)$_7$CH$_2$CH=CHCH$_2$(CH$_2$)$_6$CH$_3$]$_{1.2}$	(-SO$_3$H)$_{1.8}$
PTC 1134/231-Al/VS	Al	(-SO$_2$NHC$_6$H$_4$SO$_2$CH$_2$CH$_2$OSO$_3$H)$_{1.8}$	-
PTC 1151/94	Al	(-SO$_2$NHCH$_2$CH$_2$NHCH$_2$CH$_2$OSO$_3$H)$_{2.1}$	(-SO$_3$H)$_{2.1}$
PTC 1151/84	Al	(-SO$_2$NHCH$_2$CH$_2$NHCH$_2$CH$_2$OH)$_{2.1}$	(-SO$_3$H)$_{1.2}$
PTC 1151/105	Al	[-SO$_2$NHCH$_2$CH$_2$N(CH$_2$CH$_2$OH)MCT*]$_{2.1}$	(-SO$_3$H)$_{1.2}$
PTC 1134/294	Al	(-SO$_2$NHCH$_2$(CH$_2$)$_6$CH$_2$CH=CHCH$_2$(CH$_2$)$_6$CH$_3$	-
PTC 1145/275	Al	(-SO$_2$NHCH$_2$CH$_2$Cl)$_{1.7}$	(-SO$_3$H)$_{1.6}$
PTC 1151/219	Al	(-SO$_2$NHCH$_2$CH$_2$NHCH$_2$CH$_2$OSO$_3$H)$_{2.6}$	(-SO$_3$H)$_{0.7}$
PTC 1134/317	Al	[-SO$_2$NH(CH$_2$)$_7$CH$_2$CH=CHCH$_2$(CH$_2$)$_6$CH$_3$]$_{1.4}$	(-SO$_3$H)$_{1.9}$
PTC 1132/241	Al	(-CH$_2$N$^+$C$_5$H$_5$)$_{2.2}$ Cl$^-$	-H

*Note: MCT - 4-chloro-6-methoxy-[1,3,5]triazine-2-yl
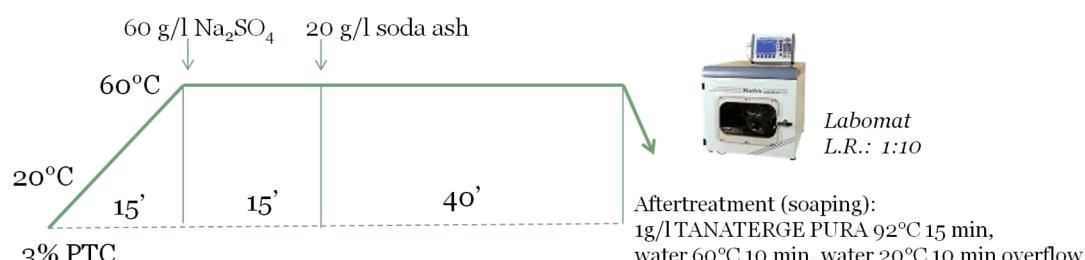
Figure 2 Reactive dyeing scheme

2.4 Antimicrobial activity of PTC dyed fabrics

Textiles finished (dyed) with the PTC derivatives (1146/75 – Zn/VS and 1134/231- Al/VS) with the best synthesis reproducibility and colouration/photoactive properties were ceded to microbiological testing performed at the National Institute of Public Health, Prague. The antimicrobial effect and its permanency were evaluated also after repeated washing (60°C) and chemo-thermo-disinfection cycles as a prescribed maintenance procedure for fabric used in health-care sector. For the antimicrobial efficiency testing according to the modified quantitative standard EN ISO 20743, following bacteria strains were used: G-negative *Escherichia coli,* CCM 4517 and G-positive *Staphylococcus aureus,* CCM 4516).

The microbiological tests were conducted under intensity of light radiation 2.1 and 5 J/cm^{-2} necessary for photocatalytic effect initiation. As light sources, two following different artificial light-sources necessary for the PTC photoactivation were selected (Figure 4):

- *Energy Saving SPIRAX SP0318 MEGAMAN, E 27, 18 W, 1200 lm 2700 K (warm white):* a lamp with a wavelength simulating light conditions in building interiors with a limited daylight access

- *NARVA LT 36 W/D65, artificial daylight, COLOURLUX proof*, a lamp-tube simulating outdoor daylight environment.

The evaluation of antimicrobial activity of textiles according to the standard EN ISO 20743 was performed using the standardized absorption method (an evaluation method in which the test bacterial suspension is inoculated directly onto samples) in Petri dishes (contact time 18 – 24 h, temperature 37°C). Antibacterial activity (*A*) was calculated according to Eq. 2:

$$A = (log\, C_t - log\, C_0) - (log\, T_t - log\, T_0) = F - G \quad (2)$$

where $F = C_t - C_0$ = Growth value on the control sample (untreated), $G = T_t - T_0$ = Growth value on the antibacterial sample (PTC finished)

3 RESULTS AND DISCUSSION

3.1 Reactive dyeing and colour-fastnesses

Resulting colour-fastnesses evaluated in INOTEX accredited lab according to relevant standards are summarized in Table 2.

From these colour-fastness results it is obvious that there are substantial differences among the used PTC derivatives. Dyeings with colour-fastnesses below 3 are generally unacceptable for health-care sector and therefore the corresponding PTCs were excluded from following testing. Only two PTC derivatives have proceeded to cotton dyeing with photoactivity and antimicrobial properties evaluation.
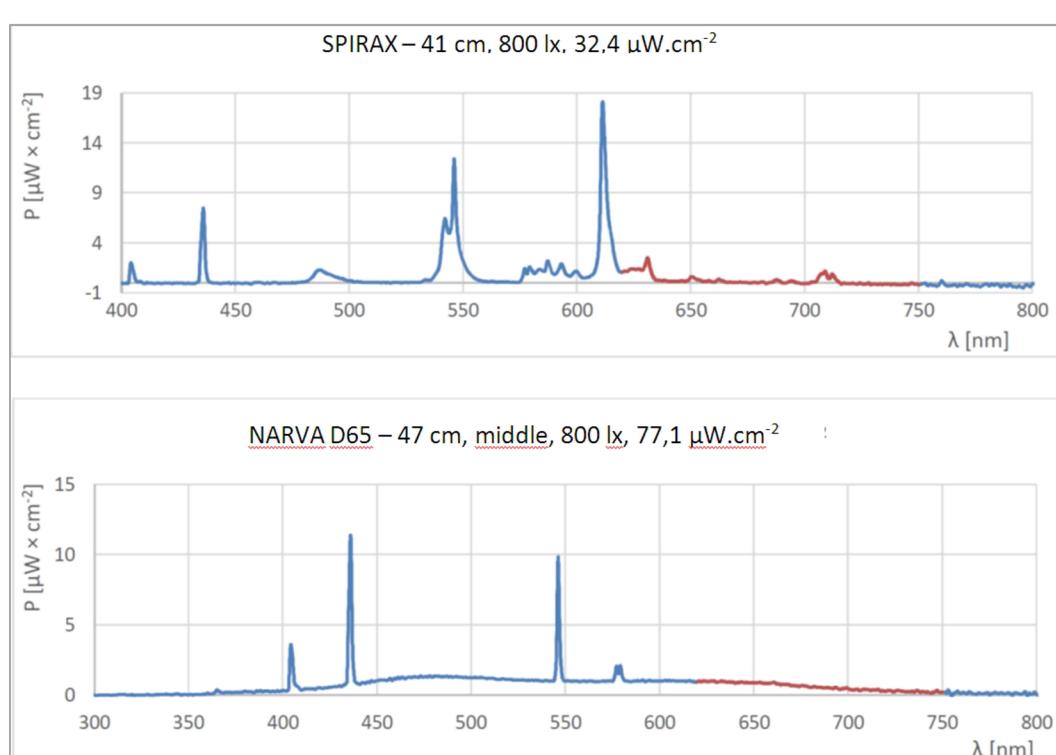

Figure 4 Emission spectra of the selected light sources

Table 2 Colour-fastnesses

3% dyeing of cotton: PTC derivative	Colour-fastness						
	in water EN ISO105-E01	in alkaline perspiration EN ISO105-E04	in acid perspiration EN ISO105-E04	in washing 60°C (C1S) EN ISO105-C06	in rubbing dry (weft) EN ISO105-X12	in rubbing wet (weft) EN ISO105-X12	light Q-SUN XE1S*
1164/75	**4-5/4/4**	**4-5/3-4/3-4**	**4/4-5/4-5**	**3-4/3/3-4**	**4**	**4-5**	**3-4D**
1146/139	4-5/4/4	4-5/4/4	4-5/4/4	3/4/4-5	4	4-5	2-3
1146/37	4/5/3-4/3	3-4/3/3-4	3/3-4/3-4	3/3-4/4	4-5	4	3D
1151/208	4/3/2-3	3-4/2/2-3	2-3/3/3	1/2-3/3-4	3-4	4-5	3-4
1134/298	4/4-5/4-5	4/4-5/4-5	4/4-5/4-5	1-2/4-5/4-5	4-5	4-5	1
1134/231	**4-5/4/4**	**4-5/3-4/4**	**4-5/4/4**	**3/3-4/4**	**4-5**	**4-5**	**3-4D**
1151/94	4-5/3-4/3-4	4-5/3/3	4-3/3-4/3-4	1/3/4	3-4	4-5	5D
1151/84	4-5/3-4/3-4	4-5/3/3	4-5/3-4/3-4	1-2/3/4	3-4	4-5	3-4D
1151/105	4-5/4/4	4-5/3-4/4	4-5/4/4	2-3/4/4-5	4	4-5	4D
1134/294	3-4/4/4	4/3-4/4	3-4/4/4	1/4-5/4-5	3-4	4	1
1145/275	3-4/3-4/3	3-4/3/3-4	3-4/3-4/3-4	3/3-4/4	4-5	3-4	4D
1151/219	4-5/3-4/3-4	4/3/3	3-4/3-4/3-4	1-2/2-3/3-4	4	4	3D
1134/317	3-4/4-5/4-5	4/4/4-5	4-5/4-5/4-5	1-2/4/4-5	4	4-5	1-2
1132/241	3-4/1-2/1-2	3/1-2/1	2-3/1-2/1	3/3-4/4	4	2	3-4D

*irradiation intensity: 60 W/m^2, time of irradiation: 16 hrs

The best colouration results and also good synthesis reproducibility were obtained in two VS reactive group-containing PTC derivatives (Zn containing PTC 1164/75 and Al containing PTC 1134/231 – Figure 5).
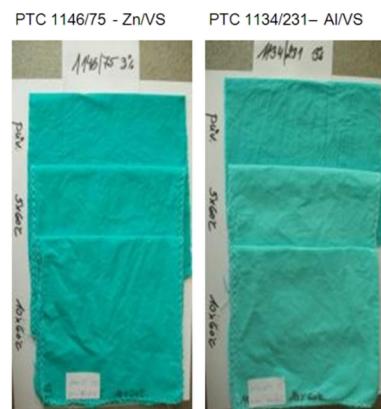

Figure 5 Phthalocyanine dyed cotton fabric (PTC 1146/75 – Zn/VS and PTC 1134/231- Al/VS)

The values of colour-fastnesses in Table 1 are usual for reactive dyeing with PTC-based dyestuffs and textiles with these colouration properties are acceptable for use in health-care sector.

3.2 Photoactivity of PTC dyed textiles

The photoactivity of fabric, in other words, singlet oxygen production, can be expressed as a slope k_{obs} of the linear dependence:

$A\ (351\ nm) = A_0 + k_{obs} \cdot f(t).$

The results of photoactivity after dyeing and after repeated washings are presented in Table 3. The washing of textiles was conducted under standardized conditions according to EN ISO 6330 (Wascator) at 60°C (process 6N).

Table 3 Photoactivity of finished and dyed fabrics as singlet oxygen production (k_{obs})

Sample (PTC)	$k_{obs} \cdot 10^2$ [min^{-1}]		
	unwashed fabric	washed 5x 60°C	washed 10x 60°C
PTC 1164/75 – Zn/VS	3.23	5.92	5.92
PTC 1134/231 – Al/VS	14.00	22.36	23.71

By these results it was confirmed that even after 10 washings, both fabrics produce singlet oxygen necessary for inhibition of microorganisms. The lower values found in unwashed samples can be explained probably by the presence of traces of an unspecified scavenger of triplet state of the PTCs (no optical brighteners were present on the dyed cotton nor in the EEC standard detergent used for washing).

The rate of production of singlet oxygen is higher at the Al-containing PTC derivative compared with Zn-PTC derivative.

3.3 Antimicrobial activity of PTC dyed fabrics

Results of the antimicrobial activity of PTC dyed textiles under indoor and outdoor light conditions (under two different light intensities) after finishing and repeated washings are summarized in Table 4.

Results of antimicrobial activity of textiles under indoor light conditions after finishing, repeated washing and chemo-thermo-disinfection cycles are summarized in Table 5. From the results in Tables 3 and 4, it is obvious that photo-induced antimicrobial activity of PTC dyed cotton fabric (derivative PTC 1146/75 – Zn/VS) is high and reliable against both G+ and G- bacterial strains even after repeated washing and thermo-disinfection cycles under indoor and outdoor light conditions.

Table 4 Antibacterial activity of PTC dyed cotton fabric after finishing and repeated washing

Antibacterial activity – A (log)					
	Cotton fabric dyed with PTC 1146/75 (3% dyeing)	Light source	Light exposition [J/cm^{-2}]	*S. aureus*	*E. coli*
1)	Unwashed	daylight indoor conditions SPIRAX	2.1	5.1	6.5
	5x washed at 60°C			1.9	2.9
	10x washed at 60°C			1.2	2.3
2)	Unwashed	daylight outdoor conditions NARVA	5.0	4.6	5.1
			2.1	4.7	3.8
	5x washed at 60°C		5.0	4.7	5.0
			2.1	4.6	3.8
	10x washed at 60°C		5.0	4.6	5.0
			2.1	4.8	3.7

Table 5 Antibacterial activity of PTC dyed cotton fabric after finishing and repeated washing and chemo-thermo-disinfection cycles (light source: SPIRAX, light exposition: 2.1 J/cm^{-2})

Antibacterial activity – A (log)			
Maintenance cycles	Cotton fabric dyed with PTC 1134/231 (3% dyeing)	*S. aureus*	*E. coli*
Washing	Unwashed	5.5	4.9
	5x washed at 60°C	5.6	4.1
	10x washed at 60°C	3.0	3.5
Washing + Chemo-thermo-disinfection	Unwashed	5.0	6.0
	5x washed at 60°C + CHT	5.0	5.5
	10x washed at 60°C + CHT	5.0	5.4

4   CONCLUSIONS

Photoactive PTC derivatives applicable as functional reactive dyes for cotton antimicrobial finishing were successfully synthesized and reactively bound to cotton fabric. Their application by conventional exhaustion dyeing process resulting in good colour-fastnesses was verified and optimized. The photoactivity of PTC finished textiles was identified and evaluated after dyeing and repeated washing.

From the results of antibacterial activity it can be concluded that cotton fabric dyed with a photosensitive PTC derivative shows a high antimicrobial effect against both G+ and G- bacteria strains. This effect is stable in repeated washings at 60°C. Moreover, the stability of the effect in repeated washing followed by a chemo-thermo-disinfection prescribed for textiles maintenance processing in the health care sector has been proved.

This barrier finishing/dyeing technology has been up-scaled and verified by semi-industrial trials and is now ready to be transferred to the industrial scale. It represents an effective non-toxic and eco-friendly alternative of antimicrobial finishing systems and is suitable for apparel textiles and bed-linen.

5   REFERENCES

1.   Schweitzer C., Schmidt R.: Physical Mechanisms of Generation and Deactivation of Singlet Oxygen, Chem. Rev. 103, 1658-1757, 2003

2.   Graf G., Hoelzle G., Reinert G.: Water-soluble phthalocyanine compounds and their use as photoactivators, From Eur. Pat. Appl., 1985, EP 153278 A2 19850828

3.   Hoelzle G., Reinert G., Polony R.: Bleaching textiles and controlling microorganisms, From Eur. Pat. Appl., 1982, EP 47716 A2 19820317

TECHNOLOGIES TO ENHANCE THE ENVIRONMENTAL PROFILE OF WOOL FLOORCOVERINGS

S. J. McNeil[1] and M. R. Sunderland[2]

[1]Textile Science and Technology Team, Food and Bio-based Products Group, AgResearch Limited
Christchurch 8140, New Zealand
[2]Formerly Textile Science and Technology Team, Food and Bio-based Products Group, AgResearch Limited
Christchurch 8140, New Zealand
steve.mcneil@agresearch.co.nz

Abstract: *This paper describes research undertaken by AgResearch New Zealand and other organisations to enhance the eco-credentials of wool floorcoverings, and thereby to help maintain or enhance wool's position within the global textile industry. Technologies recently commercialised or under development for environmentally sound wool floorcoverings will be reviewed in the areas of harvesting, protection from insect pests, wet-processing, in-use environmental impact, contribution to the built environment, and recycling.*

Key Words: *wool, carpet, built environment, closed-loop recycling, insect-resistance, entomotoxic nanocides, Lanalbin APB, Lanasan NCF*

1   INTRODUCTION

AgResearch, the New Zealand Government's agricultural research institute, undertakes research to enhance wool's eco-credentials to help maintain, or enhance, wool's position within the global textile industry. Floorcoverings are the major end-use of strong wool, consuming some 45% of global production [1]. New Zealand is a major producer of this type of wool, therefore a significant proportion of AgResearch's activity in the wool area is directed towards floorcoverings. Floorcoverings comprise tufted, woven and nonwoven, carpets and rugs, produced by hand or machine.

Figure 1 The Pazyryk carpet

Wool is a bio-based fibre with a good environmental profile compared to other textile fibres [2]. For instance, the production of wool consumes only 42% of the energy needed to manufacture polyester and 21% of the energy needed to manufacture nylon to the spun fibre stage [3]. The production of wool can have a positive effect on the environment, as grazing by sheep and other livestock can prevent desertification, reclaim degraded land and combat climate change [4].

The first manufacture of pile rugs from yarns of twisted animal fibres was well over 6000 years ago and the oldest carpet in existence; the Pazyryk carpet (Figure 1) is estimated to be over 2400 years old. However, despite this long history, research into wool floorcoverings continues to make important discoveries. For example, it is not long since it was discovered that the lipids bound on the surface of wool are attached by oxygen ester linkages [5] as well as the well-known thioester linkages [6]. This important study also increased our understanding of the structures of these bound lipids [5]. Understanding the nature of the surface of wool is important in floorcoverings, because it is the surface that controls soiling and the repulsion of water and stains [7, 8]. The surface of wool is also important for textile processing, as it affects the uptake of dyes and the application of surface coatings [9].

Wool is used in a range of environmental remediation products for removing metals [10], hydrocarbons [11] and other contaminants [12, 13]. Wool's utility for these applications stems from its hydrophobic surface, its amino acid composition and its large capacity for swelling [5, 12]. Advances in the mechanical aspects of manufacturing wool

floorcoverings can give environmental benefits, and these have been reviewed elsewhere [14]. Some chemical developments to enhance the environmental profile of wool floorcoverings are reviewed here.

2 HARVESTING

While most wool is harvested by shearing sheep, some is collected by depilation of sheepskins (fellmongering). This process typically involves sodium sulphide, calcium hydroxide and sodium hydroxide, and can create unpleasant and potentially dangerous working conditions. The resulting effluent requires significant remediation before it can be discharged. AgResearch has recently developed an enzyme-based depilatory that is considerably more benign than conventional depilatories [15]. Wool harvested with the enzyme depilatory did not show any differences in processing or end-product performance, other than an enhancement of pilling resistance, and the quality of leather produced by the two depilatories was the same.

3 PROCESSING

3.1 *Insect-Resist*

Damage by insect pests is primarily an issue for textiles made from wool, silk and sea silk. The wool industry has responded with technologies that cover a wide gamut from new-generation highly specific insecticides, non-pesticide agents, to nanoparticles.

Enhanced pyrethroids

The synthetic pyrethroid, permethrin, has been the most used insect-resist agent for wool since 1980 [16]. This is in spite of its significant aquatic toxicity [17]. Bifenthrin, also a synthetic pyrethroid, was introduced as an insect-resist agent by the Wool Research Organisation of New Zealand in conjunction with a commercial partner in the 1990s to replace permethrin [18]. The advantages of bifenthrin over permethrin include better wash fastness, greater effectiveness at low levels, no resistance problem with carpet beetles and a significantly lower environmental impact. The disadvantages of bifenthrin are that it is more expensive and has a higher mammalian toxicity than permethrin.

Permethrin has shown a remarkable synergy with the neonicotinoid compound, imidalcloprid [19]. However, the high water solubility of imidalcloprid means that it lacks the high affinity for wool that is a prerequisite for exhaust application. Therefore, this combination of insect-resist agents has not been commercialised to-date.

Enhancements in other classes of agents

A halogenated pyrrole with broad spectrum insecticide activity, chlorfenapyr (formulated as Mystox MP), was introduced by Catomance Technologies and AgResearch in 2007 as an insect-resist agent for wool [20]. There are relatively few wool textiles in existence containing this insecticide, and therefore little opportunity exists for insect populations to build-up a resistance. The vast majority of protected textiles contain pyrethroid insecticide and, at present, the only known resistance to insect-resist agents was shown by Australian carpet beetles (*Anthrenocerus australis*) towards permethrin [18]. Chlorfenapyr has a similar toxicity to aquatic life as bifenthrin, and possesses better fastness to washing and light than bifenthrin.

Microencapsulated agents

Water soluble insect-resist agents have been applied to wool in microcapsules as a way of providing adequate washfastness. For example, clothianidin and a combination of permethrin and imidacloprid were microencapsulated and applied to wool by the pad-dry-bake method [21]. The clothianidin insecticide encapsulated with polylactic acid showed the best insect-resist performance at a level of 50 ppm on wool, and gave excellent protection, even after 10 washes (i.e. 85% insect mortality and negligible wool mass loss). The fabric handle properties were only slightly affected by the application of the microcapsules. This approach may well find application in industry in the future.

Non-pesticide approaches

A surfactant-based mothproofer Ecolan CEA has been commercialised by Chemcolour New Zealand Ltd and AgResearch, eliminating the need for insecticides for some wool users. There is a significant reduction in the aquatic toxicity of wool processing effluent when using Ecolan CEA [22]. This surfactant also has a dye levelling effect in the wool dyebath, reducing, or in some cases, eliminating the need for conventional levelling agents, thus making two contributions to enhancing the environmental profile of wool floorcoverings.

Another approach to protecting wool from insect attack utilises nanocide particles [23, 24] that disrupt the water-impervious cuticle of insects, causing desiccation [25]. Titanium dioxide was bound to wool at various levels, and found to have a significant antifeedant effect against the common clothes moth (*Tineola bisselliella*) at levels as low as 0.1% on mass of wool [26]. A higher level (1.7%) was needed for significant insect mortality, and titanium dioxide did not exhibit a repelling effect in a feeding preference trial.

Some antifungal compounds have been found to exhibit an antifeedant effect on the larvae of both the common clothes moth and the Australian carpet beetle [27]. Further investigations revealed that the most effective compound, propiconazole, did not repel the Australian carpet beetle and

showed no lasting toxicity in direct contact and ingestion experiments [28]. This led to the suggestion that the antifeedant action of propiconazole on Australian carpet beetle was related to inhibition of the cytochrome P450 enzyme system, and/or the inhibition of gut enzymes involved in the digestion of wool [28].

3.2 Dyeing and Finishing

With some justification it can be said that the dyeing of wool has a lower environmental impact than the dyeing of other fibres, as wool achieves very high exhaustion of dyes and does not require the carriers or high levels of salt, sometimes employed to dye polyester and cotton, respectively. Great improvements are being made to improve the sustainability of dyeing across many types of fibres and dyes, and wool and wool dyes are no exception.

Applying ultrasound during dyeing has attracted considerable interest because of its potential to reduce the consumption of energy and chemicals. The mechanism is thought to be due to the faster movement of dye across the liquid-fibre boundary layer and reduced aggregation of dyes in solution [29]. In terms of wool processing with ultrasound, perhaps the most promising results to-date have been for the scouring of raw wool (i.e. the removal of wool grease) [30], and the application of natural dyes [31]. A study at AgResearch has showed that ultrasound can: enhance the colour of scoured wool by removing trace amounts of surface contaminants; increase the effectiveness of subsequent bleaching; and remove bound surface lipids [32].

4 INCREASING THE USEFUL LIFETIME OF WOOL FLOORCOVERINGS

Extending the useful lifetime of floorcoverings is an obvious and effective way of reducing their net environmental impacts, as well as enhancing the value proposition to consumers. Two technologies for extending the lifetime of wool floorcoverings have been developed by AgResearch, and commercialised by Chemcolour New Zealand Ltd. The Lanalbin APB (Anti Photo Bleaching) technology greatly reduces the colour changes that some wool products can undergo when exposed to strong sunlight indoors, and is used widely around the world (Figure 2) [22].

The Lanasan NCF (Nano Carpet Finish) technology increases fibre cohesion in the carpet pile and blocks the irregularities of the wool surface than can hold particles of soil [33]. This process is performed during dyeing or yarn scouring and imparts several benefits. The shedding of loose fibres is a significant cause of customer dissatisfaction with new floorcoverings, and Lanasan NCF greatly reduces shedding, by up to

85% in some cases. It also reduces soiling propensity by 35% (Figure 3).
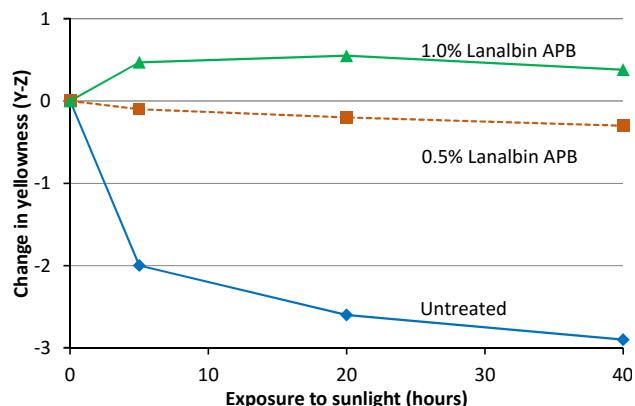
Figure 2 Effect of Lanalbin APB on photobleaching

Trials showed increases of up to 20% in carpet's ability to withstand short-term wear; results in long term trials were even more impressive, carpet made from Lanasan NCF treated yarn withstood 25,000 treads before the backing was exposed, compared to only 15,000 for the untreated sample. Lanasan NCF strengthened yarns by as much as 80% - reducing the frequency of yarn breaks and the resulting machine stoppages during tufting and weaving.

Figure 3 Carpets made from untreated yarn (left) and Lanasan NCF treated yarn (right) after Wools of New Zealand/International Wool Secretariat Rapid Soiling Test TM 267

5 ENHANCEMENTS TO THE BUILT ENVIROMMENT

Textile floorcoverings are widely recognised for their enhancements to the built environment, with their contributions to thermal comfort [34], acoustics [35] and safe walking [36] being the most well-known and appreciated [37]. The enhancement

of indoor air quality by wool products [38, 39] is an on-going area of research, which is starting to lead to the development of wool-based passive air purifiers [40, 41].

Meeting the needs of the increasing numbers of older people and people with disabilities is a major challenge for society [36, 42]. Wool floorcoverings have both subjective and objective benefits for these groups [37, 38, 43, 44]:

- reduced severity of falls and improved gait (walking speed and stride length)
- deinstitutionalisation of environments, which reduces stress
- reduced glare, noise, and indoor air pollution
- low flammability

A feature of carpets that has received little attention to-date, is the provision of visual cues to assist walking. A set of design guidelines have been developed from current knowledge of ageing vision and impaired walking, and used for the colouring and patterning of a carpet [43]. The designed carpet was shown to assist walking in a trial with people who had artificially impaired vision and gait. These design guidelines could increase the contribution of floorcoverings to the independent living of many people.

6   IN-USE ENVIRONMENTAL IMPACT

Floorcoverings are generally used for several years, so the cumulative impact of maintenance in terms of cleaning chemicals (and their emissions of volatile compounds), water, electricity and human labour are significant contributors to their cradle-to-grave environmental impact. The environmental impact of cleaning and maintenance of floorcoverings are also significant contributors to the environmental impact of buildings [45]. As there is a scarcity of such data for floorcoverings [45], AgResearch investigated the energy, time and water usage required for maintaining carpets and hard floors (solid vinyls, wood and wood laminates) in commercial buildings [46]. It was found that the electrical energy requirements for both types of flooring were similar for areas with heavy volumes of foot traffic. For areas with less traffic, carpets required slightly more electrical energy, but less human energy, water and time to clean than hard floors. The greatest difference found overall was in the consumption of water, with hard floors requiring up to 40 times more than carpet.

A study conducted by AgResearch with the University of Auckland showed that immobilising a lipase type enzyme onto wool fabric enhanced subsequent cleaning [47]. This approach could readily be extended to wool floorcoverings.

7   END-OF-LIFE

The biodegradability of wool carpets makes them useful mulch mats to supress weeds around new plantings. The carpets gradually decompose, and the nutrients released are available to the growing plants. AgResearch found that the rate of biodegradation of wool carpet mulch mats was greatly increased by applying a layer of plant material to the carpet, as this created moisture, temperature and nutrient conditions favourable to biological activity (Figure 4) [48]. The application of certain nutrients (e.g. phosphates and nitrates) to the plant mulch further increased the rate of carpet biodegradation.

Figure 4 View of mulch mat trial

Post-consumer wool carpets can be down-cycled into felted carpet underlay [49]. Shredded, post-consumer wool carpets have been incorporated into pasture at 10 Tonne/ha, (Figure 5) and the effects on the yield of ryegrass, and the levels of nutrients in the soil and grass were measured [50]. Thirteen weeks after seeding, the grass grown on areas with shredded carpet was a darker shade of green than the unfertilised grass, indicating a healthier condition (Figure 6). This colour difference was still evident after nine months and two harvests. The carpet-fertilised areas gave a 24% greater dry matter yield ten weeks after seeding. A second harvest, after a further five weeks, showed an 82% greater yield of dry matter in the areas with shredded carpet.

Grass harvested after ten weeks showed higher levels of available elements when grown on carpet-fertilised areas than in the unfertilised areas (e.g., 25% more sulphur, 17% more magnesium, 10% more nitrogen and 7% more phosphorus) and this correlated with the increased levels of nutrients measured in the soil [50]. This study demonstrated that a closed-loop cycle (wool to grass to wool) is both a feasible and efficient form of nutrient recycling that diverts used carpets from landfill and incineration, and reduces the need for inorganic fertilisers.

Figure 5 Trial plot immediately prior to seeding. Shredded carpet had been incorporated into the left and right quadrants, and a small amount of shredded carpet is visible on the surface of the soil

Figure 6 Three weeks after the first harvest (i.e. 13 weeks after seeding)

Many researchers have made important contributions to our understanding of the end-of-life options for floorcoverings. For instance, it has been shown that incorporating wool into soil increases moisture retention, yields of grain and green fodder, and the levels of available nitrogen, phosphorus and potassium, without affecting the pH, electrical conductivity and micronutrient levels of the soil [51]. Plant roots grow directly on wool fibres which had been incorporated into growing media, suggesting growth towards nutrients and/or a possible role for roots or root exudates in the decomposition of wool in soil [52]. The fertiliser value for shredded carpet applied to pasture has been estimated at 46 euros per hectare in 2009 [53].

8   CONCLUSIONS

Some of the latest research to enhance the environmental profile of wool floorcoverings has been reviewed here. It is clear that significant

research is ongoing at AgResearch and other institutes in many areas, such as harvesting, processing, extending useful lifetimes, contribution to the built environment, in-use environmental impact, and end-of-life options.

9   REFERENCES

1. Ingham P., McNeil S., Meade W., Sunderland M.: Key Engineering Materials 671, 2016, pp. 490-496

2. Potting J., Blok K.: Journal of Cleaner Production 3, 201-213, 1995

3. Barber A., Pellow G.: LCA: New Zealand Merino Wool Total Energy Use. Proceedings of the 5th Australian Life Cycle Assessment Society Conference, Melbourne Australia, November 2006

4. Savory A.: Can Sheep Save the Planet? International Wool Textile Organisation Congress, Cape Town, South Africa, April 2014

5. Rankin D.A., Carr C.M.: Journal of the Textile Institute 104(2), 197-212, 2013

6. Bryson W. G., McNeil S. J., McKinnon A. J., Rankin D. A.: The Cell Membrane Complex of Wool - A Critical Assessment of the Literature, Wool Research Organisation of New Zealand Communication C123, New Zealand 1992

7. Negri A.P., Cornell H.J., Rivett D.E.: Textile Research Journal 63(2), 109-115, 1993

8. Ingham P.E.: Australasian Textiles 9(6), 27-34, 1989

9. McNeil S.J., Standard O.C.: Textile Research Journal (in press)

10. McNeil S.J.: Asian Textile Journal 10(5-6), 88-90, 2001

11. Johnson N.A.G., Wood E.J., Ingham P.E., McNeil S.J., McFarlane I.D.: Journal of the Textile Institute 93(4), 26-41, 2003

12. Pušić T., Boban A., Dekanić T., Soljačić I.: Vlákna a Textil 18(1), 7-15, 2011

13. Leighs S.J., McNeil S.J., Meade W.J.: Wool Filtration Media Opportunities and Applications. Presented at Visions for Fibres and Textiles Conference, Melbourne, Australia, April 2012

14. Ingham P.E., Meade W., McNeil S.J.: Advances in Wool Carpet Technology, Proceedings of the 12th International Wool Research Conference, Shanghai, China, October 2010, Donghua University, Shanghai, Vol I, 14-17, 2010

15. Sunderland M., McNeil S.: Key Engineering Materials 671, 317-323, 2016

16. Lewis D.M., Shaw T.: Review of Progress in Coloration 17, 86-94, 1987

17. Stratton G.W., Corke C.T.: Environmental Pollution 24(2), 135-144, 1981

18. Barton J.: International Dyer 185(9), 14-16, 2000

19. Haas J.: Development of a Novel Insect-Resist Agent for Keratin-Digesting Insects, Proceedings of the 8th International Wool Textile Research Conference, Christchurch, New Zealand, February 1990, Wool Research Organisation of New Zealand, Christchurch, New Zealand, Crawshaw G.H. (Ed.), Vol V, 558-567, 1990

20. Mill W.: Wool Record 166(3758), 30, 2007

21. Hassan M.M., Sunderland M.: Progress in Organic Coatings 85, 221-229, 2015

22. Ingham P.E., McNeil S.J., Sunderland M.R.: Advanced Materials Research 441, 33-43, 2012

23. Ki H.Y., Kim J.H., Kwon S.C., Jeong S.H.: Journal of Materials Science 42(19), 8020-8024, 2007

24. Nazari A., Montazer M., Dehghani-Zahedani M.: Industrial & Engineering Chemistry Research 52(3), 1365-1371, 2013

25. Barik T.K., Sahu B., Swain V.: Parasitology Research 103(2), 253-258, 2008

26. McNeil S.J., Sunderland M.R.: Clean Technologies and Environmental Policy 18(3), 843-852, 2016

27. Sunderland M.R., Cruickshank R.H., Leighs S.J.: Textile Research Journal 84(9), 924-931, 2014

28. Sunderland M.R., Cruickshank R.H.: Journal of Insect Behavior 29(1), 57-68, 2016

29. Actus Grande G., Giansetti M., Pezzin A., Rovero G., Sicardi S.: Ultrasonics Sonochemistry 27, 440-448, 2015

30. Cui Y.: Journal of China Textile University, Chinese Edition 25, 50-54, 1999

31. Merdan N., Saclioglu M.Z., Kocak D., Sahinbaskan B.Y.: Advances in Environmental Biology 6(2), 750-755, 2012

32. McNeil S.J., McCall R.A.: Ultrasonics Sonochemistry 18(1), 401-406, 2011

33. Ingham P.E., Sunderland M.R., McNeil S.J., Marazzi R.: International Dyer 191(1), 23-25, 2006

34. McNeil S.: The Thermal Properties of Wool Carpet, AgResearch Technical Bulletin, New Zealand 2016

35. McNeil S.: Acoustic Advantages of Wool Carpeting, AgResearch Technical Bulletin, New Zealand 2014

36. Willmott M.: Age and Ageing 15, 119-120, 1986

37. Meade W.: Consumer Properties of Carpets, Wool Research Organisation Technical Bulletin, New Zealand 1998

38. Ingham P., Causer Z., McMillan R.: The Role of Wool Carpets in Controlling Indoor Air Pollution, Proceedings of the Textile Institute Floorcoverings Conference, Blackpool, UK, November, 1-9, 1994

39. McNeil S.: The Removal of Indoor Air Contaminants by Wool Carpet, AgResearch Technical Bulletin, New Zealand 2015

40. McNeil S.J., Zaitseva L.I.: Key Engineering Materials 671, 219-224, 2016

41. Kinney T.: Wool: Master's Design Thesis, University of Texas, Austin 2014

42. Nejedlá M.: Vlákna a Textil (3-4), 3-11, 2015

43. McNeil S.J., Tapp L.S.: Journal of the Textile Institute 107(3), 376-385, 2016

44. Martini P., Spearpoint M.J., Ingham P.E.: Fire Safety Journal 45(4), 238-248, 2010

45. Hernandez P., Kenny P.: Energy and Buildings 42(6), 815-821, 2010

46. McCall R.A., McNeil S.J.: Indoor and Built Environment 16(5), 482-486, 2007

47. An J.D., Patterson D.A., McNeil S., Hossain M.M.: Biotechnology Progress 30(4), 806-817, 2014

48. Barker R.H.T., Taylor M., Johnstone P., van Koten C.: Biodegradation of Wool Carpet Pile, AgResearch Report FBP 23243, New Zealand 2013

49. http://www.cavbrem.co.nz/environment/carpet-recycling.aspx Accessed 13 April 2016

50. McNeil S.J., Sunderland M.R., Zaitseva L.I.: Resources, Conservation and Recycling 51(1), 220-224, 2007

51. Kadam V.V., Meena L.R., Singh S., Shakyawar D.B., Naqvi S.M.K.: Indian Journal of Small Ruminants 20(2), 83-86, 2014

52. Zheljazkov V.D., Stratton G.W., Pincock J., Butler S., Jeliazkova E.A., Nedkov N.K., Gerard P.D.: Waste Management 29(7), 2160-2164, 2009

53. Gibbs P.: The Land Recycling Option for Wool Carpet. Presented at The Carpet Recycling UK Conference, Leicester UK, June 2009

ALLICIN-CONJUGATED NANOCELLULOSE AS A FINISHING FOR IMPARTING ANTIBACTERIAL PROPERTIES TO POLYESTER AND CELLULOSE-POLYESTER FABRICS

M. K. Mehrizi[1], R. Jafary[1], S. H. H. Moghaddam[2], A. Jebali[3] and A. Haji[4]

[1]*Department of Textile Engineering, Yazd University, Yazd, Iran*
[2]*Department of Laboratory Sciences, School of Par Medicine, Shahid Sadoughi University of Medical Sciences, Yazd, Iran*
[3]*Department of Medical Genetic, Shahid Sadoughi University of Medical Sciences, Yazd, Iran*
[4]*Textile Engineering Department, Birjand Branch, Islamic Azad University, Birjand, Iran*
mkhajeh@yazd.ac.ir

Abstract: *The use of antimicrobial agents on fabrics has a very long history. Although several classes of antimicrobial agents (such as phenols, halogens, quaternary ammonium salts and metal salts) have been developed for textiles, most of them are toxic. The aim of our study was to treat polyester and cellulose-polyester fabrics with allicin-conjugated nanocellulose. These fabrics were characterized by scanning electron microscopy, X-ray diffraction and Fourier transform infrared spectroscopy. Also, the antibacterial ability of treated fabrics was determined by AATCC method 100-1993. The results showed both treated fabrics had significant antibacterial activity against Staphylococcus aureus. It can be concluded that allicin-conjugated nanocellulose can be attached to polyester and cellulose-polyester fabrics to impart a stable antibacterial property.*

Key Words: *Nanocellulose, Allicin, Antibacterial, Staphylococcus aureus, Cellulose, Polyester*

1   INTRODUCTION

The use of antimicrobial agents on fabrics has started centuries ago. In recent years, antimicrobial textiles have gained much more attention from both academic researchers and textile industries. Self-sterilizing fabrics have potential benefits to reduce diseases transferred among hospital populations and other groups [1, 2]. It has long been known that microorganisms can grow on textiles and fabrics. They provide an excellent medium for transfer and propagation of infection-causing microbial species due to their characteristics and proximity to the person's body [3]. Fabrics made from natural fibers are more suitable for growth of microorganisms than synthetic fibers because their hydrophilic structure keeps water, oxygen, and nutrients. They provide a perfect environment for bacterial growth. A way to prevent microbial degradation of fabrics, limit the occurrence of bacteria, and protect against microbial agents, is the treatment of the fabric with antimicrobial compounds. Different classes of antimicrobial agents have been developed for textiles, such as phenols, halogens, quaternary ammonium salts and metal salts. These materials are toxic and allergenic, and cannot be used for long periods. There are many ways by which antimicrobial properties can be imparted to textiles, including interpolation of antimicrobial agents directly into fibers, adsorption of antimicrobials onto fiber surfaces, immobilization of antimicrobials on fibers by ionic or covalent linkages, etc. [4].

Some non-toxic natural products can inhibit the growth of microorganisms and can be considered for use in textiles [5]. For example, garlic (*Allium sativum*) is able to inhibit not only bacteria, but also fungi and viruses [6]. Allicin [S-(2-propenyl) 2-propene-1-sulfinothioate], which is one of the active ingredients of freshly-crushed garlic homogenates, is a natural antimicrobial agent. Moreover, it is an anti-oxidant, anti-carcinogenic, anti-inflammatory, anti-genotoxic, immuno-modulatory and anti-thrombotic [7]. Allicin is a foremost component in garlic generated by the enzyme alliinase, through its action on the amino acid alliin [8-10]. Based on a previous study, allicin-conjugated nanocellulose has antimicrobial activity [11]. The first aim of this study was to attach allicin-conjugated nanocellulose on polyester and cellulose-polyester fabrics. The next purpose of this study was to evaluate their antibacterial property.

2   EXPERIMENT

Materials

In this study, cellulose manufactured by the My Baby Company, Iran was used for synthesis of nanocellulose. N-ethyl-N-(dimethylaminopropyl) carbodiimide (EDC) and aminopropyl triethoxysilane (APTES) were provided by Sigma-Aldrich Co (St Louis, MO, USA). Nitric acid, sulfuric acid, amine-allicin, sodium hydroxide and dimethyl sulfoxide (DMSO) were sourced from the Merck Company (Germany). The fabrics were from

Yazdbaf Company in Yazd, Iran. On a side note, cellulose-polyester fabric contained 35% cellulose and 65% polyester.

Primary washing of fabrics

The fabrics were scoured using a bath containing distilled water and 2 g/L non-ionic detergent (Acta wash, Arak, Iran) at 60°C for 30 min. The fabric was subsequently rinsed and dried at room temperature.

Nanocellulose preparation

In our research, 0.1 g of raw cellulose was treated with 1 mL of 5 M NaOH at 37°C for 1 hour, and rinsed with distilled water (DW). Then, 1 mL of 5 M DMSO was added to the rinsed cellulose and incubated again at 37°C for 1 hour, and was washed three times with DW. In the next step, 1 mL of 70% sulfuric acid was added to wash the cellulose. Straightaway, 2 mL of 5 M NaOH were gently added to it. In the final step, hydrolyzed cellulose was centrifuged at 5,000 rpm for 5 min, and the nanocellulose pellets were washed with DW for three times. All nanocelluloses were suspended in DW, shaken for 5 min, and stored at 5°C.

Synthesis of allicin-conjugated nanocellulose and preparation of treated fabrics

Firstly, 1 g of citric acid was added to the suspension of nanocellulose, and boiled for 10 minutes, and then washed twice with DW. Then, 1 mL of 100 mg/mL EDC was added to carboxyl-nanocellulose, and incubated at 37°C for 30 min. Next, both fabrics were treated with 200 mg/mL APTES, incubated at 37°C for 30 min, washed three times with DW, dried at 37°C. Then, 1 mL of 500 µg/mL of nanocellulose conjugated with allicin was added to APTES modified fabrics, incubated at 37°C during 30 min and dried at room temperature.

3   CHARACTERIZATION TESTS

Fourier transform infrared (FTIR) spectroscopy

FTIR spectra were observed by Bomem MB100 instrument (Hartman & Braun, Canada) with compressed pellets containing potassium bromide and the sample [5].

X-ray diffraction (XRD) spectroscopy

To determine the crystal phase of the conjugated polyester and cellulose-polyester fabric, XRD measurements (Philips, The Netherlands) were carried out over the diffraction angle (2θ) 0°-100°.

Scanning electron microscopy (SEM)

The topography of the samples was analyzed by high resolution SEM (Model AIS2100, Seron technology, USA). The fabrics were evaluated before and after conjugation with allicin.

Antibacterial tests

The antibacterial property of the samples was evaluated according to the AATCC 100-1993 test method against a standard strain of *Staphylococcus aureus* (*S. aureus*) (AATCC 25923, obtained from Iranian Research Organization for Science and Technology). Briefly, circular (5 cm in diameter) sterile fabric samples were treated with 1 mL of the bacterial suspension. The suspension was in the nutrient broth medium, containing about 1.0×10^5 colony forming units (CFU)/mL (equivalent to spectrophotometric optical density of 0.2-0.3 at 580 nm). Fabrics and bacteria were incubated for 24 h at 37°C, and then 100 mL of sterile DW was poured onto the plate and agitated for one min. One mL of the diluted suspension was then placed on a nutrient agar culture plate, and incubated for 24 h at 37°C. Viable colonies of bacteria on the agar plate were counted using a magnifier, and the percentage of reduction in bacterial colonies was calculated using the equation (1):

$$R (\%) = [(A–B)/ A] \times 100 \qquad (1)$$

where *R* is the reduction rate of bacteria, *A* and *B* are the numbers of bacterial colonies from untreated and treated fabrics, respectively [12, 13].

4   RESULTS

In this study, the antimicrobial properties of polyester and cellulose-polyester fabrics finished with allicin-conjugated nanocellulose were studied. This research showed that the conjugation could induce antibacterial activity against *S. aureus*. In future, antimicrobial property of these novel modified fabrics must be evaluated against other microorganisms. Also, the reaction of human body must be investigated.

4.1 Antibacterial properties

The results of per cent reduction of colonies are shown in Table 1. The numbers are average of two experiments for each type of fabric. As is seen, there was a significant difference between raw fabrics and conjugated fabrics.

Table 1 Antibacterial activities of both fabrics against *S. aureus*

Samples	Approximate colony count (raw fabric)	Approximate colony count (conjugated fabric)	Reduction of bacteria [%]
Polyester fabric	1000 (±10)	100* (±4)	90 (±4)
Cellulose-polyester fabric	700 (±5)	36* (±4)	95 (±4)
*p<0.05 compared with raw fabric			

4.2 Characterization analysis

The FTIR spectra of raw (sample A) and conjugated (sample B) polyester fabrics are presented in Figure 1. The typical absorption peaks of raw polyester fabric (spectrum a) were shown to be at 2958.75, 1736.65, 1687.84, 1505.25, 1410.09 and 1093.01 cm^{-1} related to the stretching of C–H, C=O (carboxylic acid), C=O (carbonyl amid), C–C, C=C, and C–O–C, respectively [14-17]. The specific absorption peaks of conjugated polyester fabric were shown to be at 1735 cm^{-1} and 1687.32 cm^{-1} due to C=O (carboxylic acid) and C=O (carbonyl amid).

The FTIR spectra of raw (sample A) and conjugated (sample B) cellulose-polyester fabrics are presented in Figure 2. The typical absorption peaks of raw cellulose-polyester fabric (spectrum a) were shown to be at 3430.14, 2941.58, 1703.12, 1409.9, 1341.85, 1265.84 and 1009.66 cm^{-1} related to the stretching of O-H, C-H, –C=O (carboxylic acid), C=C, (H-C-C, H-C-O and H-O-C), C-O, and

C-C bending, respectively. The specific absorption peaks of conjugated cellulose-polyester fabric were shown to be at 1734 cm^{-1} due to C=O (carboxylic acid).

Figure 3 shows the XRD patterns of the polyester and cellulose-polyester fabrics finished with allicin-conjugated nanocellulose. There are strong peaks for polyester and cellulose-polyester fabrics finished with allicin-conjugated nanocellulose at 17.5610 and 22.4606, respectively, which are related to the crystalline phase. According to equation (2), if λ=1.54 nm, K=0.9 and $FWHM$=0.9840, the approximate size of the crystals is considered to be about 84.64 and 87.32 angstroms for polyester and cellulose-polyester fabrics finished with allicin-conjugated nanocellulose, respectively.

$$Crystal\ size\ (Å)= \frac{K \times \lambda \times 180}{FWHM \times \pi \times cos\,\theta} \qquad (2)$$
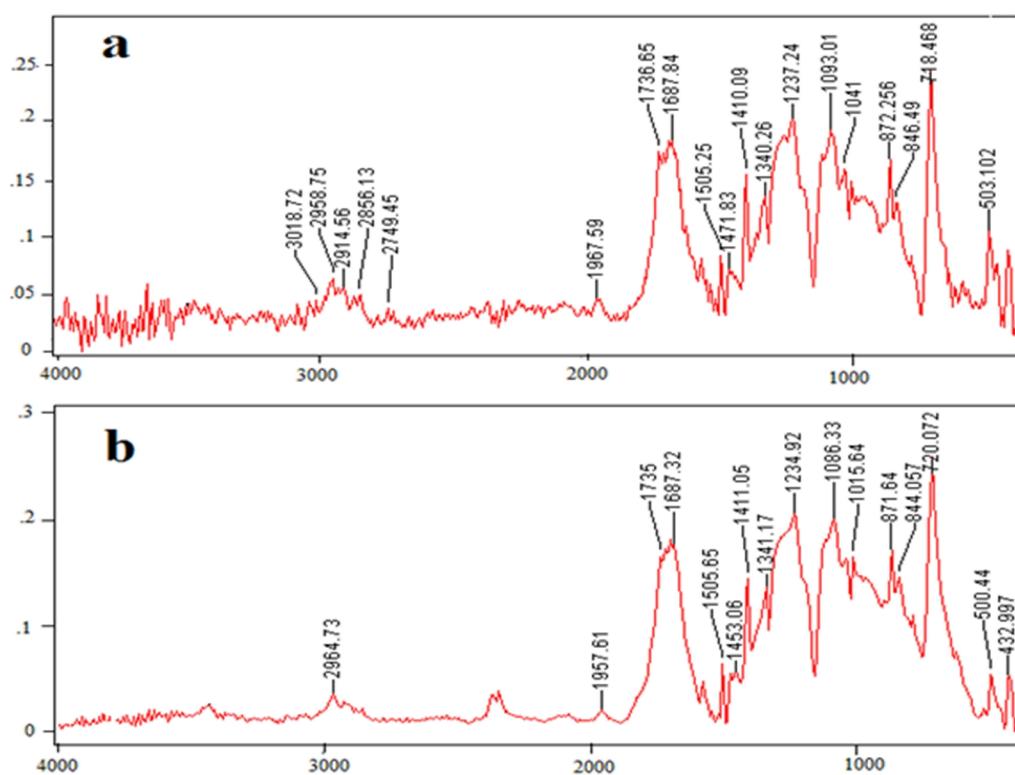

**Figure 1** The FTIR spectra of raw (A) and conjugated (B) polyester fabric
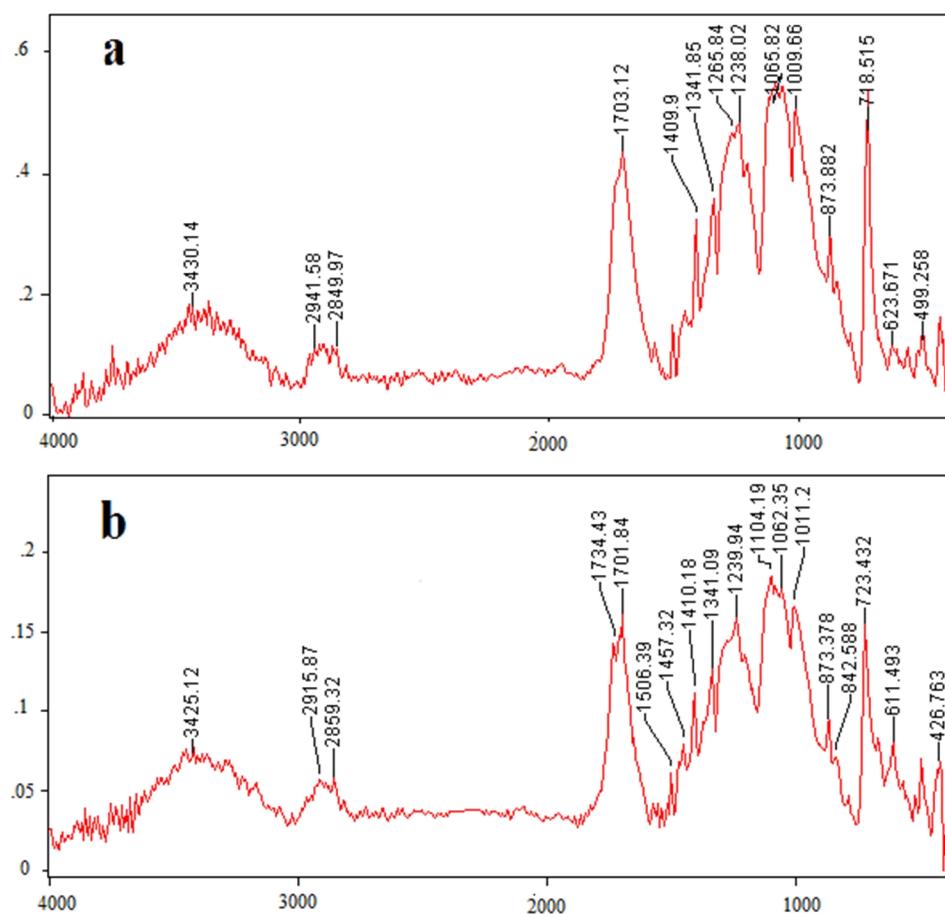
**Figure 2** The FTIR spectra of raw (A) and conjugated (B) cellulose-polyester fabric
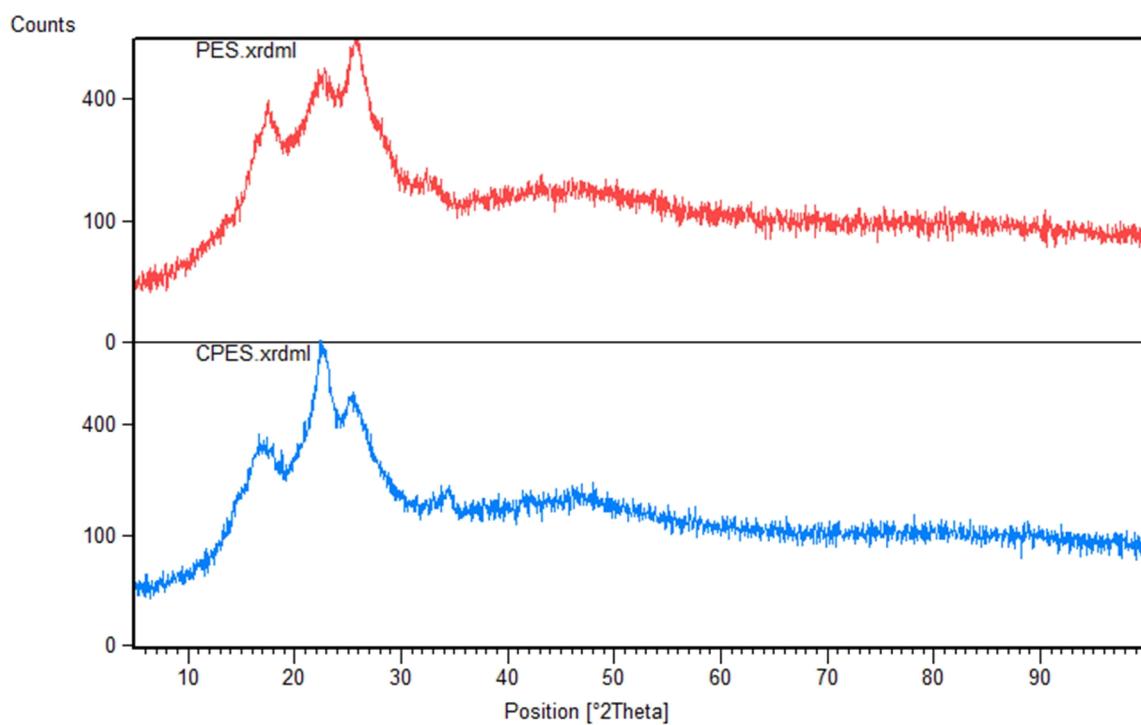
Figure 3 The XRD patterns of the polyester and cellulose-polyester fabrics
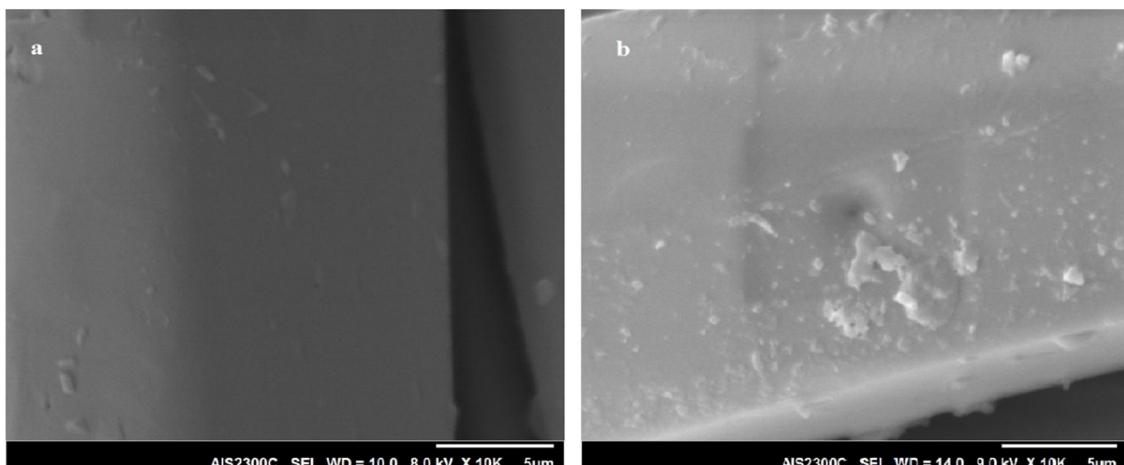
Figure 4 The SEM images of raw polyester fabric (a) and allicin conjugated polyester fabric (b)
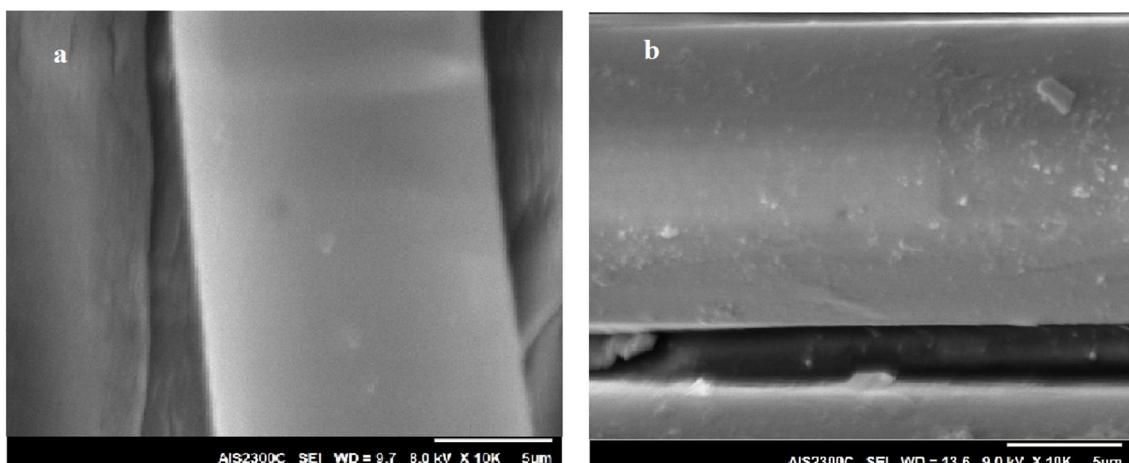

Figure 5 The SEM images of raw polyester fabric (a) and allicin conjugated cellulose-polyester fabric (b)

Figure 4 shows the SEM images of raw polyester fabric (a) and allicin conjugated polyester fabric (b). Also, Figure 5 shows the SEM images of raw cellulose-polyester fabric (a) and allicin conjugated cellulose-polyester fabric (b). Considerable differences are observed between raw fabrics and conjugated fabrics; the former has relatively smooth surface and is uniform, whereas the latter is rough, which is related to the nanocellulose conjugated with allicin mounted onto the surface of the fabrics.

5 SUMMARY

In this study, polyester and cotton-polyester fabrics were modified with APTES, and then attached to allicin-conjugated nanocellulose. As control, the fabrics, which were not exposed to any substance, were considered. The reason of choosing of this method was based on Jebali et al study. Their study showed that nanocellulose conjugated with allicin had antifungal and antibacterial properties. They proposed that this novel nanoparticle can be used on the surface of different fabrics (e.g. polyester and cellulose-

polyester) to achieve antimicrobial fabrics for use in hospitals and health centers. Here, the results showed that this method could give us a high antimicrobial property. The procedure was introduced by us for the first time, and must be compared with other methods. It is a fact that all fabrics can be antimicrobial when exposed to antibiotics, formaldehyde, metal ions (such as silver, copper, etc.), quaternary ammonium, phenols, oxidizing agents (such as chlorine, chlorine amines, ozone) [18, 12]. All of them can inhibit microbial growth by means of various mechanisms (e.g. enzyme inactivation, disruption of cell membrane). Unfortunately, most of them are toxic and can lead to allergy or hypersensitivity. These problems restrict the usage of these materials in the fabrics. We think that fabrics exposed to allicin-conjugated nanocellulose are an ideal compound because of natural origin.

Silver nanoparticle is the main antimicrobial nanoparticle which can be used on all fabrics. For example, Velmurugan et al showed that silver nanoparticles prepared by green synthesis induced antimicrobial property on the cellulose fabrics [19].

Perelshtein et al modified textile fabrics (nylon, polyester and cotton) with silver nanoparticles by sonochemical coating which showed antibacterial activity of modified textile fabrics [20]. Compared with natural allicin-conjugated nanocellulose, silver nanoparticles are synthetic and very toxic.

6 REFERENCES

1. Ackart W.B., Camp R.L., Wheelwright W.L., Byck J.S.: Antimicrobial Polymers, Biomedical Materials Research 9, 55-68, 1975

2. Varesano A., Vineis C., Aluigi A., Rombaldoni F.: Antimicrobial Polymers for Textile Products, Science against Microbial Pathogens: Communicating Current Research and Technological Advances 1, 99-110, 2011

3. Wasif A.I., Laga S.K.: Use of Nano Silver as an Antimicrobial Agent For Cotton, AUTEX Research Journal 9(1), 2009

4. Kostic J., Radic N.: Antimicrobial Textile Prepared by Silver Deposition on Dielectirc Barrier Discharge Treated Cotton/Polyester Fabric, Chemical Industry & Chemical Engineering Quarterly 14(4), 219-221, 2008

5. Ghoreishian S.M., Maleknia, L., Mirzapour H., Norouz M.: Antibacterial Properties and Color Fastness of Silk Fabric Dyed with Turmeric Extract, Fibers and Polymers 14, 201-207, 2013

6. Cho S.J., Rhee, D.K., Pyo S.: Allicin, a Major Component of Garlic, Inhibits Apoptosis of Macrophage In a Depleted Nutritional State Nutrition 22, 1177-1184, 2006

7. Weisberger A.S., Pensky J.: Tumor Inhibition by a Sulfhydryl-blocking Agent Related to an Active Principle of Garlic (Allium sativum), Cancer Research 18, 1301-1308, 1958

8. Ankri S., Miron T., Rabinkov A., Wilchek M., Mirelman D.: Allicin From Garlic Strongly Inhibits Cysteine Proteinases and Cytopathic Effects of Entamoeba Histolytica, Antimicrob Agents Chemother 41, 2286-2288, 1997

9. Aware R.S., Thorat B.N.: Garlic Under Various Drying Study and Its Impact on Allicin Retention, Drying Technology 29, 1510-1518, 2011

10. Luo D.Q., Guo J.H., JieWang F., Jin Z.X., Cheng X.L., Zhu J.C., Peng C.Q., Zhang C.: Anti-Fungal Efficacy of Polybutylcyanoacrylate Nanoparticles of Allicin and Comparison with Pure Allicin, Journal of Biomaterials Science 20, 21-31, 2009

11. Jafary R., Khajeh Mehrizi M., Hekmatimoghaddam S.h., Jebali A.: Antibacterial property of cellulose fabric finished by allicin-conjugated nanocellulose, The Journal of The Textile Institute 106, 683-689, 2015

12. Khajeh Mehrizi M., Mortazavi S.M., Abedi D.: The Antimicrobial Characteristic Study of Acrylic Fiber Treated with Metal Salts and Direct Dyes, Fibers and Polymers 10, 601-605, 2009

13. Son Y.-A., Sun G.: Durable Antimicrobial Nylon 66 Fabrics: Ionic Interactions with Quaternary Ammonium Salts, Applied Polymer Science 90, 2194-2199, 2003

14. Cheung S.Y.: A Study of New Series of Organic Compounds Synthesized from Alkoxy-Substituted Quinaldine Applied for Synthetic Fabrics, Institute of Textiles & Clothing, 2010

15. Cho L.-L.: Identification of textile fiber by Raman microspectroscopy, Forensic Science Journal 6, 55-62, 2007

16. Kusuktham B.: Surface Modification of Polyester Fabrics with Vinyltriethoxysilane, Journal of Metals, Materials and Minerals 20, 85-88, 2010

17. Siqueira G., Bras J., Dufresne A.: Luffa cylindrica as a lignocellulosic source of fiber,microfibrillated cellulose and cellulose nanocrystals, Luffa as a cellulose source 5(2), 727-740, 2010

18. Abedi D., Mortazavi S.M., Khajeh Mehrizi M., Feiz M.: Antimicrobial Properties of Acrylic Fabrics Dyed with Direct Dye and a Copper Salt, Textile Research Journal 78, 311-319, 2008

19. Ahlström B., Chelminska-Bertilsson M., Thompson R.A., Edebo L.: Long-chain Alkanoylcholines, a New Category of Soft Antimicrobial Agents that are Enzymatically Degradable, Antimicrob. Agents Chemother 39, 50-55, 1995

20. Murguia M.C., Machuca L.M., Lura M.C., Cabrera M.I., Grau R.J.: Synthesis and Properties of Novel Antifungal Gemini Compounds Derived from N-Acetyl Diethanolamines, Journal of Surfactants Deterg 11, 223-230, 2008

SORPTION PROPERTIES OF IRON IMPREGNATED ACTIVATED CARBON PREPARED FROM ACRYLIC FIBROUS WASTES

S. Naeem, V. Baheti, J. Militky and J. Wiener

Department of Material Engineering, Faculty of Textile Engineering, Technical University of Liberec, Studentska 2, Liberec 46117, Czech Republic
salman.ntu@gmail.com

Abstract: *In this work, waste acrylic fiber web was impregnated with iron chloride solution and another web without salt impregnation was carbonized by heating under a layer of charcoal through physical activation in a high temperature furnace to produce activated carbon and iron impregnated activated carbon (FeAC). After stabilization at heating rate $50°C.hr^{-1}$ the carbonization process was performed at the heating rate of $300°C.hr^{-1}$. Both the webs were heated to 1200°C with no holding time for getting a higher surface area and porosity. Both the samples were characterized by using BET surface area, SEM, EDX and TGA for determining the surface area, microscopic structure and content of different elements. Iron impregnated activated carbon (FeAC) was later used as adsorbent for the removal of methylene blue from an aqueous solution. The dye removal percentage and adsorption capacity was checked at different experimental parameters like different dye concentrations, adsorbent dosage, stirring speed and different pH.*

Key Words: *Textile recycling, Fibrous wastes Acrylic fibers, Stabilization, Carbonization, FeAC, Physical activation, Activated carbon*

1   INTRODUCTION

Dyes are synthetic or natural compounds used to add color. Synthetic dyes are increasingly used in textile industries because of their low cost. They are resistant against bio and photo-degradation because of their complex structure [1]. The commonly used synthetic dyes in textiles are basic dyes, vat dyes, direct dyes and reactive dyes. The colored solutions of synthetic dyes discharged from textile industries are aesthetically unpleasant, damage the ecosystem and disturb the biological processes in water. The colored solutions discharged into freshwater reduce the process of photosynthesis and also serious risks are associated with synthetic dyes [2, 3]. Hence the removal of colored solution (dyes) from waste water is very important before discharging them to main stream water. Different treatment methods are already in use like biological, physical and chemical methods. Physical methods are expensive and accompanied with the production of sludge and hazardous byproducts [4]. Chemical methods like flocculation and coagulation are not preferable either because of high solubility of dyes and consequently higher yield of sludge. The biological method of treatment is not preferable because of low-biodegradation behavior of synthetic dyes [5].

Among the techniques mentioned, adsorption is better because of efficiency, simple operation, cost effectiveness and recovery of adsorbent [6, 7]. The dye molecules are adsorbed onto activated carbon by chemical and physical means. Adsorption of dyes onto activated carbon takes place either by physisorption or chemisorption. The porosity, pore structure and surface area are other different structural factors that determine the adsorption (physisorption) capacity of adsorbent [8, 9]. However, the functional groups present on the surface of carbon are mainly responsible for chemisorption. Activated carbon is a commonly used adsorbent for solid/gas separation and to remove odor/taste and other impurities from waste water. For further improvement of its structural characteristics, various surface modification techniques like physical, chemical and biological methods are used [10]. In recent years, researchers have been trying to explore alternative inexpensive methods for the preparation of activated carbon. Different precursors used for the formation of activated carbon are phenolic resins [11, 12], polyacrylamides, polyimides, pitch, cellulose based fibers and polyacrylonitrile based fibers [13]. Literature shows that carbon fibers made from polyacrylonitrile precursor are better due to high strength, dust free nature and greater carbon yield [14]. Hence, the idea of using acrylic fibrous waste for activated carbon is a good approach. Different researchers have used different methods to modify the structure of activated carbon with iron or other metal oxides. Some researchers used granular activated carbon, mixing it with iron chloride to get iron impregnated activated carbon [15]. In another study, activated carbon was stirred with a $KMnO_4$ solution for 20 minutes.

After separating activated carbon from the KMnO$_4$ solution, the residual AC was mixed with iron sulfate to get FeAC [16].

In this work, surface of activated carbon was modified with iron by impregnating acrylic web with the solution of iron chloride (200 g.L^{-1}). Iron chloride was selected in this study because of its high solubility over a wide range of pH. Both the webs (iron impregnated web and acrylic web) were transformed into activated carbon through physical activation in the presence of air at high temperature using charcoal. Both activated webs were analyzed by different characterization methods like BET, EDX, SEM and TGA. The dye uptake or dye removal percentage of iron impregnated activated carbon was checked from aqueous solution.

2   EXPERIMENTAL

2.1 Materials

The acrylic waste was provided by Grund Industries, Czech Republic. The acrylic fibers are favorable for the formation of activated carbon due to low ash content and their natural structure. Methylene blue used in this work was purchased from Sigma Aldrich. Iron chloride was purchased from Biesterfeld Silcom s.r.o. Czech Republic.

2.2 Preparation of iron impregnated activated carbon non-woven web

Non-woven structure of acrylic fibers was prepared by using a carding and needle punching machine. Two smaller webs having dimensions 30 × 20 cm were cut from this web. In order to remove any impurity, one acrylic sample was washed with distilled water and heated to 100°C for 4 to 5 hours in an oven to make it completely dry. The other web was dipped in ferric chloride solution and boiled for almost 4 hours. After boiling, the web was washed with distilled water to remove extra iron content. Both the webs after drying were stabilized at 250°C at 50°C.hr^{-1}. The stabilized webs were then heated at 1200°C with a heating rate of 300°C.hr^{-1} using charcoal for physical activation.

2.2.1 Characterization of iron impregnated activated carbon web

The pH of point of zero charge of both the webs was determined by salt addition method. In different flasks, 40 mL solution (0.1 M NaNO$_3$) was taken. The solution pH was varied from 2 to 10 by using NaOH and HNO$_3$. In each flask, 0.1 g of activated carbon was added and the solution was agitated overnight at room temperature. After agitation, the final pH was measured, the difference between final and initial values of pH was plotted against initial pH. The values of pH$_{ZPC}$ of FeAC and activated carbon are 4.8 and 6.7 respectively.

SEM was employed to analyze both the activated webs, that is, with and without metal impregnation.

This helped to analyze morphology of the webs like porosity and distribution of iron particles on the surface of activated carbon. EDX analysis showed the relative proportion of different elements and their concentrations in both the webs. Thermo gravimetric analysis (TGA) was done to investigate the desorption rate of iron impregnated web and activated carbon web with methylene blue (MB).

2.3 Adsorption of methylene blue onto iron impregnated activated carbon

The solution of methylene blue was prepared with different concentrations after dissolving the required dye (MB) in distilled water. Batch method was used to find out the adsorption experiments. Equilibrium adsorption point was determined by adding a fixed amount of FeAC, that is, 0.1 g into 50 mL solution of methylene blue of different concentrations (10 ,20, 30, 40 and 50 mg.L^{-1}). The flasks having iron impregnated activated carbon web and methylene blue solutions were put on water bath shaker for 135 minutes at 200 rpm to achieve the equilibrium point. The adsorbent was removed from methylene blue solutions every 15 minutes and the remaining solution was analyzed with the help of UV-visible spectrophotometer at the wave length of 665.0 nm.

The impact of adsorbent dosage on removal efficiency of methylene blue was checked by varying adsorbent dosage from 0.05 to 0.25 g. All the flasks containing pre-weighted amount of adsorbent with 50 mL methylene blue solutions were agitated by using water bath shaker at 200 rpm for 135 minutes for analyzing adsorbent uptake and removal efficiency. The adsorption capacity and dye removal efficiency were also checked by varying the speed of rotation and changing the pH of solution as well.

The dye removal efficiency and adsorption capacity were calculated from Eq. (1) and Eq. (2), respectively.

$$Dye\ removal\ efficiency\ [\%] = \left[\frac{(C_0 - C_e)}{C_0}\right] \times 100 \quad (1)$$

where C_0 (mg.L^{-1}) is the initial concentration of dye before addition of activated carbon and C_e (mg.L^{-1}) is the dye concentration at equilibrium after addition of activated carbon (FeAC).

$$Adsorption\ capacity\ q_e = (C_0 - C_e)\frac{v}{w} \quad (2)$$

where q_e [mg.g^{-1}] is the amount of dye adsorbed, v is the volume of the solution in liters and w [g] is the mass of activated carbon (FeAC) used.

3   RESULTS AND DISCUSSION

3.1 Effect of carbonization parameters on properties of iron impregnated activated carbon web

The specific surface area of AC and FeAC was measured by using Quantachrome Instrument. Adsorption/desorption measurements were taken in relative pressure range P/P0 from 0.02 to 1. Both adsorption and desorption isotherms were recorded and specific surface area was determined. The specific area of AC and FeAC was found to be 280 $m^2.g^{-1}$ and 570 $m^2.g^{-1}$. SEM analysis was done to analyze surface morphology of AC and FeAC. The iron impregnated web was afterwards carbonized at 1200°C with different heating rates (150°C.hr^{-1}, 300°C.hr^{-1}, 450°C.hr^{-1}) and no holding time. The best results were achieved by carbonization at 1200°C with the heating rate of 300°C.hr^{-1}, as can be seen from Figure 1.
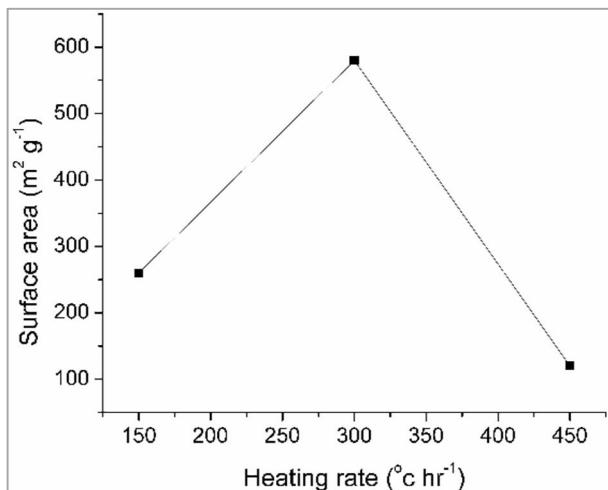

Figure 1 Effect of heating rate on specific surface area

The SEM image of activated carbon and FeAC can be seen in Figure 2 (a and b). The image of Figure 2(a) depicts iron particles distributed heterogeneously. However, very low porosity can be seen in Figure 2(b) compared with FeAC. The white particles present on the surface of this porous carbon are the complexes of iron.

The EDX analysis showed the presence of iron particles on the surface of carbon web. EDX results of activated carbon and iron impregnated carbon web can be seen from the Table 1.

TGA helped to understand the desorption behavior of both the carbon webs and dye adsorbed FeAC. Both the samples were heated up to 900°C with the heating rate of 10°C.min^{-1}. Figure 3 shows that dye adsorbed iron impregnated sample showed higher decrease in weight compared with AC and FeAC. The reason for higher weight loss is

desorption of water and adsorbed dye (MB) from the surface and pores.

Table 1 EDX analysis of AC and FeAC

| Element	App	Intensity	Mass %	Atomic %
AC				
C K	0.18	2.1094	0.09	92.49
O K	0.01	0.7448	0.01	6.61
Ca K	0.00	0.9026	0.00	0.90
FeAC				
C K	0.40	1.7227	0.25	87.81
O K	0.03	0.8288	0.04	10.23
S K	0.00	0.9635	0.00	0.62
Fe L	0.01	0.5315	0.02	1.34
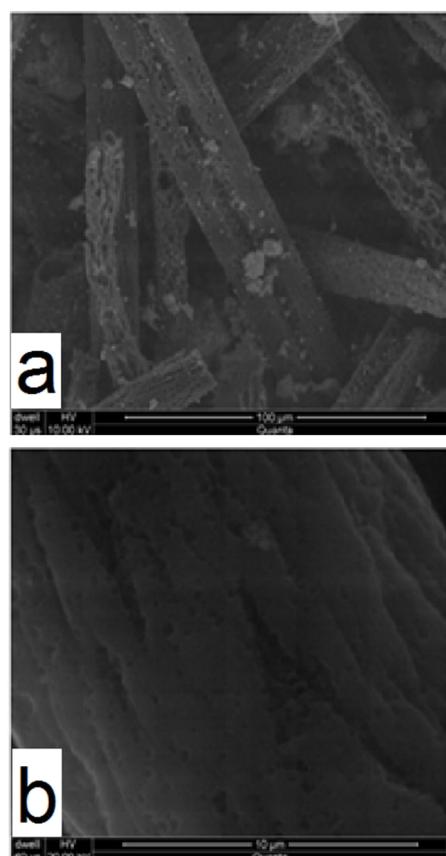
Figure 2 SEM image of carbon (a) Iron impregnated AC (b) AC

3.2 Effect of process parameters on adsorption performance

3.2.1 Effect of dye concentration

The adsorption performance of FeAC was calculated by varying the concentration from 10 mg.L^{-1} to 50 mg.L^{-1}. It can be seen from Figure 4 that removal percentage of methylene blue and adsorption capacity of adsorbent increases with the increase of time. However, as the concentration of the dye is increased, it takes more time to reach the equilibrium. The reason for shorter equilibration time at lower concentrations of the dye is due to relatively greater number of active sites available

for adsorption of dye molecules. It took around 90 minutes to reach the equilibrium when the concentration of dye was 10 mg.L^{-1}, compared to around 120 to 135 minutes when the dye concentration was increased from 40 mg.L^{-1} to 50 mg.L^{-1}.
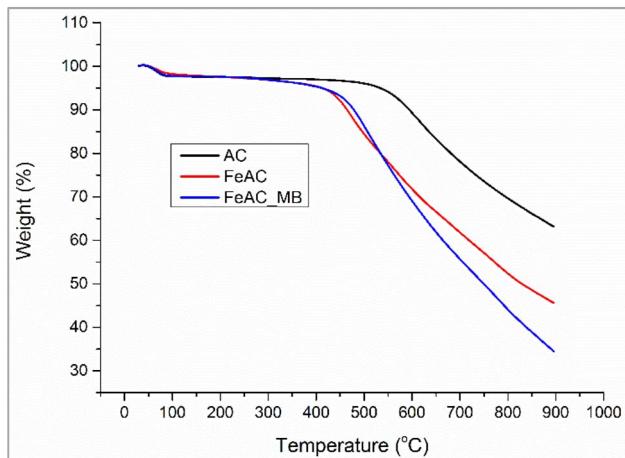

Figure 3 Comparison of desorption rate
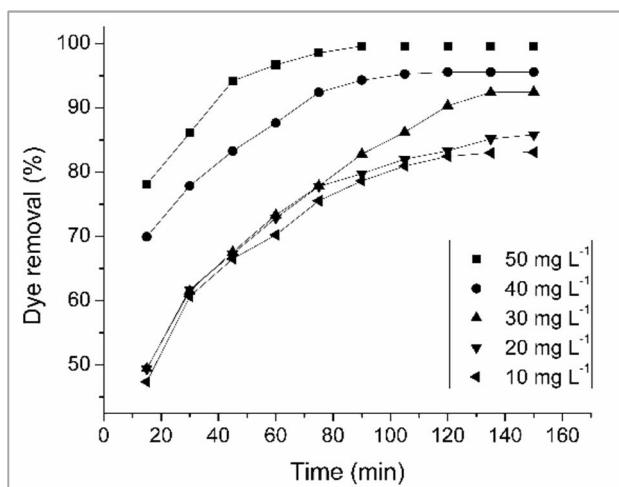
Figure 4 Effect of initial dye concentration on dye removal

As far as the removal of dye is concerned, it decreased from 97.05% to 84.41% keeping other parameters like temperature, stirring speed and adsorbent dosage constant. As far as dye accumulation on the adsorbent is concerned, it increases with the increase in the concentration of dye. The dye accumulated on iron impregnated activated carbon (FeAC) is found to increase from 3.74 mg.g^{-1} to 19.56 mg.L^{-1} when the dye concentration was increased from 10 mg.L^{-1} to 50 mg.L^{-1} as can be seen from Figure 5. This behavior is obviously due to the availability of active sites in the adsorbent for the unit quantity of methylene blue in the solution.
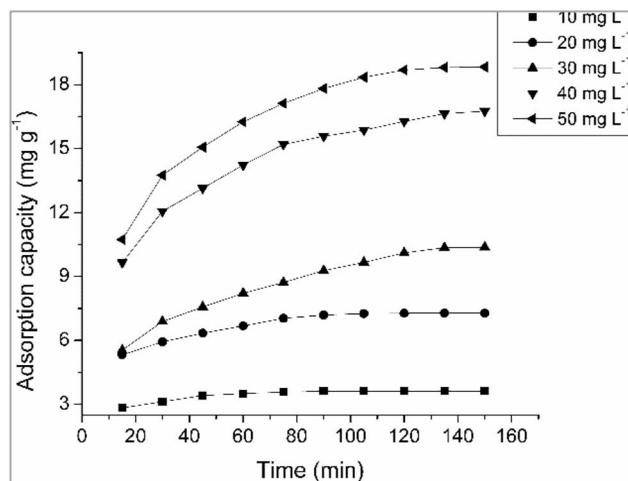

Figure 5 Effect of initial dye concentration on adsorption capacity

3.2.2 Effect of adsorbent dosage

The impact of adsorbent quantity on adsorption performance and dye removal efficiency has been investigated by taking dye concentration 50 mg.L^{-1}, contact time 135 minutes for reaching the equilibrium point, temperature 25°C at stirring speed of 200 rpm. The adsorbent dosage was varied from 1 g.L^{-1} to 5 g.L^{-1}. From Figure 6, it is clear that by increasing adsorbent quantity, an increasing trend of dye removal has been seen, however at the same time, a decreasing trend of adsorption capacity is present.
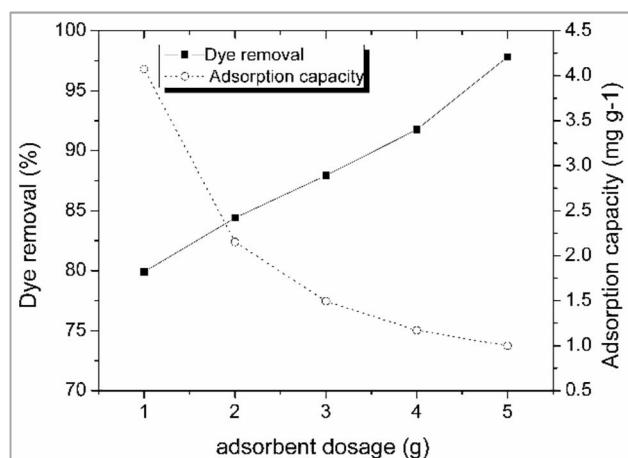

Figure 6 Effect of adsorbent dosage on adsorption performance

The dye removal percentage was 79.9% with 1 g.L^{-1} adsorbent. The trend of dye removal keeps on increasing to 84.41%, 87.94%, 91.76% and 97.84% with the increase of adsorbent dosage from 2 g.L^{-1}, 3 g.L^{-1}, 4 g.L^{-1} and 5 g.L^{-1}, respectively, due to the presence of more active sites and greater iron content on the adsorbent. However, other factors also play an important role when the inverse trend between adsorption capacity and adsorbent

dosage is analyzed as many adsorption sites in adsorbent remain unsaturated, hence a drop in adsorption capacity takes place [17].

3.2.3 Effect of pH

The pH values calculated by salt addition method showed that surface of iron impregnated activated carbon is more acidic (pH_{ZPC} = 4.8) compared with activated carbon (pH_{ZPC} = 6.7) without iron. The surface of FeAC becomes positively charged at value of pH lower than the point of zero charge of FeAC due to the accumulation of positive (H^+) ions. Hence as the pH value decreases from the point of zero charge, the dye removal efficiency keeps on decreasing as shown in Figure 7.
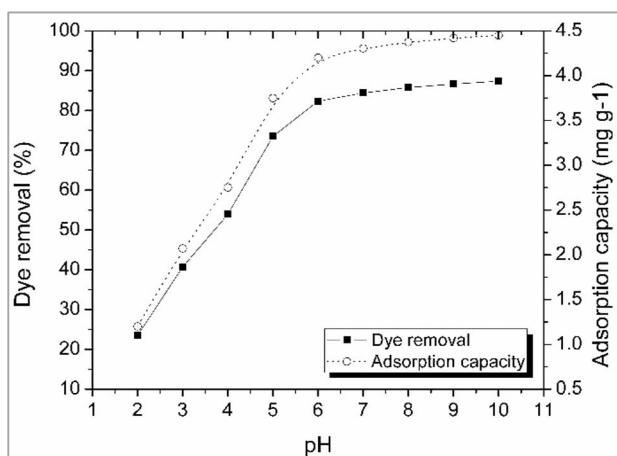
Figure 7 Effect of pH on adsorption performance

The trend is even more prominent at lower values of pH as the surface becomes more positively charged. The H^+ ions on the surface of adsorbent make it difficult to interact with cationic dye molecules (MB^+). This repulsive force is responsible for lower removal of methylene blue. However, an increase in dye removal efficiency was seen at pH above 5. From pH 7 onward, dye removal efficiency remains similar. The increase in dye removal above the point of zero charge is caused by attractive force between positively charged methylene blue molecules and negatively charged surface of FeAC.

3.2.4 Effect of stirring speed

The impact of stirring speed on adsorption performance of FeAC was calculated at 50 mg.L^{-1} methylene blue concentration, temperature 25°C, adsorbent dosage 2 g.L^{-1}, 50 mL dye solution and 135 minutes contact time for reaching the equilibrium point. The stirring speed was changed from 50 to 200 rpm. One sample for reference was checked without any stirring speed. From Figure 7, it is clear that 5.39% dye was removed when there was no stirring. However dye removal percentage of methylene blue was 38.23%, 56.27%, 71.56% and 84.41% at stirring

speeds 50 rpm, 100 rpm, 150 rpm and 200 rpm, respectively.

The adsorption capacities also increased by increasing the stirring speed while keeping adsorbent dosage the same. The increase in adsorption capacities were 1.95 mg.g^{-1}, 2.87 g.L^{-1}, 3.65 g.L^{-1} and 4.305 g.L^{-1} when the stirring speed was increased from 50 to 200 rpm, respectively. This trend is obviously due to increased interaction of methylene blue with the adsorbent by the increase of stirring speed.
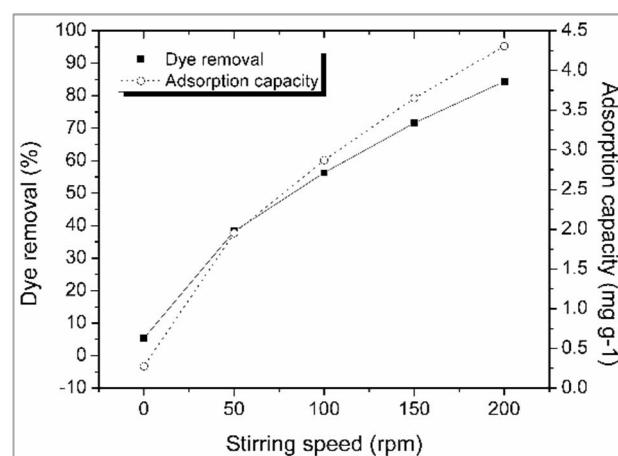
Figure 8 Effect of stirring speed on adsorption performance

4   CONCLUSION

The acrylic waste was converted into AC and iron impregnated activated carbon (FeAC) through physical activation by using thermal treatment process in a high temperature furnace. The surface area was also increased with FeAC (570 m^2.g^{-1}) when compared with AC. The high temperature carbonization was carried out at 1200°C.hr^{-1} with no holding time. Controlled atmospheric oxygen reacted with the carbon under a slow heating rate for achieving maximum surface area. In the case of iron impregnated web, the breaking of carbon-carbon bonds occurred and iron deposited on AC through physical and chemical attachment. The surface charge of activated carbon decreased from 6.7 to 4.8, due to iron impregnation and surface oxidation. This acidic nature of FeAC is important for the uptake of cationic dyes like methylene blue from waste water. The adsorption phenomenon in terms of adsorption capacity and dye removal percentage was investigated by varying dye concentration, FeAC dosage, different stirring speed and pH (2-10) values of solution. The results showed that dye removal time is increased when the concentration of dye is increased in solution.

5 REFERENCES

1. Slampova A., Smela D., Vondrackova A., Jancarova I., Kuban V.: Determination of Synthetic Colorants in Foodstuffs, Chem. Listy 95, 163-168, 2012

2. Kertèsz S., Cakl J., Jiránková H.: Submerged hollow fiber microfiltration as a part of hybrid photocatalytic process for dye wastewater treatment, Desalination 343, 106-112, 2014

3. Baskaralingam P., Pulikesi M., Elango D., Ramamurthi V., Sivanesan S.: Adsorption of acid dye onto organobentonite, J. Hazard. Mater 128, 138-144, 2006

4. Gupta V. K., Carrott P.J.M., Ribeiro Carrott M.M.L., Suhas.: Low-cost adsorbents: growing approach to wastewater treatment - a review, Environ Sci Technol 39, 783-842, 2009

5. Grabowska E.L., Gryglewicz G.: Adsorption characteristics of congo red on coal-based mesoporous activated carbon, Dyes and Pigments 74, 34-40, 2007

6. Bouberka Z., Khenifi A., Sekrane F., Bettahar N., Derriche N.: Adsorption of Direct Red 2 on Bentonite Modified by Cetyltrimethylammonium Bromid, Chem Eng J 136, 295-305, 2008

7. Gupta V.K., Ali I., Saleh T.A., Nayak A., Agarwal A., Chemical treatment technologies for waste-water recycling—an overview, RSC Advances 2, 6380-6388, 2012

8. Shan H.Y., Malarvizhi R., Sulochana N.: Equilibrium isotherm studies of methylene adsorption onto activated carbon prepared from Delonixregia pods, Journal of Environmental Protection 3, 111-116, 2009

9. Ciardelli G., Ranieri N.: The treatment and reuse of wastewater in the textile industry by means of ozonation and electroflocculation, Water Res 35, 567-572, 2001

10. Zelmanov G., Semiat R.: Boron removal from water and its recovery using iron (Fe^{+3}) oxide/hydroxidebased nanoparticles (NanoFe) and NanoFe-impregnated granular activated carbon as adsorbent, Desalination 333, 107-117, 2014

11. Mangun C., Barr J., Riha S.,Lizzio A., Donnals G., Daley M.: Adsorption of SO$_2$ onto Oxidized and Heat Treated Activated Carbon Fibers (ACFS), Carbon 35, 411-417, 1997

12. Daley M., Braatz R., Economy J., Mangun C.: Effect of Pore Size on Adsorption of Hydrocarbons in Phenolic-Based Activated Carbon Fibers, Carbon 36, 123-131, 1998

13. Coleman M., Sivy G.T.: Fourier Transform IR Studies of the Degradation of Polyacrylonitrile Copolymers - IV Acrylonitrile/Acrylamide Copolymers, Carbon 19, 127-131, 1981

14. Baheti V., Militky J.: Reinforcement of wet milled jute nano/micro particles in polyvinyl alcohol films, Fiber Polym 14, 133-137, 2013

15. Chang Q., Lin W., Ying W.C.: Preparation of iron-impregnated granular activated carbon for arsenic removal from drinking water, Journal of Hazardous Materials 184, 515-522, 2010

16. Shah I., Adnan R., Ngah W., Norita M.: Iron Impregnated Activated Carbon as an Efficient Adsorbent for the Removal of Methylene Blue, Regeneration and Kinetics Studies, PLoS One 10 2015

17. Sharma D.C., Forster C.F.: Removal of hexavalent chromium using sphagnum moss peat, Water Res 27, 1201-1208, 1993

ELABORATION OF ENVIRONMENT-FRIENDLY REACTIVE DYEING PROCEDURES BY MEANS OF COMPUTER AIDED SIMULATION

H. J. Nagy[1], K. Őrsi[1], Á. Orbán[1], Á. Tóth[2], I. Rusznák[1], P.Sallay[1] and A. Víg[1]

[1]*Department of Organic Chemistry and Technology, BME, Budafoki 8, H-1111 Budapest, Hungary*
[2]*Claret Bt., Petőfi Sándor 29, H-9762 Tanakajd, Hungary*
hnagy@mail.bme.hu

Abstract: A "utility" computer program has been elaborated by us as an extension to the computer program of CLARIANT which simulates the Exhaust and Pad-Batch dyeing procedures. By the program of CLARIANT, the fixed proportion of selected reactive dyes could be predicted as the function of the applied dying technology. Our utility program is appropriate for a rapid calculation and demonstration of the characteristics of the waste water (Chemical Oxygen Demand (COD), Biological Oxygen Demand (BOD$_5$) produced in the course of simulated dyeings.

Key Words: computer-aided simulation, DRIMAREN dyes, environmental load, cucurbituril, inclusion complex, competitive complex formation

1   INTRODUCTION

Environmental requirements in the European Union are among the strictest ones in the world. Based on surveys of EU citizens, the most important tasks of the protection of environment are keeping the good quality of drinking water as well as keeping the impact of chemicals on the environment as little as possible [1]. The water demand is extremely high in textile finishing, because it is the only solvent of chemicals, dyes and finishing agents used in it. The mentioned dissolved harmful agents are to be removed from the wastewater. Numerous chemical treatments of wastewater generated in textile finishing have been studied at our Department (Department of Organic Chemistry and Technology, BME) in the last decade [2, 3].

DRIMAREN reactive dyes have been studied for environment-friendly optimisation in exhaust and pad-batch procedures according to the optimization program of CLARIANT (Archroma).

Environmental impact of mono- and bifunctional reactive dyes has been simulated and the financial efficiency of the applied dyeing procedures has been evaluated.

2   MATERIALS AND METHODS

2.1   The studied dyes

DRIMAREN „K"- mono- and „HF-CL" bifunctional reactive dyes have been the targets of simulation under different technological conditions. Exhausting and pad-batch procedures have been applied according to the optimization program of CLARIANT.

The named dyes are highly reactive and well applicable in dyeing procedures even at room temperature. The optimal fixation temperature in the exhausting dyeing technologies is 60°C (the used dyeing program followed that of CLARIANT-Standard at 40/60°C).

For producing pale and moderate colours as trichromatic system, different mixtures *DRIMAREN* Yellow K-2R, *DRIMAREN* Red K-4BL and *DRIMAREN* Blue K-2RL dyes are suggested. For producing deep shades, *DRIMAREN* Yellow K-2R, *DRIMAREN* Red K-8B and *DRIMAREN* Navy K-BNN have to be mixed [4].

2.2   Methods for evaluations

2.2.1   CLARIANT's Optimization Software

Our dyeing experiments have been simulated by the means of the above mentioned software. This software established correlations among the dyeing conditions and the fixed proportion of the *DRIMAREN* dye.

Simulated dyeings under pad-batch and exhaust conditions have been studied. The technological parameters as well as the fixed proportion of dyes have been optimised for different shades of colours (Figures 1 and 2).
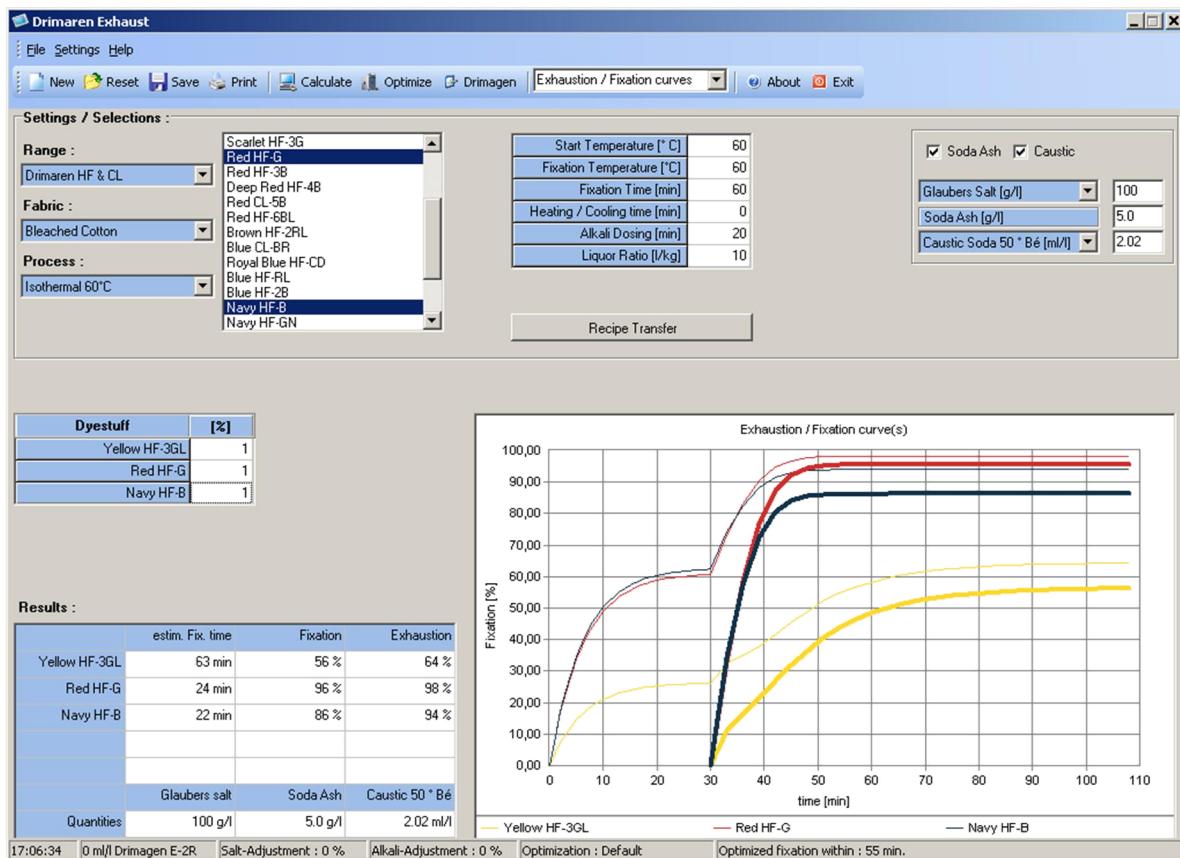
Figure 1 CLARIANT Exhaust software
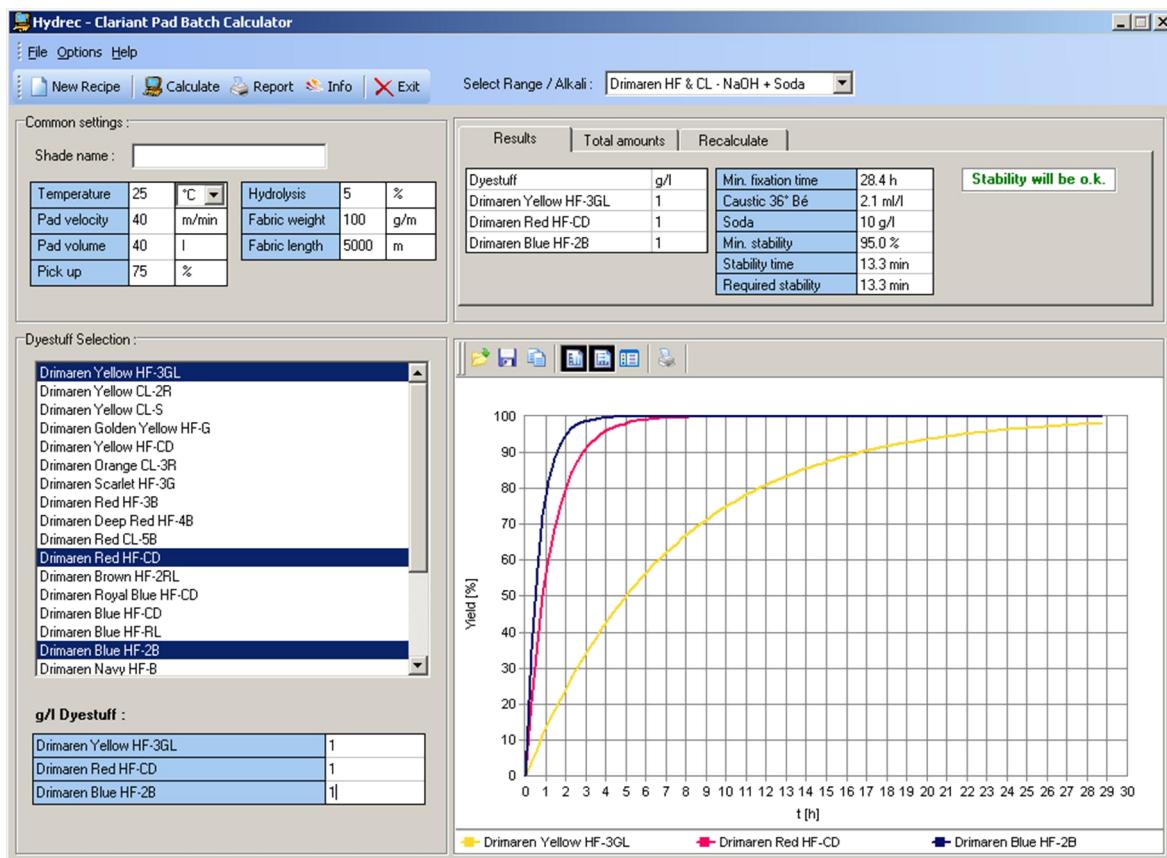
Figure 2 CLARIANT Pad-Bach Calculator software

2.2.2 Software for evaluation of the quality and concentration of wastewater

Optimised dyeing conditions have been elaborated by means of CLARIANT's Exhaust and Pad-Batch software (Figures 1 and 2). To calculate the impact of the dyeing procedures on the environment, one has to know the composition of the wastewater from them. To arrive at the wanted data, a new computer program had to be elaborated [5].

The following data are needed: mass of the fabric to be dyed, liquor ratio, the mass of the added sodium salt, the mass of the added NaOH and/or Na_2CO_3, the number of the dyeing procedure followed rinsing treatments. The mentioned data are provided by the software of CLARIANT.

Using the above formulated data, our new computer program allowed for calculating the following characteristics of the produced wastewater:

- volume (with and without rinsing water), [m^3]
- pH
- following concentrations: dye, salts, NaOH and/or Na_2CO_3), [g/l]
- chemical oxygen demand (COD), [mg/L]
- biochemical oxygen demand (BOD), [mg/L]
- sulphate-content, [mg/L]
- total salt-content, [mg/L], [5].
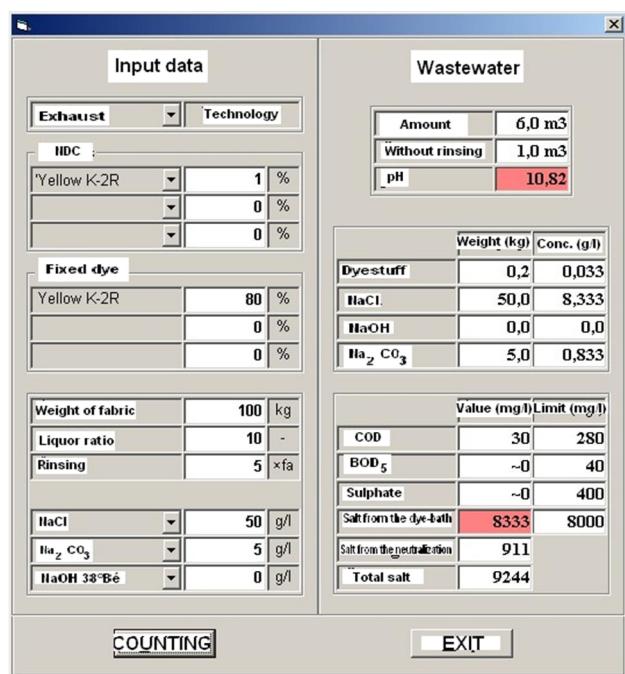
Figure 3 One example for the demonstration about the calculation of characteristic data of wastewater

The computer program has been produced at *Delphi* programming language. One example of elaborated and calculated data gained by analyses of produced wastewater after using the mentioned program is shown by Figure 3.

The expense of an industrial dyeing procedure also has to include the cost of the treatment of the simultaneously occurred wastewater.

The following detailed costs have to be known:

- materials (dyes, auxiliaries, salts, Na_2CO_3, NaOH, wetting agent, equalising chemicals)
- chemicals necessary for treating of wastewater (neutralisation, chemical oxidation)
- running of equipment (heating)
- cost of environment protection (cleaning of wastewater)
- expenses of the use of environment (possible penalties)
- expenses for supporting the quality requirements [5].

3   RESULTS AND DISCUSSION

The use of the two demonstrated computer programs is discussed for exhaust dyeing of cotton fabric with *DRIMAREN* Yellow K-2R (Standard Depth(SD)=1/1), dye uptake from 66% through 79%. Figure 4 demonstrates that by increasing salt concentration in the dyebath, the dye concentration in the wastewater was decreased whereas that of the salt was significantly increased.

Based upon Figure 4, optimal data for dye fixation might be calculated. The optimum might be based either upon the expenses or on the proportion of fixed amount of the dye, or on the least concentration of polluting compounds in the wastewater. The changes of the expenses for the unfixed dye and total amount of salt calculated for the dyeing of 1 kg cotton fabric is shown in Figure 5 in the function of the fixed proportion of the dye. The least amount of expenses occurred at 74% of dye fixation.

The changes of the polluting compounds are expressed in proportion of the permissible limits % in the function of fixed amount of dye for the dyeing procedure with *DRIMAREN* Yellow K-2R dye (SD 1/1) in Figure 6.

The studied dyeing procedure might be optimised by two possible aspects. If our goal is to arrive at the maximised dye fixation (79%), then the wastewater discharge was 72%; if the goal was the minimization of the wastewater discharge (45%), then the achieved dye fixation was only 66%. The expense for the unfixed amount of dye and that of the salt was 50 Ft/kg fabric at the highest achieved dye fixation, whereas it was 52 Ft/kg fabric at the least wastewater discharge.

Under the use of different elaborated dyeing procedures, the pollution of the environment proved to be inevitable. A new procedure has been elaborated by us, under the condition of which the concentration of the dye in the wastewater could be significantly reduced. The application for disperse dyeing are as follows.
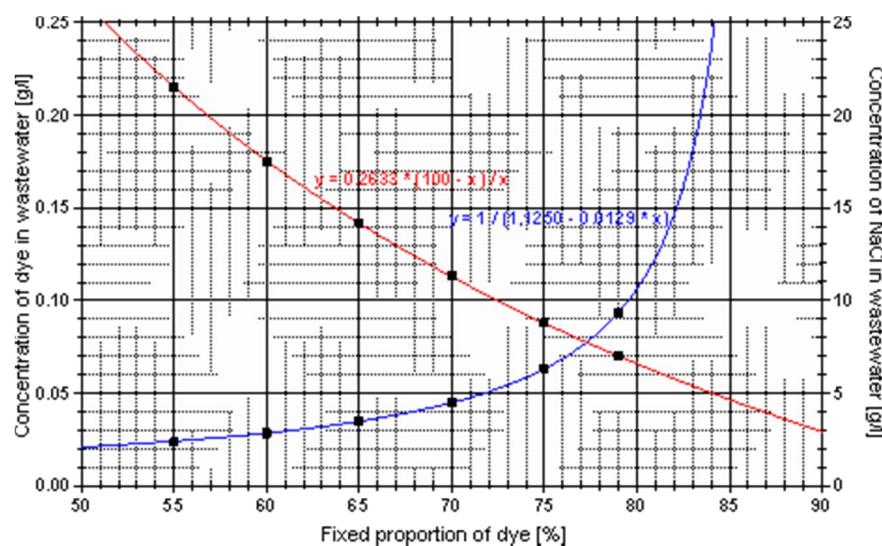
**Figure 4** Wastewater pollution by *DRIMAREN* Yellow K-2R (SD 1/1) as the function of the fixed proportion of the dye
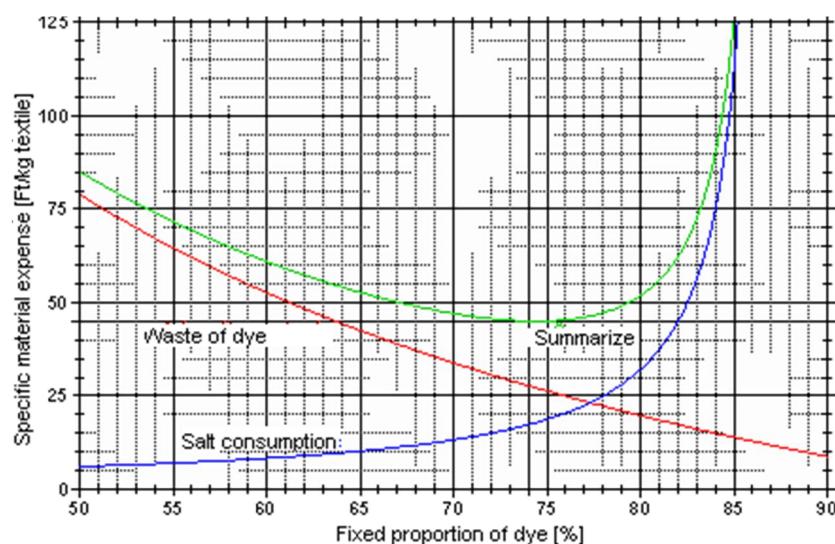

Figure 5 The changes of expenses as the function of fixed amount of dye (*DRIMAREN* Yellow K-2R dye (SD 1/1))
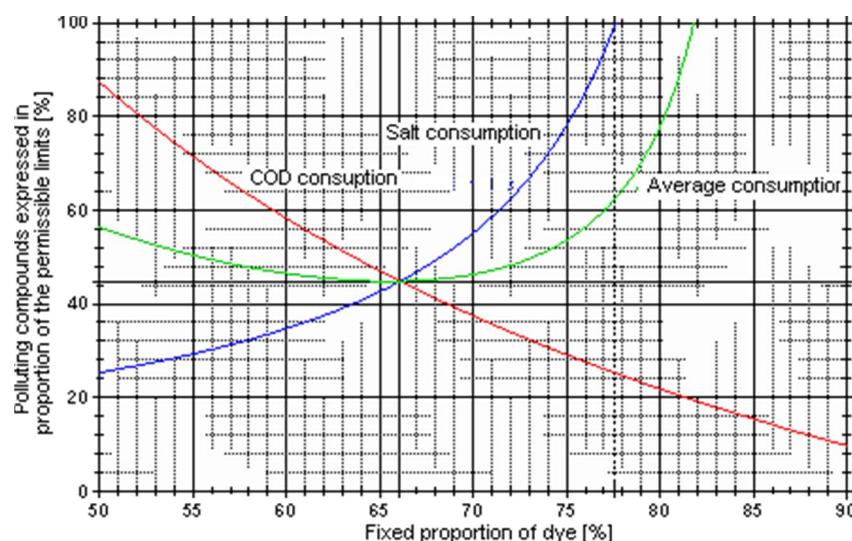

Figure 6 The changes of the polluting compounds expressed in proportion of the permissible limits % in the function of fixed amount of dye (*DRIMAREN* Yellow K-2R dye (SD 1/1))

4   CONCLUSIONS

The advantage of the cold pad-batch procedure compared to the exhaust one is the lower amount of produced wastewater but its disadvantage is the higher concentration of included chemicals dangerous for the environment in it.

The proportion of the fixed-dye content might be significantly influenced by the variation of parameters in both technologies. The loss of dye can be minimised for all the dyes by proper selection of the dyeing parameters in both dyeing procedures. Also, in such cases, the concentrations of the components in the wastewater must not exceed the prescribed limits. Relative optimum between the fixed dye content and the dye and chemical concentration in the wastewater might be calculated so that the maximum in the fixed dye content may not be optimal in all the cases. The directive is the lowest cost.

5   REFERENCES

1. http://europa.eu/ Accessed: 2016-04-25
2. Nagy H.J., Rusznák I., Sallay P., Víg A.: Journal of Hungarian Chemists 63(4), 116-121, 2008
3. Nagy H.J., Kristály E., Lele I., Lele M., Gere P., Rusznák I., Sallay P., Víg A.: Journal of Hungarian Chemists 69(3), 70-73, 2014
4. CLARIANT dyes - Internal reports 2010
5. Nagy H.J., Őrsi K., Orbánné Á, Tóth Á., Rusznák I., Sallay P., Víg A.: Hungarian Textile Technology 1, 16-23, 2011

REDUCTION OF THE AMOUNT OF UNFIXED DISPERSE DYES IN WASTEWATER BY COMPLEXATION WITH CUCURBITURILS

H. J. Nagy, M. L. Varga, Á. Orbán, I. Rusznák, P. Sallay and A. Víg

Department of Organic Chemistry and Technology, BME, Budafoki 8, H-1111 Budapest, Hungary
hnagy@mail.bme.hu

Abstract: *Two cucurbiturils [6] and [8] as well as randomly-methylated β-cyclodextrin (RAMEB) have been applied for reducing the originally generated disperse dye concentration in wastewater. Three disperse dyes (C.I. Disperse Orange 30, C.I Disperse Red 60 and C.I. Disperse Yellow 42) have been the studied ones. Prior to complexation the disperse dyes by cucurbituril, the dyes had been dissolved in aqueous solution of RAMEB. When cucurbiturils (CU[6] or CU[8]) were added to the aqueous solution of disperse dye-RAMEB complex, competition occurred between the two "hosts" (RAMEB and CU) for the dyes. It can be concluded that in efficiency of complexing disperse dyes, both cucurbiturils were more efficient than RAMEB and CU[8] has been markedly more efficient than CU[6].*

1   INTRODUCTION

Chemical wastewater treatments have been performed by means of cucurbiturils. Cucurbiturils are macrocyclic molecules made of glycoluril ($=C_4H_2N_4O_2=$) monomers linked by methylene-bridges ($-CH_2-$), forming a partly enclosed cavity [1]. The name is derived from the resemblance of this molecule with a pumpkin of the family of Cucurbitaceae (Figure 1).


a)   Cucurbitaceae   b)   Cucurbituril
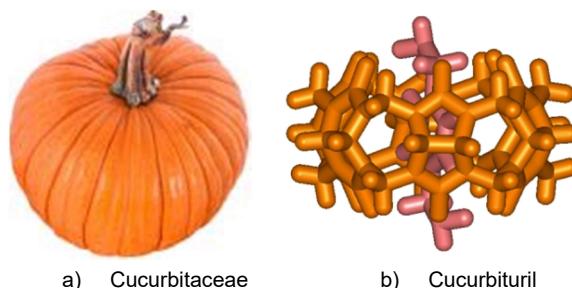
Figure 1 Name and structure of cucurbiturils

2   MATERIALS AND METHODS

2.1   Inclusion complex forming compounds

We have been working with randomly-methylated β-cyclodextrin (RAMEB) which was a generous gift of Cyclolab (Budapest, Hungary) to us (Figure 2). Cucurbiturils have been synthesized by Buschman's [2] and Behrend's [3] methods (Figure 3).

2.2   Disperse dyes

Three disperse dyes have been studied by us from which *FORON* Yellow has been the product of CLARIANT and *SIRIUS* Orange and *SIRIUS* Red

were BAYER AG's products (Table 1). The interaction of the mentioned dyes with cyclodextrins had not yet been published by any researchers so far. The competitive complexation of randomly-methylated β-cyclodextrin (RAMEB) (Figure 2) and cucurbit[6]uril or cucurbit[8]uril (CU[6] or CU[8])) (Figure 3) has first been elaborated by us.
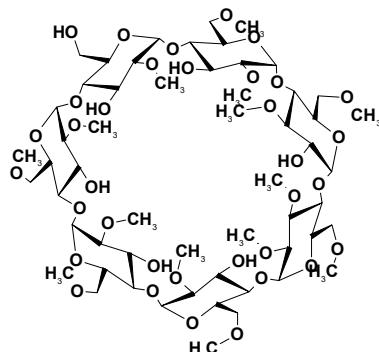

**Figure 2** RAMEB (diameter of cavity: 0.6-0.65nm [2])
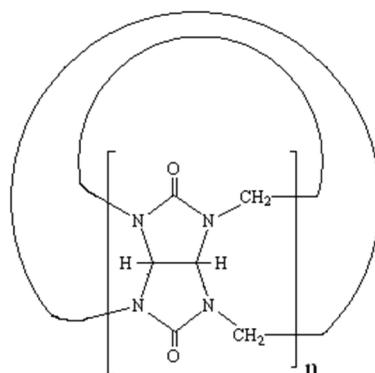
Figure 3 Cucurbituril (CU[6] n=6, CU[8] n=8) (diameter of cavities are: CU[6]: 0.39 nm and CU[8]: 0.69 nm [4, 5])

Table1 Disperse dyes

Number of dyes	Name of dyes	C.I. name/ C.I. constitution number	Structure	Group of dyes		Molar mass [g/mol]
				According to structure	According to application	
1	**Disperse orange**	*C.I. Disperse Orange 30 / 11119*		monoazo	disperse	379
2	**Disperse yellow**	*C.I. Disperse Yellow 42 / 10338*		mononitro	disperse	324
3	**Disperse red**	*C.I. Disperse Red 60 / 60756*		anthraquinoid	disperse	331

C.I. - Color Index

2.3 Competitive complexation between cyclodextrin and cucurbiturils

The three above-mentioned disperse dyes practically insoluble in water could, however, be dissolved with the help of inclusion complex forming RAMEB. The concentration of the aqueous RAMEB solution was $(2.3*10^{-2}$ mol/dm^3) and those of the RAMEB assisted dye solutions were (C.I. Disperse Orange 30 $(1.44*10^{-3}$ mol/dm^3), C.I. Disperse Yellow 42 $(3.94*10^{-4}$ mol/dm^3) C.I. Disperse Red 60 $(1.33*10^{-4}$ mol/dm^3) [11]. Into 50% of the discussed three dye solutions, 10^{-4} mol/dm^3 CU[6] has been mixed, and the same concentration of CU[8], to the other 50%. The produced dispersions were separately stirred for 4 days at room temperature. The suspensions were filtered thereafter, and the concentrations of the obtained assisted dye solutions were measured by UV-VIS spectrophotometry [6, 7].

3 RESULTS AND DISCUSSION

What happened actually? Competition for complex formation with the dye occurred between RAMEB and CU[6] and CU[8], respectively [13]. The actual goal was to remove the highest amount of the polluting dye from the wastewater with cucurbituril. In this respect, CU[8] was much more efficient than CU[6]. CU[6] removed 16% of the red, 30% of the orange and 49% of the yellow polluting dyes, whereas the efficiency of the CU[8] was higher, thus 60% removal of red, 61% of the orange and 79% of the yellow dye occurred (Figure 4).
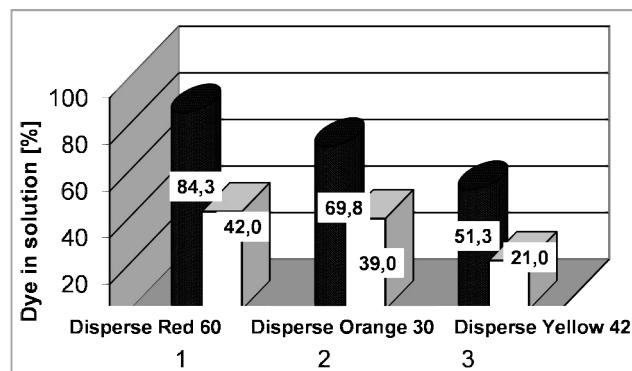
Figure 4 One by one proportion of the three studied dissolved disperse dyes after their complexation for 4 days by CU[6] (red) and CU[8] (blue), respectively

4 CONCLUSIONS

When cucurbiturils (CU[6] or CU[8]) were added to the aqueous solution of disperse dye-RAMEB complex, there was a competition between the two hosts (RAMEB and CU) for the dyes.

It can be concluded that in complexing disperse dyes, CU[8] was markedly more efficient than CU[6]. The efficiency of complex formation sensitively depends also on the structure of the CU and those of the disperse dyes (Figures 2 and 3, Table 1).

5   REFERENCES

1. Karcher S., Kornmüller A., Jekel M.: Water Research 35, 3309-3316, 2001

2. Buschmann H.J.; Schollmeyer E.: Journal of Inclusion Phenomena 29, 167-174, 1997

3. Behrend R.; Meyer E.; Rusche F.: Liebigs Annalen Chemie 339, 1-137, 1905

4. Lagona J., Mukhopadhyay P., Chakrabarti S., Isaacs L.: Angewandte Chemie Int. Ed. 44, 4844-4870, 2005

5. Assaf K.I., Nau W.M.: Chemical Society Reviews 44, 394-418, 2015

6. Nagy H.J., CD News 23(9), 1-9, 2009

7. Nagy H.J., Rusznák I., Sallay P., Víg A.: Hungarian Textile Technology 5, 143-144, 2007

8. Nagy H.J., Sallay P., Varga M.L., Rusznák I., Bakó P.: Textile Research Journal 79(14), 1312-1318, 2009

COMPARATIVE STUDY OF DYEING PERFORMANCE OF SOYBEAN FIBRE AND WOOL

A. K Patra[1] and Astha[2]

[1]*The Technological Institute of Textile & Sciences, Bhiwani 127021, India*
[2]*Panipat Institute of Engineering and Technology, Panipat 132102, India*
arunkpatra@rediffmail.com

Abstract: *In the present work, dyeability of soybean fibre is studied using four different classes of dyes, namely acid dyes, metal complex dyes, vinylsulphones and bromoacrylamide reactive dyes. In each class, three different dyes of red, blue and yellow colours were used and the dyeing with each of them was carried out in shades ranging from light to heavy dark. Identical experiments were also carried out on wool fibre for comparative purposes, both being protein fibres although differing in source and composition of amino acids. The results were evaluated in terms of % exhaustion, K/S and % fixation. The exhaustion values were calculated by measuring the optical densities of the bath while the % fixation was determined based on colour strength of substrate at relevant stages. Both wash and light fastness were studied for all the dyes. Further, process optimization was done for dyeing with metal complex dye using Box-Behnken design of experiments. The dyeing results for soybean fibre were quite satisfactory, particularly with 1:2 metal complex dyes and Lanasol reactive dyes under acidic conditions. The regenerated protein fibre showed comparable dyeing behavior and wash fastness as that of wool with these two dye classes.*

Key Words: *absorbance, colour strength, exhaustion, fixation, soybean*

1 INTRODUCTION

In last two decades, many new fibres came into existence, but only a few could become commercially successful. The idea behind the innovations has mainly revolved around economy, ecology and special properties. Soybean fibre is one such fibre which, although claimed to have been investigated in the 1930s, got first commercially launched in 2003. In fact, China is the first country to achieve production of the fibre on industrial scale. It is a regenerated protein fibre and in some ways can substitute the expensive natural protein fibres like wool and silk. This 21st century fibre, other than being eco-friendly, has special attributes like biodegradability, non-allergenic, microbiocidal and anti-ageing properties. Moreover, it has softness and featheriness of cashmere and silk-like lustre and is marketed as 'artificial cashmere', 'vegetable cashmere' and 'soy silk'.

The fibre often referred to as soya fibre is obtained by wet-spinning process. The raw material for the fibre is available as a byproduct of large scale food production and is a renewable, sustainable resource. Soybean fibre contains as many as 18-20 amino acids similar to those found in wool and silk although the proportions are different. The main components are glutamic acid (23.7%), aspartic acid (13.0%) and leucine (9.2%) [1, 2].

The moisture absorption and air permeability of soya fibre are superior to those of silk and many synthetic fibres while its heat insulation properties are similar to those of cotton [1]. The fibre has bacterial resistance to *Staphylococcus aureus*, *Coli bacillus* and *Candica albicans* [3]. Soybean fibre resistance to golden and yellow *Staphylococcus aureus* is more than 5.8 and hence it is an inherently anti-bacterial fibre [4, 5].

Use of polyvinyl alcohol (PVA) during the manufacture process adds strength and acceptable wearability characteristics to the fibre [6]. From the chemical constitution point of view, soya fibre may have chemical processability similar to that of wool and silk. To evaluate its dyeing behaviour, a detailed study using dyes of different classes has been carried out in the present study. The dyeability has been compared with that of wool by applying dyes under identical conditions. The best of the options is chosen based on the colour build up and fastness properties. This is then further optimized using design of experiments.

2 EXPERIMENTAL

2.1 Materials

Soybean protein fibre of 13.19 µ diameter, 1.5 D fineness and 38 mm staple length was used. Grey wool fibre of diameter 20.5 µ and 70 mm staple length was taken for comparative study with the former. Three dyes from each of the four classes of dyes were used to evaluate the dyeability of the two protein fibres.

Table 1 List of dyes used

Acid dyes	Metal complex dyes	Vinylsulphone dyes	Bromoacrylamide reactive dyes
Lanaset Red G	Metalan Scarlet SLP	RemazolBrillliant Red P-5B	Lanasol Red 6G
Lanaset Yellow 2R	Metalan Yellow S-2GLP	RemazolBrillliant Yellow 3GL	Lanasol Yellow 4G
Lanaset Blue 2R	Metalan Navy Blue S-DNLIP	RemazolBrillliant Blue BB	Lanasol Blue 3G

Acid dyes and bromoacrylamide based reactives (Lanasol dyes) were procured from Huntsman India, while the 1:2 metal complex dyes from Atul Limited was used and the vinyl sulphone dyes applied were from Dystar. The dyes are listed in Table 1. All the chemicals used for pretreatment and dyeing were of L R grade while the auxiliaries such as non-ionic detergent (Lissapol D) and leveling agents (Albegal Set from Huntsman and Uniperol SE from BASF) were of industrial grade. All the dyeing trials were carried out in the lab scale IR dyeing machine.

2.2 Preparatory process

The soybean fibre was scoured with 2 g/L soda ash and 2 g/L non-ionic detergent at 90°C for 60 min. It was then thoroughly washed. Oxidative alkaline bleaching was done with 15 mL/L hydrogen peroxide, 4 g/L Stabilizer AWNI at pH 10 and temperature 90°C for 60 min. The pH was finally brought to neutral with acetic acid. Similar scouring and bleaching treatment was given to wool as well but at the temperature of 50°C.

2.3 Dyeing procedure

The dyeing with acid dyes was carried out as per the standard dyeing procedure. The temperature of the dyebath was set to 50°C. The fibre samples were treated with 10% Na_2SO_4 and pH maintained at 4.5-5 using acetic acid. The dyebath temperature was slowly raised to 98°C and held at that temperature for 60 min. When the dyeing was completed, the samples were taken out, rinsed, soaped, washed under running water and dried at room temperature.

In case of metal complex dyes, the dye bath was set to 40°C with salt and 1% Uniperol SE. The rest remains the same as for acid dyes. For the Lanasol reactive dyes, the dye bath was set to 50°C with 5% Glauber's salt and 1% Albegal B to promote surface levelness. The pH of the bath was maintained in the acidic range at about 4.5 using acetic acid. The temperature of the bath was then gradually raised to 98°C and dyeing was carried out for 60 min. The dyeing was followed by usual washing and soaping. For Remazols, the dyeing of protein fibres was carried out as per recommended procedure of the supplier. Soaping in all the cases was done by treating with 2 g/L non-ionic detergent for 20 min at 70-80°C.

2.4 Testing and evaluation

The percentage exhaustion %E (percentage of dye absorbed or chemically bound to the fibre) was measured by finding the optical density of the dyebath before commencing the dyeing and after completing the dyeing. The absorbance value of a dye liquor sample was measured at its wavelength of maximum absorbance using Perkin Elmer UV/VIS spectrophotometer (Lambda 25) and exhaustion % of dye was calculated by:

$$\%E = \left[\frac{A_0 - A_1}{A_0} \right] \times 100 \qquad (1)$$

where: A_0 − optical density of dye solution before dyeing, A_1 − optical density of residual dye solution after dyeing.

The dye fixation % was further determined by measuring the colour strength (K/S) of the dyed samples before and after soaping. The formula used was:

$$\%F = (K/S_1)/(K/S_0) \times 100 \qquad (2)$$

where: K/S_1 - colour strength of dyed sample after soaping, K/S_0 - colour strength of dyed sample before soaping.

The K/S values were determined by Computer Colour Matching system of Premier colour scan SS-5101A.

Then the total dye fixation %T referring to the dye chemically bound to the substrate relative to the dye applied was calculated by the following equation:

$$\%T = \frac{\%E \times \%F}{100} \qquad (3)$$

where: %E is exhaustion percentage of dye and %F is fixation percentage of the dye. This value is, however, shown for samples of the experimental design only.

The washing fastness of the samples was measured by ISO 2 method and light fastness in SDL-237 light fastness tester. A few selected samples were tested by FTIR (Fourier Transform Infra-Red) spectroscopy where the peaks were obtained by Attenuated Total Reflection (ATR). Bruker table top model spectrophotometer with ZnSe crystal was used for the measurement.

3 RESULTS AND DISCUSSION

3.1 Dyeing performance in terms of colour strength

The *K/S* values in Table 2 show good colour depth in soybean fibre with both Lanaset acid dyes and Metalan 1:2 metal complex dyes. The colour build up with increase in percentage shade is also quite satisfactory and similar in all the three dyes of the same class of dyes. In fact, the build-up appears to be better in metal-complex dyes than acid dyes, which may be attributed to better linkages with substrate in the former than the latter. In case of wool, the colour strength is much higher compared to soybean irrespective of colour, percentage shade and class of dyes. This is of course due to the greater number of reaction sites in wool as the amino acid content is quite high. However, the depth obtained in soybean fibre as observed visually is reasonably good and hence can be used.

As regards dyeing with the reactive dyes taken, the sulpho-group containing Lanasol dyes appear to give good colour effect on soybean fibre. These dyes contain bromoacrylamide reactive groups which are capable of forming covalent bonds with the nucleophilic groups of the amino acids in the protein fibre. This is the cause of retention of the dyes in the substrate and hence a good dyeability. The vinylsulphone based reactives, however, showed lesser depth except for Remazol Brilliant Yellow 3GL, where the *K/S* values are good for all percentage shades, as is evident from Table 2. The colour strengths in all cases were higher in wool compared to soybean for reasons already cited.

3.2 Exhaustion and fixation

The acid and metal complex dyes showed very good exhaustion on the regenerated protein fibre

(Table 3). The % exhaustion, however, gradually decreased with the increase in % shade, although even at 6% shade, the exhaustion levels are quite appreciable. The corresponding fixation levels are also found to be quite good, as the dye moved from dye bath onto the substrate has better chances of fixation. The terminal amino groups present in the fibre offer the chance for ionic linkage with the dye anion and hence the fixation. But since the amino acid content is lower in the soy fibre compared to that in wool, the fixation is comparatively lower in soybean. The fixation of metal complex dye is better than acid dyes, on the regenerated protein fibre.

When dyed with reactives, there is a clear difference in exhaustion levels between Remazol and Lanasol dyes, particularly at higher percentage shades (Table 4). The vinyl sulphone based dyes did not exhaust well onto the substrate as the dye bath concentration increased. Between the two types of reactives, Lansol is definitely the preferred one due to high exhaustion and subsequent fixation. Although both the dyes gave lower colour yield on soybean compared to wool, the bromoacrylamide based Lanasol reactive dyes appear to be quite suitable for soybean fibre.

3.3 Fastness properties

The wash fastness of the three acid dyes on soya fibre was found to be quite good up to 2% shade while it was around 3 at 4% and 6% shade. The fastness to washing, as shown in Table 5, was still better in case of metal complex dyes irrespective of colour and shade percentage. The fastness ratings in reactives were all acceptable while the wash fastness for all the dyes on wool was similar to soybean fibre or, in some cases, even better. The light fastness ratings were 4 or above for all the samples tested.

Table 2 Colour strength of dyed samples

Fibre	Shade [%]	*K/S* values											
		Acid dyes			1:2 Metal complex dyes			Vinylsulphone reactive dyes			Bromoacrylamide reactive dyes		
		Red	Yellow	Blue	Scarlet	Yellow	N.Blue	Red	Yellow	Blue	Red	Yellow	Blue
Soybean	0.5	2.50	1.50	1.50	1.30	1.76	1.16	0.48	1.68	0.68	1.33	1.76	0.945
	1	3.96	3.18	2.43	2.99	3.50	3.06	1.04	2.37	1.12	2.85	2.74	1.21
	2	7.0	6.0	4.70	11.0	10.0	9.50	2.65	5.2	1.73	5.24	4.10	3.75
	4	10.11	9.52	9.22	16.4	14.63	12.86	4.51	7.15	5.03	9.21	7.0	6.28
	6	14.5	13.5	13.3	18.91	17.89	18.53	8.60	9.53	6.91	10.61	8.04	9.43
Wool	0.5	6.20	5.0	4.96	6.0	7.85	5.80	4.0	3.57	4.0	6.0	5.80	5.0
	1	9.63	12.01	10.63	12.0	11.49	10.71	8.50	8.70	7.70	10.66	10.90	10.5
	2	21.0	21.07	18.60	25.0	18.5	19.5	13.6	13.0	12.52	17.88	17.05	17.0
	4	23.4	23.92	21.75	28.4	26.45	23.55	23.21	18.0	17.82	24.39	21.83	22.63
	6	29.0	28.07	23.47	30.24	30.0	28.0	26.25	22.22	19.08	31.81	28.52	25.0

Table 3 Exhaustion and fixation values for acid and metal complex dyes

Fibre	Shade [%]	Acid Dyes						1:2 Metal Complex Dyes					
		Lanaset Red G		Lanaset Yellow 2R		Lanaset Blue 2R		Metalan Scarlet		Metalan Yellow		Metalan Blue	
		Exh%	Fix%	Exh%	Fix%	Exh%	Fix%	Exh%	Fix%	Exh%	Fix%	Exh%	Fix%
Soybean	0.5	90.00	86.20	98.65	76.21	90.00	81.96	90.00	90.27	88.00	91.91	78.33	96.96
	1	88.67	86.08	95.00	78.51	85.00	79.15	89.00	89.25	81.66	91.62	74.00	93.86
	2	97.00	80.89	87.32	75.94	84.28	78.59	86.84	88.00	81.00	87.87	74.00	92.41
	4	91.17	82.16	89.09	74.37	77.50	76.19	86.95	86.31	83.63	86.05	81.17	89.24
	6	92.00	77.54	81.33	71.42	70.76	76.00	85.71	85.95	82.72	83.91	71.76	87.32
Wool	0.5	95.00	91.17	99.23	86.20	95.00	87.78	90.00	95.84	90.00	93.11	90.00	95.08
	1	94.33	90.84	97.50	85.80	85.00	84.36	90.00	95.23	90.00	91.90	82.00	96.48
	2	98.00	84.67	90.14	83.34	88.57	84.54	88.42	94.33	88.00	90.24	86.00	93.97
	4	95.88	84.47	93.63	84.13	80.00	79.93	88.69	87.41	82.27	90.11	85.88	86.90
	6	95.50	83.28	88.66	82.55	79.23	78.23	85.71	84.04	80.58	89.28	82.35	86.41

Table 4 Exhaustion and fixation values for reactive dyes

Fibre	Shade [%]	Vinylsulphone Dyes						Lanasol Reactive Dyes					
		Ramazol Bril Red P5B		Ramazol Brilliant Yellow 3GL		Ramazol Brilliant Blue BB		Lanasol Red 6G		Lanasol Yellow 4G		Lanasol Blue 3G	
		Exh%	Fix%	Exh%	Fix%	Exh%	Fix%	Exh%	Fix%	Exh%	Fix%	Exh%	Fix%
Soybean	0.5	90.00	58.53	65.00	84.00	75.00	64.15	97.50	89.26	81.42	84.61	95.00	58.33
	1	86.66	47.92	57.50	81.72	37.50	69.20	96.66	84.56	77.14	88.96	88.00	53.77
	2	54.54	49.81	57.14	76.13	31.57	67.87	93.75	70.24	50.00	65.70	87.50	57.69
	4	44.44	42.74	64.70	71.50	25.00	60.82	89.28	61.70	50.00	59.27	77.14	54.27
	6	15.00	56.46	14.28	71.97	20.00	60.70	88.23	54.55	27.27	41.20	65.71	50.64
Wool	0.5	90.00	90.49	90.00	97.80	85.00	95.01	87.50	92.30	84.28	88.01	95.00	89.44
	1	91.66	89.12	85.00	96.45	85.00	93.10	83.33	89.86	81.42	89.34	94.00	88.01
	2	95.45	86.07	84.28	83.33	87.50	91.72	81.25	87.86	83.33	85.25	90.00	84.39
	4	94.44	81.15	82.94	78.26	68.42	85.10	82.85	85.27	81.00	87.30	78.57	80.02
	6	90.00	80.57	81.25	74.81	666.66	84.61	84.70	85.75	76.36	86.63	71.42	80.85

Table 5 Wash fastness of samples dyed with different dyes

Fibre	Shade [%]	Wash fastness rating											
		Acid dyes			1:2 Metal complex dyes			Vinylsulphone reactive dyes			Bromoacrylamide reactive dyes		
		Red	Yellow	Blue	Scarlet	Yellow	N.Blue	Red	Yellow	Blue	Red	Yellow	Blue
Soybean	0.5	3-4	3-4	4-5	4-5	4-5	4	4	4	4-5	4	4-5	4
	1	3-4	3-4	4	4	3-4	4	3-4	4	4	4	4	4
	2	3-4	3-4	3-4	3-4	3-4	4	4	3-4	4	3-4	4	3-4
	4	2-3	3	3	3-4	3-4	4	3-4	4	3-4	3-4	3-4	4
	6	3	3	3	3-4	3-4	3-4	3-4	3-4	3-4	3	3-4	3-4
Wool	0.5	4-5	4-5	4-5	4-5	4-5	4-5	4-5	4-5	4-5	4-5	4-5	4-5
	1	4	4	4-5	4-5	4-5	4-5	4	4	4-5	4-5	4-5	4-5
	2	4	4-5	4-5	4-5	4	4-5	4	4	4-5	4	4	4
	4	4	4	4	4	4-5	4	3-4	4	4	4	4-5	4-5
	6	3-4	4	4	4	4	3-4	3-4	4	4	4	4	4

3.4 FTIR Spectra

IR spectra of soybean fibre dyed in 6% shade with metalan scarlet SLP, Lanaset Red G, Remazol Brilliant Red P-5B and Lanasol Red 6G dyes were tested. However, no significant changes in peaks were observed for these dyed samples except a very little variation in peak intensities at places shown in Figure 1. This indicates that no major changes in functional groups or strength properties have occurred in the fibres after the preparatory process and subsequent coloration carried out.
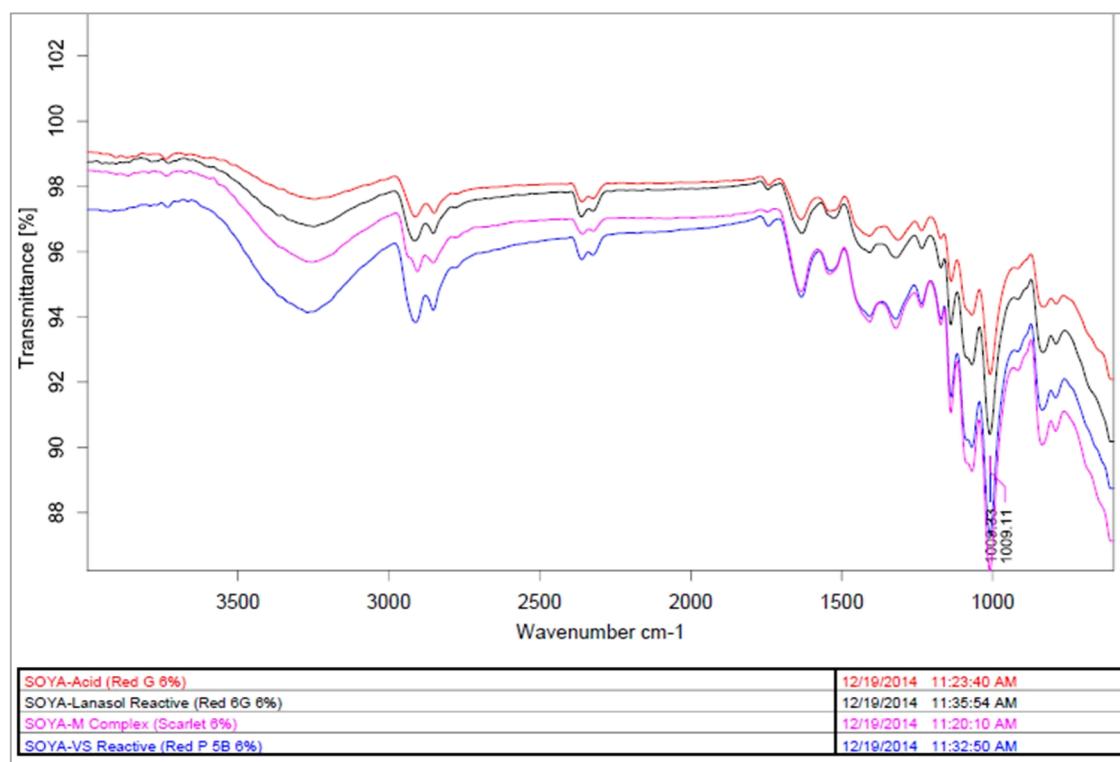
Figure 1 FTIR Spectra of Soybean fibre dyed with different classes of dyes

3.5 Design of Experiments

To study the individual interactive effects of concentration of levelling agents, pH and time of treatment, Box-Behnken factorial design was used. These three variables were chosen because they were supposed to potentially affect the dyeing process. Tables 6 and 7 list the coded values of these independent variables.

Table 6 Variables with coded levels

Variable	Coded Level		
	-1	*0*	*+1*
Levelling Agent [%]	0.5	1	1.5
pH	4	5.5	7
Time [min]	40	60	80

Colour strength (*K/S*), Exhaustion %, Fixation % obtained in treatment were taken as the response factors. Metal complex dyes being the best among all the dye classes attempted, Metalan Scarlet SLP was chosen for the study and applied at 2% shade.

The results obtained for the 15 samples dyed according to Box Behnken experimental design are given in Table 8.

Table 7 Experimental design based on coded levels

| Sample No.	Levelling Agent [%]	pH	Time [min]
E1	-1	-1	0
E2	1	-1	0
E3	-1	1	0
E4	1	1	0
E5	-1	0	-1
E6	1	0	-1
E7	-1	0	1
E8	1	0	1
E9	0	-1	-1
E10	0	1	-1
E11	0	-1	1
E12	0	1	1
E13	0	0	0
E14	0	0	0
E15	0	0	0

Regression analysis was carried out to assess the effect of independent variables on the measured responses. Using the best fit equations, contour plot diagrams were plotted to see the effect. The regression equation obtained for K/S of dyed soybean fibre is:

$$K/S = 9.657 + 0.254 \times Levelling\ agent - 2415 \times pH + 0.864 \times Time - 1.670 \times (Levelling\ agent)^2 -$$
$$-0.187 \times (pH)^2 - 1.510 \times (Time)^2 + 0 \times Levelling\ agent \times pH + 0.475 \times pH \times Time -$$
$$-0.273 \times Levelling\ agent \times Time \qquad (4)$$

Table 8 Results of experimental design

Sample No.	Levelling Agent [%]	pH	Time [min]	K/S Value	Exhaustion [%]	Fixation [%]	Total Dye Fixation [%]
E1	0.5	4	60	24.48	96.31	90.46	87.12
E2	1.5	4	60	24.87	96.31	95.20	91.68
E3	0.5	7	60	15.23	43.85	89.07	39.05
E4	1.5	7	60	19.66	54.38	83.03	45.15
E5	0.5	5.5	40	18.52	49.81	96.54	48.08
E6	1.5	5.5	40	16.84	57.89	94.01	54.42
E7	0.5	5.5	80	22.05	82.29	95.16	78.30
E8	1.5	5.5	80	24.00	73.68	92.56	68.19
E9	1	4	40	25.40	97.89	96.96	94.91
E10	1	7	40	14.34	29.81	86.39	25.75
E11	1	4	80	26.80	98.24	98.46	96.72
E12	1	7	80	21.45	65.26	89.49	58.40
E13	1	5.5	60	25.78	91.57	93.95	86.03
E14	1	5.5	60	24.67	89.47	92.33	82.60
E15	1	5.5	60	24.26	92.10	92.85	85.51

The correlation coefficient between the experimental values and the calculated values obtained from the equation is 0.996, while the standard error is as low as 0.354. This shows that the experimental data and the calculated values are in agreement with each other. According to the analysis of variance, F ratio is 63.512 and p-value 0.00, illustrating that the model is extremely significant. The contour plot generated (shown in Figure 2) indicates the optimum K/S value for levelling agent of 0.9-1% and a dyeing time of 60 min.
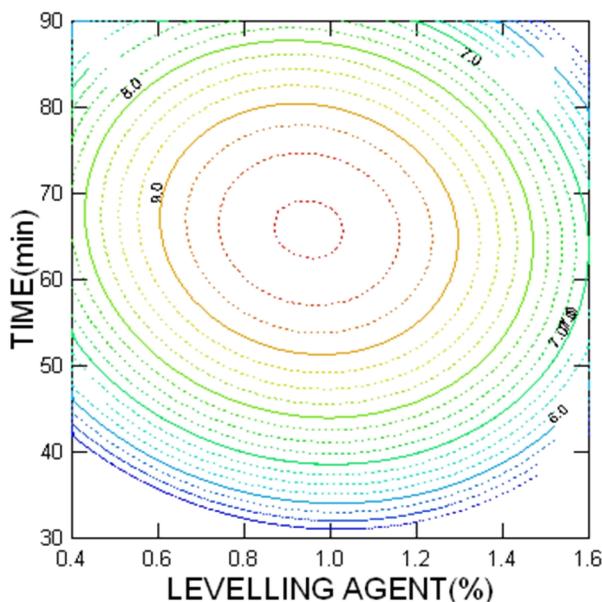
Figure 2 Contour plot of K/S vs. levelling agent [%], time [min]

As regards pH, higher dye uptake appears to happen in medium to strong acidic pH with 1% levelling agent (Figure 3). The trend can be attributed to higher substantivity of soybean fibre at low pH values. The disulphonated 1:2 metal complex dye is supposed to have higher exhaustion than a mono-sulphonated one, due to the extra sulphonic acid group in the dye molecule.
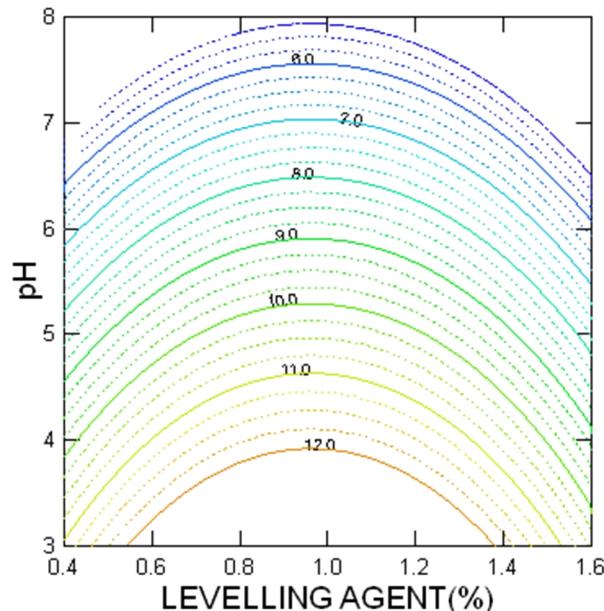
Figure 3 Contour plot of K/S vs. levelling agent [%], pH

This could be the reason for high affinity of Metalan Scarlet SLP towards the regenerated protein fibre. Adequate amount of levelling agent set promotes even exhaustion by slowing down the rate at which the dye moves towards substrate. The effect of pH and time of dyeing on K/S value of soybean fibre, shown in Figure 4, although not indicating an absolute optimized value, shows a trend favouring acidic conditions, with reasonably good colour yield in pH range of 4-5-5.
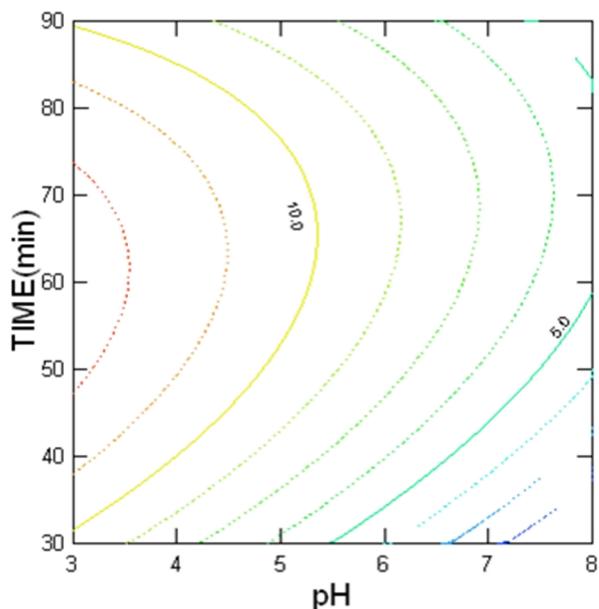
Figure 4 Contour plot of *K/S* vs. pH, time [min]

4   CONCLUSIONS

The soybean fibre under study has a good dyeability with metal complex dyes, acid dyes, bromoacrylamide based reactives and vinyl sulphones, in that order. Although the exhaustion and subsequent fixation of dyes on substrate is reasonably good in the majority of cases, the final colour yield is lower compared to that in wool. The wash and light fastness properties do not appear to be a matter of concern.

The regenerated fibre does not undergo any significant change in the wet pretreatment and coloration processes and hence is not supposed to lose strength, as observed from FTIR studies.

Application of Metalan Scarlet SLP, using design of experiments, shows 1% levelling agent, 60 min dyeing time in a pH range of 4-5.5 to be an adequate condition for dyeing soybean fibre.

5   REFERENCES

1. Chi J., Kang M. and Yoon C.: Dyeing properties of soya fibre with reactive and acid dyes, *Coloration Technology* 121(2), 81-85, 2005

2. Roy S.D., Sen A. and Gulrajani M.L.: Dyeing behavior of soybean fobre with acid dyes, *Colourage* 59(9), 37-42, 2012

3. http://swicofil.com/soybeanproteinfiberproperties.html, (Nov 2014)

4. Mathur M. and Hira M.: Special fibres – I: Soybean Protein Fibre, *Man-made Textiles in India* 47(10), 365-369, 2004

5. Mahapatra N.N.: Processing soybean fibre in textile industries, *Colourage* 55(3), 68-76, 2008

6. http://intechopen.com, Soybean Fibre: A novel fibre in the Textile Industry (Dec 2014)

OPTICAL PROPERTIES OF PHOTOCHROMIC PIGMENT INCORPORATED INTO POLYPROPYLENE FILAMENTS

A. P. Periyasamy, M. Viková and M. Vik

Faculty of Textile Engineering, Technical University of Liberec, Czech Republic
martina.vikova@tul.cz

Abstract: *This paper reviews the impact of different concentrations of photochromic pigment as well as different drawing ratios with respect to the optical properties of multifilament. Temperature variation may induce very significant and different effects on the behavior of the photochromic system, so there is a special device such as LCAM FOTOCHROM available in LCAM – TUL which helps us to measure various optical properties like kinetics of the growth and decay. The results are showing there is a significant change in the optical properties of polypropylene fibers with respect to drawing ratio.*

Key Words: *photochromism, colorimetry, functional dyes, smart fabrics, polypropylene*

1   INTRODUCTION

Photochromism denotes a reversible color change upon exposure to light [1-3]. Photochromic materials have received extensive attention since they are applicable to photoactive media, such as optical storage, optical switches, sensors, smart windows, and so forth [4-14].During the 1950's, Hirschberg suggested the term of photochromism (which comes from Greek words *phos,* meaning light, and *chroma,* meaning color) for the color changing materials [15, 16]. Photochromism is defined by IUPAC as a "Light-induced reversible change of color", the reversible color changing by the exposure to electromagnetic radiation (mainly UV irradiation) [1, 2, 17-20]. Generally, photoproducts absorb at shorter wavelengths than their precursor. This is termed negative photochromism; the photochromic mechanism is illustrated in Figure 1 [21].
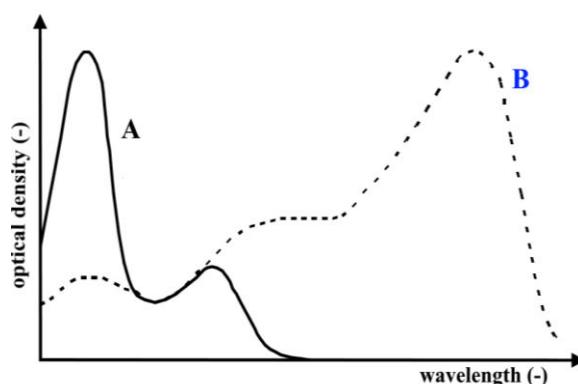

Figure 1   Reaction   scheme   and   UV-VIS spectra of a photochromic compound [36]

Chromic materials are classified in several types, of which photochromic and thermochromic materials are popular due to their wide scope [18]. Typical photochromic compounds and their color changing reactions are illustrated in Scheme 1. There are huge differences between photochromism and thermochromism: in photochromism, the color change is normally associated with electromagnetic radiation, whereas heat is responsible for change of color in thermochromism [22]. Therefore, the presence of light alone is not sufficient to induce a photochemical reaction; the light must also have the correct wavelength to be absorbed by the reactant species. The reversible change of a single chemical species between two states having distinguishably different absorption spectra can be induced in at least one direction by electromagnetic radiation [3, 18, 23-25] and furthermore, these two forms may differ in many other physical properties such as their redox potential [16, 26], fluorescent intensity, dipole moment [27, 28], molecular shape etc.

A more common scenario is that the initial photochromic species absorbs in the UV range and upon photolysis produces a colored photoproduct absorbing in the visible region of the spectrum (positive photochromism) [29, 30], and the process involves interconversion of a single molecule between two chemically distinct forms [31-35]. The activating radiation generally is in the UV region (300 to 400 nm) but could be in the visible (400 to 700 nm) [10, 32, 33].

Generally, photochromic compounds are photochemically stable in terms of absorption of radiation, but become thermodynamically metastable in state B from which they revert back to (reversible color changing) A by the absorption of electromagnetic radiation or thermal energy (Eq. 1).

$$A \underset{h\nu_2 \text{ or } \Delta T}{\overset{h\nu_1}{\rightleftarrows}} B \qquad (1)$$

Closed form   Open form (merocyanine)
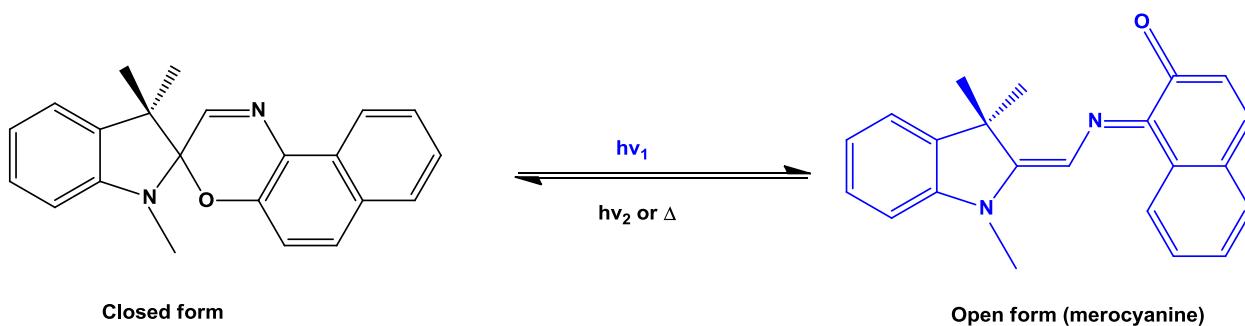
Scheme 1 Photochromic (heterolytic cleavage/photocyclization) reaction of spirooxazines [1]

Basic characteristics which are required for the photochromic materials are given below [15]:

a) Light sensitivity

b) Spontaneous reversibility (and)

c) Color changes.

The B state should be moderately stable;

a. Also B should absorb radiation in different region of the spectrum than A, and;

b. The change of $B \rightarrow A$ should occur either thermally or by exposure to electro-magnetic radiation.

Polypropylene (PP) is a polymer, which is a member of the 'polyolefin' (polymers produced from alkenes) family. It is a highly versatile material that has many beneficial physical properties. Polypropylene provides superior qualities and is the most versatile and cost effective fiber (polymer) in comparison with other thermo-forming and polyolefin materials. It has good impact strength, surface hardness, excellent abrasion resistance and resistance to a wide variety of acids, alkali and solvent solutions with a temperature range up to 93°C. For this present research work, we have produced photochromic pigment incorporated in PP multi-filaments by using four different concentrations of photochromic pigment. The filaments were produced at four drawing ratios. The main goal of this study was to find the relationship between concentration of photochromic pigments & drawing ratio with respect to the optical properties of polypropylene filaments [37-46].

2   EXPERIMENTAL PROCEDURE

The photochromic pigments incorporated in polypropylene multifilament were produced by laboratory melt spinning machine and the process parameters are illustrated in the Table 1. The produced samples are shown in Figure 2. The photochromic pigment was mechanically mixed with polypropylene granulate (chips) and the mixture added in the hopper of the extruder of the melt spinning machine. After production, the filaments were carried over for the drawing process due to inferior mechanical behavior of the proto-filaments. The drawing process was carried out at

different ratios, the process parameters for the drawing process are given in Table 2.

Figure 2 Samples of photochromic polypropylene multifilament

Table 1 Various parameters which were used in melt spinning

Polypropylene	Metallocene Polypropylene PP HM 562 R
Temperature of melt spinning	220°C
Photochromic pigment	5-Chloro-1,3-dihydro-1,3,3-trimethylspiro[2*H*-indole-2,3′-(3*H*)naphth[2,1-*b*](1,4)oxazine]
Pigment concentration in fiber	0; 0.25; 0.5; 1.5; 2.5 % (on weight basis)
Drawing temperature (T_d)	120°C
Melt flow index	26.6 g/10 min
Number of holes in spinneret	13

Table 2 Drawing ratio and concentration of photochromic pigments

Sample	Composition	Drawing ratio λ			
1	PP 562 R	2	2.5	3	3.5
2	PP 562 R + 0.25% Blue	2	2.5	3	3.5
3	PP 562 R + 0.5% Blue	2	2.5	3	3.5
4	PP 562 R + 1.5% Blue	2	2.5	3	3.2
5	PP 562 R + 2.5% Blue	2	2.5	3	3.2

After the drawing process, the multifilament's optical properties were analyzed – they were determined by using the unique spectrophotometer FOTOCHROM LCAM (often commercial spectrophotometers have limitations in finding out

optical properties of photochromic materials, due to color changing properties) which was developed by LCAM Team at the Technical University of Liberec. The scheme and picture of the instrument are shown in Figures 3 and 4, respectively. The color-measuring instrument (spectrophotometer) determines the *K/S* value of a given filament through Kubelka-Munk equation (Eq.2) [47, 48].

$$\frac{K}{S} = \frac{(1-R)^2}{2R} \qquad (2)$$

where *R* - reflectance percentage, *K* - absorption and *S* - scattering of dyes.

This unique spectrophotometer is able to measure the kinetics of color changes in exposed photochromic samples when the change is visible by the use of Kubelka-Munk function for the concentration of photochromic pigment and the drawing ratio in time. Temperature variation may induce very significant and different effects on the behavior of the photochromic system, constant temperature (20°C ± 2°C) was kept for all the samples.

3   RESULTS & DISCUSSION

The results are shown in Figures 5 to 9 and they clearly explain the relationship between Kubelka-Munk function with respect to the drawing ratio along with the concentration of photochromic pigment. It has clearly shown that increasing of drawing ratio decreases the Kubelka-Munk value.
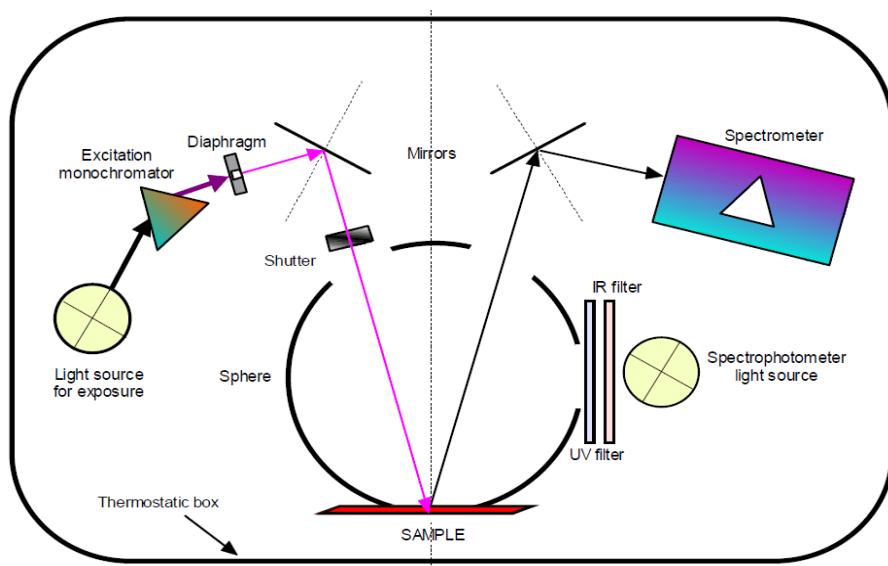

Figure 3 Scheme of LCAM FOTOCHROM

**Figure 4** Picture of LCAM FOTOCHROM
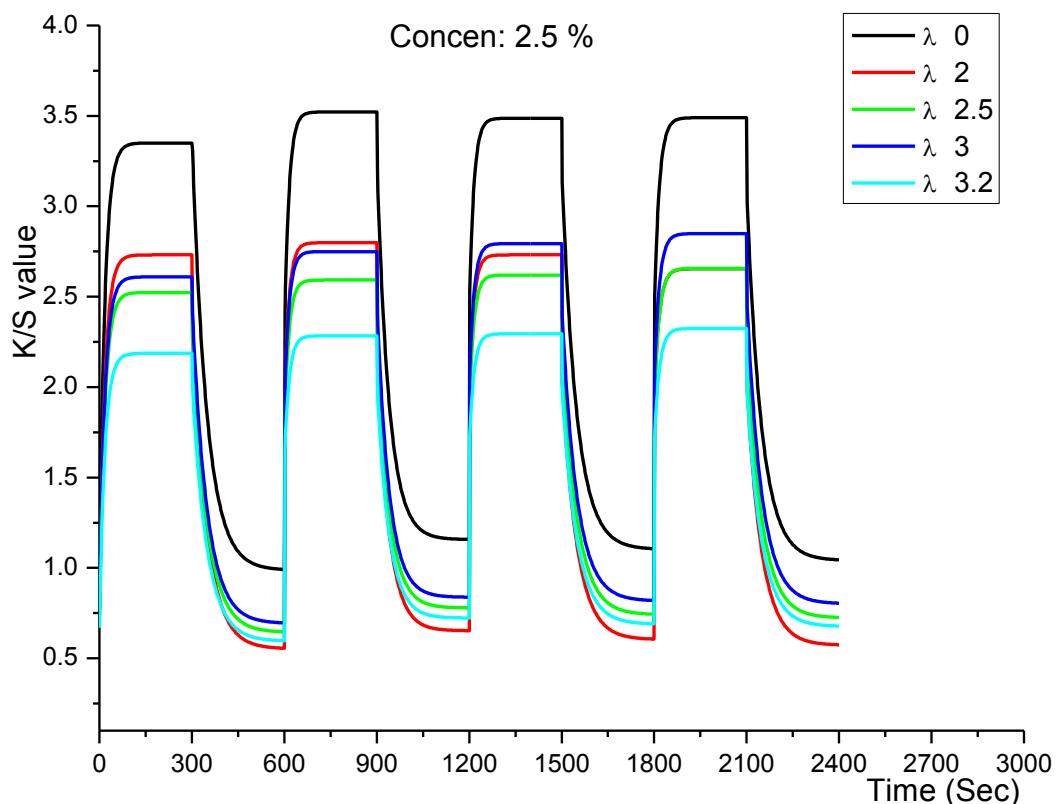
Figure 5 Impact of drawing ratios on optical properties of photochromic filaments
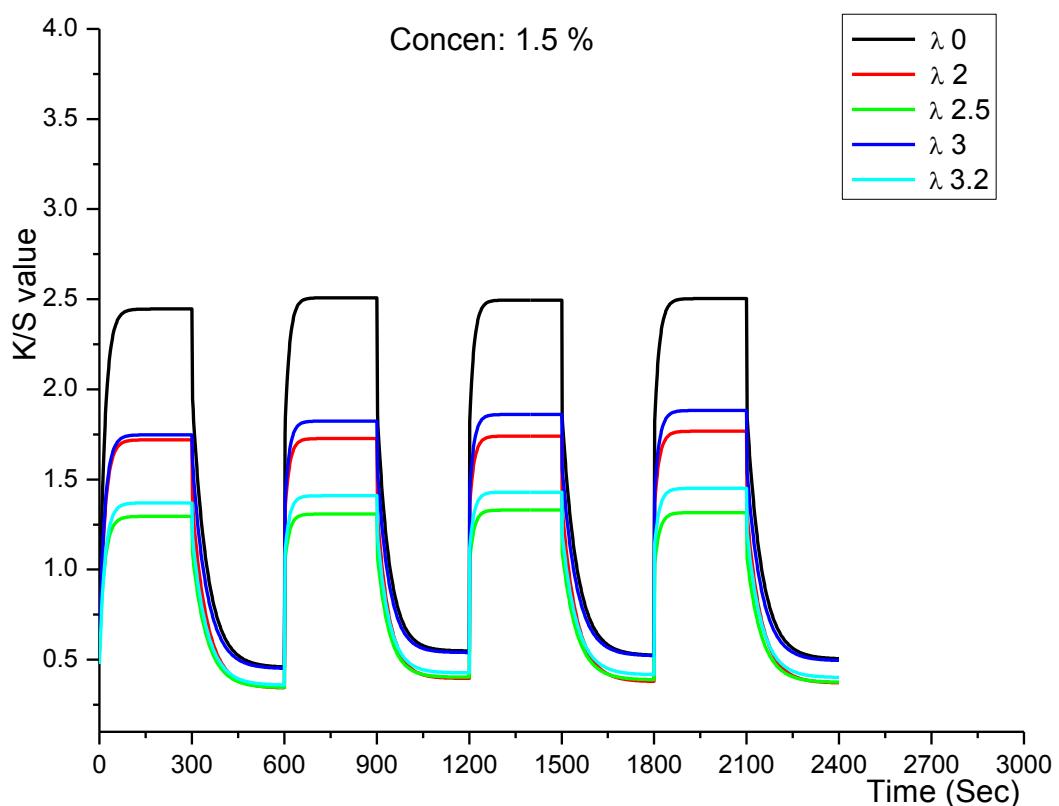

Figure 6 Impact of drawing ratios on optical properties of photochromic filaments
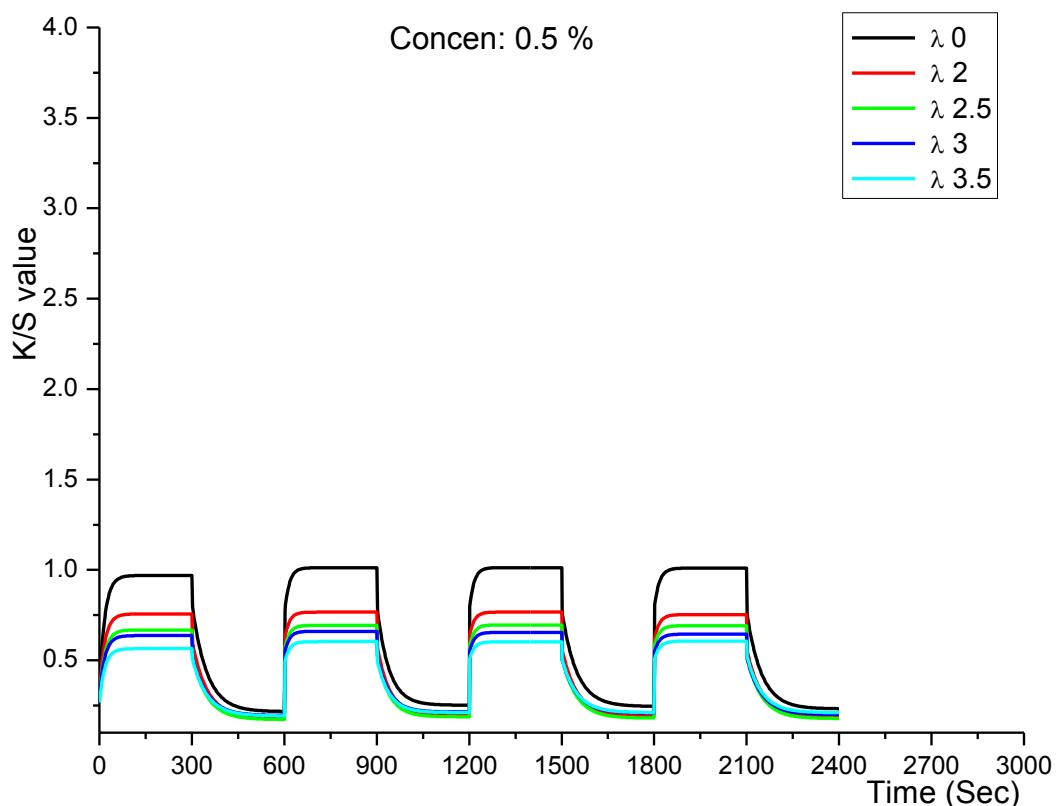
**Figure 7** Impact of drawing ratios on optical properties of photochromic filaments
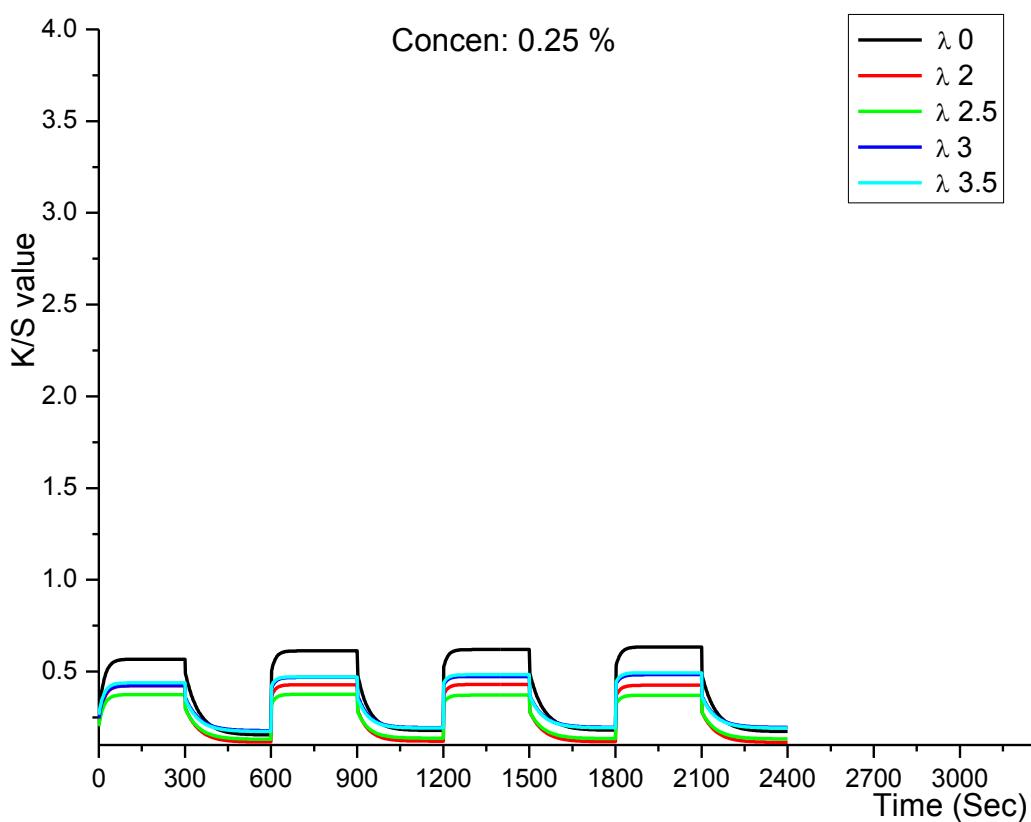
Figure 8 Impact of drawing ratios on optical properties of photochromic filaments
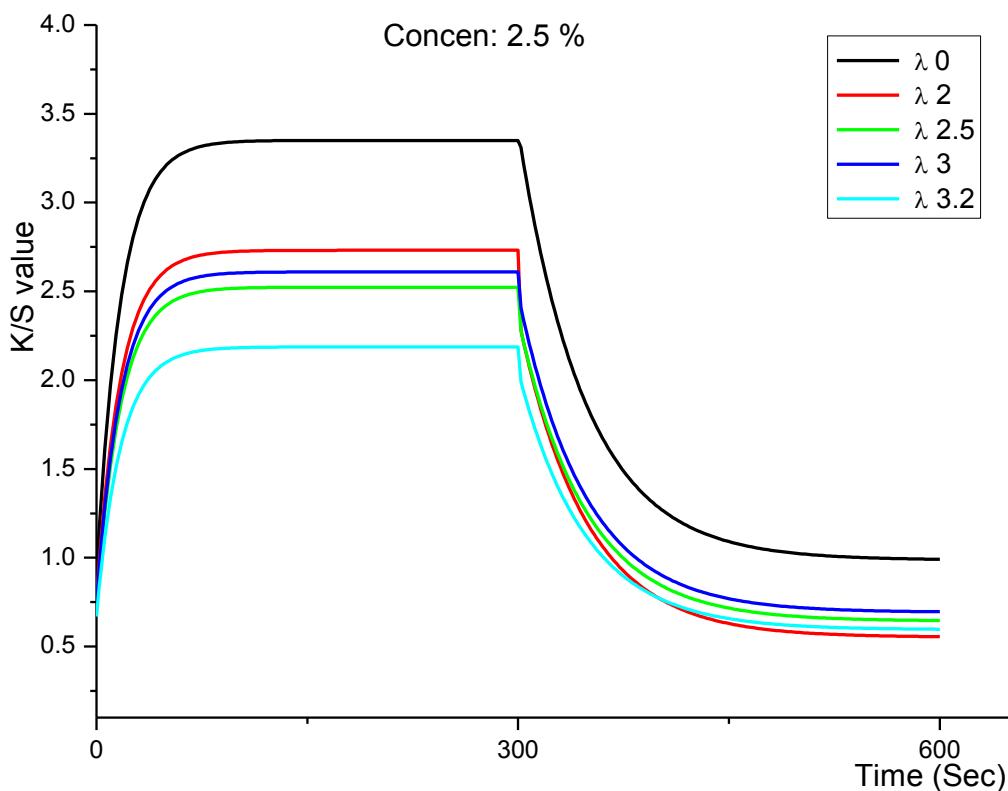
Figure 9 Dependence of K/S function on time – growth and decay phase of photochromic change for different drawing ratios λ while concentration of pigment is 2.5%
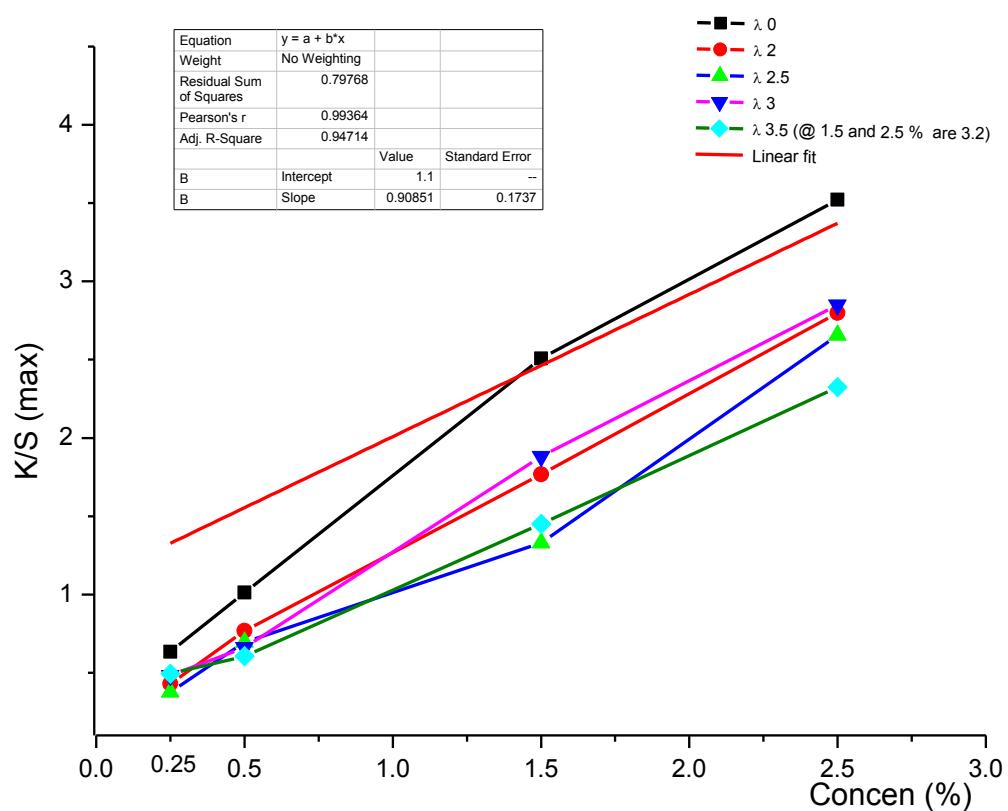

Figure 10 Dependence of the maximum K/S function of photochromic change for different drawing ratios λ and different concentrations

This situation can be described as the effect of the attenuating of multifilament and the reduction of fineness and the concentration of photochromic pigment in the mass of used polypropylene polymer. The transformations of Kubelka-Munk function maximum value with respect to the drawing ratio as well as concentration are shown in Figure 10.

4   CONCLUSION

This research work describes the dependence of K/S values on concentrations of photochromic pigment and various drawing ratios. From this work, we conclude the following points:

- Increasing the drawing ratio decreases the K/S values.
- Even though at the same concentration different K/S values are observed for different drawing ratios, it seems there is a huge impact on K/S values with respect to drawing ratio.

5   REFERENCES

1. Crano JC, Robert J. Guglielmetti: Organic Photochromic and Thermochromic Compounds Volume 1: Main Photochromic Families. vol. 1. New York, USA: Kluwer Academic Publishers, New York, USA; 1999. doi:10.1007/b115590

2. Crano JC, Robert J. Guglielmetti: Organic Photochromic and Thermochromic Compounds Volume 2: Physicochemical Studies, Biological Applications, and Thermochromism. vol. 2. First. Kluwer Academic Publishers, New York, USA; 1999

3. Christie RM.: Advances in dyes and colourants. In: M. L. Gulrajani, editor. Adv. Dye. Finish. Tech. Text., 1-37, 2013

4. Pan G., Wei J., Zhu A., Ming Y., Fan M., Yao S.: Photochromic properties and reaction mechanism of naphthopyran, Sci China Ser B Chem 44, 276-82, 2001, doi:10.1007/BF02879618

5. Little A.F., Christie R.M.: Textile applications of photochromic dyes. Part 3: Factors affecting the technical performance of textiles screen-printed with commercial photochromic dyes, Color Technol 127, 275-81, 2011,doi:10.1111/j.1478-4408.2011.00307.x

6. Smith G.P.: Photochromic Glasses : Properties and Applications, J Mater Sci 2, 139-52, 1967

7. Janus K., Sworakowski J., Luboch E.: Kinetics of photochromic reactions in a 10-membered dibenzoazo crown ether, Chem Phys 285, 47-54, 2002, doi:10.1016/S0301-0104(02)00688-2

8. Sakamoto R., Nishihara H.: 8.22 - Electrochromic and Photochromic Properties. In: Poeppelmeier JR, editor. Compr. Inorg. Chem. {II} (Second Ed. Second Edi, Amsterdam: Elsevier, 919-67, 2013, doi:http://dx.doi.org/10.1016/B978-0-08-097774-4.00814-7

9. Nigel Corns S., Partington S.M., Towns A.D.: Industrial organic photochromic dyes, Color Technol 125, 249-61, 2009, doi:10.1111/j.1478-4408.2009.00204.x

10. Chowdhury M.A., Joshi M., Butola B.S.: Photochromic and Thermochromic Colorants in Textile Applications, J Eng Fiber Fabr 9, 2014

11. Matharu A.S., Ramanujam P.S.: Photochromic Polymers for Optical Data Storage: Azobenzenes and Photodimers, In: Allen NS, editor. Handb. Photochem. Photophysics Polym. Mater., John Wiley & Sons, Ltd, USA, 209-34, 2010

12. Żmija J., Małachowski M.J.: New organic photochromic materials and selected applications, Journal of Achievements in Materials and Manufacturing Eng. 41(2), 48-56, 2010

13. Tian H., Yang S.: Recent progresses on diarylethene based photochromic switches, Chem Soc Rev 33, 2004, pp. 85–97, doi:10.1039/B302356G

14. Vikova M., Vik M.: The determination of absorbance and scattering coefficients for photochromic composition with the application of the black and white background method, Text Res J 85, 1961-71, 2015, doi:10.1177/0040517515578332

15. Rawat M.S.M., Mal S., Singh P.: Photochromism in Anils - A Review, Open Chem J 2, 7-19, 2015

16. He T., Yao J.: Photochromism in composite and hybrid materials based on transition-metal oxides and polyoxometalates, Prog Mater Sci 51, 810-79, 2006, doi:10.1016/j.pmatsci.2005.12.001

17. Dürr H., Bouas-Laurent H. (Ed.): Photochromism: Molecules and systems, Revised Edition, Elsevier Oxford, UK, 2003, doi:10.1007/s13398-014-0173-7.2

18. Bamfield P., Hutchings M.G.: Chromic Phenomena Technological Applications of Colour Chemistry, Second Edition, The Royal Society of Chemistry, UK; 2010, doi:10.1039/9781849731034

19. Dorion G.H., Canaan N., Loeffler K.O., Conn N.: Photochromic cellulose paper, synthetic paper and regenerated cellulose, US Patent 3314795, 1967

20. Muller A. (Ed.): Smart materials in architecture, interior architecture and design, Berlin: Birkhauser-Publishers for Architecture (Part of Springer Science), 2013

21. Pardo R., Zayat M., Levy D.: Photochromic organic–inorganic hybrid materials, Chem Soc Rev 40, 672, 2011, doi:10.1039/c0cs00065e

22. White M.A., Bourque A.: Colorant, Thermochromic, Encycl. Color Sci. Technol., Luo R. (Ed.), Springer New York, 1-12, 2014, doi:10.1007/978-3-642-27851-8_165-5

23. Addington M., Schodek D.: Smart Materials and New Technologies - For architecture and design professions, Elsevier Ltd, Amsterdam, NL; 2005

24. Chapman R.: Technologies and materials, Dev. Smart Fabr., Chapman R. (Ed.), Rav Lally, Pira International Ltd Cleeve Road, Leatherhead Surrey kt22 7ru UK, 1-82, 2006

25. Robert R. Mather: Intelligent textiles, Rev Prog Color 31, 36-41, 2001

26. Irie M., Yokoyama Y., Seki T. (Ed.): New Frontiers in Photochromism, Springer International Publishing; 2013, doi:10.1007/978-4-431-54291-9

27. Hadjoudis E.: Photochromic and Thermochromic Anits, Mol Eng 5, 301-37, 1995

28. El'tsov A.V.: Organic Photochromes, translated from Russsian, Consultants Bureau, New York; 1990, doi: 10.1007/978-1-4615-8585-5

29. Vikova M., Vik M.: The determination of absorbance and scattering coefficients for photochromic composition with the application of the black and white background method, Text. Res. J. 85, 1961-71, 2015, doi:10.1177/0040517515578332

30. Vikova M., Vik M.: Description of photochromic textile properties in selected color spaces, Text. Res. J. 85, 609-20, 2015, doi:10.1177/0040517514549988

31. Pardo R., Zayat M., Levy D.: Photochromic organic-inorganic hybrid materials, Chem Soc Rev 40, 672-87, 2011, doi:10.1039/c0cs00065e

32. Vikova M., Vik M.: Alternative UV Sensors Based on Color-Changeable Pigments, Adv Chem Eng Sci 01, 224-30, 2011, doi:10.4236/aces.2011.14032

33. Bouas-Laurent H., Dürr H.: Organic photochromism (IUPAC Technical Report), Pure Appl Chem 73, 639-65, 2001, doi:10.1351/pac200173040639

34. Żmija J., Małachowski M.J.: New organic photochromic materials and selected applications, Journal of Achievements in Materials and Manufacturing Eng. 41(2), 48-56, 2010

35. Shibaev V., Bobrovsky A., Boiko N.: Photoactive liquid crystalline polymer systems with light-controllable structure and optical properties, Prog Polym Sci 28, 729-836, 2003, doi:10.1016/S0079-6700(02)00086-2

36. Frick M.: Photochrome Textilien - Herstellung und Eigenschaften, Universität Stuttgart, Germany, 2008

37. Wypych G.: (PP) polypropylene, Handb. Polym. (2nd Edition), Wypych G, (Ed.), ChemTec Publishing, 497-504, 2016, doi:http://dx.doi.org/10.1016/B978-1-895198-92-8.50156-7

38. Yan Y.: Developments in fibers for technical nonwovens, Adv. Tech. Nonwovens, Kellie G. (Ed.), Woodhead Publishing, 19-96, 2016, doi:http://dx.doi.org/10.1016/B978-0-08-100575-0.00002-4

39. Crangle A.: Types of polyolefin fibres, Polyolefin Fibres: Industrial and Medical App., Ugbolue S.C.O. (Ed.), Woodhead Publishing, 3-34, 2009, doi:http://dx.doi.org/10.1533/9781845695552.1.3

40. Mather R.R.: The structural and chemical properties of polyolefin fibres Polyolefin Fibres: Industrial and Medical App., Ugbolue S.C.O. (Ed.), Woodhead Publishing, 35-56, 2009, doi:http://dx.doi.org/10.1533/9781845695552.1.35

41. Shamey R.: Improving the colouration/dyeability of polyolefin fibres, Polyolefin Fibres: Industrial and Medical App., Ugbolue S.C.O. (Ed.), Woodhead Publishing, 363-97, 2009, doi:http://dx.doi.org/10.1533/9781845695552.2.363

42. Richaud E., Verdu J., Fayolle B.: Tensile properties of polypropylene fibres, Handb. Tensile Prop. Text. Tech. Fibres, Bunsell A.R. (Ed.), Woodhead Publishing, 315-31, 2009, doi:http://dx.doi.org/10.1533/9781845696801.2.315

43. Mather R.R.: The structure of polyolefin fibres, Handb. Text. Fibre Struct. Vol. 1, Eichhorn S.J., Hearle J.W.S., Jaffe M., et al. (Ed.), Woodhead Publishing, 276-304, 2009, doi:http://dx.doi.org/10.1533/9781845696504.2.276

44. Kotek R., Afshari M., Harbison V., Gupta A.: Production methods for polyolefin fibers, Polyolefin Fibres: Industrial and Medical App., Ugbolue S.C.O. (Ed.), Woodhead Publishing, 185-261, 2009, doi:http://dx.doi.org/10.1533/9781845695552.2.185

45. Gownder M.: Properties of Syndiotactic Polypropylene Fibers Produced from Melt Spinning, Met. Technol. Commer. Appl., Benedikt G.M. (Ed.), William Andrew Publishing, Norwich, NY, 167-75, 1999, doi:http://dx.doi.org/10.1016/B978-188420776-1.50023-5

46. Maier R.D., Bidell W., Shamiri A.: Polypropylene: Gas-Phase Polymerization and Reactor Blends, Reference Module in Mater. Sci.and Mater. Eng., Elsevier; 2016, doi:http://dx.doi.org/10.1016/B978-0-12-803581-8.03757-7

47. Viková M., Christie R.M., Vik M.: A Unique Device for Measurement of Photochromic, Res J Text Appar 18, 6-14, 2014

48. Viková M., Vik M.: Colorimetric Properties of Photochromic Textiles, Appl Mech Mater 440, 260-5, 2014, www.scientific.net/AMM.440.260, doi:10.4028

NANOMATERIALS AND INNOVATIVE TECHNOLOGIES IN TEXTILE INDUSTRY

D. Rástočná Illová, J. Šesták and Ľ. Balogová

VÚTCH-CHEMITEX, spol. s r.o., Rybníky 954, 011 68 Žilina, Slovak Republic
rastocna-illova@vutch.sk

Abstract: *Researchers from the Research Institute for Textile Chemistry (VÚTCH)-CHEMITEX, spol. s r.o. in Žilina, Slovak Republic have been engaged successfully in innovative technology, namely in application of nanotechnologies in finishing textile materials, for several years already. They prepared and evaluated the application of several types of nanosol solutions, e.g. hydrophobic and hydrophilic nanosol, electroconductive and antimicrobial nanosol in the frame of an intensive industrial research. Results from application of sol-gel technology in the development of various nanosol types and their application in nanostructuring of textile surfaces are presented. Carbon nanoparticles were used, among others, to obtain positive change of electroconductive properties of textile materials. Results from the original research (protected by a patent application) concerning preparation of multifunctional fabric with a digital camouflage print, hydrophobic, self-cleaning and antimicrobial nanofinish and reduced flammability are presented in a further part of the paper. The results present a high level of innovation in an assortment of fabrics designed for special protective clothing. Application of special fibre types in construction of the textile material in combination with nanostructural modification of the textile surface can increase added value of the fabric. Achieving a multifunctional effect based on synergic effect causing change of functional parameters and performance characteristics of the fabrics can increase the level of innovation of the textile materials. Knowledge and results from the evaluation of an innovative technology for finishing textile materials using low-temperature plasma generated by DCSBD (Diffuse Coplanar Surface Barrier Discharge) under atmospheric pressure are presented in the final part of the paper. Research works performed in the field of application of low-temperature plasma in the process of dyeing textile materials focused mainly on the enhancement of dye yield on the dyed textile material and the enhancement of dye affinity to textile substrate with a subsequent reduction of waste water pollution. Results and knowledge presented in the paper are a contribution to the application of innovative technologies (nanotechnology, plasma application) and nanoproducts (nanosols) with the aim to increase added value of the textile materials.*

Key Words: *nanosols, multifunctional fabric, low-temperature plasma*

1 INTRODUCTION

At present, nanotechnologies as a high-tech trend of development increasingly find application also in such traditional segments as textile and clothing industry. Nanostructuring of textile surface and/or incorporation of additives into fibres using nanoparticles of various types enable to achieve essential change of functional properties and performance characteristics of fibres and textile materials. The above-mentioned ways enable to achieve a change of hydrophobic or hydrophilic properties of textile materials, reduce formation of electrostatic charge, increase resistance to ignition and burning, increase resistance to micro-organisms, or to achieve even a multifunctional effect of these properties by a suitable combination of nanoparticles on fibre surface and in fibre mass. An advantage is a fact that nanostructuring of textile surface and/or incorporating of additives into fibres using nanoparticles does not change physico-mechanical characteristics and/or typical textile properties of the materials e.g. dyeability, hand, drape etc.

Development of textile materials interconnected with research in the field of microsystems, nanotechnologies, information processing and communication technologies enabled miniaturization and non-invasive smart monitoring of human physiological functions using so-called „smart" materials and „intelligent" fabrics [1, 2]. The ongoing and progressing multidisciplinar research in the field of textile fibres, special yarns, biomedical textile sensors, wireless and mobile telecommunication integrated with telemedicine leads up to the development of smart biomedical clothing today [1].

The innovative technologies include also the activation of polymeric material surface using low-temperature plasma under atmospheric pressure, which is increasingly popular [3]. Plasma is conductive gas with atoms more or less ionized to positive and negative ions, electrons, excited and metastable particles as well as neutral particles [4]. Generation of non-steady plasma produces ions at low temperature and electrons with sufficient energy for the distortion of chemical bonds

in material surface layer which are in contact with the generated non-steady plasma. Distortion of chemical bonds in the surface layer of a material initializes formation of radicals and, subsequently, functional groups, and thereby physical and chemical changes of the material surface. Surface modification using plasma does not require application of water or chemical substances and therefore it is a low-cost and eco-friendly process. A great advantage of the plasma finishing processes is the reduction of contaminating substances and, this way, also saving costs spent on waste water treatment, therefore it is also an eco-friendly technology [5].

2 EXPERIMENTAL, RESULTS, DISCUSSION AND CONCLUSIONS

2.1 Nanotechnologies for application in textiles

An appropriate application of nanotechnologies on textile materials is the application of solutions, so-called nanosols, for surface nanostructuring, during which a net structure is created on textile surface, imparting desired changed properties.

So-called sol-gel technology is used to prepare nanosol solutions. A suitable additive is incorporated into a prepared solution and polycondensation reaction is induced by thermal effect and/or UV radiation for the purpose of xerogel formation and its subsequent cross-linking on the surface.

One possibility of nanosol preparation by means of sol-gel reactions is the preparation of inorganic-organic complexes using organosilanes which can be, after subsequent incorporation of carbon nanotubes (CNTs), used as nanosols with enhanced electroconductive properties. Modification (functionalization) of the carbon nanotubes is performed in dispersion medium by the means of compounds containing functional groups.

Unique physical and chemical properties of carbon materials and mainly CNTs, such as high mobility of charge carriers, high working temperature and thermal conductivity, impact strength, biocompatibility, low dielectric constant, radiation resistance, chemical inactivity and possibility to concentrate high output on a small area are the motivation for a research spreading the possibilities of their application to different fields. We used sol-gel method including the process of acidic co-hydrolysis of organosiloxane precursors to prepare nanosols. Basic precursors were TEOS (triethoxysilane) and VTES (vinyltriethoxysilane). In order to achieve better dispergation of CNTs in nanosol solution, sonication, i.e. action of ultrasound on nanosol solution, was used in the course of its preparation as well as in the course of its application on a textile material. Basic

electroconductive nanosol EVN2-TEG type was prepared after optimization of the nanosol preparation process and time of sonication. We worked with the nanosol in our further experiments. Sonication was also used in subsequent application of the prepared electroconductive solution on the selected fabric type with various selected times of ultrasound action on fabric immersed in the nanosol solution in order to ensure homogeneous dispergation of electroconductive nano- and/or microparticles on the fabric surface.

Application of CNTs in electroconductive nanosols

Basic experiment focused on the determination of the optimal concentration of content of selected CNTs type in nanosol and sonication time (CNTs dispergation) in the nanosol solution. Basic concentrations were selected as follows: 1.5, 3.0 and 5.0 g/L CNTs U type (USA origin) or G type (Greek origin). Following times of nanosol solution sonication were selected: 15, 30, 45 and 60 min. Conditions determined after performing a number of experiments in the field of preparation of EVN nanosols with various content of CNTs U and G type and after assessment of optimal time of applying ultrasound during CNTs dispergation in the nanosol in order to achieve homogeneous and stable nanosol solution (min. 24 hours stability) were as follows:

- concentration 3 g/L CNTs of selected type;
- time of nanosol solution sonication: 30 min;
- CNTs type: G – more homogeneous structure of the solution and deposit on the fabric was achieved.

After that, we started to investigate the influence of time factor on EVN nanosol sonication during its application on selected fabrics made of 100% PES, 100% cotton (ba) and blend of PES/cotton (PES/ba) fibres. Besides, values of electric surface resistance were measured on the fabrics using the instrument Teraohmmeter EO 03 type. Determined values of electric surface resistance of the standard unfinished fabrics were as follows:

a. fabric from 100% PES fibres: $4.80.10^{10}$ Ω;
b. fabric from 100% cotton: $2.35.10^{12}$ Ω;
c. fabric from PES/cotton (50/50) blend: $1.18.10^{12}$ Ω.

Usage of electroconductive carbon black in electroconductive nanosols for their application on fabrics

Optimal concentration of Timrex KS 44 additive in EVN2-TEG nanosol 10 g/L, 12.5 g/L and 15 g/L was determined in the frame of further experiments. Standard time of sonication for the preparation of the nanosol was 30 min. Then, the influence of time factor during nanosol application in time: 5, 15, 45 and 60 min was observed.
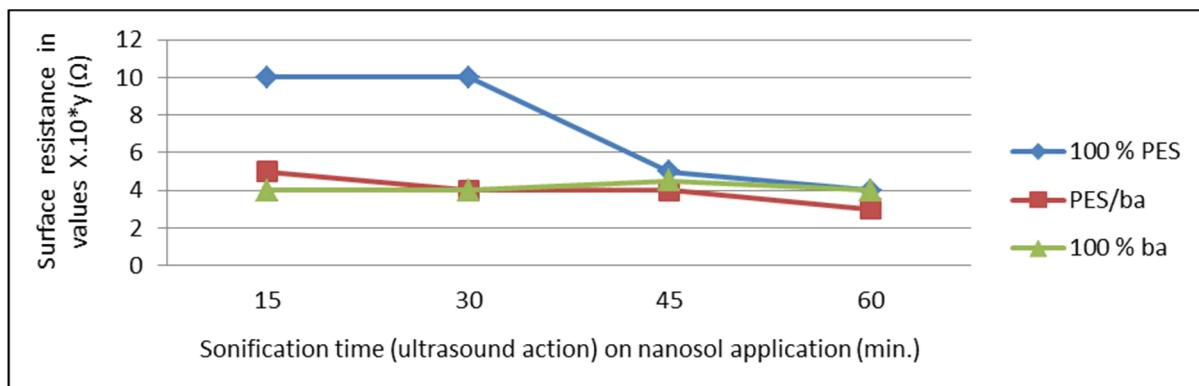
Graph 1 Surface resistance of textile fabrics after application of EVN2-TEG nanosol containing 3 g/L CNT U type
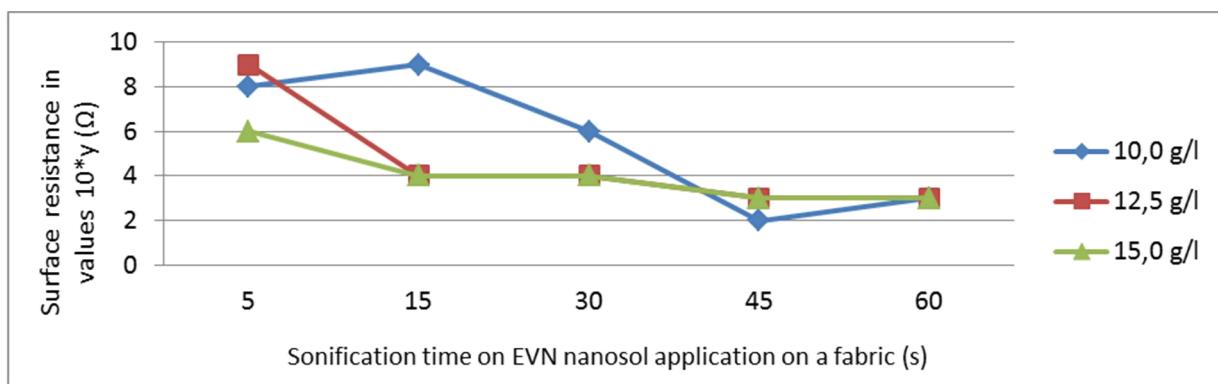
Graph 2 Relation between surface resistance and sonication time and concentration of Timrex KS 44 additive on PES/cotton blend
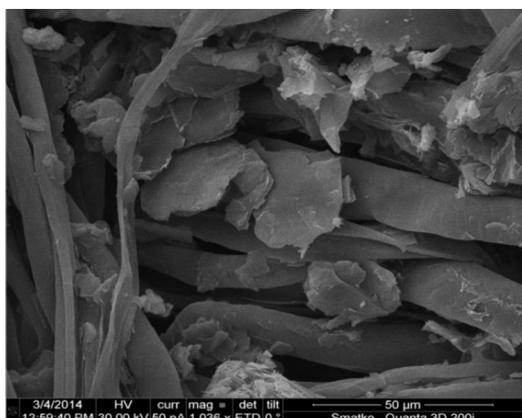

Figure 1 Surface macrostructure of 100 % cotton fabric finished with nanosol containing electroconductive carbon black
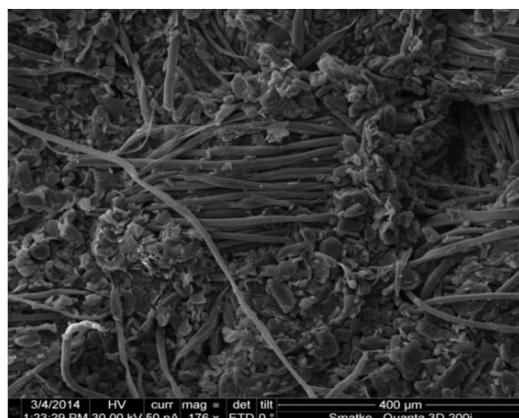

Figure 2 Surface macrostructure of PES/cotton fabric after application of electroconductive nanosol containing electroconductive carbon black

It can be stated on the base of the achieved results that fabrics made of 100% cotton or PES/cotton blend show very low surface resistance from 10^2-10^3 Ω already with the concentration of 12.5 g/L, optimally with the concentration of 15 g/L Timrex KS 44 additive. On the other hand, application of nanosol with Timrex KS 44 additive on synthetic fabrics made of 100% PES and/or 100% PP showed unsatisfactory level of surface resistance; it was by 5 to 6 orders higher.

Conclusion to nanotechnologies

The achieved results confirm the feasibility of preparation of electroconductive nanosols based on organosilanes after incorporation of additives with CNTs and/or electroconductive microparticles. Besides, examination of their application on selected types of fabrics made of 100% PES, PES/cotton and 100% cotton fibres also confirmed the feasibility of the application of this electroconductive finish on technical fabrics,

e.g. electroconductive membranes for industrial dumping sites, electroconductive layer for electrotechnical industry etc. Application of sol-gel technology in preparation of nanosols based on inorganic compounds, organosilanes, is a great benefit from the environmental viewpoint compared to organic compounds used nowadays which may present a risk for human health.

2.2 Multifunctional fabrics

Research in the field of application of progressive finishes based on nanotechnologies focused also on innovation of assortment of special protective clothing, arising from a need to ensure maximal protection of life and health of a soldier by the enhancement of qualitative and functional properties of his combat clothing. Enhancement of added value of the textile materials with functional nanostructural surface modification was achieved due to a an innovative solution based on a principal change of material composition of a standard range of textile materials (PES/cotton/Lycra, and/or 100% cotton) used up to now in the assortment of field uniforms of the Army of the Slovak Republic, type 2007. The principle of multifunctionality of the fabrics consists in synchronization of at least 5 significant properties

and in achievement of highly positive values of selected parameters in one fabric at once in comparison with 2-3 properties typical for standard fabrics (Table 1).

Flammability reduction was achieved by the application of special fibre types and/or blended yarns with reduced flammability (aramide fibres, modacrylic fibres, viscose fibres with reduced flammability). Basic starting point for the development of a new construction of the multifunctional fabric was the adjustment of a suitable combination of the fibres with reduced flammability and standard fibres (cotton, polyester). Flammability of standard and multifunctional fabrics was determined according to EN ISO 15025: 2003 „Protective clothing, protection against heat and flame". Method of test for limited flame spread", is shown in Figure 3. Results of the measurement are given in Table 2.

Enhancement of strength and air permeability, improving wearing comfort, was achieved by a new fabric construction. Results of the measurement of these parameters are given in Table 2. Formulations of specific dyes were proposed on the base of chromatographic co-ordinates and remission values specified for particular wave lengths in visible and infrared field.

Table 1 Comparison of selected parameters of a standard and multifunctional fabric.

Parameter	Standard fabric designed for field uniforms	Multifunctional fabric
Strength [N], (weft/warp)	600 / 1000	970 / 1220
Air permeability [mm/s]	130	185
Hydrophobicity – resistance to surface wetting [wetting degree]	5 (PTFE „teflon")	3 – 4 („silicon") 5 (PTFE „teflon")
Self-cleaning effect	no	yes
Flammability – ignitability [s]	4	6 up to ≥ 20
Digital print	wood, desert	wood, desert
Colour fastness [rating]	2-3 or 4	4-3 or 3

a) burning time 92 s   b) burning time **47,5 s**   c) burning time 63,7 s   d) burning time **0 - 35,4 s**
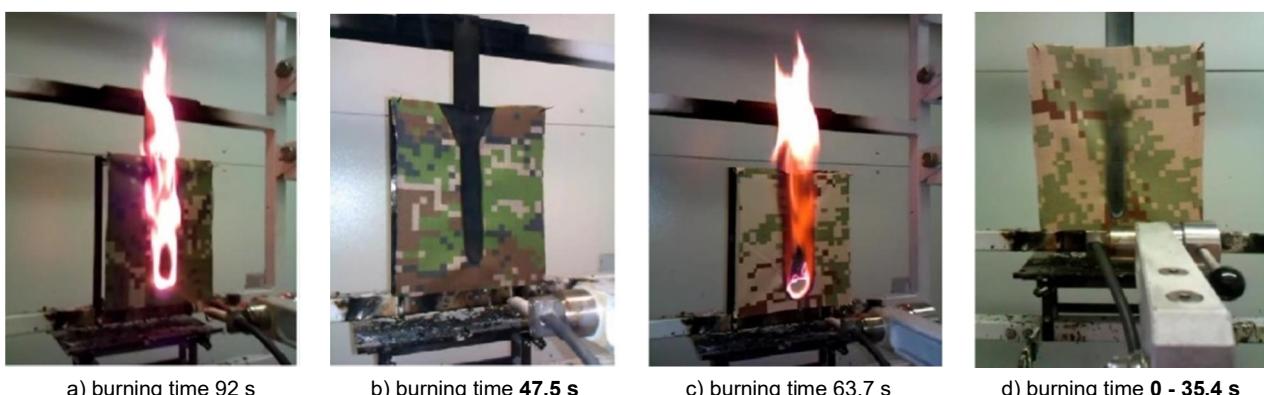
Figure 3 Limited flame spread – ignition of textile surface
a) standard fabric PES/cotton/Lycra, pattern „wood"
b) multifunctional fabric 70% aramide/VsFR // 30% cotton/PES, pattern „wood"
c/ standard fabric 100% cotton, pattern „desert"
d/ multifunctional fabric 75% modacrylics/VsFR / /25% cotton/PES, pattern „desert"

Print of the multifunctional fabric with a digitalized camouflage pattern of the Army of the Slovak Republic, „wood" and „desert", using pigment dyes, meets the requirements of camouflage effect in the field of 400-1000 nm. Hydrophobic finish with self-cleaning and antimicrobial effect on fabric surface was achieved by nanostructuring surface of the multifunctional fabric, by application of hydrophobic nanosol and/or combined finish based on hydrophobic nanosol with incorporated active antimicrobial component. Nanostructured character of the multifunctional fabric surface with hydrophobic finish was demonstrated by SEM (Scanning Electron Microscopy) analysis (Figure 4) and level of the hydrophobic nanofinish was demonstrated by the determination of contact static angle (Figure 5).

The developed unique fabric shows advanced physico-functional properties and performance characteristics due to an innovative combination of special and standard fibres together with novel fabric construction and nanofinishes. Parameters of selected types of the multifunctional fabric printed with digital camouflage pattern of the Army of the Slovak Republic, „wood" and „desert", with hydrophobic nanofinish are given in Table 2. They are compared with the characteristics of standard fabrics used for manufacture of field uniforms, type 2007, used by the Army of the Slovak Republic at present.


without hydrophobic nanofinish   with hydrophobic finish
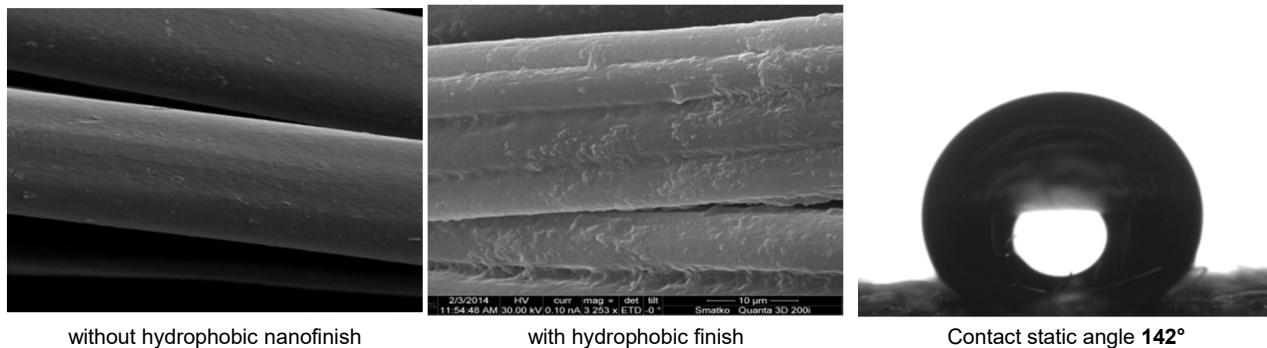
Figure 4 Surface of the multifunctional fabric: SEM image with 3253 magnification

Contact static angle **142°**

Figure 5 Contact static angle of the multifunctional fabric with hydrophobic nanofinish

Table 2 Comparison of basic structural and physico-mechanical parameters of selected types of the multifunctional fabrics printed with digitalized camouflage patterns of the Army of the Slovak Republic, „wood" and „desert", with hydrophobic nanofinish and standard fabrics used for field uniform, type 2007

Structural, physico-mechanical parameter	Multifunctional fabric type 614-K - pattern „wood"	Standard fabric used by the Army of the Slovak Republic - pattern „wood"	Multifunctional fabric type 690 - pattern „desert"	Standard fabric used by the Army of the Slovak Republic - pattern „desert"
Material composition	70% aramid/VsFR 30% cotton/PES	PES/cotton/Lycra	75% modacr./VsFR 25% cotton/PES	100% cotton
Weave	twill	twill	twill	twill
Mass per unit area	219 $g.m^{-2}$	258 $g.m^{-2}$	224 $g.m^{-2}$	200 $g.m^{-2}$
Strength (warp/weft)	1193 N / 1019 N	1000 N / 600 N	932 N / 762 N	900 N / 600 N
Air permeability	535 $mm.s^{-1}$	132 $mm.s^{-1}$	828 $mm.s^{-1}$	257 $mm.s^{-1}$
Water vapour resistance R_{et}	5.59 $m^2.Pa.W^{-1}$	4.73 $m^2.Pa.W^{-1}$	4.82 $m^2.Pa.W^{-1}$	4.17 $m^2.Pa.W^{-1}$
Resistance to surface wetting	wetting grade 3 - 4	wetting grade 5	wetting grade 3 - 4	wetting grade 4
Abrasion resistance	67,500 revolutions	52,500 revolutions	15,000 revolutions	11,000 revolutions
Flammability - ignition time	6 s	4 s	>20 s	4 s
Flammability (limit. flame spread-warp/weft) - burning time - smouldering time	47 s / 49 s 0 s / 0 s	92 s 22 s	0 s / 35 s 0 s / 0 s	64 s 29 s
Colour fastness to light - beige - green - brown - black	blue scale rating 6-7 7 7 6-7	blue scale rating 4-5 4-5 5 4	blue scale rating 6-7 7 7 7	blue scale rating 6-7 6 6-7

As for care, preservation of functional parameters and performance characteristics (including hydrophobic finish) of all types of the multifunctional fabric was confirmed after at least 5 washing cycles performed in accordance with recommended care symbols. Supposed life time of a field uniform made of the multifunctional fabric is at least 2 years providing that care instructions are observed.

Protection of intellectual property of the solution is covered by the Utility model No. 6700 registered on January 21, 2014 by the Industrial Property Office of the Slovak Republic and by SK patent application No. PP 50009-2013 published in the Official Gazette of the Industrial Property Office of the Slovak Republic No. 11-2014 from November 4, 2014 entitled „Multifunctional fabric with camouflage print, hydrophobic, self-cleaning and antimicrobial nanofinish".

Conclusion to the multifunctional fabrics

Application of special aramide fibre types and/or modacrylic fibres in blended yarns with viscose fibres characterized by reduced flammability together with standard yarns (PES/cotton) was a basic precondition of a new fabric construction which significantly improved functional parameters and wearing comfort of field uniforms. New material composition of the fabric increased safety and protection of a man in dangerous and risky environment (fire, flame, heat, explosion, high humidity etc.). Application of hydrophobic and antimicrobial nanosols based on inorganic organosilanes is an advanced technology, the novelty of which consists in surface nanostructuring of special and standard fibres. At present, hydrophobic finish of standard fabric used to manufacture field uniform, type 2007, is based on so-called teflon finish (PTFE – polytetrafluoroethylene) which is not very appropriate from the viewpoint of environmental protection. Hydrophobic finish based on nanosols from organosilanes is an environmentally acceptable alternative. Novelty of the technical solution consists in accomplishment of coloristic requirements given by remission curves and chromatic co-ordinates determined for the camouflage pattern „desert" and „wood" of the Army

of the Slovak Republic. The multifunctional fabric is a novelty on the market of textile materials with wide application possibilities due to the above-mentioned combination of functional properties and performance characteristics. It was developed for application in an assortment of soldier field uniforms to increase protection of a soldier but thanks to its multifunctionality it can be used with advantage also for manufacture of protective clothing designed for special units (police, firemen, civil protection etc.) and/or for workers working in dangerous conditions and/or in adverse atmospheric conditions (chemical industry, civil engineering, transport etc.).

2.3 Fabric finishing with low-temperature plasma

Our research focused in the first stage on the determination of the influence of low-temperature plasma under atmospheric pressure on the change of morphological structure of textile material made of 100% wool. Modification of wool surface was observed using reflection electron microscopy (REM) and Fourier transform infrared spectroscopy (FTIR). Chemical composition of wool fabric surface unfinished with plasma and wool fabric surface finished with plasma was evaluated using X-ray photoelectron spectroscopy (XPS). Surfaces of the wool textile materials were activated on both sides by low-temperature plasma under atmospheric pressure with different activation times at a semi-industrial finishing line in VÚTCH-CHEMITEX, spol. s r. o., Žilina, innovated in co-operation with the Institute of Physics, Faculty of Mathematics, Physics and Informatics in Bratislava. ZUP 400 device (Figure 6), designed for plasma application on surface of polymeric materials, is integrated into the innovated semi-industrial finishing line.

Influence of low-temperature air plasma under atmospheric pressure on morphology of wool fabric was evaluated using reflection electron microscopy (REM). Measurement was performed on an unfinished wool fabric and a wool fabric finished with plasma. Times of wool surface activation were t_{as} = 5, 30, 100 and 150 s; output of plasma electrodes was 350 W (Figure 7).


a)	b)	c)

Figure 6 Innovated semi-industrial finishing line with ZUP 400 device (a), plasma sources (b), in working mode (c)
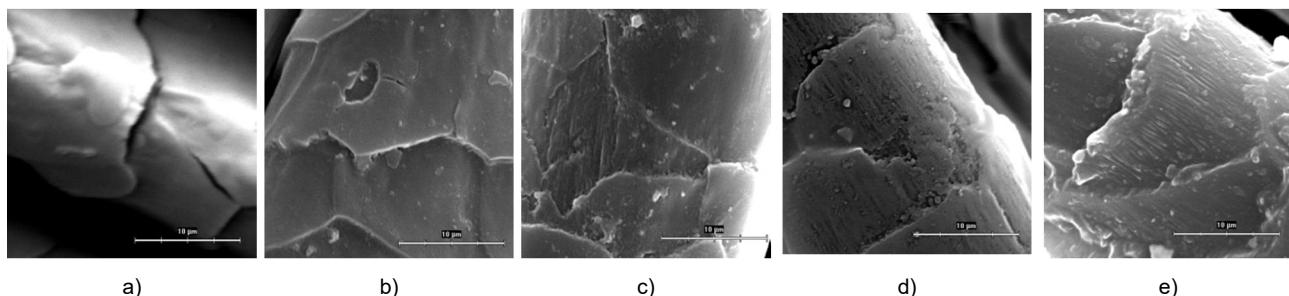
Figure 7 REM image of unfinished wool (a) and wool finished with plasma, t_{as}: 5s (b), 30s (c), 100s (d), 150s (e), resolution 10 µm

REM images of unfinished wool and wool finished with low-temperature plasma under atmospheric pressure show roughage of wool fibre surface after plasma activation (Figure 7b-e) in comparison with wool fibre without surface activation (Figure 7a). Morphologic changes occur in epicuticula of wool. The most remarkably disrupted scale structure of wool fibre can be observed on wool fibre with application of low-temperature plasma under atmospheric pressure at time of surface activation 150 s and plasma output 350 W (Figure 7e).

FTIR ATR (attenuated total reflectance Fourier transform infrared spectroscopy) was used to confirm morphological changes on wool surface caused by low-temperature plasma under atmospheric pressure determined using REM with a view to qualitative as well as quantitative analysis. The measured values were elaborated as transmittance value in dependence on wave number. Surfaces of wool fabric were activated with plasma at plasma output 350 W and different activation times t_{as} = 5, 30, 100 and 150 s. It can be states on the base of the results that FTIR ATR analysis confirmed changes in wool structure caused by low-temperature air plasma under atmospheric pressure. Distortion of epicuticle up to exocuticle A and/or B on wool fibre occurs in accordance with its structure. It is also likely that conversion of secondary structure of the protein fibre occurs as well.

XPS method, as one of the most comprehensive techniques, was used to characterize chemical composition of material surfaces after plasma activation. An unfinished wool woven fabric and a wool woven fabric finished with low-temperature plasma under atmospheric pressure was analyzed at output of plasma electrodes 350 W and surface activation time 30 and 60 s. Percentage of bonds in unfinished wool and wool finished with plasma is summarized in Table 3. In the case of the reference wool sample unfinished with plasma, carbon spectrum consists of three

peaks corresponding to aliphatic C-C/C-H bond with energy 285.0 eV, C-N/C-O bond with energy 268.5 eV and carbonyl C=O bond with energy 288.3 eV.

Table 3 Percentage of bonds in unfinished wool and wool finished with plasma

Time of plasma activation [s]	Chemical bonds [%]			
	C-C/C-H	C-O	C=O	O-C=O
0	63	20	17	0
30	51	23	25	1
60	46	24	25	5

In the case of wool fabric finished with low-temperature plasma under atmospheric pressure, a significant reduction of C-C/C-H bond occurred, on the other hand, the number of C-O and C=O bonds increased. Besides, new carbon bond appeared after plasma activation on wool surface at 289.5 eV. It corresponds to carbon bond in carboxyls, O-C=O. It seems that the number of these bonds depends considerably on the duration of plasma activation and it is characteristic especially for longer plasma activation times. It can be stated on the base of the results of XPS analysis given in Table 3 that wool surface activation with low-temperature plasma under atmospheric pressure causes a change of surface structure, functional groups are formed, which can be then used for further reactions and treatments.

Influence of low-temperature plasma under atmospheric pressure on dyeing of wool textile materials, on dye affinity to the dyed material was studied in the second stage of the research. Evaluation of influence of plasma on dyeing quality was based on the determination degree of dye exhaustion DDE [%]. Conventional exhaust dyeing method was used.
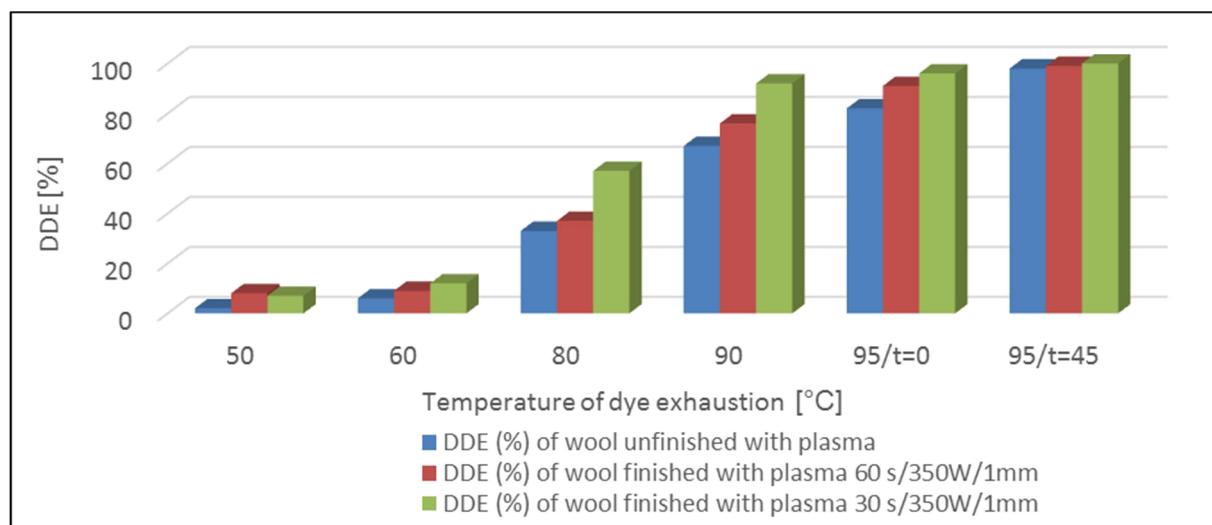
Graph 3 Degree of dye exhaustion DDE [%] for unfinished wool and wool finished with low-temperature plasma under atmospheric pressure

Table 4 DDE [%] at different dyeing temperatures (T_f) and levelling times of the dyed unfinished wool and wool finished with low-temperature plasma under atmospheric pressure

Levelling time [min]	DDE [%]					
	Unfinished wool			*Wool finished with low-temperature plasma under atmospheric pressure* **60 s/350 W/1 mm**		
	T_f [°C]			T_f [°C]		
	90°C	**93°C**	**95°C**	**90°C**	**93°C**	**95°C**
10	80.8	89.2	91.7	94.8	95.5	96.9
20	90.7	94.1	94.7	97.2	97.6	97.7
30	92.6	95.4	96.0	97.6	97.8	97.9
40	93.8	96.7	97.2	98.3	98.2	98.5
45	94.6	96.7	97.3	98.3	98.3	98.7

From the obtained results of degree of dye exhaustion DDE [%] (Graph 3) it can be deduced that DDE of wool woven fabric finished with low-temperature air plasma under atmospheric pressure increases compared to wool woven fabric unfinished with plasma in the course of the whole dyeing process as well as after completion of dyeing at the temperature of 95°C and levelling time 45 min. DDE increases significantly from temperature 80°C of the dyeing process of wool woven fabric finished with plasma compared to fabric unfinished with plasma. DDE achieved on wool woven fabric finished with low-temperature plasma under atmospheric pressure with activation time 60 s, at temperature 90°C and 95°C/t=0 compared to wool woven fabric unfinished with plasma allowed for modification of conditions of the dyeing process for wool textile materials with plasma application. Dyeing process was studied in the next stage of the research under changed conditions, namely with reduced dyeing temperature and shorter levelling time. The works were based on the results obtained in previous investigations.

For another experiment, a wool woven fabric finished with low-temperature plasma under atmospheric pressure with output 350 W, surface activation 60 s and an unfinished fabric were dyed using conventional process of exhaust dyeing on PRETEMA dyeing machine with acid dye NZ in concentration 3%, but under modified dyeing conditions, namely dyeing temperatures reduced from 95°C to 93°C and 90°C and with shortened levelling time at the specified temperatures reduced from 45 min to 40, 30, 20 and 10 min.

It can be stated on the base of the determined DDE that higher DDE was achieved at all dyeing temperatures in wool woven fabric finished with low-temperature plasma under atmospheric pressure and subsequently dyed compared to wool woven fabric unfinished with plasma. DDE achieved on a level of 97.3% on dyeing of wool woven fabric unfinished with plasma at the temperature 95°C, with levelling time 45 min increased by finish of the wool woven fabric with low-temperature plasma under atmospheric pressure at all specified dyeing temperatures 95, 93 and 90°C with levelling time 45 min. Surface activation of wool textile materials with low-temperature air plasma under

atmospheric pressure improved the dyeability of the wool woven fabrics at all dyeing temperatures 95, 93 and 90°C. DDE 97.3% of wool woven fabric unfinished with plasma was achieved, by the activation of wool surface with plasma before the dyeing process, at all dyeing temperatures 95, 93, 90°C already with the shortened levelling time of 20 min. Finishing of wool woven fabric with low-temperature air plasma under atmospheric pressure allows to reduce dyeing temperature from 95 to 90°C and to shorten levelling time from 45 to 20 min; at the same time, DDE [%] was preserved on the same level compared to wool woven fabric unfinished with plasma, dyed at the temperature 95°C with levelling time 45 min.

Conclusion to fabric finishing with low-temperature plasma

It can be stated on the base of these results that finishing of wool woven fabrics with low-temperature plasma under atmospheric pressure allows for a reduction of dyeing temperature from 95°C to 90°C and for shortening the levelling time from 45 min to 20 min without any negative influence on dye affinity to the dyed wool fibre. Besides, the finish allows to preserve the degree of dye exhaustion DDE [%]. The achieved results show that activation of wool surface with low-temperature air plasma under atmospheric pressure shows a positive influence on dyeability of wool and ultimately it may contribute to a reduction of economic costs of the dyeing process.

3   REFERENCES

1. Lymberis A., Olsson S.: Intelligent biomedical clothing for personal health and disease management: State of art and future vision, Telemedicine Journal and e-Health 9(4), 379-386, 2003

2. Smart textiles and clothing, http://www.wearable.ethz.ch

3. Shishoo R.: Plasma Technologies for Textiles, Woodhead Publishing Limited in Association with The Textile Institute, Cambridge, 2007

4. Martišovitš V.: Základy fyziky plazmy, FMFaI UK Bratislava, Bratislava, 2004

5. Carneiro N., Souto A.P., Silva E., Marimba A., Tena B., Ferreira H., Magalhaes V.: Color. Technol. 117, 298, 2001

LIGHT STABILIZATION OF REACTIVE AZO DYES
BY SCREENING OF THE PHOTOCHEMICALLY ACTIVE LIGHT

K. Sirbiladze[1], A. Vig[2], T. Sirbiladze[3] and I. Rusznak[2]

[1]Department of Light Industry, Akaki Tsereteli State University, 59 Tamar Mephe str., Kutaisi, Georgia
[2]Department of Organic Chemistry and Technology, Budapest University of Technology and Economics, Hungary
[3]Department of Chemical Technology, Akaki Tsereteli State University, 59 Tamar Mephe str., Kutaisi, Georgia
k_sirbiladze@yahoo.com; avig@mail.bme.hu

Abstract: Photostability of colored textile materials conditions service life of products, and when considering this problem, it is important to analyze the interaction of all components of the system "polymer-dye-additives". However, in most cases, special emphasis should be placed on the dyestuff, as the limiting element of photostability resource. Photochemical transformations begin as the result of light quantum absorption. The dyestuff molecule intensively absorbs the ultraviolet (UV) and visible regions of spectrum, of which the UV region has a particular influence on the molecule photodegradation process.

The cause of this may be the ratio between the energy of light ray photons and the energies of photoionization of a covalent bond in the dyestuff molecule (electron detachment from the perturbed molecule). In this case, photochemical reaction proceeds without creation of a stable disturbed state of the molecule, and it is possible to avoid it only by screening a dyestuff molecule from a photochemically active light ray. The main kinematic studies in the given research work have been carried out on the red and orange reactive azo dyes, which are characterized by the relatively low values of photostability. It has been established that the light-stabilizing effect of UV-absorption and other additives largely depends on their arrangement in a matrix, and the better results may be achieved in the case of the arrangement of the dyestuff and additives in the same regions.

Key Words: photochemical transformations, UV absorbers, free radicals, light-stabilizing effect

1   INTRODUCTION

Light stability is one of the most important characteristics of coloured textiles [1-3]. Generally, light stability of the dye is a critical characteristic in the dyed system. Absorption of a light quantum is the initial step of photochemical transformations. The dyestuff molecule intensively absorbs in the ultraviolet (UV) and visible regions, of which the UV region has a particular influence on the molecule photodegradation process. The cause of this may be the ratio between the energy of light ray photons and the energies of photoionization of a covalent bond in the dyestuff molecule (electron detachment from the perturbed molecule). In this case, photochemical reaction proceeds without creation of a stable disturbed state of the molecule, and it is possible to avoid it only by screening the dyestuff molecule from a photochemically active light ray.

The photo protection of the dyeing can be characterized by UV light screening constant γ, which is calculated as follows:

$$\gamma = \frac{\varepsilon_1 c_1 + \varepsilon_2 c_2 + \varepsilon_3 c_3}{\varepsilon_1 c_1} \times \frac{1 - e^{-\varepsilon_1 c_1 l_1}}{l - e^{-(\varepsilon_1 c_1 + \varepsilon_2 c_2 + \varepsilon_3 c_3)}} \quad (1)$$

where: ε - the absorption coefficient; c - concentration; l - absorption layer thickness.

The indices 1, 2 and 3 correspond to dye, fibre forming polymer and additive, accordingly.

In certain cases, the use of $1/\gamma$ instead of y may be favourable. $1/\gamma$ expresses the reduced proportion of the absorbed light quantum.

UV absorbers can be applied as screeners for irradiating UV light [1]. The following compounds are usually used as UV absorbers: benzophenone derivatives, benzotriazoles, acrylonitriles, piperidines and organometallic compounds.

2   EXPERIMENTAL

The main kinetic studies of the following azo-dyes have been performed: Brilliant Red 5BX, Brilliant Red 6B and Orange GT. Plasticizer-free cellulose hydrate film (CHF) (thickness 35-45 mcm) and scoured, bleached and mercerized cotton fabric (138 g/m^2) were used in the experiments. The mentioned substrates were dyed with reactive dyes by standard method of discontinuous dyeing.

The dyed substrates were then treated with light stabilizers, either with UV absorber (2-oxo-4-octoxy-benzophenone (UVA 1), or with 2-(2-hydroxy-5-methylphenyl)benzotriazole (UVA 2)), or with "nitroxyl free radical" (2,2,6,6-tetramethyl-4-oxo piperidin-1-oxyl (N-1)), or with (2,2'-azobis-isobutyronitrile (N-2)). Water or an organic solvent was applied in dissolving the mentioned chemicals

preparing solutions of 4 g/L concentration for the after-treatment.

The impact of the selected textile auxiliary substances (surfactant OP-10 (alkylphenolpolyethyl glycol ether), levelling agent A (ionic active substance), dispersing agent (disodium-methylene-bis-naphthyl-sulfonate)) on the lightfastness of coloured polymer substrates have also been studied. The coloured polymeric substrates were after-treated at the temperature of 80°C for 2 hours in 4 g/L stabilizer, as well as 2 g/L textile auxiliary substance containing aqueous solutions. The processed samples were dried at room temperature. Furthermore, the coloured polymeric substrates were after-treated from organic solvents (chloroform (30 min.) and heptane (24 h)) at room temperature.

The obtained samples were irradiated by "Xenotest 450" or by a super high-pressure mercury vapour lamp DRS-250.

Kinetics of the occurred photo-fading were followed either by UV-VIS absorption spectrophotometer HP UV-VIS or by UV-VIS photoluminescence spectrophotometer UV-1800 or by a reflection spectrophotometer "Datacolor". Light stability of dyed textiles was also evaluated visually by a blue scale of 8 grades.

Free radicals have been detected by electron spin resonance (ESR) using a "Radiopan" ESR-spectrometer SE/X 2543.

3   RESULTS AND DISCUSSION

In preliminary experiments, it has been established that the applied UV absorbers and nitroxyl free radicals change the photo-degradation kinetics of the studied systems [4]. Observed photo stabilizing effect is inconsistent. The obtained slight positive effect of photo stabilizer could be explained by its uneven distribution in the substrates.

These results could be evaluated from the photo-degradation kinetic curves on CHF (Figure 1). No significant changes could be observed. Photo-fading was slightly accelerated by adding N-1 or slightly decelerated by adding UVA1. When both additives are applied simultaneously, a slightly increased deceleration of photo-fading is observed. In Table 1, as regards the light fastness of differently treated coloured cotton fabrics, the same tendency can be observed. In most cases, there are no changes, or only a very small increase (0.5-1 grade) in the light-fastness can be observed.
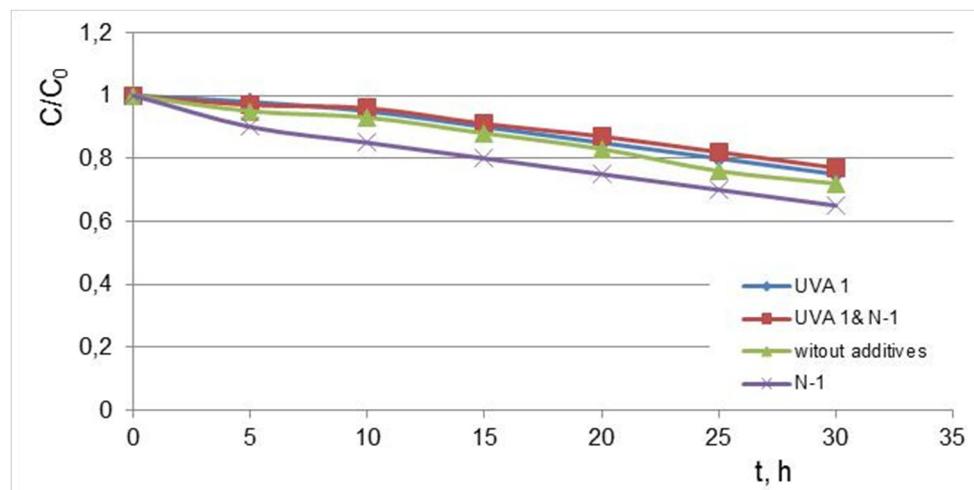

Figure 1 Photo-degradation kinetic curves of CHF films dyed with reactive Brilliant red 6B (C=10^{-2} mol/kg) under irradiation with the light of "Xenotest 450" in the absence and in the presence of UVA1 or N-1 or both of them

Table 1 Lightfastness of cotton fabric dyed with different reactive dyes in the presence of different additives

	Reactive azo-dye	Textile auxiliary substance	Light stabilization (by 8-point scoring system)						
			Without additives	UVA 1	UVA 2	UVA 1 N-1	UVA1 N-2	UVA 2 N-1	UVA2 N-2
1	Brilliant Red 5BX	levelling substance A	3	3	3	3-4	3	3-4	3
2	Brilliant Red 6B		3	3	3	3-4	3	4	3-4
3	Orange GT		3	3	3	3	3	3	3-4
4	Brilliant Red 5BX	OP-10	3-4	3-4	3	4	4	3-4	3-4
5	Brilliant Red 6B		3	3	3	3	3	3	3
6	Orange GT		3	3	3	3-4	3	3	3
7	Brilliant Red 5BX	dispersing agent	2-3	2-3	2-3	3	3	3	3
8	Brilliant Red 6B		3	3	3	3-4	3-4	4	3-4
9	Orange GT		2-3	2-3	3	3	3	3	3

A more equal distribution of the light stabilizers could be achieved by introducing them in the polymer substrates from organic solvents.

Significant changes could be observed (Figure 2). Photo-fading was highly decelerated both in the presence of UVA1 & N-1 and in the presence of UVA2 & N-2, respectively. However, due to the fact that dissolubility of additives in heptane solution is limited, the processing duration is long (24 hours), we preferred to use chloroform as the solvent.

Effect of nitroxyl free radicals on the light-stability of the reactive Brilliant Red 6B dyed cellulose hydrate film could be evaluated from the photo-degradation

kinetic curves (Figure 3). Significant changes could be observed. Photo-fading was highly decelerated (by approximately 4 times) by the addition of N-1 whose effect was slightly increased in the case of the presence of UVA1 in the system.

From the luminescence spectra of the reactive Brilliant Red 6B dyed CHF (Figure 4), it can be assumed that the detected light-stabilizing effect occurs due to the uniform distribution of the dye and light-stabilizer molecules in the system. The luminescence of the dye has been decreased by 40-50 percent both in the presence of N-1 and in the presence of UVA1 & N-1.
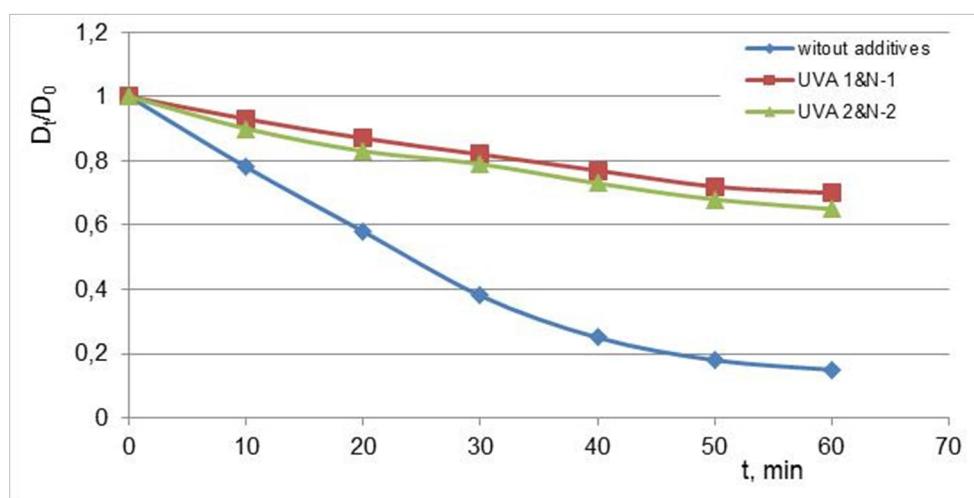

Figure 2 Photo-degradation kinetic curves of the reactive Brillant red 6B dyed cellulose hydrate film (irradiation: DRS lamp; D_o = initial optical density of CHF, D_t = optical density of CHF at t - time of irradiation)
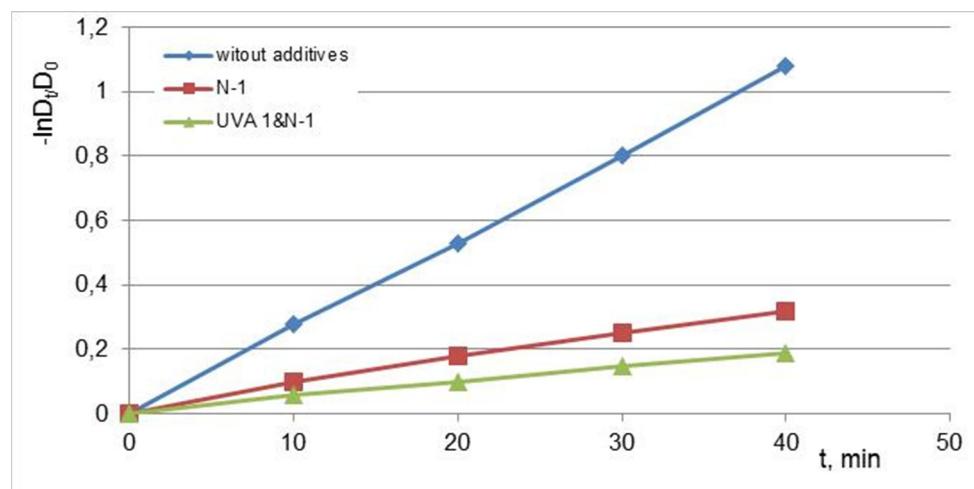

Figure 3 Photo-degradation kinetic curves of the reactive Brilliant Red 6B dyed cellulose hydrate film (CHF) (irradiation: DRS lamp, D_o = initial optical density of CHF, D_t = optical density of CHF at t - time of irradiation).
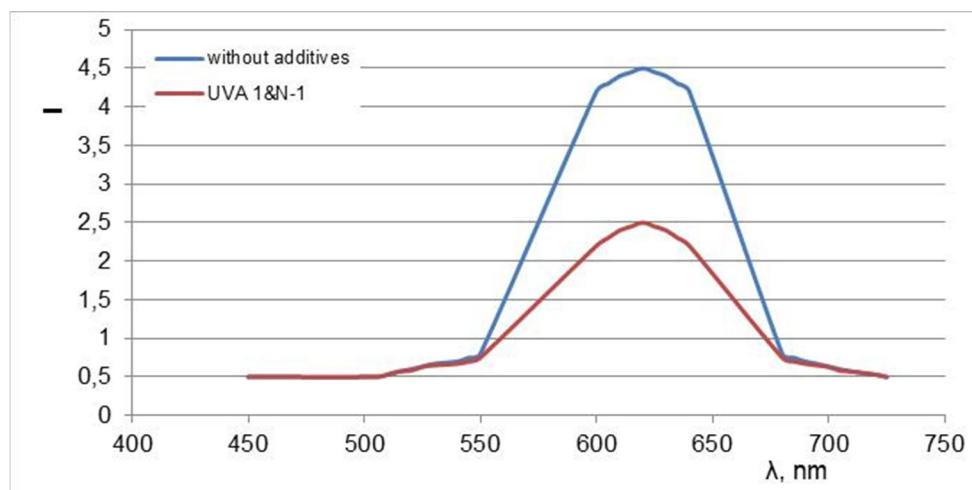
Figure 4 Luminescence spectra of the reactive Brilliant Red 6B dyed CHF ($C=4 \cdot 10^{-2}$ mol/L): 1. Without additive; 2. In the presence of UV absorber and free nitroxyl radical.
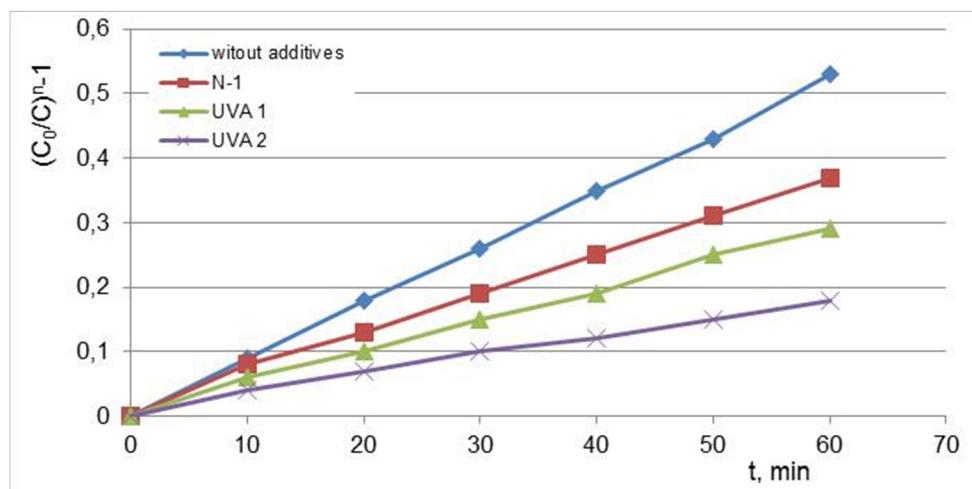

Figure 5 Photo-degradation kinetic curves of the reactive Brilliant Red 6B dyed cotton fabrics (irradiation: DRS lamp)

The same results have been obtained for the reactive dyed cotton fabrics (Figure 5). It could be demonstrated that all photo stabilizers showed a significant lightfastness-improving effect. It is Important to note that in the case of applying both additives simultaneously, a synergic enhancement effect occurs.

Washing (2 g/L surfactant, 40°C, 10 minutes) the nitroxyl free radical containing cotton fabric resulted in decreasing the free radical concentration by approximately 50%. However, their photo stabilizing effect was changed imperceptibly. It could be assumed that the stable free nitroxyl radicals were removed mostly from the surface area of the substrate.

It could be proved that mixture of UV absorbers and free nitroxyl radicals was the most effective luminescence extinguisher on both CHF and cotton fabric. Approximately a 60%-drop in luminescence could be observed.

4   CONCLUSIONS

It has been established that the light-stabilizing effect of UV absorbers and stable free nitroxyl radicals largely depends on the method of their introduction in a polymeric substrate. A much better photostabilizing effect could be demonstrated in the case of adding the additives into the polymeric substrate from organic solvent. Using this method resulted in a reduction of dye luminescence. Also, light-stability can be improved by 1-1.5 grades.

5   REFERENCES

1. Sirbiladse K., Rusznak I., Vig A.: The impact of UV irradiation on the radical iniatiating capacity of dissolved dyes, Radiation Physics and Chemistry 67(3-4), 2003

2. Vig A., Nagy H.J., Aranyosi P., Sirbiladze K., Rusznak I., Sallay P.: The light stability of azo dyes and dyeings V. The impact of the atmosphere on the light stability of dyeings with heterobifunctional reactive azo dyes, Dyes and Pigments 72(1), 16-22, 2007

3. Sirbiladze K., Vig A., Sirbiladze T., Rusznak I.: Synthesis of New Reactive Monoazo Dyes Extended by Studies of Photodestruction Mechanism and Light Stabilization, 16th Blue Danube Symposium on Heterocyclic Chemistry, Balatonalmadi, Hungary, June 14-17, 2015

4. Sirbiladze K., Sirbiladze T.: The Synthesis of Vinilsulphonic Reactive Dyes and the Reseach of their Photocemical Features, XXIII. International Congress, Hungary, Budapest, 8-13 May 2013

CHITOSAN NANOFIBERS AND NANOPARTICLES FOR IMMOBILIZATION OF MICROBIAL COLLAGENASE

M. Slováková[1], V. Kratochvilová[1], J.Palarčík[1], R. Metelka[1], P. Dvořáková[1], J. Srbová[1], M. Munzarová[2] and Z. Bílková[1]

[1]*Faculty of Chemical Technology, University of Pardubice, Studentská 95, 532 10 Pardubice, Czech Republic*
[2]*Nanovia Ltd., Podkrušnohorská 271, 436 03 Litvínov - Chudeřín, Czech Republic*
marcela.slovakova@upce.cz

Abstract: The purpose of the paper is to describe the production and characterization of electrospun chitosan nanofibers and chitosan/TPP nanoparticles as carriers for microbial collagenase. These proteolytic highly active and stable carriers have a potential of advanced bioactive wound dressings. The morphology and the microstructure of nanofibers and nanoparticles were examined using a scanning electron microscopy and dynamic light scattering. Low molecular weight chitosan/TPP nanoparticles prepared at the ratio 2:1 showed a size range of 130 - 142 nm. Specific collagenase activity 0.545×10^{-3} U/mg for chitosan nanofibers and 0.684×10^{-3} U/mg of nanoparticles was quantified using the hydrolysis of a peptidic substrate (Pz-peptide) and is expressed per mass of chitosan biomaterial. Storage stability and reusability of collagenase chitosan nanofibers and collagenase chitosan nanoparticles did not fall below 73% of their original activity.

Key Words: chitosan, nanofibers, nanoparticles, collagenase, stability

1 INTRODUCTION

Chitosan (CS) is a derivative of chitin and is a natural polyaminosacharide offering a set of unique characteristics that include biocompatibility, biodegradability, nontoxicity, antibacterial properties, and hydrophilicity [1]. In the past decades, CS has been extensively used as a carrier candidate in biomedicine because of its excellent stability, mucoadhesive property, and being a suitable carrier of nucleic acids, enzymes and antigens [2-6].

The nanofibrous form of CS brings additional attractive features like large surface area and porosity leading to good permeability for oxygen and water [7, 8]. These properties support cell respiration, skin regeneration, moisture retention, removal of exudates, and hemostasis [9]. The formation of CS nanoparticles is a process based on the complexation of oppositely charged molecules by electrostatic interactions [10]. Nanoparticles can easily be constructed using an ionic gelation process which involves sodium tripolyphosphate as a negatively charged molecule and CS as polycation [11, 12]. Low molecular weight chitosan is popular primarily due to its better solubility in the neutral aqueous solvents with low viscosity and rapid degradation than is chitosan having a higher molecular weight [2, 13].

Nanofibrous scaffolds fabricated via electrospinning represent a potential delivery vehicle. In this well-established process, fibers that are hundreds of nanometers in diameter can be formed and compiled into a non-woven 3-D scaffold [14].

An example of a suitable delivery system is collagenase stored inside electrospun poly(ethylene oxide) nanofibers releasing active molecules upon hydration [15]. Collagenases are used for a broad spectrum of biotechnological applications; they are suitable for the isolation of a broad variety of cell types, especially fibroblasts, human and rodent hepatocytes, frog oocytes and epithelial cells [16]. Clostridial collagenases are capable of degrading various types of collagen and gelatine, which is the essence of an enzymatic debridement, a frequently used technique for the removal of necrotic tissue from wounds. Microbial collagenase is already used as an active ingredient ointment (Iruxol® Mono Ointment), where it is a safe and effective choice for the debridement of cutaneous ulcers and burn wounds [17-19].

This work describes the production and characterization of electrospun chitosan nanofibers and chitosan nanoparticles as carriers for microbial collagenase. Covalent linkage used in this work is used to effectively prevent both the denaturation and leaching of enzyme molecules [20]. In particular, immobilizing the proteases by covalent bond additionally decreases autocatalysis and controls proteolysis [21, 22]. Carbodiimide chemistry for grafting the collagenase from *Clostridium histolyticum* was used. Both chitosan nanofibers and nanoparticles were compared in terms of immobilized collagenase activity, stability and reusability. Collagenase activity, being a fundamental proof of the enzyme

occurring in its active form, was quantified using the hydrolysis of a peptidic substrate.

2   EXPERIMENTAL

Chemicals

KiOnutrime-CS (Kitozyme, Belgium), polyethylene oxide (Scientific Polymer Products, NY, USA), chitosan I (MW 47 kDa, deacetylation 80%) (Contipro, Dolni Dobrouc), collagenase NB 4G from *Clostridium histolyticum* (70 - 120 kDa, contains class I and class II collagenase, PZ activity (Wünsch): ≥ 0.18 U/mg) and Pz-peptide (4-phenylazobenzyloxycarbonyl-Pro-Leu-Gly-Pro-D-Arg, Mr = 776.9) were purchased from Serva Electrophoresis GmbH, Germany, sodium tripolyphosphate (TPP) and other pure chemicals were purchased from Sigma-Aldrich (St. Louis, MO, USA).

Manufacturing the nanofibers

CS nanofibers, described in detail in [23], were prepared using the modified needleless technology NanospiderTM in an NS LAB 500 S electrospinning laboratory device (Nanovia Ltd. Litvínov, Czech Republic) [24]. Briefly, CS nanofibers were prepared from the polymer solution of CS (5 wt% to 20 wt%) and polyethylene oxide (1 wt% to 10 wt%), in acetic acid by an electrospinning methodology and were crosslinked by heating to 130°C for 1 hour.

Chitosan/tripolyphosphate (CS/TPP) nanoparticles preparation under stirring according to [Biswas]. 15 mL of 2.3 mM TPP was mixed with 30 mL of 0.2% CS in 25 mM acetate buffer pH 5.2 (CS:TPP ratio 2:1) for 30 minutes at room temperature. Dialysis followed using the 3.5 kDa molecular weight cut-off dialysis tubing (Serva Electrophoresis) to 0.1 M acetate buffer pH 5.5. For further analysis, the nanoparticles were stored at 4°C and 0.1 M acetate buffer pH 5.5 or lyophilized from distilled water using the Scan Vac CoolSafe (Labogene, Denmark).

Dynamic light scattering

The average particle size and size distribution of the prepared nanoparticles in different media were determined by dynamic light scattering (DLS) using a Zetasizer and software 7.03 version (Malvern Instruments Ltd., UK). The measurements were performed at 25°C, with a scattering angle of 173°, using disposable cuvettes. Amount of nanoparticles per sample was 0.25 mg in 1.5 mL. Each measurement was performed in 12 repeats after 30 s. Data were statistically processed.

Scanning electron microscopy

Scanning electron microscopy of prepared particles was performed using VEGA3 SBU apparatus and backscattered electron detector (Tescan, Czech Republic). Samples were coated with a conductive layer of gold (thickness of 0.2 nm) in Balzers sputter coater to prevent charging of the specimen.

Collagenase immobilization

The enzyme collagenase was immobilized onto 1.5×1.5 cm CS squares or 2 mg of CS/TPP nanoparticles according to [23]. Briefly, the zero-length crosslinker EDC (7.5 mg) and sulfo-NHS (1.25 mg) reagent (each dissolved in 0.2 mL of 0.01 M phosphate buffer (pH 7.3)) were quickly added to the nanofibers. Immediate addition of collagenase solution followed (unless stated otherwise, 3 mg of collagenase dissolved in 0.5 mL of 0.01 M phosphate buffer (pH 7.3)) and 0.1 mL of the same buffer was added. The immobilization proceeded at 4°C for 16 h under mild rotation. All measurements were repeated a minimum of two times the calculated means and SD values of which are shown in the graphs.

Determination of soluble and immobilized collagenase activity

The enzymatic activity of the soluble or immobilized collagenase was estimated by measuring the hydrolysis yield of a standard solution of a freshly prepared chromogenic substrate, Pz-peptide, in 0.03 M TRIS-HCl buffer (pH 7.0) containing 0.2 M NaCl and 5 mM $CaCl_2$ according to [25]. 1 U according to Wünsch catalyzes the hydrolysis of 1 µmole of 4-phenylazobenzyloxycarbonyl-L-prolyl-L-leucylglycyl-L-prolyl-D-arginine per minute at 25°C, pH 7.1. The resulting 4-phenylazobenzyloxycarbonyl-Pro-leucin, after its extraction with ethylacetate, changed to a yellow product which was measured spectrophotometrically. Specifically, the activity of the 0.02 mL soluble or immobilized enzyme was determined in terms of micrograms (µg). The hydrolysis of 1.29 mM Pz-peptide was performed in a 0.03 M TRIS-HCl buffer (pH 7.0) containing 0.2 M NaCl and 5 mM $CaCl_2$ at 37°C (final reaction volume 2 mL). The enzymatic reaction occurred under mild stirring and was stopped after 25 min by the addition of 0.25 mL 22 wt% citric acid per 2 mL of supernatant. 2 mL of ethylacetate was added, the product was vigorously shaken and the absorbance of the organic phase was measured at 320 nm in a quartz cuvette using a Biochrom LIBRA S22 UV/VIS spectrophotometer (Thermo Fisher, CR). Collagenase activity per mg of nanofibers was then calculated. The activity of soluble collagenase was determined by the same method using the corresponding quantity of immobilized collagenase (4 µg).

3   RESULTS AND DISCUSSION

In this study, a strategy for covalent biofunctionalization of CS nanofibers and CS/TPP nanoparticles with collagenase from *Clostridium histolyticum* is presented. The work was carried out

with the aim to prepare proteolytic highly active and stable nanofibers with the potential of advanced bioactive wound dressings.

For the preparation of the nanofibers we used modified needleless Nanospider[TM] technology [26]. This technology enables flexibly the formation of fibers tens of nanometers to tens of micrometers in diameter and the preparation of nanofibers with masses per unit area ranging from 1 to 100 g/m^2. Nanofiber structure was analysed by scanning electron microscopy (Figure 1) using a TESCAN VEGA3 microscope.
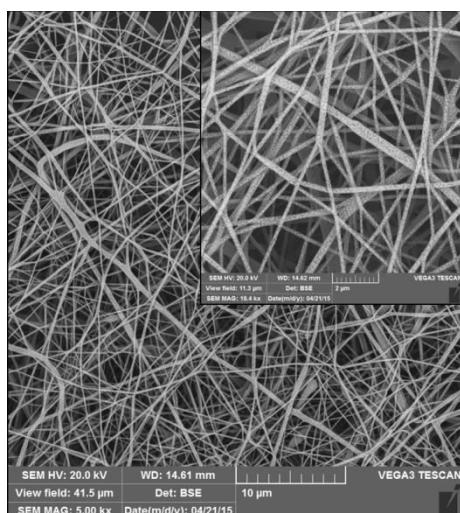

Figure 1 Scanning electron microscopy of CS nanofibers. Magnification 5,000× and 18,000× for inset. VEGA3 TESCAN instrument

CS/TPP nanoparticles were prepared according to the procedure first reported by Calvo et al. [11] with suitable modifications based on the ionotropic gelation of CS with TPP anions [2]. To achieve the nanoparticle sizes around a hundred nm, different

ratios of CS to TPP were carried out and the composition of this optimisation was chosen as CS/TPP ratio 2:1. The hydrodynamic diameter of the prepared CS/TPP nanoparticles dialyzed against the same buffer was determined by the means of dynamic light scattering (DLS). Resulting hydrodynamic sizes (Table 1) were close for the CS/TPP nanoparticles freshly prepared (sample **1**) and those dialyzed to 0.1 M acetate buffer pH 5.5 (sample **2**).

Furthermore, the effect of the storage to the nanoparticles was monitored using the DLS and size distribution. Results on Figure 2 and Table 1 show that nanoparticles stored at the conditions of 4°C and 0.1 M acetate buffer pH 5.5 did not change in hydrodynamic size (sample **3**). Size distribution also remained unchanged.

Table 1 Results of DLS measurement of CS/TPP nanoparticles (**1 - 3**). Concentration of sample particles 16.67%, vortex before measurement, 25°C, 0.1 M acetate buffer pH 5.5

Particle sample	Mean D_H (nm)	SD
(**1**) CS/TPP nanoparticles, no dialysis	132.4	1.57
(**2**) CS/TPP nanoparticles, dialysis	139.3	1.78
(**3**) CS/TPP nanoparticles, stored for 7 weeks, dialysis	142.6	1.31

The morphology of the CS/TPP nanoparticle lyophilized from distilled water studied from scanning electron microscopy images (Figure 3) revealed that the nanoparticles have particle character. During application and gilding lyophilized sample on a slide pad, distinct formation of aggregates with a porous structure takes place.
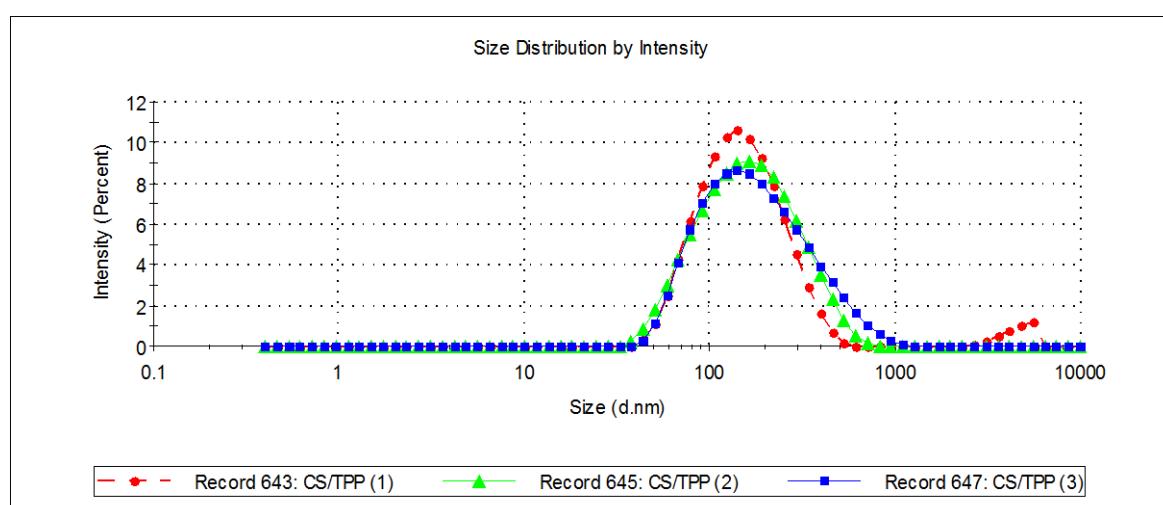

Figure 2 Size distributions by intensity of samples (**1-3**) of CS/TPP nanoparticles (circle – no dialysis (**1**), triangles – dialysis (**2**), storage 7 weeks and dialysis (**3**))
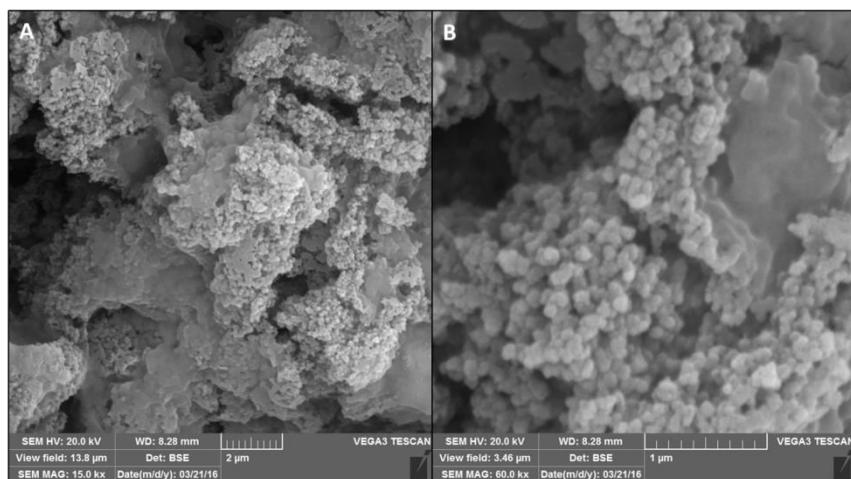
**Figure 3** Scanning electron micrograph of CS/TPP nanoparticles. Magnification **A)** 15,000×, **B)** 60,000×

Immobilization method applied in this study is based on the formation of amide and ester linkages mediated by the zero-length crosslinker carbodiimide (EDC). The addition of sulfo-NHS to the EDC-mediated reaction increases the solubility and stability of the active intermediate O-acylisourea subsequently reacting with the amino and hydroxyl group of chitosan. EDC/sulfo-NHS-coupled reactions are generally considered highly efficient [27]. CS nanofibers of basis weight 20 (g/m^2) were cut into squares (1.5×1.5 cm). Prior to biofunctionalization of the nanofibers, polypropylene spunbonds were torn off and all squares were weighed. Dialyzed CS/TPP nanoparticle suspensions (2 mg of solid) were washed and supernatants were removed before carbodiimide immobilization method of the collagenase occurred. The collagenase CS nanoparticles were sonicated for 10 minutes before immobilization and activity assays. Specific enzyme activity in units is expressed per mass of CS biomaterial (Table 2). The resulting values for immobilized collagenase activities on nanofibers are lower by 20.3% compared to the activity of the enzyme on nanoparticles. Possible explanation for the difference is a different form, size, or specific surface.

Table 2 Immobilized collagenase activity

Particle sample	Specific enzyme activity (U/mg of biomaterial)
Collagenase CS nanofibers	0.545×10^{-3}
Collagenase CS/TPP nanoparticles	0.684×10^{-3}

Storage stability and reusability are the main advantages of immobilized enzymes. This also testifies about the quality of the binding of the enzyme to the carrier. To demonstrate the long-term usability of immobilized collagenase, the prepared collagenase CS nanofibers and collagenase CS nanoparticles were stored at 4°C in 30 mM Tris-HCl buffer pH 7.0 with 0.2 M NaCl a 5 mM $CaCl_2$ and monitored for 4 weeks. The collagenase CS nanoparticles were sonicated for 10 minutes before activity assay. The results of specific enzyme activity for collagenase CS nanofibers showed no decrease (still at 100%) after 4 weeks, collagenase CS nanoparticles activities decrease to 73% of original values (Figure 4). An increase in collagenase CS nanofibers activity recorded after 1 week of storage is a commonly observed phenomenon caused by the restoration of functional conformation leading to enzyme reactivation [28]. These experiments repeatedly confirmed high and sufficient proteolytic activity of stored collagenase CS nanofibers and CS/TPP nanoparticles.

The reusability of collagenase CS nanofibers and CS/TPP nanoparticles were measured 8 times in a row during one day. Excellent results of collagenase CS nanofibers were observed (Figure 5), activity per mg of nanofibers did not decrease below 100%. Collagenase CS/TPP nanoparticles activity after the last run did not fall below 78% of its original value. These results show the ability of immobilized collagenase to repeatedly cleave the target substrate without any substantial activity loss.
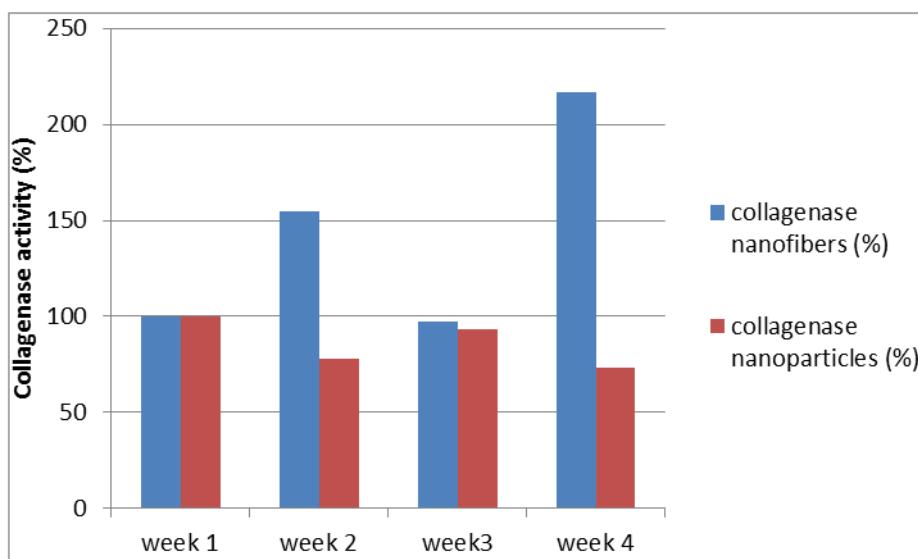
Figure 4 Storage stability of immobilized collagenase on CS nanofibers and on nanoparticles
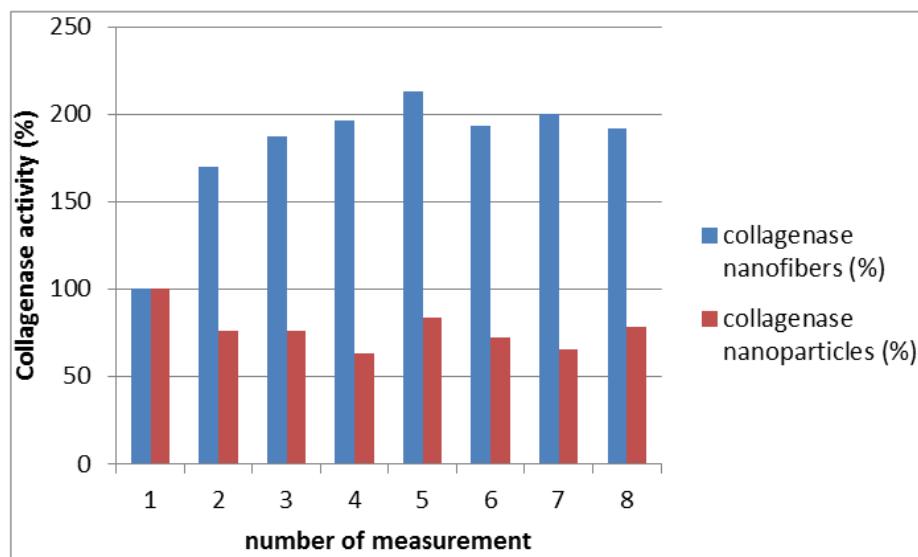

Figure 5 Reusability of immobilized collagenase on CS nanofibers and on nanoparticles

4   CONCLUSIONS

In this work, biocompatible chitosan electrospun nanofibers and chitosan/tripolyphosphate nanoparticles were biofunctionalized with the enzyme collagenase from *Clostridium histolyticum*. In comparison, higher collagenase activity per mg was achieved when using the chitosan/TPP nanoparticles.

This resulted in an activity of up to 0.545×10^{-3} U/mg of nanoparticles and 0.684×10^{-3} U/mg of nanofibers, respectively. This study confirmed comparable results of chitosan biomaterials in its different forms. The excellent stability and reusability of collagenase immobilized on chitosan carriers suggests their potential in enzyme debridement for skin regeneration.

5   REFERENCES

1. Krajewska B.: Enzyme Microb. Technol. 35, 126-139, 2004
2. Biswas S., Chattopadhyay M., et al.: Carbohydrate Polymers 121, 403-410, 2015
3. Xie Z., Paras C.B., et al.: Acta Biomaterialia 9(12), 9351-9359, 2013
4. Alessandro N., Noha M.Z., et al.: Pharmaceutical Research 26(8), 1918-1930, 2009
5. Shao T., Li X., et al.: Diagnostic Pathology 6(64), 1-5, 2011
6. Jain A., Jain S.K.: European Journal of Pharmaceutical Sciences 35(5), 404-416, 2008

7. Ding F., Deng H., Du Y., Shi X., Wang Q.: Nanoscale 6(16), 9477-9493, 2014

8. Kubinova S., Sykova E.: Minim. Invasive Ther. Allied Technol. 19, 144-156, 2010

9. Rieger K.A., Birch N.P., Schiffman J.D.: Journal of Materials Chemistry B1, 4531-4541, 2013

10. Csaba N., Koeping-Hoeggard M., Jose Alonso M.: Int J Pharm 382, 205-214, 2009

11. Calvo P., RemunanLopez C., VilaJato J., Alonso M.: Pharm Res 14, 1431-1436, 1997

12. Nasti A., Zaki N.M., de Leonardis P., et al.: Pharm Res 26, 1918-1930, 2009

13. Kumar P.T.S., Raj M., et al.: Tissue Engineering: Part A 19(3-4), 380-392, 2013

14. Qu F., Pintauro M.P., Haughan J.E., Henning E.A., et al.: Biomaterials 39, 85-94, 2015

15. Qu F., Lin J.G., Esterhai J.L., Fisher M.B., Mauck R.L.: Acta Biomaterialia 5(9), 6393-402, 2013

16. Eckhard U., Schoenauer E., Ducka P., Briza P., et al.: Biological Chemistry 390(1), 11-18, 2009

17. Payne W.G., Salas R.E., et al.: EPlasty 8, 151-156, 2008

18. Ramundo J., Gray M.: Journal of Wound, Ostomy & Continence Nursing 36(6S), S4–S11, 2009

19. Tallis A., Motley T.A., Wunderlich R.P., Dickerson Jr. J.E., Waycaster C., Slade H.B.: Collagenase Diabetic Foot Ulcer Study Group: Clinical Therapeutics 35(11), 1805-1820, 2013

20. Mozhaev V.V., Melik-Nubarov N.S., Sergeeva M.V., Šlkšnis V., Martinek K.: Biocatalysis and Biotransformation 3(3), 179−187, 1990

21. Mukhopadhyay A., Chakrabarti K.: RSC Advances 5, 89346-89362, 2015

22. Li D., Teoh W.Y., Gooding J.J., Selomulya C., Amal R.: Advanced Functional Materials 20, 1767-1777, 2010

23. Srbová J., Slováková M., Křípalová Z., Žárská M., Špačková M., Stránská D., Bílková Z.: Reactive and Functional Polymers Accepted in Mai, 2016

24. Dubsky M., Kubinova S., Sirc J., Voska L., Zajicek R., Zajicova A., et al.: Journal of Materials Science-Materials in Medicine 3(4), 931-41, 2012

25. Wünsch E.A., Heinrich H.G.: Hoppe-Seyler´s Zeitschrift für physiologische Chemie. 333, 149-51, 1963

26. Jirsak O., Sanetrnik F., Lukas L., Kotek K., Martinova L., Chaloupek J.: U.S. patent (2005) WO 205024101

27. Hermanson G.T.: Bioconjugate Techniques, third ed., Academic Press, Boston, 2013

28. Ye P., Xu Z., Wu J., Innocent C., Seta P.: Macromolecules 39, 1041-1045, 2006

CONTROLLED MINIMAL APPLICATION ON KNITWEAR

P. Tolksdorf

A. Monforts Textilmaschinen GmbH & Co, KG, Blumenberger Str. 123-143, 41061 Mönchengladbach, Germany
tolksdorf@monforts.de

Abstract: *Due to volatile commodity and energy prices as well as requirements from brands, retailers, consumers and governments, sustainability has become a significant competitive factor for textile manufacturers. The minimal application of finishing liquors in the textile industry is a very effective way to significantly reduce the energy consumption in continuous finishing processes. Minimal application on dimension stable woven fabric is a common technique and different methods are available in the market. Because of curling selvages and instable dimension in running and cross direction, reliable minimal application methods for knitted fabric can be hardly found in the market. These kinds of fabrics are usually treated in padding processes with very high wet pick up.*

The paper will report about a new and unique way of treating knitted fabric with minimal application technique. More than 50% of heating energy can be saved with the Eco Applicator process for knitwear. Wet-in-Wet processes are also possible with a precise and reproducible Add On of the required products without any tailing effects.

Key Words: *Knitwear, Sustainability*

1   INTRODUCTION

Sustainable production is in the focus of the textile industry:

- Volatile prices for commodities and energy force the industry to pay highest attention to resource saving and energy efficiency.
- Furthermore, sustainability is a subject with which the textile industry is increasingly confronted by legislation, by brands and retailers and by consumers.

To put it in a nutshell: Sustainability is an issue with hard economic aspects. It has become a significant competitive factor. Technological upgrading is one of the keys to realising sustainable textile production and so to remain competitive.

The German mechanical engineering industry plays a prominent role in developing and realising sustainable solutions. For example:

- effective solutions for new energy concepts and
- effective handling of scarce resources.

Textile machines are usually designed for the different demand profiles of the textile manufacturer. These profiles result from the textile product to be manufactured and the specific process to be performed. In other words, the textile producer directly affects the specific energy use in many ways.

Energy efficiency

Energy efficiency is an integral part of sustainability. Monforts' energy management has been one of Monforts' primary goals for many years, driving the company to develop energy efficient and resource conserving solutions. For many years, textile finishing has operated with chemical and thermal processes which, by present-day standards, can have a severe impact on the environment. The energy costs are high, and the use of chemicals absolutely essential. But with innovative ranges and advanced auxiliaries, Monforts has succeeded in optimising these processes. The savings benefits that have been achieved in recent years are, in some cases, quite considerable.

2   MONFORTS ECO APPLICATOR

An excellent example highlighting Monforts' R&D activities concerning sustainable machines and processes is the Matex Eco Applicator; a unit which significantly reduces the moisture content before the drying process. The challenge of sustainability is to save natural resources without compromising production quality of the final products. The ECO Applicator ensures minimised energy consumption in subsequent drying processes, faster drying and higher productivity compared with standard equipment such as padding systems. Padding is a process employed in the textile industry for wet treatment of textiles. The fabric, or 'substrate', is transported through a trough containing the finishing or dying liquor. The term 'liquor' is generally used to refer to an aqueous liquid in which textiles are washed, bleached, dyed or impregnated. It contains all the dissolved,

emulsified or dispersed constituents such as dyestuffs, pigments or chemicals.

During the further course of the production process, the substrate is transported through squeezing rollers to remove the excess liquor. A liquor absorption of 70% - which is a typical value in standard padding application on woven fabric - means that 100 kg of textile fabric has to absorb 70 kg of liquor. After the impregnation process, the wetted fabric is dried in a final step by means of a Montex stenter.

For this process, drying energy is required which, in the textile finishing industry, is a major cost factor. Influencing factors for the energy consumption and costs of drying processes are the initial moisture content, residual moisture content, drying temperature and relative water vapour content of the ambient air. The degree of initial moisture is the crucial point for determining how much evaporation heat and energy is necessary for drying.

Facts

Reducing the liquor pick up which is the means of operation of the Monforts Matex ECO applicator results in lower evaporation heat and lower operating costs. With the ECO Applicator, the liquor is not applied to the fabric by dipping it through a trough but by using steel rollers which transfer the required amount of liquor onto the fabric. With lower waste water contamination, the application unit becomes a resource-conserving alternative to padding. The ECO Applicator has a wide range of potential uses: The liquor can be applied to one or both sides of the substrate, or different liquors can be applied to the front and rear sides. Small liquor contents mean low residual liquor volumes. The possibility to apply different liquors at the same time allows for creating multi-functional products. This could be for instance a sportswear fabric that provides rain protection outside whilst it has hydrophilic properties inside (Figure 1).

In addition to the traditional dry in wet application, the Eco Applicator is also suitable for wet in wet applications. Compared with conventional systems, an extremely precise application without any diluting effects can be achieved. No intermediate drying step is necessary, which results in higher production capacity and saving of natural resources. Since ITMA 2011 at Barcelona, the Minimal Application on dimension stable woven fabric has been available in the market and in the meantime a common and customer approved technique.

Controlled minimal application on knitwear

A significant advantage of the Eco Applicator technology is the defined liquor application using microwave measuring technology combined with a Monforts control unit for an automatic adjustment of the targeted wet pick up. Opposite to padding application, where the final pick up depends on many different parameters such as fabric quality, production speed, surrounding temperature and so on, the Eco Applicator technology always ensures constant liquor add on independently of the mentioned influences. This is valid for any kind of dimension stable fabrics due to a constant fabric weight (g/m²) during the application process. Because of curling selvages and instable dimension in running and cross direction, reliable minimal application methods for knitted fabric could be hardly found in the market. These kinds of fabrics are therefore usually treated in padding processes with very high wet pick up. Additionally to the before mentioned variables influencing the wet pick up in padding processes, knitted fabrics are often very sensitive to tension in length and cross direction. This particular property results in unreliable liquor pick up and limited reproducibility also in padding processes. In the often practiced "wet-in-wet" application for knitted fabrics, the above mentioned properties become even more significant with negative effects on reproducibility, fabric quality and chemical consumption (Figure 2).

**Figure 1** Multi-functional textile
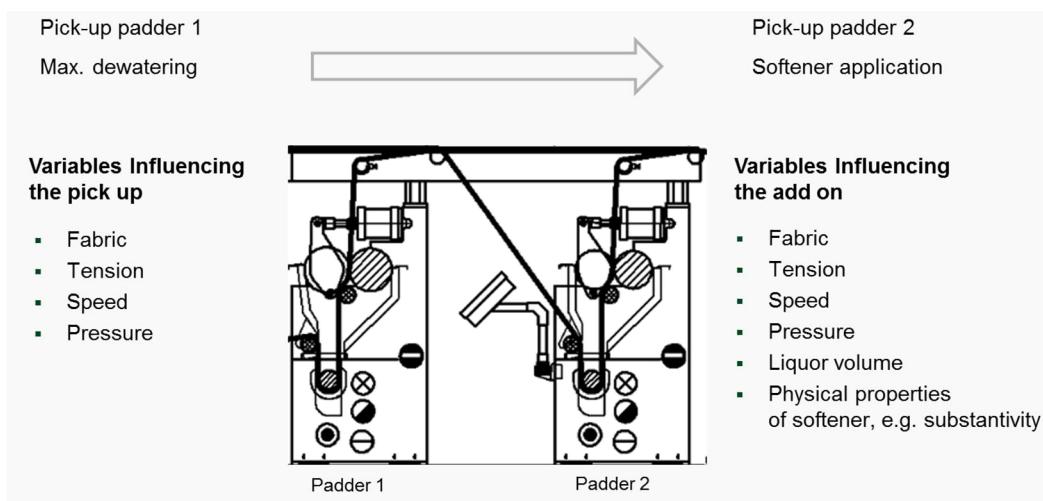
**Figure 2** The scheme of classical wet in wet application
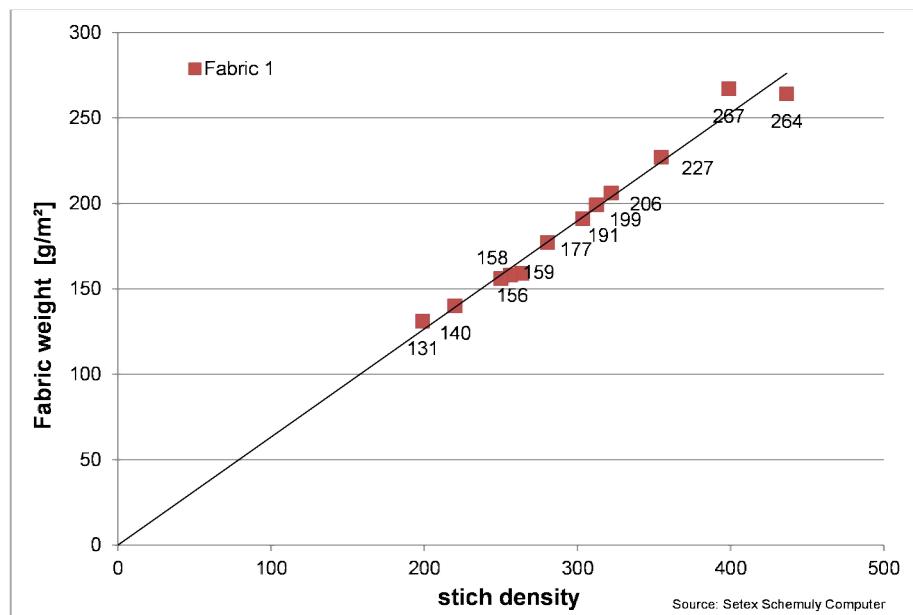
Figure 3 The relation between stitch density and fabric weight

Fabric weight during processing

A reliable online liquor pick up measurement requires precise information about the fabric weight during processing. The specific weight of elastic fabrics is influenced by tension, which is unavoidable in continuous finishing. Therefore standard measuring methods are not suitable for those fabrics. An accurate measuring of the liquor load on elastic fabrics requires parallel information about the fabric weight at this stage. A comprehensive evaluation in the Monforts R&D centre has proved a linear relation between the numbers of meshes or cross points on an elastic fabric as displayed in Figure 3.

Based on this evaluation jointly carried out with Setex Schermuly Computer, Monforts has developed a method to control the liquor add on

precisely related to the current fabric weight. Comprehensive trials have proved significant reduction of liquor load on knitted fabrics by keeping the finishing effects.

3   CONCLUSIONS

Besides knitted and elastic fabrics, the Matex ECO Applicator can be used in a very wide range of applications: home textiles, smart clothes, building textiles, medicine/hygiene and further Techtex areas. The new unit achieves a maximum energy saving of more than 50% because moisture that is not applied to the textile fabric does not have to be dried. Additionally, water and in some cases chemicals will be saved. The ecological benefit due to CO_2 reduction is significant.

ADVANCED TEXTILES WITH ENHANCED ELECTRICAL CONDUCTIVITY

V. Tunáková and J. Militký

Faculty of Textile Engineering, Technical University of Liberec, Studentská 2, 46117 Liberec, Czech Republic
veronika.tunakova@tul.cz

Abstract: *The purpose of the paper is to describe the present state of a fabrication and characterization of advanced multifunctional lightweight, flexible and porous textile structures with significantly increased electrical conductivity. First of all, electrical properties and electromagnetic shielding effectiveness of traditional nonconductive textile materials are introduced. Further three of today's most commonly used methods for preparation of electrically conductive textile structures or transforming a nonconductive textile substrate to a conductive one are described. These planar textile structures with enhanced electric conductivity are studied in terms of their functionality which is represented by surface resistivity and the ability to shield electromagnetic field. Because of disparity of used methods, benefits and disadvantages associated with utility properties including chosen physiological comfort properties and durability in use are also discussed.*

Key Words: *textile structures, electric conductivity, electromagnetic shielding, utility properties*

1   INTRODUCTION

In recent years, conductive fabrics have attracted increased attention especially for electromagnetic shielding, creation of conductive paths, wearable antennas and heating elements or anti-electrostatic purposes. This is mainly due to their desirable flexibility and light weight compared to traditional materials based commonly on metal sheets or metal wires. Therefore the main aim of many researchers is to find a way of preparing an electrically conductive textile structure (fibre, yarn, fabric) preserving main characteristics of traditional fabrics such as handle, drape, elasticity, appearance, low weight, transport properties (water vapour and air permeability) and also process ability involving cutting, sewing, printing etc.

Most synthetic fibers used in the textile industry are electrical insulators with specific resistance (resistivity) of the order of 10^{12} to 10^{14} Ω.m depending on humidity and temperature of air. This is inconvenient for static electricity discharge needs or electromagnetic shielding in areas where it is necessary to eliminate electromagnetic radiofrequency radiation. E.g. resistivity for antistatic materials ranges from 10^2 to 10^9 Ω.m (corresponding to the surface resistivity of about 10^5-10^{12} Ω), while materials intended to shield the electromagnetic field have to have a resistivity lower than 10 Ω.m (corresponding to surface resistivity lower than 10^4 Ω).

One way of creating conductive fabrics is using minute electrically conductive fibers (metal, carbon or conductive polymer fibers). They can be produced in filament or staple lengths and can be incorporated into traditional non-conductive fibers to create yarns or nonwovens that possess varying degrees of conductivity [1-5]. Incorporation of metal fiber or metal wire is a very common method for improving electrical conductivity of fabric now. Even if very fine metal fibers (8 μm diameter) are commercially available today, their flexural rigidity is still higher compared with traditional fibers, either natural or polymeric. That is why ends of metal fibers jutting from textile structure can cause skin irritation. Totally different density of metal fibers compared to traditional fibers (e.g. 910 kg/m^3 for polypropylene and ca 8000 kg/m^3 for stainless steel) can cause another problem especially during the mixing stage of spinning process, leading to a significant irregularity of yarn. Another way represents conductive coatings which can transform substrates into electrically conductive materials without significantly altering the existing substrate properties. They can be applied to the surface of fibers, yarns or fabrics. The most common are metals [6] and conductive polymer coatings [7]. Main disadvantages are that plated metal or conductive polymer coating can be easily peeled off the fiber during processing and usage and therefore they have a poor durability in use. Their color (metallic or conductive polymer color – e.g. polypyrrole is black) is also sometimes undesirable for textile use. Fibers containing carbon black or other conductive particles within can also be used [8]. To gain proper conductivity of conductive fiber, it is necessary to use a large amount of at least 15 wt % conductive particles. This large amount of conductive particles causes the fiber-producing process to be difficult, complex and expensive. Also, it is impossible to contain the

carbon black in the inside of natural fibers. Especially when preparing electrically conductive fabrics for clothing, we have to face some limitations and difficulties. The conductive component has to be embedded in textiles in such a way that the flexibility and comfort of the fabrics be retained. Fibers and fabrics have to meet special requirements concerning not only conductivity but also processability and wearability: (a) the fibers have to be able to withstand handling that is typical for textiles, for example weaving, washing and wrinkling, without damaging of their functionality, (b) fibers used for clothing have to be fine and somewhat elastic in order to be comfortable to wear, (c) fabrics need to have low mechanical resistance to bending and shearing so that they can be easily deformed and draped. The closer the textiles are to the body, the more flexible and lightweight they have to be. Fabrics have to be lightweight (preferably no more than 250 g/m^2), permeable to air and water vapor and washable like other cloths without impairment of the electric conductivity. Moreover, fabrics should be dyeable so that pleasing and fashionable articles of clothing can be made of it.

This paper introduces the present state of fabrication and characterization of different multifunctional lightweight, flexible and electrically conductive textile structures developed within our research. Three most common methods of the preparation of electrically conductive fabrics will be described, their functionality will be evaluated by the help of measuring electric resistivity and electromagnetic shielding effectiveness and also comfort properties together with durability in use will be discussed.

2   EXPERIMENTAL

Materials

The set of total 12 fabrics of different material composition and structure (woven, knitted, nonwoven) was investigated.

The first group of six samples represents nonconductive woven fabrics with different weave, thickness and material composition to show electric and electromagnetic shielding ability of traditional textile materials.

The second group of four samples is made of so-called hybrid yarns. These yarns were composed of conventional polypropylene (PP) fiber and different content of staple BEKINOX stainless steel (SS) metal fibers. The aspect ratio (length/diameter ratio, l/d) of the SS used in this study is 6250, since the diameter of the SS is 8 µm and the fiber length of the SS is 50 mm. In this study, TREVON polypropylene fiber with a fineness 2.2 dtex and 50 mm length was used as the nonconductive component. The two components were mixed at the drawing frame and a ring spinning system was used to produce blended yarns. Hybrid yarns were prepared in two different linear densities: (a) single yarn (fineness of yarns was 25 tex), (b) two ply yarns (fineness of yarns was 2x25 tex). Woven samples (W1, W10, W20) were made of 100% hybrid yarn (T=2x25 tex) containing different portion of conductive phase, namely 1%, 10% and 20%. Knitted sample (K15) was also made of 100% hybrid yarn (T=25 tex) containing 15% of stainless steel fiber.

The third group of samples is represented by polyester fabric/polypyrrole composite (PES/PPy) prepared by chemical oxidative polymerization of pyrrole onto a 100% polyester textile substrate. In this experiment, pyrrol monomer concentration was 5.8 g/L, polymerization temperature was 6.7°C and polymerization time was 10 h. The weight ratio among monomer, oxidizing agent (iron (III) chloride hexahydrate) and dopant (p-toluenesulfonic acid monohydrate) was 1:5:3.

The fourth group of samples is represented by very thin 100% polyester filament cross laminated nonwoven metallized with copper (PES/Cu).

Table 1 Characteristics of the sample set

| Sample	Composition	Warp/weft count [tex]	Fabric structure	Thickness [mm]	Mass per unit area [g/m^2]
100% PES	100% polyester	-	woven	-	-
100% CV	100% viscose	-	woven	-	-
100% CO	100% cotton	-	woven	-	-
100% LI	100% linen	-	woven	-	-
100% WO	100% wool	-	woven	-	-
50%PES/50% WO	50% PES/50% WO	-	woven	-	-
W1	1% SS/99% PP	25x2/ 25x2	woven	0.78	233.5
W10	10% SS/90% PP		woven	0.75	221.0
W20	20% SS/80% PP		woven	0.71	208.8
K15	15% SS/85% PP	25	knitted	0.65	149.9
PES/PPy	100% PES+PPy	35	woven	0.51	195.6
PES/Cu	100% PES+Cu	10µm filament	nonwoven	0.07	16.6
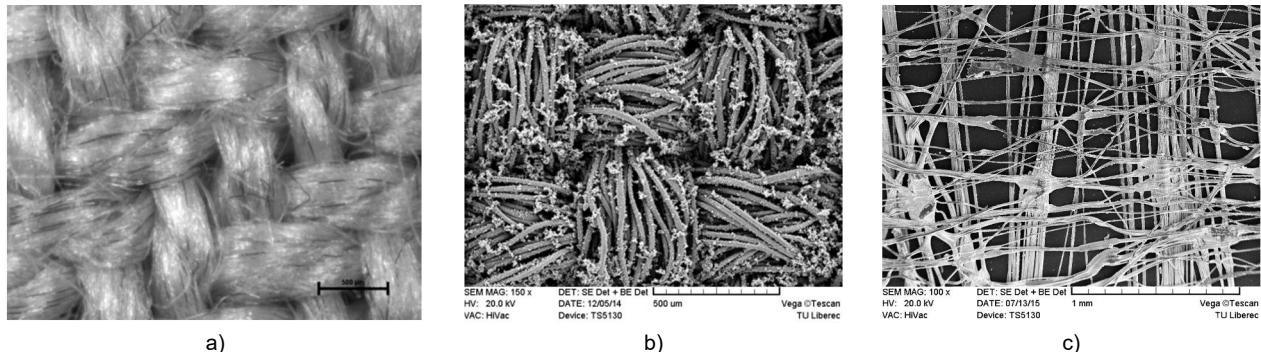
Figure 1 Microscopic images of sample: (a) W20 woven fabric containing 20% of conductive component, (b) PES/PPy woven fabirc (c) PES/Cu nonwoven fabric

Prior to the metallization of nonwoven filaments, plasma pre-treatment of the sample was used to get a higher surface tension. Samples were then autocatalytically activated with tin and silver. Finally, metallization of the sample was performed from copper salt solution; consumption of copper was 3 g/m^2. The characteristics of the sample set are shown in Table 1. Microscopic images of fabrics with incorporated conductive component (metal fiber, polypyrrole and copper particles) are shown in Figure 1.

Statistical analysis of small samples

Due to the very small sample sizes $4 \leq n \leq 20$ available for the evaluation process of electrical and electromagnetic shielding properties, a procedure based on order statistics introduced by Horn [9] was used. It is based on the depths which correspond to the sample quartiles. The pivot depth is expressed by:

$$H_L = \frac{int\left(\frac{n+1}{2}\right)}{2} \quad or \quad H_L = \frac{int\left(\frac{n+1}{2}+1\right)}{2} \qquad (1)$$

according to which H_L is an integer. The lower pivot is $x_L = x_{(H)}$ and the upper one is $x_U = x_{(n+1-H)}$. Note that the $x_{(i)}$ are ordered statistics i.e. $x_{(i)} <= x_{(i+1)}$. The estimate of the parameter of location is then expressed by the pivot half sum:

$$P_L = \frac{x_L + x_U}{2} \qquad (2)$$

and the estimate of the parameter of spread is expressed by the pivot range:

$$R_L = x_U - x_L \qquad (3)$$

The random variable:

$$T_L = \frac{P_L}{R_L} = \frac{x_L + x_U}{2(x_U - x_L)} \qquad (4)$$

has an approximately symmetric distribution and its quantiles are given in [9].

The 95% confidence interval of the mean is expressed by pivot statistics as

$$P_L - R_L t_{L,0.95}(n) \leq \mu \leq P_L + R_L t_{L,0.95}(n) \qquad (5)$$

and analogously, hypothesis testing may also be carried out. For small samples ($4 \leq n \leq 20$), the pivot statistics lead to more reliable results than the application of Student's F-test or robust t-tests.

Electric conductivity evaluation

Electric conductivity is a measure of the electron mobility in a material, with the units of Siemens per meter [S/m]. Usually it is calculated from its inverse: the electric resistivity [Ω.m]. When measuring planar materials of undetermined thickness, such as coatings on textiles, it is preferred to approximate it in terms of surface resistivity. This parameter is measured by contacting only the surface of the material, neglecting the thickness entirely, yielding the resistance of a square of any size, Ω. The electrical surface resistivity of the samples was measured according to the standard of the AATCC Test Method 76-2000, using two concentric ring electrodes, at the read voltage of 1 V, at temperature 22.3°C and relative humidity 40.7%. Measurement results were recorded 60 s after the moment of placing the electrodes on the textile sample. Surface resistivity is measured by applying a voltage potential between two electrodes of specified configuration which are in contact with the same side of the material under test. Surface resistivity ρ_S [Ω] was calculated from the relation:

$$\rho_S = R_S \frac{2\pi}{ln\left(\frac{R_2}{R_1}\right)} \qquad (6)$$

where R_S [Ω] is surface resistance reading, R_1 outer radius of the center electrode [m], R_2 inner radius of the outer ring electrode [m]. The measurement was carried out at 20 different places of textile samples because of subsequent statistical analysis, $\alpha=0.05$, $t_{L,0.95}(20) = 0.266$.
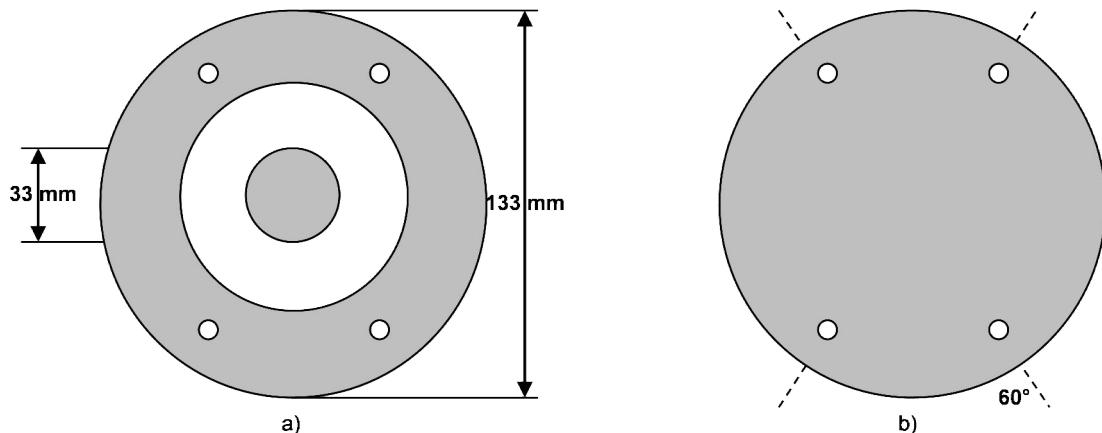
Figure 2 Illustrations of a) reference and b) load sample

Electromagnetic shielding ability

Electromagnetic shielding effectiveness (SE) of the multifunctional lightweight, flexible and porous fabrics was measured according to ASTM D4935-10, for planar materials using a plane-wave, far-field EM wave. SE of samples was measured over frequency range of 30 MHz to 1500 MHz. The set-up consisted of a sample holder with its input and output connected to the network analyzer. An electromagnetic shielding effectiveness test fixture (Electro-Metrics, Inc., model EM-2107A) was used to hold the sample. The design and dimension of sample holder follows the ASTM method mentioned above. Network analyzer Rohde & Schwarz model ZNC3 was used to generate and receive the electromagnetic signals. The standard mentioned above determines the electromagnetic shielding effectiveness of the fabric using the insertion-loss method. A reference measurement for the empty cell was required for the electromagnetic shielding effectiveness assessment. A "through" calibration by the help of the reference sample was made first. A load measurement was performed on a solid disk shape sample subsequently. The reference and load specimens must be of the same material and thickness. Sample (both reference and load) geometries according to ASTM D4935-10 are shown in Figure 2. The measurement was carried out at the temperature of 22.3°C, relative humidity 40.7% and at 5 different places of textile samples because of subsequent statistical analysis, α=0.05, $t_{L,0.95}(5) = 1.37$.

Chosen comfort properties

Thickness, mass per unit area, air permeability, stiffness, appearance, drape and handle were evaluated by the help of conventional measurement techniques.

3   RESULTS AND DISCUSSION

Electric conductivity

The mean values estimator (pivot half sums) and confidence intervals for means of surface resistivity ρ_S are summarized in Table 2. Comparison of surface resistivity for all samples is displayed in Figure 3. It is clearly visible that fabrics made totally of traditional natural or synthetic fibers have the highest surface resistivity (more than 10^{12} Ω) and hence the lowest electric conductivity from whole sample set. When using some conductive component (metal fiber, polypyrrole or metal particles), surface resistivity decreases even down to 184 Ω for metal coated fabric. This decrease is ten orders of magnitude compared with traditional textiles. When investigating woven fabrics containing metal fiber, it was confirmed that there is a rapid decrease in surface resistivity with increasing metal fibers content - about four orders of magnitude between 1% and 20% metal fiber content in these hybrid fabrics. It can also be observed from this sample set (fabrics with incorporated metal fiber) that knitted structure containing 15% of metal fiber has higher surface resistivity compared to woven fabric containing only 10% of metal fiber. This phenomenon is caused by their more open structure, higher porosity and therefore greater amount of air (which is a very good insulator) inside the structure of knitted fabric compared with woven ones.

Table 2 Mean values and 95% confidence intervals of mean for surface resistivity and electromagnetic shielding effectiveness for frequency 1.5 GHz

Sample	Surface resistivity ρ_S [Ω]		Electromagnetic shielding effectiveness SE [dB]	
	P_L	95% CI	P_L	95% CI
100% PES	>1E+12	-	0	-
100% CV	>1E+12	-	0	-
100% CO	>1E+12	-	0	-
100% LI	>1E+12	-	0	-
100% WO	>1E+12	-	0	-
50%PES/50% WO	>1E+12	-	0	-
W1	3.16E+07	±2.37E+07	13.16	±0.86
W10	3.61E+04	±6.25E+03	28.89	±0.32
W20	1.87E+03	±4.18E+02	34.59	±0.33
K15	9.93E+06	±2.62E+06	9.65	±1.10
PES/PPy	6.26E+07	±9.01E+06	17.92	±0.72
PES/Cu	1.84E+02	±8.07E+01	47.46	±2.80
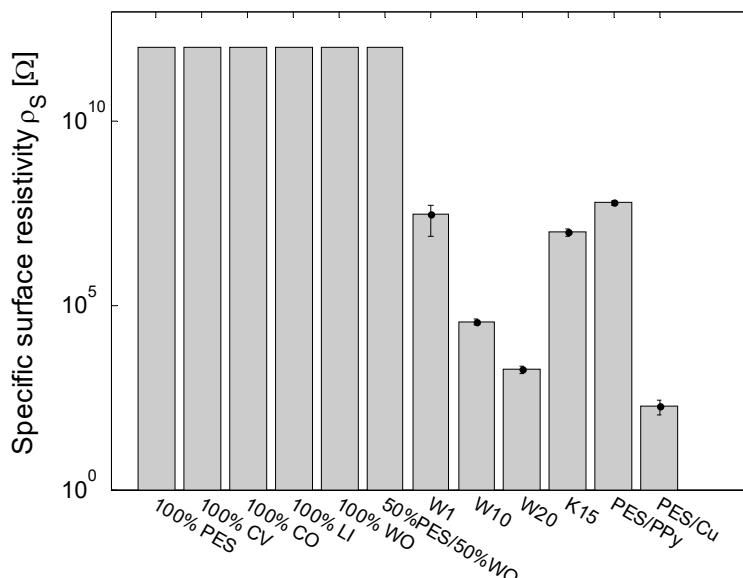
Figure 3 Comparison of surface resitivity (mean values represented by pivot half sums and 95% confidence intervals of means) for whole sample set

Electromagnetic shielding ability

The mean values estimator (pivot half sums) and confidence intervals for the means of electromagnetic shielding effectiveness SE for frequency 1.5 GHz are summarized in Table 2. This particular frequency was chosen from the measured frequency range (30 MHz – 1.5 GHz) because it is close to the working frequency of communication networks including GPS navigation devices, cell phones (GSM 1800) and radars. It is visible that all nonconductive traditional fabrics in dry state are totally transparent to electromagnetic wave and that is why they have zero shielding ability as shown in Figure 4a), where frequency dependence of electromagnetic shielding effectiveness (SE) for nonconductive textile structures is displayed.

Figure 4b) shows the variation in SE for all groups of conductive fabrics with incident frequency in the range 30-1500 MHz. It is visible that samples which

contain some conductive component are able to shield electromagnetic field with different efficiency.

The highest shielding effectiveness is provided by metal coated sample (almost 50 dB at frequency 1.5 GHz). SE is almost constant throughout the whole measured frequency range for this sample.

Very good results can be also achieved by mixing nonconductive fibers with extremely thin stainless steel fibers during spinning process, especially for more compact (less porous) woven structures with higher amount of metal fiber (>5%). It was confirmed that the electromagnetic shielding effectiveness increased logarithmically with the increasing frequency for these hybrid woven samples. As the frequency increases, the wavelength of the electromagnetic wave decreases and becomes closer to the size of the metal fiber. At higher frequencies, waves are more likely to encounter fiber embedded in the polymer matrix and hence, SE increases as the frequency

increases. Dependence of SE on frequency for hybrid knitted sample behaves differently compared with hybrid woven samples. Frequency dependence of knitted samples SE was approximated by cubic spline function with smoothing parameter p → 0, which possesses a sufficiently high degree of smoothness. The position of the SE global maximum can be observed at the frequency of about 1.1 GHz for the sample K15. Generally, knitted samples have lower SE compared to woven ones because of higher porosity and its special structure which does not create a conductive grid as woven structures do.

Application of conductive polymers onto nonconductive textile structure represents another

way of preparing fabrics with some level of shielding ability (about 17 dB at 1.5 GHz). Also in this case, SE is almost constant throughout the whole measured frequency range. It seems that this phenomenon can be observed in systems where the conductive component is present in particle/ nanoparticle form.

In Figure 5, there is a comparison of measured values of electromagnetic shielding effectiveness for all functional samples especially for frequencies 600, 1000 and 1500 MHz. These three frequencies were found interesting because they cover measured frequency range well and they are close to the working frequency of particular electric devices.
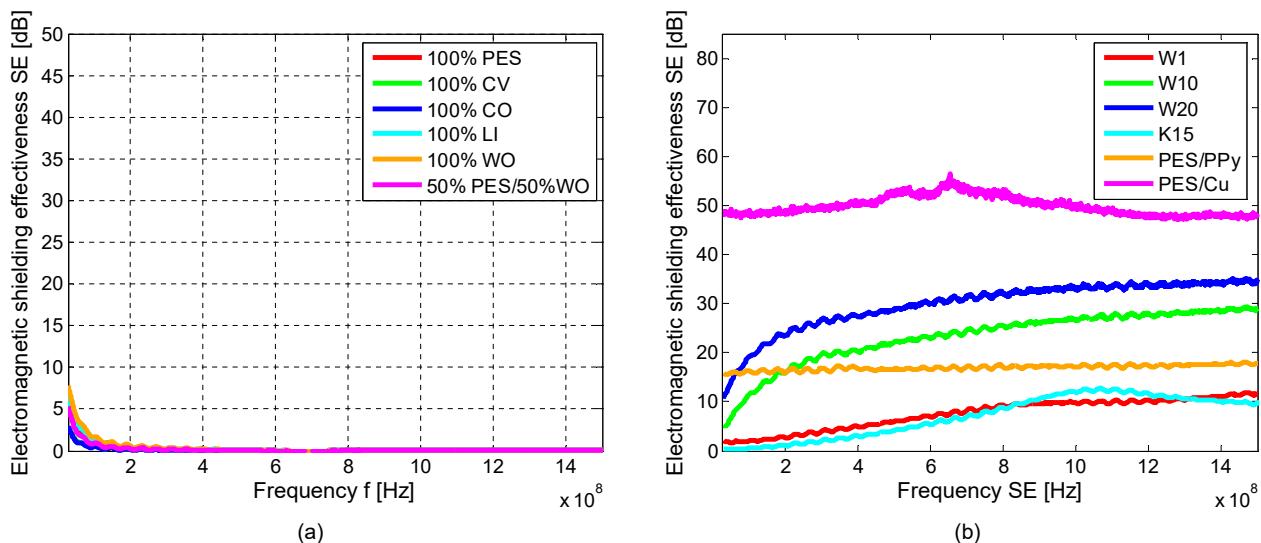

Figure 4 Electromagnetic shielding effectiveness of: (a) traditional nonconductive textile structures, (b) different conductive textile materials measured in frequency range 30 MHz – 1.5 GHz
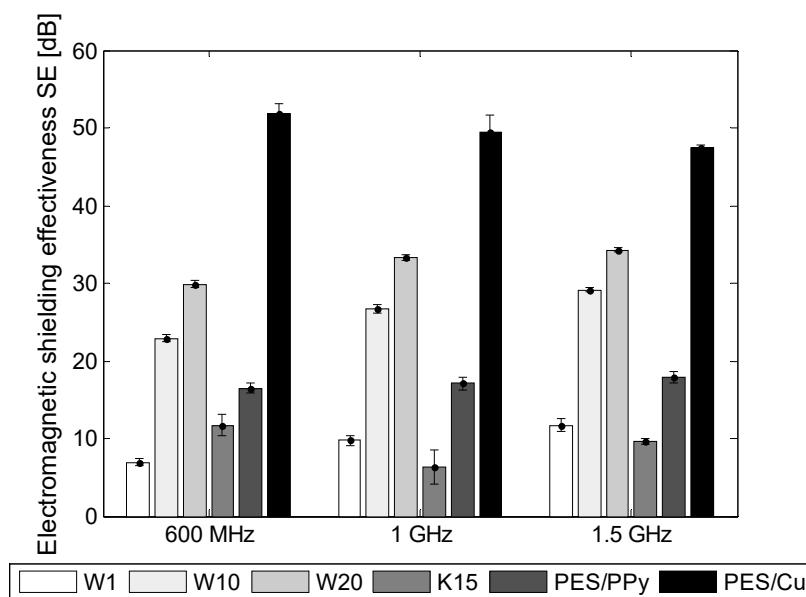

Figure 5 Comparison of electromagnetic shielding effectiveness (mean values represented by pivot half sums and 95% confidence intervals of means) for conductive sample set for different frequencies (600 MHz, 1 GHz and 1.5 GHz)

Many GSM phones support 850 MHz, 900 MHz, 1800 MHz and 1900 MHz band, while Wireless LAN protocols, such as Bluetooth or Wi-Fi uses 900 MHz or 2400 MHz. Based on this graphical evaluation, appropriate sample for given final use can be chosen based on the value of the electromagnetic shielding effectiveness for particular frequency.

Correlation between electric conductivity and electromagnetic shielding ability

It is well known that the SE increases as electric conductivity as well as the permittivity of shielding material increases based on the electromagnetic shielding theory [10] but there is a lack of experimental verification and exploration of this dependence for fiber structures. In addition, direct measurement of fabrics electromagnetic shielding effectiveness is quite complicated especially because of the need for special devices and time consuming preparation of samples. Employing the presumption that the electrical part of electromagnetic field dominates for sufficiently high frequencies seems to be simpler. Knowledge of the electrical characteristics, which are easily measurable, could therefore be used for establishment of electromagnetic shielding effectiveness of textile samples. That is why correlation between surface or volume resistance and electromagnetic shielding efficiency is studied. The dependence of total shielding effectiveness SE for the frequency 1.5 GHz on natural logarithm of surface resistivity is shown in Figure 6. The approximate linearity is visible. The solid line in this graph corresponds to the linear regression model with parameters obtained by the minimizing sum of squared differences. Corresponding correlation coefficient r = 0.963 indicates a good quality of the fit. This graph clearly indicates that for sufficiently high frequencies, it is sufficient to measure only the electric field characteristics. In this graphical evaluation, electromagnetic shielding efficiency at only one frequency (1.5 GHz) was studied. This particular frequency is the maximum one for measuring SE by the coaxial transmission line method. During the research it was confirmed that linear regression model is applicable also for other studied frequencies (900 MHz – 1.5 GHz) with a good quality of fit ($r \sim$ 0.94).

Chosen comfort properties

Fabrics have to meet special requirements concerning not only functionality which is represented by conductivity and electromagnetic shielding measurements in this study, but also processability and wearability. That is why permeability to air and bending rigidity of these advanced textiles were evaluated. Other requirements such as processability, eye appeal, dyeability and washability will be discussed.

Air permeability describes the rate of flow of a fluid through porous media. Air permeability of the textile sample set was measured by FX 3300 instrument according to standard ASTM D737-96 using air pressure differential 100 Pa, area 20 cm^2. The measurement was carried out at 10 different places of textile samples because of subsequent statistical analysis, α=0.05, $t_{L,0.95}$(10) = 0.523. The mean values estimator (pivot half sums) and confidence intervals for means of air permeability are summarized in Table 3. Comparison of air permeability for all samples is displayed in Figure 7.

It is clear that the copper coated extremely thin nonwoven sample has the highest air permeability (> 4400 L/m^2/s) of whole sample set. Air permeability increases (from 100 to 300 L/m^2/s) with increasing metal fiber content for woven samples. Metal fibers are finer than polypropylene fibers and therefore yarn with higher content of metal fiber embodies lower diameter and that is why bigger pores are formed in fabric, allowing easier transport of air (air permeability).

It was confirmed that knitted sample containing staple metal fiber has higher air permeability compared with woven samples (about three times). This output was expected because the knitted fabric was made of finer yarn (25 tex), had lower mass per unit area (150 g/m^2 on the average), and lower thickness (0.65 mm) and therefore higher porosity compared with woven fabrics (T = 50 tex, m = 221 g/m^2, t = 0.75 mm). On the other hand, polypyrrole coated sample has the lowest air permeability from whole sample set. During chemical polymerization process, polypyrrole particles are deposited not only on fiber surface creating a layer, but also in granular form in the yarn interstices (this phenomenon is visible in microscopic images 1b)), which decreases porosity of the substrate significantly. It is expected that there is a correlation between air and water vapour permeability – higher air permeability means higher water vapour permeability.

Bending rigidity is important for both consumer and industrial application of fabrics. While fabric stiffness may not be wanted to be high for a good drape in apparel and garment fabrics, it may be an important requirement especially for industrial fabrics widely used in heavy duty applications such as geotextiles and forming fabrics. Bending rigidity was evaluated using cantilever test. This test was proposed by Pierce and consists simply of allowing a 3 cm wide strip of fabric project as a cantilever from a horizontal platform and of measuring the angle between horizontal line and the chord from the edge of the platform to the tip of the fabric. The length of overhang was 1, 2, 3, 4, 5, 6, 7, 8 and 9 cm. The bending rigidity was calculated for each overhang and, finally, mean value was computed both warpwise and weftwise, see Table 3.
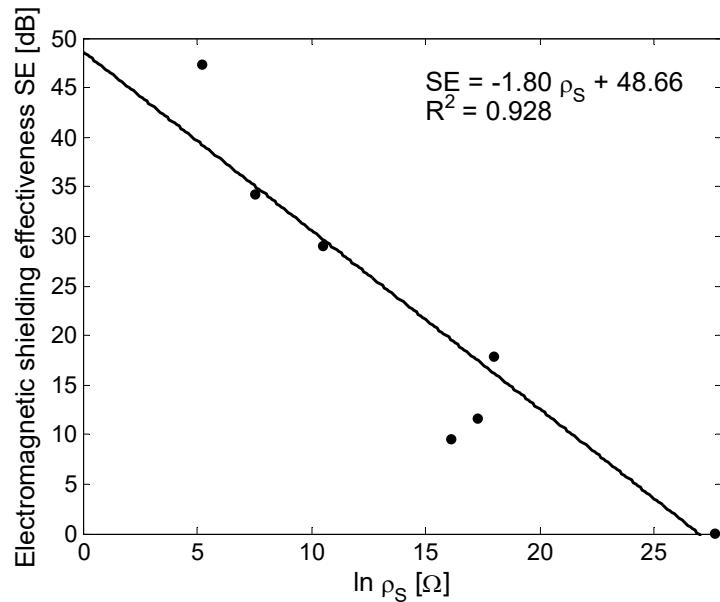
Figure 6 Dependence of electromagnetic shielding effectiveness (f = 1.5 GHz) on logarithm of surface resistivity aproximated by linear model

Table 3 Mean values and 95% confidence intervals of mean for air permeability and mean value of bending rigidity measured in warp and weft direction.

Sample	Air permeability A [l/m^2/s]		Bending rigidity B [10^{-7}Nm^2]	
	P_L	95% CI	warpwise	weftwise
W1	109.90	±3.66	13.70	12.40
W10	190.30	±8.89	8.23	6.99
W20	309.40	±9.77	4.18	3.89
K15	1096.30	±44.12	-	-
PES/PPy	55.88	±6.57	2.83	2.40
PES/Cu	4430.00	±77.74	0.153	
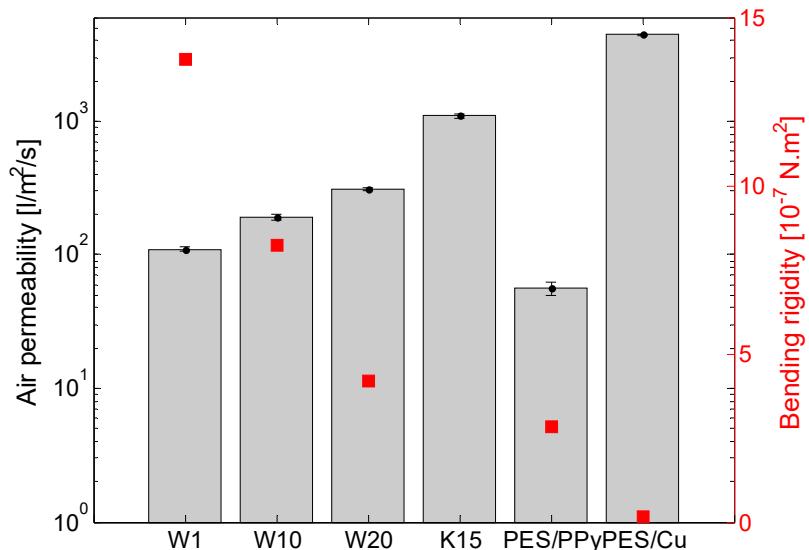
Figure 7 Comparison of air permeability (bars) and bending rigidity (square marker) of all studied samples

Three samples were tested in each case. Bending rigidity of knitted sample was not evaluated, because of edge curling. Comparison of bending rigidity for all studied samples (bending rigidity of woven samples measured in warp direction was chosen as representative) is shown in Figure 7 (red colour). It is visible from this figure that the copper coated extremely thin nonwoven sample has not only the highest air permeability, but also very low bending rigidity ($B \sim$ 1.5E-8 N.m^2). This effect is caused by very low thickness and very low areal density of the sample. The highest stiffness was found in the woven sample with the lowest metal fiber content ($B \sim$ 1.3E-6 N.m^2). It was confirmed that the higher areal density of the sample is, the higher is its bending rigidity.

From the point of view of processability, all studied samples can be easily cut and joined by traditional techniques. Hybrid fabrics with metal fiber content withstand repeated application of wet processing comprising washing and drying very well [10], their colour is light grey and therefore they can be easily dyed or printed. Dark black colour of polypyrrole coated sample can be a limiting factor and also its resistance to washing is not really satisfactory. Metal coated samples generally exhibit a typical metal colour. Adhesion of the coating to the substrate seems to be strong and therefore durability is expected to be favourable. This assumption still has to be proven. It seems that very conductive copper coated extremely thin and lightweight polyester nonwoven substrate can be a good candidate for the production of conductive textile structures, especially due to its low weight, very high permeability to air and therefore the possibility to create sandwich systems with different functional layers.

4   CONCLUSIONS

This paper introduced the present state of fabrication and characterization of different multifunctional lightweight, flexible and electrically conductive textile structures developed within our research. During this research, functionality and chosen comfort properties were evaluated. In addition, processability and other important parameters of conductive textile structures were discussed. It seems that hybrid textile structures are the best choice when producing apparel and garment fabric because they look and behave totally the same as traditional textile fabrics. Due to relatively low electric conductivity they can be used not only for electromagnetic shielding, but also for heating applications or antistatic purposes. On the other hand, metal coated thin nonwoven fabric could be suitable for industrial applications, especially considering sandwich systems, because it has high electrical conductivity while preserving the properties of the substrate – in our case, very low weight, low stiffness and high

transport properties. Due to their relatively high electric conductivity, they can be considered for creation of conductive paths or wearable antennas.

5   REFERENCES

1. Neruda M., Vojtech L.: Heating Ability of Electrically Conductive Textile Materials, In Proceedings of the 16th International Conference on Mechatronics, 631-634, 2014

2. Zhang T., et al.: Evaluation of Electromagnetic Shielding and Wearability of Metal Wire Composite Fabric Based on Grey Clustering Analysis, Journal of the Textile Institute 107(1), 1-8, 2014

3. Safarova V., Militky J.: Analysis of the Electrical and Mechanical Properties of Hybrid Yarns Designated for Protection Against Electromagnetic Field, Vlakna a Textil (Fibres and Textiles) 21(3), 70-73, 2014

4. Ozen M.S., Sancak E., Akalin M.: The Effect of Needle-Punched Nonwoven Fabric Thickness on Electromagnetic Shielding Effectiveness, Textile Research Journal 85(8), 804-815, 2015

5. Jagatheesan K., et al.: Fabrics and their Composites for Electromagnetic Shielding Applications, Textile Progress 47(2), 87-161, 2015

6. Duran D., Kadoglu H.: Electromagnetic Shielding Characterization of Conductive Woven Fabrics produced with Silver-Containing Yarns, Textile Research Journal 85(10), 1009-1021, 2015

7. Varesano A., Dall'Acqua L., Tonin C.: A Study on the Electrical Conductivity Decay of Polypyrrole Coated Wool Textiles, Polymer Degradation and Stability 89, 125-132, 2005

8. Hu T., Wang J., Wang J.: Electromagnetic Interference Shielding Properties of Carbon Fiber Cloth Based Composites with Different Layer Orientation, Materials Letters 158(1), 163-166, 2015

9. Horn P.S.: Some easy t statistics, J. Amer. Statist. Assoc. 78, 930-936, 1983

10. Ott H.W.: Electromagnetic compatibility engineering, New York: John Wiley & Sons, 2009

11. Tunakova V., Technikova L., Militky J.: Influence of Washing/Drying Cycles on Fundamental Properties of Metal Fiber-Containing Fabrics Designed for Electromagnetic Shielding Purposes, Textile Research Journal 2016, In Press

NOVEL METHOD OF ON-LINE COLOR MEASUREMENT

M. Vik[1], F. Founě[2] and P. Škop[2]

[1]*Faculty of Textile Engineering, Technical University of Liberec, Studentská 2, 461 17 Liberec, Czech Republic*
[2]*VÚTS, a.s. Svárovská 619, 460 01 Liberec, Czech Republic*
michal.vik@tul.cz; frantisek.foune@vuts.cz; petr.skop@vuts.cz

Abstract: Dyeing and finishing, being an end of the line process for a textile, traditionally bears a large proportion of the cost of faults. In order to minimize customer rejections and returns, dyers and finishers are forced to suffer the high labor costs associated with detailed manual inspection. And manual inspection is not always a guaranteed solution to the problem. Computer vision systems are large and complex, typically involving multiple planes of cameras with several cameras on each plane, and numerous lighting arrangements. The operation of such machines has, in the past, been an unwieldy task. Traditionally, the process of setting up such systems used to be long and arduous with multiple sets of parameters needing to be set for each differing material, color, customer or batch number. Such number of parameters together with the variability of present day cameras and the technologies available on the market today vary widely. Based on that, VÚTS has developed a new color sensor for the on-line textile quality control system focusing on high traceability of measured data between on-line and off-line measuring systems. This paper describes the features of this color sensor and a deep analysis of factors influencing measured colorimetric data.

Key Words: colorimetry, spectrophotometer, on-line color measurement, quality control, textile

1   INTRODUCTION

In-line color monitoring, properly configured and used, can produce substantial savings in dyeing and finishing operations. When continuous dyer has to make an adjustment to correct a shade variation, it would be of great benefit for him to know whether the change had originated on or before the dye range [1]. Such work would be a part of a larger study to help the continuous dyer to rapidly distinguish between the color variations which he can control and those which he cannot. Some companies utilize on-line systems for measuring and, in some cases, controlling color. Because of this movement, there are ever-increasing opportunities to compare on-line and laboratory measurements [2]. Since a number of companies produce both laboratory and in-line systems for different industrial applications such as pulp and paper, food industry, we get a lot of questions related to why lab and on-line measurements do not agree. There are several reasons for which the instruments can disagree; yet each reading is, in itself, "correct". What are those reasons? The geometry differences between sensors, product backing difference, calibration basis difference, product condition difference at the time of measurement, effect of different light source spectral content on fluorescent dyestuff or FWA and sensor differences [3].

The conditions surrounding on-line color measurement make it fundamentally different from measurement in the laboratory. The basic requirement of on-line measurement is the fact it must be contact-free. Moreover, the distance between the optical measuring head and the object to be measured is unfortunately difficult to fix and is often subject to variations.

The color of the ideal diffuse surface does not depend on the geometry of the measurement. Therefore it is enough to measure it at one viewing angle and one illumination angle in order to characterize the surface reflection of the diffuse surface. Traditionally, it is measured in on-line measurement at following geometries: 0°:0° and 45°:0° or 0°:45° either directional (45°x:0° or 0°:45°x) or circumferential (45°a:0° or 0°:45°a). One of the known exceptions is X-Rite VeriColor Spectro with 30°x:0° measuring geometry and ERX130 with 0°:0° geometry on the 22.5° angle to the product [4]. The measurement geometries are shown in Figure 1.

How many measuring geometries are used in the production lab? The answer is typically two, but exactly, more. Because diffuse measuring geometries are used in two modes: specular component included (di:8°) and specular excluded (de:8°); as an addition, in pulp and paper industry, a special diffuse measuring geometry d:0°, which is specular excluded. Of course, directional geometries are also used [5].

It is necessary to understand that treatment of non-diffuse reflection is different for each measuring geometry. Consider a high gloss – it is not captured by the receptor of directional geometries (45°:0° or 0°:45°), only diffusely reflected light.
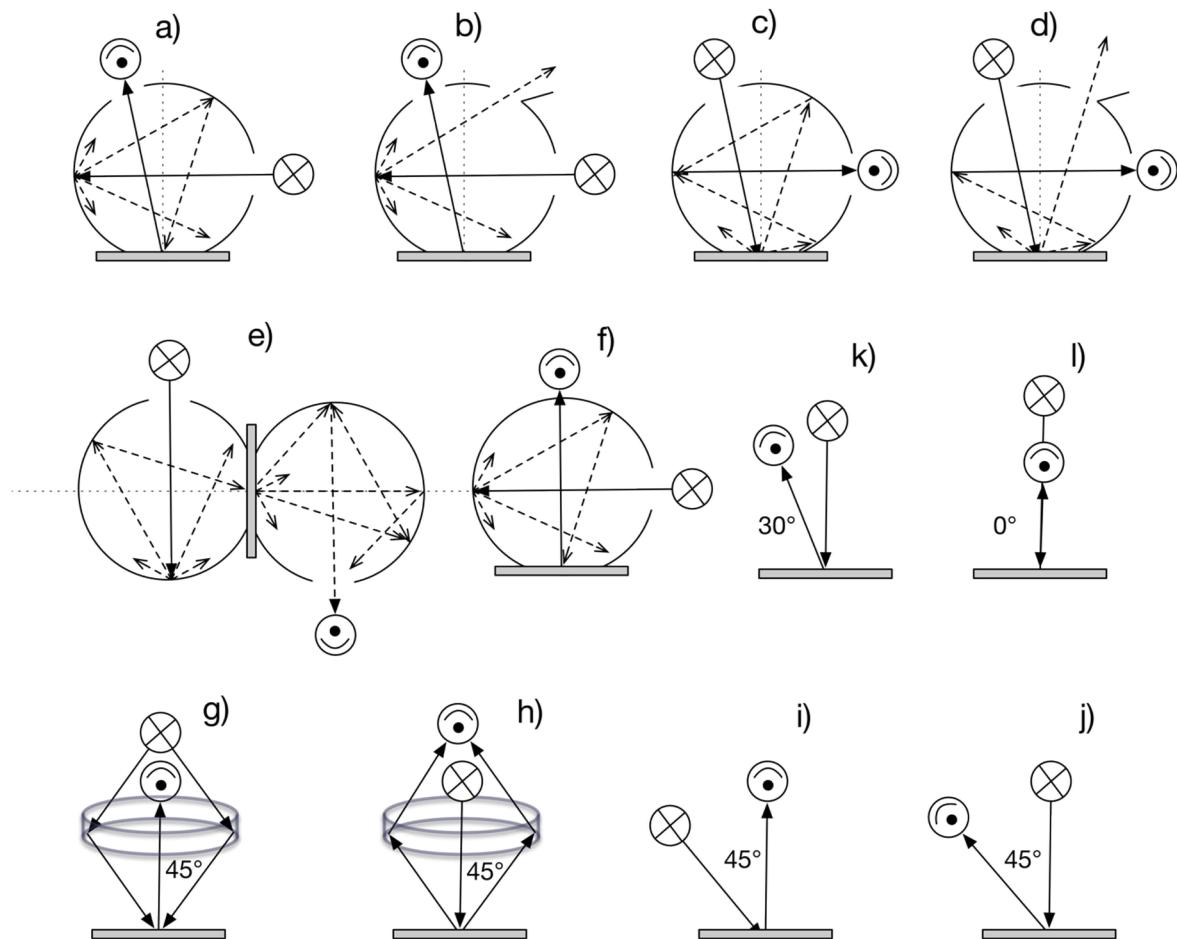
Figure 1 Schematic representation of geometries used in the color measurement

When compared with measurements made by a di:8°measuring geometry of a lab instrument, the readings will be different. In the same fashion, color difference measurements between the standard and the product could be different depending on the gloss difference between the product and the standard. For example, color appearance of glossy samples will appear duller on a di:8°device in comparison with a device equipped with 45°a:0° viewing geometry.

The physical data on reflection that are obtained from the device is the radiance of the surface. The radiance of the surface is converted into reflectance by dividing it by the radiance value of the white reference. The reflectance of the surface R_λ at each wavelength λ is supposed to be independent of the light source. Subtracting the radiance of the dark surface compensates the offset due to dark current [6]. But in practice, entirely closing the light source and blocking any light from entering, the lens measures the radiance of dark surface. Equation (1) gives the reflectance of the surface relative to the white surface used. The reflectance is independent of the illumination and sensitivity of the detector.

$$R_\lambda = \frac{sample_\lambda - dark_\lambda}{white_\lambda - dark_\lambda} \qquad (1)$$

If the reflectance factor f_λ of the available white reference surface with respect to the perfectly diffuse white surface is known, Equation (1) is written as follows:

$$R_\lambda = \frac{sample_\lambda - dark_\lambda}{white_\lambda - dark_\lambda} f_\lambda \qquad (2)$$

Here $sample_\lambda$, $white_\lambda$ and $dark_\lambda$ are the radiance values at each wavelength of the measured sample, white and dark reference, respectively. Similarly, f_λ is the reflectance factor of the white reference. The reflectance factor of the white reference is the ratio of the radiance of the white reference to the ratio of the perfectly diffuse white surface. In laboratory, calibration procedure is relatively simple because the operator can place individual standards on the measuring aperture. In case of on-line systems, it is necessary to use an overall solution, which means that the auto calibration feature has been integrated into the measuring head and is controlled by the actual

measuring system. Obvious design contains a rotary plate, which includes a black standard, white standard and, frequently, validation standard. Depending on the ambient conditions, calibration interval ranges between 30 minutes and several hours [7].

Another difference from color measurement in the laboratory consists in single-layer material used in production which, in case of thin fabric, gives rise to the problem of translucency and hence to a certain fluctuation in the measured data resulting from minor differences in local fabric texture, as will be visible in Figure 3.

The environment in which the process is performed necessitates systematic adaptation of the hardware. Apart from the problems caused by high ambient temperatures, contamination, vibrations, electrostatics, etc., it is necessary to take into account that the measuring procedure must be fully automatic and that manual intervention, e.g. for system calibration, is not possible. As a result, exacting technical demands are made on the stability and the degree of automation of such a measuring system; fast and easy maintenance involving as little handling as possible of the components installed in the machine is also essential.

2   EXPERIMENTAL

VÚTS has developed a new color sensor for the on-line textile quality control system, which tries to solve all above-mentioned problems. The simplified optical scheme of this new concept can be seen in Figure 2. Contrary to off-line measurement, where measured sample is in close contact with the measuring aperture, here a controlled gap between integrating sphere and fabric loop is used. That means that diffuse measuring geometry is used (di:8°). This dual beam spectrophotometer measures the reflectance value of each color at every 10 nanometers across the visible spectrum, 31 points of information to define the color. As the entire spectrum 380 nm to 780 nm commonly used in color measurement is simultaneously imaged and recorded on a diode array, the actual measuring time lies in the range of thousands of seconds, thus the corresponding area of the measured loop is near to the area of entrance aperture. A directly connected PC calculates the basic physical data, i.e. the reflectance spectrum from which the tristimulus values are determined in accordance with the relevant CIE or ISO standards. The VUTS in-line spectrophotometer eliminates the need for a "correction algorithm for ambient light", which can cause metamerism [8] or "look up tables" for *L*a*b** data, or "special calibration for Status T" as needed by camera solutions or by long distance measuring systems. The whole prototype of VUTS

measuring system was for more than one year tested in Textile Company Nova Mosilana, member of MARZOTTO Group. In this initial implementation of on-line color measurement, however, we have opted for an overall solution within our system, which means that the auto calibration feature and positioning of measuring head was semi-automatic.
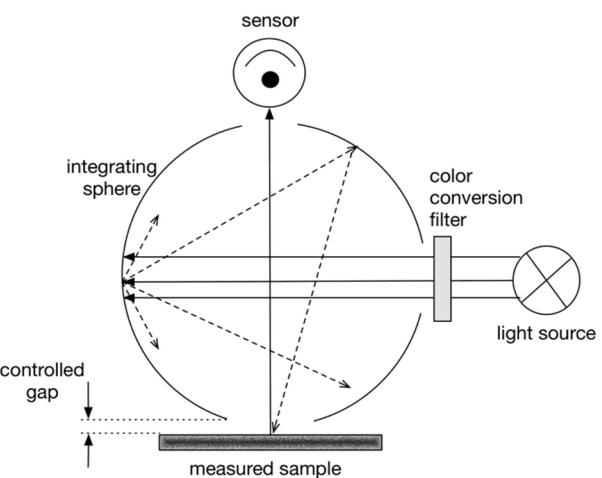

Figure 2 Schematic representation of geometries used in the color measurement

As mentioned above, one of the focal points in the development was to find a measuring geometry which would permit the implementation of a large number of additional, process-specific features: contact-free measurement, large measuring area, oscillation tolerance, enclosed design, automatic calibration, insensitivity to electric discharges in the kV range, etc. These requirements were met with a robust design of on-line system, which is represented in Figure 3. Table 1 gives an overview of the technical data of the on-line color measuring system from VUTS.
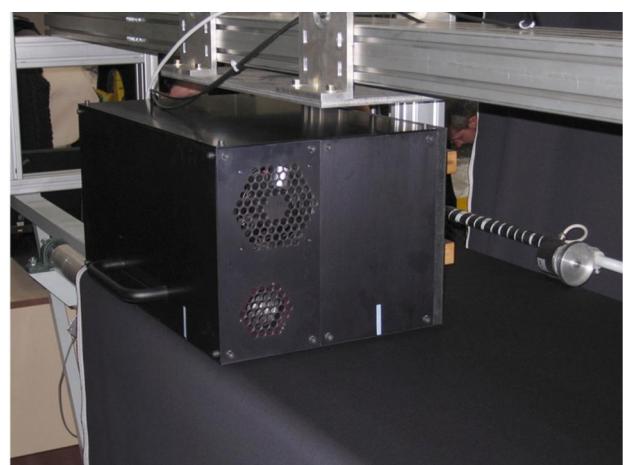

Figure 3 Schematic representation of geometries used in the color measurement

**Table 1** VUTS on-line measuring system technical specification

Feature	Description	Feature	Description
Instrument Type	Dual-beam spectrophotometer	Photometric Range	0 to 200%
Measurement Geometry	Diffuse illumination and 8° viewing	Aperture diameter	40 mm
Sphere Diameter	152 mm / 6.0 inch	Interface	USB 2.0 and higher
Spectral Analyser	Two independent spectral channels of spectrograph which are arranged in one housing, and an embedded linear detector with 2x2048 pixels	Power Requirements	850 to 1250 VAC, 47 to 63 Hz, 300 VA peak, 220 VA typical
Spectral Range	400 nm to 700 nm (extended version 380 - 780 nm)	Absolute Operating Range	10° to 40 °C, 20% to 80% noncondensing rel. humidity
Reporting Interval	10 nm (measured 2.5)		

3   RESULTS AND DISCUSSION

In-line measurement, in contrary to off-line measurements, is designed for the measurement of moving fabric. It is simple to understand that the speed of movement can vary due to time and position of fabric in respect to the measuring head. Based on that, sensitivity of colorimetric data on speed variability of the measured fabric was tested. In the graph in Figure 4 it is visible that the measured data are more sensitive at short frequencies in speed variability in comparison to high difference of speed at the start of the measurement. This effect confirms the backing problem, as was mentioned before. That means speed variability will cause difference in fabric

tension and consequently, difference in opacity. Based on that, considering the measuring conditions (individual measurements, not exactly identical measuring points), the measurement on stationary and moving material displays a very high degree of correspondence, as visible in the chart in Figure 5. The measuring speed has no effect on the results.

The problem of oscillation tolerance in particular, however, must be given special attention in optical design and mentioned data filtering. In our system, such problem was solved by FFT filtering of measured data based on known frequency, speed variability from the speed sensor of the measuring device.
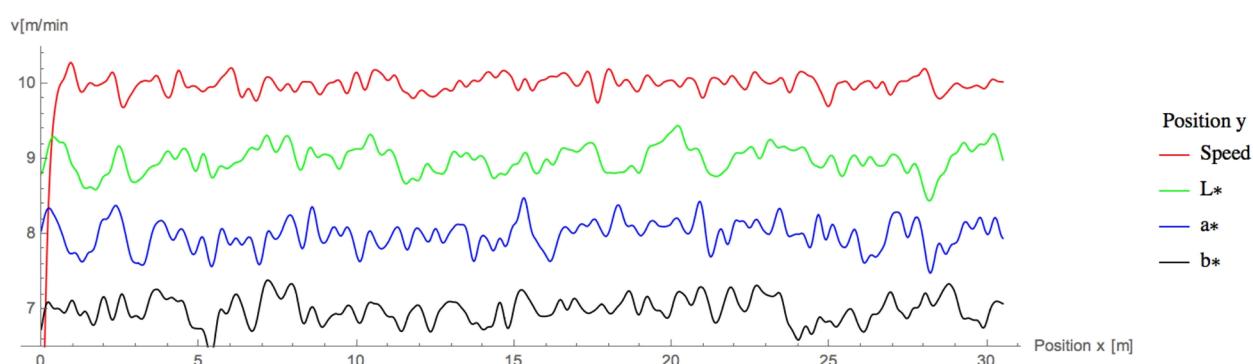
Figure 4 Comparison of colorimetric parameters of deep blue shade woolen fabric and its speed variability
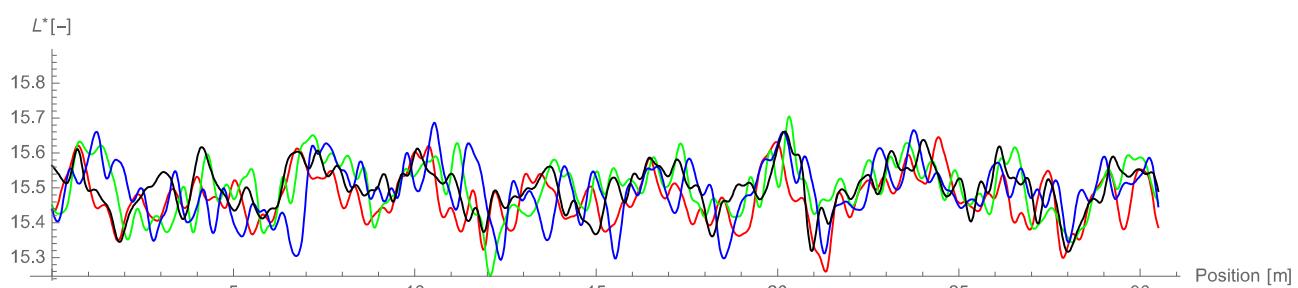
Figure 5 Comparison of lightness $L*$ of deep blue shade woolen fabric measured at different speed levels: red line: 10 m/min, green line: 16 m/min, blue line: 22 m/min and black line: repetition of 10 m/min
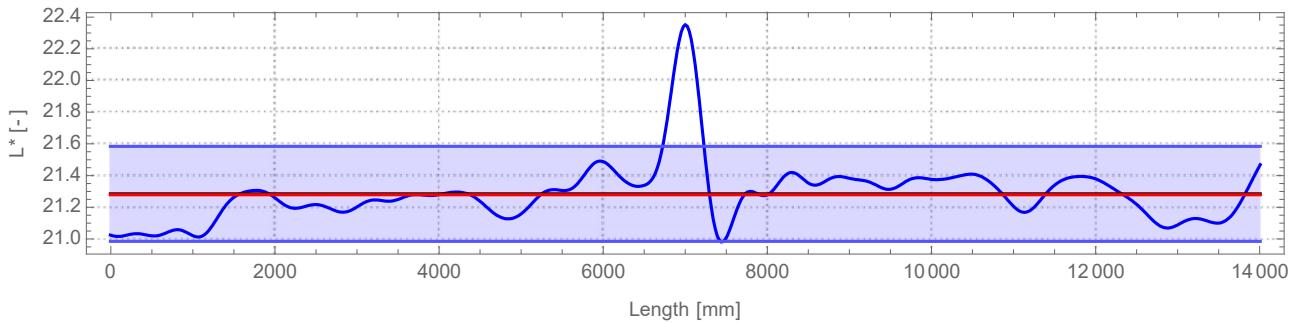
Figure 6 Filtered lightness *L** data of deep grey fabric sewn in the middle from two parts (the seam causes a peak of lightness value at distance of 7 meters)

Another important parameter in on-line is the insensitivity of the measured data to distance fluctuation between the measuring head and the textile fabric to be measured. The obvious optical design allows variation of 3 to 4 mm without causing a change in the lightness value of more than *ΔL**=0.25. This does not apply to our solution, due to the request of a customer to be able to measure color difference near to just noticeable limit [9] with 95% probability. Considering the measuring results to be with improved traceability

with laboratory measurement, we use a thin gap between the fabric and the measuring head, which is controlled by a laser sensor for displacement and position. The results show that lightness value is dependent on short range of distance nearly linearly, as visible in chart in Figure 7. Following charts in Figures 8 and 9 show that increasing distance influences more chroma than hue, nevertheless, the effect is not as strong as in lightness direction.
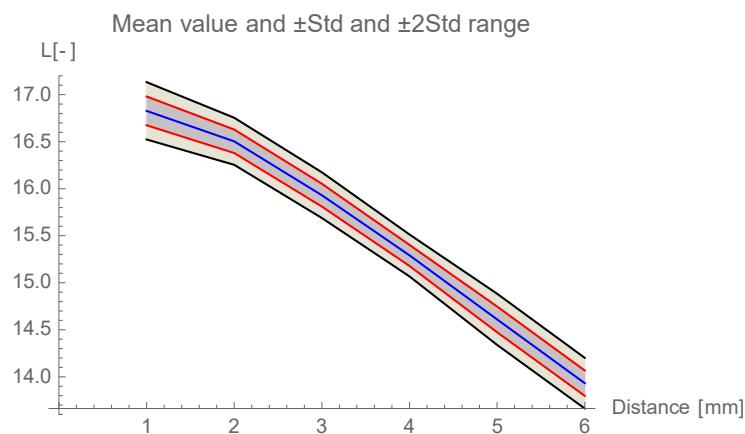

Figure 7 Sensitivity of measured lightness L* on distance between fabric and entrance aperture of deep blue woolen fabric
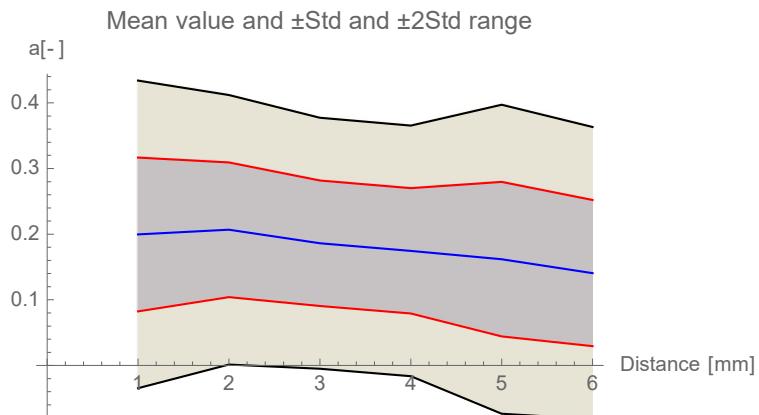

Figure 8 Sensitivity of measured redness-greenness a* on distance between fabric and entrance aperture of deep blue woolen fabric
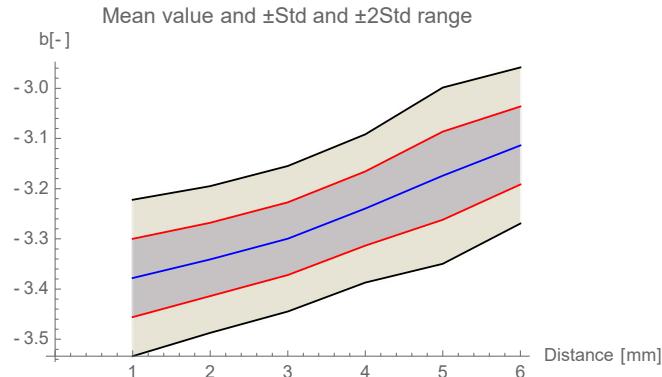
Figure 9 Sensitivity of measured yellowness-blueness b* on distance between fabric and entrance aperture of deep blue woolen fabric

Following the results of distance sensitivity, we implemented two functions into the evaluation software, which allows us to stay at a controlled distance (see Figure 10) and in case of fluctuations due to unexpected movement of measured fabric (in case of presented example in chart in Figure 10, data peak at length 11900 mm), the measured data are corrected based on presented relations.

Contrary to other on-line systems where information about measuring points is scattered due to usage of xenon short arc flash lamps or its alternatives, VUTS system allows a reading sequence near to 50 milliseconds. The resulting huge amount of output data can be represented after reduction of reading sequence by a set of bar charts, as is obvious. Nevertheless, a big part of the data output is lost. Color maps are used as the important output of the measurement made by VUTS on-line system, which represent the result of measured data at different positions of fabric loop (see Figures 11-16). Due to this simplification, local distribution of uneven dyeing is immediately visible. Operator of stenter or inspection machine is able to immediately recognize upcoming troubles.
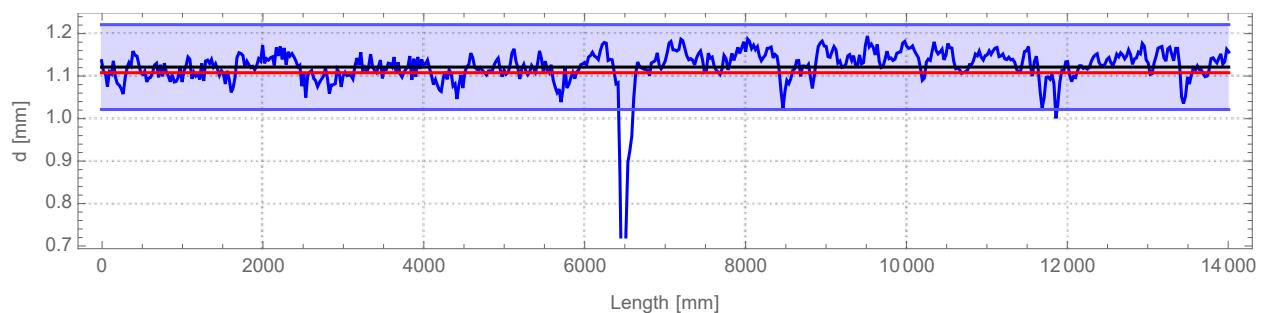

**Figure 10** Sensitivity of measured yellowness-blueness b* on distance between fabric
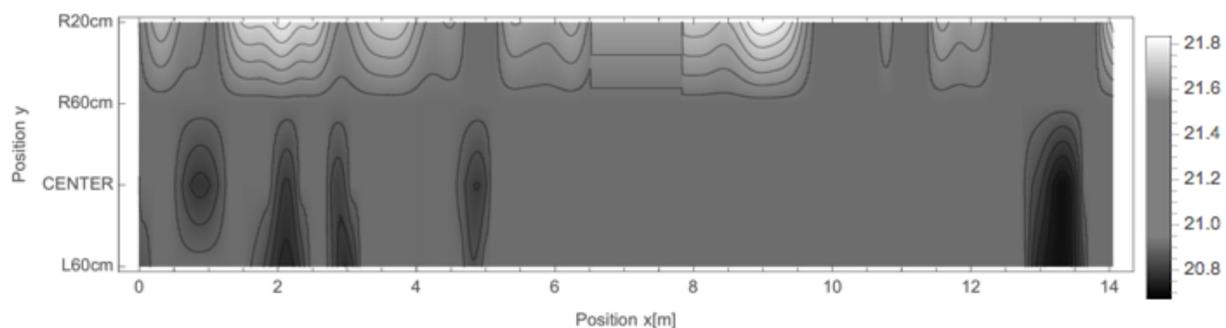
Figure 11 Color map of lightness difference of irregular blue shade woolen fabric - *L**
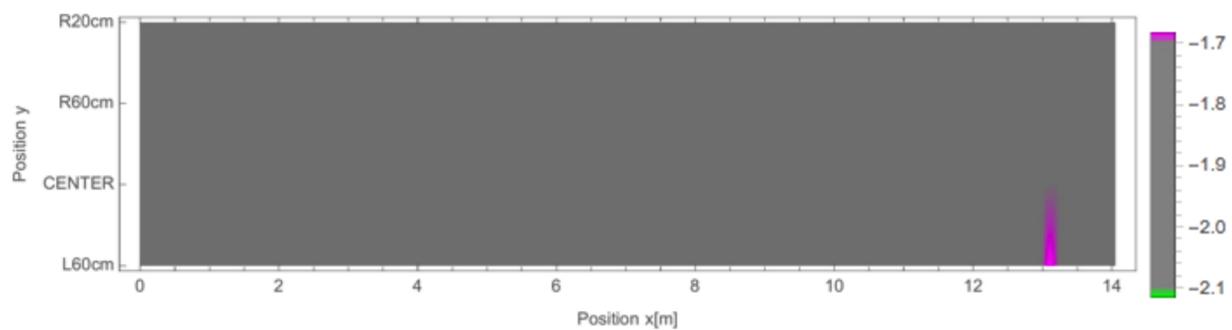
Figure 12 Color map of lightness difference of irregular blue shade woolen fabric - *a**
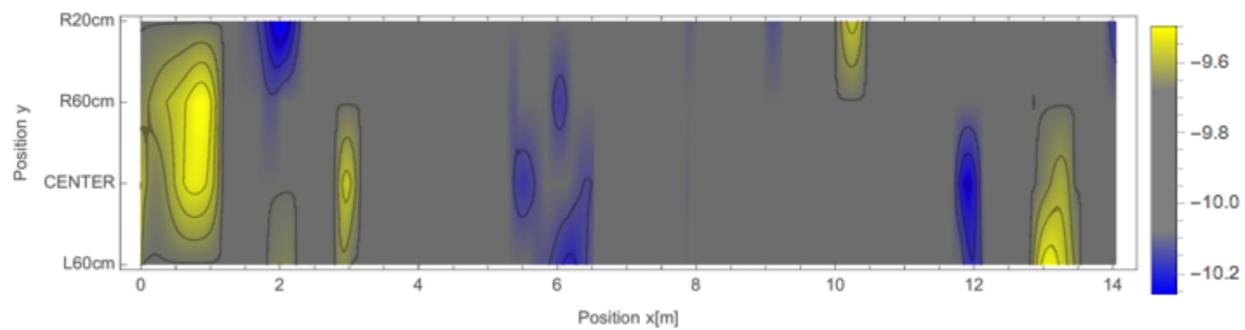
Figure 13 Color map of lightness difference of irregular blue shade woolen fabric - *b**
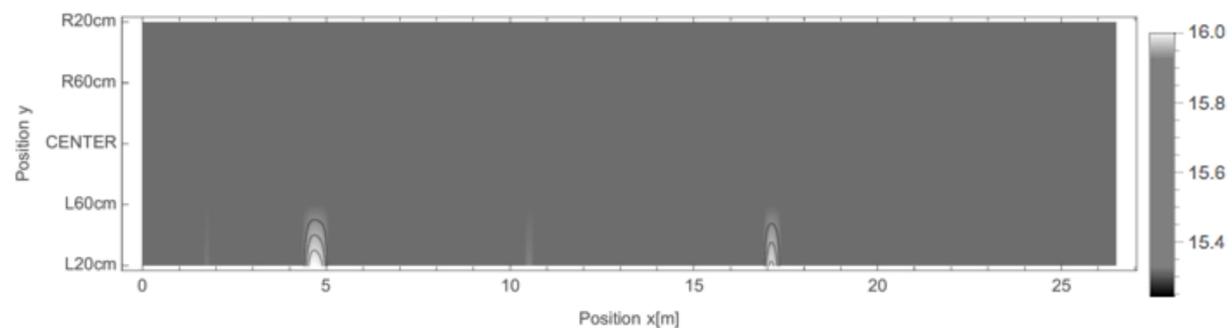
Figure 14 Color map of lightness difference of regular black shade woolen fabric - *L**
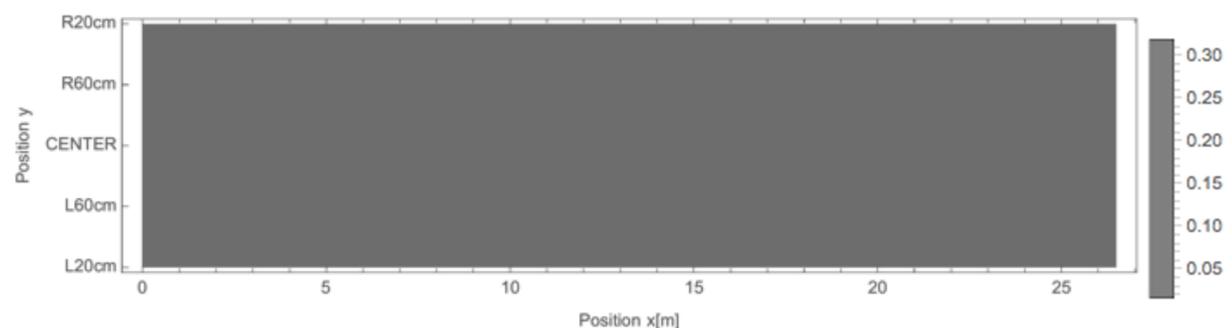

Figure 15 Color map of lightness difference of regular black shade woolen fabric - *a**
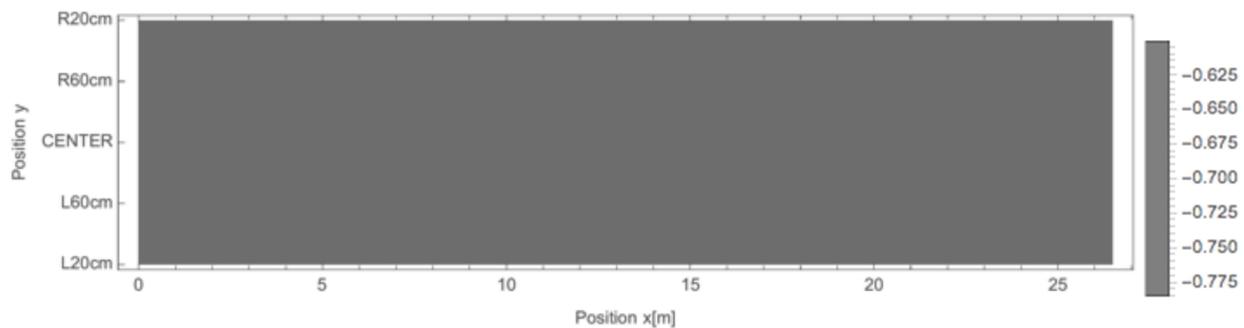
Figure 16 Color map of lightness difference of regular black shade woolen fabric - *b**

It is necessary to point out that the presented results were obtained from standard production and show tolerance limits which are near to just noticeable color difference. Obvious industrial tolerance of color difference is three times as high. There is no point in discussing measurement results here in any further detail, as no additional new information could be deduced. We consider it more important to outline the conclusion we have drawn from the trial runs and the problems which had been established.

1. The measuring frequency does not need to be adapted to the speed of the fabric. Instead, it is necessary to establish an appropriate relation with the control constants of the machine (the time and position at which a specific change can be brought about).

2. Reliable information is only provided by the average of at least 3 (4) individual measurements (position of measuring head), as individual values measured on in-process single layer fabric and with additional contamination conveyance etc. are not sufficiently representative. Just like in any on-line measurement, there is the risk of an absurd amount of data being produced, which is of no practical use.

3. With translucent fabric, the stability of the measured data can be considerably improved by using a pale grey backing and optical translucence measurement by a supportive sensor.

4. The measuring system must be shielded very effectively against electrical currents.

4   CONCLUSIONS

VUTS has developed a new on-line color measuring system for use especially in textile and paper industry. The system has a robust design whose main difference from the known instruments is the measuring sphere with a controlled gap. This permits improved traceability between on-line and off-line measuring systems. The optical unit has been specially developed to ensure a high

oscillation tolerance and a sufficient measuring area. The connection to a double-beam spectrometer and the continuous stable light source is made for high stability of measured parameters. The complete system is fully automatic thanks to computer control. Several test installations in the testing labs and a textile factory show that the measuring system does in fact come up to expectations and supplies good results.

5   REFERENCES

1. Imbault J.: A remote system for on-line color measurement, American Dyestuff Reporter 77(11), 34-38, 1988

2. Kryštůfek J., Militký J., Vik M., Wiener J.: Textile Dyeing Theory and Applications, TU Liberec 2013

3. Vik M., Čejka V., Founě F., Škop P.: Factors influencing reliability of on-line color measurements. Vlákna a Textil 22(1), 64-67, 2015

4. Vik M., Čejka V., Founě F.: Traceability problem of on-line color measurement, Speakers Platform conference on ITMA 2015, Milan, Italy, November 2015

5. Vik M: Color and Appearance Measurement in Industry, VÚTS Liberec 2015 (in Czech)

6. Keesee S.H., Aspland J.R.: Factors affecting the potential of on-line color measurement, Textile Chemist and Colorist 20(4), 15-18, 1988

7. Van Wersch K.: On-line-Farbmessung in der Kontinuefaerberei aus der Sicht des Maschienenbauers, ITB Veredlung 2/90, 21-40, 1990

8. Vik M., Vikova M.: Colour-appearance phenomena – metamerism, Vlákna a Textil 7(2), 126-127, 2000

9. Abbasi A.M.R., Vik M., Vikova M.: Color difference formulae evaluation by method of adjustment, World Journal of Engineering 11(1), 89-94, 2014

REMOVAL OF ACID DYES FROM AQUEOUS EFFLUENTS USING IONIC LIQUIDS

T. Weidlich and J. Martinková

Chemical Technology Group, Institute of Environmental and Chemical Engineering, Faculty of Chemical Technology
Studentska 573, University of Pardubice, CZ-532 10, Czech Republic
tomas.weidlich@upce.cz

Abstract: *The decolorization efficiency of three anionic dyes dissolved in aqueous solution using four quaternary phosphonium salts with bulk cation has been investigated by spectroscopic measurements. NMR spectroscopy suggests a replacement of sodium cations bound to sulfo groups in anionic dyes with tetrasubstituted phosphonium cations in a structure of isolated ion pairs. According to the obtained results, the tetraphenylphosphonium salt, which contains a more hydrophobic and bulky cation, exhibited a lower aqueous solubility of the produced ion pair.*

Key words: *ion exchange; wastewater treatment; precipitation; cationic surfactant; anionic dye; ion pair; ^{1}H and ^{13}C NMR spectroscopy*

1   INTRODUCTION

Water is the common green solvent used for the production and application of anionic (or acid) dyes. Sulfonic acid groups bonded in the structures of acid dyes make these colorants very polar and water soluble. The main method applied for the isolation of acid dyes from the reaction mixture is the precipitation of produced dyes by salting out and subsequent filtration. The obtained mother liquors are a saturated solution of the mentioned anionic dye in brine. The produced aqueous mother liquors contain high loads of refractory COD (Chemical Oxygen Demand caused by dissolved polar aromatic compounds) and AOX (Adsorbable Organic Halogens, if halogenated starting materials are used) and high salt loads from salting out process [1].

Over the past few decades, manufacturers and users of synthetic colorants have faced increasingly stringent regulations promulgated by agencies established to safeguard human health and the environment. This has meant that much of the emerging technology in these two areas arose from the need to comply with the regulations enacted. A significant proportion of this technology has been designed, specifically, to remove color and priority pollutants from wastewater effluents and to circumvent pollution problems by eliminating their sources. The main treatment methods applicable for the removal of colorants from aqueous effluents are carbon adsorption, chemical oxidation or chemical reduction accompanied by subsequent biodegradation in a wastewater treatment plant [1, 2]. However, anionic dyes are not readily adsorbed onto charcoal and moreover, the removal efficiency strongly depends on pH value [3].

Recently, chelating resins represent an important category of promising adsorbents [4, 5]. They are highly selective and efficient as compared with other adsorbent materials. However, the simple recovery of used chelating resins saturated by anionic dyes has not been satisfactorily solved.

The ultimate goal of this study is to describe the effect of quaternary phosphonium halides (R_4PX, ionic liquids [6]) containing a large tetra-alkylated cation on the effective removal of acid dyes from aqueous solutions. These ionic liquids serve as a liquid anion exchanger. We observed that the replacement of halide anions of ionic liquids by larger anions (anions of the acid dyes) proceeds smoothly even at room temperature [11, 13]:

$$R_4P^+X^- + dye\text{-}SO_3^-Na^+ \rightarrow dye\text{-}SO_3^-R_4P^+ + Na^+ + X^-$$
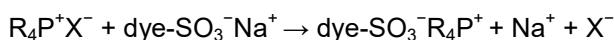
The anionic dyes Acid Yellow 17, Mordant Blue 9 and Reactive Orange 16 are commonly used aquatoxic acid dyes [9, 10] and were chosen as target pollutants. The interaction of these dyes with R_4PX salts gives slightly soluble ionic salts which can settle after a long contact time or can be removed more efficiently by the action of common inorganic flocculants aluminum or ferric sulphate.

2   MATERIALS AND METHODS

Dyes and reagents

Acid Yellow 17 (AY17), Mordant Blue 9 (MB9) and Reactive Orange 16 (RO16) were supplied by Sigma-Aldrich Co. These dyes belong among monoazo compounds bearing two sulfonate groups ($dye(SO_3Na)_2$), see Table 1. Stock solutions of the dyes (1×10^{-2} M) were prepared in distilled water.

Table 1 Description of used anionic dyes

Anionic dye	Chemical structure
Acid Yellow 17 (AY17) CAS: 6359-98-4 C.I. No.: 18965 $C_{16}H_{10}Cl_2N_4Na_2O_7S_2$ M = 551.28 A_{400} = 0.289 (10 µM sol.)	
Mordant Blue 9 (MB9) CAS: 3624-68-8 C.I. No.: 14855 $C_{16}H_9ClN_2Na_2O_8S_2$ M = 502.8 A_{516} = 0.250 (10 µM sol.)	
Reactive Orange 16 (RO16) CAS: 12225-83-1 C.I. No.: 17757 $C_{20}H_{17}N_3Na_2O_{11}S_3$ M = 617.52 A_{492} = 0.417 (10 µM sol.)	

Phosphonium-based ionic liquids trihexyltetradecyl-phosphonium chloride (Hex$_3$C$_{14}$PCl), tetraoctylphosphonium bromide (Oct$_4$PBr), tributyltetradecylphosphonium chloride (Bu$_3$C$_{14}$PCl), tetraphenylphosphonium chloride (Ph$_4$PCl) were Sigma-Aldrich Co. products (Table 2).

All other chemicals were Lach-Ner Co. (Czech Republic) products and were used as received. Stock solutions of two water soluble ionic liquids Ph$_4$PCl (5×10^{-2} M) and Bu$_3$C$_{14}$PCl (5×10^{-2} M) were prepared in distilled water.

Table 2 Description of phosphonium-based ionic liquids used for removal of dyes from aqueous solutions

Phosphonium-based ionic liquid	Chemical structure
Trihexyltetradecylphosphonium chloride (Hex$_3$C$_{14}$PCl) CAS No.: 258864-54-9 M = 519.31	
Tetraoctylphosphonium bromide (Oct$_4$PBr) CAS No.: 23906-97-0 M = 563.76	
Tributyltetradecylphosphonium chloride (Bu$_3$C$_{14}$PCl) CAS No.: 81741-28-8 M = 435.15	
Tetraphenylphosphonium chloride (Ph$_4$PCl) CAS No.: 2001-45-8 M = 374.84	

Instruments

A UV-visible spectrophotometer Libra S22 (Biochrom, Great Britain) was used to measure the absorbance values of the dyes to establish their λ_{max} and concentrations. A magnetic stirrer HeiTEC (Heidolph Instruments GmbH&Co.) was used for stirring of solutions. ^{1}H NMR and ^{31}P NMR spectra of the azo dyes were measured in CDCl$_3$ or DMSO-d$_6$ at 500.13 MHz and 202.45 MHz, respectively, using a Bruker Avance 500 spectrometer (Bruker BioSpin, Germany). The elemental analyses of phosphorus in filtered samples of treated aqueous solutions were carried out with the sequential, radially viewed ICP (Inductively Coupled Plasma) atomic emission spectrometer INTEGRA XL 2 (GBC, Dandenong Australia) equipped with a ceramic V-groove nebulizer and a glass cyclonic spray chamber (both Glass Expansion, Australia). The AOX (adsorbable organically bound halogens) analyses were performed according to European ISO 9562 standard.

Precipitation of dyes

An aliquot of neat room temperature ionic liquid (Hex$_3$C$_{14}$PCl, Oct$_4$PBr) or of the above-mentioned aqueous solution of ionic liquid was added into a beaker (400 mL) with the same 100 mL of 1×10^{-2} M dye solution, and the volume of solution in each beaker was replenished up to 200 mL. After 16 hours of stirring at the speed of 400 rpm and the temperature of 20±1°C, filtration by suction and measuring dye concentration in filtrates, the maximum decolorization efficiency (*DE %*) of dyes was determined from absorbance measurements, according to the concentration-absorbance standard curves at the respective maximum adsorption wavelength of the individual dye solutions. Afterwards, *DE %* was calculated from Eq.1:

$$DE\ \% = \left(1 - \frac{A}{A_0}\right) \times 100\% \qquad (1)$$

where *A* and *A$_0$* denote the absorbance in the solution after and before precipitation, respectively. Oily precipitates of R$_4$P-dye salts were washed with 50 mL distilled water and dissolved in dichloromethane. The CH$_2$Cl$_2$ solutions were evaporated to dryness, and the evaporation residues were dissolved in CDCl$_3$ to give saturated solutions for NMR spectroscopy measurements.

^{1}H and ^{31}P NMR spectroscopy was measured using saturated CDCl$_3$ solutions of precipitated quaternary phosphonium salts of the dyes.

AY17(SO$_3$PPh$_4$)$_2$:

^{1}H NMR (CDCl$_3$, δ(TMS) = 0.00 ppm): 13.4 bs (1H, OH); 8.24 s (1H, H-*arom.*); 8.04-7.89 m (4H, H-*p*); 8.00-7.98 d (2H, H-*arom.*); 7.88-7.86 m (4H, H-*p* of *Ph$_4$P*); 7.77-7.75 m (8H, H-*m* of *Ph$_4$P*); 7.68-

7.58 m (8H, H-*o* of *Ph$_4$P*); 7.41-7.40 bs (1H, H-*arom.*); 7.28-7.26 d (2H, H- *arom.*); 2.42 s (3H, CH$_3$).

^{13}C NMR (δ(CDCl$_3$) = 76.90 ppm): 157.5 C$_q$; 148.8 C$_q$; 145.4 C$_q$; 145.1 C$_q$; 140.6 C$_q$; 135.5 4 x C$_{arom}$.H; 134.7 CH; 134.1 8 x C$_{arom}$.H; 131.1 CH; 130.6 8 x C$_{arom}$.H; 130.4 CH; 128.0 C$_q$; 127.9 CH; 127.0 C$_q$; 117.0 4xC$_q$-arom.; 114.7 CH; 11.7 CH$_3$.

^{31}P NMR (CDCl$_3$, δ(H$_3$PO$_4$) = 0.00 ppm): 23.60.

Ph$_4$PBr:

^{31}P NMR (CDCl$_3$, δ(H$_3$PO$_4$) = 0.00 ppm): 23.30.

MB9(SO$_3$PC$_{14}$Bu$_3$)$_2$:

^{1}H NMR (CDCl$_3$, δ(TMS) = 0.00 ppm): 8.47-8.44 d (1H); 8.36-8.34 d (1H); 8.26-8.22 d (1H); 7.81 bs (1H); 7.54 bs (1H); 7.38-7.30 m (1H); 7.20-7.10 d (1H).

^{13}C NMR (δ(CDCl$_3$) = 76.90 ppm): 176.9 C$_q$; 143.6 C$_q$; 142.4 C$_q$; 134.0 2xC$_q$; 116.2 CH; 31.8 4xCH$_2$; 30.9 *n* xCH$_2$; 30.3 CH$_2$; 30.2 CH$_2$; 29.5 CH$_2$; 29.4 4 x CH$_2$; 29.2 4 x CH$_2$; 28.8 CH$_2$; 22.5 CH$_2$; 22.2 CH$_2$; 21.6 CH$_2$; 21.5 CH$_2$; 19.0 CH$_2$; 18.4 CH$_2$; 17.8 CH$_3$.

^{31}P NMR (CDCl$_3$, δ(H$_3$PO$_4$) = 0.00 ppm): 33.64.

Bu$_3$C$_{14}$PCl:

^{31}P NMR (CDCl$_3$, δ(H$_3$PO$_4$) = 0.00 ppm): 33.47.

3   RESULTS AND DISCUSSION

In the preliminary experiments, it was found that used phosphonium-based ionic liquids have the desired ability to precipitate the tested dyes from aqueous solution. MB9 was used as model dye for the study of influence of R$_4$PX quantity on *DE* (Table 3).

Table 3 Dependence of DE on the amount of R$_4$PX added to MB9 dye

Molar ratio MB9 : R$_4$PX	MB9 [mmol]	R$_4$PX [mmol]	DE [%]
1 : 1	1	Bu$_3$C$_{14}$PCl (1)	43
1 : 2	1	Bu$_3$C$_{14}$PCl (2)	93
1 : 2.1	1	Bu$_3$C$_{14}$PCl (2.1)	94
1 : 4	1	Bu$_3$C$_{14}$PCl (4)	84
1 : 1	1	Hex$_3$C$_{14}$PCl (1)	13
1 : 2	1	Hex$_3$C$_{14}$PCl (2)	92
1 : 2.1	1	Hex$_3$C$_{14}$PCl (2.1)	93
1 : 4	1	Hex$_3$C$_{14}$PCl (4)	99

We described earlier [7, 8] that the quantity of sulphonate groups bound in dye structure (number of -SO$_3$Na, n SO$_3$Na) plays a crucial role in calculation of optimal dose of R$_4$PX. In the case of dye(SO$_3$Na)$_2$, the addition of two moles of R$_4$PX per mol of dye(SO$_3$Na)$_2$ induces rapid ion pair formation which is accompanied by precipitation. The increase of molecular mass of produced ion pair in combination with drop in polarity cause a significant decrease of solubility of the corresponding ion pair dye(SO$_3$PR$_4$)$_2$.

On the other hand, an excess of R_4PX negatively influences the quality of the treated wastewater because some quaternary phosphonium salts have biocidal properties [11]. As we tested using NMR spectroscopy, the ion pair corresponding to dye$(SO_3PR_4)_2$ structure arose even using molar ratio $SO_3Na : R_4PX$ lower than 1 (see Materials and methods, Precipitation of dyes chapter). Hence, molar ratio n $SO_3Na : R_4PX = 1 : 1$ was chosen as the optimum for the treatment of model aqueous dye solutions.

The interaction between dye and R_4PX can be affected by the pH value of aqueous solution because of the charge on the dye and R_4PX molecules. The sulphonate groups bound in the dye structure would be protonated at low pH values. On the other hand, the part of the dye-SO_3^- groups is probably not closely associated with bulky R_4P^+ cations at high pH values, which causes the partial solubility of dyes in strongly alkaline aqueous solutions even in the presence of R_4PX. However, the pH dependence of DE using R_4PX show that the maximum DE did not vary significantly in the pH range 6-9 typical for the neutralized wastewater, as we published earlier [7].

As could be seen in Figure 1 and Table 4, DE varies mainly with structure of the dissolved dye. In general, R_4PX containing a more hydrophobic cation with high mass is better dye scavengers than IL having a smaller and lighter cation.
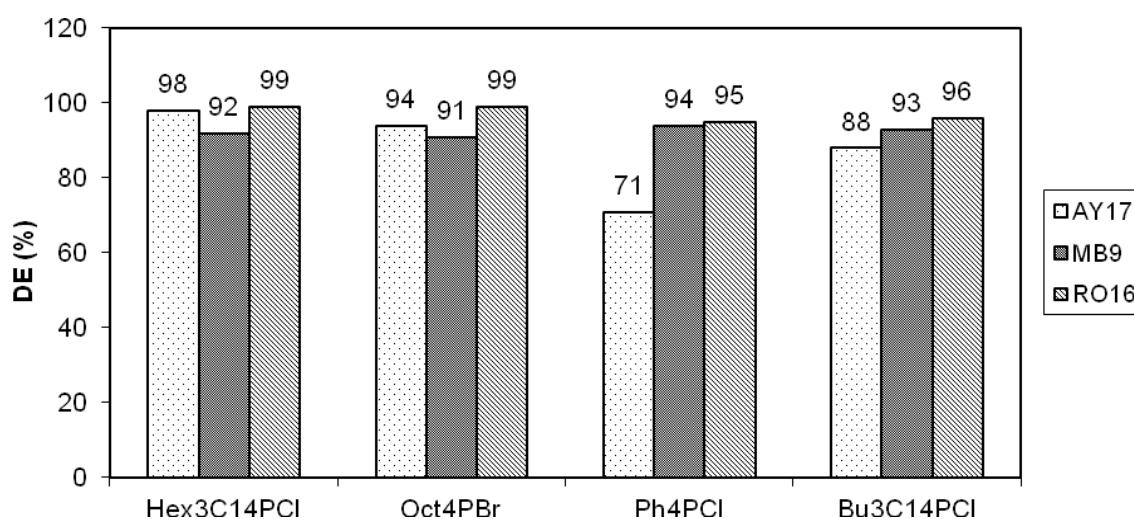

Figure 1 Effect of different R_4PX on DE of three tested acid dyes in 5 mM aq. solution

Table 4 Changes in relative molar mass (M_r) of dyes caused by ion exchange of cations and determined DE related to aqueous solubility of obtained dye$(SO_3PR_4)_2$ ion pair

Used anionic dye dye$(SO_3Na)_2$	Applied IL	Produced ion pair	M_r of ion pair	DE [%]
AY17 (551.28 g/mol)	Hex$_3$C$_{14}$PCl	AY17(SO$_3$PC$_{14}$Hex$_3$)$_2$	1473.03 g/mol	98
AY17 (551.28 g/mol)	Oct$_4$PBr	AY17(SO$_3$POct$_4$)$_2$	1473.03 g/mol	94
AY17 (551.28 g/mol)	Bu$_3$C$_{14}$PCl	AY17(SO$_3$PC$_{14}$Bu$_3$)$_2$	1304.71 g/mol	88
AY17 (551.28 g/mol)	Ph$_4$PCl	AY17(SO$_3$PPh$_4$)$_2$	1184.09 g/mol	71
MB9 (502.8 g/mol)	Hex$_3$C$_{14}$PCl	MB9(SO$_3$PC$_{14}$Hex$_3$)$_2$	1424.56 g/mol	92
MB9 (502.8 g/mol)	Oct$_4$PBr	MB9(SO$_3$POct$_4$)$_2$	1424.56 g/mol	91
MB9 (502.8 g/mol)	Bu$_3$C$_{14}$PCl	MB9(SO$_3$PC$_{14}$Bu$_3$)$_2$	1256.23 g/mol	93
MB9 (502.8 g/mol)	Ph$_4$PCl	MB9(SO$_3$PPh$_4$)$_2$	1135.62 g/mol	94
RO16 (617.52 g/mol)	Hex$_3$C$_{14}$PCl	RO16(SO$_3$PC$_{14}$Hex$_3$)$_2$	1539.27 g/mol	99
RO16 (617.52 g/mol)	Oct$_4$PBr	RO16(SO$_3$POct$_4$)$_2$	1539.27 g/mol	99
RO16 (617.52 g/mol)	Bu$_3$C$_{14}$PCl	RO16(SO$_3$PC$_{14}$Bu$_3$)$_2$	1370.95 g/mol	96
RO16 (617.52 g/mol)	Ph$_4$PCl	RO16(SO$_3$PPh$_4$)$_2$	1250.34 g/mol	95

The quantity of dissolved phosphorus in treated water was determined using ICP-OES technique (Table 5) after isolation of dye$(SO_3PR_4)_2$ ion pairs from treated aqueous solutions.

Table 5 Phosphorus content in obtained aqueous filtrates after R_4PX treatment

Obtained aqueous filtrate	Content of P [mg.L^{-1}]
50 mM aq. $Bu_3C_{14}PCl$ solution	1549
5 mM aq. RO16 solution	Less than 0.5
5 mM aq. AY17 solution	Less than 0.5
5 mM aq. MB9 solution	Less than 0.5
2 $Bu_3C_{14}PCl$ + AY17	7.257
2 $Bu_3C_{14}PCl$ + RO16	6.364
2 $Bu_3C_{14}PCl$ + MB9	9.451
2 Oct_4PBr + RO16	Less than 0.5
2 $Hex_3C_{14}PCl$ + RO16	0.844

However, the produced dye$(SO_3PR_4)_2$ ion pairs are viscous precipitates (viscosity of MB9$(SO_3PC_{14}Hex_3)_2$ is 116.7 Pa.s). Hence removal of this tar-like matter from the aqueous phase is a major problem in all the cases when precipitation occured. To solve this problem, coagulation was tested as a simple and low-cost process to facilitate separation of the ion pair from the treated aqueous dye solution.

For practical reasons, mixed aqueous solutions of soluble $Bu_3C_{14}PCl$ together with $Al_2(SO_4)_3$ were used for simple removal of anionic dyes [8]. Determination of an appropriate dose of coagulant is considered as one of the most important parameters for its performance in the dye$(SO_3PR_4)_2$ ion pair removal process. Moreover, an optimum dosage of coagulant also minimises the concentration of R_4P^+ salts and dye residues in treated water. For dye RO16, the *DE* 99% and content of phosphorus in aqueous filtrate less than 0.5 mg/L were obtained using molar ratio dye : RO16$(SO_3PC_{14}Bu_3)_2$: $Al_2(SO_4)_3$ = 1 : 2 : 16. Using sole inorganic $Al_2(SO_4)_3$ coagulant for the removal of RO16 in molar ratio dye : $Al_2(SO_4)_3$ = 1 : 16 from 5 mM aqueous solution, the obtained DE was only 63.5%.

In the case of 5 mM aqueous solution MB9 (AOX = 155 mg Cl/L), even using the molar ratio of reactants dye : MB9 $(SO_3PC_{14}Bu_3)_2$: $Al_2(SO_4)_3$ = 1 : 1 : 2, the *DE* 94.5% was obtained, the content of phosphorus in colorless aqueous filtrate was less than 0.5 mg/L and the content of absorbable organic halogens is AOX 17.8 mg Cl/L [8].

4   CONCLUSIONS

A new technique was investigated for the simple treatment of model waste water contaminated with anionic dyes. It was shown that the addition of nonpolar phosphonium-based ionic liquids enables efficient removal of dyes from aqueous solutions by precipitation.

For simplifying the treatment process, the produced tarry-like precipitates of dye$(SO_3PR_4)_2$ ion pairs were removed by adsorption on hydrated aluminum oxide surface produced by the addition of aqueous solution of 50 mM $Bu_3C_{14}PCl$ in 0.4 M aqueous aluminum sulphate in the form of rapidly sedimenting coloured particles.

5   REFERENCES

1.   Reife A., Freeman H.S.: Environmental Chemistry of Dyes and Pigments, 1996, Wiley and Sons, New York, ISBN: 0-471-58927-6

2.   Integrated Pollution Prevention and Control, Reference Document on Best Available Techniques for the Manufacture of Organic Fine Chemicals, August 2006, available on: www.icct.cz

3.   Malik P.K.: Use of activated carbons prepared from sawdust and rice-husk for adsorption of acid dyes: a case study of Acid Yellow 36, Dyes and Pigments 56, 239-249, 2003

4.   Karcher S.; Kornmüller A., Jekel M.: Anion exchange resins for removal of reactive dyes from textile wastewaters, Water Research 36, 4717-4724, 2002

5.   Dragan E.S.; Dinu I.A.: Interaction of Dis-azo Dyes with Quaternized Poly(dimethylaminoethyl methacrylate) as a Function of the Dye Structure and Polycation Charge Density, Journal of Applied Polymer Science 112(2), 728-735, 2009

6.   Welton T.: Room-Temperature Ionic Liquids. Solvents for Synthesis and Catalysis, Chemical Review 99(8), 2071-2084, 1999

7.   Weidlich T., Martinková J.: Application of Tetraphenyl- and Ethyltriphenylphosphonium Salts for Separation of Reactive Dyes from Aqueous Solution, Separation Science and Technology 47(9), 1310, 2012

8.   Weidlich T., Martinková J.: Dye precipitation process from aqueous solutions, Czech Patent No. CZ303942 (B6) (2013)

9.   De Luna L.A.V., da Silva T.H.G., Nogueira R.F.P., Kummrow F., Umbuzeiro G.A.: Aquatic toxicity of dyes before and after photo-Fenton treatment, Journal of Hazardous Materials 276, 332-338, 2014

10. Mansour H.B., Corroler D., Barillier D., Ghedira K., Chekir L., Mosrati R.: Evaluation of genotoxicity and pro-oxidant effect of the azo dyes: Acid yellow 17, violet 7, orange 52, and of their degradation products by Pseudomonas putida mt-2, Food and Chemical Toxicology 45, 1670-1677, 2007

11. Schlüsener M.P., Kunkel U., Ternes T.A.: Quaternary Triphenylphosphonium Compounds: A New Class of Environmental Pollutants, Environmental Science & Technology 49(24), 14282-14291, 2015

INSTRUCTIONS FOR AUTHORS

The journal ,,**Vlákna a textil**" (**Fibres and Textiles**) is the scientific and professional journal with a view to technology of fibres and textiles, with emphasis to chemical and natural fibres, processes of fibre spinning, finishing and dyeing, to fibrous and textile engineering and oriented polymer films. The original contributions and works of background researches, new physical-analytical methods and papers concerning the development of fibres, textiles and the marketing of these materials as well as review papers are published in the journal.

Manuscript

The original research papers are required to be written in English language with summary. Main results and conclusion of contribution from Slovak and Czech Republic may be in Slovak or Czech language as well. The advertisements will be published in a language according to the mutual agreement.

The first page of the manuscript has to contain:

The title of the article (16 pt bold, capital letters, centred)

The full *first name* (s) and also *surnames* of all authors (11 pt, bold, centred).

The complete address of the working place of the authors, e-mail of authors (9 pt, italic, centred)

Abstract (9 pt, italic)

Key words (9 pt, italic)

The manuscript has to be written in A4 standard form, in **Arial, 10 pt**.

The text should be in ***double-column format (width 8.1 cm) in single line spacing.***

Page margins: up and down 2.5 cm; left and right 2.0 cm.

Do not number the pages and do not use footnotes. Do not use business letterhead.

Figures, tables, schemes and photos (centered) should be numbered by Arabic numerals and titled over the table and under the figure or picture.

Photos and schemes have to be sufficiently contrastive and insert in text as pictures.

Figures, tables, schemes and photos, please, send in separate file.

Mathematical formulae should be centred on line and numbered consecutively on the right margin.

Physical and technical properties have to be quantified in SI units, names and abbreviations of the chemical materials have to be stated according to the IUPAC standards.

References in the text have to be in square brackets and literature cited at the end of the text.

References (9 pt), have to contain names of all authors.

[1]   Surname N., Surname N.: Name of paper or Chapter, In Name of Book, Publisher, Place of Publication, YYYY, pp. xxx-yyy

[2]   Surname N., Surname N.: Name of paper, Name of Journal Vol. (No.), YYYY, pp. xxx-yyy

[3]   Surname N., Surname, N.: Title of conference paper, Proceedings of xxx xxx, conference location, Month and Year, Publisher, City, Surname N. (Ed.), YYYY, pp. xxx-yyy

[4]   Surname N., Surname N.: Name of Paper, Available from http://www.exact-address-of-site, Accessed: YYYY-MM-DD

The final template of manuscript is available on **http://www.ft.tul.cz/mini/Vlakna_a_textil**

Authors are kindly requested to deliver the paper (in Word form) to be published by e-mail: marcela.hricova@stuba.sk

GOLDEN SPONSORS

ARCHROMA — LIFE ENHANCED

Synthesia

Veba

SILVER SPONSORS

inoTEX®

CONTIPRO PHARMA

LENZING

LORIS BELLINI Dyeing machines

TEXCOLOUR

MENZEL

COOLTRANS

BRONZE SPONSORS

DyStar

SedoTreepoint

monforts

COFFEE BREAK SPONSORS

SETEX
www.setex-germany.com

OTHER SPONSORS & EXHIBITORS

pernikjanos.cz

Q-LAB

gb

datacolor international

LABIMEX CZ

MEDIA SPONSORS

Prima

CHEMAGAZÍN

ORGANISERS

STCHK

The Czech Association
of Textile Chemists
and Colourist

IFATCC

International Federation of
Associations of Textile
Chemists and Colourist

---

in cooperation with

clutex
cluster technical textiles
2006 - 2016

Office of the Government
of the Czech Republic

ATOK

University
of Pardubice
Centre for Technology
and Knowledge Transfer

University
of Pardubice
Faculty
of Chemical Technology

---

and with financial support
of the Pardubice Region, City of Pardubice, Hradec Králové Region

PARDUBICKÝ KRAJ

Pardubice

HRADEC KRÁLOVÉ REGION